

2013

# Structural and synthesis studies of the Pro<sup>143</sup> region Skp1 in *Dictyostelium discoideum*

Chamini V. Karunaratne

*Louisiana State University and Agricultural and Mechanical College*, ckarun2@lsu.edu

Follow this and additional works at: [https://digitalcommons.lsu.edu/gradschool\\_dissertations](https://digitalcommons.lsu.edu/gradschool_dissertations)



Part of the [Chemistry Commons](#)

---

## Recommended Citation

Karunaratne, Chamini V., "Structural and synthesis studies of the Pro<sup>143</sup> region Skp1 in *Dictyostelium discoideum*" (2013). *LSU Doctoral Dissertations*. 2218.

[https://digitalcommons.lsu.edu/gradschool\\_dissertations/2218](https://digitalcommons.lsu.edu/gradschool_dissertations/2218)

This Dissertation is brought to you for free and open access by the Graduate School at LSU Digital Commons. It has been accepted for inclusion in LSU Doctoral Dissertations by an authorized graduate school editor of LSU Digital Commons. For more information, please contact [gradetd@lsu.edu](mailto:gradetd@lsu.edu).

STRUCTURAL AND SYNTHESIS STUDIES OF THE PRO<sup>143</sup> REGION OF SKP1 IN  
*DICTYOSTELIUM DISCOIDEUM*

A Dissertation

Submitted to the Graduate Faculty of the  
Louisiana State University and  
Agricultural and Mechanical College  
in partial fulfillment of the  
requirements for the degree of  
Doctor of Philosophy

in

The Department of Chemistry

by  
Chamini Vichithra Karunaratne  
B.S., University of Colombo, 2006  
December 2013

*To My Family...*

*To my parents Irine and Upali Karunaratne and to my brother Yahal Karunaratne, for supporting, encouraging and believing in me in all my endeavors.*

*To my husband Waruna Jinadasa, whose love, encouragement and profound understanding helped me to reach this accomplishment.*

*To my son Yevin, for being adorable and make me feel spectacular.*

## ACKNOWLEDGMENTS

I would like to express my sincere gratitude to my advisor, Dr. Carol Taylor, for her invaluable guidance, support, and encouragement that I have received throughout my graduate career at LSU. Dr. Taylor has always made herself available despite her busy schedule. Thank you very much for taking the time to proofread my dissertation chapters and patiently correcting my writing.

My deepest appreciation goes to my committee members Dr. Graca Vicente, Dr. William Crowe and Dr. Bin Chen for their help and meaningful suggestions. I would also like to thank my Dean's Representative, Dr. Gregg Henderson for taking the time to read my work and attend my examinations.

I would like to thank our collaborator Dr. Christopher West at the Oklahoma Health Sciences Center for testing our compounds for biological activity and for sharing biological data. Sincere thanks to Dr. Thomas Weldeghiorghis and the late Dr. Dale Treleven for their help with NMR studies and Connie David for help with mass spectrometry studies.

I am also grateful to my labmates Benson, Doug, Ning, Saroj, Chyree, and Molly for their discussions, friendship and encouragement. Completing this work would have been more difficult were it not for the support and friendship provided by all of you. I also thank Jarret for synthesizing some amino acid building blocks for me.

Finally, my gratitude goes to the Department of Chemistry, Louisiana State University and the National Institutes of Health for their financial support.

## TABLE OF CONTENTS

ACKNOWLEDGMENTS.....	iii
LIST OF TABLES.....	vii
LIST OF FIGURES .....	ix
LIST OF SCHEMES.....	xiii
LIST OF ABBREVIATIONS AND SYMBOLS .....	xvii
ABSTRACT.....	xxi
CHAPTER 1: THE SKP1 PROTEIN.....	1
1.1 Ubiquitination.....	1
1.2 The E3 Ubiquitin Ligase Complex.....	2
1.3 Skp1 of <i>Dictyostelium</i> .....	3
1.3.1 Prolyl Hydroxylase Enzyme.....	5
1.3.2 Skp1 Glycosylation in <i>Dictyostelium</i> .....	6
1.4 Conformational Changes in Skp1 Associated with Post-translational Modifications.....	9
1.5 Post-Translational Modifications of Skp1 as a Therapeutic Target.....	9
1.6 Enzyme Kinetics of Gnt1.....	11
1.7 Goals of the Project .....	13
CHAPTER 2: SYNTHESIS OF A BISUBSTRATE ANALOG AS A PUTATIVE INHIBITOR OF GNT1.....	15
2.1 Skp1 Glycosylation .....	15
2.2 Inhibitors of Glycosyltransferases .....	15
2.3 Potential Inhibitors of Gnt1.....	17
2.4 Design of a Bisubstrate Analog.....	19
2.4.1 Retrosynthetic Analysis of Bisubstrate Analog.....	19
2.4.2 Synthesis of Bisubstrate Analog .....	20
2.5 Experimental Section.....	26
2.5.1 Experimental procedures.....	27
2.5.2 <sup>1</sup> H and <sup>13</sup> C NMR Spectra .....	36
CHAPTER 3: THERMODYNAMICS AND KINETICS STUDIES OF CONFORMATIONAL CHANGES IN A DIPEPTIDE MODEL SYSTEM FOR THE POST-TRANSLATION MODIFICATIONS OF PRO <sup>143</sup> IN SKP1 OF DICTYOSTELIUM .....	60
3.1 Conformational Concepts Relevant to Proline-Containing Peptides.....	60
3.1.1 Prolyl Hydroxylation in Proteins Other than Skp1 .....	62
3.1.2 Traditional Views of <i>Cis</i> → <i>Trans</i> Isomerism and Collagen Stability .....	63
3.2 Recent Advances in Understanding Factors Affecting <i>Cis</i> → <i>Trans</i> Isomerism in Pro-Containing Peptides .....	64
3.2.1 Lubell and coworkers - Steric and Stereochemical Effects of a Substituent at Cδ.....	64

3.2.2	Raines and coworkers – Inductive Effect of a Substituent at Cy .....	65
3.2.3	Moroder <i>et al.</i> – More Evidence for the Inductive Effect and the Importance of Stereochemistry at Cy.....	67
3.2.4	Taylor <i>et al.</i> – Factors Affecting Conformation in Proline and Hydroxylated Prolines.....	68
3.2.5	Schweizer and Coworkers – Glycosylation of Hydroxyproline.....	71
3.3	Synthesis of Dipeptide and Glycopeptide Model Systems to Study the Conformational Changes Associated with Prolyl Hydroxylation and Glycosylation in Skp1.....	72
3.4	NMR Spectroscopic Studies .....	76
3.4.1	Proton NMR Spectra .....	76
3.4.2	Inductive Effect on Cy Chemical Shift.....	78
3.4.3	Measurement of $K_{trans/cis}$ and Thermodynamics Studies of Dipeptides <b>61-63</b> .....	89
3.4.4	Kinetics Studies of Proline-Containing Peptides .....	85
3.4.4.1	Magnetization Inversion Transfer NMR Experiments .....	85
3.4.4.2	Rabenstein and Coworkers – Studies of <i>Cis</i> → <i>Trans</i> Isomerization of Cysteine-Proline Peptide Bonds.....	86
3.4.4.3	Lubell and Coworkers – Effect of Substituents on C $\delta$ on Amide <i>Cis</i> → <i>Trans</i> Isomerization .....	87
3.4.4.4	Moroder and coworkers – Studies of <i>Cis</i> → <i>Trans</i> Isomerization of Fluoroproline .....	89
3.4.4.5	Schweizer and coworkers – Studies of <i>Cis</i> → <i>Trans</i> Isomerization of Glycosylated Hydroxyproline Derivative .....	89
3.4.4.6	Raines and coworkers – Effect of the Electronegative Substituents at Cy on <i>Cis</i> → <i>Trans</i> Isomerization .....	91
3.4.4.7	Williams <i>et al.</i> – an Undergraduate Magnetization Transfer Experiment.....	91
3.5	Kinetics Study of Skp1 Relevant Peptides - Isomerization of the Prolyl Amide Bond .....	92
3.6	Study of Hyp-Cy Stereochemistry of the Native Skp1 Protein .....	94
3.7	2 <i>S</i> ,4 <i>S</i> -Fluoroproline (flp).....	96
3.7.1	Previous studies of fluoroproline .....	96
3.7.2	Synthesis of flp .....	98
3.8	Experimental Section.....	101
3.8.1	Synthetic Procedures.....	101
3.8.2	Variable temperature NMR experiments .....	126
3.8.3	Magnetization Transfer NMR Experiments.....	131
3.8.4	$^1\text{H}$ and $^{13}\text{C}$ NMR Spectra.....	151

#### CHAPTER 4:

SYNTHESIS OF AN $\alpha$ -HELICAL MIMETIC FOR THE 143-151 FRAGMENT OF SKP1 .....		211
4.1	The $\alpha$ -Helix in Peptides and Proteins.....	211
4.2	$\alpha$ -Helical Mimetics .....	211
4.2.1	Helical Surface Mimetics.....	212
4.2.2	Helical Foldamers.....	214
4.2.3	Helix Stabilization Methods - Hydrogen Bond Surrogates .....	215
4.3	The $\alpha$ -Helix of Skp1 .....	218
4.4	A HBS $\alpha$ -Helical Mimetic for the 143-151 Peptide of Skp1.....	219
4.5	Retrosynthetic Analysis of an Arora-Type $\alpha$ -Helical Mimetic for Skp1 .....	220

4.6	Synthesis of the C-Terminal Fmoc-QIRK-NH <sub>2</sub> Tetrapeptide 132.....	221
4.7	Synthesis of Fmoc-IKNDFT-OBn hexapeptide <b>171</b> .....	222
4.7.1	Synthesis of Fmoc-Asp(O <sup>t</sup> Bu)-Phe-Thr( <sup>t</sup> Bu)-OBn ( <b>150</b> ) .....	222
4.7.2	Synthesis of Fmoc-Ile-Lys(Boc)-Asn(Trt)-OBn ( <b>157</b> ) .....	222
4.7.3	[3+3] Fragment coupling .....	225
4.8	The Central Peptidomimetic Fragment: Previous Alkylation of Related β- Ketoesters.....	225
4.9	Synthesis of Triflate <b>136</b> .....	228
4.10	Synthesis of the β-Ketoester Dipeptide Isostere .....	228
4.11	Ethylene Isostere Approach of Vernall <i>et al.</i> for an α-Helical Mimetic for the 143-151 Peptide of Skp1.....	232
4.11.1	Synthesis of an α-Helical Mimetic by Vernall <i>et al.</i> .....	232
4.11.2	Synthesis of the Dipeptide Isostere <b>216</b> .....	235
4.11.3	Synthesis of the Tetrapeptide Isostere <b>213</b> .....	237
4.11.4	Peptide cyclization.....	241
4.11.5	Cyclization of the tetrapeptide mimetic <b>234</b> .....	243
4.12	Experimental Section .....	245
4.12.1	Synthetic Procedures .....	245
4.12.2	<sup>1</sup> H and <sup>13</sup> C NMR Spectra .....	263
CHAPTER 5:		
FUTURE WORK .....		298
5.1	Coupling of N-terminal and C-terminal Oligopeptides to the Cyclic Pentapeptide Mimetic .....	298
5.2	Circular Dichroism.....	300
5.3	Enzyme Assays .....	301
5.4	P4H1 Substrates.....	302
5.5	Future Inhibitors.....	304
REFERENCES .....		306
APPENDIX: LETTERS OF PERMISSION.....		316
THE VITA.....		326

## LIST OF TABLES

Table 1.1	Skp1 sequence in different organisms .....	10
Table 1.2	$K_m$ and $V_{max}$ values.....	13
Table 2.1	Attempted glycosylation of <b>18</b> with electrophiles <b>23-26</b> .....	22
Table 2.2	Glycosylation of <b>18</b> .....	23
Table 3.1	Energy barriers for amide bond isomerization of <i>N</i> -Acetyl-5- <i>tert</i> -butylproline Methyl Amide Derivatives at 25 °C.....	64
Table 3.2	Thermodynamics parameters for compounds <b>39-43</b> .....	68
Table 3.3	Thermodynamics parameters for compounds <b>38a</b> , <b>39</b> , and <b>44-47</b> .....	69
Table 3.4	Thermodynamics parameters for compounds <b>47-54</b> .....	70
Table 3.5	<i>Cis</i> → <i>trans</i> isomerization of glycosylated Ac-Hyp-NHMe .....	71
Table 3.6	Prolyl amide <i>cis</i> → <i>trans</i> isomerism of glycosylated Ac-hyp-OMe .....	72
Table 3.7	Coupling constant and ring pucker assignment for compounds <b>61-63</b> .....	78
Table 3.8	<sup>13</sup> Cy chemical shifts for compounds <b>40</b> , <b>86</b> and <b>87</b> .....	78
Table 3.9	<sup>13</sup> Cy chemical shifts for compounds <b>40</b> , <b>86α/β</b> , <b>59</b> and <b>60α/β</b> .....	79
Table 3.10	<sup>13</sup> Cy chemical shifts for compounds <b>60</b> - <b>62</b> .....	79
Table 3.11	Thermodynamics parameters for compounds <b>61-63</b> .....	82
Table 3.12	Thermodynamics data of peptides <b>61-63</b> and <b>89</b> .....	84
Table 3.13	Prolyl amide bond isomerization rates constants for compounds <b>38a</b> , <b>55</b> and <b>101-104</b> .....	88
Table 3.14	Prolyl amide bond isomerization rate constants for compounds <b>38a</b> , <b>55</b> <b>105</b> and <b>57α/β</b> .....	90
Table 3.15	Prolyl amide isomerization rate constants for compounds <b>59</b> , <b>60α/β</b> .....	90
Table 3.16	Prolyl peptide bond isomerization rates for compounds <b>62</b> and <b>89</b> .....	93
Table 3.17	Chemical shifts differences of the <i>cis</i> and <i>trans</i> isomer proton signal.....	93
Table 3.18	Thermodynamics data derived from Van't Hoff plots .....	126
Table 3.19	Thr-Pro amide isomer equilibrium constant $K_{v/c}$ at various temperatures of Ac-Thr Pro-NHMe ( <b>61</b> ).....	127
Table 3.20	Thr-Pro amide isomer equilibrium constant $K_{v/c}$ at various temperatures of Ac-Thr-Hyp-NHMe ( <b>62</b> ).....	128



Table 3.21	Thr-Pro amide isomer equilibrium constant $K_{t/c}$ at various temperatures of Ac-Thr-[( $\alpha$ ,1-4)GlcNAc]Hyp-NHMe ( <b>63</b> ).....	129
Table 3.22	Thr-Pro amide isomer equilibrium constant $K_{t/c}$ at various temperatures of Ac-[( $\alpha$ ,1-4)GlcNAc]-NHMe ( <b>89</b> ) .....	130
Table 3.23	Integration vs. $d_2$ for Ac-Thr-Hyp-NHMe ( <b>62</b> ) at 60 °C.....	132
Table 3.24	Integration vs. $d_2$ for Ac-Thr-Hyp-NHMe ( <b>62</b> ) at 65 °C.....	133
Table 3.25	Integration vs. $d_2$ for Ac-Thr-Hyp-NHMe ( <b>62</b> ) at 70 °C.....	134
Table 3.26	Integration vs. $d_2$ for Ac-Thr-Hyp-NHMe ( <b>62</b> ) at 75 °C.....	135
Table 3.27	Data for Eyring Analysis for Ac-Thr-Hyp-NHMe ( <b>62</b> ) .....	136
Table 3.28	Integration vs. $d_2$ for Ac-Hyp[( $\alpha$ ,1-4)GlcNAc]-NHMe ( <b>89</b> ) at 60 °C.....	137
Table 3.29	Integration vs. $d_2$ for Ac-Hyp[( $\alpha$ ,1-4)GlcNAc]-NHMe ( <b>89</b> ) at 65 °C.....	138
Table 3.30	Integration vs. $d_2$ for Ac-Hyp[( $\alpha$ ,1-4)GlcNAc]-NHMe ( <b>89</b> ) at 70 °C.....	139
Table 3.31	Integration vs. $d_2$ for Ac-Hyp[( $\alpha$ ,1-4)GlcNAc]-NHMe ( <b>89</b> ) at 75 °C.....	140
Table 3.32	Integration vs. $d_2$ for Ac-Hyp[( $\alpha$ ,1-4)GlcNAc]-NHMe ( <b>89</b> ) at 80 °C.....	141
Table 3.33	Data for Eyring Analysis for Rotation about the Prolyl Amide Bond of Ac-Hyp[( $\alpha$ ,1-4)GlcNAc]-NHMe ( <b>89</b> ) .....	142
Table 3.34	Integration vs. $d_2$ for Ac-Thr-Pro-NHMe ( <b>61</b> ) at 60 °C.....	143
Table 3.35	Integration vs. $d_2$ for Ac-Thr-Pro-NHMe ( <b>61</b> ) at 65 °C.....	144
Table 3.36	Integration vs. $d_2$ for Ac-Thr-Pro-NHMe ( <b>61</b> ) at 70 °C.....	145
Table 3.37	Integration vs. $d_2$ for Ac-Thr-Pro-NHMe ( <b>61</b> ) at 75 °C.....	146
Table 3.38	Integration vs. $d_2$ for Ac-Thr-Hyp(GlcNAc)-NHMe ( <b>63</b> ) at 60 °C .....	147
Table 3.39	Integration vs. $d_2$ for Ac-Thr-Hyp(GlcNAc)-NHMe ( <b>63</b> ) at 65 °C .....	148
Table 3.40	Integration vs. $d_2$ for Ac-Thr-Hyp(GlcNAc)-NHMe ( <b>63</b> ) at 70 °C .....	149
Table 3.41	Integration vs. $d_2$ for Ac-Thr-Hyp(GlcNAc)-NHMe ( <b>63</b> ) at 75 °C .....	150
Table 4.1	Enzyme kinetics parameters for the glycosyltransferase Gnt1 .....	219
Table 4.2	Alkylation of $\beta$ -keto esters .....	227
Table 4.3	Conditions used for the alkylation of <b>135</b> .....	230

## LIST OF FIGURES

Figure 1.1	Amino acid sequence of Ub ( <b>1</b> ) .....	1
Figure 1.2	Schematic diagram of the E3 SCF complex and E2, Ub and substrate .....	3
Figure 1.3	Skp1 in <i>Dictyostelium</i> .....	3
Figure 1.4	Post-translational modifications of Pro <sup>143</sup> of Skp1: the glycosidic linkages.....	7
Figure 1.5	Detection of Skp1- $\alpha$ GlcNAcT-like activity in S100 extracts of <i>Toxoplasma gondii</i> .....	11
Figure 2.1	(a) The first bisubstrate analog inhibitor of $\alpha$ -1,2-FucT, (b) predicted transition state of $\alpha$ -1,2-Fucc.....	16
Figure 2.2	The trisubstrate analog synthesized by van Boom <i>et al.</i> .....	17
Figure 2.3	Inhibitors of ppGalNAcTs .....	17
Figure 2.4	Structure of thioglycoside bisubstrate analog .....	19
Figure 3.1	Gauche effect and hyperconjugative interactions in Hyp .....	61
Figure 3.2	(a) Chemical structure of collagen and (b) hydrophobic pentapeptide sequence of elastin ( <b>37</b> ) .....	62
Figure 3.3	Proline derivatives .....	65
Figure 3.4	Effect of temperature on the conformational stability of (Pro-Fip-Gly) <sub>10</sub> , (Pro-Hyp-Gly) <sub>10</sub> and (Pro-Pro-Gly) <sub>10</sub> triple helices.....	66
Figure 3.5	Hydrogen bonding in triple helical collagen .....	67
Figure 3.6	Microcolin A isolated from <i>Lyngbya majuscula</i> .....	72
Figure 3.7	Dipeptides and glycopeptide synthesized.....	73
Figure 3.8	(a) <sup>1</sup> H NMR spectrum of Ac-Thr-Hyp-NHMe ( <b>62</b> ) in D <sub>2</sub> O at 297 K (b) 2D COSY spectrum of Ac-Thr-Hyp-NHMe ( <b>62</b> ) in D <sub>2</sub> O at 297 K.....	77
Figure 3.9	1.1-1.4 ppm range of <sup>1</sup> H NMR spectra showing the resolution of Thr-Hy signals of (a) Ac-Thr-Hyp-NHMe ( <b>62</b> ) and (b) Ac-Thr-[( $\alpha$ ,1-4)GlcNAc]Hyp-NHMe ( <b>63</b> ) at temperatures of 25, 55 and 75 and 85 °C. ....	80
Figure 3.10	Van't Hoff plots for <i>cis</i> $\rightarrow$ <i>trans</i> isomerization of dipeptides <b>61-63</b> .....	81
Figure 3.11	Potential additional target molecules .....	82
Figure 3.12	Van't Hoff plots for <b>61</b> , <b>62</b> , <b>63</b> , and <b>89</b> .....	84

Figure 3.13	Structures of (a) oxytocin ( <b>99</b> ) and (b) arginine vasopressin ( <b>100</b> ).....	86
Figure 3.14	<i>N</i> -Acetyl-5- <i>tert</i> -butylproline <i>N</i> '-methylamides .....	88
Figure 3.15	Proline derivatives.....	91
Figure 3.16	Peptides <b>61-63</b> and <b>89</b> .....	92
Figure 3.17	Dipeptide standards for structure determination .....	94
Figure 3.18	<sup>1</sup> H NMR spectra of <b>62</b> , the 13-mer and <b>106</b> showing 3.7-4.6 ppm region .....	96
Figure 3.19	Flp and flp conformations. Newman projection formula are depicted looking Downthe C $\gamma$ -C $\delta$ bond axis .....	97
Figure 3.20	Van't Hoff plot for the <i>cis</i> → <i>trans</i> isomerization of Thr-Pro amide bond of Ac-Thr-Pro-NHMe ( <b>61</b> ) in D <sub>2</sub> O.....	127
Figure 3.21	Van't Hoff plot for the <i>cis</i> → <i>trans</i> isomerization of Thr-Pro amide bond of Ac-Thr-Hyp-NHMe ( <b>62</b> ) in D <sub>2</sub> O.....	128
Figure 3.22	Van't Hoff plot for the <i>cis</i> → <i>trans</i> isomerization of Thr-amide bond of Ac-Thr-[( $\alpha$ ,1-4)GlcNAc]Hyp-NHMe ( <b>63</b> ) in D <sub>2</sub> O.....	129
Figure 3.23	Van't Hoff plot for the <i>cis</i> → <i>trans</i> isomerization of proline amide bond of Ac- Hyp(GlcNAc)-NHMe ( <b>89</b> ) in D <sub>2</sub> O.....	130
Figure 3.24	Inversion recovery of (A) inverted <i>trans</i> Thr-H $\gamma$ doublet and (B) non-inverted <i>cis</i> Thr-H $\gamma$ doublet of compound <b>62</b> at 60 °C .....	132
Figure 3.25	Inversion recovery of (A) inverted <i>trans</i> Thr-H $\gamma$ doublet and (B) non-inverted <i>cis</i> Thr-H $\gamma$ doublet of compound <b>62</b> at 65 °C .....	133
Figure 3.26	Inversion recovery of (A) inverted <i>trans</i> Thr-H $\gamma$ doublet and (B) non-inverted <i>cis</i> Thr-H $\gamma$ doublet of compound <b>62</b> at 70 °C .....	134
Figure 3.27	Inversion recovery of (A) inverted <i>trans</i> Thr-H $\gamma$ doublet and (B) non-inverted <i>cis</i> Thr-H $\gamma$ doublet of compound <b>62</b> at 75 °C .....	135
Figure 3.28	Eyring plot for rotation about the Thr-Hyp amide bond of Ac-Thr-Hyp-NHMe ( <b>62</b> ) .....	136
Figure 3.29	Inversion recovery of (A) inverted <i>trans</i> GlcNAc-H1 doublet and (B) non-inverted <i>cis</i> Thr-H $\gamma$ doublet of compound <b>89</b> at 60 °C .....	137
Figure 3.30	Inversion recovery of (A) inverted <i>trans</i> GlcNAc-H1 doublet and (B) non-inverted <i>cis</i> Thr-H $\gamma$ doublet of compound <b>89</b> at 65 °C .....	138

Figure 3.31	Inversion recovery of (A) inverted <i>trans</i> GlcNAc-H1 doublet and (B) non-inverted <i>cis</i> Thr-Hy doublet of compound <b>89</b> at 70 °C .....	139
Figure 3.32	Inversion recovery of (A) inverted <i>trans</i> GlcNAc-H1 doublet and (B) non-inverted <i>cis</i> Thr-Hy doublet of compound <b>89</b> at 75 °C .....	140
Figure 3.33	Inversion recovery of (A) inverted <i>trans</i> GlcNAc-H1 doublet and (B) non-inverted <i>cis</i> Thr-Hy doublet of compound <b>89</b> at 80 °C .....	141
Figure 3.34	Eyring plot for rotation about Ac-Hyp amide bond of Ac-Hyp[( $\alpha$ ,1-4)GlcNAc]-NHMe ( <b>89</b> ) .....	142
Figure 3.35	Inversion recovery of (A) inverted <i>trans</i> Ac-Thr singlet and (B) non-inverted <i>cis</i> Ac-Threonine singlet of compound <b>61</b> at 60 °C .....	143
Figure 3.36	Inversion recovery of (A) inverted <i>trans</i> Ac-Thr singlet and (B) non-inverted <i>cis</i> Ac-Threonine singlet of compound <b>61</b> at 65 °C .....	144
Figure 3.37	Inversion recovery of (A) inverted <i>trans</i> Ac-Thr singlet and (B) non-inverted <i>cis</i> Ac-Threonine singlet of compound <b>61</b> at 70 °C .....	145
Figure 3.38	Inversion recovery of (A) inverted <i>trans</i> Ac-Thr singlet and (B) non-inverted <i>cis</i> Ac-Threonine singlet of compound <b>61</b> at 75°C .....	146
Figure 3.39	Inversion recovery of (A) inverted <i>trans</i> Thr-Hy doublet and (B) non-inverted <i>cis</i> Thr-Hy doublet of compound <b>63</b> at 60 °C .....	147
Figure 3.40	Inversion recovery of (A) inverted <i>trans</i> Thr-Hy doublet and (B) non-inverted <i>cis</i> Thr-Hy doublet of compound <b>63</b> at 65 °C .....	148
Figure 3.41	Inversion recovery of inverted <i>trans</i> Thr-Hy doublet (A) and non-inverted <i>cis</i> Thr-Hy doublet (B) at 70 °C .....	149
Figure 3.42	Inversion recovery of (A) inverted <i>trans</i> Thr-Hy doublet and (B) non-inverted <i>cis</i> Thr-Hy doublet of compound <b>63</b> at 75 °C .....	150
Figure 4.1	Hydrogen bonding pattern in an $\alpha$ -helix.....	211
Figure 4.2	X-ray crystal structure of the helical Bak BH3 domain of Bcl-xL protein. Copyright 2006, John Wiley and Sons, reprinted with permission. Hamilton's $\alpha$ -helix mimetic, terphenyl scaffold <b>123</b> .....	213
Figure 4.3	X-ray crystal structure of smMLCK binding region of the CaM (Copyright 2006, John Wiley and Sons, reprinted with permission) and the $\alpha$ -helical mimetic <b>124</b> .....	214
Figure 4.4	The indane template mimicking an $\alpha$ -helix.....	214

Figure 4.5	$\alpha$ -Helices derived from foldamers:(a) peptoids,(b) $\beta$ -peptides. Copyright 2008, ACS publications, reprinted with permission .....	215
Figure 4.6	$\alpha$ -Helices derived from helix stabilization: (a) HBS $\alpha$ -helices, (b) Side chain crosslinked $\alpha$ -helices. Copyright 2008, ACS Publications, reprinted with permission .....	215
Figure 4.7	Hydrogen bond mimetics: (a) Native peptide highlighting the ( <i>i</i> , <i>i</i> +4) H-bond (b) <i>N</i> -terminal hydrazone mimetic.....	216
Figure 4.8	CD spectra of unconstrained peptide, Ac-QVARQLAEIY-NH <sub>2</sub> ( <b>125</b> ), and HBS $\alpha$ -helix mimetic <b>126</b> used to demonstrate proof of principle for the hydrogen bond surrogate strategy by Arora. Copyright 2008, ACS Publications, reprinted with permission.....	217
Figure 4.9	(a) Galanin sequence in humans; (b) Peptide partial sequence GYLLG showing <i>i</i> $\rightarrow$ <i>i</i> +4 H-bond; (c) H-bond mimetic with an internal ethylene bridge....	218
Figure 4.10	(a) Crystal structure of the Skp1 alpha helix of <i>Arabidopsis thaliana</i> , (b) Glu-rich $\alpha$ -helix stabilized by hydrogen bonds ( <b>128</b> ); (c) $\alpha$ -helical mimetic with covalent bonds ( <b>129</b> ) .....	220
Figure 4.11	The $n \rightarrow \pi^*$ interaction .....	236
Figure 5.1	CD spectra of an $\alpha$ -helix and a random coil.....	301
Figure 5.2	Kinetic analysis of the Skp1-HypPro GlcNAc transferase with respect to Skp1 adapted from Teng-umnuay <i>et al.</i> (a) Plot for the Michaelis-Menten Kinetics, (b) Lineweaver-Burke analysis .....	302
Figure 5.3	Alexa Fluor-488 C5-aminoxyacetamide.....	304
Figure 5.4	Schmidt's $\alpha(1-3)$ GalT inhibitor <b>263</b> .....	304
Figure 5.5	Futuristic target .....	305

## LIST OF SCHEMES

Scheme 1.1	The ubiquitination pathway .....	2
Scheme 1.2	<i>Dictyostelium</i> development and O <sub>2</sub> -dependence.....	4
Scheme 1.3	Post-translational modifications of Pro <sup>143</sup> of Skp1: the enzymatic pathway.....	5
Scheme 1.4	Enzyme-catalyzed hydroxylation of proline .....	6
Scheme 1.5	Formation of the GlcNAc-Hyp Linkage (*H = 3H) .....	8
Scheme 1.6	Proposed conformational changes in Skp1 .....	9
Scheme 1.7	Possible mechanisms of action for Gnt1 .....	12
Scheme 2.1	GlcNAc transferases from <i>Dictyostelium discoideum</i> .....	18
Scheme 2.2	(a) Oxazoline formation, (b) synthesis of NAG-thiazoline .....	18
Scheme 2.3	Retrosynthetic analysis of S-glycoside bisubstrate analog. ....	20
Scheme 2.4	Synthesis of α-thiosugar .....	20
Scheme 2.5	Synthesis of proline electrophiles.....	21
Scheme 2.6	Synthesis of thioester <b>29</b> .....	22
Scheme 2.7	Synthesis of α-thiomethyl glycoside .....	23
Scheme 2.8	Synthesis of thioglycoside <b>27</b> .....	24
Scheme 2.9	Synthesis of the first generation inhibitor.....	25
Scheme 2.10	Synthesis of the first generation inhibitor.....	26
Scheme 3.1	Pyrrolidine ring conformational changes .....	60
Scheme 3.2	<i>Cis</i> → <i>trans</i> isomerism about the prolyl amide bond in Hyp .....	61
Scheme 3.3	Enzyme-catalyzed hydroxylation of proline. ....	63
Scheme 3.4	Synthesis of dipeptide <b>61</b> .....	73
Scheme 3.5	Synthesis of dipeptide <b>62</b> .....	74
Scheme 3.6	Synthesis of glycosyl donor <b>78</b> .....	75
Scheme 3.7	Synthesis of Ac-Thr-Hyp(GlcNAc)-NHMe ( <b>63</b> ) .....	75
Scheme 3.8	Ac-Hyp-NHMe synthesis.....	83

Scheme 3.9	Synthesis of Ac-[( $\alpha$ ,1-4)GlcNAc]Hyp-NHMe ( <b>89</b> ).....	83
Scheme 3.10	<i>N</i> -methylformamide <i>cis</i> $\rightarrow$ <i>trans</i> isomerization .....	91
Scheme 3.11	Synthesis of <b>106</b> .....	95
Scheme 3.12	Formation of 4-oxopropyl product.....	97
Scheme 3.13	Synthesis of flp by Raines and coworkers.....	98
Scheme 3.14	Synthesis of Boc-flp-OBn ( <b>117</b> ).....	98
Scheme 3.15	Mechanism for fluorination using DAST .....	99
Scheme 3.16	Synthesis of Fmoc-flp-OBn ( <b>118</b> ).....	99
Scheme 3.17	Synthesis of Fmoc-flp-OBn ( <b>118</b> ).....	100
Scheme 3.18	Synthesis of H-flp-OH ( <b>121</b> ) .....	100
Scheme 3.19	Synthesis of H-flp-OH ( <b>123</b> ) .....	100
Scheme 3.20	Synthesis of H-flp-OH ( <b>123</b> ) .....	101
Scheme 4.1	HBS Strategy .....	217
Scheme 4.2	Retrosynthetic analysis of HBS system.....	220
Scheme 4.3	Synthesis of QIRK peptide <b>132</b> .....	221
Scheme 4.4	Synthesis of <b>150</b> .....	222
Scheme 4.5	Synthesis of <b>157</b> .....	223
Scheme 4.6	Model studies.....	223
Scheme 4.7	Synthesis of dipeptide <b>167</b> .....	224
Scheme 4.8	Synthesis of the tripeptide <b>157</b> .....	224
Scheme 4.9	Synthesis of Fmoc-Ile-Lys(Boc)-Asn(Trt)-Asp(O <sup>t</sup> Bu)-Phe-Thr( <sup>t</sup> Bu)-OBn ( <b>171</b> )..	225
Scheme 4.10	Retrosynthetic analysis of the diene precursor <b>130</b> .....	226
Scheme 4.11	Synthesis of $\alpha$ -alkyl- $\gamma$ -keto esters.....	226
Scheme 4.12	Synthesis of $\alpha$ -alkyl- $\gamma$ -keto esters.....	227
Scheme 4.13	Synthesis of triflate ester <b>136</b> .....	228
Scheme 4.14	Synthesis of $\beta$ -keto-ester <b>135</b> .....	229

Scheme 4.15	Attempted Synthesis of <b>133</b> .....	229
Scheme 4.16	Synthesis of electrophiles <b>192</b> and <b>193</b> .....	230
Scheme 4.17	Methylation of <b>135</b> .....	231
Scheme 4.18	Methylation of <b>135</b> .....	231
Scheme 4.19	Alkylation of <b>196</b> .....	231
Scheme 4.20	Alkylation of <b>135</b> .....	232
Scheme 4.21	Retrosynthetic analysis $\alpha$ -helical mimetic for Galanine 1-16.....	233
Scheme 4.22	Retrosynthetic analysis of second generation $\alpha$ -helical mimetic with a saturated ethylene bridge.....	234
Scheme 4.23	Synthesis of the <b>217</b> .....	235
Scheme 4.24	Conjugate addition of <b>217</b> .....	235
Scheme 4.25	Synthesis of <b>216</b> .....	236
Scheme 4.26	Synthesis of <b>213</b> .....	237
Scheme 4.27	Synthesis of <b>224</b> .....	238
Scheme 4.28	Attempted synthesis of tetrapeptide mimetic .....	238
Scheme 4.29	Attempted synthesis of tetrapeptide mimetic <b>213</b> .....	239
Scheme 4.30	Reductive amination .....	240
Scheme 4.31	Reductive amination of <b>216</b> .....	240
Scheme 4.32	Cyclization of $\alpha$ -Peptoids .....	241
Scheme 4.33	Cyclization of peptoids .....	242
Scheme 4.34	Cyclization of <b>202</b> .....	243
Scheme 4.35	Cyclization of <b>253</b> .....	244
Scheme 5.1	Preparation of fragment <b>255</b> and <b>256</b> .....	298
Scheme 5.2	Coupling of <b>255</b> and <b>256</b> .....	299
Scheme 5.3	Preparation of fragment <b>258</b> .....	299
Scheme 5.4	Plan to complete the synthesis of <b>211</b> .....	300



Scheme 5.5	GlcNAc-Hyp linkage with the $\alpha$ -helical mimetic <b>211</b> .....	302
Scheme 5.6	Trapping of ketoproline with aminoxy-biotin <b>261</b> .....	303

## LIST OF ABBREVIATIONS AND SYMBOLS

Å	Angstrom
Ac	Acetyl
ADDP	azodicarboxylatedipiperidine
AMP	adenosine monophosphate
Bn	benzyl
Boc	<i>tert</i> -butyloxycarbonyl
BOP	benzotriazol-1-yloxytris(dimethylamino)-phosphonium hexafluorophosphate
<sup>t</sup> Bu	<i>tert</i> -butyl
° C	degrees Celsius
CAM	calmodulin
CD	circular dichroism
COSY	correlation spectroscopy
<i>m</i> CPBA	<i>meta</i> -chloroperoxybenzoic acid
DAST	Diethylaminosulfur trifluoride
DCC	dicyclohexylcarbodiimide
DCM	dichloromethane
<i>Dd</i>	<i>Dictyostelium discoideum</i>
DIAD	diisopropyl azodicarboxylate
DIEA	<i>N,N</i> -diisopropylethylamine
DFT	density functional theory
DMAP	4-dimethylaminopyridine
DNA	deoxyribonucleic acid
DMF	dimethylformamide
<i>E. Coli</i>	<i>Escherichia coli</i>

EDC	1-(3-dimethylaminopropyl)-3-ethylcarbodiimide hydrochloride
EGFP	Enhanced Green Fluorescent Protein
ESI	electrospray ionization
Fmoc	9-fluorenylmethoxycarbonyl
FucT	fucosyl transferase
Gal	galactose
GlcNAc	<i>N</i> -acetyl glucosamine
GT	Glycosyltransferase
HATU	<i>O</i> -(7-azabenzotriazol-1-yl)-1,1,3,3-tetramethyluronium
HBS	hydrogen bond surrogates
HBTU	<i>O</i> -(benzotriazol-1-yl)-1,1,3,3-tetramethyluronium hexafluorophosphate
HIF $\alpha$	hypoxia-inducible factor- $\alpha$
HMBC	heteronuclear multiple bond coherence
HOAt	1-hydroxy-7-azabenzotriazole
HOBt	1-hydroxybenzotriazole
HPLC	high performance liquid chromatography
HRGP	hydroxyproline-rich glycoproteins
HRMS	high resolution mass spectrometry
HRP	horseradish peroxidase
HSQC	heteronuclear single quantum correlation
Hyp	<i>trans</i> -4-L-hydroxyproline
Me	methyl
MS	mass spectrometry
NIS	<i>N</i> -iodosuccinimide
NMR	nuclear magnetic resonance

nOe	nuclear Overhauser effect
P4H1	prolyl-4-hydroxylase
PHD	prolyl hydroxylase domain
PMA	phosphomolybdic acid
PMB	<i>para</i> -methoxybenzyl
ppm	parts per million
PRP	proline-rich proteins
PTM	post translational modification
PyBOP	benzotriazol-1-yloxytri(pyrrolidino)phosphonium hexafluorophosphate
PyBroP	bromotris(pyrrolidino)phosphonium hexafluorophosphate
q	quartet
RCM	ring closing metathesis
$R_f$	retention factor
rt	room temperature
s	singlet
smMLCK	smooth muscle myosin light chain kinase
Ser	serine
TBAF	tetra- <i>n</i> -butylammonium fluoride
TBAH	tetra- <i>n</i> -butylammonium hydroxide
TBTU	<i>O</i> -benzotriazol-1-yl-1,1,3,3-tetramethyluronium tetrafluoroborate
Tf <sub>2</sub> O	triflic anhydride
TFA	trifluoroacetic acid
TFFH	tetramethylfluoroformamidinium hexafluorophosphate
THF	tetrahydrofuran
TLC	thin layer chromatography

TOF	time of flight
TR	tachykinin receptors
Ub	ubiquitin
UDP	uridine diphosphate
UPP	Ub-proteasome pathway
UV	ultraviolet

## ABSTRACT

In Skp1 of *Dictyostelium discoideum* (*Dd*), Pro<sup>143</sup> is located at the *N*-terminus of an  $\alpha$ -helix with four consecutive Glu residues immediately following Pro. Preceding Pro<sup>143</sup> is a segment of random coil. The proline residue undergoes post-translational modifications: hydroxylation and glycosylation. A cytoplasmic prolyl hydroxylase (P4H1) delivers a hydroxyl group to Pro<sup>143</sup> and *N*-acetylglucosamine transferase 1 (Gnt1) transfers GlcNAc from UDP to Hyp<sup>143</sup> of Skp1. The installation of the first GlcNAc residue in Skp1 in *Dictyostelium* is important for the organism to differentiate into a fruiting body to disperse spores. We describe herein some structural and synthesis studies of the Pro<sup>143</sup> region of the Skp1 protein.

We report the synthesis of the bisubstrate analog Ac-Thr-[( $\alpha$ -1,4-GlcNAc)-2*S*,4*R*-4-thioproline]-OH (**17**). Enzyme assays showed that **17** was not an inhibitor for Gnt1 under assay conditions optimized for the full length Skp1 substrate.

*Cis*  $\rightarrow$  *trans* isomerization about the prolyl amide bond was studied by NMR for a series of peptides. Equilibrium constants ( $K_{c/t}$ , 25 °C) increased in the order: Ac-Thr-Pro-NHMe (**61**) (2.3) < Ac-[( $\alpha$ -1,4)GlcNAc]-NHMe (**89**) (3.25) < Ac-Thr-Hyp-NHMe (**62**) (8.7) < Ac-[( $\alpha$ -1,4)GlcNAc]-NHMe (**89**) (13.2). Hydroxylation, glycosylation and extension of the peptide in the *N*-terminal direction all favor the *trans* conformation. Magnetization transfer experiments were possible for Ac-Thr-Hyp-NHMe (**62**) ( $k_{c/t} = 0.94 \text{ s}^{-1}$ , 60 °C) and Ac-[( $\alpha$ -1,4)GlcNAc]-NHMe (**89**) ( $k_{c/t} = 0.45 \text{ s}^{-1}$ , 60 °C) at 60-75 °C. Insufficient resolution of signals for the other two compounds precluded kinetic analysis.

Synthesis of dipeptides Ac-Thr-Hyp-NHMe (**62**) and Ac-Thr-hyp-NHMe (**106**) enabled us to determine the *C $\gamma$*  stereochemistry of the Skp1 Hyp<sup>143</sup> by comparing the <sup>1</sup>H NMR spectra of both dipeptides with that of a 13-mer obtained by enzymatic degradation of the native protein.

The lack of inhibition of Gnt1 by bisubstrate analog **17** may be attributable to an adjacent glutamic acid rich  $\alpha$ -helix recognition element in the full length protein. The synthesis of a 15-mer substrate incorporating an  $\alpha$ -helical mimetic is advanced to test this hypothesis. Three fragments are presented: Fmoc-IKNDFT-OBn (**171**), Cbz-[HypE]\*EEE-OAll (**253**), and Fmoc-QIRK-NH<sub>2</sub> (**132**) where [HypE]\* represents turn inducing mimetic for the HypE dipeptide.

## CHAPTER 1: THE SKP1 PROTEIN

### 1.1 Ubiquitination

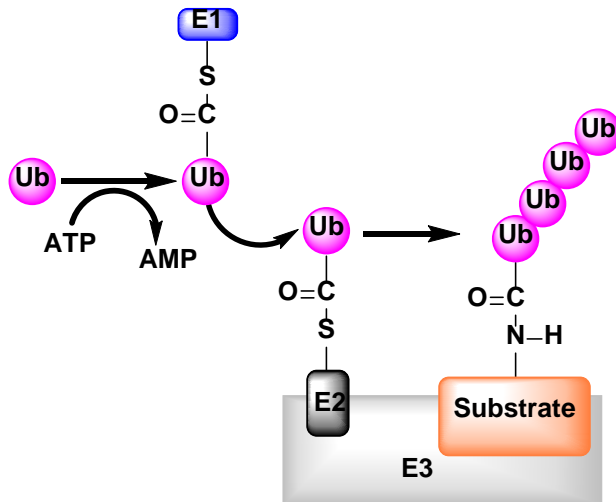
Ubiquitin (Ub) is a small protein (8565 Da) found in all eukaryotes. It consists of 76 amino acids (Figure 1.1) and exists both as a free protein and covalently attached to many other proteins.<sup>1</sup> When bound to proteins, ubiquitin directs them to the proteasome for their degradation.

H-<sup>1</sup>Met-Gln-Ile-Phe-Val-Lys-Thr-Leu-Thr-Gly-Lys-Thr-Ile-Thr-Leu-  
<sup>16</sup>Glu-Val-Glu-Pro-Ser-Asp-Thr-Ile-Glu-Asn-Val-Lys-Ala-Lys-Ile-  
<sup>31</sup>Gln-Asp-Lys-Glu-Gly-Ile-Pro-Pro-Asp-Gln-Gln-Arg-Leu-Ile-Phe-  
<sup>46</sup>Ala-Gly-Lys-Gln-Leu-Glu-Asp-Gly-Arg-Thr-Leu-Ser-Asp-Tyr-Asn-  
<sup>61</sup>Ile-Gln-Lys-Glu-Ser-Thr-Leu-His-Leu-Val-Leu-Arg-Leu-Arg-Gly-Gly-OH

Figure 1.1: Amino acid sequence of Ub (1)

Ubiquitination is a post-translational modification of proteins. Ubiquitination is the process that covalently links the C-terminal glycine 76 of ubiquitin to the side chain amine of a lysine residue on the target molecule.<sup>2</sup> Ubiquitination of proteins proceeds through an enzyme-mediated pathway known as the Ub-proteasome pathway (UPP) (Scheme 1.1).<sup>3</sup> The initial activation of Ub involves adenylation of Ub's C-terminal glycine via adenosine triphosphate (ATP) and subsequent transferring of Ub to the active site cysteine of E1 (ubiquitin-activating enzyme), thus Ub is bound to E1 via a thioester linkage. Then E1 covalently transfers the activated ubiquitin to E2 (ubiquitin-conjugating enzyme). E2 delivers Ub to the E3 enzyme (ubiquitin ligase). The E3 ubiquitin ligase is a complex with thousands of variations. The role of E3 is to transfer Ub from E2 to the target protein to form an isopeptide bond between specific lysine side chains of the target protein to the Ub carboxyl terminus.<sup>3-4</sup>





Scheme 1.1: The ubiquitination pathway

Ubiquitination is responsible for fundamental cellular processes that control numerous aspects of protein function such as degradation, DNA repair, phosphorylation of proteins rich with Pro, Glu, Ser, and Thr (PEST) target proteins. It is also responsible for the glycosylation of PEST proteins with *N*-acetylglucosamine.

## 1.2 The E3 Ubiquitin Ligase Complex

The E3 multiprotein complex consists of four major polypeptide subunits: Skp1, Cullin, F-box-containing protein, and Rbx1 (Figure 1.2). The SCF- and SCF-like complexes are the largest family of ubiquitin-protein ligases.<sup>4a</sup> The complex is a highly elongated structure wherein the Rbx1 and Skp1-F-box subunits are fixed at opposite ends. Cullin is the protein which serves as a rigid scaffold that holds the Rbx1, Skp1-F-box subunits 100 Å apart.<sup>4a</sup> Skp1 serves as an adaptor linking the F-box protein and the Cullin-1/Rbx1 complex. Each subunit is important for the overall functionality of the complex. The SCF complex participates in the ubiquitination of cell cycle regulatory proteins and their degradation by the 26S proteasome.

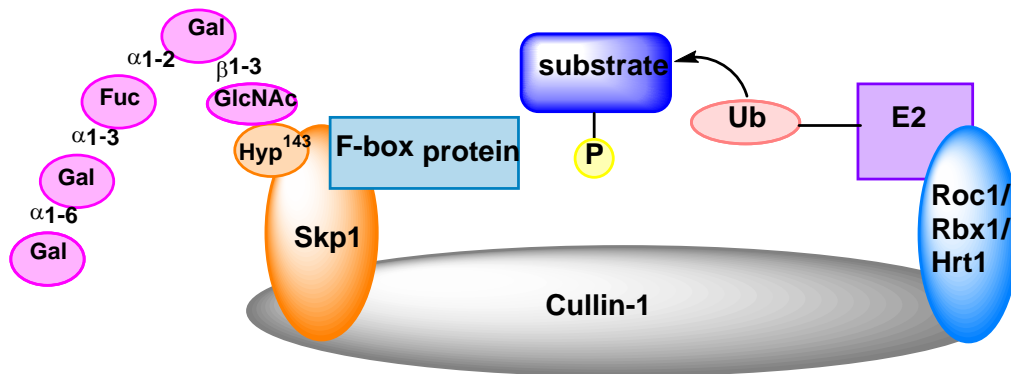


Figure 1.2: Schematic diagram of the E3 SCF complex and E2, Ub and substrate<sup>5</sup>

### 1.3 Skp1 of *Dictyostelium*

Skp1 is a small glycoprotein consisting of 163 amino acids and has a molecular weight of 21 kDa. It is found in the cytoplasm and nucleus of all eukaryotes<sup>6</sup> (Figure 1.3). Skp1 is a multifunctional protein responsible for F-box recognition and binding and may also assist in the selection of other proteins for ubiquitination.

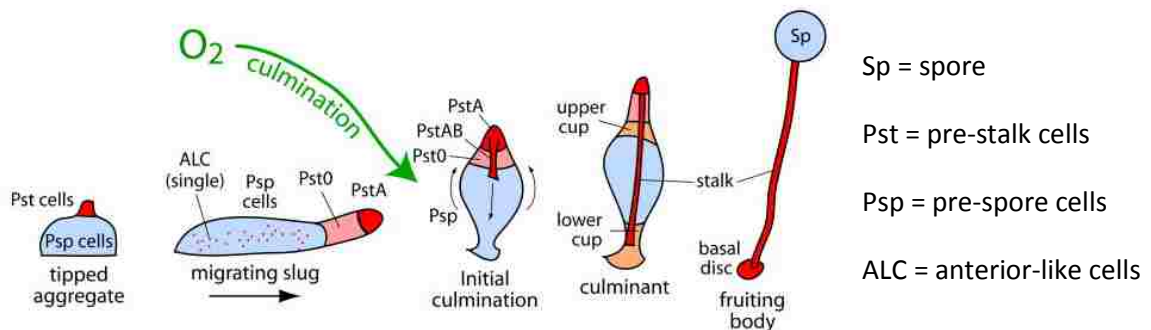


2

Figure 1.3: Skp1 in *Dictyostelium*. Copyright 2011, ACS publications, reprinted with permission

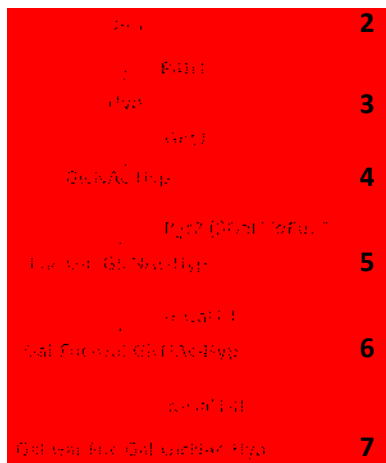
3

*Dictyostelium*, a soil amoeba in the mycetozoon group of unicellular eukaryotes, is an important model organism for cell signaling and motility.<sup>7</sup> *Dictyostelium* proliferates as a solitary amoeba and aggregates to form a multicellular slug that migrates to the soil surface for culmination and subsequent dispersal of spores (Scheme 1.2). Studies by West and coworkers have shown that the growth of *Dictyostelium* is oxygen-dependent. *Dictyostelium* normally requires 2.5% oxygen for growth but requires elevated oxygen to culminate, *i.e.*, coming together of ALCs (anterior-like cells) at the baseline and sporulation (production of spores).<sup>7-8</sup>



Scheme 1.2: *Dictyostelium* development and O<sub>2</sub>-dependence. Copyright 2010, Elsevier, reprinted with permission

In *Dictyostelium*, the proline residue at position 143 of Skp1 is post-translationally modified by hydroxylation and complex glycosylation. These post-translational modifications involve a prolyl-4-hydroxylase (P4H1) and five sequentially acting cytoplasmic glycosyltransferase activities encoded by three genes<sup>8b</sup> (Scheme 1.3). The hydroxylation and glycosylation are important for culmination and spore formation of *Dictyostelium*. Biochemical and genetic studies showed that Skp1 is the only substrate for P4H1 and the glycosyltransferase Gnt1 in cells.<sup>9</sup>



Scheme 1.3: Post-translational modifications of Pro<sup>143</sup> of Skp1: the enzymatic pathway

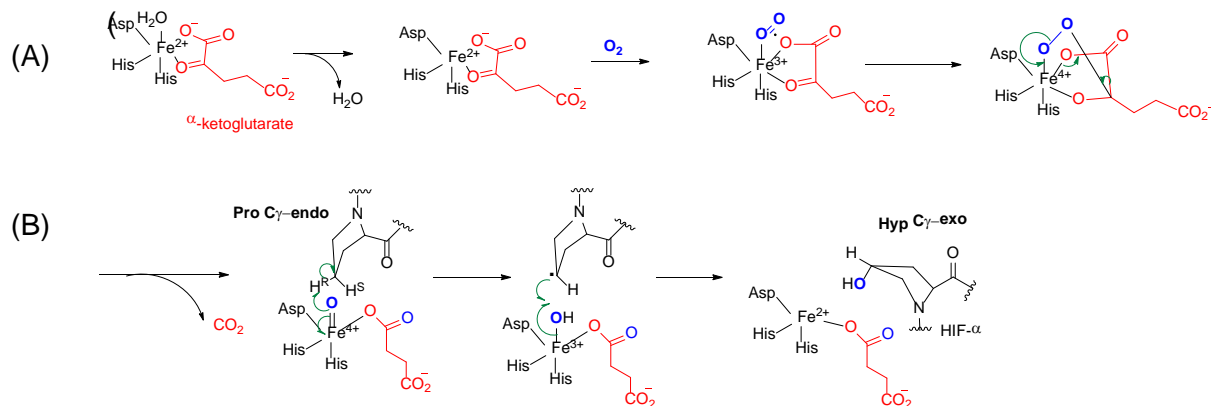
### 1.3.1 Prolyl Hydroxylase Enzyme

*Dictyostelium* expresses the ortholog of animal hypoxia-inducible factor- $\alpha$  (HIF- $\alpha$ ) like prolyl-4-hydroxylase, P4H1, which is involved in oxygen sensing in animals.<sup>10</sup> The hydroxylation of Skp1 is oxygen-dependent and regulates the reproduction of *Dictyostelium*, enabling it to differentiate into a fruiting body. The P4H1 enzyme has a high  $K_m$  for oxygen *in vitro*. Elevated oxygen levels are required for P4H1-null cells to culminate into a fruiting body, while reduced oxygen is sufficient for cells in which P4H1 is overexpressed.

Recent studies on the prolyl-4-hydroxylase of collagen by Raines' group<sup>11</sup> and the prolyl-4-hydroxylase of HIF $\alpha$  by the Schofield group<sup>12</sup> have revealed interesting details of the mechanism of proline hydroxylation by these enzymes. In humans, HIF- $\alpha$  is a key regulator in the cellular response to critically low oxygen concentrations.

Hydroxylation of HIF- $\alpha$  is catalyzed by enzymes containing a prolyl hydroxylase domain (PHD).<sup>11-12</sup> The reaction has two stages as detailed in Scheme 1.4: (A) Formation of a highly reactive Fe(IV)=O species, without the direct participation of the proline; and (B) abstraction of the *pro-R* hydrogen atom from C-4 of the proline residue by the Fe(IV) species. During the

hydroxylation of proline,  $\alpha$ -ketoglutarate is oxidized to succinate and one atom of molecular oxygen is incorporated into proline and the other into succinate.<sup>11</sup> After the pyrrolidine ring of Pro<sup>564</sup> in HIF- $\alpha$  is hydroxylated by a *trans*-4-hydroxylase, the ring conformation shifts from C $\gamma$ -*endo* to C $\gamma$ -*exo*.



Scheme 1.4: Enzyme-catalyzed hydroxylation of proline<sup>11</sup>

### 1.3.2 Skp1 Glycosylation in *Dictyostelium*

After hydroxylation, the Skp1 protein of *Dictyostelium* is known to be further modified by a pentasaccharide chain<sup>6</sup> (Figure 1.4). Gonzalez-Yanes *et al.* discovered *Dictyostelium* Skp1 glycosylation for the first time by metabolic labeling of cells with <sup>3</sup>H fucose.<sup>13</sup> The attachment of a pentasaccharide to Hyp<sup>143</sup> was recognized by Edman degradation analysis of peptides from the purified protein and the carbohydrate sequence was confirmed by exoglycosidase studies using MALDI-TOF mass spectrometric analysis.<sup>14</sup> The results showed that the sequence of the pentasaccharide is Gal( $\alpha$ ,1-6)-Gal( $\alpha$ ,1-3)-Fuc( $\alpha$ ,1-2)-Gal( $\beta$ ,1-3)-GlcNAc. The reducing end of the pentasaccharide is attached to hydroxyproline at position 143 (Figure 1.4). The attachment of Hyp<sup>143</sup> to GlcNAc was confirmed by three pieces of evidence:<sup>6</sup> (1) observation of a small decrease in apparent  $M_r$  (relative molecular mass) after treating cells with inhibitors of prolyl-4-hydroxylases;<sup>15</sup> (2) observation of a similar reduction in apparent  $M_r$  of Skp1 after substitution of

Hyp<sup>143</sup> of Skp1 with Ala; (3) a synthetic peptide with a Hyp<sup>143</sup> was shown to be a good substrate for the Gnt1 enzyme of the pathway. Given the homology of Gnt1 with GT27 polypeptide  $\alpha$ -GalNAc-transferases (ppGalNAcTs), the key carbohydrate-protein linkage was considered highly likely to be  $\alpha$ . Since *trans*-4-hydroxyproline is the most common isomer of hydroxyproline,<sup>16</sup> the linkage was similarly presumed to be GlcNAc( $\alpha$ ,1-4)-*trans*-4-Hyp. Collaborating with West's group, we confirmed that the hydroxyproline residue is *trans*-4-Hyp.<sup>17</sup> This will be discussed in detail in Chapter 3.

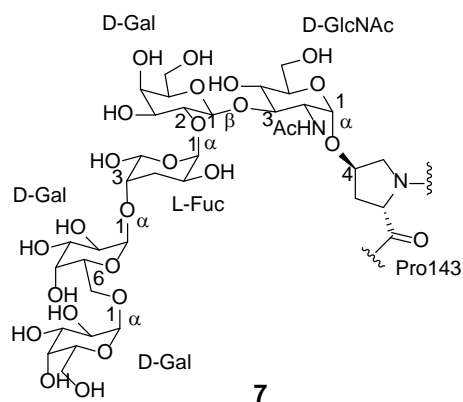
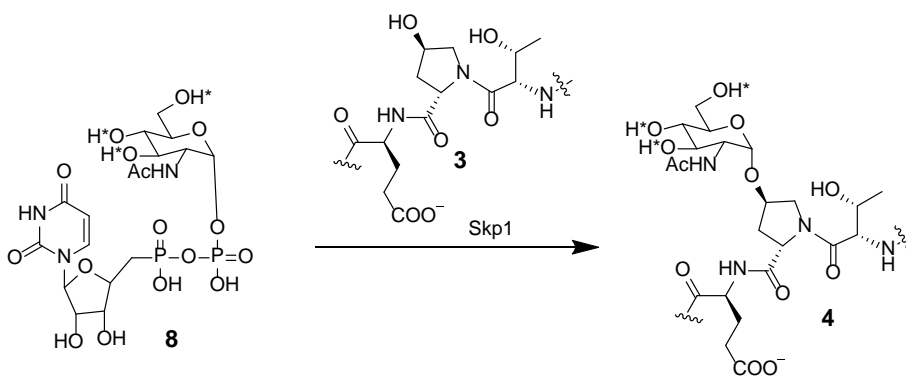


Figure 1.4: Post-translational modifications of Pro<sup>143</sup> of Skp1: the glycosidic linkages

In 1999, a report by West and coworkers described their study of the GlcNAc-Hyp<sup>143</sup> glycosidic linkage. They found that the Skp1 isoform with Pro at position 143 was not a substrate for the GlcNAc transferase, providing further evidence that the sugar is linked via Hyp.<sup>18</sup> They studied the formation of the GlcNAc-Hyp linkage by measuring the transfer of radioactivity from UDP-[<sup>3</sup>H]GlcNAc to Skp1 (Scheme 1.5). The optimized conditions for the enzyme were found to be 30 °C, pH 7.5-8.0, 5-10 mM Mg<sup>2+</sup> and 1-5 mM dithiothreitol.



Scheme 1.5: Formation of the GlcNAc-Hyp Linkage (\*H =  $^3\text{H}$ )

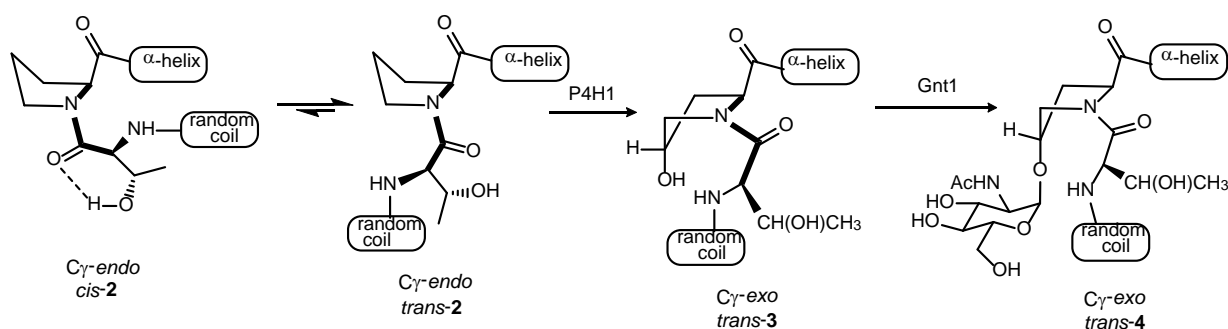
These two post-translational modifications are vital to the regulatory function of Skp1. We hypothesized that conformational changes associated with these post-translational modifications of Skp1 induce changes in the rest of the protein and allow recognition and binding of the F-box-target complex which leads to successful ligation of the target molecule to ubiquitin. West *et al.* have shown that without post-translational hydroxylation and glycosylation, the organism is no longer able to culminate and reproduce. This suggests that in the absence of these post-translational modifications, the ubiquitin pathway fails and that in-turn leads to inadequate protein metabolism and inability of the organism to reproduce.<sup>17, 19</sup>

The first GlcNAc residue may also be involved in oxygen regulation, and is a prerequisite for further glycosylation.<sup>18-19</sup> The second and third sugars [Gal( $\beta$ ,1-3) and Fuc( $\alpha$ ,1-2)] are added to Skp1 by PgtA, a two-domain diglycosyltransferase. The *N*-terminal domain of the PgtA protein controls the action of Gal( $\beta$ ,1-3)transferase activity and the *C*-terminal domain is associated with the Fuc( $\alpha$ ,1-2)transferase activity. Formation of the Fuc( $\alpha$ ,1-2)Gal( $\beta$ ,1-3)GlcNAc linkages was confirmed by the sensitivity of the diglycosyltransferase to  $\beta$ 3-galactosidase and  $\alpha$ 2-fucosidase respectively towards the model substrates.<sup>6, 8b</sup> The galactose residue is necessarily added before the fucose residue.<sup>19</sup> The Fuc-Gal disaccharide must be present in the folded Skp1 glycoprotein for further elaboration to take place. Under such circumstances, the fourth sugar, Gal-I is added to the sequence by the AgtA enzyme resulting in the Gal( $\alpha$ ,1-3)-Fuc

linkage. Addition of the final sugar is also mediated by AgtA. The addition of the second Gal residue (Gal-II) by AgtA is likely subject to different kinds of constraints and have the effect of rendering the Gal-I addition irreversible.<sup>8b</sup>

#### 1.4 Conformational Changes in Skp1 Associated with Post-translational Modifications

Before hydroxylation, the Pro<sup>143</sup> residue of Skp1 likely adopts a C $\gamma$ -endo ring pucker and the *cis*  $\rightarrow$  *trans* equilibrium of the prolyl peptide bond slightly favors the *trans* isomer (Scheme 1.6). Once Pro<sup>143</sup> is hydroxylated by P4H1, the pyrrolidine ring will change its conformation to a C $\gamma$ -exo pucker and the peptide bond will adopt predominantly the *trans* orientation. After GlcNAc is attached Hyp<sup>143</sup> stays largely in the C $\gamma$ -exo conformation and will likely still favor the *trans* peptide bond. We believed that the changes in torsional angles around the glycosidic bond of the protein likely contribute to its recognition by PgtA, the enzyme that introduces the next two monosaccharides.<sup>8b</sup> These conformational changes in the proline peptide bond associated with the proline hydroxylation and glycosylation will be elaborated in Chapter 3.



Scheme 1.6: Proposed conformational changes in Skp1

#### 1.5 Post-Translational Modifications of Skp1 as a Therapeutic Target

All unicellular eukaryotes (including some parasites and invertebrates and most multicellular organisms) bear the equivalent of Pro<sup>143</sup> in their Skp1 sequence (Table 1.1).<sup>20</sup> The



lack of Pro<sup>143</sup> in the Skp1 of higher eukaryotes, including humans, makes these post-translational modifications a potentially valuable therapeutic target. Toxoplasmosis, a disease caused by *Toxoplasma gondii* is the most clinically compelling example.<sup>21</sup> According to the Center of Disease Control website, toxoplasmosis is the third leading cause of death from foodborne illnesses in the USA.

Table 1.1: Skp1 sequence in different organisms

Organism	Comment	Skp1 Sequence (133-155) ↓
<i>Dictyostelium discoideum</i>	amoebazoan	KIFNIKNDFT PEEEEQIRKENEW
<i>Saccharomyces cerevisiae</i>	yeast	RTFNIVNDFT PEEEEAIRRENEW
<i>Cryptosporidium parvum</i>	diarrheal pathogen	QIFNIENDFT PEEESAIREENKW
<i>Toxoplasma gondii</i>	toxoplasmosis	RIFNIVNDF TPEEEAQVREENKW
<i>Enterocella nidulans</i>	amoebic dysentery	RTFNIVNDFT PEEEEAIRRENEW
<i>Anopholes gambiae</i>	malaria vector	KTFNIKNDFT PAEEEQVRKENEW
<i>Tetraodon nigroviridis</i>	puffer fish	KTFNIKNDFT EEEEAQVRKENQW
<i>Homo sapiens</i>	man	KTFNIKNDFT EEEEAQVRKENQW

Studies by West and coworkers utilizing UDP-[<sup>3</sup>H]-GlcNAc showed that the Skp1 of *Toxoplasma gondii* undergoes post-translational modifications, as observed for *Dictyostelium* Skp1.<sup>21</sup> The assay results shown in Figure 1.5 demonstrate that extracts of *T. gondii* (Tg-S-100) exhibit an activity that is like Gnt1 of *Dictyostelium discoideum*. Parasites (200 million organisms) were isolated from human foreskin fibroblasts and Skp1 was extracted from them. An equal amount of protein was prepared from the fibroblast itself and these proteins samples were compared. The parasites' Skp1 was treated with UDP-[<sup>3</sup>H]-GlcNAc with or without the recombinant *Dictyostelium discoideum* Skp1 bearing a His-tag (*Dd*-His<sub>10</sub>Skp1). After incubation for 2 h at 29 °C, mixtures were separated on a SDS-PAGE gel. Figure 1.5 demonstrates that a significant level of [<sup>3</sup>H]GlcNAc incorporation was observed for Skp1 of *Toxoplasma gondii* (*Tg*-Skp1) and the addition of *Dd*-His<sub>6</sub>P4H1 increased the incorporation. Also *Dd*-His<sub>10</sub>Skp1 is modified by radiolabeled sugar and it is significantly higher in the presence of *Dd*-His<sub>6</sub>P4H1.

These results suggest that *Toxoplasma gondii* expresses a GlcNAc transferase which attaches GlcNAc to a Hyp residue by analogy to *Dictyostelium* Gnt1.

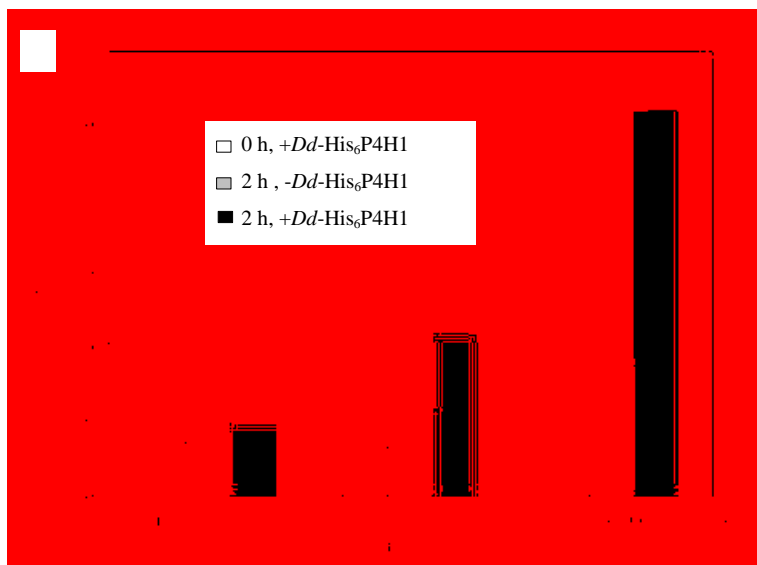


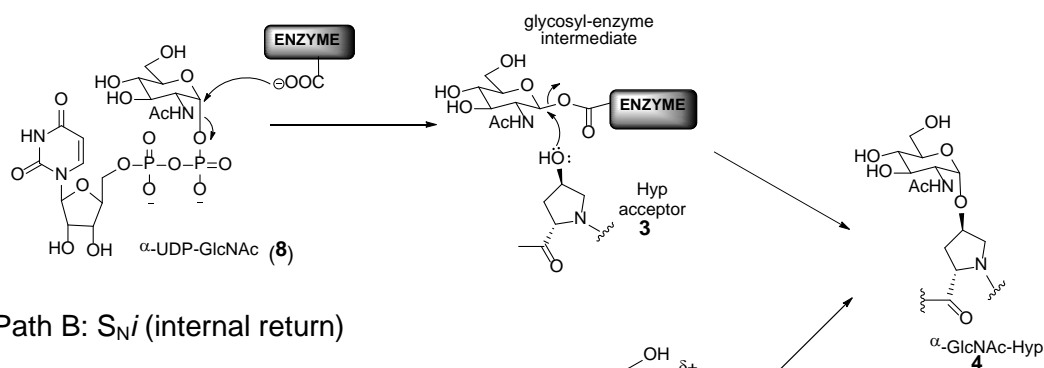
Figure 1.5: Detection of Skp1- $\alpha$ GlcNAcT-like activity in S100 extracts of *Toxoplasma gondii*. The Y-axis represents radioactivity in disintegrations per minute (Dpm). Copyright 2006, Elsevier, reprinted with the permission

Assuming that the addition of the GlcNAc residue to the Hyp of Skp1 is vital for *T. gondii* to propagate, as is the case for *Dictyostelium*, inhibitors of the associated glycosyltransferase enzyme might serve as selective drugs.

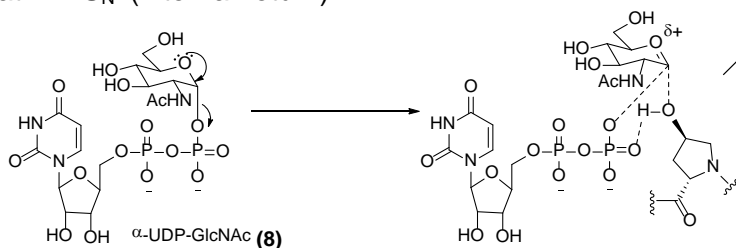
## 1.6 Enzyme Kinetics of Gnt1

Kinetics studies showed that glycosylation by Gnt1 is first order in both UDP-GlcNAc and the synthetic 23-mer peptide (KIFNIKNDFTPEEEEEQIRKENEW) substrate. Therefore, the peptide, or the protein, must be involved in the rate determining step of the reaction. Two possible pathways for the Gnt1-catalyzed reaction are proposed in Scheme 1.7: one via a ping-pong mechanism and the other through the internal return mechanism. Initially, it was assumed that the glycosyltransferase process was analogous to that of a glycosyl hydrolase enzyme proceeding via a covalent enzyme substrate intermediate (Scheme 1.7A).<sup>22</sup> Recently, Lairson *et al.* proposed a mechanism that has a short-lived oxacarbenium ion intermediate. In this mechanism, the phosphate leaving group serves as the base (Scheme 1.7B).<sup>23</sup>

### Path A: Ping-Pong



### Path B: $S_Ni$ (internal return)



Scheme 1.7: Possible mechanisms of action for Gnt1

Teng-umnuay *et al.* explored the behavior of Gnt1 toward Skp1A1-Myc, a full length protein from strain HW120 that is hydroxylated, but not glycosylated at Pro<sup>143</sup> and the synthetic 23-mer that corresponding to residues 135-157 of Skp1 with Hyp at the center of the peptide. Their results showed that the Gnt1 enzyme exhibits unusually low  $K_m$  values, in the submicromolar range, for both its natural donor (UDP-GlcNAc) and acceptor substrate (Skp1A-Myc) (Table 1.2). The low  $K_m$  value for UDP-GlcNAc is similar to the relatively low  $K_m$  values for the substrates of two cytoplasmic glycosyltransferases, the Skp1 Fuc-transferase and the general Ser/ThrGlcNAc-transferase.<sup>18</sup> This is consistent with Gnt1 being a cytoplasmic enzyme. The apparently higher  $K_m$  value of Skp1A-Myc (full length protein) compared to UDP-GlcNAc is due to the presence of some unhydroxylated isoform of Skp1A-Myc in the preparation that inhibits the enzyme by 50%.<sup>18</sup> The  $V_{max}$  value of Skp1A-Myc is higher than that estimated for the UDP-GlcNAc. This is probably because Skp1A-Myc was not present at saturation in the reaction. The  $V_{max}$  value of the synthetic 23-mer is one third that of the full length protein which

is a small difference compared to the 3000-fold difference in apparent  $K_m$  values between those two substrates. These kinetic data suggest that the 23-mer lacks structure that is important for highly effective recognition by the enzyme but it contains the necessary functionality for interacting with the catalytic site of the enzyme. Our hypothesis was that the low binding affinity is due to a lack of secondary structure in the 23-mer.

Table 1.2:  $K_m$  and  $V_{max}$  values

Substrate	$K_m$ ( $\mu\text{M}$ )	$V_{max}$ (nmol/h/mg)
UDP-GlcNAc ( <b>8</b> )	0.16	8.0
Skp1A-Myc ( <b>3</b> )	0.56	12.6
23-mer Peptide ( <b>9</b> )	1600	4.2

## 1.7 Goals of the Project

The aim of this project was to investigate the role of the post-translational modification pathway; specifically the prolyl 4-hydroxylation and glycosylation of Skp1. Research was focused on the synthesis of small peptides and peptidomimics to assess the importance of conformational and configurational control elements in Skp1 recognition by the P4H1 and Gnt1 enzymes.

Experiments are organized in three chapters: (1) *Synthesis of a bisubstrate analog as a putative inhibitor of Gnt1*: Reliant on circumstantial evidence, we prepared a S-glycoside bisubstrate analog. This has been assessed in West's laboratory, for its ability to inhibit the transfer of N-acetylglucosamine from UDP-GlcNAc to Hyp. (2) *Use of Ac-Thr-Pro\*-NHMe dipeptides to assess conformational and stereochemical consequences of prolyl hydroxylation and glycosylation*: These peptides have been used to assess the pyrrolidine ring pucker preference and *cis-trans* preference of the proline peptide bond. Peptides were examined using NMR experiments to determine the equilibrium constant and rate constants for prolyl peptide bond isomerization have been calculated to find the effect of hydroxylation and glycosylation on Skp1. (3) *Synthesis of an  $\alpha$ -helical mimetic*: We proposed to synthesize an Skp1 mimetic by inducing  $\alpha$ -helical formation by replacing the  $i, i+4$

H-bond of natural peptide with a covalent linkage. This will have the local secondary structural elements characteristic of the full-length protein. The amino acid sequence that we attempt to mimic in the  $\alpha$ -helix is IKNDFTPEEEEQIRK.

## CHAPTER 2: SYNTHESIS OF A BISUBSTRATE ANALOG AS A PUTATIVE INHIBITOR OF GNT1

### 2.1 Skp1 Glycosylation

As described in Chapter 1, after Skp1 Pro<sup>143</sup> is hydroxylated by P4H1 this residue undergoes five consecutive glycosylations to attach the linear pentasaccharide (Scheme 1.3). West and coworkers determined the sequence of the linear pentasaccharide to be Gal( $\alpha$ ,1-6)-Gal( $\alpha$ ,1-3)-Fuc( $\alpha$ ,1-2)-Gal( $\beta$ ,1-3)-GlcNAc by MALDI-MS, with uncertainty remaining about the position and stereochemistry of the last two residues.<sup>14</sup> After Gnt1 has introduced the GlcNAc residue to the Hyp<sup>143</sup>, conformational changes in this region of the protein will likely contribute to recognition by PgtA, the enzyme that attaches the next two monosaccharides.<sup>24</sup> After these modifications, the appropriately folded Skp1 polypeptide undergoes further glycosylation to attach the last two Gal residues by GalT-I and GalT-II (Figure 1.4).

### 2.2 Inhibitors of Glycosyltransferases

Glycosyltransferase (GT) enzymes transfer an activated sugar from a nucleotide to an acceptor, which could be an oligosaccharide, a protein or a lipid.<sup>25</sup> Glycosyltransferases are responsible for the biosynthesis of oligosaccharides and bioconjugates. Thus, GTs play key roles in many biological processes such as cell signaling, carcinogenesis and cell wall biosynthesis in human pathogens.<sup>26</sup> These enzymes have therefore become an attractive target for development of inhibitors in drug discovery.<sup>25</sup>

Glycosyltransferase inhibitors have been designed based on the donor and acceptor structures and the principles of transition state analog inhibition. Such inhibitors are designed to mimic either the ground state or the transition state of the natural substrates by replacing the glycosidic oxygen atom by a different heteroatom or by a carbon atom.<sup>25a, 27</sup> The rational design of glycosyltransferase inhibitors is difficult because the process is best informed by the three-

dimensional structure of the glycosyltransferase enzyme and currently only a little information is available on their three-dimensional structure. Moreover, it is hard to design an selective inhibitor based on the donor structure, as glycosyltransferase enzymes use a common glycosyl donor and glycosyl acceptors typically have millimolar-range affinity for these enzymes.<sup>25</sup>

The synthesis of compound **10**, the first bisubstrate analog inhibitor of a fucosyl transferase (FucT) was reported in 1989 by Hindsgaul *et al.*<sup>28</sup> This bisubstrate analog consisted a nucleotide covalently linked to an acceptor domain but with none presentation of the donor sugar residue (Figure 2.1a). The design was intended to mimic the transition state of  $\alpha$ -1,2-FucT (Figure 2.1b). The transition state mimic showed competitive inhibitory activity with respect to both guanidine diphosphate GDP-Fuc ( $K_i$  of 16  $\mu$ M) and acceptor phenyl  $\beta$ -D galactopyranoside ( $K_i$  of 2.3  $\mu$ M).<sup>28</sup>

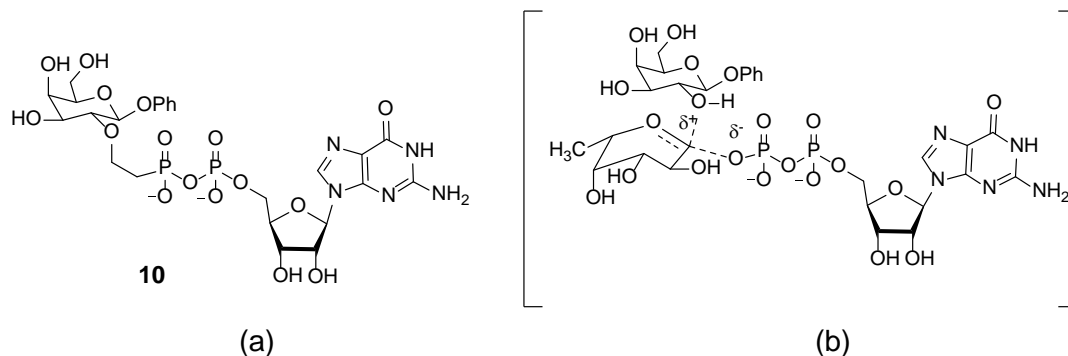


Figure 2.1: (a) The first bisubstrate analog inhibitor of  $\alpha$ -1,2-FucT, (b) predicted transition state of  $\alpha$ -1,2-FucT

In 1995 van Boom *et al.* reported the synthesis of a trisubstrate analog for  $\alpha$ -1,3-FucT.<sup>29</sup> Their analog design was based on the proposed transition state of the FucT reaction and consisted of all three components: donor, with nucleotide moiety, and acceptor (Figure 2.2). They replaced the diphosphate with a malondiamide linker between the guanosine and fucose moieties to facilitate membrane transport. However they did not report the inhibitory activity of the synthesized analog.<sup>29</sup>

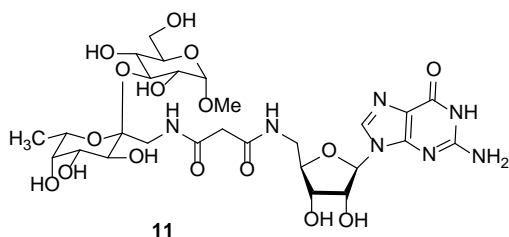


Figure 2.2: The trisubstrate analog synthesized by van Boom *et al.*

### 2.3 Potential Inhibitors of Gnt1

Bertozzi and coworkers developed the first inhibitors of ppGalNAcT: the glycosyltransferase that catalyzes the addition of GalNAc to Ser/Thr sidechains from UDP-GalNAc.<sup>30</sup> Compounds **12** and **13** (Figure 2.3) were identified from a library of 1338 uridine-based compounds in which the spacer X and the C=N linkage replaces the diphosphate linkage the nature of the linker and the precursor aromatic aldehyde to the imine (2,3,4-trihydroxybenzaldehyde depicted) were varied. The trihydroxybenzene ring mimics the flattened out donor sugar in the transition state. The inhibitors bound to ppGalNAc twice as strongly as UDP-GalNAc and 30-fold stronger than UDP alone. These inhibitors (**12** and **13**) were found to have broad activity for a range of UDP-sugar-utilizing enzymes.

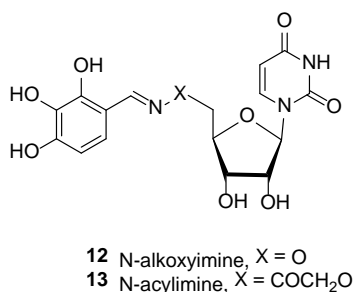
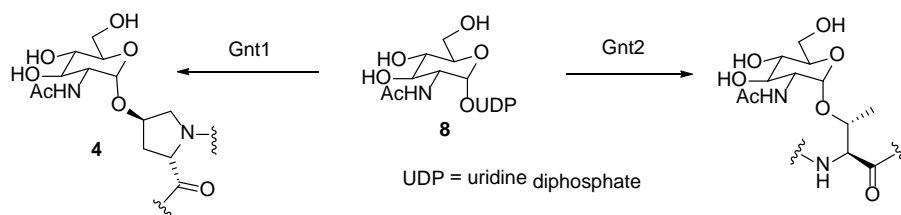


Figure 2.3: Inhibitors of ppGalNAcTs

West and coworkers tested Bertozzi's compounds **12** and **13** (Figure 2.3) as potential inhibitors of Gnt1 and Gnt2 (an enzyme that transfers GlcNAc to Ser/Thr) from *Dictyostelium*

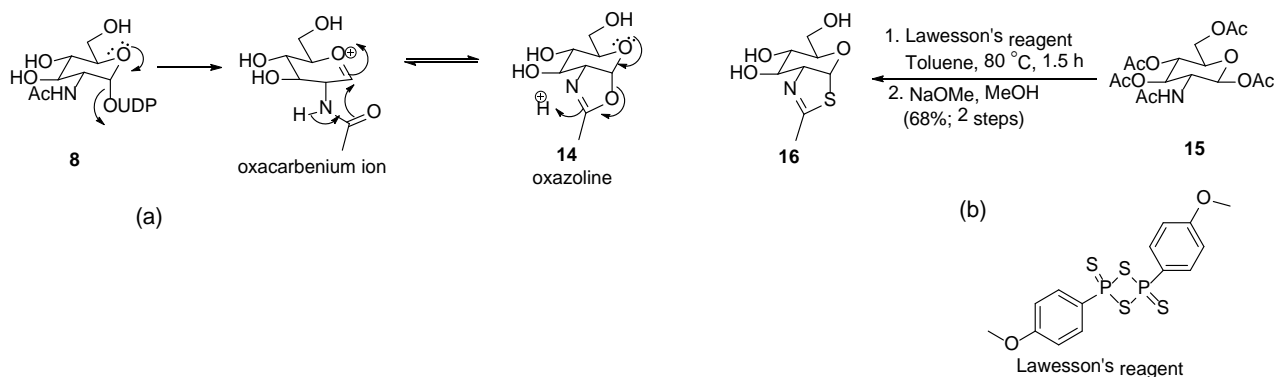


(Scheme 2.1). They observed that both compounds **12** and **13** inhibited Gnt2 with  $K_i$  values of 35  $\mu\text{M}$  for **12** and 70  $\mu\text{M}$  for **13** but no inhibition of Gnt1 was seen.<sup>31</sup> This implies that despite the difference in configuration at C4 of GlcNAc and GalNAc the 2,3,4-trihydroxybenzene ring can mimic the transition state of the reaction in the case of Gnt2. Since **12** and **13** are ineffective as inhibitors of Gnt1, this suggests the enzyme mechanism is considerably different.



Scheme 2.1: GlcNAc transferases from *Dictyostelium discoideum*

Knapp's NAG-thiazoline **16** is a proven inhibitor of *N*-acetyl- $\beta$ -hexosaminidase ( $K_i = 280$  nM).<sup>32</sup> This observation provides evidence for neighboring group participation of the *N*-acetamido group and formation of an oxazoline intermediate in the mechanism of hydrolysis by the *N*-acetyl- $\beta$ -hexosaminidase (Scheme 2a).<sup>33</sup> NAG-thiazoline might also serve as an inhibitor of Gnt1 if there is neighboring group participation by the *N*-acetamido group as UDP-GlcNAc interacts with the enzyme.



Scheme 2.2: (a) Oxazoline formation, (b) synthesis of NAG-thiazoline

We prepared **16** according to the Scheme 2.2b and the enzyme assays were carried out in West's Laboratory. Their results demonstrated that NAG-thiazoline (**16**) was inactive against

both Gnt1 and the *Trypanosoma cruzi* analog of Gnt2.<sup>10</sup> The negative results with NAG-thiazoline and the Bertozzi inhibitors indicate that the peptide in the native protein might be an important in the acceptor substrate and/or the glycosyl transfer mechanism is very different.

## 2.4 Design of a Bisubstrate Analog

For three reasons we designed the bisubstrate analog **17** (Figure 2.4) to be an S-glycoside instead of an O-glycoside: (a) relative stability towards glycosidase enzymes; (b) longer C-S bond lengths reminiscent of the transition state for glycosyl transfer; and (c) they are likely easier to prepare than the corresponding O-glycosides.

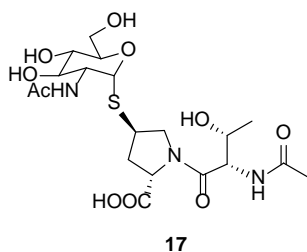
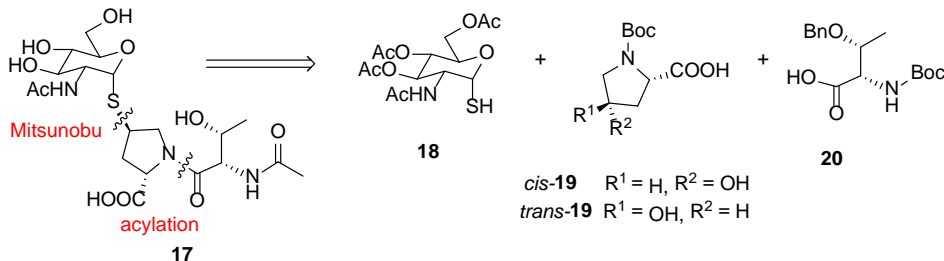


Figure 2.4: Structure of thio glycoside bisubstrate analog

### 2.4.1 Retrosynthetic Analysis of Bisubstrate Analog

Our approach to the synthesis the thio glycoside inhibitor is depicted in Scheme 2.3. There are two key disconnections, the glycosidic linkage and the peptide linkage, that lead to the sugar thiol **18**, hydroxyproline **19** and threonine **20**. The sugar thiol **18** is a known compound that has been synthesized from *N*-acetyl glucosamine tetraacetate by Knapp and coworkers.<sup>34</sup> The Hyp-Thr fragment can be synthesized starting with commercially available Boc-Hyp-OH (**19**) and Boc-L-Thr(OBn)-OH (**20**). The stereochemistry at C4 of the proline residue in the bisubstrate analog **17** could be approached via a Mitsunobu reaction with the  $\alpha$ -SH monosaccharide as nucleophile. A Mitsunobu product would demonstrate inversion of stereochemistry at the C4 of the proline residue, therefore we employed *cis*-4-hydroxyproline,

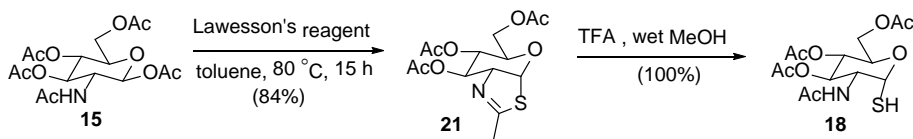
hyp. Mitsunobu reaction with the sulfur nucleophiles depends on the acidity of SH-groups and there are precedents for displacement of OH by thiols and with  $\beta$ -thio-sugars via Mitsunobu chemistry.<sup>35</sup>



Scheme 2.3: Retrosynthetic analysis of S-glycoside bisubstrate analog.

#### 2.4.2 Synthesis of Bisubstrate Analog

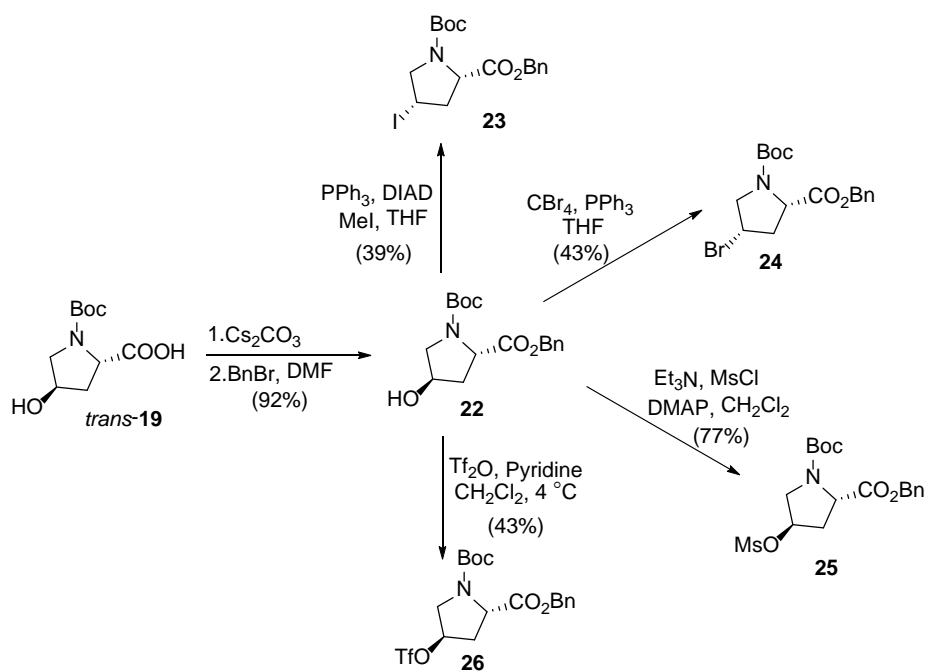
We synthesized the  $\alpha$ -thiosugar **18** from commercially available *N*-acetyl glucosamine tetraacetate **15** with Lawesson's reagent to give the thiazoline **21**, followed by hydrolysis promoted by TFA (Scheme 2.4). This sequence had been reported previously by Knapp's group.<sup>34</sup>



Scheme 2.4: Synthesis of  $\alpha$ -thiosugar

Our initial efforts to develop a synthesis of the bisubstrate analog employed  $S_N2$  chemistry. A range of leaving groups were introduced at C4 of Pro; some with  $4R$  configuration, and some with  $4S$  configuration depending upon their mechanism of formation. The synthesis of 4-substituted prolines began with the conversion of commercially available Boc-*trans*-4-Hyp-OH (**19**) to its benzyl ester **22** using cesium carbonate and benzyl bromide (Scheme 2.5). We synthesized various proline electrophiles: iodide **23**, bromide **24**, mesylate **25**, and triflate **26**,

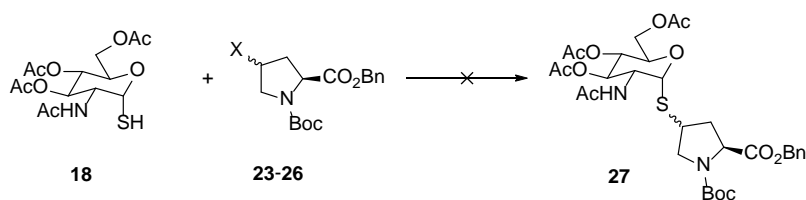
from building block **22** (Scheme 2.5). Initially we were probing chemical reactivity of these electrophiles and didn't concern ourselves with the stereochemistry of C4 of the proline residue.



Scheme 2.5: Synthesis of proline electrophiles

With a range of building blocks in hand, next we tried to form the thioglycosidic linkage. The electrophiles (**23-26**) were treated with  $\alpha$ -GlcNAc thiol **18** in the presence of different bases (Table 2.1), according to close literature precedents.<sup>36</sup> All reaction conditions gave complex mixtures of products and the desired product **27** was not isolated from any of these reaction mixtures.

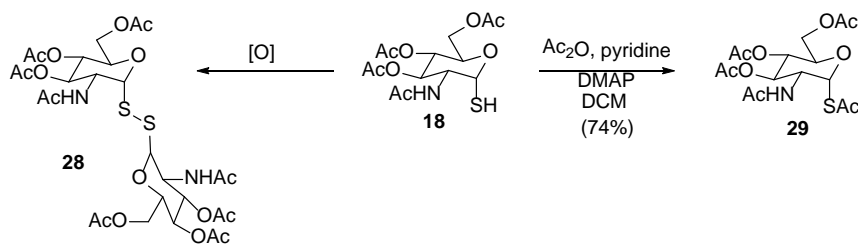
Table 2.1: Attempted glycosylation of **18** with electrophiles **23-26**



(Table 2.1 continued)

Electrophile	Conditions	Reference
Iodide <b>23</b>	Et <sub>3</sub> N, CH <sub>2</sub> Cl <sub>2</sub>	15e
Bromide <b>24</b>	Et <sub>3</sub> N, CH <sub>2</sub> Cl <sub>2</sub>	15e
Bromide <b>24</b>	K <sub>2</sub> CO <sub>3</sub> , <sup>n</sup> Bu <sub>4</sub> NBr	15a, 15d, 15e
Mesylate <b>25</b>	NaH, MeOH; DMF	15b, 15c
Triflate <b>26</b>	1M NaOH, MeOH	15f, 15g

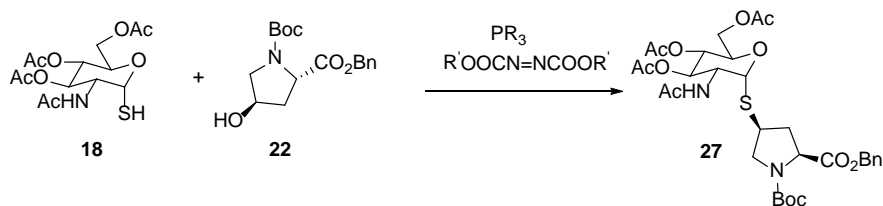
The thiosugar **18** could potentially be oxidized to form a disulfide **28**<sup>8</sup> and, if so, this would mean no nucleophilic thiol, accounting for the above failures. To test this hypothesis we subjected the alleged thiol **18** to acetylation conditions, according Knapp *et al.*,<sup>34</sup> and obtained **29** (Scheme 2.6). This tells us that our thiosugar **18** does exist as a monomer and is nucleophilic.



Scheme 2.6: Synthesis of thioester **29**

Since we failed to synthesize the  $\alpha$ -glycosides by direct nucleophilic substitution, we sought to apply the Mitsunobu reaction. This was appealing because we could couple the alcohol **22** to the thiosugar **18** in a single step, without going through electrophilic proline derivatives, with associated stereochemical consequences. Initially, we carried out the reaction of the  $\alpha$ -1-thiosugar **18** and the *trans*-4-Hyp derivative **22** under traditional Mitsunobu conditions, but we were unable to isolate compound **27** (Table 2.2, Entry 1). We investigated different conditions for the Mitsunobu reaction as listed in Table 2.2.

Table 2.2: Glycosylation of **18**



Entry	Ratios*	Solvent	Reagents	Temp °C	Results
1	1:1.3:2.2:2.2	THF	PPh <sub>3</sub> /DIAD	0	-
2	1:1.3:2.2:2.2	THF	PMe <sub>3</sub> /ADDP	0	-
3	1:1.3:1.3:1.3	THF	PPh <sub>3</sub> /DIAD	50	+
4	1:1.3:2.2:2.2	THF	PPh <sub>3</sub> /DIAD	50	+
5	1:1.3:2.2:2.2	THF	PMe <sub>3</sub> /ADDP	60	+
6	1:1.3:2.6:2.6	THF	PPh <sub>3</sub> /DIAD	60	+
7	1:1.3:2.6:2.6	dioxane	PPh <sub>3</sub> /DIAD	90	+
8	1:1.3:2.6:2.6	toluene	PPh <sub>3</sub> /DIAD	60	+++

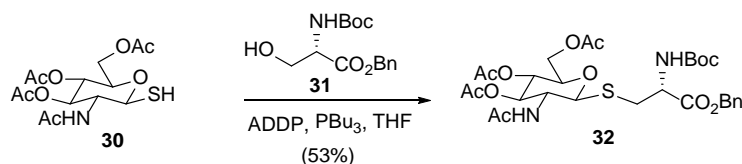
\*Hyp: thiol: phosphine:dialkylazodicarboxylate

DIAD = diisopropyl azodicarboxylate

ADDP = 1,1'-(azodicarbonyl)dipiperidine

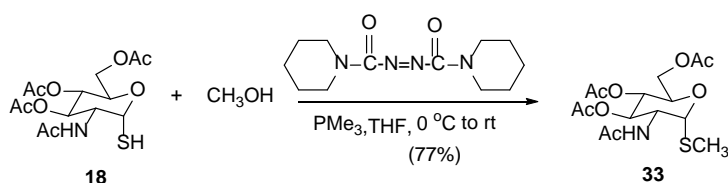
(-) =no product, (+) =trace amount of product, (+++) =considerable amount of product

Swarmy *et al.* reported that for the Mitsunobu reaction to proceed satisfactorily, the pK<sub>a</sub> of the nucleophile (the thiosugar in this case) has to be less than 11. For acidic pronucleophiles with pK<sub>a</sub> >13 it appears necessary to use modified Mitsunobu reagents in order to increase the basicity of the reaction intermediate and overcome this limitation.<sup>35a, 37</sup> To our knowledge, there have been no reports of the Mitsunobu reaction with α-1-thio sugars. In 2000, Ohnishi and coworkers<sup>38</sup> synthesized β-*N*-acetylglucosaminyl-1-*N*-Boc-cysteine (**32**) utilizing modified Mitsunobu conditions (Scheme 2.7).



Scheme 2.7: Synthesis of β-thio sugar using modified Mitsunobu reaction by Ohnishi and coworkers

In 1999 Toth and coworkers<sup>39</sup> reported the preparation of alkyl 1-thioglycosides from  $\beta$ -1-thiosugars and a series of alcohols using trimethylphosphine in combination with azodicarboxylatedipiperidine (ADDP) in good yields. We successfully applied the reaction conditions of Toth *et al.* to our  $\alpha$ -1-thiosugar **18**, to produce an  $\alpha$ -thiomethyl glycoside **33** (Scheme 2.8). This experiment led us to conclude that our thiosugar **18** is sufficiently nucleophilic under modified Mitsunobu conditions. Unfortunately reaction of thiosugar **18** and Hyp **22** using these conditions did not give the desired product **27** (Table 2.2, Entry 2).

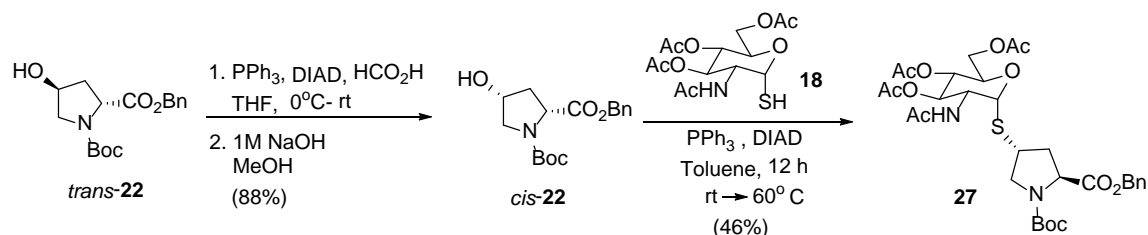


Scheme 2.8: Synthesis of  $\alpha$ -thiomethyl glycoside

Most often, the Mitsunobu reaction is conducted at room temperature, or below. There are examples that invoke high temperatures for hindered alcohols. Shi and coworkers<sup>40</sup> have carried out the Mitsunobu reaction with tertiary alcohols and phenols to produce ethers at elevated temperatures. They used traditional Mitsunobu reagents (DIAD and triphenylphosphine) and toluene as the solvent at high temperatures (80 °C to 100 °C). We also carried out the reaction using different ratios of DIAD and triphenylphosphine and THF as the solvent at high temperature (Table 2.2, Entries 3, 4, 6). After two days, the reaction was not complete, but we were able to isolate the desired product **27** and recover starting material **22**. The purification of the product was troublesome due to the presence of triphenylphosphine oxide. The identity of compound **27** was confirmed by NMR and mass spectrometry data. We also tried the reaction using modified reagents and high temperature at the same time (Table 2.2, Entry 5), but there was no improvement relative to Entries 3, 4 and 6. In order to further raise the temperature we carried out the same reaction in anhydrous dioxane at 90 °C, but the

yield was lower (Table 2.2, Entry 7). We switched the solvent to toluene because our reactants and reagents were soluble in toluene and we obtained a higher yield of desired **30** at 60 °C (Table 2.2, Entry 8).

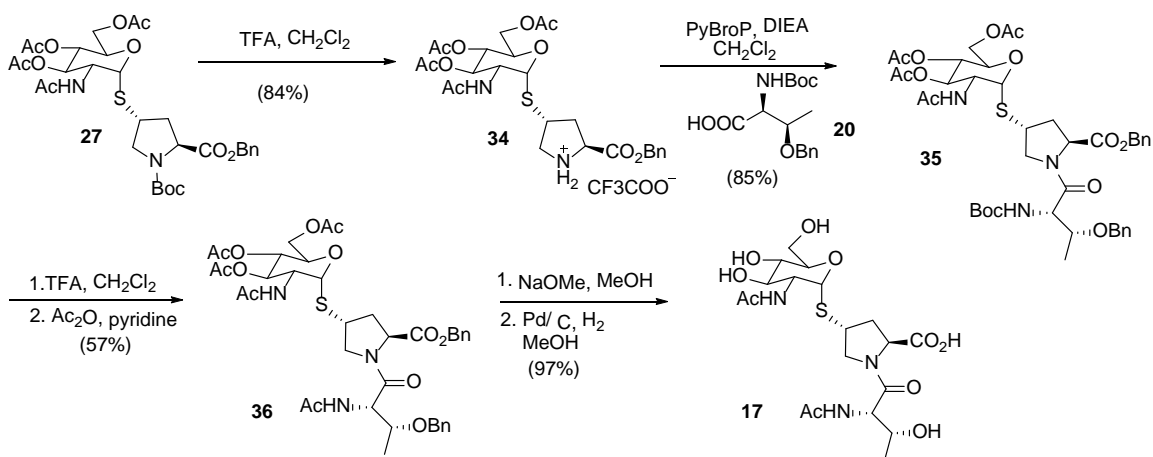
The studies in Table 2.2 were carried out on the readily available *trans*-hydroxyproline building block *trans*-**22**, but we need *cis*-hydroxyproline building block *cis*-**22** to prepare our bisubstrate analog **17** with the correct configuration at C4 of the proline residue. We prepared *cis*-**22** in two steps from *trans*-**22**. To invert the stereochemistry at C $\gamma$  of **22**, the formate ester was prepared using a Mitsunobu reaction, then hydrolyzed with sodium hydroxide to give the alcohol. Compound *cis*-**22** was then coupled with **18** under the optimized conditions. After purification by repetitive flash chromatography we obtained the product **36** in 46% yield (Scheme 2.8).



Scheme 2.9: Synthesis of thioglycoside **27**

Our next task, according to our retrosynthetic analysis, was to attach the threonine residue. Cleavage of the Boc group from **27** was carried out with TFA. Amine **34** was coupled with Boc-*L*-Thr(OBn)-OH (**20**) using PyBroP as the coupling reagent to give **35**. Compound **36** was synthesized by Boc removal followed by acetylation. Finally, acetate ester methanolysis and subsequent debenzoylation afforded the first generation inhibitor of Gnt1 **17** in 23% overall yield starting from Mitsunobu product **27** (Scheme 2.10).





Scheme 2.10: Synthesis of the first generation inhibitor

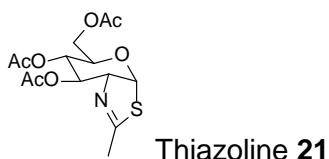
Compound **17** has been assessed in West's laboratory at University of Oklahoma Health Sciences Center, for its ability to inhibit the transfer of *N*-acetylglucosamine from UDP-GlcNAc to Hyp in the 23-mer (peptide representing the 133-157 sequence of Skp1). Experimental results showed that compound **17** was inactive as an inhibitor for Gnt1.

## 2.5 Experimental Section

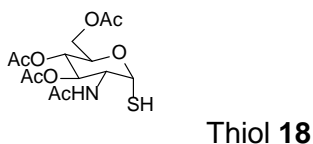
**GENERAL METHODS:** All reactions were performed under a dry nitrogen atmosphere unless otherwise noted. Reagents were obtained from commercial sources and used directly; exceptions are noted. Triethylamine, diisopropylethylamine and pyridine were dried and distilled from CaH<sub>2</sub> and stored over KOH pellets. Methanol was distilled from Mg turnings and stored over 4 Å molecular sieves. Flash chromatography was performed using flash silica gel (32-63 μ) from Dynamic Adsorbents Inc. Reactions were followed by TLC on precoated silica plates (200 μm, F-254 from Dynamic Adsorbents Inc.). The compounds were visualized by UV fluorescence or by staining with anisaldehyde, ninhydrin, phosphomolybdic acid, potassium permanganate stains or 10% sulfuric acid in ethanol stains. NMR spectra were recorded on a Bruker DPX-250, DPX-400 and AV-400 spectrometer. Proton NMR data is reported in ppm downfield from TMS as an internal standard. \*Some compounds reported in this chapter exist as

mixture of rotomers about the prolyl amide bond on the time scale of  $^1\text{H}$  NMR. Signals in square parentheses refer to those of the minor rotomer. High resolution mass spectra were recorded using either an Agilent 6210 time-of-flight MS, or a Hitachi MS-8000 3DQ LC-ion trap mass spectrometer with electrospray ionization.

### 2.5.1 Experimental Procedures

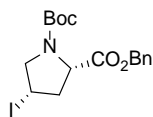


A solution of 2-acetamido-2-deoxy- $\beta$ -D-glucopyranose-1,3,4,6-tetraacetate **15** (2.00 g, 5.14 mmol, 1.5 equiv.) in toluene (20 mL) was treated with Lawesson's reagent (1.38 g, 3.42 mmol, 1 equiv.) and stirred for 1.5 h at 80 °C under nitrogen. The reaction mixture was allowed to cool to rt, then neutralized by the addition of solid  $\text{Na}_2\text{CO}_3$  (200 mg), filtered through a plug of cotton, concentrated and purified by flash chromatography (7:3  $\text{CH}_2\text{Cl}_2$ :EtOAc) affording thiazoline **21** as a yellow syrup (1.49 g, 84%).  $R_f$  0.43 (19:1  $\text{CH}_2\text{Cl}_2$ :MeOH).  $[\alpha]_D^{25} = +0.38$  ( $c$  1.0, MeOH).  $^1\text{H}$  NMR ( $\text{CDCl}_3$ , 400 MHz)  $\delta$  2.10 (s, 3H), 2.09 (s, 3H), 2.14 (s, 3H), 2.32 (d,  $J = 2.2$  Hz, 3H), 3.55 (dt,  $J = 9.1, 4.4$  Hz, 1H), 4.13 (d,  $J = 6.0$  Hz, 2H), 4.47-4.49 (m, 1H), 4.96 (dd,  $J = 9.5, 1.3$  Hz, 1H), 5.57 (dd,  $J = 3.2, 1.7$  Hz, 1H), 6.25 (d,  $J = 7.2$  Hz, 1H);  $^{13}\text{C}$  NMR ( $\text{CDCl}_3$ , 100 MHz)  $\delta$  20.8, 20.9, 21.0, 21.1, 63.4, 68.5, 69.4, 70.8, 76.8, 88.9, 168.3, 169.4, 169.7, 170.7.



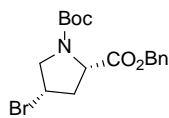
A solution of GlcNAc-thiazoline triacetate **21** (100 mg, 0.29 mmol) in MeOH (1 mL) was cooled to 0 °C and treated with trifluoroacetic acid (2 drops from a 20 G syringe needle) and water (2 drops from a 20 G syringe needle). The reaction mixture was gradually warmed to rt,

stirred for 5.5 h, and concentrated to provide the  $\alpha$ -mercaptan **18** as a colorless foam (106 mg, quantitative yield).  $R_f$  0.37 (19:1  $\text{CH}_2\text{Cl}_2$ :MeOH).  $[\alpha]_D^{25} = +0.05$  ( $c$  1.0, MeOH).  $^1\text{H NMR}$  ( $\text{CDCl}_3$ , 400 MHz)  $\delta$  1.96 (s, 3H), 2.03 (s, 3H), 2.04 (s, 3H), 2.09 (s, 3H), 4.10 (dd,  $J = 12.3, 2.2$  Hz), 4.25 (dd,  $J = 12.3, 4.2$  Hz), 4.30 (ddd,  $J = 9.4, 4.2, 2.2$ , Hz, 1H), 4.44-4.50 (m, 1H), 5.06-5.14 (m, 2H), 5.76 (dd,  $J = 7.0, 5.2$  Hz, 1H), 5.89 (d,  $J = 8.4$  Hz, 1H);  $^{13}\text{C NMR}$  ( $\text{CDCl}_3$ , 100 MHz)  $\delta$  20.8, 20.9, 23.3, 52.7, 61.9, 68.1, 69.2, 70.8, 79.0, 169.4, 170.2, 170.9, 171.9.



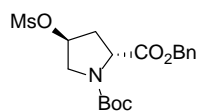
Electrophile **23** (Following conditions reported by Joullie and coworkers<sup>41</sup> for iodide formation)

Triphenylphosphine (220 mg, 0.84 mmol, 1.5 equiv.) was added to a stirred solution of Boc-Hyp-OBn (**22**) (180 mg, 0.56 mmol, 1 equiv.) in anhydrous THF (3 mL). The solution was cooled to 0 °C, stirred for 15 min under nitrogen. A solution of DIAD (165  $\mu\text{L}$ , 169 mg, 0.84 mmol, 1.5 equiv.) in anhydrous THF (2 mL) was added dropwise over 10 min to the reaction mixture, stirred for 30 min maintaining the temperature at 0 °C. Methyl iodide (70  $\mu\text{L}$ , 159 mg, 1.12 mmol, 2.0 equiv.) was added, the reaction mixture was gradually warmed to the RT and stirred for 3.5 h under nitrogen. The reaction mixture was concentrated and the residue was applied to a flash column eluting with 1:1 hexanes:EtOAc to give **23** (95 mg, 39%).  $R_f$  0.70 (1:1 hexanes:EtOAc).  $^1\text{H NMR}$  ( $\text{CDCl}_3$ , 400 MHz)  $\delta$  1.33 [1.45] (s, 9H), 2.29-2.43 (m, 1H), 2.82-2.91 [2.53-2.63] (m, 1H), 3.67 (apt.t,  $J = 8.7$  Hz, 1H), 4.02-4.14 [3.92-3.99] (m, 2H), 4.27 [4.37] (t,  $J = 7.7$  Hz, 1H), 5.08-5.31 (m, 2H); 28.15 [28.38], 41.8 [42.1], 42.9 [43.2], 56.7 [59.1], 57.1 [58.7], 67.1, 80.7, 128.2, 128.3, 128.5, 128.7, 135.3, 135.5, 152.7, 153.3, 171.2, 171.5.



Electrophile **24** (Following conditions reported by Webb *et al.*<sup>42</sup> and Berger *et al.*<sup>43</sup> for bromide formation.)

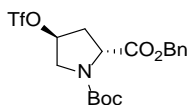
Triphenylphosphine (190 mg, 0.73 mmol, 2.2 equiv.) was added to a stirred solution of carbon tetrabromide (241 mg, 0.73 mmol, 2.2 equiv.) in anhydrous THF (1 mL), and the mixture was stirred for 10 min under nitrogen. A solution of Boc-Hyp-OBn (**22**) (99 mg, 0.33 mmol, 1 equiv.) in anhydrous THF (2 mL) was added to the reaction mixture over 5 min and stirred overnight. The reaction mixture was concentrated and the residue was applied to a flash column eluting with 3:1 hexanes:EtOAc to give **24** (50 mg, 43%).  $R_f$  0.38 (3:1 hexanes:EtOAc).  $^1\text{H}$  NMR ( $\text{CDCl}_3$ , 400 MHz)  $\delta$  1.33 [1.46], 2.40-2.47 (m, 1H), 2.77-2.88 (m, 1H), 3.68-3.75 (m, 1H), 4.08 (dd,  $J = 11.9, 6.4$  Hz, 0.5H) [4.02 (dd,  $J = 11.9, 6.4$  Hz, 0.5H)], 4.28 (p,  $J = 6.3$  Hz, 1H), 4.35 [4.47] (dd,  $J = 8.5, 5.5$  Hz, 1H), 5.08-5.31 (m, 2H), 7.33-7.37 (m, 5H);  $^{13}\text{C}$  NMR ( $\text{CDCl}_3$ , 100 MHz)  $\delta$  28.3 [28.5], 41.1 [40.1], 41.6 [42.5], 55.4 [55.8], 58.5 [58.2], 67.3, 80.8, 128.4, 128.6, 128.7, 128.8, 135.5, 135.7, 153.3 [153.8], 171.7 [171.4]; HRMS (+ESI) calcd for  $\text{C}_{17}\text{H}_{22}\text{BrNNaO}_4$  ( $\text{M}+\text{Na}$ ) $^+$ : 406.0624; obsd: 406.0643.



**Electrophile 25** (Following conditions reported by Knapp *et al.*<sup>34</sup> Lange *et al.*<sup>44</sup>, Qui *et al.*<sup>45</sup> and Oh *et al.*<sup>46</sup> mesylate formation.)

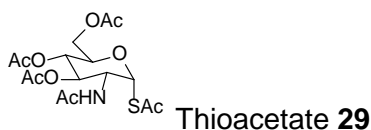
Triethylamine (377  $\mu\text{L}$ , 274 mg, 2.70 mmol, 2.2 equiv.) was added to a solution of Boc-Hyp-OBn (**22**) (395 mg, 1.23 mmol, 1 equiv.) in dichloromethane (5 mL) at 0  $^\circ\text{C}$ . This was stirred for 5 min under nitrogen, *N,N*-dimethylaminopyridine (150 mg, 1.23 mmol, 1 equiv.) was added and stirring continued for another 10 min at 0  $^\circ\text{C}$ . Methanesulfonyl chloride (105  $\mu\text{L}$ , 155 mg, 1.35 mmol, 1.1 equiv.) was added, the mixture warmed to rt and stirred overnight under  $\text{N}_2$ . The mixture was concentrated, diluted with dichloromethane (40 mL) and washed with water (2  $\times$  20 mL). The aqueous layer was back-extracted with  $\text{CH}_2\text{Cl}_2$  (25 mL). The organic layers were combined, dried over  $\text{MgSO}_4$ , filtered and concentrated. The residue was purified by flash column chromatography, eluting with 19:1  $\text{CH}_2\text{Cl}_2$ :MeOH to give **25** (380 mg, 77%).  $R_f$  0.66 (19:1  $\text{CH}_2\text{Cl}_2$ :MeOH).  $^1\text{H}$  NMR ( $\text{CDCl}_3$ , 400 MHz)  $\delta$  1.35 [1.46]\* (s, 9H), 2.20-2.28 (m, 1H), 2.59-

2.69 [2.54-2.57] (m, 1H), 3.03 (s, 3H), 3.75 [3.72] (d,  $J = 4.3$  Hz, 1H), 3.85 [3.88] (s, 1H), 4.44 [4.52] (t,  $J = 7.8$  Hz, 1 H), 5.09-5.29 (m, 3H), 7.33-7.35 (m, 5H);  $^{13}\text{C}$  NMR ( $\text{CDCl}_3$ , 100 MHz)  $\delta$  28.3 [28.5], 37.6 [36.4], 38.8, 52.3 [52.7], 57.6 [57.4], 67.3, 78.0 [78.3], 81.1, 128.3, 128.5, 128.6, 128.7, 128.8, 135.3, 135.6, 153.5 [154.0], 172.2 [171.9].



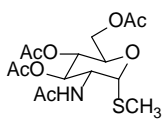
Triflate **26** (Following conditions reported by Raines and coworkers<sup>47</sup> triflate formation.)

Pyridine (102  $\mu\text{L}$ , 100 mg, 1.26 mmol, 2 equiv.) was added to a solution of *N*-Boc-*trans*-4-hydroxy-*L*-proline benzyl ester (**22**) in dry  $\text{CH}_2\text{Cl}_2$  (5 mL) at 4  $^\circ\text{C}$  under  $\text{N}_2$ . The mixture was stirred for 10 min then triflic anhydride (159  $\mu\text{L}$ , 267 mg, 0.95 mmol, 1.5 equiv.) was added dropwise and the resulting yellow solution was stirred at -10  $^\circ\text{C}$  for 2 h. The mixture was gradually warmed to rt, stirred for another 2.5 h, concentrated and the residue purified by flash column chromatography, eluting with 3:1 hexanes:EtOAc, to give **26** as yellow oil (91 mg, 43%).  $R_f$  0.41 (3:1 Hexanes:EtOAc).  $^1\text{H}$  NMR ( $\text{CDCl}_3$ , 400 MHz)  $\delta$  1.33 [1.47]\* (s, 9H), 2.26-2.36 (m, 1H), 2.56-2.76 (m, 1H), 3.78 (dd,  $J = 13.4, 3.3$  Hz, 1H), 3.86 (d,  $J = 11.9$  Hz, 0.5H) [3.96 (d,  $J = 13.5$  Hz, 0.5 H)], 4.47 [4.56] (t,  $J = 8.0$  Hz, 1H), 5.08-5.27 (m, 2H), 5.44 (app. s, 1H), 7.32-7.35 (m, 5H);  $^{13}\text{C}$  NMR ( $\text{CDCl}_3$ , 100 MHz)  $\delta$  28.2 [28.4], 37.6 [36.4], 52.5 [52.7], 57.4 [57.2], 67.4 [67.6], 81.5, 86.2 [86.7], 119 (q,  $J_{\text{C-F}} = 319.7$  Hz), 128.3, 128.6, 128.7, 128.8, 135.1, 135.4, 153.3 [153.8], 171.7 [171.5].



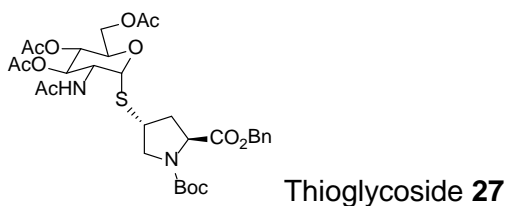
A solution of **18** (155 mg, 0.43 mmol, 1 equiv.) in a 3:2 mixture of pyridine:dichloromethane (8 mL) was treated with acetic anhydride (405  $\mu\text{L}$ , 438 mg, 4.27 mmol, 1.08 equiv.) and a crystal of 4-(*N,N*-dimethylamino)pyridine. The reaction mixture was

stirred overnight at rt, concentrated and applied to a flash column eluting with 39:1 CH<sub>2</sub>Cl<sub>2</sub>: MeOH to give **29** (84 mg, 74%) as a colorless solid. *R<sub>f</sub>* 0.20 (39:1 CH<sub>2</sub>Cl<sub>2</sub>: MeOH). <sup>1</sup>H NMR (CDCl<sub>3</sub>, 400 MHz) δ 1.92 (s, 3H), 2.04 (s, 3H), 2.05 (s, 3H), 2.09 (s, 3H), 2.46 (s, 3H), 3.91 (dt, *J* = 10.1, 3.0 Hz, 1H), 4.06 (dd, *J* = 12.5, 2.2 Hz, 1H), 4.25 (dd, *J* = 12.6, 4.0 Hz, 1H), 4.66 (ddd, *J* = 11.2, 8.9, 5.2 Hz, 1H), 4.89 (app.t, *J* = 9.7 Hz, 1H), 5.18 (apt.t, *J* = 9.7 Hz, 1H), 5.52 (d, *J* = 8.7 Hz, 1H), 6.13 (d, *J* = 5.1 Hz, 1H); <sup>13</sup>C NMR (CDCl<sub>3</sub>, 100 MHz) δ 20.6, 20.7, 23.1, 31.6, 51.6, 61.6, 67.5, 71.8, 72.1, 82.3, 169.1, 169.8, 170.7, 171.7, 190.6. HRMS (+ESI) calcd for C<sub>16</sub>H<sub>23</sub>NO<sub>9</sub>SNa (M+Na)<sup>+</sup>: 428.0991; obsd: 428.1005.

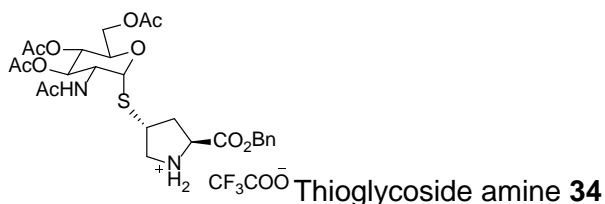


α-Methyl thioglycoside **33**

Methanol (4 μL, 3 mg, 0.09 mmol, 1 equiv.) was added to a solution of azodicarbonyldipiperidine (44 mg, 0.17 mmol, 2 equiv.) and trimethyl phosphine (18 μL, 13 mg, 0.17 mmol, 2 equiv.) in THF (2 mL) at 0 °C. The reaction mixture was warmed to rt and stirred for 10 min. A solution of thiol **18** (41 mg, 0.11 mmol, 1.3 equiv.) in THF (1 mL) was added and stirred overnight under nitrogen. The reaction mixture was concentrated, diluted with hexane (5 mL), filtered and concentrated. The residue was applied to a flash column eluting with 9:1 EtOAc:hexanes to give **33** (33 mg, 77%). *R<sub>f</sub>* 0.50 (9:1 EtOAc:hexanes). <sup>1</sup>H NMR (CDCl<sub>3</sub>, 400 MHz) δ 1.97 (s, 3H), 2.04 (s, 3H), 2.05 (s, 3H), 2.10 (s, 3H), 2.14 (s, 3H), 4.10 (dd, *J* = 12.2, 2.1 Hz, 1H), 4.28 (dd, *J* = 12.2, 4.6 Hz, 1H), 4.34 (ddd, *J* = 9.3, 4.6, 2.1 Hz, 1H), 4.49- 4.56 (m, 1H), 5.08-5.16 (m, 2H), 5.36 (d, *J* = 5.4 Hz, 1H), 5.8 (d, *J* = 8.7 Hz, 1H); <sup>13</sup>C NMR (CDCl<sub>3</sub>, 100 MHz) δ 13.6, 20.8, 20.9, 21.0, 23.4, 52.6, 62.2, 68.3, 68.4, 71.5, 85.4, 169.5, 170.2, 170.9, 171.9. HRMS (+ESI) calcd for C<sub>15</sub>H<sub>23</sub>NNaO<sub>8</sub>S (M+Na)<sup>+</sup>: 400.1042; obsd: 400.1069.

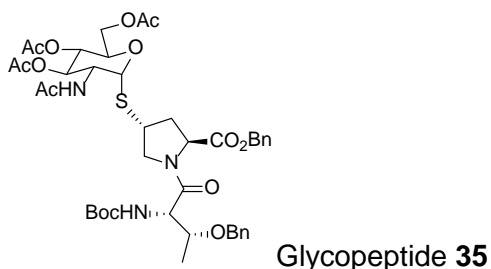


Diisopropylazodicarboxylate (254  $\mu$ L, 261 mg 1.29 mmol, 2.6 equiv.) was added to a solution of triphenylphosphine (339 mg, 1.29 mmol, 2.6 equiv.) in dry toluene (3 mL). The mixture was stirred at rt under  $N_2$  for 10 min. Boc-*cis*-4-Hyp-OBn *cis*-**22** (160 mg, 0.49 mmol, 1.0 equiv.) in dry toluene (2 mL) was added to the reaction mixture, followed by the addition of **18** (235 mg, 0.65 mmol, 1.3 equiv.) in dry toluene (2 mL). The reaction mixture was heated at 60  $^{\circ}$ C and stirred overnight under  $N_2$ . The mixture was concentrated. After three flash columns, eluting with 2:1 EtOAc:Hexanes, compound **27** was obtained as a colorless foam (152 mg, 46%).  $R_f$  0.36 (2:1 EtOAc:hexanes).  $[\alpha]_D^{25} = +0.48$  ( $c$  1.0, MeOH).  $^1H$  NMR ( $CDCl_3$ , 400 MHz)  $\delta$  1.34 [1.46]<sup>\*</sup> (s, 9H), 1.96 (s, 3H), 2.03 (s, 3H), 2.04 (s, 3H), 2.05 (s, 3H), 2.21-2.42 (m, 2H), 3.40 [3.30] (dd,  $J = 10.9, 7.0$  Hz, 1H), 3.51 (sextet,  $J = 6.9$  Hz, 1H), 3.86-3.94 (m, 1H), 4.02-4.07 (m, 1H), 4.24 (dd,  $J = 12.3, 7.2$  Hz, 1H), 4.31-4.38 (m, 1H), 4.45-4.54 (m, 1H), 4.96-5.03 (m, 1H), 5.07-5.24 (m, 4H), 5.47 (5.50) (d,  $J = 5.3$  Hz, 1H), 5.70 (t,  $J = 7.3$  Hz, 1H), 7.33-7.38 (m, 5H);  $^{13}C$  NMR ( $CDCl_3$ , 100 MHz)  $\delta$  20.8 [20.9], 23.4, 28.3 [28.6], 38.6 [37.5], 42.0 [41.9], 52.3 [52.7], 52.5, 58.9 [58.7], 62.3 [60.6], 67.2, 68.3 [68.2], 69.1 [69.0], 71.3, 80.8, 85.4 [84.8], 128.3, 128.5, 128.8, 128.9, 135.5 [135.7], 153.5 [154.0], 169.4, 170.1 [170.0], 170.8, 171.7, 172.1 [171.9], 172.3 [172.1]. HRMS (+TOF) calcd for  $C_{31}H_{43}N_2O_{12}S$  ( $M + H$ )<sup>+</sup>: 667.2531; obsd: 667.2550.



Trifluoroacetic acid (1.5 mL) was added to a solution of glycopeptide **27** (154 mg, 0.23 mmol) in  $CH_2Cl_2$  (3 mL) at 0  $^{\circ}$ C. The reaction mixture was gradually warmed to rt, stirred for 2 h

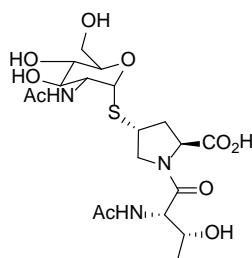
under nitrogen, concentrated and applied to a flash column, eluting first with 2:1 EtOAc:hexanes, and then with 9:1 CH<sub>2</sub>Cl<sub>2</sub>:MeOH to give **34** as a colorless foam (110 mg, 84%). *R<sub>f</sub>* 0.52 (9:1 CH<sub>2</sub>Cl<sub>2</sub>:MeOH). <sup>1</sup>H NMR (CD<sub>3</sub>OD, 400 MHz) δ 1.94 (s, 3H), 1.97 (s, 3H), 1.98 (s, 3H), 2.01 (s, 3H), 2.46-2.53 (m, 1H), 2.64 (p, *J* = 7.0 Hz, 1H), 3.24-3.34 (m, 2H), 3.68 (p, *J* = 6.6 Hz, 1H), 3.80 (dd, *J* = 12.0, 7.1 Hz, 1H), 4.10 (d, *J* = 12.0 Hz, 2H), 4.24 (dd, *J* = 12.3, 5.2 Hz, 1H), 4.39-4.42 (m, 1H), 4.47 (dd, *J* = 11.3, 5.5 Hz, 1H), 4.68 (t, *J* = 7.9 Hz, 1H), 4.97 (t, *J* = 9.4 Hz, 1H), 5.10 (dd, *J* = 11.1, 9.1 Hz, 1H), 5.25 (d, *J* = 12.0 Hz, 1H), 5.30 (d, *J* = 12.0 Hz, 1H), 5.63 (d, *J* = 5.4 Hz, 1H), 7.36-7.40 (m, 5H); <sup>13</sup>C NMR (CD<sub>3</sub>OD, 100 MHz) δ 20.7, 22.5, 37.2, 42.3, 52.4, 53.3, 60.3, 63.6, 69.6, 69.7, 70.2, 70.8, 71.8, 85.8, 129.8, 129.9, 130.0, 136.4, 169.9, 171.4, 171.9, 172.3, 173.7.



Diisopropylethylamine (85 μL, 63 mg, 0.485 mmol, 2.5 equiv.) was added to a solution of **34** (110 mg, 0.19 mmol, 1 equiv.) in CH<sub>2</sub>Cl<sub>2</sub> (3 mL) at 0 °C, followed by the addition of Boc-L-Thr(OBn).OH (69 mg, 0.22 mmol, 1.15 equiv.) and PyBroP (136 mg, 0.29 mmol, 1.5 equiv.). The reaction mixture was gradually warmed to rt, stirred overnight under nitrogen, and concentrated. The residue was purified by flash column eluting first with 2:1 EtOAc:hexanes, then with 9:1 CH<sub>2</sub>Cl<sub>2</sub>:MeOH to give **35** as a colorless foam (142 mg, 85%). *R<sub>f</sub>* 0.54 (9:1 CH<sub>2</sub>Cl<sub>2</sub>:MeOH). [α]<sub>D</sub><sup>25</sup> = +0.40 (c 1.0, MeOH). <sup>1</sup>H NMR (CDCl<sub>3</sub>, 400 MHz) δ 1.21 [1.25]<sup>\*</sup> (d, *J* = 6.0 Hz, 3H), 1.44 [1.45] (s, 9H), 1.75-1.89 (m, 0.5 H), 1.75-1.89 (m, 0.5H), 1.97 [1.95] (s, 3H), 2.04 [2.03] (m, 9H), 2.24-2.44 (m, 1.5H), 3.30-3.55 (m, 1H), 3.60-3.68 (m, 1H), 3.77-3.87 (m, 1H), 4.02-4.07 (m, 1H), 4.11-4.16 (m, 1H), 4.17-4.25 (m, 1H), 4.28-4.38 (m, 1H), 4.44-4.64 (m,



2H), 4.72 (dd,  $J = 8.0, 4.3$  Hz, 1H), 5.10 [4.94] (dd,  $J = 9.1, 19.2$ , 1H), 5.14 [5.13] (s, 2H), 5.20 (s, 2H), 5.47 [5.59] (d,  $J = 5.4$  Hz, 1H), 5.75 (d,  $J = 8.3$  Hz, 1H), 7.26-7.35 (m, 10H);  $^{13}\text{C}$  NMR ( $\text{CDCl}_3$ , 100 MHz)  $\delta$  16.2 [16.6], 20.8 [20.9], 23.3 [24.2], 28.6 [28.5], 36.7 [35.9], 43.1 [42.4], 46.9 [46.3], 52.7 [52.8], 53.1 [52.9], 56.2, 58.8 [59.8], 62.3, 67.3 [67.9], 68.3 [68.1], 69.1 [69.3], 71.1 [71.3], 71.6, 80.0 [79.7], 84.8, 85.4 [85.2], 127.8, 127.9, 128.0, 128.3, 128.4, 128.5, 128.6, 128.8, 128.9, 135.5 [135.2], 138.5 [137.8], 155.8 [155.9], 169.4 [169.3], 169.6 [169.9], 170.2, 170.7, 172.2, 171.7 [172.0]; HRMS (+ESI) calcd for  $\text{C}_{42}\text{H}_{56}\text{N}_3\text{O}_{14}\text{S}$  (M+H) $^+$ : 858.3477; obsd: 858.3464.



Bisubstrate Analog **17**

Trifluoroacetic acid (1 mL) was added to a solution of **35** (142 mg, 0.17 mmol, 1 equiv.) in  $\text{CH}_2\text{Cl}_2$  (3 mL) at 0 °C under  $\text{N}_2$ . The mixture was stirred for 2 h, concentrated, and then concentrated twice more from  $\text{CH}_2\text{Cl}_2$ . The residue was dissolved in a mixture of pyridine (1 mL) and acetic anhydride (1 mL) and stirred at rt under  $\text{N}_2$  overnight. The red solution was concentrated, diluted with EtOAc (20 mL) washed with 1N HCl (20 mL) and brine (20 mL). The organic layer was dried over  $\text{MgSO}_4$ , filtered concentrated and the residue purified using flash chromatography, eluting with 9:1  $\text{CH}_2\text{Cl}_2$ :MeOH to isolate crude compound **36** (75 mg, 57%).  $R_f$  0.41 (9:1  $\text{CH}_2\text{Cl}_2$ :MeOH).

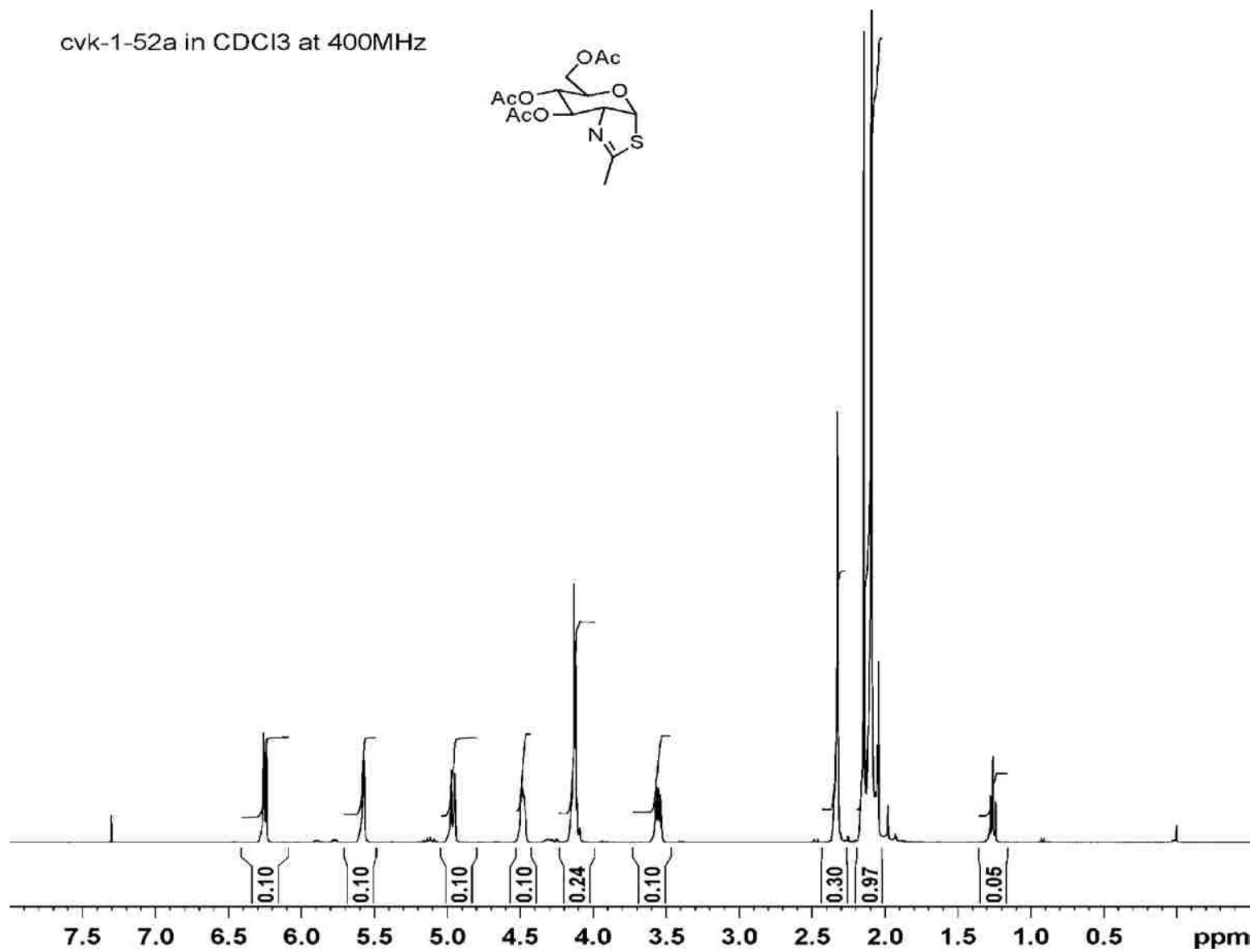
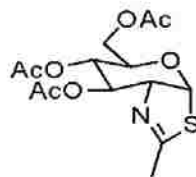
A 25% solution of sodium methoxide in MeOH (two drops from a 20 G syringe needle) was added to a solution of **36** (24 mg, 0.03 mmol) in MeOH (2 mL) at 0 °C. The reaction mixture was stirred for 2 h at rt, followed by the addition of IR-120H $^+$  resin and stirred for a further 15 min. The mixture was filtered and concentrated. The residue was dissolved in MeOH (2 mL).

and palladium on carbon (10%, 25 mg) was added in one portion. The reaction flask was evacuated, then opened to an atmosphere of H<sub>2</sub> and stirred overnight. The catalyst was removed by filtering through a plug of Celite<sup>®</sup> in a Pasteur pipet. The filtrate was concentrated to give **17** (17 mg, 97%). *R<sub>f</sub>* 0.74 (6:4:1 CH<sub>3</sub>Cl:MeOH:H<sub>2</sub>O). <sup>1</sup>H NMR (CD<sub>3</sub>OD, 400 MHz) δ 1.26 [1.16]\* (d, *J* = 6.3 Hz, 3H), 1.99 [1.97] (s, 6H), 1.95-2.06 (m, 1H), 2.37 (app.t, *J* = 6.8 Hz, 1H), 3.46-3.60 (m, 1H), 3.61-3.67 (m, 1H), 3.82-3.89 (m, 2H), 3.92-3.96 (m, 2H), 4.05 (dd, *J* = 11.0, 5.4 Hz, 1H), 4.14 (dd, *J* = 10.5, 6.8 Hz, 1H), 4.45 (d, *J* = 6.7 Hz, 1H), 4.52 (t, *J* = 6.7 Hz, 1H), 4.62 (s, 1H), 5.60 (d, *J* = 5.1 Hz, 1H), 8.09-8.11, (m, 2H); <sup>13</sup>C NMR (CDCl<sub>3</sub>, 100 MHz) δ 19.3, 22.4, 22.8, 37.5, 43.4, 53.0, 54.8, 55.9, 58.7, 60.1, 63.0, 68.8, 72.7, 75.1, 86.0, 91.3, 171.7, 173.6, 173.9.

## 2.5.2 $^1\text{H}$ and $^{13}\text{C}$ NMR Spectra

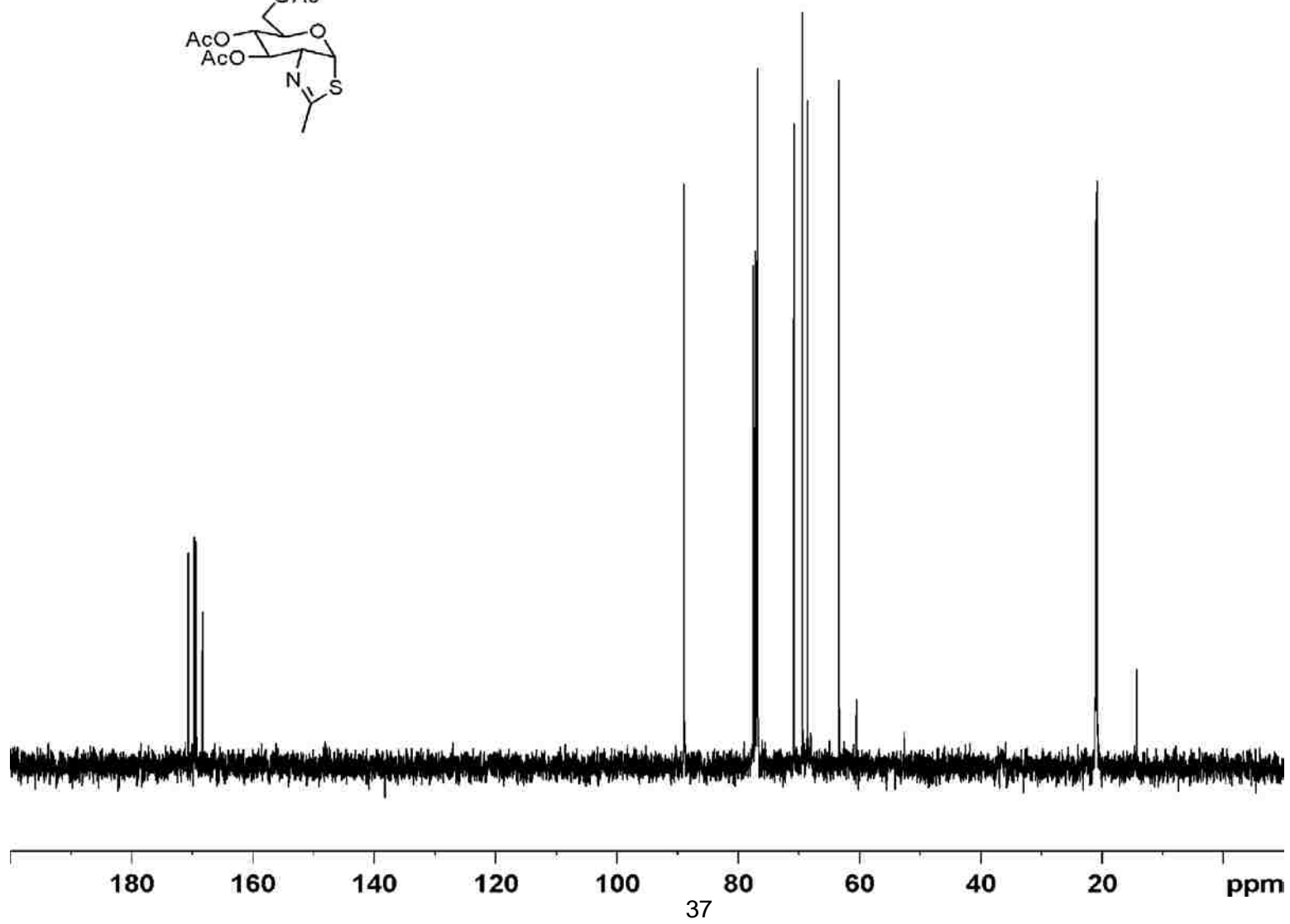
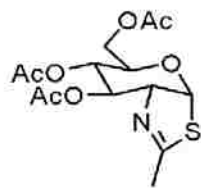
### Thiazoline 21

cvk-1-52a in  $\text{CDCl}_3$  at 400MHz



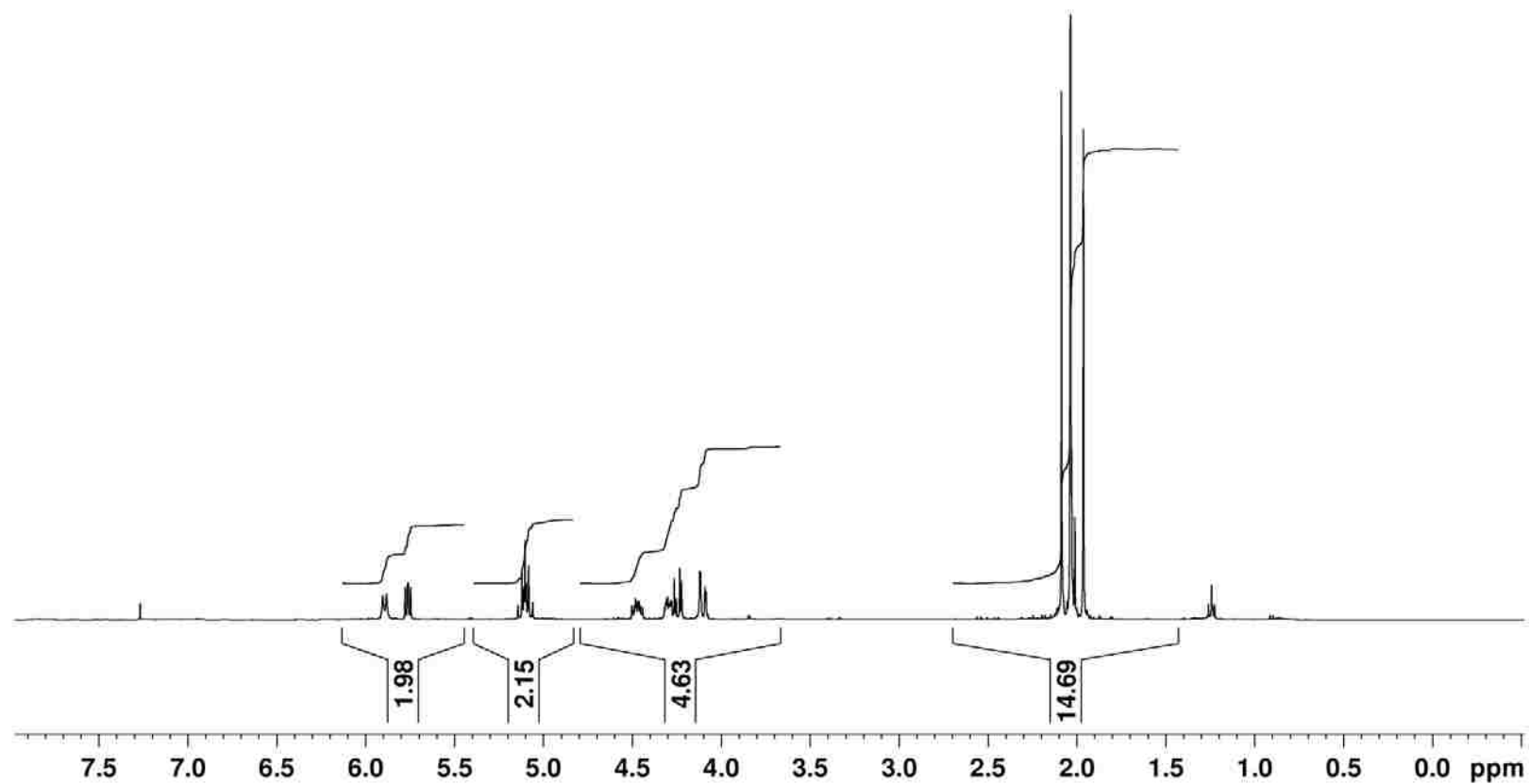
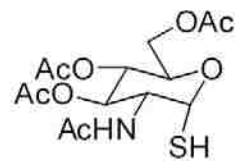
# Thiazoline 21

cvk-1-52a in CDCl<sub>3</sub> at 100MHZ



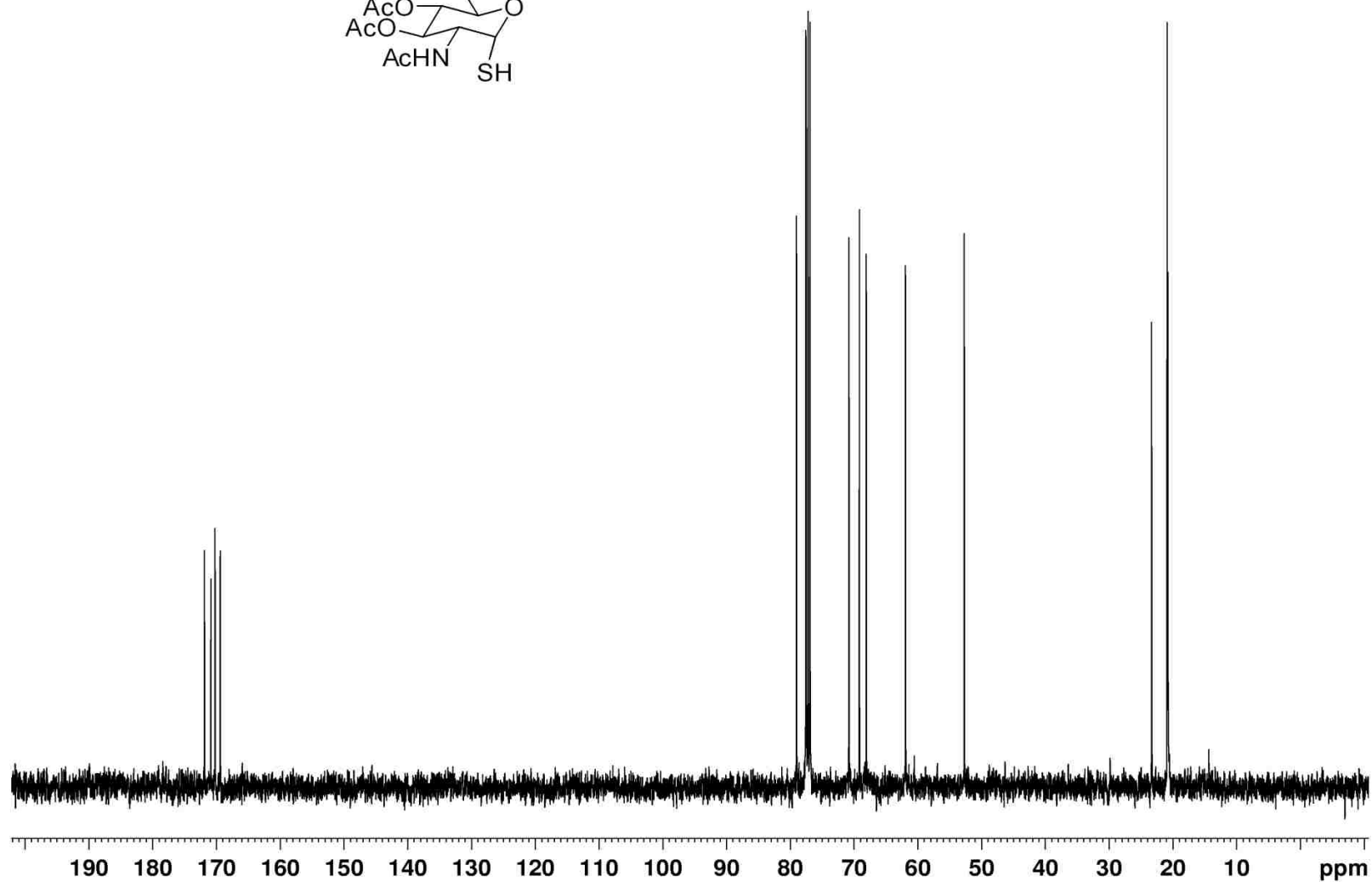
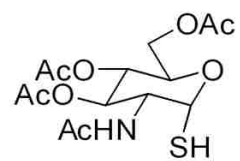
Thiol **18**

cvk-1-47a CDCl<sub>3</sub> 400MHz



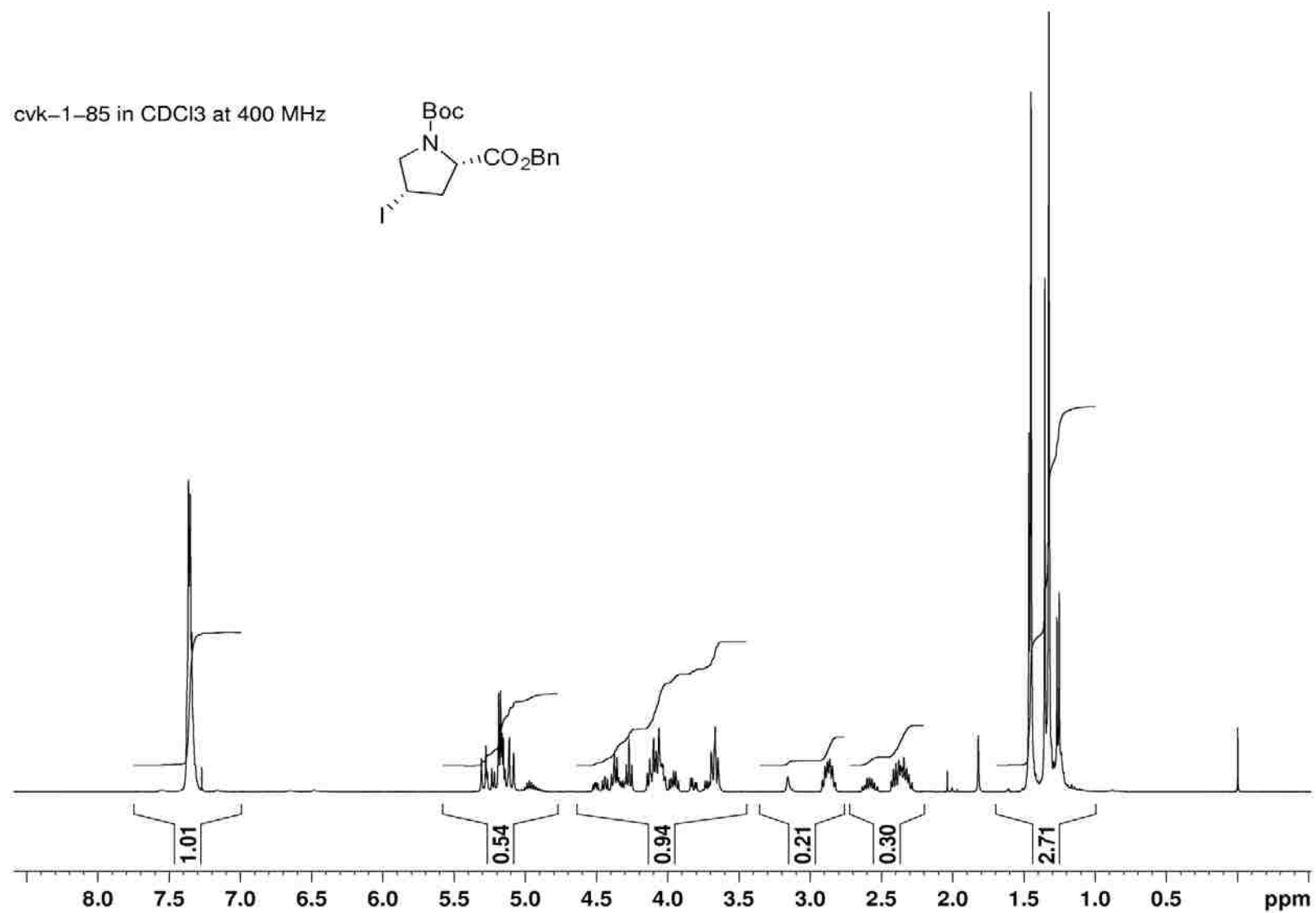
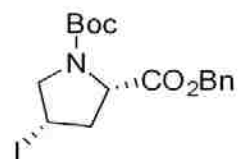
Thiol **18**

cvk-1-47a CDCl<sub>3</sub> 100MHz



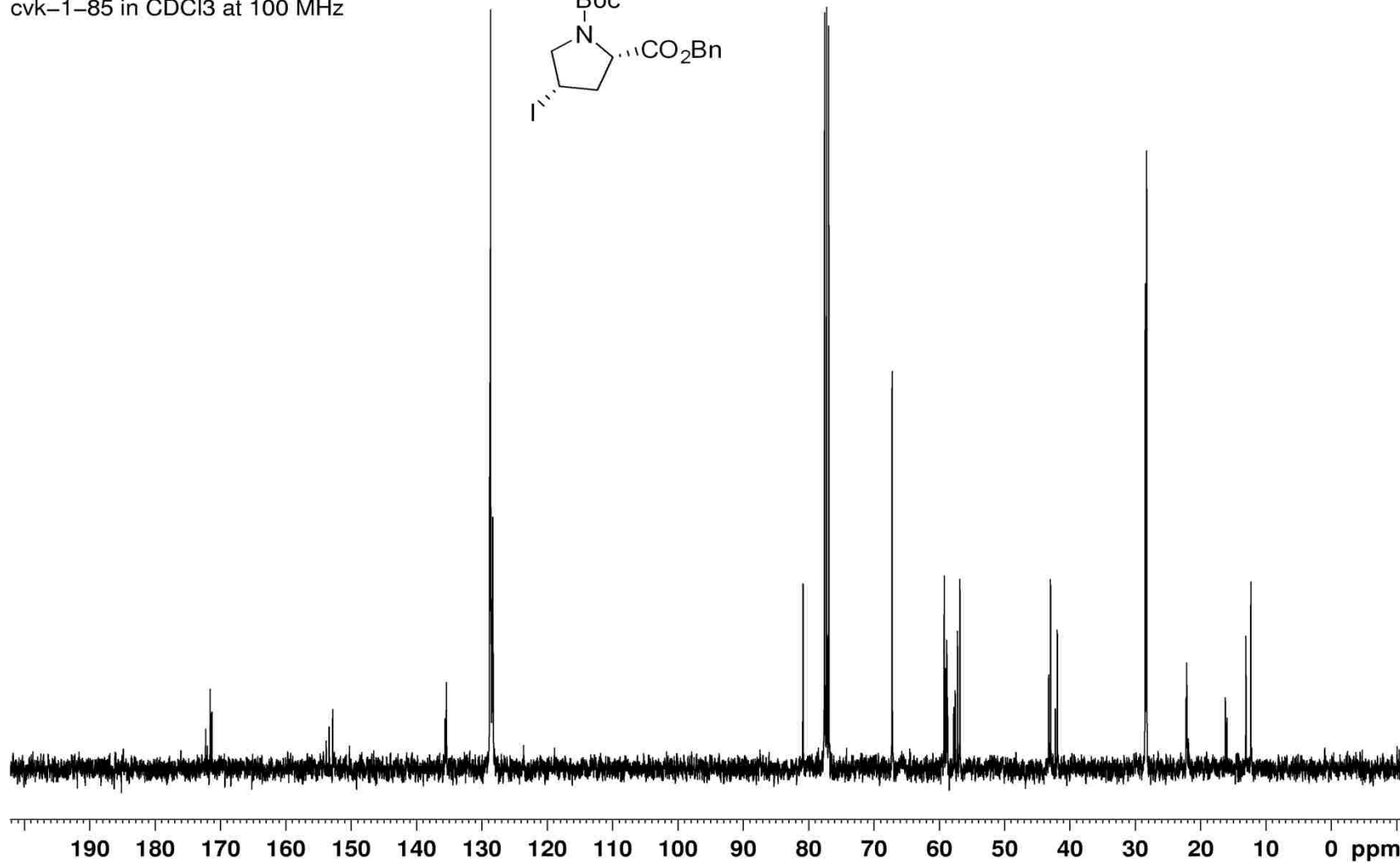
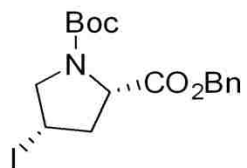
Electrophile **23**

cvk-1-85 in CDCl<sub>3</sub> at 400 MHz



Electrophile **23**

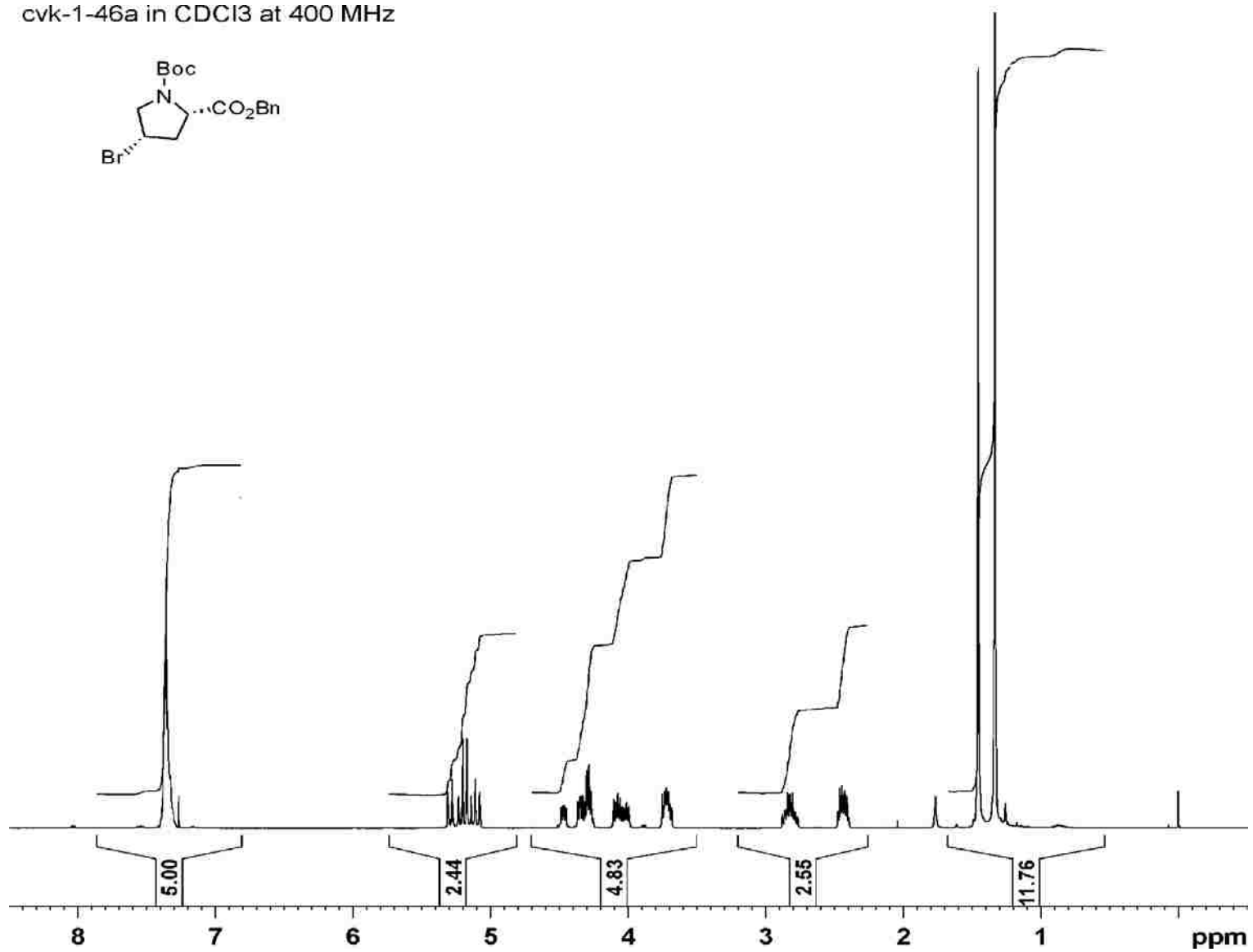
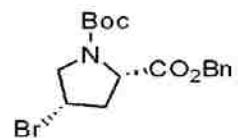
cvk-1-85 in CDCl<sub>3</sub> at 100 MHz





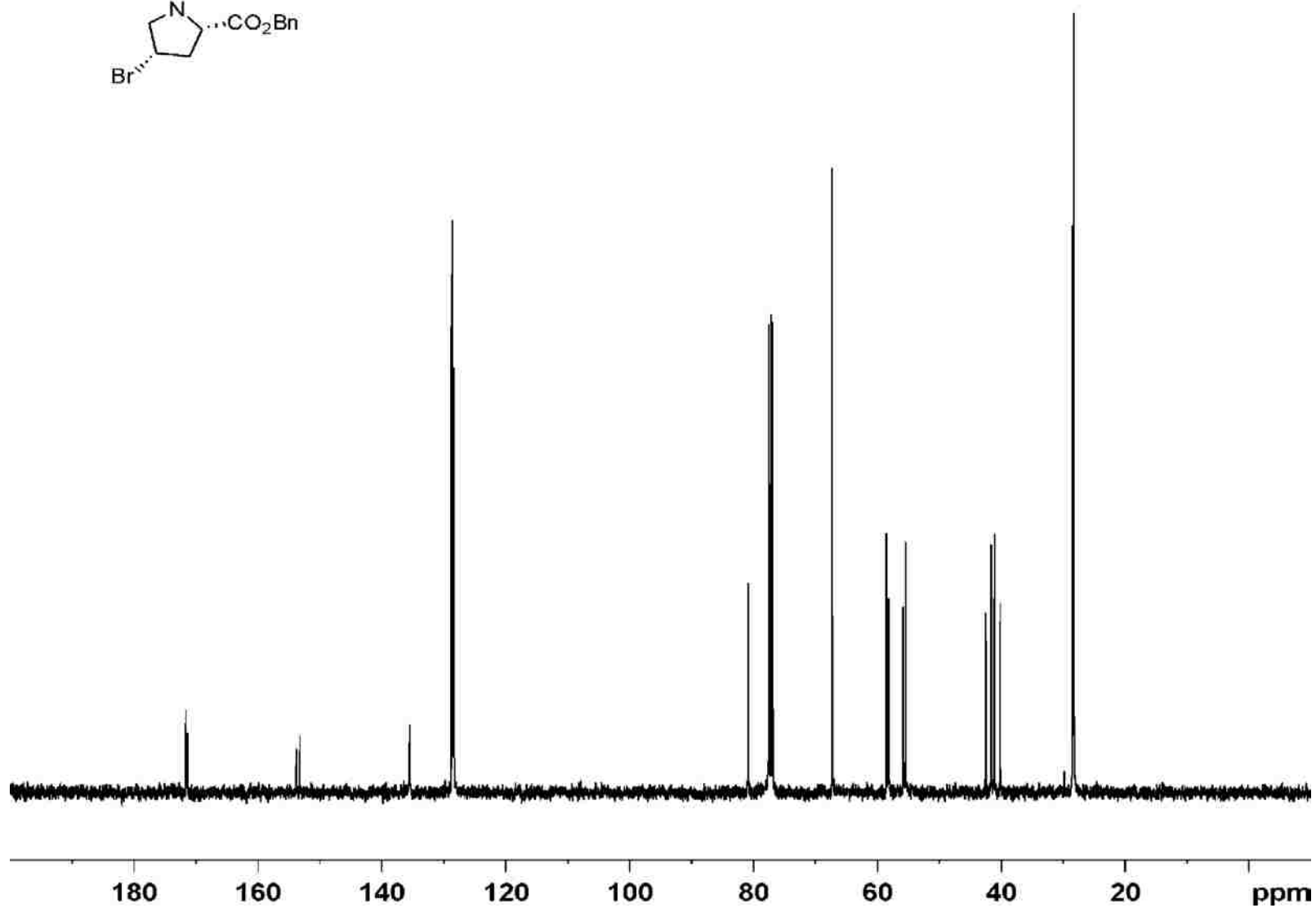
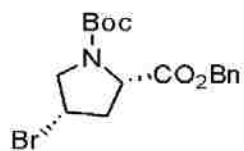
Electrophile **24**

cvk-1-46a in CDCl<sub>3</sub> at 400 MHz



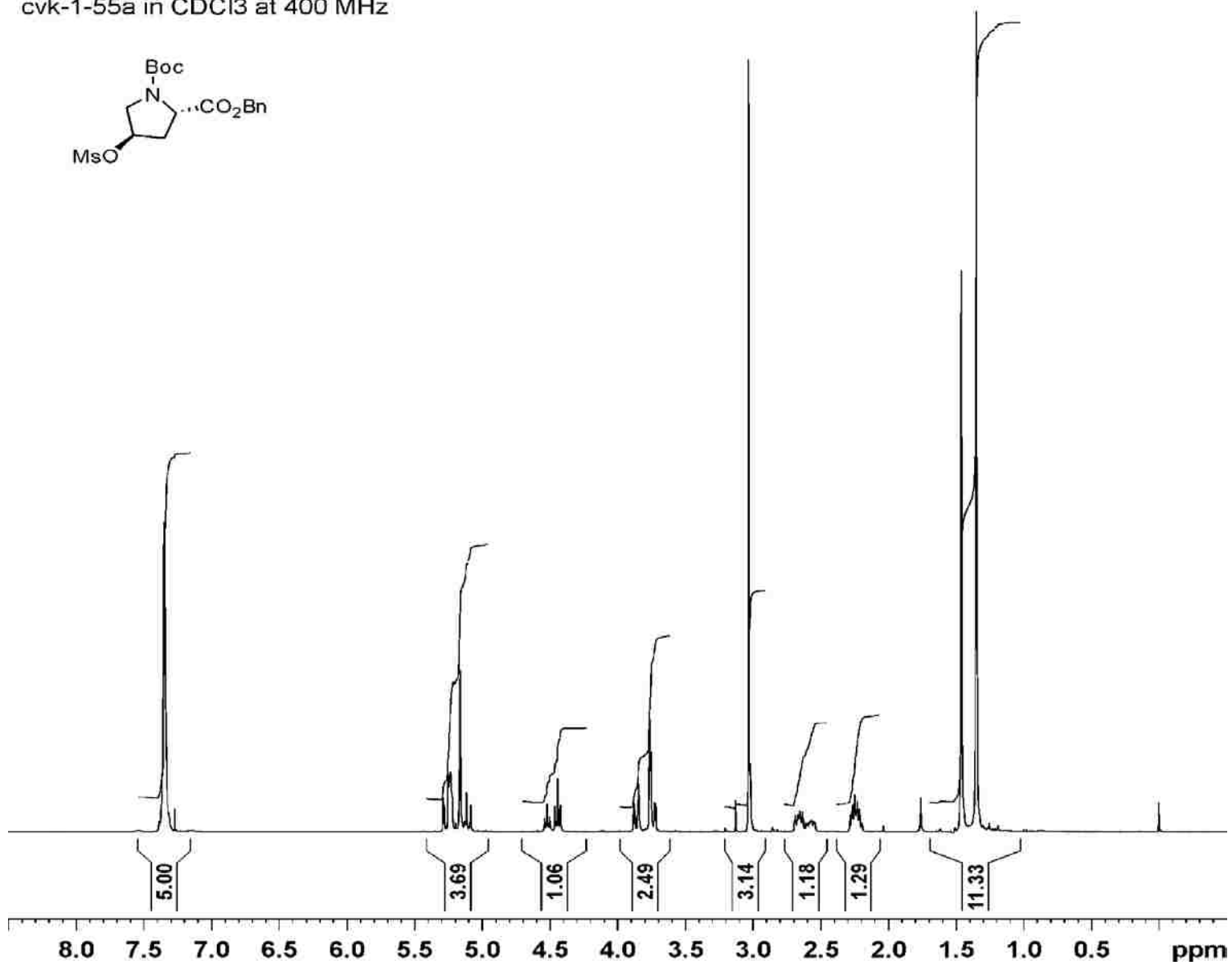
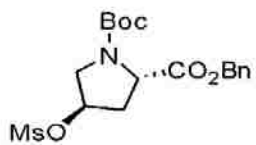
Electrophile **24**

cvk-1-46a in CDCl<sub>3</sub> at 100 MHz



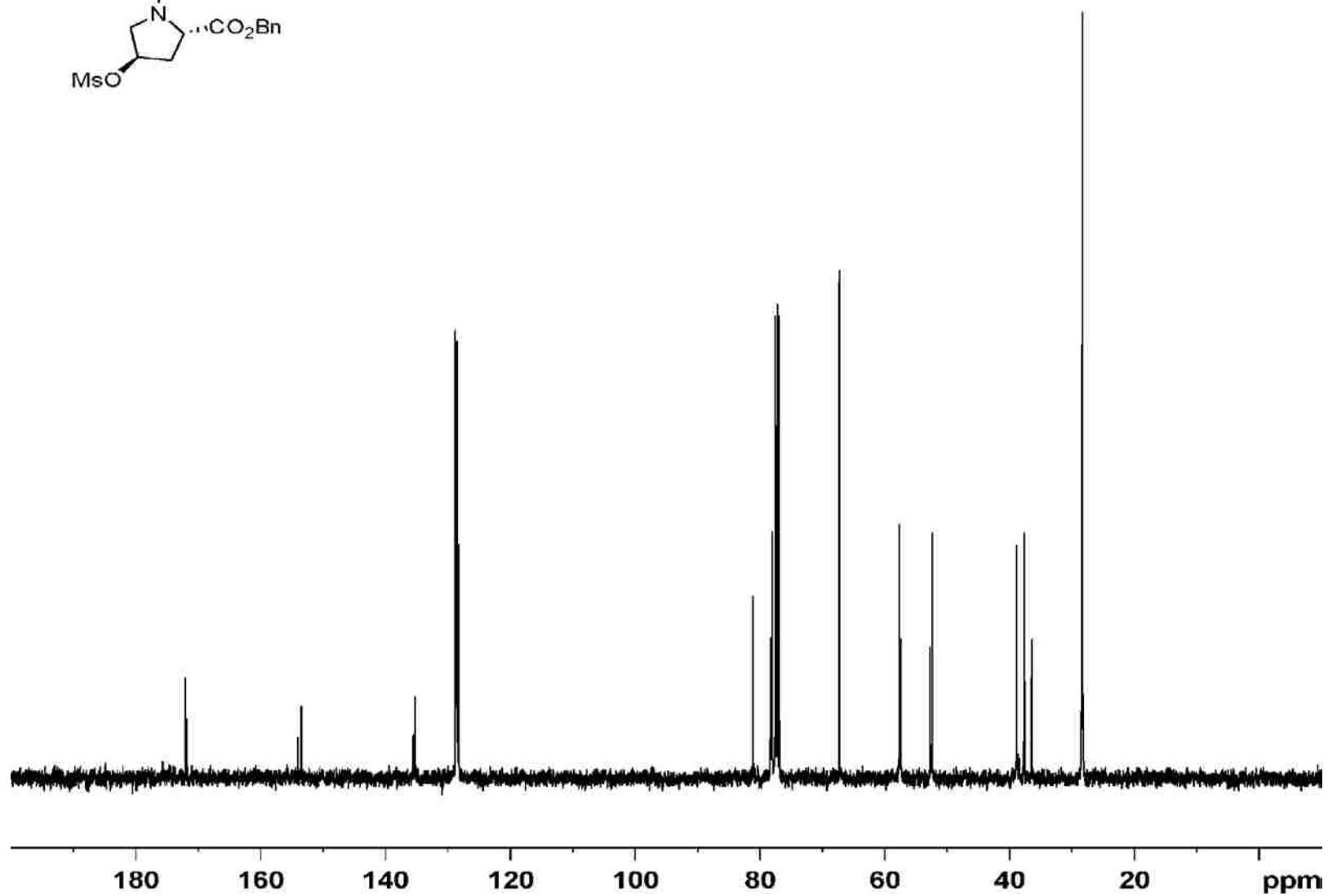
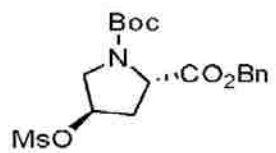
Electrophile 25

cvk-1-55a in CDCl<sub>3</sub> at 400 MHz



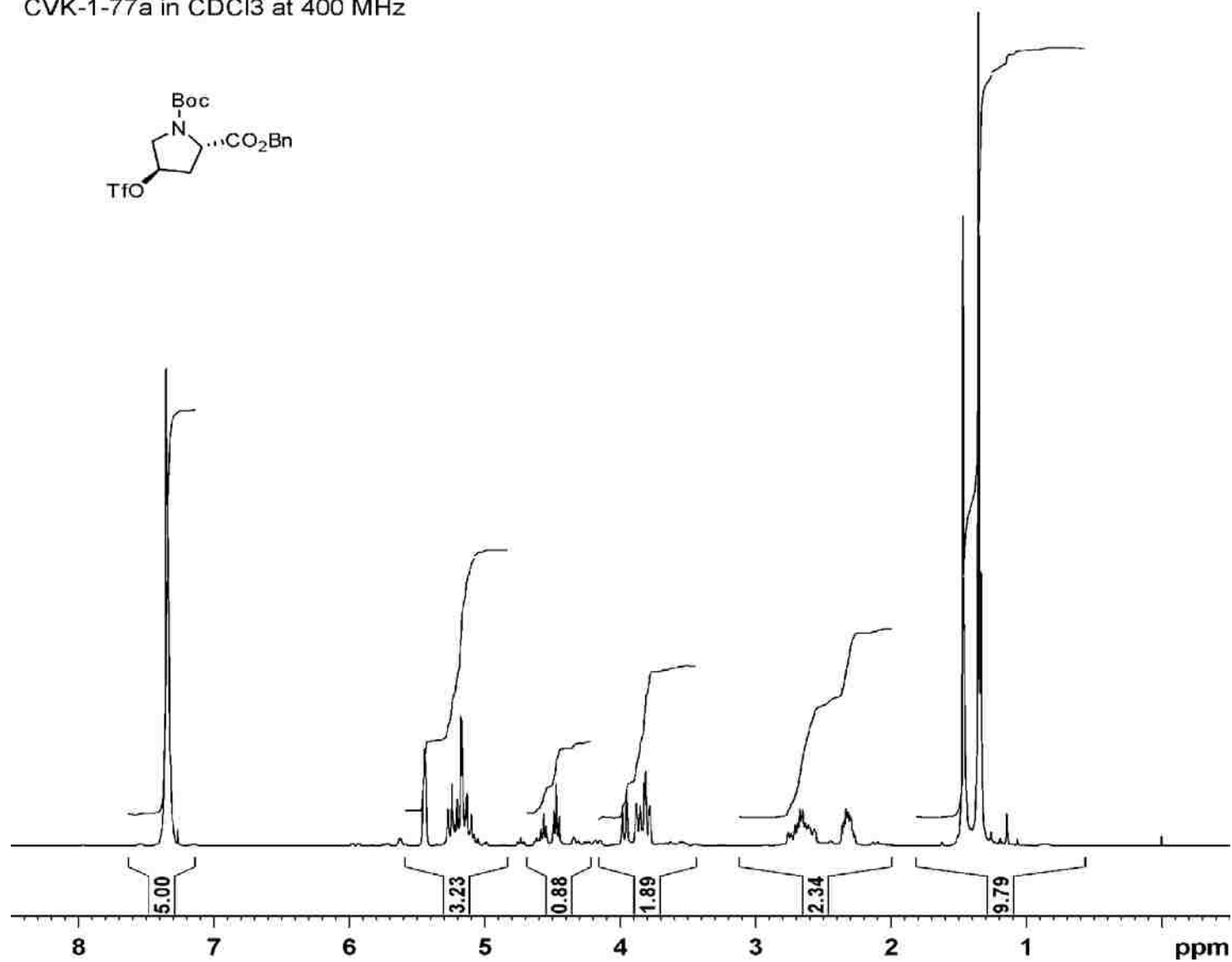
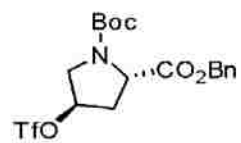
Electrophile **25**

CVK-1-55a in CDCl<sub>3</sub> at 100 MHz



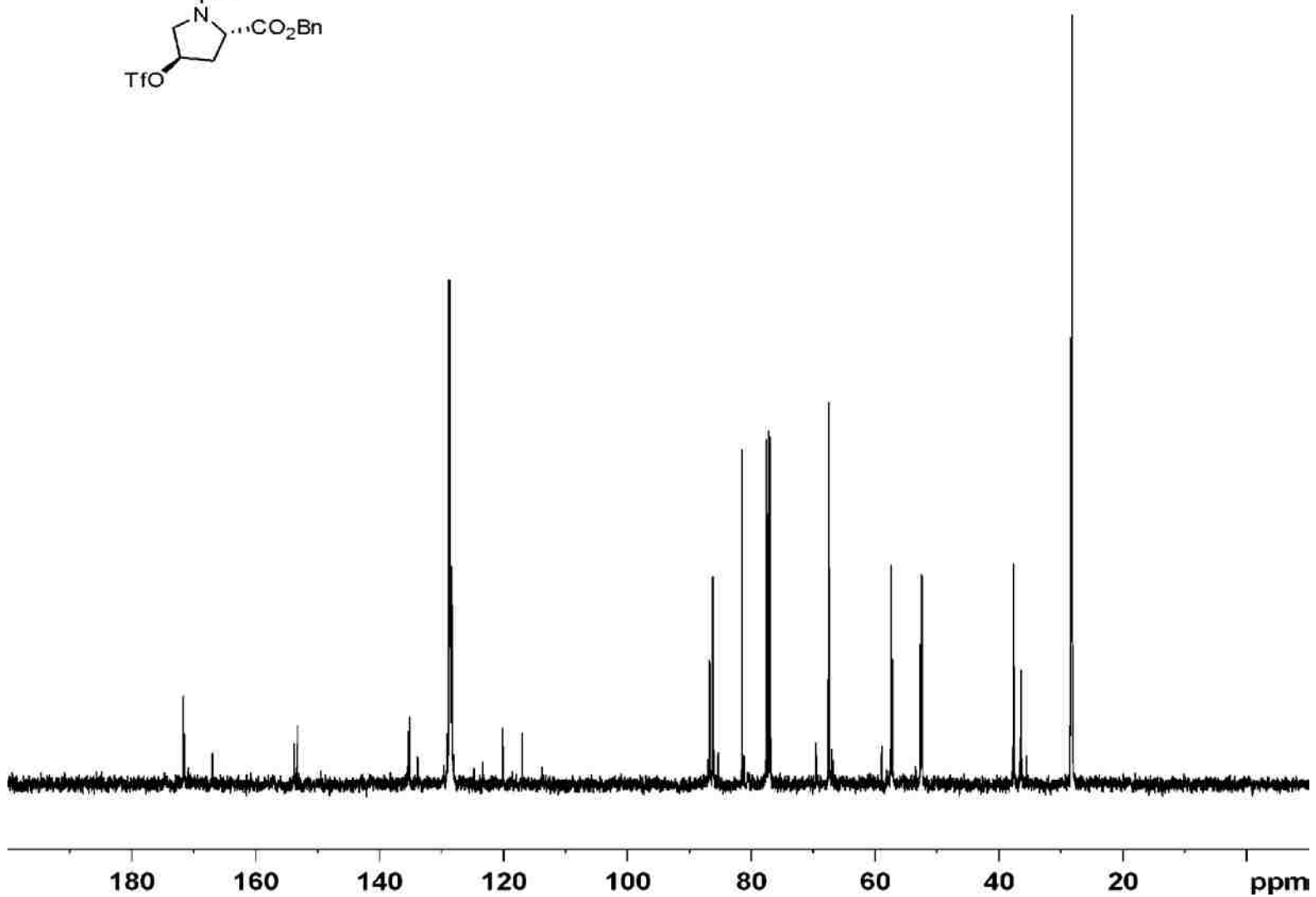
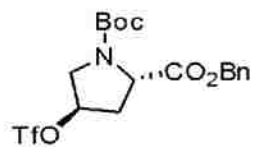
Electrophile **26**

CVK-1-77a in CDCl<sub>3</sub> at 400 MHz



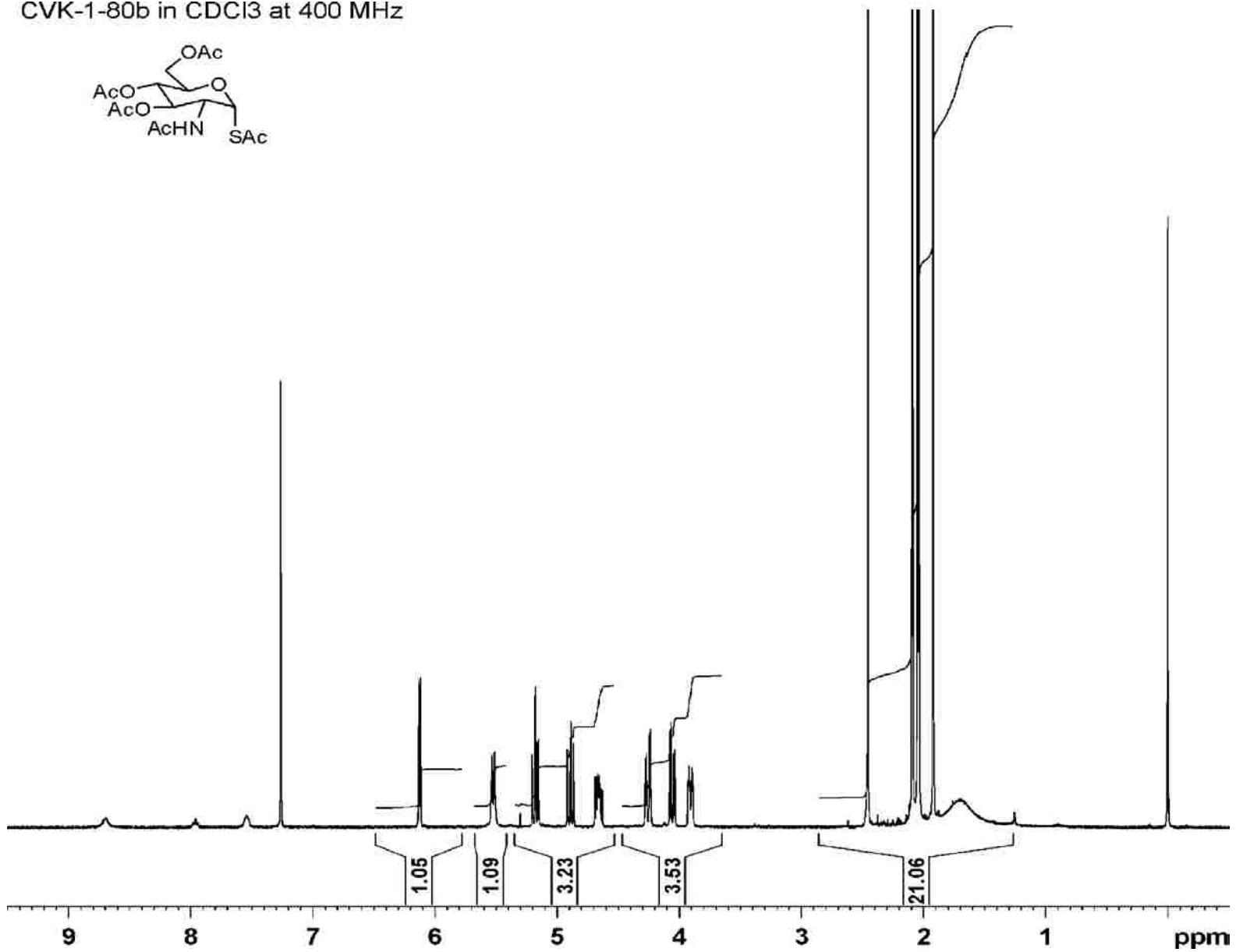
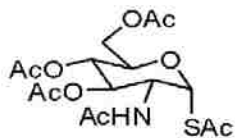
Electrophile **26**

CVK-1-77a in CDCl<sub>3</sub> at 100 MHz



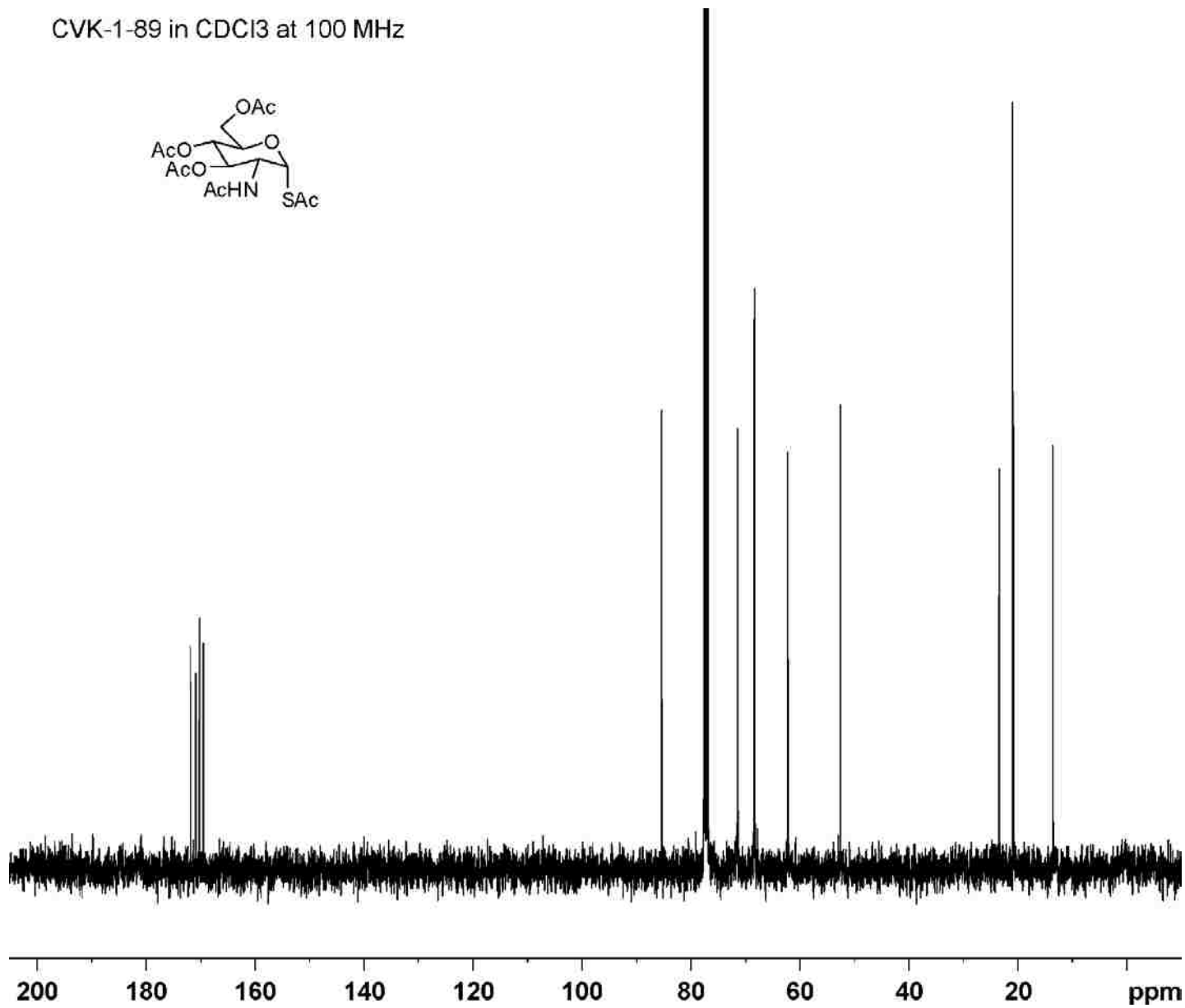
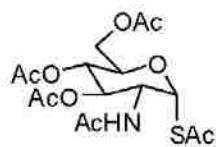
CVK-1-80b in CDCl<sub>3</sub> at 400 MHz

Thioacetate **29**



Thioacetate **29**

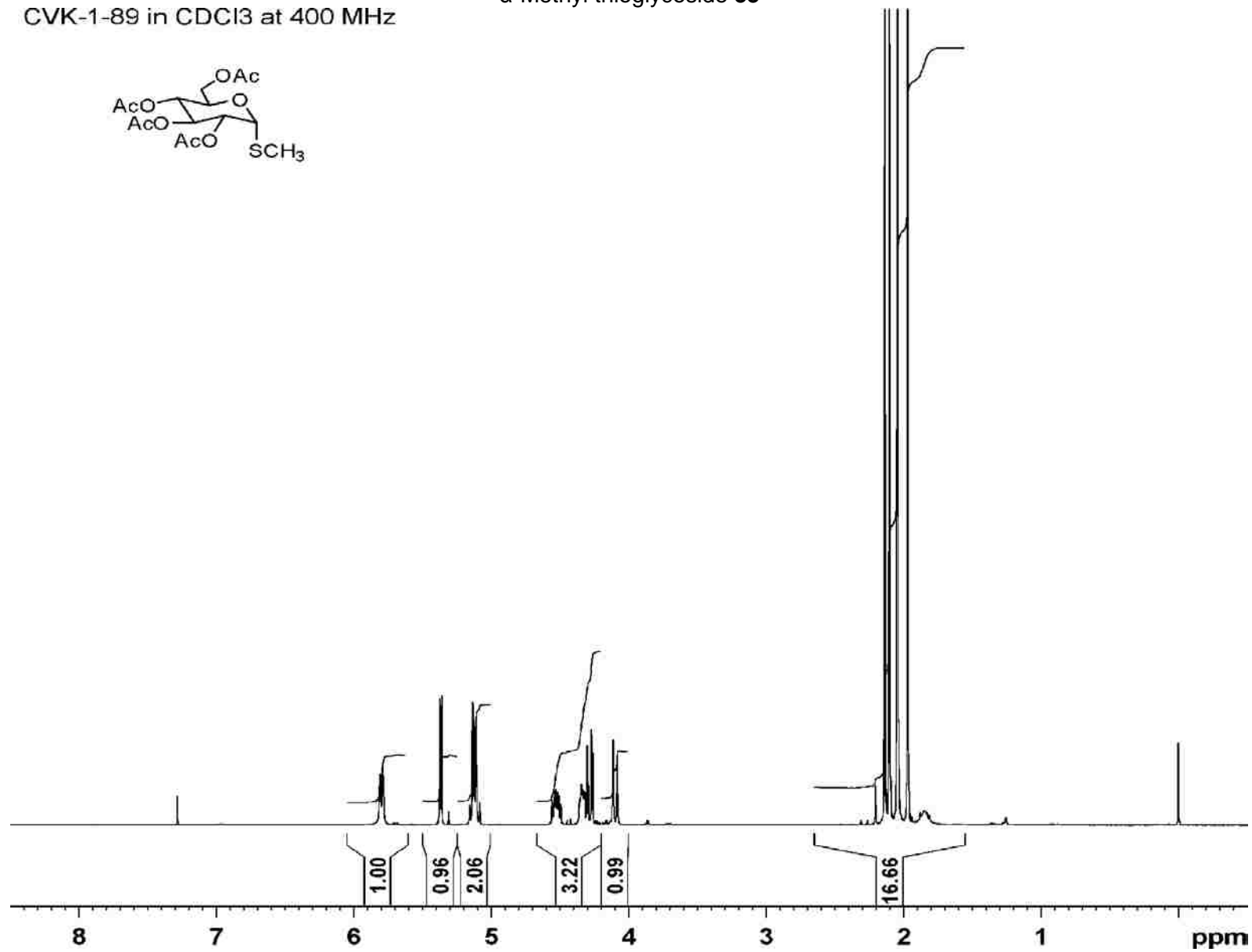
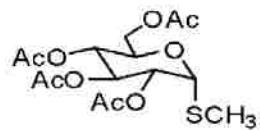
CVK-1-89 in CDCl<sub>3</sub> at 100 MHz





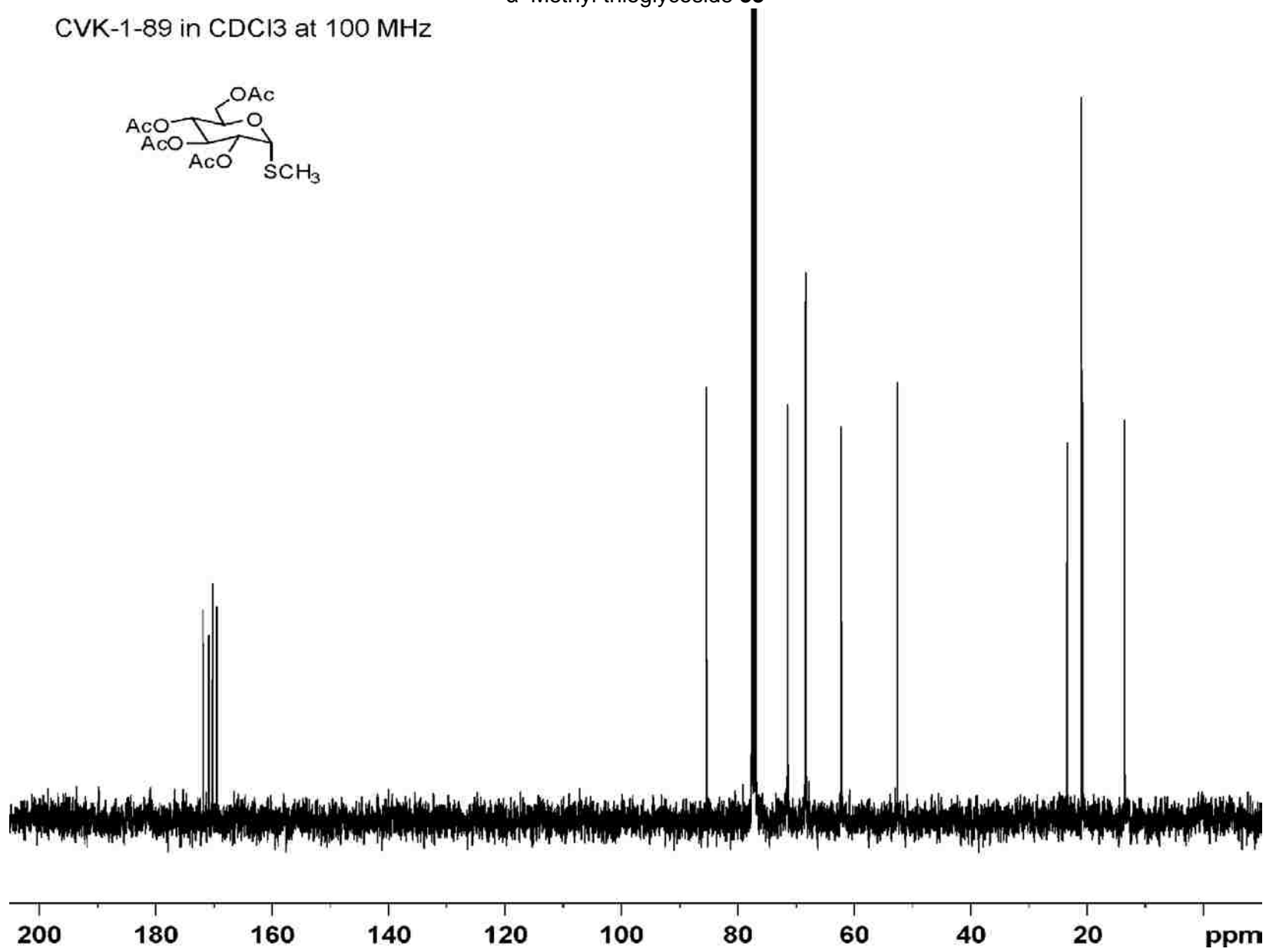
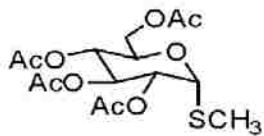
CVK-1-89 in CDCl<sub>3</sub> at 400 MHz

$\alpha$ -Methyl thioglycoside **33**



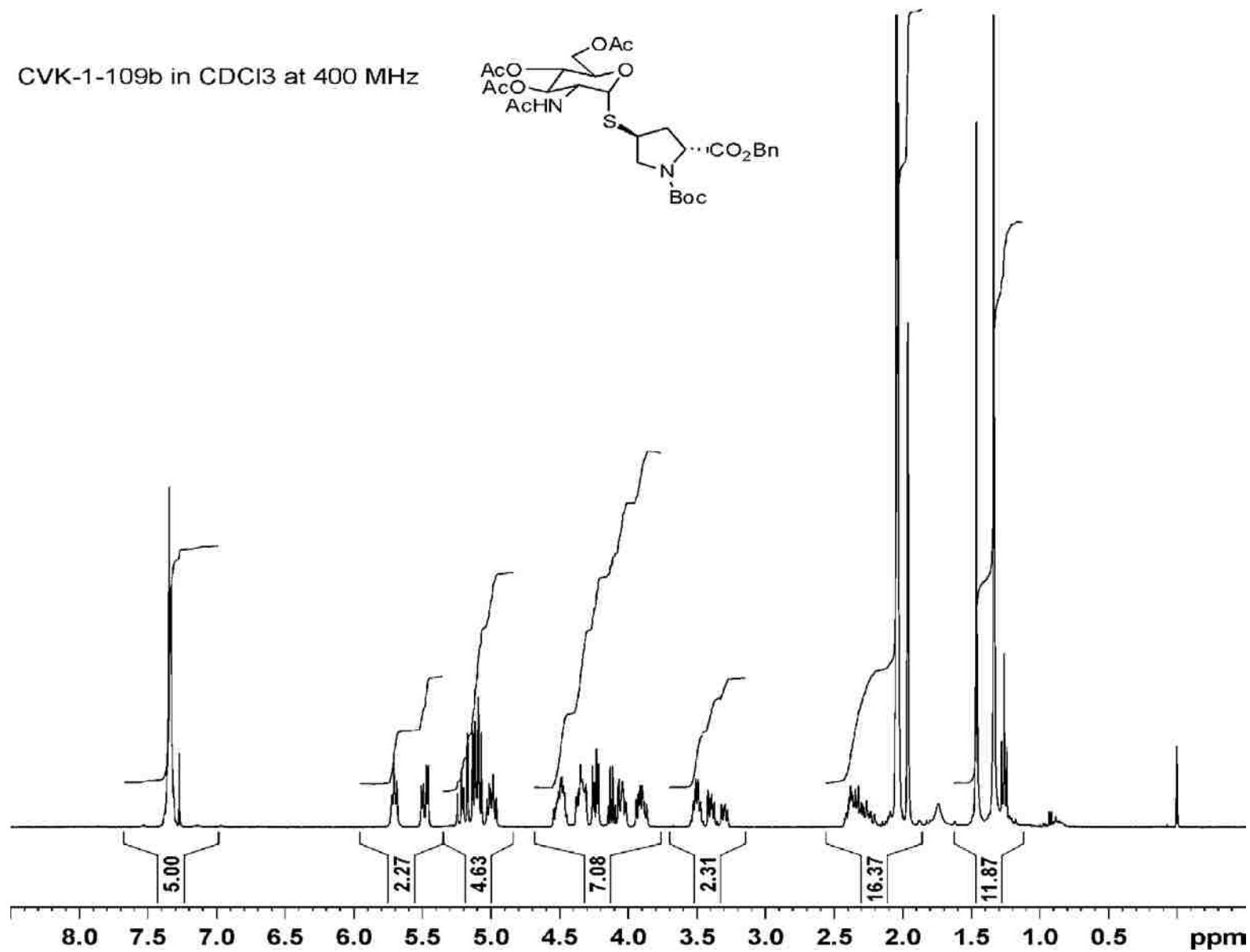
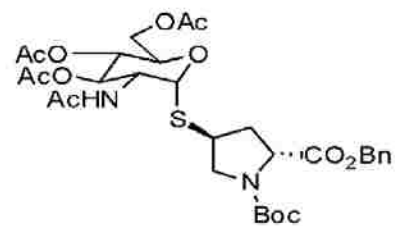
$\alpha$ - Methyl thioglycoside **33**

CVK-1-89 in CDCl<sub>3</sub> at 100 MHz



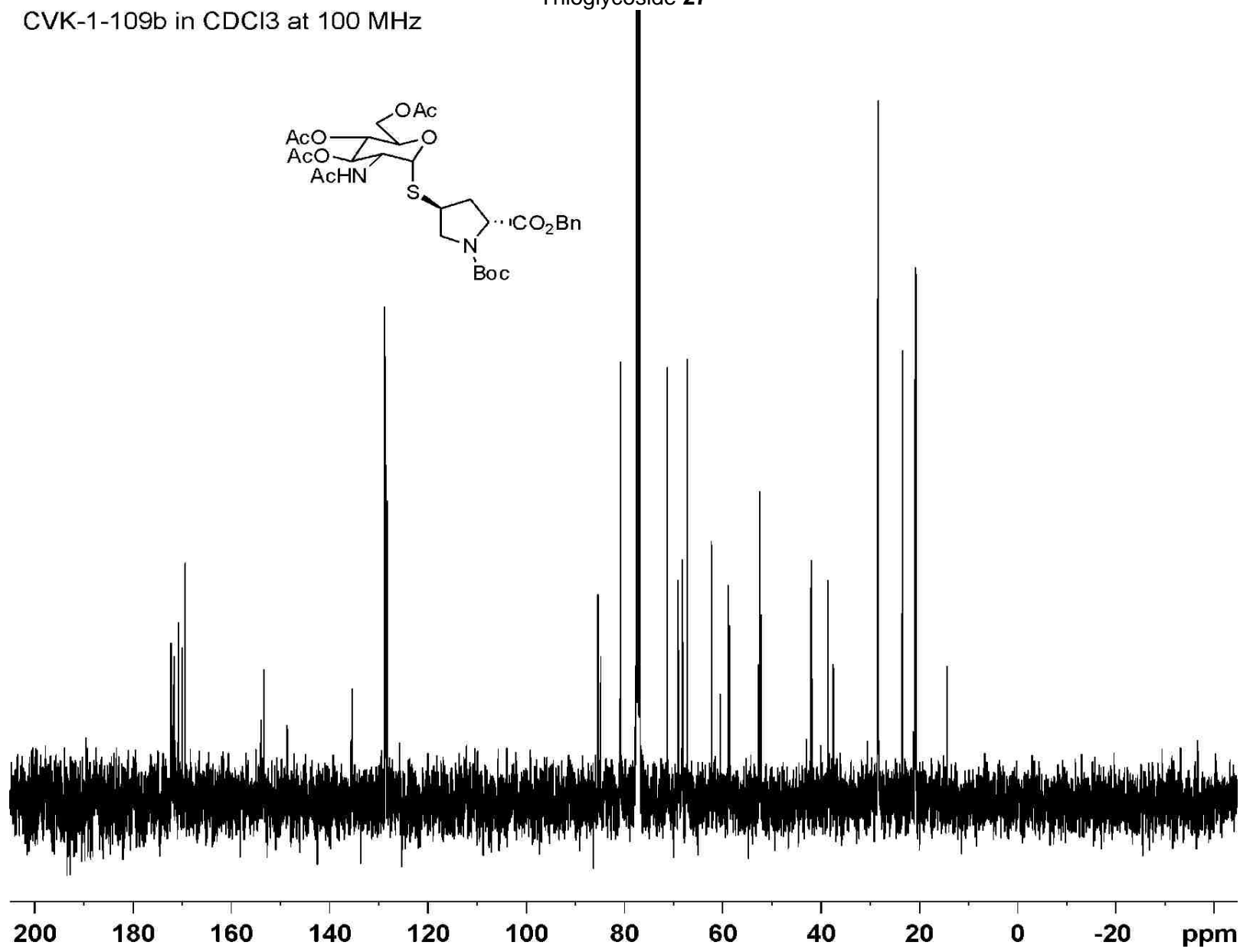
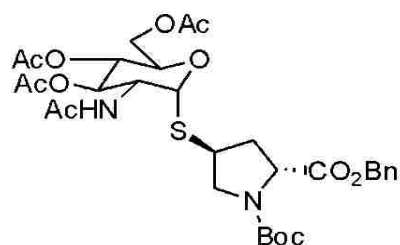
Thioglycoside 27

CVK-1-109b in CDCl<sub>3</sub> at 400 MHz



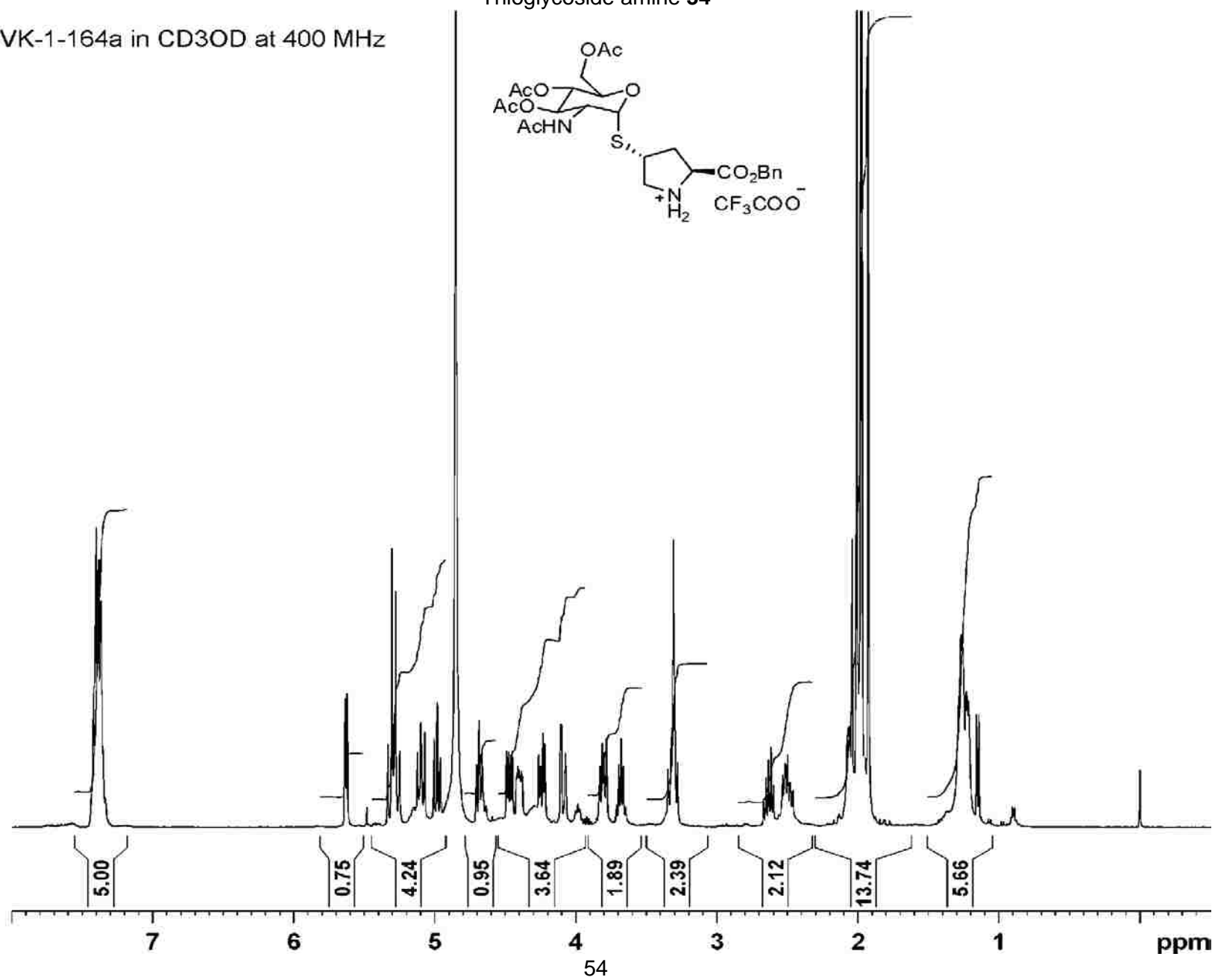
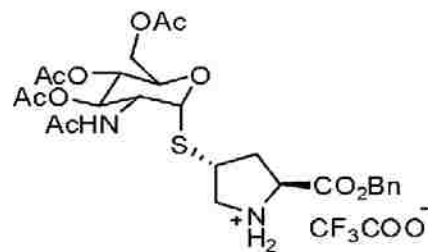
CVK-1-109b in CDCl<sub>3</sub> at 100 MHz

Thioglycoside 27



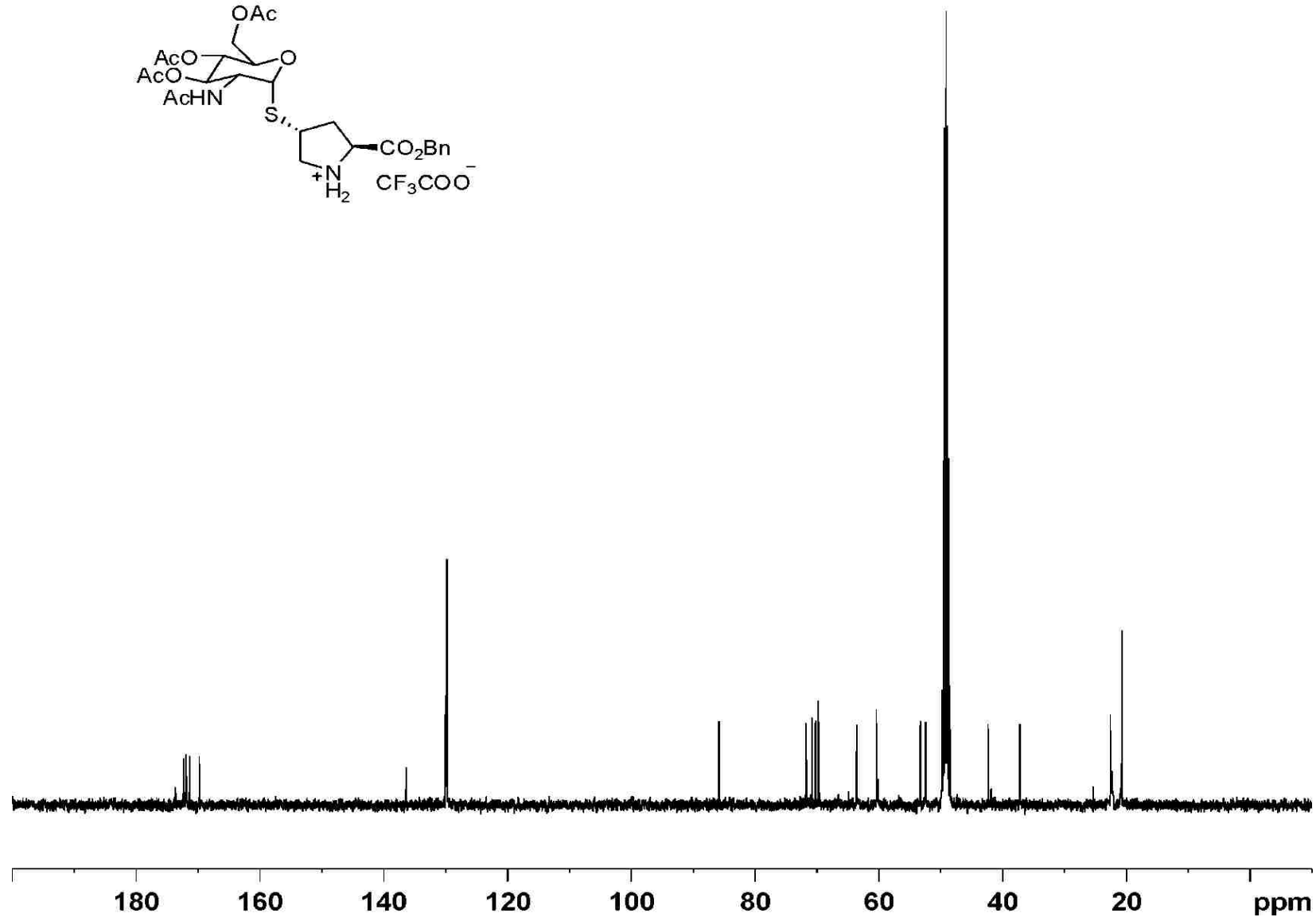
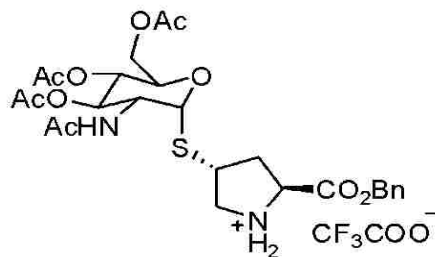
CVK-1-164a in CD3OD at 400 MHz

Thioglycoside amine **34**



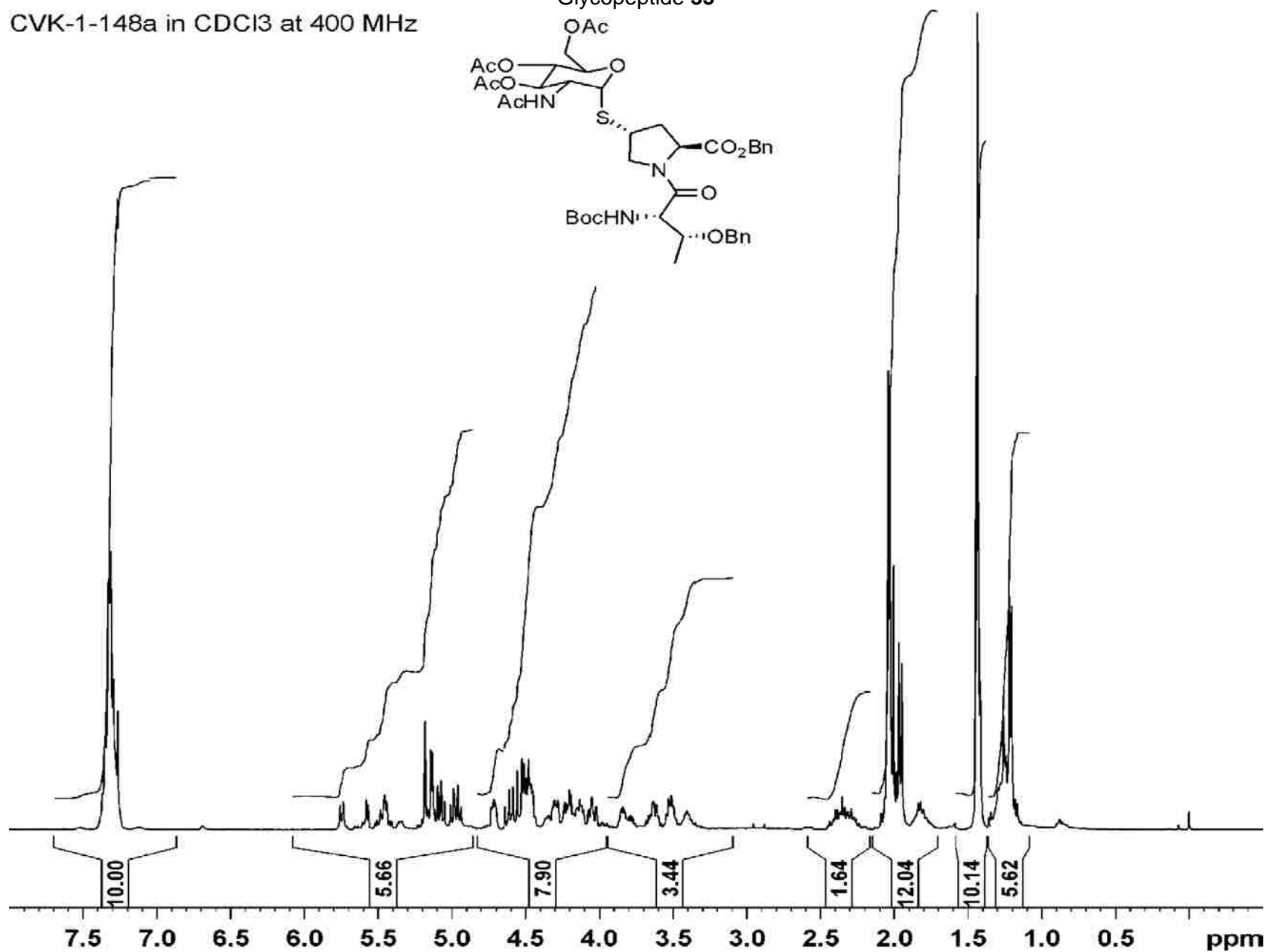
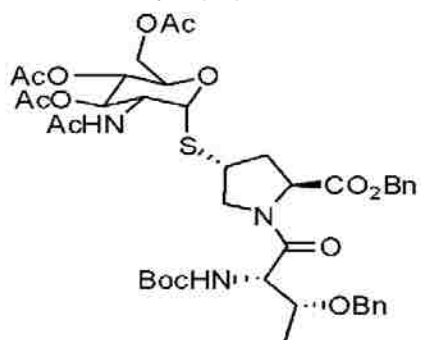
CVK-1-64a in CD3OD at 100 MHz

Thioglycoside amine **34**



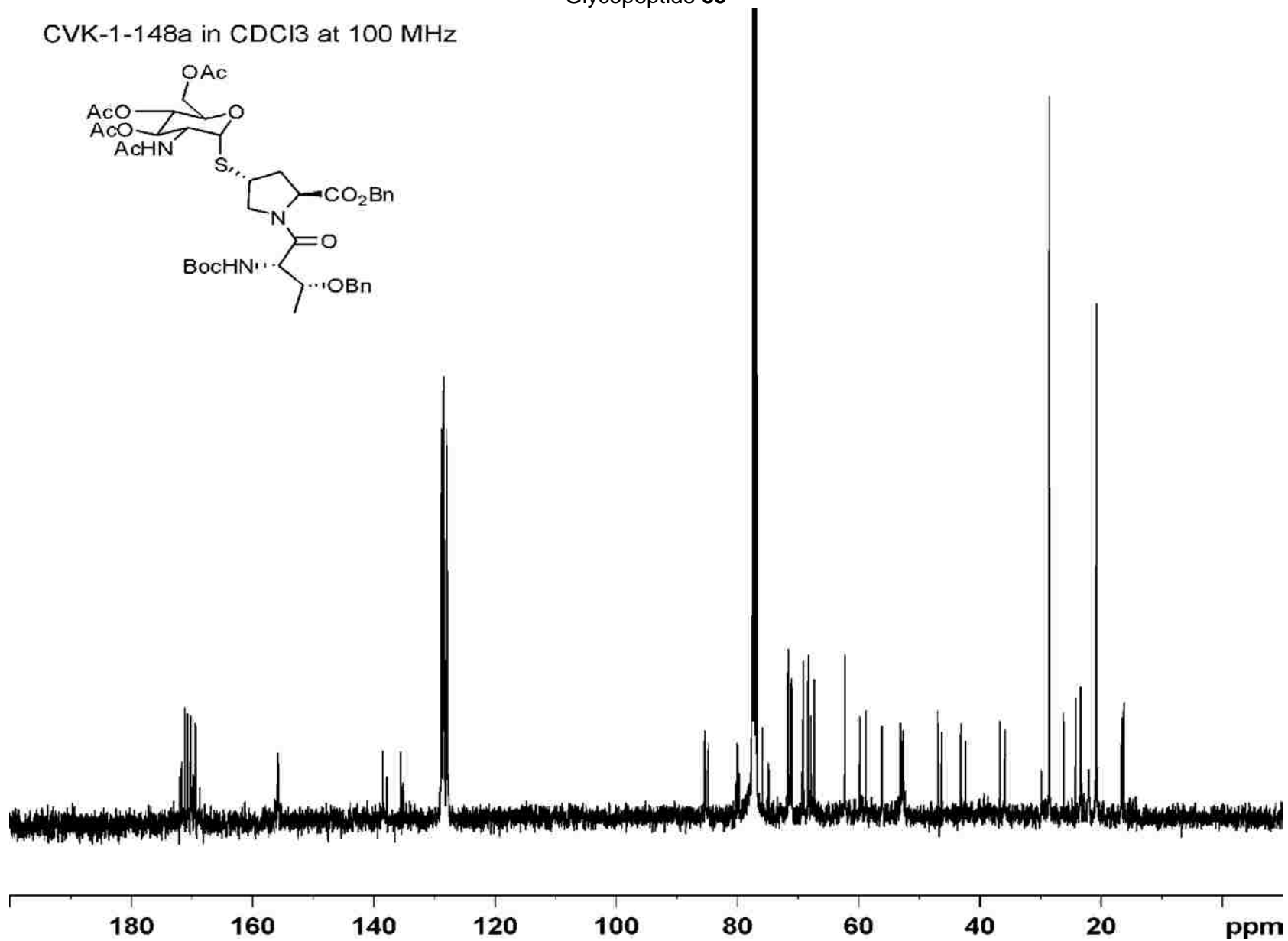
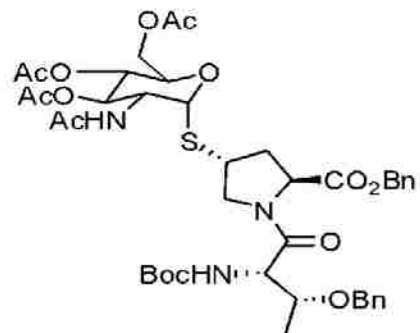
CVK-1-148a in CDCl<sub>3</sub> at 400 MHz

Glycopeptide 35



Glycopeptide 35

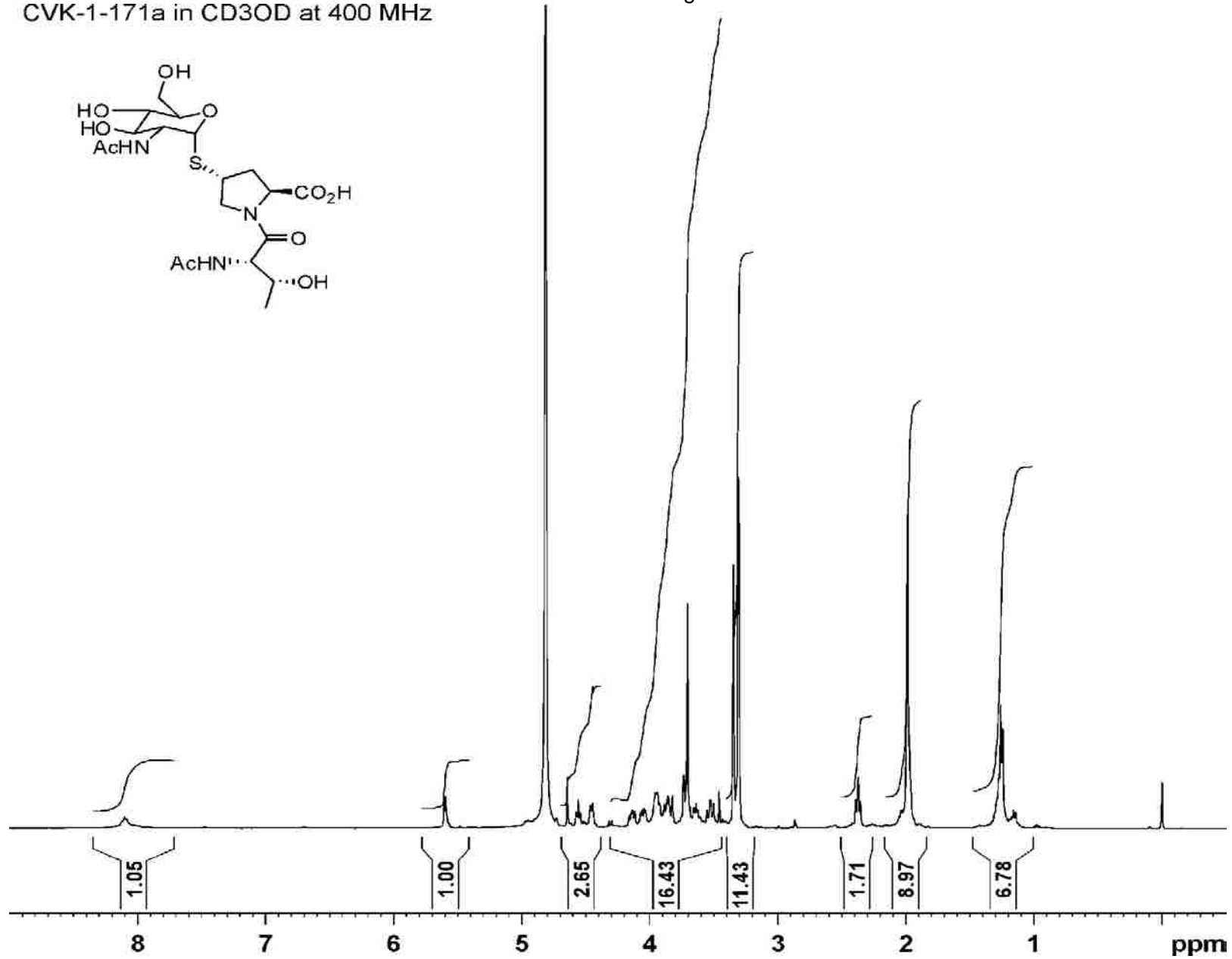
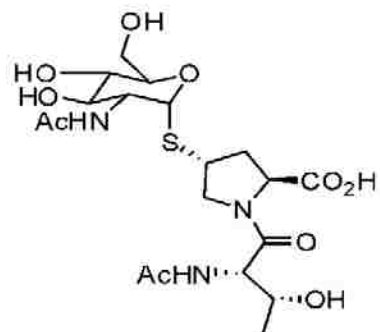
CVK-1-148a in CDCl<sub>3</sub> at 100 MHz





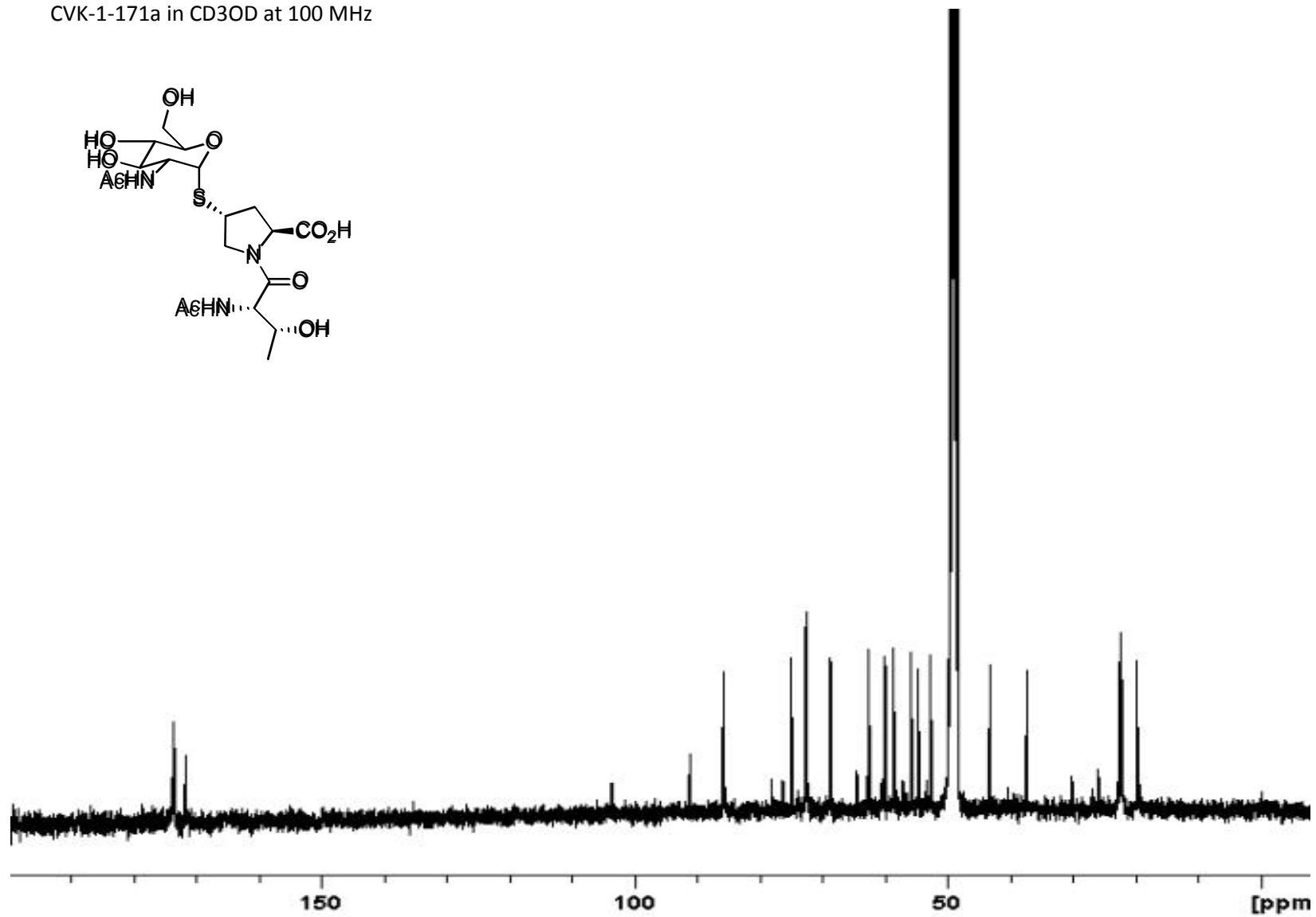
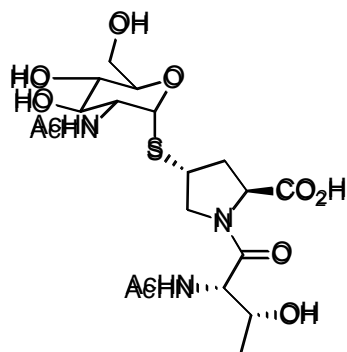
CVK-1-171a in CD3OD at 400 MHz

Bisubstrate Analog 17



# Bisubstrate Analog 17

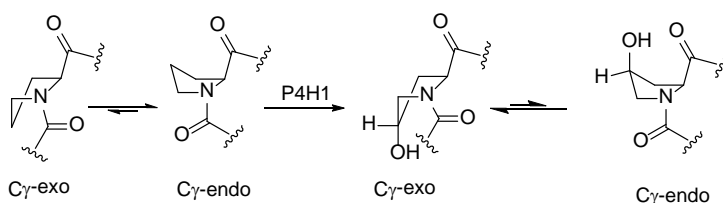
CVK-1-171a in CD3OD at 100 MHz



**CHAPTER 3: THERMODYNAMICS AND KINETICS STUDIES OF CONFORMATIONAL  
CHANGES IN A DIPEPTIDE MODEL SYSTEM FOR THE POST-  
TRANSLATIONAL MODIFICATIONS OF PRO<sup>143</sup> IN SKP1 OF  
*DICTYOSTELIUM***

### 3.1 Conformational Concepts Relevant to Proline-Containing Peptides

Proline plays a unique role in the conformation of peptides and proteins. The pyrrolidine ring of a proline residue exists in predominantly two ring pucker: *C $\gamma$ -exo* (“up”) and *C $\gamma$ -endo* (“down”) (Scheme 3.1).<sup>48</sup> The conformation of the pyrrolidine ring is influenced by substituents on the ring. In unsubstituted proline the *C $\gamma$ -endo* pucker is slightly favored over the *C $\gamma$ -exo* pucker. Electronegative substituents at *C $\gamma$*  with the *R*-configuration stabilize the *C $\gamma$ -exo* pucker. Electronegative substituents at *C $\gamma$*  with the *S*-configuration favor the *C $\gamma$ -endo* pucker.<sup>49</sup>



Scheme 3.1: Pyrrolidine ring conformational changes  
P4H1 = Prolyl-4-hydroxylase 1

These conformational preferences are a result of the gauche effect and related hyperconjugation.<sup>50</sup> The gauche effect is a general phenomenon.<sup>51</sup> Specifically, this becomes manifest when there are two electronegative atoms on the  $\gamma$  and  $\delta$  carbons of the proline residue. The  $\sigma$  orbitals of the  $C\beta$ -H and  $C\delta$ -H bonds (H being a more electropositive substituent) and the  $\sigma^*$  orbital of the  $C\gamma$ -O bond (O being a more electronegative substituent) adopt a torsional angle of  $180^\circ$ . This hyperconjugative interaction between  $\sigma(C\beta$ -H),  $\sigma(C\delta$ -H) and  $\sigma^*(C\gamma$ -O) leads to a preference for the *C $\gamma$ -exo* conformation (Figure 3.1) in *2S,4R*-hydroxyproline (Hyp). The *C $\gamma$ -endo* conformation in *2S,4R*-hydroxyproline does not permit such stabilizing effects. The opposite is true for the *2S,4S*-hydroxyproline where these stabilizing effects are present in the *C $\gamma$ -endo* conformation and absent in the *C $\gamma$ -exo* conformation.

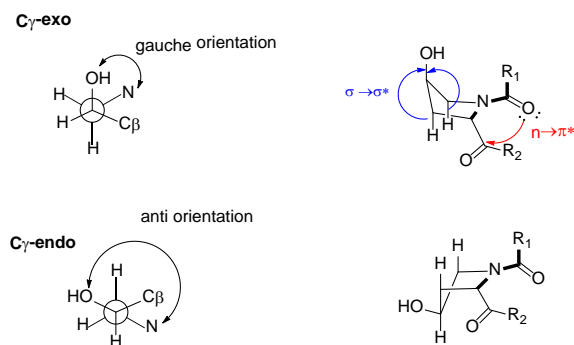
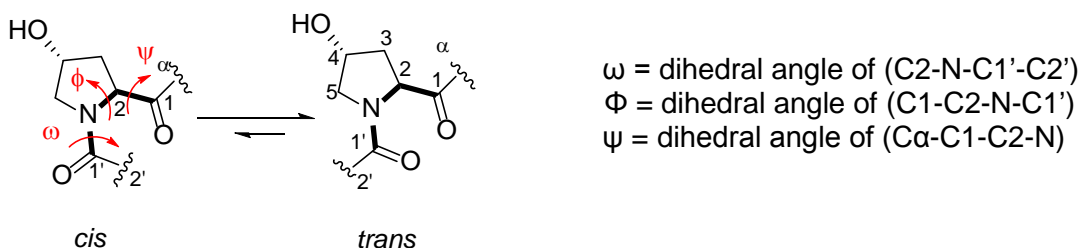


Figure 3.1: Gauche effect and hyperconjugative interactions in Hyp

In nature, planar peptide bonds occur predominantly in the *trans* conformation because the energy difference between the *cis* and *trans* conformations is about 2.6 kcal/mol.<sup>52</sup> However in prolyl peptide bond isomerization this energy difference is reduced to 0.5 kcal/mol<sup>53</sup> (Scheme 3.2). As a result of the side chain being cyclized onto the nitrogen in Pro and Hyp there is restricted rotation about the C $\alpha$ -N bond, confining the  $\Phi$  dihedral angle. This sets Pro and Hyp apart from other amino acids and leads to a reduction in energy difference between *cis* and *trans* conformational isomers rendering them nearly isoenergetic.



Scheme 3.2: *Cis*  $\rightarrow$  *trans* isomerism about the prolyl amide bond in Hyp

Electron withdrawing groups on the pyrrolidine ring of proline residues affect the *cis*  $\rightarrow$  *trans* isomerization through related inductive and stereoelectronic effects.<sup>47</sup> The *trans/cis* ratio for the conformational isomers is correlated with pyrrolidine ring conformation. The  $n \rightarrow \pi^*$  interaction between the oxygen lone pair of the *N*-terminal amide C=O ( $n$ , nonbonding) and the antibonding orbital ( $\pi^*$ ) of the following amide C=O (Figure 3.1) has a major influence on *cis*  $\rightarrow$

*trans* isomerization<sup>54</sup> (Scheme 3.2). The C $\gamma$ -*exo* pucker allows this n $\rightarrow$  $\pi^*$  interaction and stabilizes the *trans* amide bond. Lack of significant n $\rightarrow$  $\pi^*$  interaction in the C $\gamma$ -*endo* conformation leads to a higher population of the *cis* peptide bond when this ring conformation is favored.

### 3.1.1 Prolyl Hydroxylation in Proteins Other than Skp1

One of the most common post-translational modifications of 2S-proline (L-Pro) in humans is hydroxylation by prolyl 4-hydroxylase (P4H) to give 2S,4R-4-hydroxyproline (Hyp). Collagen is the most common protein in animals and has a characteristic triple-helical secondary structure. Hydroxylation of the Pro in collagen (Figure 3.2a) is essential for the stability of the collagen triple helix. Moreover Hyp can also be found in elastin (Figure 3.2b), conotoxins, and argonaute 2 protein which has a collagen-like domain.<sup>11</sup>

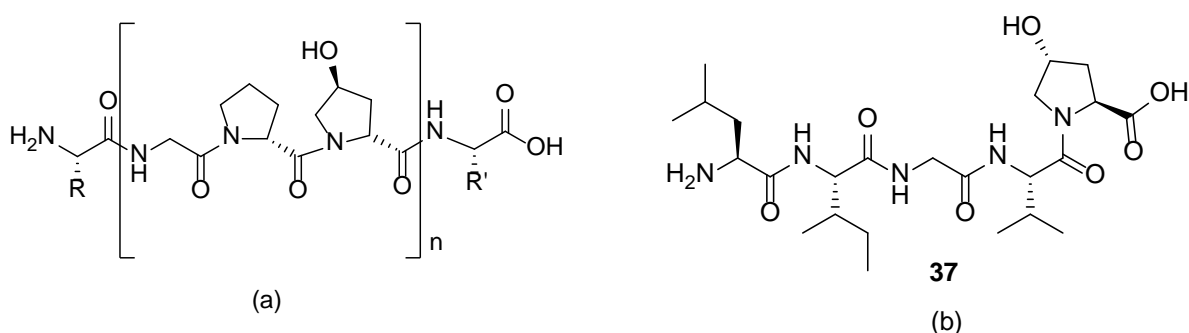
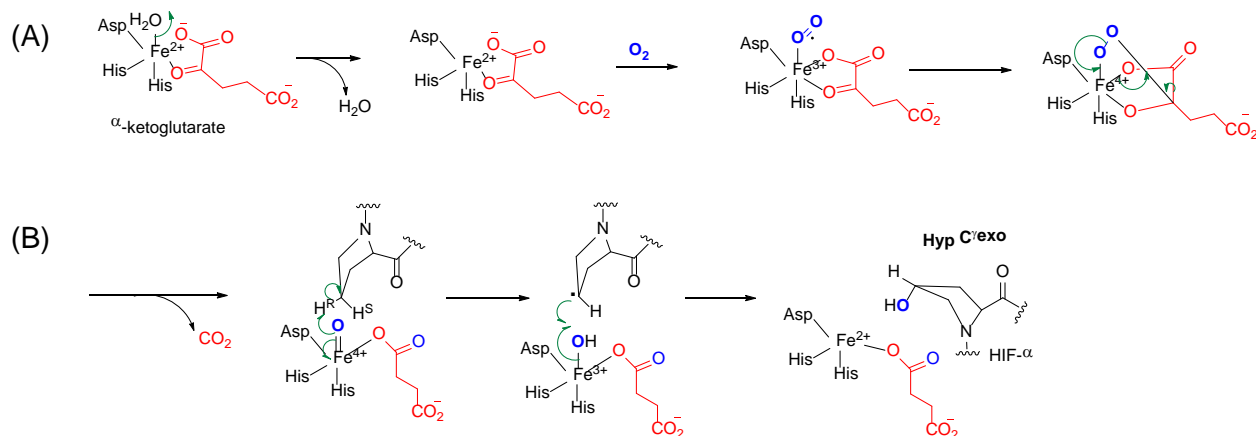


Figure 3.2: (a) Chemical structure of collagen and (b) hydrophobic pentapeptide sequence of elastin (**37**)

Recent studies on the prolyl-4-hydroxylase of collagen by Raines' Group,<sup>11</sup> and the prolyl-4-hydroxylase of the hypoxia-inducible factor- $\alpha$  (HIF $\alpha$ ) by the Schofield Group,<sup>12</sup> have revealed interesting details of the mechanism of hydroxylation. In humans, HIF- $\alpha$  is a key regulator in the cellular response to critically low oxygen concentrations.

Hydroxylation of HIF- $\alpha$  is catalyzed by enzymes containing a prolyl hydroxylase domain (PHD).<sup>11-12</sup> The reaction has two stages (Scheme 3.3): (A) Formation of a highly reactive

Fe(IV)=O species, without the direct participation of the proline; and (B) abstraction of the *pro-R* hydrogen atom from C-4 of the proline residue by the Fe(IV) species. During the hydroxylation of proline,  $\alpha$ -ketoglutarate is oxidized to succinate and one atom of molecular oxygen is incorporated into proline and the other into succinate.<sup>11</sup> After the pyrrolidine ring of Pro<sup>564</sup> in HIF- $\alpha$  is hydroxylated by a *trans*-4-hydroxylase the ring conformation shifts from *C $\gamma$ -endo* to *C $\gamma$ -exo*.



Scheme 3.3: Enzyme-catalyzed hydroxylation of proline. Adapted from Schofield<sup>11</sup>

### 3.1.2 Traditional Views of *Cis*→*Trans* Isomerism and Collagen Stability

Collagen consists of three polypeptide chains that are arranged into a triple helix. These polypeptide chains are composed of repeating units of Gly-Pro-Hyp residues. In 1973 Prockop and coworkers reported that the hydroxyl group of Hyp intensely increased the thermal stability of the collagen triple helix.<sup>55</sup> One explanation for the Hyp-mediated collagen stability was the arrangement of water molecules around the Hyp hydroxyl group to form inter-strand hydrogen bonds.<sup>56</sup> In 1990 Berman *et al.* discovered by X-ray diffraction analysis that water molecules form bridges between the Hyp hydroxyl group and the main chain amide carbonyl groups.<sup>57</sup>

In collagen, 25% of the residues are Pro or Hyp and the stability of the collagen triple helix inevitably depends on the properties of these residues. All peptide bonds in the collagen

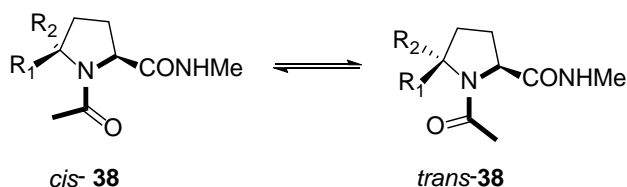
triple helix exist in the *trans* conformation. The *trans/cis* ratio of the prolyl amide bonds in the unfolded state of collagen has a direct influence on the stability of the triple helix.<sup>58</sup> All the *cis* amide bonds have to convert to *trans* amide bonds in the transition from the unfolded state to the folded triple helix. Therefore factors that affect  $K_{vc}$  of a prolyl amide bond influence the stability of collagen.

### 3.2 Recent Advances in Understanding Factors Affecting *Cis*→*Trans* Isomerism in Pro-Containing Peptides

#### 3.2.1 Lubell and coworkers - Steric and Stereochemical Effects of a Substituent at C $\delta$

In 1996 Lubell and coworkers reported steric effects on the amide *cis* → *trans* equilibrium of prolyl peptides.<sup>59</sup> This was explored by synthesizing the two diastereoisomers of *N*-acetyl-5-*tert*-butylproline methyl amide (Table 3.1) and analyzing the relative populations of *cis* and *trans* isomers and the energy barriers to amide isomerization.

Table 3.1: Energy barriers for amide bond isomerization of *N*-Acetyl-5-*tert*-butylproline methyl amide derivatives at 25 °C.



Proline derivative	$\Delta G^\circ$ (kcal/mol)
<b>38a</b> = R <sub>1</sub> , R <sub>2</sub> = H	0.57
<b>38b</b> = R <sub>1</sub> = <sup>t</sup> Bu, R <sub>2</sub> = H	0.03
<b>38c</b> = R <sub>1</sub> = H, R <sub>2</sub> = <sup>t</sup> Bu	0.38

The kinetics and thermodynamics data showed that the steric bulk and the stereochemistry at the proline C $\delta$  influence the amide geometry. Their results indicated that the C $\delta$  substituents decrease the barrier for amide isomerization and thereby significantly increase the *cis* isomer population in water because the C $\delta$  *tert*-butyl substituent skews the amide bond

way from planarity such that a twisted amide conformation appears to be in lower energy and makes it easier to rotate around.

### 3.2.2 Raines and coworkers – Inductive Effect of a Substituent at C $\gamma$

In 1996 Raines and coworkers put forward a new hypothesis that electronegative substituents stabilize the collagen triple helix via an inductive effect.<sup>60</sup> Their studies on Ac-Pro-OMe, AcHypOMe and Ac-(4*R*)-4-fluoroproline-OMe (AcFlpOMe) (Figure 3.3) showed that the ring nitrogen becomes increasingly pyramidalized in the series due to the increasing electron-withdrawing ability of oxygen and fluorine. An increase in pyramidalization also increases the  $sp^3$  character of the proline nitrogen and thereby the AcFlpOMe prolyl nitrogen has more  $sp^3$  character than that in the Hyp derivative and the amide bond isomerization rate is greater for AcFlpOMe. These results implied that the inductive effect was responsible for higher amide C=O bond order and lower C-N amide bond order.

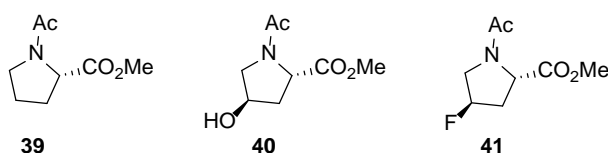


Figure 3.3: Proline derivatives

In 1998 they reported that a synthetic (Pro-Flp-Gly)<sub>10</sub> collagen mimic formed a triple helix and that the Flp residue enhanced its stability relative to Hyp in the analogous oligopeptide.<sup>61</sup> Based on their experimental results looking at the effect of temperature on conformational stability, they showed that (Pro-Flp-Gly)<sub>10</sub> required higher temperatures to unfold the triple helix (Figure 3.4).



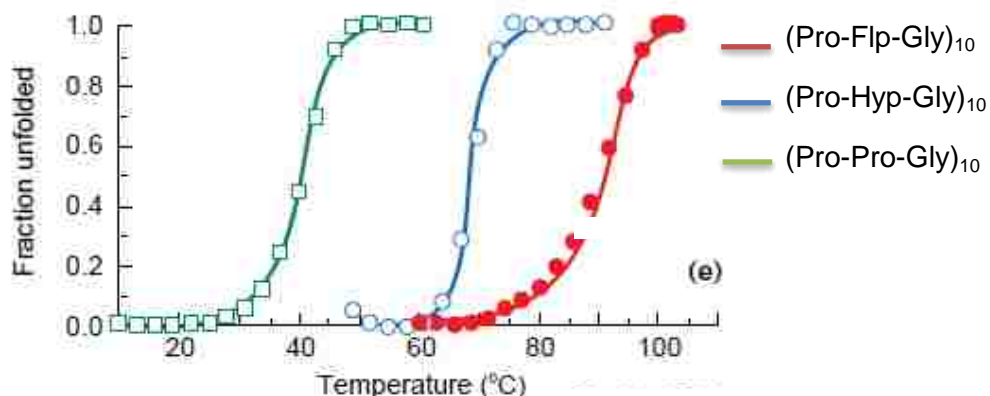


Figure 3.4: Effect of temperature on the conformational stability of (Pro-Flp-Gly)<sub>10</sub>, (Pro-Hyp-Gly)<sub>10</sub> and (Pro-Pro-Gly)<sub>10</sub> triple helices. Copyright 1999, Elsevier, reprinted with the permission

They explained the hyperstability of this collagen mimic based on three factors.

(1) Preorganization of the prolyl peptide bond conformation:

The inductive effect of the hydroxyl group of (4*R*)-hydroxyproline residues increases the pyramidalization of the pyrrolidine nitrogen and thereby increases the population of *trans* conformer which is lower in energy than the *cis* conformer. This hypothesis was supported by the crystal structures of AcProOMe having a *cis* amide bond conformation and those of AcHypOMe and AcFlpOMe having a *trans* amide bond conformation.<sup>61</sup> Moreover, the values of  $K_{vc}$  (measured directly by NMR spectroscopy) increased in the order AcProOMe < AcHypOMe < AcFlpOMe at 37 °C in deuterated water or dioxane.<sup>62</sup>

(2) Dipole-dipole interactions governed by a gauche effect: Fluorine is the most electro-negative element and installing fluorine in the C $\gamma$  position of proline will have a stronger inductive effect than the hydroxyl group in hydroxyproline. The dipole of the C $\gamma$ -F bond of the Flp residue is stronger than that of the C $\gamma$ -O bond of Hyp and this leads to stronger dipole-dipole interactions.<sup>63</sup> This will increase the stabilization of the C $\gamma$ -*endo* pucker due to a strong gauche effect.

(3) Pro C=O---HNGLy hydrogen bond strength.

In collagen, hydrogen bonds are associated with oxygen of the Pro and the NH proton of Gly (Figure 3.5). Comparing the oligopeptides containing Hyp and Flp residues, hydrogen bond strength is higher in the triple helix in the presence of the higher inductive effect of fluorine. This increases the acidity of the NHGly proton and increases the H-bond strength in the triple helix.

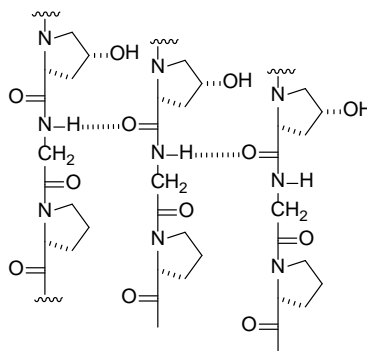


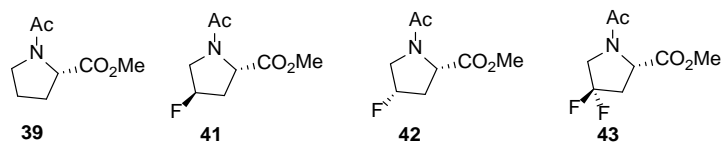
Figure 3.5: Hydrogen bonding in triple helical collagen

### 3.2.3 Moroder *et al.* – More Evidence for the Inductive Effect and the Importance of Stereochemistry at C $\gamma$

In 2001 Moroder *et al.* reported the thermodynamics and kinetics of the *cis*  $\rightarrow$  *trans* isomerization of the amide bond in Ac-Pro-OMe, Ac-Flp-OMe, Ac-flp-OMe, and Ac-(4)-F<sub>2</sub>Pro-OMe proline derivatives (Table 3.2).<sup>64</sup>

Their observation was also that the fluorine substituents accelerate the *cis*  $\rightarrow$  *trans* isomerization. With the difluoro derivative the equilibrium is shifted further towards the *trans* isomer than in the monofluorinated derivative. The *cis*  $\rightarrow$  *trans* equilibrium constant ( $K_{tc}$ ) for Flp was different to flp due to the different pucker preferences of the pyrrolidine ring. In the difluoro derivative the gauche effect of both fluorine atoms counteract each other resulting in an C $\gamma$  *endo* pucker. The energy difference between the *cis* and *trans* isomers is significantly higher in the *exo* conformation than the *endo* conformation. This explains their experimental observation of a smaller free energy difference for the flp derivative (Table 3.2).

Table 3.2: Thermodynamics parameters for compounds **39** and **41-43**



Entry	Proline derivative	$\Delta H^\circ$ (kJ mol <sup>-1</sup> )	$\Delta S^\circ$ (J mol <sup>-1</sup> K <sup>-1</sup> )	$\Delta G^\circ, 300K$ (kcal mol <sup>-1</sup> )
1	<b>39</b>	-5.04	-3.82	-0.93
2	<b>41</b>	-7.73	-9.81	-1.14
3	<b>42</b>	-3.04	-2.47	-0.55
4	<b>43</b>	-5.21	-7.32	-0.72

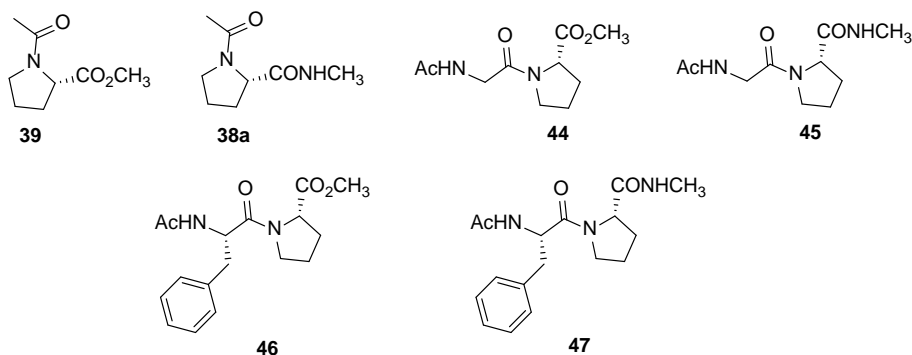
### 3.2.4. Taylor *et al.* – Factors Affecting Conformation in Proline and Hydroxylated Prolines

In 2003 Taylor *et al.* reported six proline derivatives (Table 3.3) to investigate the various factors affecting the *cis* → *trans* equilibrium. They compared *C*-terminal esters with amides vis-à-vis the position of the isomerization equilibrium. Replacement of the methyl ester with a methyl amide significantly dropped the magnitude of the  $K_{i/c}$  (Entries 1-4, Table 3.3). This is due to the strong  $n \rightarrow \pi^*$  interaction in the ester relative to the amide as the ester carbonyl carbon is more electron deficient.

They also studied the effect of steric bulk of the *N*-terminal residue on the prolyl peptide bond conformation. This was demonstrated upon adding a Gly residue *N*-terminal to the Pro residue (**44** and **45**, Table 3.3) and comparing  $K_{i/c}$  with the *N*-acetyl proline derivatives (**39** and **38a**, Table 3.3). Their results showed that increasing the steric bulk of the *N*-terminal residue favors the *trans* conformation of the prolyl peptide bond.<sup>65</sup>

The dipeptide containing a Phe-Pro amide bond showed a reduction in the magnitude of  $K_{i/c}$  compared to peptides **44** and **45**. This is due to the nonbonding hydrophobic interaction of pi-electrons of the aromatic ring with the proline. The Ar-Pro interaction stabilizes the *cis* conformation and brings it closer in energy to its *trans* counterpart.<sup>65</sup>

Table 3.3: Thermodynamics parameters for compounds **38a**, **39** and **44-47**



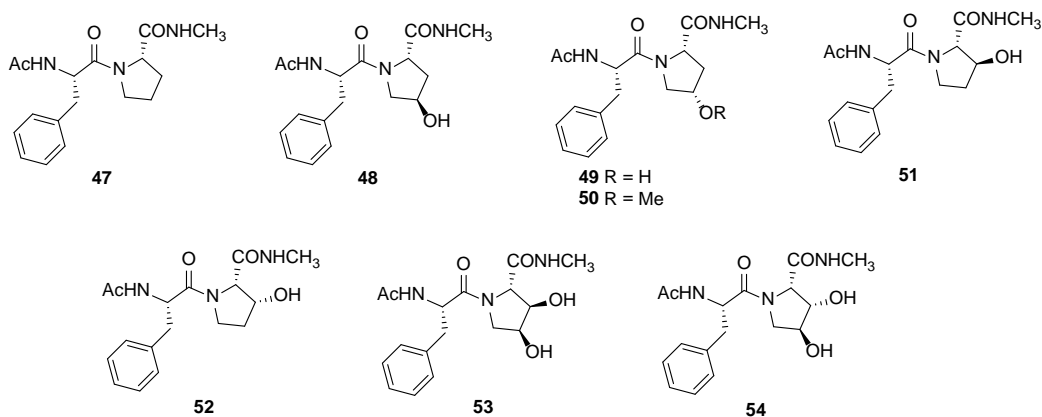
Entry	Proline derivative	$K_{t/c}$ D <sub>2</sub> O, 298 K	$\Delta H$ (kcal mol <sup>-1</sup> )	$\Delta S$ (cal mol <sup>-1</sup> K <sup>-1</sup> )	$\Delta G^\circ$ (kcal mol <sup>-1</sup> K <sup>-1</sup> )
1	<b>39</b>	5.40	-1.17	-0.62	-0.99
2	<b>38a</b>	2.56	-0.97	-1.34	-0.57
3	<b>44</b>	7.20	-1.27	-0.25	-1.20
4	<b>45</b>	5.54	-0.89	0.41	-1.01
5	<b>46</b>	4.20	-0.25	1.96	-0.83
6	<b>47</b>	2.10	0.25	2.29	-0.43

In 2005, a report by Taylor *et al.* demonstrated that the regiochemistry, stereochemistry and degree of hydroxylation of a proline residue has an impact on peptide conformation.<sup>66</sup> They studied the thermodynamics of *cis*  $\rightarrow$  *trans* isomerization of the central amide bond in a series of dipeptides (Table 3.4).

Their results showed that introducing a 4*R*-OH substituent to the proline residue significantly stabilizes the *trans* peptide bond, whereas introducing a 4*S*-OH substituent leads to little change compared to the parent compound (Entries 1-3, Table 3.4). To study the effect of the regiochemistry of hydroxylation they looked at the 3*R*-OH and 3*S*-OH substituents. The C3 substituents had a smaller effect on the conformation of the peptide bond relative to substituents at C4. In C4-substituted prolines the shorter C $\gamma$ -C $\delta$  bond length and the inherent partial double bond character probably account for the stronger inductive effect relative to substituents at C3. Moreover the X-ray crystal structure of *N*-(<sup>13</sup>C<sub>2</sub>-acetyl)-3(*S*)-hydroxyproline methyl ester showed

a typical single bond length (1.536 Å) for C $\alpha$ -C $\beta$  bond and a relatively short bond length for C $\beta$ -C $\gamma$  (1.512 Å).<sup>67</sup>

Table 3.4: Thermodynamics parameters for compounds **47-54**



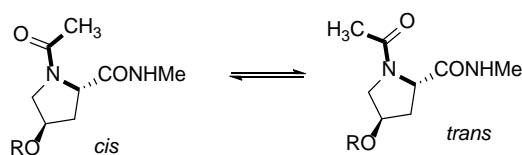
Entry	Compound	$K_{t/c}$ D <sub>2</sub> O, 298 K	$\Delta H$ (kcal mol <sup>-1</sup> )	$\Delta S$ (cal mol <sup>-1</sup> K <sup>-1</sup> )	$\Delta G^\circ$ (kcal mol <sup>-1</sup> K <sup>-1</sup> )
1	<b>47</b>	2.1	0.25	2.3	-0.44
2	<b>48</b>	5.0	-0.24	2.2	-0.90
3	<b>49</b>	1.9	1.21	5.4	-0.40
4	<b>50</b>	1.4	1.40	5.3	-0.18
5	<b>51</b>	2.4	0.65	3.9	-0.51
6	<b>52</b>	2.2	0.48	3.2	-0.47
7	<b>53</b>	5.6	-0.41	2.0	-1.01
8	<b>54</b>	2.5	0.80	4.6	-0.57

To study how the degree of hydroxylation impacts the peptide bond isomerization equilibrium they incorporated two isomers of 3,4-dihydroxyproline into the dipeptides. Peptide **53**, containing 2,3-*trans*-3,4-*cis*-3,4-dihydroxyproline showed similar behavior to the *trans*-4-hydroxyproline and gave the largest equilibrium constant in the series (Entry 7), but diastereoisomer **54** having opposite C $\beta$  configuration showed a lower equilibrium constant. Their explanation for this was the additional hydroxyl group at the C3 position enhances the pyramidalization of nitrogen and the electrophilicity of the Pro C=O group.

### 3.2.5 Schweizer and Coworkers – Glycosylation of Hydroxyproline

Glycosylation is a post-translational modification of proteins that attaches a carbohydrate moiety to a protein molecule. Glycosylation affects peptide and protein conformation. In the plant kingdom, glycosylation of Hyp occurs in hydroxyproline rich glycoproteins (HRGPs).<sup>68</sup> In the early 1990s, studies were conducted using small glycopeptides to study the effects of glycosylation on the peptide backbone.<sup>62</sup> In 2007, a paper by Schweizer and coworkers reported the structural impact of glycosylation on a Hyp derivative.<sup>69</sup> In their study they compared the thermodynamics and kinetics for *cis* → *trans* isomerization of Ac-Hyp-NHMe with 4-O-alkylated and both α- and β-galactosides of Ac-Hyp-NHMe (Table 3.5). They found that there were no significant differences in the thermodynamics and kinetics of the alkylated and glycosylated derivatives. However, the proline and galactose rings showed close contacts in nuclear Overhauser effect (nOe) experiments. Therefore they suggested that glycosylation could impact backbone conformation in HRGP in this manner.

Table 3.5: *Cis* → *trans* isomerization of glycosylated Ac-Hyp-NHMe



Entry	R	$K_{t/c}$ (37 °C)	$k_{ct}$ (s <sup>-1</sup> )*	$k_{tc}$ (s <sup>-1</sup> )*
1	<b>55</b> H	3.52 ± 0.05	0.73 ± 0.01	0.25 ± 0.01
2	<b>56</b> <sup>t</sup> Bu	3.34 ± 0.15	0.77 ± 0.02	0.27 ± 0.01
3	<b>57α</b> α-D-Gal	3.41 ± 0.30	0.83 ± 0.05	0.27 ± 0.02
4	<b>57β</b> β-D-Gal	3.37 ± 0.28	0.61 ± 0.04	0.21 ± 0.02

\*Phosphate buffer, pH 7.4 at 67 °C.

In nature, 2S,4S-hydroxyproline (hyp) is found rarely, but has been isolated from *Santalum album* (sandalwood tree), phalloidin (phallotoxins produced by *Amanita phalloides*) and *Lyngbya majuscula* (cyanobacteria)<sup>16</sup> (Figure 3.6). To-date there have been no reports of O-glycosylation of hyp from natural sources.

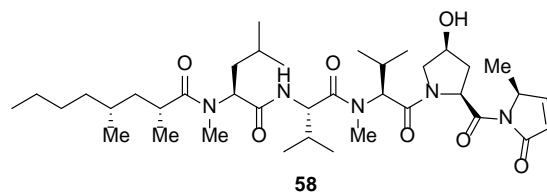
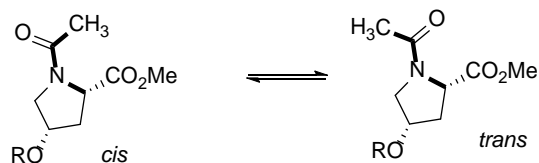


Figure 3.6: Microcolin A isolated from *Lyngbya majuscula*<sup>70</sup>

In 2009, Schweizer and coworkers reported that glycosylation of hyp (the diastereomer of Hyp) does lead to an increase in rates and the equilibrium constant of prolyl amide *cis* → *trans* isomerization compared to the rates of the corresponding non-glycosylated residue (Table 3.6).<sup>71</sup> Furthermore using nOe experiments they showed that in both α- and β-galactosides of Ac-hyp-OMe, galactose is oriented away from the proline residue.

Table 3.6: Prolyl amide *cis* → *trans* isomerism of glycosylated Ac-hyp-OMe



Entry	R	$K_{c/t}$ (24.8 °C)	$k_{ct}$ (s <sup>-1</sup> )*	$k_{tc}$ (s <sup>-1</sup> )*
1	<b>59</b> H	2.4 ± 0.1	0.44 ± 0.04	0.20 ± 0.01
2	<b>60α</b> α-D-Gal	2.9 ± 0.3	0.59 ± 0.06	0.25 ± 0.03
3	<b>60β</b> β-D-Gal	2.9 ± 0.1	0.71 ± 0.04	0.30 ± 0.02

\*Phosphate buffer, pH 7.2, 0.1 M at 67.3 °C.

### 3.3 Synthesis of Dipeptide and Glycopeptide Model Systems to Study the Conformational Changes Associated with Prolyl Hydroxylation and Glycosylation in Skp1.

After looking at the published results described above we wanted to study the conformational changes associated with the Thr-Pro dipeptide as occurs in Skp1. Initially we synthesized two dipeptides, Ac-Thr-Pro-NHMe and Ac-Thr-Hyp-NHMe and one glycosylated dipeptide Ac-Thr-[(α,1-4)GlcNAc]Hyp-NHMe (Figure 3.7) to study the conformational preferences of the pyrrolidine ring and the peptide bond as a consequence of hydroxylation and

subsequent glycosylation. These peptides were synthesized by standard peptide coupling techniques as described below.

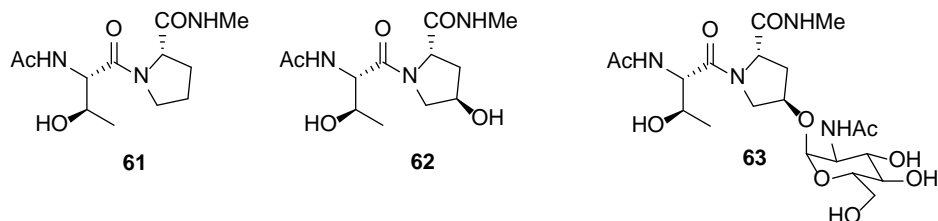
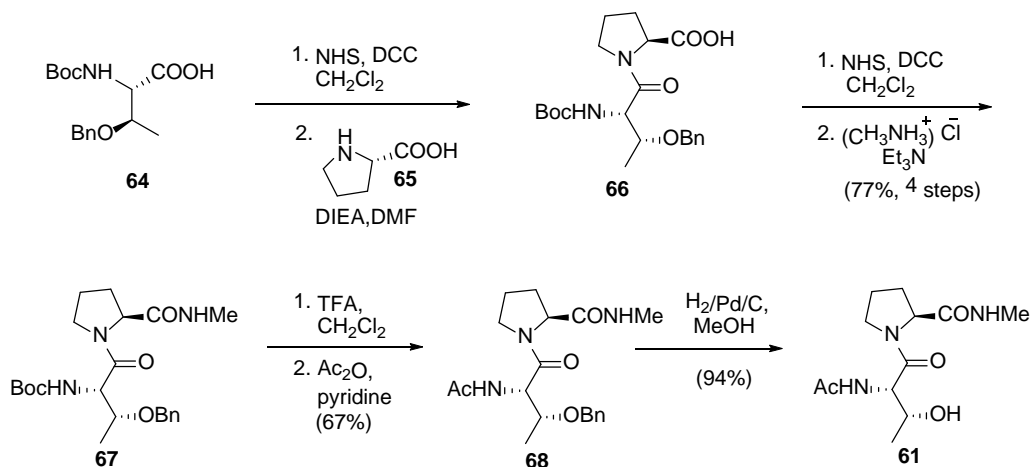


Figure 3.7: Dipeptides and glycopeptide synthesized

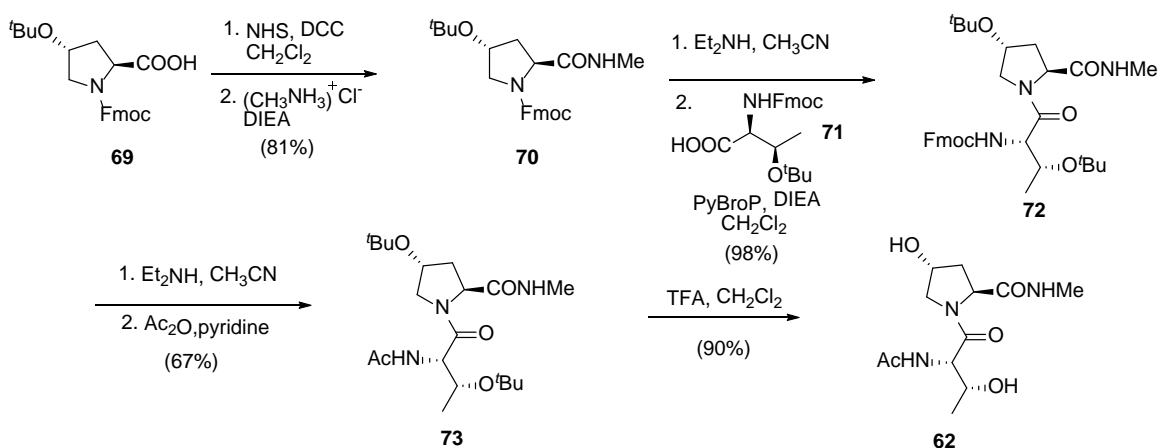
Our synthesis of the Thr-Pro dipeptide **61** was performed by analogy to procedures published previously by Taylor *et al.*<sup>65</sup> We prepared the dipeptide **66** by activating the acid of Boc-Thr(OBn)-OH (**64**) and coupling to proline **65**. The methylamide **67** was obtained by activating the acid in compound **66** and then treating with methylamine in the presence of a base. We used TFA to cleave the Boc group and subsequently acetylated the amine with acetic anhydride to afford **68**. Compound **61** was obtained in good yield after hydrogenolysis of **68** (Scheme 3.4). This was pure enough to perform NMR studies.



Scheme 3.4: Synthesis of dipeptide **61**



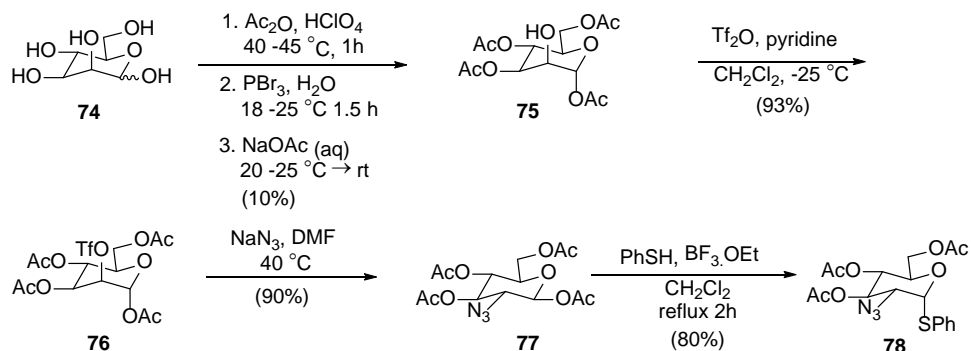
Synthesis of the Thr-Hyp dipeptide **62** started with commercially available Fmoc-Hyp(O<sup>t</sup>Bu)-OH (**69**) and Fmoc-Thr(O<sup>t</sup>Bu)-OH (**71**). We achieved the synthesis of **62** in seven linear steps and 48% overall yield (Scheme 3.5). We started our synthesis by activating the acid in compound **69** to introduce the methylamide, affording compound **70**. Removal of the Fmoc carbamate from compound **70** and coupling with Fmoc-Thr(O<sup>t</sup>Bu)-OH (**71**) gave **72** in quantitative yield. Deprotection of the amine in compound **72** and acetylation with acetic anhydride and pyridine gave **73**. Cleavage of the *tert*-butyl ethers of **73** was achieved with TFA to give **62** (Scheme 3.5), that was purified by RP-HPLC.



Scheme 3.5: Synthesis of dipeptide **62**

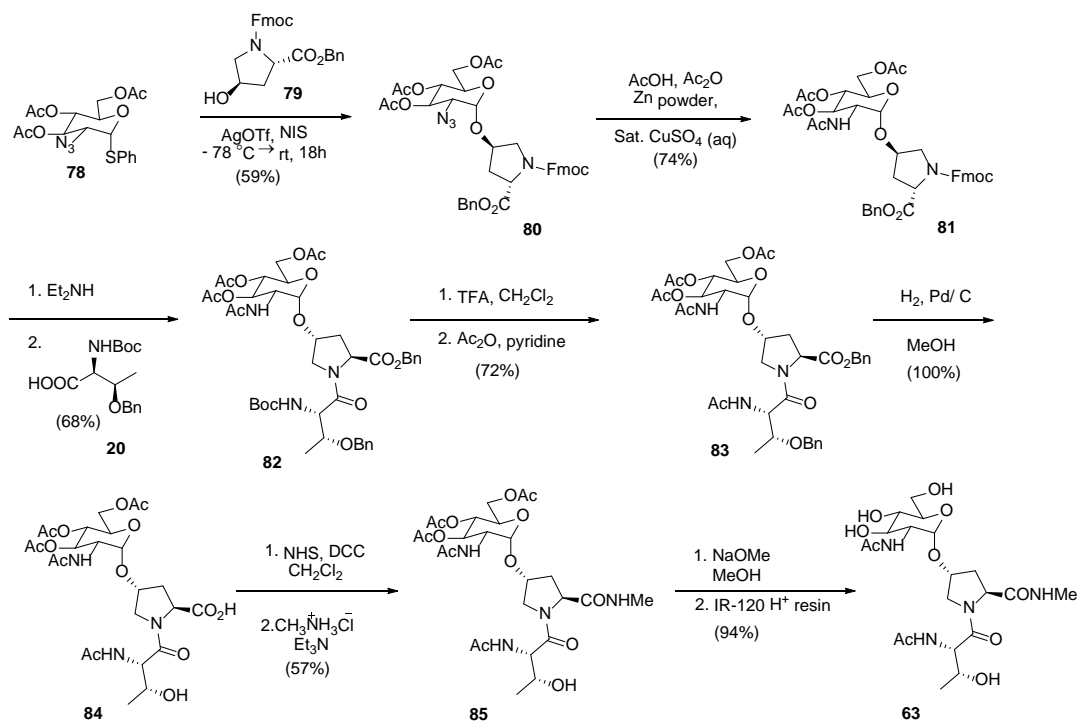
For the synthesis of the glycopeptide **63** we first needed to prepare a glycosyl donor; we started with commercially available *D*-mannose (**74**) (Scheme 3.6). We followed the one pot procedure of Deferrari *et al.*<sup>72</sup> to acetylate elsewhere, but leaving the free C-2 alcohol **75**. The overall yield of free C-2 alcohol **75** is poor, but the procedure requires negligible purification at each step and pure C-2 alcohol can be simply precipitated out from ether. The third step of the one pot sequence requires a lower reaction temperature than that recommended by Deferrari *et al.* to avoid getting the 2,3,4,6-tetra-*O*-acetyl derivative as the major product. The C-2 triflate **76** was converted to the C-2 azide **77** with inversion of configuration. Lewis acid catalyzed reaction with thiophenol gave anomeric  $\alpha$ -sulfide **78** as the major isomer (3:1  $\alpha$ : $\beta$ ). We chose a

thioglycoside glycosyl donor because they are robust and can be activated easily by *N*-iodosuccinimide (NIS).



Scheme 3.6: Synthesis of glycosyl donor **78**

The thioglycoside **78** was then coupled with the Fmoc-Hyp-OBn (**79**) to afford the *O*-glycoside **80**. The C2-azide in compound **80** was then reduced and acylated to produce the *N*-acetamide. Removal of Fmoc from **81** and coupling with Boc-Thr(O<sup>t</sup>Bu)-OH (**20**) gave **82** (Scheme 3.7).



Scheme 3.7: Synthesis of Ac-Thr-Hyp(GlcNAc)-NHMe (**63**)

To couple the threonine we followed the same procedure we used to synthesize the regular dipeptides. The amine of compound **82** was then deprotected and acetylated to give **83**. The acid **84** obtained from hydrogenolysis of **83** was then converted to its methylamide **85**. Finally the removal of acetate esters from **85** gave compound **63** in good yield (Scheme 3.7).

### 3.4 NMR Spectroscopic Studies

#### 3.4.1. Proton NMR Spectra

Proton NMR spectra were recorded for 0.01-0.04 M solutions of each compound in D<sub>2</sub>O over the temperature range 25-80 °C. The <sup>1</sup>H NMR spectra were assigned on the basis of COSY and HSQC experiments. The spectra of the Hyp-containing dipeptide **62** are discussed for illustration (Figure 3.8).

As shown in Figure 3.8(a) a number of relayed connectivities were observed in the COSY spectrum of Ac-Thr-Hyp-NHMe. The Hyp-H $\beta$  protons show expected cross peaks to H $\alpha$  and H $\gamma$ . The threonine methyl group (H $\gamma$ , 1.18 ppm) shows a cross peak to Thr- $\beta$  (4.13 ppm). This allows the assignment of Hyp- $\alpha$ , Hyp- $\gamma$ , Thr- $\alpha$  and Thr- $\beta$ . The Thr-Me doublet (H $\gamma$ ) for the *cis* and *trans* conformations are well resolved compared to the Thr- $\beta$  multiplet. Proton NMR signals for H $\beta$  and H $\delta$  of the *cis* conformation can also be seen on the spectrum but they are not as strong as the Thr-Me signal. The *trans* and *cis* conformations of Ac-Thr-Hyp-NHMe exist in a 9:1 ratio at 298 K.

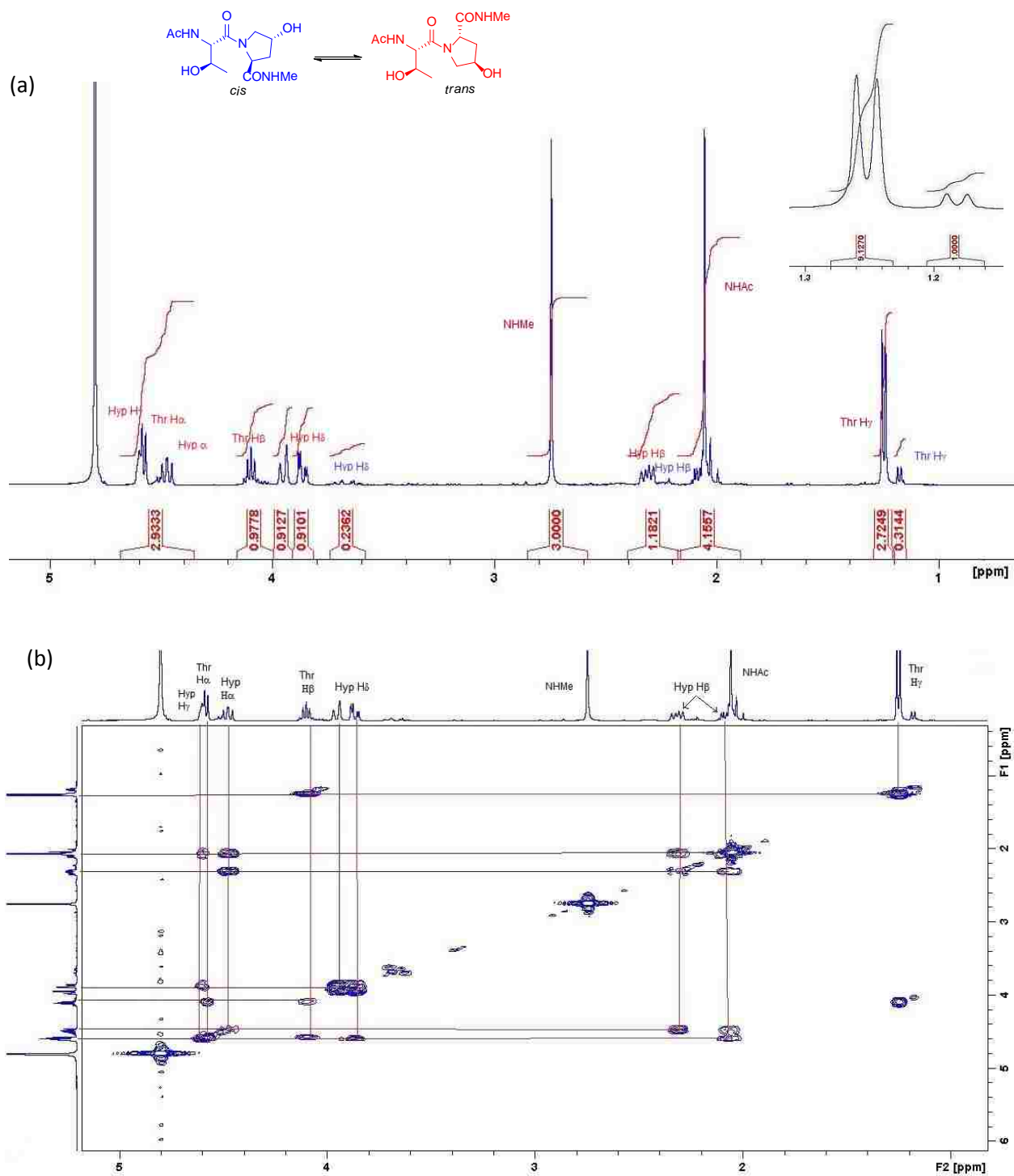


Figure 3.8: (a)  $^1\text{H}$  NMR spectrum of Ac-Thr-Hyp-NHMe (**62**) in  $\text{D}_2\text{O}$  at 297 K (b) 2D COSY spectrum of Ac-Thr-Hyp-NHMe (**62**) in  $\text{D}_2\text{O}$  at 297 K

The pyrrolidine ring pucker of the major conformational isomer of compounds **61**, **62** and **63** was assigned by comparison of  $^1\text{H}$  NMR coupling constants  $^3J_{\alpha,\beta 1}$  and  $^3J_{\alpha,\beta 2}$  with literature values<sup>73</sup> (Table 3.7). Coupling constants for the Cy-*exo* pucker are expected to be 7-10 Hz and 7-11 Hz respectively and for the Cy-*endo* pucker they are between 6-10 and 2-3 respectively.

Table 3.7: Coupling constant and ring pucker assignment for compound **61-63**

Compound	$J_{\alpha\beta 1}, J_{\alpha\beta 2}$	Ring pucker
Ac-Thr-Pro-NHMe ( <b>61</b> )	6.6, 4.3	<i>endo</i>
Ac-Thr-Hyp-NHMe ( <b>62</b> )	7.6, 9.6	<i>exo</i>
Ac-Thr-[( $\alpha$ ,1-4)GlcNAc]Hyp-NHMe ( <b>63</b> )	7.5, 9.8	<i>exo</i>

### 3.4.2 Inductive Effect on Cy Chemical Shift

In 2005, Raines *et al.* reported  $^{13}\text{C}$  chemical shifts as a measure of the electron withdrawing effect of substituents on the proline. Their study was based on Hyp derivatives esterified with an acetyl group or a trifluoroacetyl group. They observed 3-8 ppm difference in the Cy chemical shift for the proline derivative with trifluoroacetate substituent relative to **40** (Table 3.8).<sup>74</sup>

Table 3.8:  $^{13}\text{C}_\gamma$  chemical shifts for compounds **40**, **56** and **87**

Compound	$\delta(^{13}\text{C}_\gamma)$ ppm
Ac-Hyp-OMe ( <b>40</b> )	70.7
Ac-Hyp(COCH <sub>3</sub> )-OMe ( <b>86</b> )	73.7
Ac-Hyp(COCF <sub>3</sub> )-OMe ( <b>87</b> )	78.6

In 2009 Schweizer *et al.* used the same concept to estimate the electron withdrawing effects of glycosylation in hydroxy-proline derivatives.<sup>71</sup> Their results showed a downfield shift of 9-12 ppm for the Cy carbon of the glycosylated proline derivatives (Table 3.9).

Table 3.9:  $^{13}\text{C}_\gamma$  chemical shifts for compounds **40**, **88 $\alpha/\beta$** , **59** and **60 $\alpha/\beta$**

Compound	$\delta(^{13}\text{C}_\gamma)$ ppm
Ac-Hyp-OMe ( <b>40</b> )	69.9
Ac-Hyp-( $\alpha$ -Gal)-OMe ( <b>88<math>\alpha</math></b> )	78.9
Ac-Hyp-( $\beta$ -Gal)-OMe ( <b>88<math>\beta</math></b> )	77.6
Ac-hyp-OMe ( <b>59</b> )	69.9
Ac-hyp( $\alpha$ -Gal)-OMe ( <b>60<math>\alpha</math></b> )	80.3
Ac-hyp-( $\beta$ -Gal)-OMe ( <b>60<math>\beta</math></b> )	80.6

By analogy, to assess the impact of the electron withdrawing substituents upon proline hydroxylation and glycosylation in our dipeptides we used the  $^{13}\text{C}_\gamma$  chemical shift of compounds **61**, **62**, and **63**. Significant changes in the  $\text{C}_\gamma$  chemical shift were found to occur on hydroxylation and glycosylation of proline (Table 3.10).

Table 3.10:  $^{13}\text{C}_\gamma$  chemical shifts for compounds **60-62**

Compound	$\delta(^{13}\text{C}_\gamma)$ ppm
Ac-Thr-Pro-NHMe ( <b>60</b> )	23.6
Ac-Thr-Hyp-NHMe ( <b>61</b> )	69.7
Ac-Thr-Hyp(GlcNAc)-NHMe ( <b>62</b> )	79.7

### 3.4.3 Measurement of $K_{trans/cis}$ and Thermodynamics Studies of Dipeptides 61-63

The activation energy barrier for the *cis*  $\rightarrow$  *trans* isomerization of amides and peptides is around 20 kcal/mol. This is a relatively high energy barrier and so the process is usually slow on the NMR time scale. Therefore both species can be observed by NMR, sometimes with sufficient spectral resolution for integration.

The equilibrium constants for *cis*  $\rightarrow$  *trans* interconversion of **61**, **62**, and **63** were determined by integrating as many well resolved signals as possible for each isomer. For example, for Ac-Thr-Hyp-NHMe (**62**) the resolution of the threonine methyl group (Hy) protons, and the Hyp-H $\delta$  protons in the two conformations was good through the temperature range used (Figure 3.9). For the Ac-Thr-[( $\alpha$ ,1-4)GlcNAc]Hyp-NHMe (**63**), integration at higher temperatures was compromised due to poor resolution of the *cis* and *trans* isomer signals.

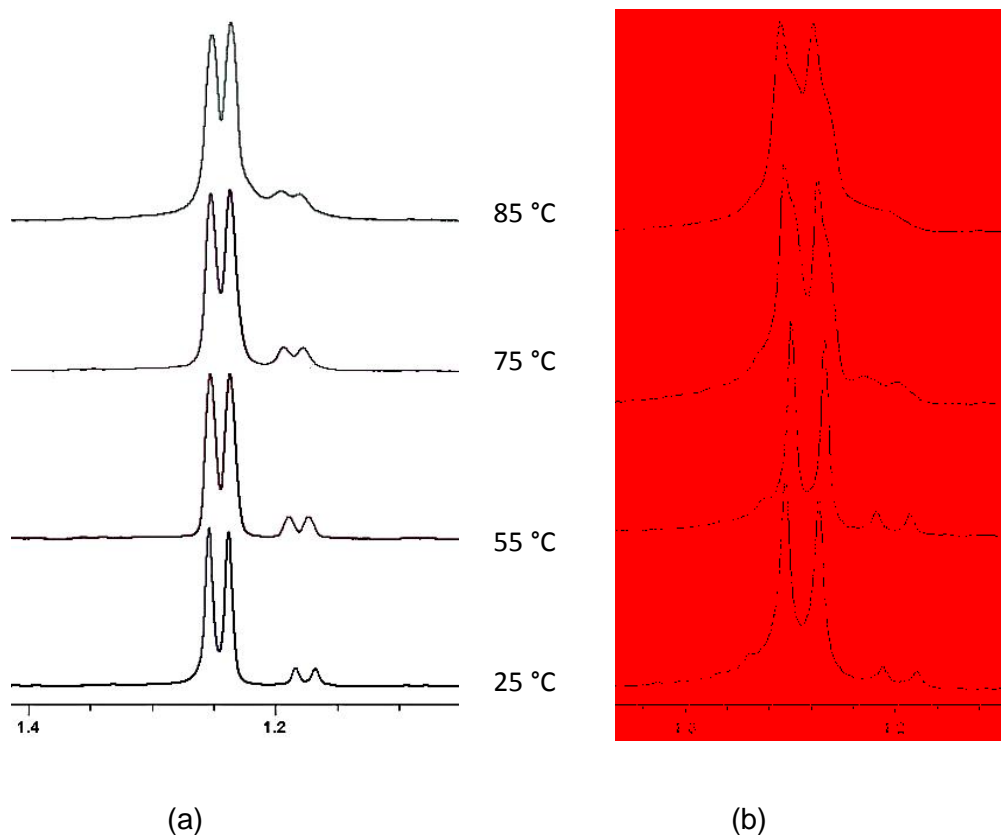


Figure 3.9: 1.1-1.4 ppm range of <sup>1</sup>H NMR spectra showing the resolution of Thr-H $\gamma$  signals of (a) Ac-Thr-Hyp-NHMe (**62**) and (b) Ac-Thr-[( $\alpha$ ,1-4)GlcNAc]Hyp-NHMe (**63**) at temperatures of 25, 55 and 75 and 85 °C.

Experiments were run over a range of temperatures (25 to 85 °C) and the resulting van't Hoff plots are shown in Figure 3.10. For all three peptides  $K_{t/c}$  is dependent on temperature and the magnitude of  $K_{t/c}$  decreases with increasing temperature. At higher temperature there is more energy to populate the *cis* species. A slightly positive gradient was observed for Ac-Thr-Pro-NHMe (**61**) and the gradient was steeper for Ac-Thr-Hyp-NHMe (**62**) and even steeper for the Ac-Thr-Hyp(GlcNAc)-NHMe (**63**). The hydroxylation and glycosylation of the proline led to a significant increase in the magnitude of the equilibrium constant.

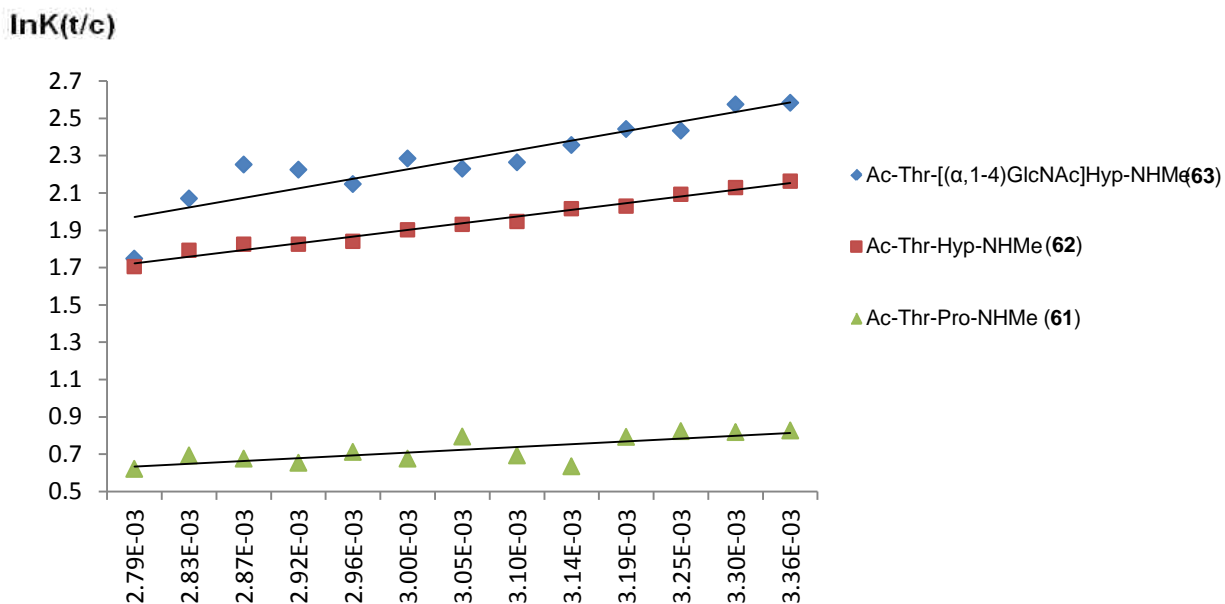


Figure 3.10: Van't Hoff plots for *cis* → *trans* isomerization of dipeptides **61-63**

The linear nature of the van't Hoff plots indicates that the enthalpic and entropic energy differences between the *cis* and *trans* prolyl amide isomers are independent of temperature. Accordingly,  $\Delta H^\circ$  and  $\Delta S^\circ$  could be calculated from the linear least squares fitting of the van't Hoff plots to the equation  $\ln K_{t/c} = (-\Delta H^\circ/R) (1/T) + \Delta S^\circ/R$ . For all three compounds  $\Delta H^\circ$  was a negative value, as reported by others for model peptides containing proline.<sup>65-66, 75</sup> The values of  $\Delta H^\circ$  and  $\Delta S^\circ$  are more negative for the dipeptide containing Hyp than for proline and even more negative in the dipeptide containing glycosylated Hyp (Table 3.11). The negative  $\Delta S^\circ$  implies that hydroxylation and glycosylation cause the *trans* amide isomer to become more ordered. The free energy difference ( $\Delta G^\circ$ ) between the *trans* and *cis* species can be calculated from  $\Delta G^\circ = \Delta H^\circ - T\Delta S^\circ$  and the values demonstrate that the *trans* amide isomer is increasingly favored in the order of Ac-Thr-Pro-NHMe (**61**) < Ac-Thr-Hyp-NHMe (**62**) < Ac-Thr-[( $\alpha$ ,1-4)GlcNAc]Hyp-NHMe (**63**).



Table 3.11: Thermodynamics parameters for compounds **61-63**

Dipeptide	$\Delta H^\circ$ (kJ/mol)	$\Delta S^\circ$ (J/mol/K)	$\Delta G^\circ$ (298 K) (kJ/mol/K)	$K_{t/c}$ (298 K)
Ac-Thr-Pro-NHMe ( <b>61</b> )	-2.67	-2.17	-2.03	2.3
Ac-Thr-Hyp-NHMe ( <b>62</b> )	-6.36	-3.34	-5.36	8.7
Ac-Thr-Hyp(GlcNAc)-NHMe ( <b>63</b> )	-9.04	-8.67	-6.45	13.2

Our results showed that hydroxylation and glycosylation do impact the *cis*  $\rightarrow$  *trans* isomerization of the prolyl amide bond whereas the 2007 Schweizer report concluded that glycosylation of Hyp does not affect the *N*-terminal amide *trans/cis* ratio or the rates of amide isomerization in model amides.<sup>69</sup> The differences between our system and Schweizer's were the nature of the sugar (GlcNAc vs Gal) and the *N*-terminal substituent investigated (Thr vs Ac). Either of these factors could explain the differences in the conclusions of the studies. This could be investigated by conducting analogous thermodynamic studies for either **89** or **90** (Figure 3.11). Analysis of Ac-[( $\alpha$ ,1-4)GlcNAc]Hyp-NHMe (**89**), would permit direct comparison of the Pro  $\alpha$  substituents. Alternatively Ac-Thr-Hyp(Gal)-NHMe would probe whether the nature of the sugar contributed to the differences. We synthesized Ac-[( $\alpha$ ,1-4)GlcNAc]Hyp-NHMe (**89**) as we already had the reagents and the synthesis was shorter than that for the proposed dipeptide **90**.

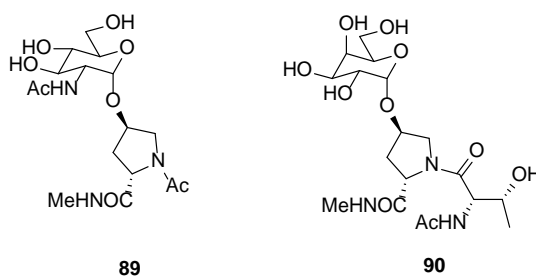
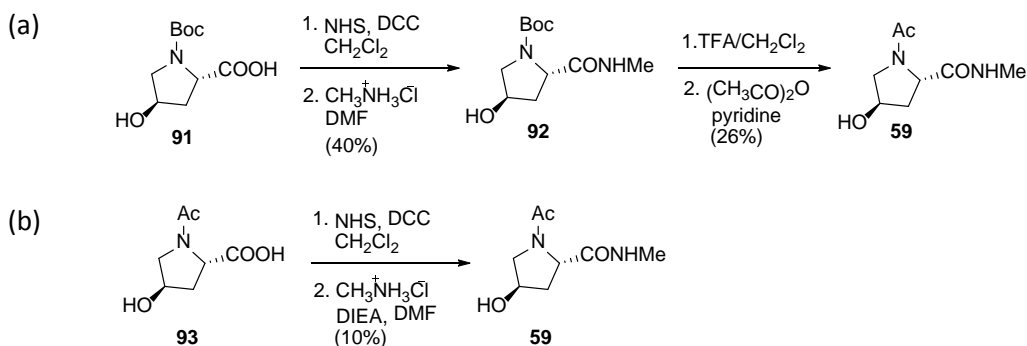


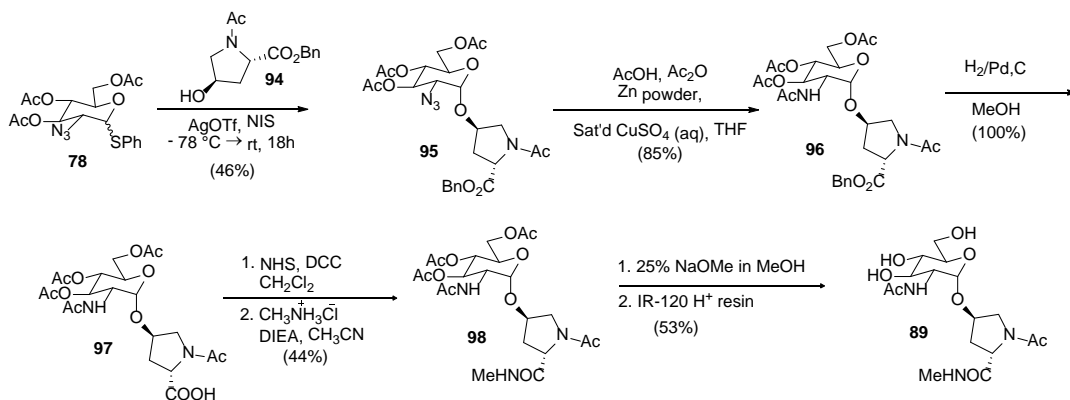
Figure 3.11: Potential additional target molecules

Initially our plan was to perform an O-glycosylation of Ac-Hyp-NHMe (**59**) with thioglycoside (**78**). Unfortunately we were unable to produce a good yield of pure Ac-Hyp-NHMe (**59**) via the routes depicted in Scheme 3.8.



Scheme 3.8: Ac-Hyp-NHMe synthesis

Therefore we prepared Ac-Hyp-OBn (**94**) and then glycosylated with thioglycoside **78**. We followed the same kind of manipulations as described earlier to produce the final Ac-[( $\alpha$ ,1-4)GlcNAc]Hyp-NHMe (**89**) (Scheme 3.9).



Scheme 3.9: Synthesis of Ac-[( $\alpha$ ,1-4)GlcNAc]Hyp-NHMe (**89**)

Variable temperature  $^1\text{H}$  NMR experiments were performed for the glycosylated amino acid Ac-[( $\alpha$ ,1-4)GlcNAc]Hyp-NHMe (**89**) and the resulting van't Hoff plot was added to the

series. (Figure 3.12) The thermodynamics data was compared with those of the dipeptides **61**, **62** and **63**.

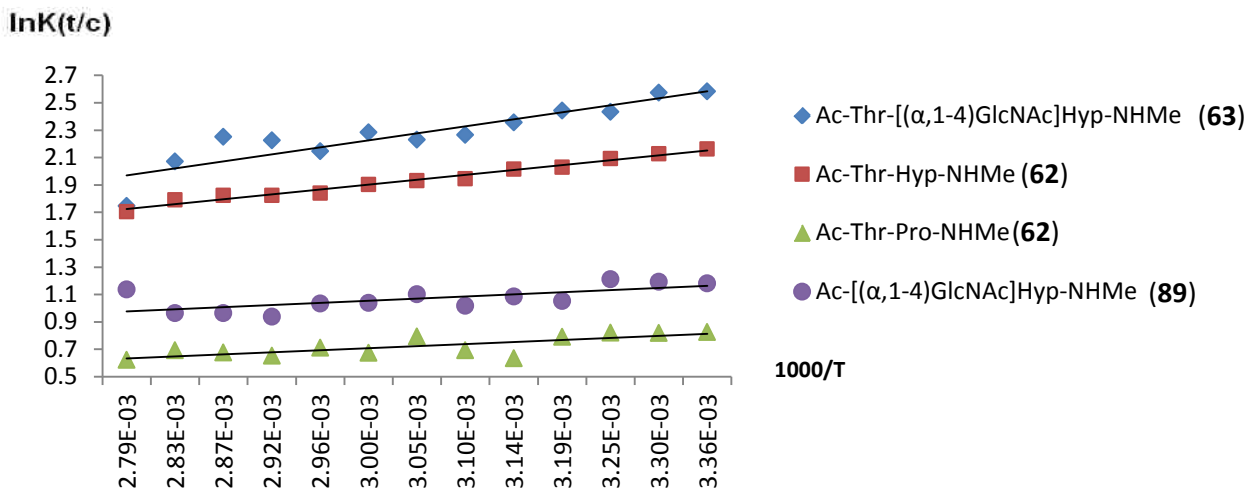


Figure 3.12: Van't Hoff plots for **61**, **62**, **63**, and **89**

The van't Hoff plot for compound **89** gave a positive gradient as observed for the other three compounds. The  $K_{t/c}$  values for Ac-[( $\alpha$ ,1-4)GlcNAc]Hyp–NHMe (**89**) were slightly higher than for Ac-Thr-Pro-NHMe (**61**), but not high as Ac-Thr-Hyp-NHMe (**62**) or Ac-Thr-[( $\alpha$ ,1-4)GlcNAc]Hyp-NHMe (**63**). Also the  $\Delta H^\circ$  and the  $\Delta G^\circ$  values of Ac-[( $\alpha$ ,1-4)GlcNAc]Hyp-NHMe (**89**) (Table 3.12) are close to the value of Ac-Thr-Pro-NHMe (**61**), but the value of  $\Delta S^\circ$  is positive which implies that the *trans* amide isomer of Ac-[( $\alpha$ ,1-4)GlcNAc]Hyp-NHMe (**89**) is more disordered than the slightly extended dipeptide.

Table 3.12: Thermodynamics data of peptides **61**, **62**, **63** and **89**

Dipeptide	$\Delta H^\circ$ (kJ/mol)	$\Delta S^\circ$ (J/mol/K)	$\Delta G^\circ$ (298 K) (kJ/mol/K)	$K_{t/c}$ (298 K)
Ac-Thr-Pro-NHMe ( <b>61</b> )	-2.67	-2.17	-2.03	2.3
Ac-Thr-Hyp-NHMe ( <b>62</b> )	-6.36	-3.34	-5.36	8.7
Ac-Thr-Hyp[( $\alpha$ ,1-4)GlcNAc]-NHMe ( <b>63</b> )	-9.04	-8.67	-6.45	13.2
Ac-[( $\alpha$ ,1-4)GlcNAc]Hyp-NHMe ( <b>89</b> )	-2.78	0.25	-2.70	3.25

These data signify that the addition of Ac-Thr at *N*-terminus has a bigger effect than glycosylation of the Hyp residue and that glycosylation **does** affect the *trans/cis* ratio of the prolyl amide bond isomerization and the effect is greater when there is large group *N*-terminal to the proline residue.

#### 3.4.4 Kinetics Studies of Proline-Containing Peptides

It is well known that for several proteins, denaturation and renaturation involve isomerization of one or several Xaa-Pro bonds.<sup>68b</sup> Studies on kinetics of the prolyl peptide bond *cis* → *trans* isomerization is important because this isomerization may be the rate determining step in polypeptide folding.<sup>68a</sup>

In the past, several studies have been conducted to find the rate of proline *cis* → *trans* isomerization. However most of these studies have been done for model compounds such as *N*-acetylproline and *N*-monosubstituted amides and studies on true prolyl peptide bond isomerization is rare. In these studies the most common technique used to determine the rates ( $k_{t/c}$ ) of *cis* → *trans* amide isomerization was magnetization inversion transfer <sup>1</sup>H, <sup>13</sup>C, <sup>19</sup>F NMR experiments. These experiments were performed at high temperature because at room temperature the rate of the isomerization is too slow to be measured by this method.

##### 3.4.4.1 Magnetization Inversion Transfer NMR Experiments

The magnetization inversion transfer technique in NMR spectroscopy is a useful method to determine the rates of slow chemical interconversions. Peptide bond rotation is one of the processes to which this technique has been applied successfully. In general, in magnetization transfer experiments the spin of one proton signal in an equilibrium mixture is selectively labeled by inversion. While this spin relaxes during a mixing time ( $d_2$ ) the response of all exchange coupled resonances is then determined by measuring the resonance intensities. Acquiring

spectra with different mixing times enables the determination of the spin-lattice relaxation time ( $T_1$ ) and the rate constant ( $k$ ) for the chemical interconversion.<sup>70</sup> Over the past years several groups have applied this technique to determine the  $k_{ct}$  and  $k_{tc}$  of proline-containing model compounds. These studies are summarized in the following section.

#### 3.4.4.2 Rabenstein and Coworkers – Studies of *Cis* → *Trans* Isomerization of Cysteine-Proline Peptide Bonds

In 1993, Rabenstein and coworkers reported the dynamics of *cis* → *trans* isomerization of the cysteine-proline peptide bonds in oxytocin (OT) and arginine-vasopressin (AVP) (Figure 3.13) in aqueous and methanol solutions. In their study they used the inversion transfer method to calculate the rate constants for *trans* → *cis* interconversion ( $k_{tc}$ ). They selectively inverted a signal of the *trans* isomer and the *cis* → *trans* isomerization of the Cys<sup>6</sup>-Pro peptide bond was observed. To characterize the *cis* → *trans* isomerization of OT, the Cys<sup>6</sup>-NH proton [Figure 3.13 (a), blue dotted circles] was considered and for AVP the Phe-NH and Gln-NH protons (Figure 3.13 (b), blue dotted circles) were used.

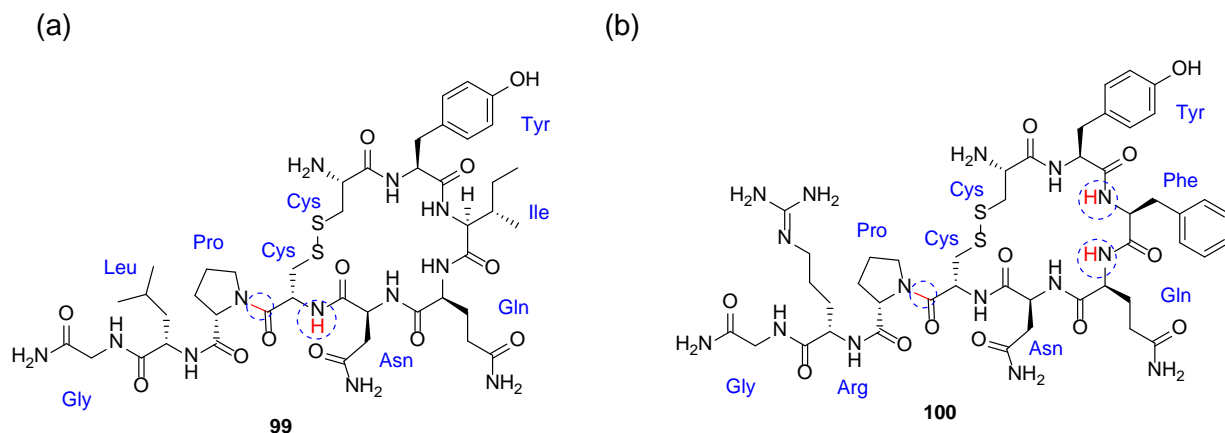


Figure 3.13: Structures of (a) oxytocin (**99**) and (b) arginine vasopressin (**100**). Blue dotted circles represent the peptide bonds and the amide protons to calculate the *cis* → *trans* isomerization

Rate constants for the *trans* → *cis* interconversion of the prolyl peptide bond in both OT and AVP,  $k_{tc} = 1/\tau_{tc}$  ( $\tau_{tc}$  = life time of the *trans* → *cis* interconversion) were determined at 5 °C temperature intervals over the temperature range 21-35 °C and 58-72 °C for OT and 21-49 °C for AVP. All the experiments for OT and AVP were carried out in aqueous solution and CD<sub>3</sub>OD solution. Their mixing time ( $d_2$ ) values ranged from 0.0001 s to  $> 5T_1$ . The  $T_1$  (spin lattice relaxation time constant) values were estimated by the inversion recovery method. In each experiment the inversion transfer spectra was measured at 14-21  $t$  ( $d_2$ ) values. The rate constant  $k_{tc}$  was calculated from the life times ( $\tau_t$  and  $\tau_c$ ) and  $k_{ct}$  was then calculated from  $K_{t/c}$  and  $k_{ct}$ . They used the pulse sequence of  $\frac{\pi}{2(x)} - \tau - \frac{\pi}{2(x)} - t - \frac{\pi}{2(x,y,-x,-y)}$  for the inversion recovery experiments.<sup>73a</sup> Their results showed that the rate of isomerization around the Cys<sup>6</sup>-Pro peptide bond is significantly faster for both OT and AVP in CD<sub>3</sub>OD solution than in water and the rate constants for *cis* → *trans* ( $k_{ct}$ ) and *trans* → *cis* ( $k_{tc}$ ) interconversions for both OT and AVP are in the range  $6.8 \times 10^{-2}$ , and  $4.3 \times 10^{-3} \text{ s}^{-1}$  respectively.

#### 3.4.4.3 Lubell and Coworkers – Effect of Substituents on C $\delta$ on Amide *Cis* → *Trans* Isomerization

In 1996 Lubell and coworkers reported the steric effects on amide *cis* → *trans* isomerization of *N*-acetyl-5-*tert*-butylproline *N*-methylenamides (Figure 3.14). In their study the energy barriers ( $\Delta G^\ddagger$ ) for *cis* → *trans* isomerization of the prolyl amide bond were measured using <sup>13</sup>C NMR magnetization transfer experiments. They performed the experiments over several temperatures between 60-85 °C for each compound and selectively inverted the C $\alpha$  carbon signal of the *trans* isomer. In their experiments they used relaxation delays of 20 s and inversion recovery delays between 1 ms and 20 s.<sup>76</sup> Their results showed that the *tert*-butyl groups at the C $\delta$  position disfavor the *trans* conformation.

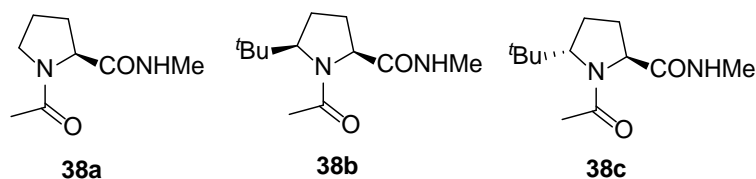


Figure 3.14: *N*-Acetyl-5-*tert*-butylproline *N*-methylamides

In their 1998 paper they studied the influence of alkyl substituents in the C $\beta$ -position on the rate of amide isomerization via synthesizing prolyl and hydroxyprolyl derivatives (Table 3.13). Again they used  $^{13}\text{C}$  magnetization transfer experiments to study the rates of *cis*  $\rightarrow$  *trans* isomerization of the prolyl amide bond. The signal for C $\alpha$  of the major amide isomer was selectively inverted.

Table 3.13: Prolyl amide bond isomerization rates for compounds **38a**, **59** and **101-104**

Proline derivative	$k_{ct}$ (s $^{-1}$ )	$k_{tc}$ (s $^{-1}$ )
<b>38a</b>	2.01	0.82
<b>59</b>	1.46	0.47
<b>101</b>	2.05	0.82
<b>102</b>	0.32	0.12
<b>103</b>	0.81	0.27
<b>104</b>	1.39	0.47

Their results showed that the  $k_{ct}$  of dimethylproline amide **102** was by 7-fold slower than that of Ac-Pro-NHMe (**38a**) (Table 3.13). Also the  $k_{ct}$  of Ac-(3,3-dimethyl)-hyp-NHMe (**104**) was 2-fold slower than that of Ac-hyp-NHMe (**101**). In addition the isomerization rate of Ac-(3,3-dimethyl)-Hyp-NHMe (**103**) was slower than that of Ac-Hyp-NHMe (**55**). This demonstrates that alkylation in the 3-position slows the isomerization of prolyl and hydroxyprolyl amides in water.<sup>77</sup>

#### 3.4.4.4 Moroder and coworkers – Studies of *Cis* → *Trans* Isomerization of Fluoroprolines

In 2001 Moroder and coworkers reported the kinetics of fluoroprolines (Ac-Pro-OMe **(39)**, Ac-Flp-OMe **(41)**, Ac-flp-OMe **(42)**, Ac-(4)-F<sub>2</sub>Pro-OMe **(43)**, Table 3.2).<sup>64</sup> They used 2D NOESY spectra to determine the rate constant for *cis* → *trans* isomerization of the Ac-Pro amide bond. For the Pro, Flp and flp derivatives cross peaks between H<sub>α<sub>trans</sub></sub> and H<sub>α<sub>cis</sub></sub> in the <sup>1</sup>H-<sup>1</sup>H NOESY spectrum were used because only these signals were resolved well in the spectra. The cross peak to diagonal peak ratios were obtained and scaled according to the following equation which accounts for differential relaxation behavior of the resonances.

$$k_{EZ} = \left( \frac{I_{ct}}{I_{cc}} + \left( \frac{I_{tc}}{I_{tt}} \right) K_{ZE} \right) / (2\tau_m)$$

$$k_{ZE} = \frac{\left( \frac{I_{ct}}{I_{cc}} \right)}{K_{ZE}} + \frac{\left( \frac{I_{tc}}{I_{tt}} \right)}{2\tau_m}$$

$I_{xx}$  denotes the peak integrals from the 2D NOESY. The first subscript is for the F1 frequency and the second subscript is for the F2 frequency. NOESY mixing times  $\tau_m$  at each temperature were chosen such that  $I_{ct} \ll I_{cc}$  and  $I_{tc} \ll I_{tt}$ .

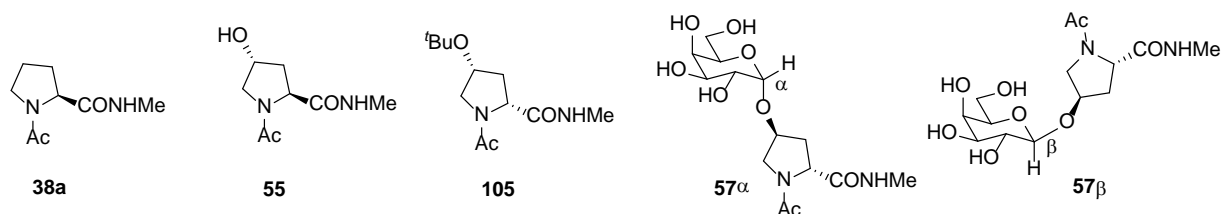
#### 3.4.4.5 Schweizer and coworkers – Studies of *Cis* → *Trans* Isomerization of Glycosylated Hydroxyproline Derivative

In 2007, Schweizer and coworkers reported the kinetics of prolyl amide bond isomerization in glycosylated Ac-Hyp-NHMe derivatives (Table 3.14). They also performed magnetization inversion transfer experiments. They used <sup>1</sup>H NMR spectroscopy in preference to <sup>13</sup>C NMR because the signal/noise ratio is much higher for <sup>1</sup>H than <sup>13</sup>C. Also they stated that the heating effects caused by decoupling for <sup>13</sup>C causes uncertainty in the temperature of the sample.



Selective inversion of the *N*-methylamide signal of the *trans* isomer was performed. Their experiments were run over the temperature range of 60 °C to 80 °C.<sup>69</sup> The error values were obtained from the linear least squares fit of the data of inversion transfer recovery plots.

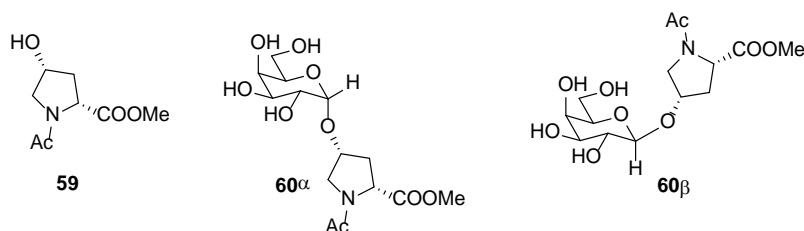
Table 3.14: Prolyl amide bond isomerization rate constants for compounds **38a**, **55**, **57 $\alpha/\beta$**  and **105**<sup>69</sup>



Entry	Compound	$k_{tc}$ (s <sup>-1</sup> )	$k_{ct}$ (s <sup>-1</sup> )
1	Ac-Hyp-OMe ( <b>38a</b> )	0.18 ± 0.01	0.81 ± 0.01
2	Ac-Hyp( $\alpha$ -Gal)-NHMe ( <b>57<math>\alpha</math></b> )	0.19 ± 0.01	0.85 ± 0.01
3	Ac-Hyp( $\beta$ -Gal)-NHMe ( <b>57<math>\beta</math></b> )	0.18 ± 0.02	0.77 ± 0.02

In 2009 Schweizer and coworkers reported the kinetics of prolyl amide isomerization of Ac-hyp-NHMe and glycosylated derivatives (Table 3.15).<sup>71</sup> They used magnetization transfer experiments to determine the rate of amide bond isomerization and used the same experimental conditions as described in their 2007 report. In their supporting information they say they the used NHMe *trans* signal even though there is no NHMe in these molecules. In their figures they refer to inversion of the *trans* *N*-amide signal to collect the data, presumably meaning the methyl singlet of CH<sub>3</sub>C(=O)-N.

Table 3.15: Prolyl amide bond isomerization rate constants for compounds **59** and **60 $\alpha/\beta$** <sup>71</sup>



Entry	Compound	$k_{tc}$ (s <sup>-1</sup> )	$k_{ct}$ (s <sup>-1</sup> )
1	Ac-hyp-OMe ( <b>59</b> )	0.20 ± 0.01	0.44 ± 0.04
2	Ac-hyp( $\alpha$ -Gal)-OMe ( <b>60<math>\alpha</math></b> )	0.25 ± 0.03	0.59 ± 0.06
3	Ac-hyp( $\beta$ -Gal)-OMe ( <b>60<math>\beta</math></b> )	0.30 ± 0.02	0.71 ± 0.04

### 3.4.4.6 Raines and coworkers – Effect of the Electronegative Substituents at C $\gamma$ on *Cis* $\rightarrow$ *Trans* Isomerization

Raines and coworkers used magnetization transfer  $^{13}\text{C}$  NMR to study the rates of the Pro and Hyp derivatives, and for the Flp derivative they used  $^{19}\text{F}$  NMR inversion transfer experiments. The experiments were conducted at 37-87  $^{\circ}\text{C}$ .

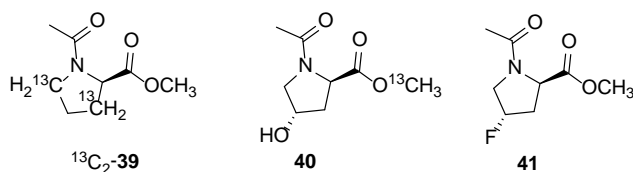


Figure 3.15: Proline derivatives

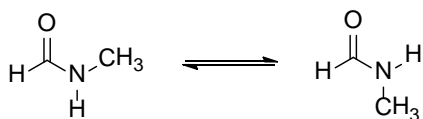
Decreasing the concentration of the Hyp derivative from 0.1 M to 1.0 mM they observed an increase in the isomerization rates and an increase in error from <10% to >60% depending on the temperature. For the Flp derivative they could not run the experiment in water because at most of the temperatures the two  $^{19}\text{F}$  resonances were overlapped.<sup>60</sup>

All the above mentioned groups used following two equations to calculate the rate constant after they collected the data from magnetization inversion transfer experiments.

$$k_{t/c} = \frac{(C_1\lambda_1 + C_2\lambda_2) + k_{itrans}(C_3 + C_4)}{\alpha(C_1 + C_2)}$$

### 3.4.4.7 Williams *et al.* – an Undergraduate Magnetization Transfer Experiment

In 2011, Williams *et al.* described an inversion recovery experiment for the undergraduate laboratory.<sup>70</sup> For this magnetization transfer experiment they used *N*-methylformamide (Scheme 3.10). This is a very different system compared to the peptide amide bond. Once the data was acquired they used the CIFIT program<sup>76</sup> to fit the kinetic magnetization transfer data and the resulting values for the chemical exchange rate were given by CIFIT.



Scheme 3.10: *N*-methylformamide *cis* → *trans* isomerization

### 3.5 Kinetics Study of Skp1 Relevant Peptides - Isomerization of the Prolyl Amide Bond

The effect of proline hydroxylation and glycosylation on the kinetics of prolyl amide bond isomerization was determined using magnetization inversion transfer experiments. For all four compounds (Figure 3.16) these experiments were performed over several temperatures (60-75 °C) depending on the resolution of the proton signals for the two isomers. Below 60 °C the rates were too slow to determine by this experiment and above 75 °C *cis* and *trans* isomer signals were not well resolved. To acquire the NMR data the parameters for these experiments were set up following the detailed instructions of Williams *et al.* including a relaxation delay of 20s.

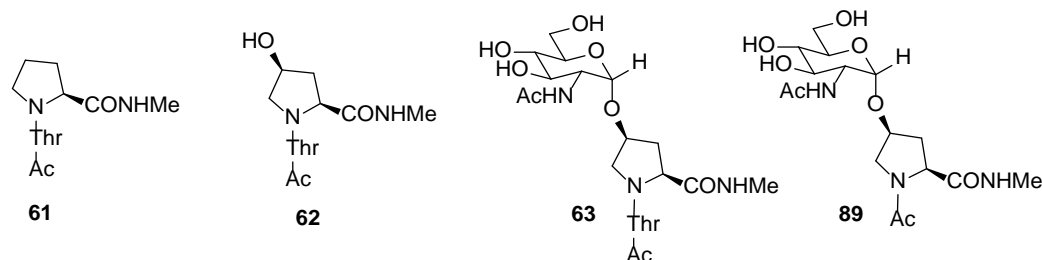


Figure 3.16: Peptides **61-63** and **89**

Except for the larger peptides studied by Rabenstein and coworkers, all other examples discussed above have an acetyl group *N*-terminal to the proline residue. Our system has an acetyl-threonine group that is more sterically demanding than an acetyl group alone.

Initially the magnetization transfer experiments were run for compounds **61**, **62**, and **63** inverting the Thr-H $\gamma$  of the *trans* isomer and for **89** inverting the H1 (anomeric proton of GlcNAc) for the *trans* isomer. After fitting the data using the CIFIT program only compounds **62** and **89**

gave positive values for the rate (Table 3.16). The isomerization rate  $k_{tc}$  was calculated using the equation of  $K_{t/c} = k_{ct}/k_{tc}$ . Magnetization inversion transfer data acquired for compound **61** gave negative rate for temperature 75 °C and compound **63** gave negative values for the rates for temperatures 65-75 °C after fitting by the CIFIT program. This is possibly when temperature raised the two isomer signals were getting closer and inversion of *trans* isomer proton was also effecting partial inversion of the *cis* isomer proton.

Table 3.16: Prolyl peptide bond isomerization rates

Temperature (°C)	Ac-Thr-Hyp-NHMe ( <b>62</b> ), $k_{tc}$ (s <sup>-1</sup> )	Ac-Thr-Hyp-NHMe ( <b>62</b> ), $k_{ct}$ (s <sup>-1</sup> )	Ac[(α,1-4)GlcNAc]Hyp-NHMe ( <b>89</b> ), $k_{tc}$ (s <sup>-1</sup> )	Ac[(α,1-4)GlcNAc]Hyp-NHMe ( <b>89</b> ), $k_{ct}$ (s <sup>-1</sup> )
60	0.14 ± 0.08	0.94 ± 0.08	0.15 ± 0.02	0.45 ± 0.02
65	0.21 ± 0.10	1.32 ± 0.10	0.18 ± 0.03	0.54 ± 0.03
70	0.31 ± 0.10	1.92 ± 0.10	0.46 ± 0.08	1.20 ± 0.08
75	0.49 ± 0.14	3.04 ± 0.14	0.50 ± 0.11	1.30 ± 0.11

Table 3.17 displays the chemical shift difference ( $\Delta\delta$ ) of the *cis* and *trans* isomer signals we attempted to selectively invert in the experiment. The  $\Delta\delta$  values are larger for Ac-Thr-Hyp-NHMe (**62**) and Ac[(α,1-4)GlcNAc]Hyp-NHMe (**89**) compared to those in Ac-Thr-Pro-NHMe (**61**) and Ac-Thr-Hyp(αGlcNAc)-NHMe (**63**). The smaller values of  $\Delta\delta$  did not give a good resolution in this experiment at elevated temperatures.

Table 3.17: Chemical shifts differences of the *cis* and *trans* isomer proton signal

	Ac-Thr-Pro-NHMe ( <b>61</b> )	Ac-Thr-Hyp-NHMe ( <b>62</b> )	Ac-Thr-Hyp(αGlcNAc)-NHMe ( <b>63</b> )	Ac[(α,1-4)GlcNAc]Hyp-NHMe ( <b>89</b> )
Proton inverted	NHCOCH <sub>3</sub>	Thr-H <sub>γ</sub>	Thr-H <sub>γ</sub>	H1
$\Delta\delta$ (ppm)	0.05	0.07	0.03	0.08
$\Delta\delta$ (Hz)	35	49	21	56
$\tau$ (ms)	14	10	24	9

Compared to Schweizer's data, the rate constants at 67 °C for Ac-Hyp-NHMe (**55**) with Ac-Thr-Hyp-NHMe (**62**) at 65 °C, values of  $k_{ct}$  is higher for Ac-Thr-Hyp-NHMe, but  $k_{tc}$  is similar. This tells that dipeptide which resembles an actual peptide *cis* → *trans* isomerization is faster to get the more stable *trans* isomer. The  $k_{ct}$  of Ac[( $\alpha$ ,1-4)GlcNAc]Hyp-NHMe (**89**) at 65 °C is smaller compared to Schweizer's  $k_{ct}$  value of Ac( $\alpha$ -Gal)Hyp-NHMe (**57 $\alpha$** ) at 67 °C but  $k_{tc}$  is similar. This may be due to the difference of the sugar moiety in **89** and **57 $\alpha$** .

### 3.6 Study of Hyp-C $\gamma$ Stereochemistry of the Native Skp1 Protein

As mentioned in Chapter 1 when we started this project the stereochemistry of the Hyp-C $\gamma$  of the native Skp1 was not known. We synthesized two dipeptides (compounds **62** and **106**, Figure 3.17) with both possible stereochemistries at C $\gamma$  of the Hyp that could serve as standards to help determine the stereochemistry of the native Skp1 Hyp-C $\gamma$ . This study was conducted in collaboration with Professor Christopher M. West (Oklahoma Health Sciences Center) and Professor Brad Bendiak (University of Colorado, Boulder).

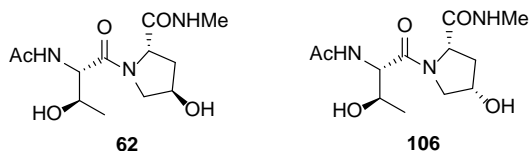
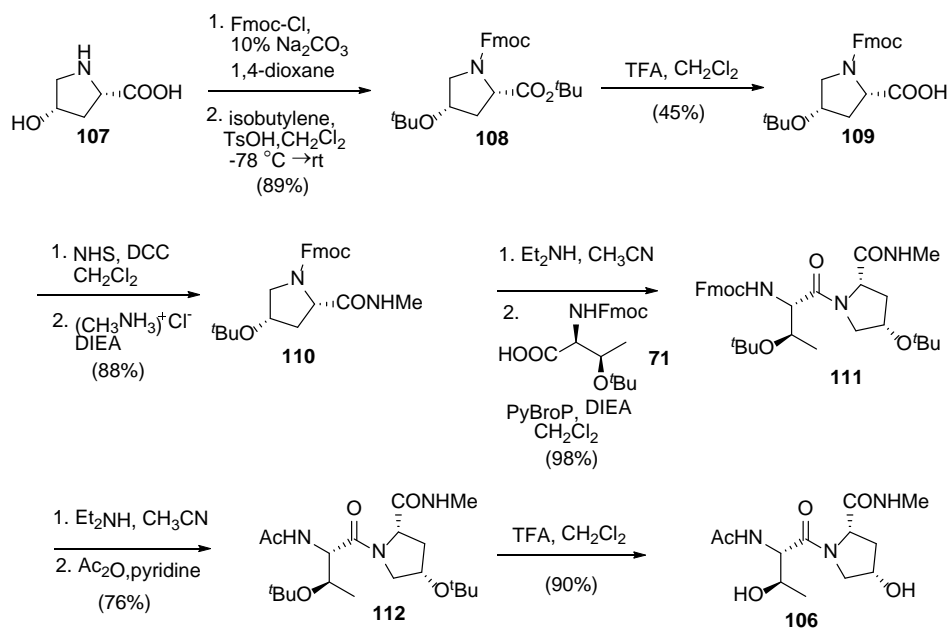


Figure 3.17: Dipeptide standards for structure determination

The synthesis of **62** has already discussed in Section 3.3. We synthesized the diastereomer of dipeptide **62**, Ac-Thr-hyp-NHMe (**106**) as depicted in Scheme 3.11. Our synthesis of **106** began with expensive, but commercially available, *cis*-4-hydroxyproline **107**. We protected the amine using Fmoc-Cl and both acid and alcohol groups using isobutylene under acidic conditions.<sup>78</sup> Selective removal of the *tert*-butyl ester was achieved using a dilute solution of TFA in CH<sub>2</sub>Cl<sub>2</sub> to get **109** in 45% yield. For the conversion of **109** to **106** we followed the same route as in the synthesis of the diastereomer.



Scheme 3.11: Synthesis of **106**

The dipeptides **62** and **106** were sent to Bendiak at the University of Colorado, Boulder. The 13-mer sequence NDFTHypEEEEQIRK was obtained by enzymatic degradation of Skp1 followed by *in vitro* enzymatic hydroxylation. This was then purified by HPLC. The <sup>1</sup>H NMR spectra of both diastereomers and the 13-mer were compared (Figure 3.18).<sup>17</sup> The <sup>1</sup>H NMR signals of H<sub>α</sub> in compounds **62** and **106** show two different coupling patterns. For the dipeptide **62** which has the 2*S*,4*R*-hydroxyproline the H<sub>α</sub> signal is an apparent triplet and for the dipeptide **106** which has 2*S*,4*S*-hydroxyproline the H<sub>α</sub> signal is a doublet of doublets. For the Skp1-derived oligopeptide the H<sub>α</sub> signal is a triplet. This strongly suggests that 2*S*,4*R* stereochemistry could be assigned to the Skp1 hydroxyproline residue. Also <sup>1</sup>H NMR signals of the two H<sub>δ</sub> protons of dipeptide **62** are very close together, which is also true for the H<sub>δ</sub> proton signal of the Skp1 peptide. By comparison, for dipeptide **106** the two H<sub>δ</sub> proton signals are separated by 0.35 ppm. In conclusion the <sup>1</sup>H NMR of the 13-mer derived from Skp1 closely matches the <sup>1</sup>H NMR of the synthetic dipeptide with 2*S*,4*R* stereochemistry (**62**). We thereby conclude the Cy stereochemistry of the Skp1 hydroxyproline to be 4*R*.<sup>17</sup>

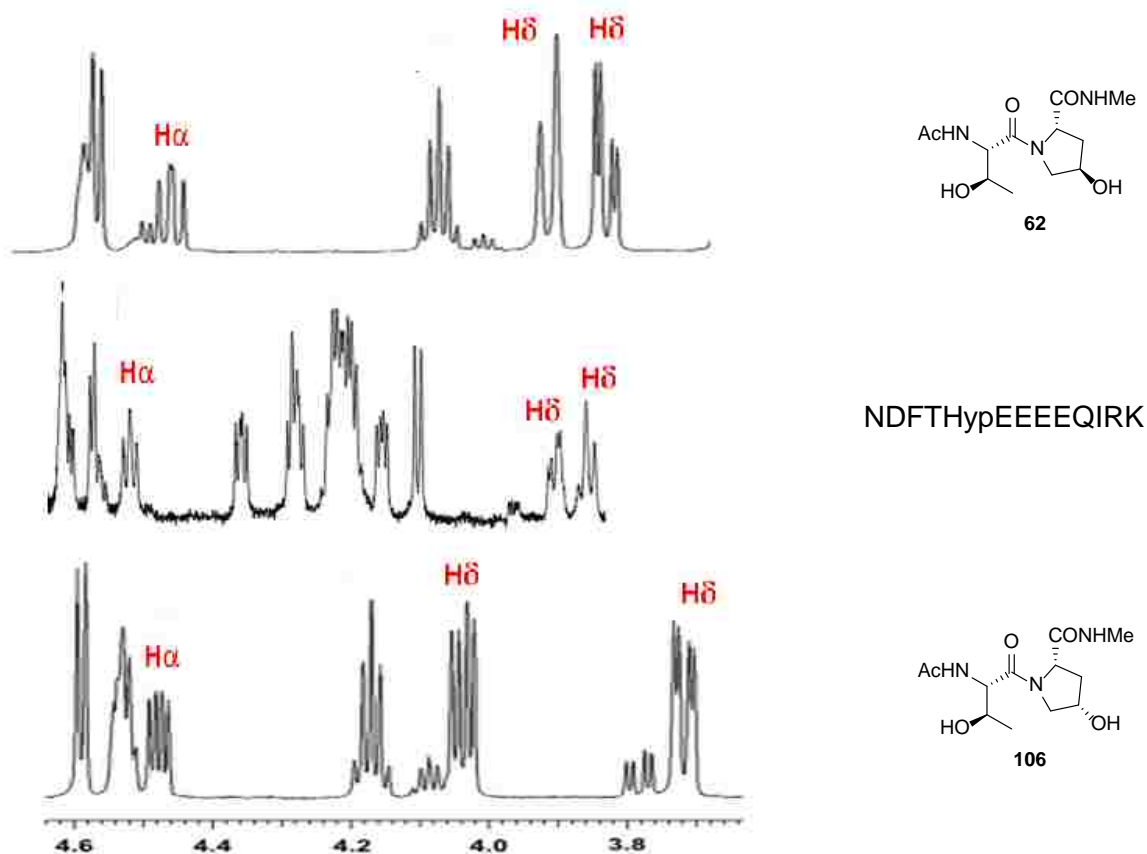


Figure 3.18:  $^1\text{H}$  NMR spectra of **62**, the 13-mer and **106** showing 3.7-4.6 ppm region

### 3.7 2S,4S-Fluoroproline (flp)

We have synthesized another derivative of hydroxyproline, 2S,4S-fluoroproline (flp) with the intention of exploring the Skp1 prolyl-4-hydroxylase (P4H1) preference for pyrrolidine conformation and C4 configuration.

#### 3.7.1 Previous studies of fluoroproline

Studies by Raines' Group demonstrated that 4R-fluoroproline enhances the conformational stability of collagen sequences relative to those containing 2S,4R-hydroxyproline.<sup>79</sup> As described in §3.2.2, the conformational preferences of 2S,4R-fluoroproline

(Flp) and 2*S*,4*S*-fluoroproline (flp) arise as a result of stereoelectronic and gauche effects.<sup>79-80</sup>

The preferred conformation of flp is *C $\gamma$ -endo* and for Flp it is *C $\gamma$ -exo* (Figure 3.19).

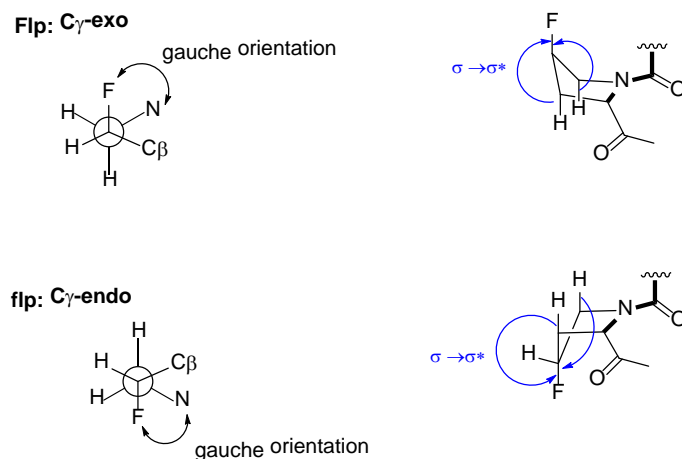
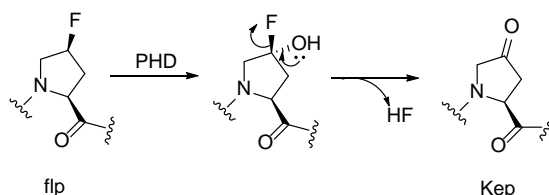


Figure 3.19: Flp and flp conformations. Newman projection formula are depicted looking down the *C $\gamma$ -C $\delta$*  bond axis.

Studies of the HIF- $\alpha$  prolyl-4-hydroxylase enzyme by the Schofield Group showed that flp can be processed by P4H1;<sup>12a</sup> indeed hydroxylation of prolyl analogs by this particular P4H1 prefers substrates that adopt a *C $\gamma$ -endo* conformation over *C $\gamma$ -exo*. In these mechanistic studies of prolyl hydroxylation the 4-oxo-prolyl product (Ketoproline, Kep) was observed with both 2*S*,4*S*-hydroxyproline (hyp) and flp (Scheme 3.12). Ketoproline (Kep) presumably arises by hydroxylation of flp to afford an intermediate fluorohydrin, followed by elimination of HF (Scheme 3.12). In contrast to flp, 2*S*,4*R*-fluoroproline (Flp) does not have a hydrogen in the 4*R* position to be abstracted by P4H1, therefore Flp is not a substrate for P4H1.

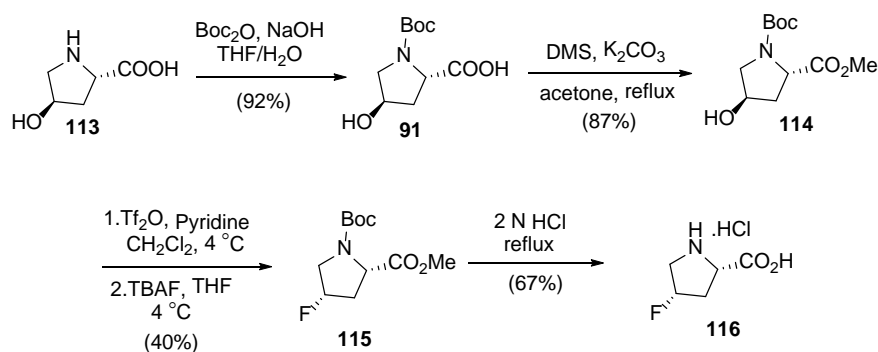


Scheme 3.12: Formation of 4-oxoprolyl product



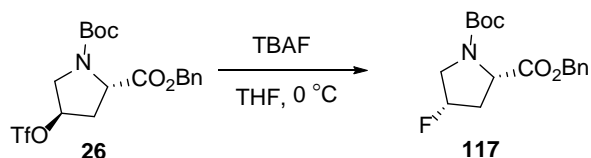
### 3.7.2 Synthesis of flp

A number of studies have reported the synthesis of flp derivatives. In our first attempt to synthesize flp we followed a procedure published by Raines and coworkers<sup>79</sup> (Scheme 3.13). This route involves activation of the 4-hydroxyproline derivative **113** with trifluoromethanesulfonic anhydride (Tf<sub>2</sub>O) to form the triflate ester followed by the S<sub>N</sub>2 displacement by fluoride ion to get inversion of configuration at C4.



Scheme 3.13: Synthesis of flp by Raines and coworkers.<sup>79</sup>

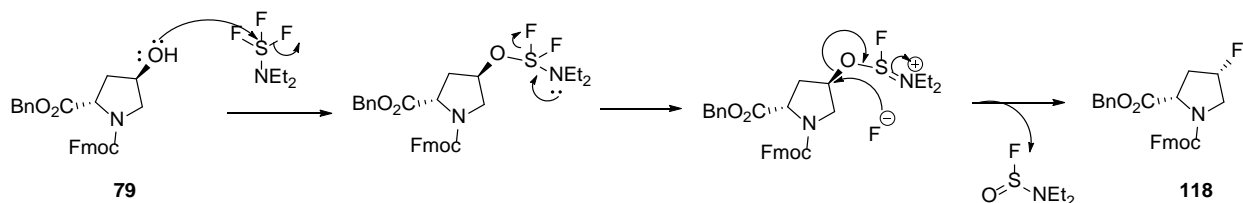
For the synthesis of flp we utilized Boc-Hyp(OTf)-OBn (**26**) that we had prepared previously for the bisubstrate analog project (§2.3.2, Scheme 2.6). We treated triflate **26** with tetrabutylammonium fluoride (TBAF) to afford Boc-flp-OBn (**117**) (Scheme 3.14). Thin layer chromatography showed the formation of the product **117**, but purification was difficult due to traces of tetrabutylammonium triflate.



Scheme 3.14: Synthesis of Boc-flp-OBn (**117**)

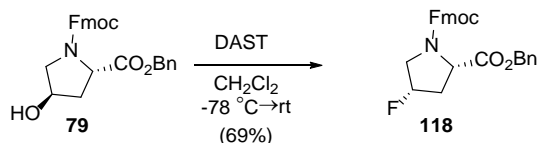
Our next attempt employed diethylaminosulfur trifluoride (DAST) as the fluorinating reagent. This route eliminates the extra step of synthesizing the triflate as DAST itself both

activates the hydroxyl group and introduces the fluoride ion (Scheme 3.15). There are reports published utilizing DAST as the fluorinating reagent in fluoroproline synthesis and their reported yields are good.<sup>80-81</sup>



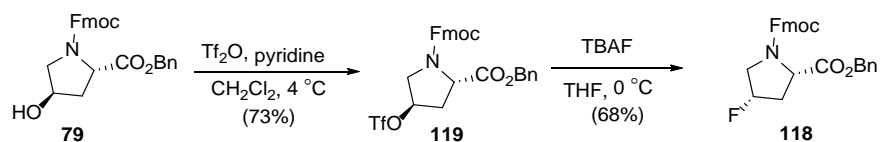
Scheme 3.15: Mechanism for fluorination using DAST

We thus began our synthesis anew with Fmoc-Hyp-OBn (**79**) which was available from the glycopeptide project (§3.3). This was treated with DAST (Scheme 3.16) to give compound **118**. The <sup>1</sup>H NMR of **118** showed extra peaks around 0.8-1.5 and 3.5 ppm region which are due to the ethyl groups of DAST or byproducts thereof. We were unable to remove these impurities by flash chromatography to get pure **118**.



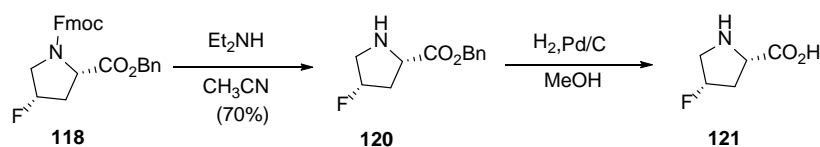
Scheme 3.16: Synthesis of Fmoc-flp-OBn (**118**)

Our next approach to flp was via a triflate formed from the Fmoc-Hyp-OBn (**118**) building block. We hoped that changing the carbamate protecting group on the pyrrolidine would result in a change in polarity and allow us to perform more effective purification. We made the triflate ester of **79** by treating with triflic anhydride (Scheme 3.17). The triflate **119** was then treated with TBAF to get Fmoc-flp-OBn (**118**), that was successfully purified using flash chromatography.



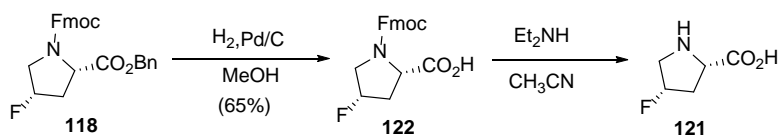
Scheme 3.17: Synthesis of Fmoc-flp-OBn (**118**)

With compound **118** in-hand our next plan was to remove the Fmoc protecting group. We treated **118** with diethylamine (Scheme 3.18) and the free amine was purified using flash chromatography. Next we subjected benzyl ester **120** to catalytic hydrogenolysis to obtain **121** which, once again was not of satisfactory purity.



Scheme 3.18: Synthesis of H-flp-OH (**121**)

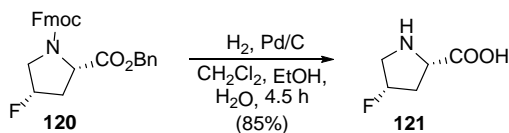
We thought it might be advantageous to swap the order of deprotections. First we did the hydrogenolysis of **118** to get free acid **122** (Scheme 3.19). The acid **122** was purified by flash chromatography and then treated with diethylamine to remove the Fmoc protecting group. Formation of the product **121** was confirmed by TLC. For the purification of **121** we used an ion exchange column, but unfortunately **121** eluted with excess diethylamine and once again we were unable to obtain pure flp.



Scheme 3.19: Synthesis of H-flp-OH (**121**)

In 2000, a paper published by Boons *et al.* reported removal of Fmoc and benzyl ester protecting groups simultaneously by catalytic hydrogenolysis using a mixture of solvents. We decided to test their procedure on Fmoc-flp-OBn (**118**). To our delight this method gave us pure

H-flp-OH (**121**) in good yield (Scheme 3.20). We sent compound **121** to West's laboratory for further investigation. We propose two studies using flp; (1) Feed flp to *Dictyostelium discoideum* and look for its incorporation into Skp1. (2) Incorporation of flp into a short peptide sequence and study processing by the P4H1 of *Dictyostelium discoideum*.

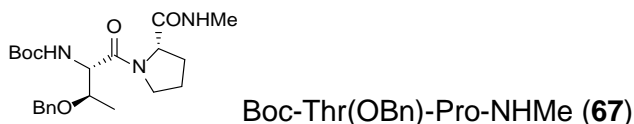


Scheme 3.20: Synthesis of H-flp-OH (**121**)

### 3.8 Experimental

#### 3.8.1 Synthetic Procedures

**General Methods:** As for Chapter 2, with the following additions. Methylamine hydrochloride was recrystallized in ethanol. HPLC was performed on Waters 600E multisolvent delivery system (Waters 2487 dual  $\lambda$  absorbance detector). NMR spectra were recorded on a Bruker DPX-400, or Varian-700 spectrometer. Many of the compounds reported in this chapter exist as mixture of rotomers about the prolyl amide bond on the time scale of  $^1\text{H}$  NMR. Signals in square parentheses refer to those of the minor rotomer.

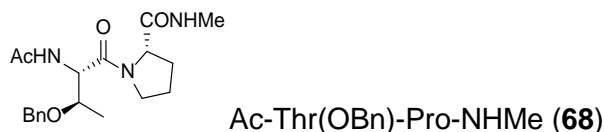


**Boc-Thr(OBn)-Pro-OH (66).** *N*-Hydroxysuccinimide (75 mg, 0.65 mmol, 1 equiv.) and DCC (133 mg, 0.65 mmol, 1 equiv.) were added sequentially to a solution of Boc-Thr(OBn)-OH (**64**) (200 mg, 0.65 mmol, 1 equiv.) in  $\text{CH}_2\text{Cl}_2$  (5 mL), at 0 °C. The solution was stirred at 0 °C for another 15 min, warmed to rt and stirred overnight under  $\text{N}_2$ . The suspension was filtered through a plug of cotton in a Pasteur pipet. The filtrate was concentrated to 2 mL and refrigerated 5 h. The suspension was again filtered and the filtrate was concentrated. The

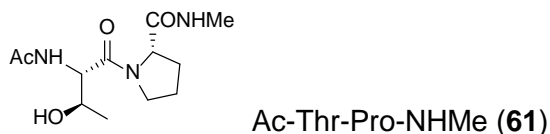
residue was dissolved in DMF (2 mL) and cooled to 0 °C. Proline (**65**) (74 mg, 0.65 mmol, 1 equiv.) was added, as a solid in one portion, followed by the addition of diisopropylethylamine (113  $\mu$ L, 84 mg, 0.65 mmol, 1 equiv.). The reaction mixture was gradually warmed to rt and stirred overnight under N<sub>2</sub>. The solution was concentrated and dissolved in water (25 mL) and washed with diethyl ether (25 mL). The aqueous layer was acidified with conc. HCl (pH = 2) and extracted with EtOAc (2 x 25 mL). The organic layers were combined, dried over MgSO<sub>4</sub>, filtered and concentrated to give **66** that was used directly in the next step, without purification. *R*<sub>f</sub> 0.20 (4:1 CH<sub>2</sub>Cl<sub>2</sub>:MeOH).

*Boc-Thr(OBn)-Pro-NHMe (67)*. Compound **66** was dissolved in CH<sub>2</sub>Cl<sub>2</sub> (5 mL) and cooled to 0 °C. *N*-Hydroxysuccinimide (75 mg, 0.65 mmol, 1.0 equiv.) was added, followed by the addition of DCC (133 mg, 0.65 mmol, 1.0 equiv.). The solution was stirred for 30 min at 0 °C, then gradually warmed to RT and stirred a further 6 h. The suspension was filtered through a plug of cotton in a Pasteur pipet. The filtrate was concentrated to 2 mL and refrigerated overnight. The suspension was again filtered and the filtrate was concentrated. The residue was dissolved in DMF (3 mL), cooled to 0 °C. Methylamine hydrochloride (44 mg, 0.65 mmol, 1.0 equiv.) was added as a solid in one portion, followed by the addition of triethylamine (225  $\mu$ L, 163 mg, 1.62 mmol, 2.5 equiv.). The solution was gradually warmed to rt and stirred overnight under N<sub>2</sub>. This was diluted with EtOAc (30 mL), washed with brine (30 mL). The aqueous layer was back-extracted with EtOAc (30 mL). The organic layers were combined, dried over MgSO<sub>4</sub>, filtered and concentrated. Dipeptide **67** was isolated by flash chromatography, eluting with 4:1 EtOAc:hexanes (209 mg, 81% over 2 steps). *R*<sub>f</sub> 0.22 (4:1 EtOAc:hexanes). <sup>1</sup>H NMR (CDCl<sub>3</sub>, 400 MHz)  $\delta$  1.16 [1.21]\* (d, *J* = 6.1, 3H), 1.45 [1.44] (s, 9H), 1.58-1.96 (m, 4H), 2.81 (d, *J* = 4.7 Hz, 3H), 3.35-3.57 (m, 2H), 3.77-3.81 (m, 0.5H), 4.18-4.25 (m, 1.5H), 4.48-4.64 (m, 3H), 5.50 (d, *J* = 6.4 Hz, 0.5H) [5.59 (d, *J* = 8.5 Hz, 0.5H)], 6.53 (s, 1H); <sup>13</sup>C NMR (CD<sub>3</sub>OD, 100 MHz)  $\delta$  16.1

[15.8], 24.2 [25.1], 26.4 [26.3], 28.4 [28.5], 34.1, 46.8 [46.2], 56.1, 58.0, 71.8 [71.0], 75.0 [74.7], 80.0 [80.2], 127.8, 127.9, 128.0, 128.5, 128.6, 138.2 138.3, 155.8 [156.0], 168.6, 170.7.

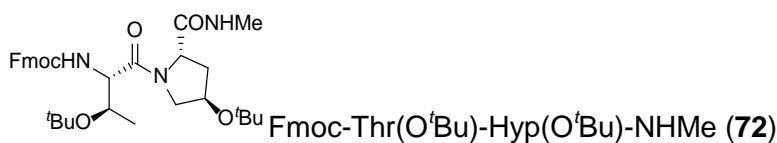


Trifluoroacetic acid (1 mL) was added to a solution of Boc-Thr(OBn)-Pro-NHMe (**67**) (93 mg, 0.222 mmol) in CH<sub>2</sub>Cl<sub>2</sub> (2 mL) at 0 °C. The reaction mixture was gradually warmed to RT and stirred for 2 h under N<sub>2</sub>. The solution was concentrated and then concentrated three times from CH<sub>2</sub>Cl<sub>2</sub>. The residue was dissolved in pyridine (1 mL) and cooled to 0 °C. Acetic anhydride (1 mL) was added, the mixture warmed to RT and stirred under N<sub>2</sub> overnight. The solution was concentrated and applied to a flash column, eluting first with 4:1 EtOAc:hexanes and then with 9:1 CH<sub>2</sub>Cl<sub>2</sub>:MeOH to give **68** (54 mg, 67%). *R<sub>f</sub>* 0.48 in 9:1 CH<sub>2</sub>Cl<sub>2</sub>:MeOH. <sup>1</sup>H NMR (CD<sub>3</sub>OD, 400 MHz)\* δ 1.18 [1.21] (d, *J* = 6.3 Hz, 3H), 1.75-1.90 (m, 1H), 1.95-2.05 (m, 2H), 2.03 [1.99] (s, 3H), 3.33-3.44 (m, 1.5H) [3.62-3.68 (m, 0.5H)], 4.08 (ddd, *J* = 12.6, 6.4, 3.2 Hz, 0.7H) [3.86 (dt, *J* = 11.4, 6.3 Hz, 0.3H)], 4.38 (d, *J* = 3.1 Hz, 1H), 4.43 (d, *J* = 11.8 Hz, 0.7H) [4.46 (d, *J* = 12.0 Hz, 0.3H)], 4.57 (d, *J* = 11.8 Hz, 0.7H) [4.62 (d, *J* = 12.0 Hz, 0.3H)], 4.70 (d, *J* = 5.1 Hz, 1H), [4.70-4.72 (m, 0.7H)] 7.23- 7.26 (m, 5H); <sup>13</sup>C NMR (CD<sub>3</sub>OD, 100 MHz) δ 16.8 [16.6], 22.7 [22.5], 25.1, 26.6, 27.1, 48.2 [47.4], 57.3, 59.5, 72.5 [72.0], 75.8 [75.1], 128.8 [128.9], 129.1 [129.2], 129.4 [129.5], 139.8, 170.4, 173.3 [173.4], 174.0.



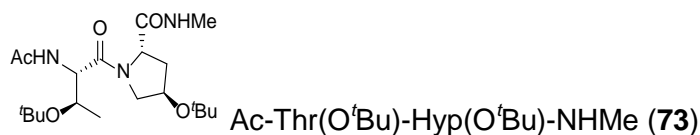
Palladium on carbon (10%, 15 mg) was added in a single portion to a solution of Ac-Thr(OBn)-Pro-NHMe (**68**) (17 mg, 0.05 mmol) in MeOH (2.5 mL). The reaction flask was evacuated, then opened to an atmosphere of H<sub>2</sub> and stirred overnight. The catalyst was removed by filtering through a plug of Celite<sup>®</sup> in a Pasteur pipet. The filtrate was concentrated,

the brown residue was subjected to the RP-HPLC (gradient: 50%-80% acetonitrile in H<sub>2</sub>O, C<sub>18</sub> 4.6 mm x 250 mm column 1 mL/min) (*R*<sub>T</sub> = 16 min) to give **61** (12 mg, 94%). *R*<sub>f</sub> 0.24 (9:1 CH<sub>2</sub>Cl<sub>2</sub>:MeOH). [α]<sub>D</sub><sup>25</sup> -5.4 (*c* 0.5, MeOH). <sup>1</sup>H NMR (D<sub>2</sub>O, 400 MHz) δ 1.24 [1.26]\* (d, *J* = 5.9 Hz, 3H), 1.91-1.97 (m, 2H), 2.02 (dd, *J* = 12.3, 5.8 Hz, 2H), 2.14 [2.11] (s, 3H), 2.80 (s, 3H), 3.41 (dd, *J* = 12.0, 6.6 Hz, 0.5H), 3.50 (dd, *J* = 12.0, 6.6 Hz, 0.5 H), 3.62-3.81 (m, 1H), 4.15 (app. p, *J* = 6.3 Hz, 0.5 H), 4.27-4.30 (m, 2H), 4.60 (d, *J* = 5.9 Hz, 0.5 H); <sup>13</sup>C NMR (D<sub>2</sub>O, 100 MHz) δ 18.7 [18.4], 21.7 [21.5], 23.6, 25.4, 25.8, 47.4 [46.5], 57.1, 59.3, 66.8 [66.9]169.7, 172.5, 174.8 [174.2].

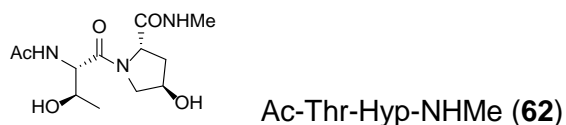


Diethylamine (800 μL) was added to a solution of Fmoc-Hyp-(O<sup>t</sup>Bu)-NHMe (**70**) (65 mg, 0.15 mmol, 1 equiv.) in acetonitrile (3 mL). The solution was stirred at 0 °C under N<sub>2</sub> for 30 min, concentrated and then concentrated twice more from acetonitrile. The residue was suspended in dichloromethane (2 mL), and cooled to 0 °C. Fmoc-Thr(O<sup>t</sup>Bu)OH (**71**) (71 mg, 0.18 mmol, 1.5 equiv.) was added followed by the addition of diisopropylethylamine (68 μL, 50 mg, 0.39 mmol, 2.5 equiv.) and PyBroP (108 g, 0.23 mmol, 1.5 equiv.). The solution was gradually warmed to rt and stirred overnight under N<sub>2</sub>. The mixture was concentrated and the residue applied to a flash column, eluting with 4:1 EtOAc:hexanes to give **72** (87 mg, 98%). *R*<sub>f</sub> 0.41 (4:1 EtOAc:hexanes). <sup>1</sup>H NMR (CD<sub>3</sub>OD, 400 MHz) δ 1.16 (d, *J* = 8.4 Hz, 3H), 1.19 (s, 9H), 1.23 (s, 9H), 2.03-2.18 [2.20-2.27]\* (m, 2H), 2.75 [2.77] (s, 3H), 3.62 (dd, *J* = 10.5, 3.5 Hz, 1H) [3.43 (dd, *J* = 12.2, 4.2 Hz)], 3.94 (dd, *J* = 10.5, 5.3 Hz, 1H) [3.75 (dd, *J* = 12.2, 5.8 Hz)], 3.98 (p, *J* = 6.0 Hz, 1H), 4.19 (t, *J* = 6.4 Hz, 1H), 4.39-4.42 (m, 1H), 4.44 (d, *J* = 2.3 Hz, 2H), 4.44 (d, *J* = 2.3 Hz, 1H), 4.54 (t, *J* = 7.4 Hz, 1H), 7.29-7.33 (m, 2H), 7.39 (t, *J* = 7.4 Hz, 2H) 7.65 (d, *J* = 7.4 Hz, 2H), 7.78 (d, *J* = 7.5 Hz, 2H); <sup>13</sup>C NMR (CD<sub>3</sub>OD, 100 MHz) δ 19.6 [20.1], 26.3 [26.4], 28.6 [28.7], 38.6 [40.7],

47.0 [47.1], 48.5, 56.5 [55.4], 58.9 [58.5], 60.6 [60.9], 67.9 [68.0], 69.8 [69.2], 75.5 [75.3], 76.2 [75.8], 121.0, 126.2, 128.2, 128.9, 142.6, 145.1 [145.3], 158.2, 171.5, 174.6. HRMS (+ESI) calcd for C<sub>33</sub>H<sub>46</sub>N<sub>3</sub>O<sub>6</sub> (M+H)<sup>+</sup>: 580.3381; obsd: 580.3395.



Diethylamine (2 mL) was added to a solution of **72** (119 mg, 0.21 mmol, 1 equiv.) in acetonitrile (3 mL). The solution was stirred at 0 °C under N<sub>2</sub> for 30 min, concentrated, and then concentrated twice more from acetonitrile. The residue was applied to a flash column, eluting first with 2:1 EtOAc:hexanes to remove Fmoc byproducts and then with 9:1 CH<sub>2</sub>Cl<sub>2</sub>:MeOH to isolate the ninhydrin active primary amine (*R<sub>f</sub>* 0.36 in 9:1 CH<sub>2</sub>Cl<sub>2</sub>:MeOH) as a pale yellow oil (**73** mg). This was dissolved in a mixture of pyridine (1 mL) and acetic anhydride (1 mL), stirred at rt under N<sub>2</sub> overnight. The red solution was concentrated and purified using flash chromatography, eluting with 9:1 CH<sub>2</sub>Cl<sub>2</sub>:MeOH to isolate compound **73** as a colorless foam (71 mg, 93%). *R<sub>f</sub>* 0.40 (9:1 CH<sub>2</sub>Cl<sub>2</sub>:MeOH). <sup>1</sup>H NMR (CDCl<sub>3</sub>, 400 MHz) δ 1.09 (d, *J* = 6.4 Hz, 3H), 1.19 (s, 9H), 1.28 (s, 9H), 2.01 (s, 3H), 2.05 (dt, *J* = 12.3, 8.4 Hz, 1H), 2.37 (ddd, *J* = 12.7, 6.1, 3.0 Hz, 1H), 2.75 [2.83]\* (d, *J* = 4.7 Hz, 3H), 3.42 (dd, *J* = 10.2, 6.2 Hz, 1H), 4.07-4.13 (m, 2H), 4.28 (p, *J* = 6.8 Hz, 1H), 4.75 (dd, *J* = 9.0, 2.9 Hz, 1H), 4.81 (dd, *J* = 7.4, 4.8 Hz, 1H), 6.62 [6.68] (d, *J* = 4.4 Hz, 1H), 6.93 [7.05] (d, *J* = 8.0 Hz, 1H); <sup>13</sup>C NMR (CDCl<sub>3</sub>, 100 MHz) δ 17.5, 23.1, 25.9, 28.0, 28.2, 36.5, 54.5, 54.6, 58.7, 68.0, 69.1, 74.2, 75.4, 169.2, 169.8, 171.7. HRMS (+ESI) calcd for C<sub>20</sub>H<sub>38</sub>N<sub>3</sub>O<sub>5</sub> (M)<sup>+</sup>: 400.2806; obsd: 400.2802.



Trifluoroacetic acid (1.5 mL) was added to a solution of Ac-Thr(O<sup>t</sup>Bu)-Hyp(O<sup>t</sup>Bu)-NHMe (**73**) (130 mg, 0.325 mmol) in CH<sub>2</sub>Cl<sub>2</sub> (1.5 mL) at 0 °C. The mixture was gradually warmed to rt



and stirred under N<sub>2</sub> for two days. The solution was concentrated and then concentrated three times from CH<sub>2</sub>Cl<sub>2</sub>. The brown residue was subjected to the RP-HPLC (gradient: starting with 80% H<sub>2</sub>O in acetonitrile to 20% H<sub>2</sub>O in acetonitrile) (*R*<sub>T</sub> = 4 min) to isolate **62** as a colorless oil (84 mg, 90%). [ $\alpha$ ]<sub>D</sub><sup>25</sup> -17.1 (*c* 0.3, MeOH). <sup>1</sup>H NMR (D<sub>2</sub>O, 400 MHz)  $\delta$  1.23 [1.18]\* (d, *J* = 4.2 Hz, 3H), 2.06 (s, 3H), 2.08 (dd, *J* = 9.7, 4.3 Hz, 1H), 2.31 (dd, *J* = 13.8, 7.6 Hz, 1H), 2.75 (s, 3H), 3.86 (dd, *J* = 11.6, 3.6 Hz, 1H), 3.95 (d, *J* = 11.6 Hz, 1H), 4.10 (app.p, *J* = 6.3 Hz, 1H), 4.48 (dd, *J* = 9.6, 7.8 Hz, 1H), 4.57-4.60 (m, 2H); <sup>13</sup>C NMR (D<sub>2</sub>O, 100 MHz)  $\delta$  18.5, 21.5, 25.8, 37.0, 56.0, 57.2, 59.5, 67.1, 69.7, 171.0, 173.8, 174.2; HRMS (+ESI) calcd for C<sub>12</sub>H<sub>22</sub>N<sub>3</sub>O<sub>5</sub> (M+H)<sup>+</sup>: 288.1554; obsd: 288.1553.

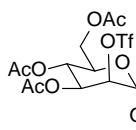


D-Mannose (**74**) (about 100 mg), followed by perchloric acid (2 drops from a Pasteur pipette), were added to acetic anhydride (20 mL) in a two-neck, 250 mL round-bottomed flask fitted with a thermometer. D-Mannose (total of 5 g, 28 mmol, 1.0 equiv.) was then added in small portions over a period of 1 h, keeping the reaction temperature in the range of 40-45 °C. Once the addition was complete, the dark yellow solution was stirred for 1 h at RT.

The reaction mixture was cooled to 8 °C and phosphorus tribromide (4 mL, 11.4 g, 42 mmol, 1.5 equiv.) was added dropwise. Water (2 mL, 2 g, 126 mmol, 4.5 equiv.) was added dropwise. The internal temperature of the reaction mixture was maintained in the range 18-25 °C. Once the addition was complete the orange brown solution was stirred at room temperature for 1.5 h. The resulting anomeric bromide (*R*<sub>f</sub> 0.49, 1:1 Hexane/EtOAc) was use directly to the next step.

The reaction mixture was cooled to 5 °C and a cooled (5 °C) solution of sodium acetate (9.2 g, 112 mmol, 4.0 equiv.) in water (20 mL) was added dropwise over 30 min, maintaining the

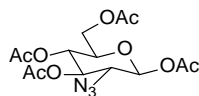
internal temperature at 20-25 °C. The mixture was stirred at RT for 20 min then poured onto ice and extracted with chloroform (2 x 100 mL). The extracts were combined and washed with ice-water (200 mL), saturated aqueous NaHCO<sub>3</sub> containing ice (200 mL) and ice water again. The yellow-orange organic layer was dried over MgSO<sub>4</sub>, filtered and concentrated. Diethyl ether (80 mL) was added and the solution was left overnight in the freezer. The crystallized product was collected by filtration and washed with ice-cold ether to give 1,3,4,6-tetra-*O*-acetylmannose (**75**) as a colorless crystalline solid (947 mg, 10% yield). *R<sub>f</sub>* 0.4 (4:1 EtOAc/Hexane).  $[\alpha]_D^{25} - 24.3$  (*c* 1.0, MeOH). <sup>1</sup>H NMR (CDCl<sub>3</sub>, 400 MHz)  $\delta$  2.05 (s, 3H), 2.09 (s, 3H), 2.12 (s, 3H), 2.18 (s, 3H), 2.47 (d, *J* = 3.9 Hz, 1H), 3.79 (ddd, *J* = 9.8, 4.8, 2.3 Hz, 1H), 4.13 (dd, *J* = 12.4, 2.2 Hz, 1H), 4.20 (app. t, *J* = 3.1 Hz, 1H), 4.30 (dd, *J* = 12.5, 5.0 Hz, 1H), 5.04 (dd, *J* = 9.8, 3.0 Hz, 1H), 5.39 (t, *J* = 9.8 Hz, 1H), 5.79 (d, *J* = 0.4 Hz, 1H); <sup>13</sup>C NMR (CDCl<sub>3</sub>, 100 MHz)  $\delta$  20.8, 20.9, 21.0, 21.1, 62.2, 65.4, 68.6, 73.0, 73.3, 91.9, 168.8, 169.8, 170.3, 171.0.



OAc 1,3,4,6-Tetra-*O*-acetyl-trifluorosulfonyl- $\beta$ -*D*-manopyranose (**76**)

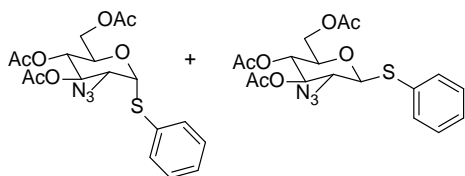
Triflic anhydride (625  $\mu$ L, 1.048 g, 3.72 mmol, 2.0 equiv.) was added dropwise to a solution of 1,3,4,6-tetra-*O*-acetylmannose (**75**) (647 mg, 1.86 mmol, 1.0 equiv.) and pyridine (376  $\mu$ L, 4.65 mmol, 2.5 equiv.) in CH<sub>2</sub>Cl<sub>2</sub> (10 mL) at -25 °C. Once the addition was complete, the mixture was stirred at -25 °C for 45 min, diluted with CH<sub>2</sub>Cl<sub>2</sub> (200 mL) and washed with water (400 mL), saturated aqueous NaHCO<sub>3</sub> (400 mL) and water (400 mL) again. The organic layer was dried over MgSO<sub>4</sub>, filtered and concentrated to give the triflate **76** (834 mg, 93% yield) as a yellow foam. *R<sub>f</sub>* 0.56 (1:1 Hexane:EtOAc).  $[\alpha]_D^{25} -14.3$  (*c* 1.0, MeOH). <sup>1</sup>H NMR (CDCl<sub>3</sub>, 400 MHz)  $\delta$  2.07 (s, 3H), 2.10 (s, 3H), 2.12 (s, 3H), 2.17 (s, 3H), 3.86 (ddd, *J* = 7.5, 5.2, 2.4 Hz, 1H), 4.17 (dd, *J* = 12.5, 2.2 Hz, 1H), 4.25 (dd, *J* = 12.5, 5.2 Hz, 1H), 5.16 (d, *J* = 2.8 Hz, 1H), 5.22 (dd, *J* = 10.1, 2.8 Hz, 1H), 5.30 (app. t, *J* = 9.9 Hz, 1H), 5.95 (s, 1H); <sup>13</sup>C NMR (CDCl<sub>3</sub>, 100

MHz)  $\delta$  20.6 (2C), 20.7, 20.8, 61.8, 64.7, 69.8, 73.6, 81.6, 89.3, 118.6 (q,  $J_{CF} = 319.5$  Hz), 168.2, 169.4, 170.1, 170.8. HRMS (+ESI) calcd for  $C_{15}H_{19}F_3NaO_{12}S$  ( $M+Na$ )<sup>+</sup>: 503.0442; obsd: 503.0444.



2-Azido-1,3,4,6-tetra-O-acetyl- $\beta$ -D-glucopyranose (**77**)

Sodium azide (226 mg, 3.5 mmol, 2.0 equiv.) was added to a solution of triflate **76** (834 mg, 1.74 mmol, 1.0 equiv.) in DMF (6 mL). The solution warmed to 40 °C and stirred for 2 h under nitrogen. The mixture was cooled to RT, diluted with  $CH_2Cl_2$  (200 mL), washed with water (300 mL) and brine (300 mL). The organic layer was dried over  $MgSO_4$ , filtered and concentrated. The residue was applied to a flash column, eluting with 1:1 Hexane:EtOAc to give the azide **77** (582 mg, 90%).  $R_f$  0.64 (1:1 Hexane:EtOAc).  $[\alpha]_D^{25} +9.2$  (c 1.0, MeOH).  $^1H$  NMR ( $CDCl_3$ , 400 MHz)  $\delta$  2.03 (s, 3H), 2.08 (s, 3H), 2.10 (s, 3H), 2.20 (s, 3H), 3.67 (app.t,  $J = 9.2$  Hz, 1H), 3.83 (ddd,  $J = 9.6, 4.2, 1.9$  Hz, 1H), 4.08 (dd,  $J = 12.6, 1.6$  Hz, 1H), 4.31 (dd,  $J = 12.5, 4.4$  Hz, 1H), 5.05 (app. t,  $J = 9.6$  Hz, 1H), 5.11 (app. t,  $J = 9.6$  Hz, 1H), 5.58 (d,  $J = 8.6$  Hz, 1H);  $^{13}C$  NMR ( $CDCl_3$ , 100 MHz)  $\delta$  20.6, 20.7, 20.8, 21.0, 61.5, 62.7, 67.9, 72.7, 72.8, 92.7, 168.6, 162.7, 169.9, 170.6. HRMS (+ESI) calcd for  $C_{14}H_{19}N_3NaO_9$  ( $M+Na$ )<sup>+</sup>: 396.1019; obsd: 396.0994.



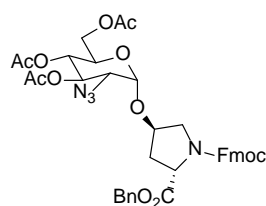
Thiobenzyl [2-azido-tri-O-acetylgluco]pyranose (**78**)

$BF_3 \cdot OEt_2$  (1.44 mL, 1.654 g, 12 mmol, 15 equiv.) was added to a solution of **77** (290 mg, 0.777 mmol, 1 equiv.) and thiophenol (198  $\mu$ L, 214 mg, 1.94 mmol, 2.5 equiv.) in  $CH_2Cl_2$  (6 mL) at RT. The reaction mixture was heated at reflux for 2 h under nitrogen, cooled to RT and stirred overnight. The reaction was quenched by the dropwise addition of water (2 mL). The mixture was diluted with  $CH_2Cl_2$  (75 mL) and washed with water (75 mL), then brine (75 mL). The

organic layer was dried over MgSO<sub>4</sub>, filtered and concentrated. The residue was applied to a flash column eluting with 2:1 Hexanes:EtOAc to give the thioglycoside **78** (262 mg, 80%) as a 3:1 mixture of anomers ( $\alpha$ : $\beta$ ) which cannot be distinguished by TLC.  $R_f$  0.70 (1:1 Hexanes:EtOAc). For clarity data are reported separately for two isomers.

Data for  $\alpha$ -anomer (major): <sup>1</sup>H NMR (CDCl<sub>3</sub>, 400 MHz)  $\delta$  2.02 (s, 3H), 2.05 (s, H), 2.10 (s, 3H), 4.03 (dd,  $J$  = 12.4, 2.0 Hz, 1H), 4.09 (dd,  $J$  = 10.3, 5.5 Hz, 1H), 4.24 (dd,  $J$  = 12.4, 5.2 Hz, 1H) 4.60 (ddd,  $J$  = 10.0, 5.2, 2.0 Hz, 1H), 5.34 (dd,  $J$  = 10.2, 9.5 Hz, 1H), 5.34 (dd,  $J$  = 10.2, 9.5 Hz, 1H), 5.65 (d,  $J$  = 5.5 Hz, 1H), 7.30-7.34 (m, 5H); <sup>13</sup>C NMR (CDCl<sub>3</sub>, 100 MHz)  $\delta$  20.6, 20.7, 20.8, 61.6, 62.0, 68.6, 68.8, 72.1, 86.5, 128.1, 129.3, 132.3, 134.2, 169.7, 169.8, 170.5.

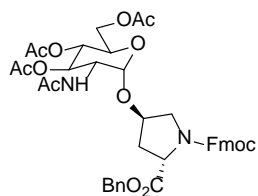
Data for  $\beta$ -anomer (minor): 2.01 (s, 3H), 2.03 (s, 3H), 2.08 (s, 3H), 3.41 (app.t,  $J$  = 9.9 Hz, 1H), 3.71 (ddd,  $J$  = 10.1, 4.8, 2.4 Hz, 1H), 4.09-4.78 (m, 1H), 4.17 (dd,  $J$  = 12.3, 2.3 Hz, 1H), 4.24 (dd,  $J$  = 12.3, 4.8 Hz, 1H), 4.51 (d,  $J$  = 10.2 Hz, 1H)], 7.30-7.34 (m, 5H); <sup>13</sup>C NMR (CDCl<sub>3</sub>, 100 MHz)  $\delta$  20.6, 20.7, 20.8, 62.1, 62.7, 68.1, 74.5, 75.6, 85.8, 129.0, 129.2, 130.3, 132.5, 169.7, 169.8, 170.5. HRMS (+ESI) calcd for C<sub>18</sub>H<sub>21</sub>N<sub>3</sub>NaO<sub>7</sub>S (M+Na)<sup>+</sup>: 446.0998; obsd: 446.0568.



Fmoc-Hyp-4-O-(2-azido-3,4,6-tetra-O-acetyl- $\alpha$ -D-glucopyranosyl)-OBn (**80**)

A solution of thioglycoside **78** (68 mg, 0.16 mmol, 1.0 equiv.) and Fmoc-Hyp-OBn (**79**) (78 mg, 0.18 mmol, 1.1 equiv.) in CH<sub>2</sub>Cl<sub>2</sub> (6 mL) was stirred with activated, powdered 4Å molecular sieves for 25 min at RT under nitrogen. The mixture was cooled to -78 °C, NIS (54 mg, 0.24 mmol, 1.5 equiv.) and silver triflate (21 mg, 0.09 mmol, 0.5 equiv.) were added. The mixture was allowed to reach 0 °C over 3 h, quenched with Et<sub>3</sub>N (1 mL), diluted with EtOAc (75

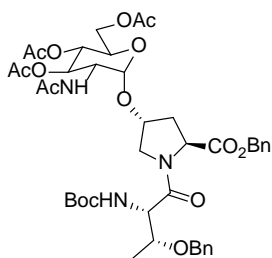
mL), washed with 10% aq. Na<sub>2</sub>S<sub>2</sub>O<sub>3</sub> (75 mL), and brine (75 mL). The organic layer was dried over MgSO<sub>4</sub>, filtered, concentrated and submitted directly to flash chromatography, eluting with 1:1 Hexane:EtOAc to give the α-O-glycoside **80** (71 mg, 59% yield). *R<sub>f</sub>* 0.36 (1:1 Hexane:EtOAc). [α]<sub>D</sub><sup>25</sup> +49.7 (*c* 1.0, MeOH). <sup>1</sup>H NMR (CDCl<sub>3</sub>, 400 MHz) δ 2.01(s, 3H), 2.05 (s, 2H) [2.06 (s, 1H)]\*, 2.07 (s, 1.8 H) [2.08 (s, 1.2H)], 2.15-2.25 (m, 1H), 2.50-2.55 (m, 1H), 3.25 (2xddd, *J* = 10.7, 3.6, 1H), 3.68-3.91 (m, 2H), 3.96-4.0 (m, 0.5H), 4.01-4.10 (m, 2H), 4.20-4.29 (m, 2.5H), 4.41-4.46 (m, 3H), 4.58 (t, *J* = 7.7 Hz, 1H), 4.98-5.08 (m, 2H), 5.12-5.26 (m, 2H), 5.45 (ddd, *J* = 12.8, 10.7, 3.5 Hz, 1H), 7.23-7.51 (m, 9H), 7.53-7.60 (m, 2H), 7.72-7.78 (m, 2H); <sup>13</sup>C NMR (CDCl<sub>3</sub>, 100 MHz) δ 20.8, 20.9, 36.3 [37.6], 47.3, 51.8, 58.0 [58.3], 60.5 [60.7], 62.1 [62.3], 67.3 [67.4], 68.0, 68.5, 68.7, 70.1 [70.0], 75.0 [77.6], 96.9 [97.9], 101.2, 120.2, 120.0, 125.2, 125.3, 125.4, 127.2, 127.3, 127.9, 127.8, 128.4, 128.6, 128.5, 128.8 128.7, 135.6, 135.4, 141.4, 141.5, 144.0, 143.9, 144.2, 144.1, 154.7, [154.9], 169.7, [169.8], 170.1, [170.2], 170.7, 172.1, [172.2]. HRMS (+ESI) calcd for C<sub>39</sub>H<sub>40</sub>N<sub>4</sub>NaO<sub>12</sub> (M+Na)<sup>+</sup>: 779.2540; obsd: 779.2556.



Fmoc-Hyp-[(α,1-4)GlcNAc(OAc)<sub>4</sub>]-OBn (**81**)

Zinc powder (50 mg) and saturated aqueous CuSO<sub>4</sub> (20 μL) were added to a solution of **80** (135 mg, 0.18 mmol) in THF (2 mL) at RT. Acetic acid (0.5 mL) and acetic anhydride (0.5 mL) were added and the mixture stirred overnight at RT. The reaction mixture was filtered and the filtrate concentrated and applied directly to a flash column, eluting with 4:1 EtOAc:Hexane to give the N-acetylated product **81** (114 mg, 83% yield). *R<sub>f</sub>* 0.45 (4:1 EtOAc:Hexanes). [α]<sub>D</sub><sup>25</sup> +17.72 (*c* 1.0, MeOH). <sup>1</sup>H NMR (CDCl<sub>3</sub>, 400 MHz) δ 1.87 (s, 1.7H) [1.88 (s, 1.3 H), 2.02 (s, 3H), 2.04 (s, 3H), 2.05 (3H), 2.18-2.24 (m, 1H), 2.48-2.54 (m, 1H), 3.51-3.77 (m, 2H), 3.95 (ddd, *J* = 9.7, 5.0, 2.2 Hz, 01H), 4.02 (t, *J* = 6.7 Hz, 0.3 H), 4.10 (d, *J* = 12.2 Hz, 1H), 4.20-4.46 (m, 5.7H),

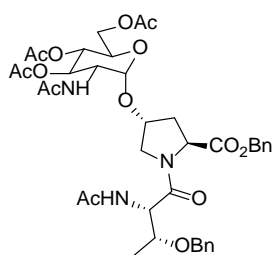
4.51-4.6 (m, 1H), 4.91 (d,  $J = 13.0, 3.1$  Hz, 0.6H) [4.95 (d,  $J = 13.0, 3.1$  Hz, 0.4H)], 4.95-5.24 (m, 5H), 5.61-5.73 (m, 1H);  $^{13}\text{C}$  NMR ( $\text{CDCl}_3$ , 100 MHz)  $\delta$  20.8, 20.9, 20.9, 23.3, 37.5 [36.3], 47.3, 51.7 [52.4], 51.8 [52.1], 58.0 [58.4], 62.3, 67.4, 68.1 [68.2], 68.4, 68.7, 71.0, 76.1 [76.8], 97.3 [97.0], 120.2, 125.1, 125.3, 127.3, 128.0, 128.4, 128.6, 128.7, 128.8, 135.3, 141.5, 143.7, 144.1, 144.3, 154.8, 169.5, 170.2, 170.8 [170.4], 171.6, 172.0. HRMS (+ESI) calcd for  $\text{C}_{41}\text{H}_{44}\text{N}_2\text{NaO}_{13}$  ( $\text{M}+\text{Na}$ ) $^+$ : 795.2741; obsd: 795.2700.



Boc-Thr(OBn)-Hyp-[( $\alpha,14$ )GlcNAc(OAc) $_4$ ]-OBn (**82**)

Diethylamine (0.5 mL) was added to a solution of glycoside **81** (114 mg, 0.15 mmol, 1.0 equiv.) in dry  $\text{CH}_3\text{CN}$  (3 mL), at 0 °C. The mixture was stirred 1 h at 0 °C. The mixture was concentrated and the residue dissolved in dry  $\text{CH}_2\text{Cl}_2$  (3 mL), cooled to 0°C and Boc-Thr(OBn)-OH (**20**) (68 mg, 0.22 mmol, 1.5 equiv.) was added, followed by the addition of diisopropylethylamine (65  $\mu\text{L}$ , 48 mg, 0.38 mmol, 2.5 equiv.) and PyBroP (103 mg, 0.22 mmol, 1.5 equiv.). The mixture was stirred overnight under nitrogen, concentrated and applied to a flash column, eluting with 4:1 EtOAc:Hexane, and then with 9:1 EtOAc :Hexanes to give **82** as a colorless foam (86 mg, 68% yield).  $R_f$  0.51 (9:1 EtOAc:Hexane).  $[\alpha]_D^{25} +12.4$  ( $c$  0.9, MeOH).  $^1\text{H}$  NMR ( $\text{CDCl}_3$ , 400 MHz)  $\delta$  1.21 (d,  $J = 6.2$  Hz, 3H), 1.41 (s, 9H), 1.95 (s, 3H), 1.99 (s, 3H), 2.01 (s, 3H), 2.02 (s, 3H), 2.08-2.14 (m, 1H), 2.42-2.45 (m, 1H), 3.78-3.82 (m, 1H), 3.80 (d,  $J = 11.2$  Hz, 1H), 3.88 (d,  $J = 11.2$  Hz, 1H), 3.39-3.97 (m, 1H), 4.07 (d,  $J = 12.2$  Hz, 1H), 4.11-4.20 (m, 1H), 4.32-4.35 (m, 2H), 4.42 (dd,  $J = 7.7, 5.1$  Hz, 1H), 4.50 (d,  $J = 11.5$  Hz, 1H), 4.56 (d,  $J = 11.5$  Hz, 1H), 4.73 (t,  $J = 8.1$  Hz, 1H), 4.90 (d,  $J = 3.4$  Hz, 1H), 5.06 (apt. t,  $J = 8.8$  Hz, 1H), 5.15 (apt. d,  $J = 11.5$  Hz, 1H), 5.17 (s, 2H), 5.42-5.52 (m, 1H), 6.15 (d,  $J = 9.0$  Hz, 1H), 7.26-

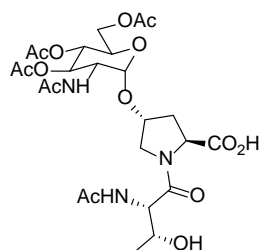
7.34 (m, 10H);  $^{13}\text{C}$  NMR ( $\text{CDCl}_3$ , 100 MHz)  $\delta$  16.5, 20.8, 20.9, 21.0, 23.2, 28.6, 35.8, 51.7, 53.4, 56.6, 58.3, 62.4, 67.4, 68.6, 68.7, 71.0, 71.5, 75.7, 78.1, 80.3, 98.2, 128.0, 128.1, 128.4, 128.5, 128.6, 128.7, 128.9, 135.6, 138.4, 156.1, 169.6, 169.9, 170.7, 170.8, 171.2, 171.6. HRMS (+ESI) calcd for  $\text{C}_{42}\text{H}_{56}\text{N}_3\text{O}_{15}$  ( $\text{M}+\text{H}$ ) $^+$ : 842.3706; obsd: 842.3698.



Ac-Thr(OBn)-Hyp-[( $\alpha$ ,1-4)GlcNAc(OAc) $_4$ ]-OBn (**83**)

Trifluoroacetic acid (0.5 mL) was added to a solution of **82** (42 mg, 0.05 mmol) in dry  $\text{CH}_2\text{Cl}_2$  (2 mL) at 0 °C. The reaction mixture was gradually warmed to RT and stirred for 2 h. Solvent was evaporated and the residue dissolved in pyridine (1.5 mL). The mixture cooled to 0 °C and acetic anhydride (1 mL) was added. The mixture was stirred overnight under  $\text{N}_2$ . The reaction mixture was diluted with ethyl acetate (20 mL), washed with 1M HCl (20 mL) and brine (20 mL). The organic layer was dried over  $\text{MgSO}_4$ , concentrated and the residue applied to a flash column eluting with 9:1 ( $\text{CH}_2\text{Cl}_2$ :MeOH) to give **83** (28 mg, 72%).  $R_f$  0.74 (4:1  $\text{CH}_2\text{Cl}_2$ :MeOH).  $^1\text{H}$  NMR ( $\text{CD}_3\text{OD}$ , 400 MHz)  $\delta$  1.16 (d,  $J$  = 3.8 Hz, 3H), 1.88 (s, 3H), 1.89 (s, 3H) [1.82 (s, 3H)], 1.90 (s, 3H), 1.93 (s, 3H) [1.94 (s, 3H), 1.97 (s, 3H)], 2.03-2.10 (m, 1H), 2.53 (dd,  $J$  = 13.5, 7.9 Hz, 1H), 3.74 (dd,  $J$  = 11.3, 3.8 Hz, 1H), 3.79 (app. t,  $J$  = 6.4 Hz, 1H), 3.95 (dd,  $J$  = 6.0, 2.1 Hz, 0.5 H), 3.98 (dd,  $J$  = 5.6, 2.1 Hz, 0.5 H), 4.01-4.06 (m, 1H), 4.13 (dd,  $J$  = 12.3, 5.7 Hz, 1H), 4.19-4.25 (m, 1H), 4.31 (d,  $J$  = 11.3 Hz, 1H), 4.40 (s, 1H), 4.47 (d,  $J$  = 11.3 Hz, 1H), 4.55 (d,  $J$  = 11.3, 1H), 4.61 (d,  $J$  = 6.7 Hz, 1H), 4.63 (app. t,  $J$  = 8.8 Hz, 1H), 4.87 (app.t,  $J$  = 9.5 Hz, 1H), 4.92 (d,  $J$  = 4.6 Hz, 1H), 5.05 (d,  $J$  = 5.25 Hz, 1H), 5.10 (s, 2H) 7.20-7.31 (m, 10H), 8.02 (d,  $J$  = 9.6 Hz, 1H), 8.17 (d,  $J$  = 7.34 Hz, 1H);  $^{13}\text{C}$  NMR ( $\text{CD}_3\text{OD}$ , 100 MHz)  $\delta$  16.9, 20.7, 20.8, 22.4, 22.7, 36.9, 52.9, 53.4, 57.9, 59.6, 63.9, 68.2, 69.8, 70.5, 72.3, 72.4, 76.6,

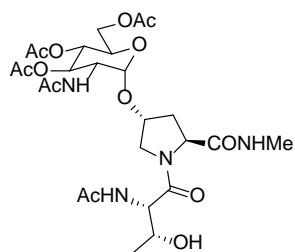
79.6, 78.5, 99.1, 128.8, 129.1, 129.5, 129.6, 129.8, 137.3, 140.0, 171.5, 171.7, 171.9, 172.5, 172.9, 173.5, 173.9. HRMS (+ESI) calcd for  $C_{39}H_{49}N_3NaO_{14}$  ( $M+Na$ )<sup>+</sup>: 806.3112; obsd: 806.3123.



Ac-Thr-Hyp-[( $\alpha$ ,1-4)GlcNAc(OAc)<sub>4</sub>]-OH (**84**)

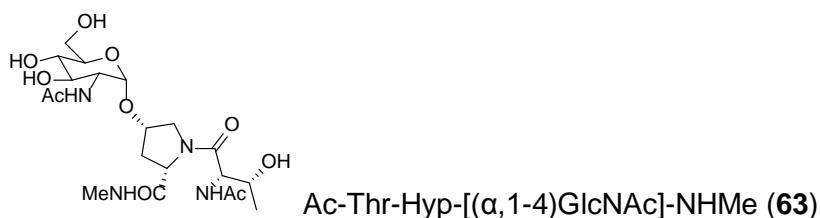
Palladium on carbon (10% w/w, 15 mg) was added in a single portion to a solution of **83** (27 mg, 0.03 mmol) in MeOH (2.5 mL). The reaction flask was evacuated, then opened up to an atmosphere of H<sub>2</sub> and stirred overnight. The catalyst was removed by filtering through a plug of Celite<sup>®</sup> in a Pasteur pipet. The filtrate was concentrated, to give **84** (21 mg, 99%). *R<sub>f</sub>* 0.24 (4:1 CH<sub>2</sub>Cl<sub>2</sub>:MeOH). [ $\alpha$ ]<sub>D</sub><sup>25</sup> -7.0 (c 0.5, MeOH). <sup>1</sup>H NMR (CD<sub>3</sub>OD, 400 MHz)  $\delta$  1.19 (d, *J* = 6.2 Hz, 3H), 1.88 (s, 3H), 1.89 (s, 3H), 1.90 (s, 3H), 1.93 (s, 3H), 1.99 (s, 3H), 2.03-2.12 (m, 1H), 2.54 (apt. dd, *J* = 10.2, 7.7 Hz, 1H), 3.70-3.72 (dd, *J* = 11.1, 3.2 Hz, 1H), 3.89-3.92 (m, 1H), 3.95-3.99 (m, 1H), 4.05 (d, *J* = 12.2 Hz, 1H), 4.15 (dd, *J* = 12.2, 5.6 Hz, 1H), 4.27 (ddd, *J* = 13.7, 10.3, 3.6 Hz, 1H), 4.35-4.38 (m, 1H), 4.43 (apt.d, *J* = 11.2 Hz, 1H), 4.43-4.44 (m, 1H), 4.49 (apt.t, *J* = 8.6 Hz, 1H), 4.89 (t, *J* = 9.7 Hz, 1H), 4.95 (d, *J* = 3.48 Hz, 1H), 5.08 (app. t, *J* = 10.0 Hz, 1H), 8.13 (d, *J* = 9.5 Hz, 1H), 8.15 (d, *J* = 6.8 Hz, 1H); <sup>13</sup>C NMR (CD<sub>3</sub>OD, 100 MHz)  $\delta$  20.1, 20.6, 20.7, 20.8, 22.4, 22.7, 37.2, 53.0, 54.7, 59.4, 63.9, 68.7, 69.8, 70.5, 70.6, 72.4, 80.0, 99.4, 171.5, 171.9, 172.3, 172.5, 173.6, 173.9. HRMS (+ESI) calcd for  $C_{25}H_{38}N_3O_{14}$  ( $M+H$ )<sup>+</sup>: 604.2322; obsd: 604.2348.



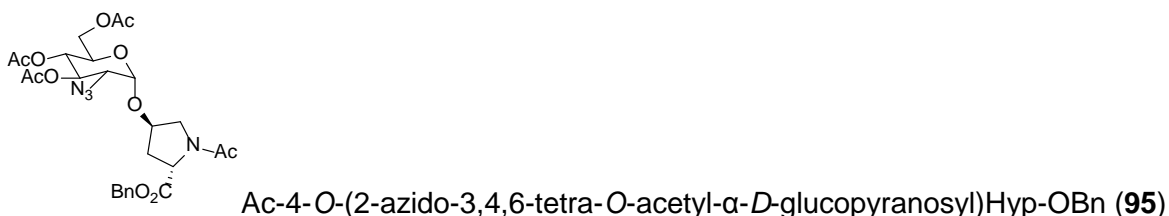


Ac-Thr-Hyp-[( $\alpha$ ,1-4)GlcNAc(OAc)<sub>4</sub>]-NHMe (**85**)

*N*-Hydroxysuccinimide (4 mg, 0.04 mmol, 1 equiv.) and DCC (8 mg, 0.04 mmol, 1 equiv.) were added sequentially to a solution of **84** (21 mg, 0.04 mmol, 1 equiv.) in CH<sub>2</sub>Cl<sub>2</sub> (2 mL) at 0 °C. The solution was stirred for 30 min at 0 °C, gradually warmed to RT and stirred overnight. The suspension was filtered through a plug of cotton in a Pasteur pipet. The filtrate was concentrated to 2 mL and refrigerated for 6 h. The suspension was filtered again and the filtrate concentrated. The residue was dissolved in CH<sub>3</sub>CN (2 mL) and cooled to 0 °C. Methylamine hydrochloride (3 mg, 0.04 mmol, 1 equiv.) was added as a solid in one portion, followed by the addition of diisopropylethylamine (6  $\mu$ L, 5 mg, 0.04mmol, 1 equiv.). The solution was gradually warmed to RT and stirred overnight under N<sub>2</sub>. The mixture was concentrated and the product was isolated by flash chromatography, eluting with 4:1 CH<sub>2</sub>Cl<sub>2</sub>:MeOH to give **85** (14 mg, 77%). *R<sub>f</sub>* 0.31 (4:1 EtOAc:hexanes). <sup>1</sup>H NMR (CD<sub>3</sub>OD, 400 MHz)  $\delta$  1.18 (d, *J* = 6.3 Hz, 3H), 1.87 (s, 3H), 1.89 (s, 3H), 1.94 (s, 3H), 1.90 (s, 3H), 2.00 (s, 3H), 2.04 (ddd, *J* = 13.7, 9.3, 4.4 Hz, 1H), 2.40 (dd, *J* = 13.6, 7.6 Hz, 1H), 2.68 (s, 3H), 3.74 (dd, *J* = 11.2, 3.8 Hz, 1H), 3.96 (t, *J* = 6.4 Hz, 1H), 4.01 (ddd, *J* = 10.1, 5.0, 2.4 Hz, 1H), 4.06 (dd, *J* = 12.2, 2.4 Hz, 1H), 4.19 (dd, *J* = 9.7, 4.4 Hz, 1H), 4.22 (dd, *J* = 7.1, 3.8 Hz, 1H), 4.36 (d, *J* = 11.4 Hz, 1H), 4.39-4.41 (m, 2H), 4.45 (t, *J* = 8.4 Hz, 1H), 4.94 (appt, *J* = 9.6 Hz, 1H), 4.94 (d, *J* = 3.5 Hz, 1H), 5.09 (dd, *J* = 10.8, 9.4 Hz, 1H); <sup>13</sup>C NMR (MeOD, 100 MHz)  $\delta$  20.1, 20.7, 20.8, 22.4, 22.6, 26.4, 37.7, 52.9, 55.2, 59.2, 60.7, 63.7, 68.6, 69.6, 70.6, 72.4, 80.1, 99.7, 171.4, 172.0, 172.4, 172.6, 173.6, 173.9, 174.5. HRMS (+ESI) calcd for C<sub>26</sub>H<sub>40</sub>N<sub>4</sub>NaO<sub>13</sub> (M+Na)<sup>+</sup>: 639.2490; obsd: 639.2463.

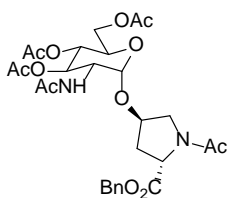


A solution of NaOMe in MeOH (25% w/v, one drop from a 20G needle) was added to a solution of glycoside **85** (8 mg, 0.013 mmol) in MeOH (2 mL) at 0 °C. The mixture was gradually warmed to RT and stirred for 2 h. Amberlite IR-120 H<sup>+</sup> resin was added to the reaction mixture and stirred for 15 min. The reaction mixture was filtered through a plug of cotton and concentrated to give the glycoside **63** (6 mg, 94%).  $[\alpha]_D^{25} +73.2$  (*c* 1.0, MeOH). <sup>1</sup>H NMR (D<sub>2</sub>O, 400 MHz)\* δ 1.27 (d, *J* = 6.3 Hz, 3H), 2.00 (s, 3H), 2.07 (s, 3H), 2.05-2.15 (m, 1H) 2.53 (dd, *J* = 13.5, 7.5 Hz, 1H), 2.76 (s, 3H), 3.49 (app.t, *J* = 9.5 Hz, 1H), 3.68-3.74 (m, 2H), 3.79 (dd, *J* = 12.3, 5.6 Hz, 1H), 3.84 (dd, *J* = 12.1, 3.2 Hz, 1H), 3.90 (dd, *J* = 12.3, 1.6 Hz, 1H), 3.95 (dd, *J* = 10.6, 3.6 Hz, 1H), 4.10 (app.p, *J* = 6.3 Hz, 1H), 4.17 (d, *J* = 12.1 Hz, 1H), 4.51 (dd, *J* = 9.7, 1.6 Hz, 1H), 4.57 (brs, 1H), 4.61 (d, *J* = 6.3 Hz, 1H), 5.01 (d, *J* = 3.6 Hz, 1H); <sup>13</sup>C NMR (D<sub>2</sub>O, 100 MHz) δ 18.5, 21.6, 21.8, 25.8, 35.7, 53.0, 53.4, 57.2, 59.8, 60.6, 67.3, 69.9, 70.8, 72.5, 75.7, 95.8, 171.0, 173.7, 173.9, 174.1. HRMS (ESI+) calcd for C<sub>20</sub>H<sub>34</sub>N<sub>4</sub>O<sub>10</sub> (M+H)<sup>+</sup>: 490.2275; obsd: 491.2349.



A solution of thioglycoside **78** (259 mg, 0.61 mmol, 1.0 eq.) and Ac-Hyp-OBn (**94**) (177 mg, 0.67 mmol, 1.1 equiv.) in CH<sub>2</sub>Cl<sub>2</sub> (3 mL) was stirred with activated 4 Å molecular sieves (35 mg) for 15 min at RT under nitrogen and then the mixture was cooled to -78 °C. *N*-Iodosuccinimide (206 mg, 0.915 mmol, 1.5 equiv.) and silver triflate (78 mg, 0.3 mmol, 0.5 equiv.) were added. The mixture was allowed to warm to RT and stirred overnight. The reaction

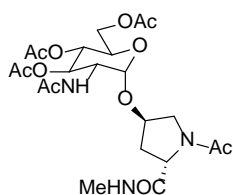
mixture was quenched with Et<sub>3</sub>N (1 mL) diluted with EtOAc (75 mL), washed with 10% Na<sub>2</sub>S<sub>2</sub>O<sub>3</sub> (75 mL), and brine (75 mL). The organic layer was dried over MgSO<sub>4</sub>, filtered, concentrated and submitted directly to flash chromatography eluting with 1:1 Hexane:EtOAc to give the α-O-glycoside **95** (161 mg, 46% yield). *R<sub>f</sub>* 0.19 (4:1 EtOAc: Hexane). [α]<sub>D</sub><sup>25</sup> +71.7 (*c* 1.0, MeOH). <sup>1</sup>H NMR (CDCl<sub>3</sub>, 400 MHz) δ 2.00 (s, 3H), 2.05 (s, 3H), 2.08 (s, 3H), 2.12 (s, 3H), 2.14 (app. ddd, *J* = 13.5, 7.2, 5.3 Hz, 0.7 H) [2.21-2.32 (m, 0.3H)], 2.48-2.54 (m, 0.7 H) [2.55-2.61 (m, 0.3H)], 3.29 (dd, *J* = 10.7, 3.6 Hz, 0.7H) [3.17 (dd, *J* = 10.7, 3.6 Hz, 0.3H)], 3.60-3.80 (m, 0.7H) [3.52-3.56 (m, 0.3H)], 3.87 (d, *J* = 11.1, 5.0 Hz, 1H), 4.00-4.11 (m, 2H), 4.18-4.27 (m, 1H), 4.47-4.52 (m, 0.7H) [4.43-4.46 (m, 0.3H)], 4.56-4.70 (m, 1H), 4.95 (t, *J* = 9.6 Hz, 1H), 5.05 (d, *J* = 3.7 Hz, 1H), 5.18 (s, 1.5H) [5.24 (s, 0.5H)], 5.41 (app. t, *J* = 9.4 Hz, 1H), 7.34-7.37 (m, 5H); <sup>13</sup>C NMR (CDCl<sub>3</sub>, 100 MHz) δ 20.7, 20.8, 20.9, 22.4 [21.8], 35.8 [38.1], 53.2 [50.8], 57.7 [58.9], 60.7 [60.4], 62.3 [62.1], 67.3 [67.2], 68.6 [6], 68.7 [68.4], 68.6, 68.7, 70.1 [69.8], 74.0, 78.5, 98.3 [96.7], 128.4, 128.6, 128.7, 128.8, 129.0, 135.6, 169.7, 169.8, 170.1, 170.3, 170.7, 171.9, 172.0. HRMS (ESI+) calcd for C<sub>22</sub>H<sub>34</sub>N<sub>3</sub>O<sub>11</sub> (M+H)<sup>+</sup>: 516.2188; obsd: 516.2189.



Ac-[(α,1-4)GlcNAc(OAc)<sub>4</sub>]Hyp-OBn (**96**)

Zinc powder (50 mg) and saturated aqueous CuSO<sub>4</sub> (50 μL) were added to a solution of **95** (57 mg, 0.19 mmol) in THF (2 mL) at RT. Acetic acid (0.5 mL) and acetic anhydride (0.5 mL) were added and the mixture stirred overnight at RT. The reaction mixture was filtered, the filtrate concentrated and the residue applied directly to a flash column, eluting with 9:1 CH<sub>2</sub>Cl<sub>2</sub>:MeOH to give the *N*-acetylated product **96** (50 mg, 85% yield). *R<sub>f</sub>* 0.33 (9:1 CH<sub>2</sub>Cl<sub>2</sub>:MeOH). <sup>1</sup>H NMR (CDCl<sub>3</sub>, 400 MHz) δ 1.93 (s, 3H), 2.02 (s, 3H), 2.03 (s, 3H), 2.03 (s, 3H), 2.10 (s, 3H), 2.12-2.18 (m, 1H), 2.42-2.48 (m, 1H), 3.58 (d, *J* = 11.4 Hz, 1H), 3.77 (dd, *J* = 11.4, 4.6 Hz, 1H), 3.94 (ddd,

$J = 9.6, 5.1, 2.3$  Hz, 1H), 4.07 (dd,  $J = 12.3, 2.1$  Hz, 1H), 4.19 (dd,  $J = 12.3, 5.1$  Hz, 1H), 4.28 (ddd,  $J = 10.3, 8.8, 3.6$  Hz, 1H), 4.44-4.48 (m, 1H), 4.63 (app. t,  $J = 7.9$  Hz, 1H), 5.02 (d,  $J = 3.7$  Hz, 1H), 5.08 (app. t,  $J = 9.6$  Hz, 1H), 5.11-5.21 (m, 3H), 6.02 (d,  $J = 8.6$  Hz, 1H), 7.33-7.38 (m, 5H);  $^{13}\text{C}$  NMR ( $\text{CDCl}_3$ , 100 MHz)  $\delta$  20.7, 20.8, 20.9, 22.4, 23.1, 35.8, 52.3, 52.7, 57.8, 62.2, 67.3, 68.2, 68.6, 70.8, 76.4, 96.3, 128.3, 128.6, 128.8, 128.9, 129.0, 135.6, 169.4, 169.9, 170.5, 170.8, 171.7, 171.8. HRMS (ESI+) calcd for  $\text{C}_{28}\text{H}_{36}\text{N}_2\text{NaO}_{12}$  ( $\text{M}+\text{Na}$ ) $^+$ : 615.2160; obsd: 615.2111.

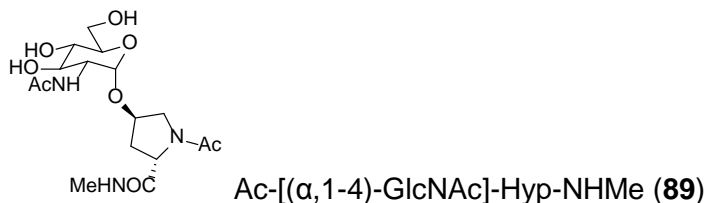


Ac-[( $\alpha,1$ -4)GlcNAc(OAc) $_4$ ]Hyp-NHMe (**98**)

Palladium on carbon (10%, 35 mg) was added in a single portion to a solution of **96** (50 mg, 0.08 mmol) in MeOH (3.0 mL). The reaction flask was evacuated, then opened to an atmosphere of  $\text{H}_2$  and stirred overnight. The catalyst was removed by filtering through a plug of Celite<sup>®</sup> in a Pasteur pipet. The filtrate was concentrated, to give Ac-[( $\alpha,1$ -4)GlcNAc(OAc) $_4$ ]Hyp-OH (**97**) (40 mg, 94%).  $R_f$  0.32 (4:1  $\text{CH}_2\text{Cl}_2$ :MeOH).  $[\alpha]_D^{25} +41.7$  (c 1.0, MeOH).

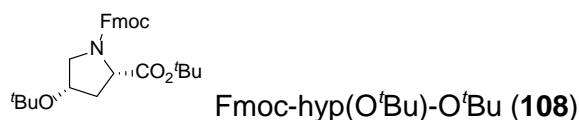
*N*-Hydroxysuccinimide (9.2 mg, 0.08 mmol, 1 equiv.) was added to a solution of **97** (40 mg, 0.08 mmol, 1 equiv.) in dry  $\text{CH}_2\text{Cl}_2$  (2 mL), at 0 °C. The mixture was stirred for 15 min under  $\text{N}_2$  at 0 °C. Then DCC (17 mg, 0.08 mmol, 1 equiv.) was added and the mixture gradually warmed to RT and stirred overnight. The reaction mixture was filtered and the filtrate was concentrated to reduce the volume of  $\text{CH}_2\text{Cl}_2$  to 0.5 mL and this was kept in the freezer for 6 h. The solution was filtered again and concentrated. The resulting NHS ester was dissolved in dry acetonitrile (2 mL), cooled to 0 °C and methylamine hydrochloride (5.4 mg, 0.08 mmol, 1 equiv.) was added, followed by the addition of DIEA (14  $\mu\text{L}$ , 10.3 mg, 0.08 mmol, 1 equiv.). The reaction mixture was gradually warmed to RT, stirred overnight, concentrated, applied to a flash

column and eluted with 9:1 CH<sub>2</sub>Cl<sub>2</sub>:MeOH. The product **98** eluted, along with free NHS. This was further purified by flash chromatography eluting with 4:1 CH<sub>2</sub>Cl<sub>2</sub>: MeOH (More polar eluent leads to low band broadening and afforded a better separation of the compound and free NHS) to afford product **98** (10 mg, 24%). *R<sub>f</sub>* 0.82 (4:1 CH<sub>2</sub>Cl<sub>2</sub>: MeOH). [ $\alpha$ ]<sub>D</sub><sup>25</sup> +29.5 (*c* 1.0, MeOH). <sup>1</sup>H NMR (CDCl<sub>3</sub>, 400 MHz)  $\delta$  1.94 (s, 3H), 2.03 (s, 3H), 2.04 (s, 3H), 2.09 (s, 3H), 2.10 (s, 3H), 2.06-2.16 (m, 1H (H $\beta$  from cosy)), 2.70 (dt, *J* = 13.2, 5.4 Hz, 1H), 2.78 (d, *J* = 4.9 Hz, 3H), 3.49 (dd, *J* = 11.0, 3.5 Hz, 1H), 3.67 (dd, *J* = 11.0, 5.2 Hz, 1H), 3.97 (ddd, *J* = 9.4, 5.0, 2.6 Hz, 1H), 4.11 (dd, *J* = 12.3, 2.6, 1H), 4.23 (dd, *J* = 12.3, 7.3 Hz, 1H), 4.29 (ddd, *J* = 10.3, 9.0, 3.8, 1H), 4.55 (app. p, *J* = 5.0 Hz, 1H), 4.63 (dd, *J* = 8.2, 5.2 Hz, 1H), 4.92 (d, *J* = 3.8 Hz, 1H), 5.10 (app. t, *J* = 9.5 Hz, 1H), 5.16 (app. t, *J* = 9.5 Hz, 1H), 5.75 (d, *J* = 9.0 Hz, 1H), 6.97 (app. q, *J* = 4.8 Hz, 1H); <sup>13</sup>C NMR (CDCl<sub>3</sub>, 100 MHz)  $\delta$  20.8, 20.9, 22.8, 23.3, 26.5, 34.0, 52.3, 52.4, 58.3, 62.3, 68.3, 68.5, 71.1, 75.8, 96.2, 169.5, 170.2, 170.8, 170.9, 171.0, 171.9. HRMS (ESI+) calcd for C<sub>22</sub>H<sub>34</sub>N<sub>3</sub>O<sub>11</sub> (M+H)<sup>+</sup>: 515.2188; obsd: 516.2196.



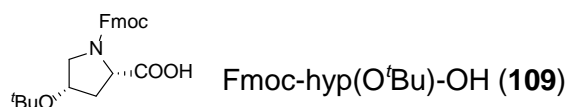
A solution of NaOMe in MeOH (25% w/v, two drops from a 20G needle) was added to a solution of glycoside **98** (10 mg, 0.02 mmol) in dry MeOH (1.5 mL) at 0 °C. The mixture was gradually warmed to RT and stirred for 1 h. Dowex 50WX2 H<sup>+</sup> resin (5 mg) was added to the reaction mixture and stirred for 15 min. The reaction mixture was filtered through a plug of cotton and concentrated to give the glycoside **99** (4 mg, 53%). [ $\alpha$ ]<sub>D</sub><sup>25</sup> +2.0 (*c* 0.2, MeOH). <sup>1</sup>H NMR (D<sub>2</sub>O, 400 MHz)  $\delta$  2.03 (s, 2.4H) [2.01 (s, 0.6 H)], 2.05-2.18 (m, 0.8H) [2.23-2.31 (m, 0.2 H)], 2.15 (s, 2.4H) [2.05 (s, 0.6H)], 2.52 (dd, *J* = 13.8, 7.8 Hz, 0.7 H) [2.60-2.69 (m, 0.2 H), 2.8 (s, 2.4 H) [2.82 (s, 0.6 H)], 3.5 (app. t, *J* = 9.3 Hz, 1H), 3.75 (dd, *J* = 13.4, 6.2 Hz, 1.6 H) [3.58 (dd, *J* = 11.8, 6.5 Hz, 0.4H)], 3.78 (app. t, *J* = 4.7 Hz, 1H), 3.79-3.81 (m, 1H), 3.82 (d, *J* = 11.8

Hz, 1H), 3.89 (dd,  $J = 11.8, 2.0$  Hz, 0.8H) [3.68 ( $J = 11.8, 4.4$  Hz, 0.2 H)], 3.93 (dd,  $J = 10.6, 3.8$  Hz, 1H), 4.50 (t,  $J = 8.5$  Hz, 0.8H) [4.70 (t,  $J = 8.5$  Hz, 0.2H)], 4.54 (s, 0.8H) [4.71 (s, 0.2 H)], 5.10 (d,  $J = 3.7$  Hz, 0.8H) [5.00 (d,  $J = 3.7$  Hz, 0.2 H)];  $^{13}\text{C}$  NMR ( $\text{CDCl}_3$ , 100 MHz)  $\delta$  21.6 [20.6], 21.7, 36.2 [37.9], 52.9 [51.4], 53.6 [53.5], 59.2, 60.6 [60.5], 70.0, 70.6 [70.5], 72.3, 74.8 [74.0], 95.0, 95.3, 173.2, 174.1, 174.2. HRMS (ESI+) calcd for  $\text{C}_{16}\text{H}_{28}\text{N}_3\text{O}_8$  ( $\text{M}+\text{H}$ ) $^+$ : 389.17871; obsd: 390.1874.

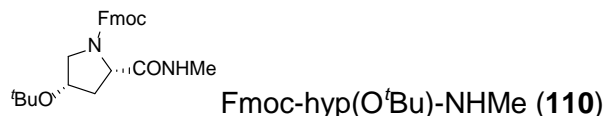


A solution of Fmoc-Cl (1.036 g, 4.00 mmol, 1.05 equiv.) in 1,4-dioxane (1 mL) was added dropwise to a solution of *cis*-4-hydroxyproline (**107**) (500 mg, 3.81 mmol, 1 equiv.) in 1,4-dioxane (5 mL) and 10% aqueous sodium carbonate (10 mL) at 0 °C. The mixture was gradually warmed to rt, stirred overnight, poured on to ice cold water (100 mL) and extracted with diethyl ether (2 x 60 mL). The aqueous layer was acidified by the addition of conc. HCl (pH=2) and extracted with EtOAc (3 x 50 mL). The organic layers were combined, dried over  $\text{MgSO}_4$ , filtered and concentrated to give Fmoc-*cis*-4-hydroxyproline as a colorless foam (1.425 g, 100%). Isobutylene (approximately 30 mL) was condensed into a two-necked flask at -78 °C. In a separate flask a solution of *p*-toluenesulfonic acid hydrate (3.222 g, 17 mmol, 4.2 equiv.) in  $\text{CH}_2\text{Cl}_2$  (20 mL) was added to Fmoc-protected *cis*-4-hydroxyproline (1.425 g, 4.03 mmol, 1 equiv.) in  $\text{CH}_2\text{Cl}_2$  (20 mL). This mixture was added to the isobutylene over 15 min, maintaining the temperature around -78 °C. The mixture was gradually warmed to rt, stoppered, and stirred for 3 d. The reaction mixture was diluted with  $\text{CH}_2\text{Cl}_2$  (10 mL), washed with sat'd aqueous  $\text{NaHCO}_3$  solution (2 x 30 mL). The combined aqueous layers were back-extracted with  $\text{CH}_2\text{Cl}_2$  (40 mL). The organic layers were combined, dried over  $\text{MgSO}_4$ , filtered and concentrated. The residue was applied to a flash column and eluted with 1:1 Hexanes:EtOAc to give **108** (1.249 g, 76%).  $R_f$  0.74 (1:1 Hexane:EtOAc).  $^1\text{H}$  NMR ( $\text{CDCl}_3$ , 400 MHz)  $\delta$  1.18 [1.20]\*, 1.44 [1.46], 1.92-

2.07 (m, 1H), 2.36-2.49 (m, 1H), 3.36 (p,  $J = 5.4$  Hz, 1H), 3.75 (dd,  $J = 10.4, 6.6$  Hz, 0.5 H) 3.83 (dd,  $J = 10.8, 6.4$  Hz, 0.5 H), 4.10-4.21 (m, 2H), 4.23-4.32 (m, 2H), 4.44-4.49 (m, 1H), 7.30 (t,  $J = 7.4$  Hz, 2H), 7.38 (t,  $J = 7.3$  Hz, 2H), 7.59 (t,  $J = 7.0$  Hz, 1H), 7.64 (t,  $J = 7.4$  Hz, 1H), 7.74 (d,  $J = 7.4$  Hz, 1H);  $^{13}\text{C}$  NMR ( $\text{CDCl}_3$ , 100 MHz)  $\delta$  28.1, 28.4, 38.8 [37.8]\*, 47.4 [47.3], 53.8 [53.2], 58.2 [58.4], 67.8 [67.5], 68.6 [69.4], 74.2, 81.5 [81.3], 120.0, 125.2, 125.6 125.4, 127.1, 127.2, 127.7, 127.8, 141.4, 141.3, 143.7, 143.9, 144.4, 144.5, 154.6 [154.8], 171.2 [170.8].

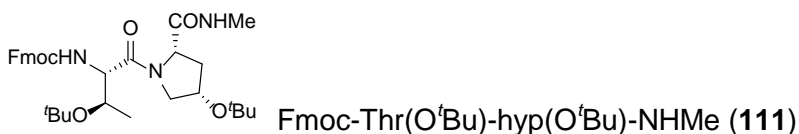


Trifluoroacetic acid (100  $\mu\text{L}$ ) was added to a solution of **108** (98 mg, 0.21 mmol) in  $\text{CH}_2\text{Cl}_2$  (4 mL) at 0  $^\circ\text{C}$ . The reaction mixture was gradually warmed to rt and stirred overnight, neutralized with  $\text{NaHCO}_3$  (500 mg), and stirred for another 15 min. The solution was filtered through a plug of cotton. The filtrate was evaporated, the residue was applied to a flash column and eluted with 9:1 EtOAc:hexanes to give **109** as a colorless foam (38 mg, 44 %).  $R_f$  0.2 (19:1  $\text{CH}_2\text{Cl}_2$ : $\text{CH}_3\text{OH}$ ).  $^1\text{H}$  NMR ( $\text{CDCl}_3$ , 400 MHz)  $\delta$  1.19 (s, 9H), 2.11-2.17 (m, 1H), 2.33-2.44 (m, 1H), 3.39 (dd,  $J = 10.6, 3.8$  Hz, 0.5H) 3.48 (d,  $J = 11.8$  Hz, 0.5 H), 3.63-3.68 (m, 1H), 4.16-4.52 (m, 5H), 7.26-7.29 (m, 2H), 7.30-7.40 (m, 2H), 7.54-7.61 (m, 2H), 7.70 (dd,  $J = 7.4$  Hz, 2H), 7.75 (dd,  $J = 7.4$  Hz, 2H);  $^{13}\text{C}$  NMR ( $\text{CDCl}_3$ , 100 MHz)  $\delta$  28.2 [28.3]\*, 37.4 [38.4], 47.3, 53.9 [54.5], 58.2, 67.9 [68.2], 69.7 [69.1], 75.0, 75.5, 120.1, 125.3, 125.4, 127.2, 127.3, 127.9, 141.4, 141.5, 143.9, 144.2, 144.3, 154.9 [155.6], 175.5. HRMS (+ESI) calcd for  $\text{C}_{24}\text{H}_{27}\text{NNaO}_5$  ( $\text{M}+\text{Na}$ ) $^+$ : 432.1787; obsd: 432.1784.



*N*-Hydroxysuccinimide (18 mg, 0.16 mmol, 1 equiv.) and DCC (33 mg, 0.16 mmol, 1 equiv.) were added sequentially to a solution of **109** (65 mg, 0.16 mmol, 1 equiv.) in  $\text{CH}_2\text{Cl}_2$  (2

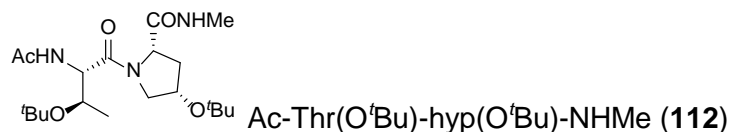
mL) at 0 °C. The solution was stirred for 30 min at 0 °C, gradually warmed to rt and stirred overnight. The suspension was filtered through a plug of cotton in a Pasteur pipet. The filtrate was concentrated to 2 mL and refrigerated for 6 h. The suspension was again filtered and the filtrate was concentrated. The residue was dissolved in DMF (2 mL) and cooled to 0 °C. Methylamine hydrochloride (11 mg, 0.16 mmol, 1 equiv.) was added as a solid in one portion, followed by the addition of diisopropylethylamine (28  $\mu$ L, 21 mg, 0.16 mmol, 1 equiv.). The solution was gradually warmed to RT and stirred overnight under N<sub>2</sub>. The mixture was diluted with EtOAc (25 mL) and washed with brine (25 mL). The aqueous layer was back-extracted with EtOAc (25 mL). The organic layers were combined, dried over MgSO<sub>4</sub>, filtered and concentrated. The product was isolated by flash chromatography, eluting with 2:1 EtOAc:hexanes to give **110** (52 mg, 77%). *R*<sub>f</sub> 0.35 (4:1 EtOAc:hexanes). <sup>1</sup>H NMR (CD<sub>3</sub>OD, 400 MHz)  $\delta$  1.14 (s, 9H), 1.82-1.98 (m, 1H), 2.21-2.36 (m, 1H) 2.68 (s, 3H), 3.14 (dd, *J* = 10.7, 3.4 Hz, 0.5H) [3.30-3.32 (m, 0.5H)]\*, 3.44 (dd, *J* = 10.5, 4.7 Hz, 0.5H) [3.64 (dd, *J* = 10.8, 5.2 Hz, 0.5H)], 4.08-4.23 (m, 3H), 4.32 (d, *J* = 6.4 Hz, 2H), 4.40-4.49 (m, 1H), 7.27-7.37 (m, 4H), 7.53-7.63 (m, 2H), 7.77 (t, *J* = 6.0 Hz, 2H); <sup>13</sup>C NMR (CD<sub>3</sub>OD, 400 MHz)  $\delta$  26.7 [26.5], 28.6, 34.9 [37.1], 40.3 [39.2], 56.0 [55.4], 61.2, 69.2 [68.5], 70.2 [70.8], 75.1, 121.1, 126.2, 128.3, 129.0, 142.7, 145.3, 145.5, 157.0, [157.1], 175.7 [175.4].



Diethylamine (800  $\mu$ L) was added to a solution of Fmoc-*cis*-4-Hyp-(O<sup>t</sup>Bu)-NHMe **110** (52 mg, 0.12 mmol, 1 equiv.) in acetonitrile (3 mL). The solution was stirred at 0 °C under N<sub>2</sub> for 30 min, concentrated, and then concentrated twice more from acetonitrile. The residue was suspended in dichloromethane (2 mL) and cooled to 0 °C. Fmoc-Thr(O<sup>t</sup>Bu)OH (**71**) (73 mg, 0.18 mmol, 1.5 equiv.) was added, followed by the addition of diisopropylethylamine (54  $\mu$ L, 400 mg,

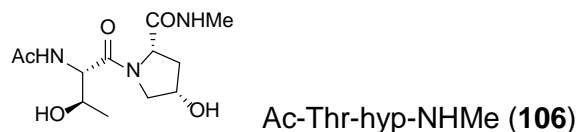


0.31 mmol, 2.5 equiv.) and PyBroP (86 mg, 0.18 mmol, 1.5 equiv.). The solution was gradually warmed to RT stirred overnight under N<sub>2</sub>. The mixture was concentrated and the residue applied to a flash column eluting with 4:1 EtOAc:hexanes to give **111** (80 mg, 100%). *R<sub>f</sub>* 0.38 (4:1 EtOAc:hexanes). <sup>1</sup>H NMR (CDCl<sub>3</sub>, 400 MHz) δ 1.14 (d, *J* = 7.0, 3H), 1.14 (s, 9H), 1.32 (s, 3H), 2.17-2.28 (m, 2H), 2.73 (d, *J* = 4.2 Hz, 3H), 3.77-3.86 (m, 2H), 4.09-4.14 (m, 2H), 4.21 (d, *J* = 6.8 Hz, 1H), 4.38 (d, *J* = 6.6 Hz, 2H), 4.59 (dd, *J* = 7.5, 5.2 Hz, 1H), 4.76 (dd, *J* = 8.4, 3.2 Hz, 1H), 5.81 [5.73] (d, *J* = 7.8 Hz, 1H), 7.03 (q, *J* = 4.4 Hz, 1H), 7.30 (t, *J* = 7.4 Hz, 2H), 7.39 (t, *J* = 7.4, 2H), 7.58 (dd, *J* = 7.2, 4.4 Hz, 2H), 7.75 (d, *J* = 7.5 Hz, 2H); <sup>13</sup>C NMR (CDCl<sub>3</sub>, 100 MHz) δ 17.1 [14.3]\*, 26.0 [25.9], 28.2, 28.3, 37.8, 47.3, 55.7, 56.5 [60.6], 59.2, 67.2, 68.7, 70.1, 74.3, 75.7, 120.2, 120.2, 125.2, 125.3, 127.2, 127.9, 141.4, 143.8, 144.0, 155.8, 169.0, 172.3. HRMS (+ESI) calcd for C<sub>33</sub>H<sub>45</sub>N<sub>3</sub>NaO<sub>6</sub>S (M + Na)<sup>+</sup>: 602.3206; obsd: 602.3242.

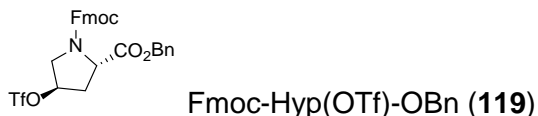


Diethylamine (2 mL) was added to a solution of **111** (119 mg, 0.21 mmol, 1 equiv.) in acetonitrile (2 mL). The solution was stirred at 0 °C under N<sub>2</sub> for 30 min, concentrated, and then concentrated twice more from acetonitrile. The residue was dissolved in a mixture of pyridine (1 mL) and acetic anhydride (1 mL) at 0 °C, warmed to rt and stirred under N<sub>2</sub> overnight. The red solution was concentrated and purified by flash chromatography, eluting with 4:1 EtOAc:hexanes to remove Fmoc byproducts and then with 9:1 CH<sub>2</sub>Cl<sub>2</sub>:MeOH to isolate **112** as a colorless foam (27 mg, 93%). <sup>1</sup>H NMR (CDCl<sub>3</sub>, 400 MHz) δ 1.10 (d, *J* = 6.4 Hz, 3H), 1.15 (s, 9H), 1.31 (s, 9H), 2.0 (s, 3H), 2.22-2.25 (m, 2H), 2.73 [2.79]\* (d, *J* = 4.8 Hz, 3H), 3.79 (dd, *J* = 10.7, 5.3 Hz, 1H), 3.86 (dd, *J* = 10.7, 2.6 Hz, 1H), 4.12 (dt, *J* = 11.6, 6.4 Hz, 1H), 4.21-4.25 (m, 1H), 4.74 (dd, *J* = 8.2, 4.1 Hz, 1H), 4.84 (dd, *J* = 7.7, 5.1, 1H), 6.61 (d, *J* = 7.5 Hz, 1H), 7.02, (d, *J* = 8.0 Hz, 1H); <sup>13</sup>C NMR (CDCl<sub>3</sub>, 400 MHz) δ 17.3, 23.3, 26.1, 28.2, 28.3, 37.9, 54.4, 56.6,

59.3, 68.2, 70.1, 74.4, 75.8, 169.4, 170.0, 172.3. HRMS (+ESI) calcd for C<sub>20</sub>H<sub>37</sub>N<sub>3</sub>NaO<sub>5</sub>S (M + Na)<sup>+</sup>: 422.2631; obsd: 422.2709.

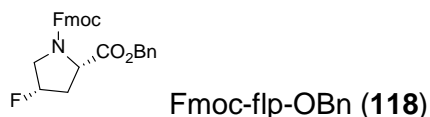


Trifluoroacetic acid (1.0 mL) was added to a solution of Ac-Thr(<sup>t</sup>Bu)-*trans*-4-Hyp(O<sup>t</sup>Bu)-NHMe (**112**) (17 mg, 0.04 mmol) in CH<sub>2</sub>Cl<sub>2</sub> (1.0 mL) at 0 °C. The mixture was gradually warmed to rt and stirred overnight under N<sub>2</sub>. The solution was concentrated and then concentrated three times from CH<sub>2</sub>Cl<sub>2</sub>. The brown residue was subjected to the RP-HPLC (gradient: 0-100% acetonitrile in H<sub>2</sub>O over 60 min, C<sub>18</sub> 10.0 mm column 3 mL/min) (*R*<sub>T</sub> = 4 min) to isolate **106** as a colorless oil (6 mg, 50%). [α]<sub>D</sub><sup>25</sup> +71.7 (*c* 1.0, MeOH). <sup>1</sup>H NMR (D<sub>2</sub>O, 400 MHz) δ 1.15 [1.23] (d, *J* = 6.4 Hz, 3H), 1.99 (dt, *J* = 4.5, 3.6 Hz, 1H), 2.04 [2.03] (s, 3H), 2.44-2.51 (m, 1H), 2.73 [2.71] (s, 3H), 3.69 (dd, *J* = 11.0, 3.5 Hz, 0.7 H) [3.75 (dd, *J* = 13.4, 5.0 Hz, 0.3 H), 4.03 (dd, *J* = 11.1, 5.2 Hz, 0.7 H) [4.07 (dd, *J* = 5.8, 5.3 Hz, 0.3H), 4.15 (p, *J* = 6.3 Hz, 1H), 4.46 (dd, *J* = 9.5, 4.6 Hz, 1H), 4.49-4.53 (m, 1H), 4.56 (d, *J* = 5.9 Hz, 1H), 4.84-4.89 (m, 1H); <sup>13</sup>C NMR (CDCl<sub>3</sub>, 100 MHz) δ 18.4 [18.1], 21.5 [21.6], 25.8 [26.1], 36.2 [38.9], 55.1 [55.8], 56.9, 59.6 [59.9], 66.9 [67.4], 69.5 [67.9], 171.2, 174.0, 174.2. HRMS (+ESI) calcd for C<sub>12</sub>H<sub>21</sub>N<sub>3</sub>O<sub>5</sub> (M)<sup>+</sup>: 287.1481; obsd: 287.1352.



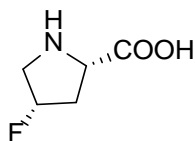
Pyridine (705 μL, 690mg, 8.72 mmol, 4 equiv.) was added to a solution of *N*-Fmoc-*trans*-4-hydroxy-*L*-proline benzyl ester (**79**) (979 mg, 2.18 mmol, 1equiv.) in dry CH<sub>2</sub>Cl<sub>2</sub> (5 mL) at 4 °C under N<sub>2</sub>. The mixture was stirred for 10 min then triflic anhydride (550 μL, 923 mg, 3.27 mmol, 1.5 equiv.) was added dropwise and the resulting yellow solution was stirred at -10 °C for 2 h.

The mixture was gradually warmed to rt, stirred for another 1 h, concentrated and the residue purified by flash column chromatography, eluting with 3:1 hexanes:EtOAc, to give **119** (1.9 g, 73%).  $R_f$  0.60 (3:1 Hexanes:EtOAc).  $^1\text{H}$  NMR ( $\text{CDCl}_3$ , 400 MHz)  $\delta$  2.25-2.34 (m, 1H), 2.62-2.72 (m, 1H), 3.83 (2d,  $J = 13.6$  Hz, 1H), 3.97 (t,  $J = 6.6$  Hz, 0.5H), 4.57 (d,  $J = 13.6$  Hz, 0.5H), 4.23 (t,  $J = 6.8$  Hz, 1H), 4.34 (app. d,  $J = 7.4$  Hz, 1H), 4.42 (dd,  $J = 7.4, 3.3$  Hz, 1H), 4.48 (t,  $J = 8.0$  Hz, 0.5H), 4.60 (t,  $J = 8.0$  Hz, 0.5H), 4.99-5.22 (m, 2H), 5.42 (app.d,  $J = 11.8$  Hz, 1H), 7.20-7.48 (m, 13H);  $^{13}\text{C}$  NMR ( $\text{CDCl}_3$ , 100 MHz)  $\delta$  36.4 [37.7], 47.1 [47.2], 52.6 [53.0], 57.4 [57.1], 67.5 [67.6], 68.0 [68.1], 86.5 [85.8], 117.0, 120.1, 120.2, 125.0, 125.1, 125.1, 127.2, 127.8, 127.9, 128.3, 128.5, 128.6, 128.8, 135.1 [135.2], 141.3 [141.4], 143.6 [143.4], 144.0 [143.9], 154.3 [154.0], 171.1.



*Tetra*-*n*-butylammonium fluoride (638  $\mu\text{L}$ , 1M solution in THF, 0.64 mmol, 1.25 equiv) was added dropwise to a solution of triflate **119** (295 mg, 0.51 mmol, 1.00 equiv.) in dry THF over 15 minutes period at 0  $^\circ\text{C}$ . The reaction mixture was stirred 4.5 h under nitrogen maintaining the temperature between 0-5  $^\circ\text{C}$ . The reaction mixture was concentrated and applied to a flash column, eluted with 3:1 Hexanes:EtOAc to give **118** as colorless oil (170 mg, 69%).  $R_f$  0.62 (1:1 EtOAc: Hexane).  $^1\text{H}$  NMR ( $\text{CDCl}_3$ , 400 MHz)  $\delta$  2.26-2.46 (m, 1H), 2.51 (app. t,  $J = 16.6$  Hz, 1H), 3.63 (dtd,  $J = 34.9, 12.05, 4.0$  Hz, 1H), 3.88 (ddd,  $J = 26.6, 13.2, 3.4$ , 1H), 4.06 (t,  $J = 6.4$  Hz, 0.5H), 4.25 (t,  $J = 7.0$  Hz, 0.5H), 4.30-4.42 (m, 2H), 4.48-4.55 (m, 0.5H), 4.66 (d,  $J = 9.6$  Hz, 0.5H), 5.17 (d,  $J = 12.3$  Hz, 1H), 5.12-5.17 (m, 1H), 5.22 (d,  $J = 12.4$  Hz, 1H), 5.28 (dt,  $J = 15.8, 3.8$  Hz, 1H), 7.24-7.41 (m, 9H), 7.50 (d,  $J = 7.3$  Hz, 1H), 7.58 (dd,  $J = 7.3, 3.3$  Hz, 1H), 7.75 (t,  $J = 7.4$  Hz, 2H);  $^{13}\text{C}$  NMR ( $\text{CDCl}_3$ , 100 MHz)  $\delta$  36.8 [37.9] ( $J_{\text{C-F}} = 22$  Hz), 47.4, 53.2 [53.7] ( $J_{\text{C-F}} = 25$  Hz), 57.8 [58.1], 67.3, 67.8 [67.9], 90.8 [92.6] ( $J_{\text{C-F}} = 104$  Hz), 120.1, 125.1, 125.2, 125.3, 127.3, 127.9, 128.3, 128.3, 128.4, 128.5, 128.7, 135.7, 135.6, 141.5, 141.6, 143.8, 143.9, 144.3,

154.5 [154.5], 171.0 [171.2]; HRMS (+ESI) calcd for C<sub>27</sub>H<sub>24</sub>FNO<sub>4</sub> (M+H)<sup>+</sup> 446.1767; obsd: 446.1761.



2S,4S-fluoroproline (**121**)

Palladium on carbon (10%, 20 mg) was added in one portion to a solution of Fmoc-flp-OBn (**118**) in (102 mg, 0.23 mmol) in EtOH (2 mL), H<sub>2</sub>O (1mL), and CH<sub>2</sub>Cl<sub>2</sub> (1mL). The reaction flask was evacuated, then opened to an atmosphere of H<sub>2</sub> and stirred 4.5 h. The catalyst was removed by filtering through a plug of Celite<sup>®</sup> in a Pasteur pipet. The filtrate was concentrated to give flp (**121**) (26 mg, 85%). *R<sub>f</sub>* 0.20 (6:4:1 CH<sub>2</sub>Cl<sub>2</sub>:CHCl<sub>3</sub>:H<sub>2</sub>O). [α]<sub>D</sub><sup>25</sup> -16.6 (c 0.75, MeOH). <sup>1</sup>H NMR (D<sub>2</sub>O, 400 MHz) δ 2.49-2.56 (m, 1H), 2.66 (app. d, *J* = 4.1 Hz, 1H), 3.50 (d, *J* = 13.3 Hz, 0.5H), 3.60 (d, *J* = 11.7 Hz, 0.5H), 3.84 (dd, *J* = 19.0, 14.0 Hz, 1H), 4.39 (d, *J* = 7.6 Hz, 1H), 5.41 (s, 1H), 5.54 (s, 1H); <sup>13</sup>C NMR (CDCl<sub>3</sub>, 100 MHz) δ 35.8 [36.0], 51.8 [52.0], 59.8, 91.4 [93.1], 173.8.

### 3.8.2 Variable temperature NMR experiments

Samples of **61**, **62**, **63**, and **89** were prepared in D<sub>2</sub>O at concentrations between 0.02 M and 0.03 M. Experiments were performed over several temperatures (25-85 °C) on a Bruker 400 MHz NMR spectrometer. The ratio of *trans/cis* isomer was determined by integrating well resolved <sup>1</sup>H NMR signals. Thermodynamics data Δ*H*<sup>°</sup> and Δ*S*<sup>°</sup> (Table 3.18) were calculated by fitting the data of the Van't Hoff plots to the following equation;

$$\ln K_{tc} = (-\Delta H^{\circ}/R)(1/T) + \Delta S^{\circ}/R$$

Δ*G*<sup>°</sup> was calculated from Δ*G*<sup>°</sup> = Δ*H*<sup>°</sup> – *T*Δ*S*<sup>°</sup>

Δ*H*<sup>°</sup>= standard enthalpy

Δ*S*<sup>°</sup>= standard entropy

$\Delta G^\circ$ =standard Gibbs free energy

$R$ = gas constant (8.314 J K<sup>-1</sup>mol<sup>-1</sup>)

Table 3.18: Thermodynamics data derived from Van't Hoff plots

Dipeptide	Equation	Slope	Intercept	$\Delta H^\circ$ (kJ/mol)	$\Delta S^\circ$ (J/mol/K)	$\Delta G^\circ$ (298 K) (kJ/mol/K)
<b>61</b>	$y=322.144x-0.2615$	322.144	-0.2615	-2.67	-2.17	-2.03
<b>62</b>	$y=764.926x-0.4019$	764.926	-0.4019	-6.36	-3.34	-5.36
<b>63</b>	$y=1086.956x-1.0473$	1086.956	-1.0473	-9.04	-8.67	-6.45
<b>89</b>	$y=333.9919x-0.0304$	333.992	-0.0304	-2.78	-0.25	-2.70

Tables 3.19-3.22 show the equilibrium constants at various temperatures for compounds **61**, **62**, **63** and **89** and figures 3.20-3.23 display the relevant Van't Hoff plots for the *cis*→*trans* isomerization of the prolyl peptide bond of each dipeptide.

Table 3.19: Thr-Pro amide isomer equilibrium constant  $K_{t/c}$  at various temperatures for Ac-Thr-Pro-NHMe (**61**)

T (°C)	T (K)	1000/T	Integration of methylamide CH <sub>3</sub>		$K_{t/c}$	$\ln K_{t/c}$
			<i>trans</i>	<i>cis</i>		
85	358	2.79	5.4	2.9	1.9	0.62
80	353	2.83	2.2	1.1	2.0	0.69
75	348	2.87	5.7	2.9	2.0	0.68
70	343	2.92	5.0	2.6	1.9	0.65
65	338	2.96	5.5	2.7	2.0	0.71
60	333	3.00	5.5	2.8	2.0	0.68
55	328	3.05	4.2	1.9	2.2	0.79
50	323	3.10	5.0	2.5	2.0	0.69
45	318	3.14	4.9	2.6	1.9	0.63
40	313	3.19	6.4	2.9	2.2	0.79
35	308	3.25	6.6	2.9	2.3	0.82
30	303	3.30	6.8	3	2.3	0.82
25	298	3.36	4.8	2.1	2.3	0.83

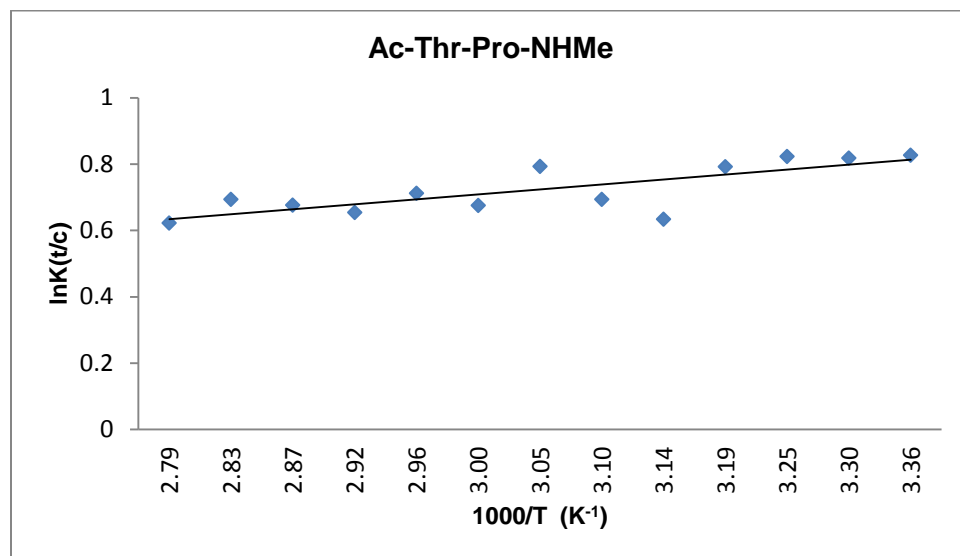


Figure 3.20: Van't Hoff plot for the *cis*→*trans* isomerization of Thr-Pro amide bond of Ac-Thr-Pro-NHMe (**61**) in D<sub>2</sub>O

Table 3.20: Thr-Pro amide isomer equilibrium constant  $K_{t/c}$  at various temperatures for Ac-Thr-Hyp-NHMe (**62**)

T (°C)	T (K)	1000/T	Integration of Thr-Hy		$K_{t/c}$	$\ln K_{t/c}$
			<i>trans</i>	<i>cis</i>		
85	358	2.79	8.8	1.6	5.5	1.70
80	353	2.83	4.8	0.8	6.0	1.79
75	348	2.87	8.7	1.4	6.2	1.82
70	343	2.92	8.7	1.4	6.2	1.82
65	338	2.96	8.2	1.3	6.3	1.84
60	333	3.00	8.7	1.3	6.7	1.90
55	328	3.05	8.3	1.2	6.9	1.93
50	323	3.10	8.4	1.2	7.0	1.95
45	318	3.14	8.3	1.1	7.5	2.01
40	313	3.19	8.4	1.1	7.6	2.03
35	308	3.25	8.1	1.0	8.1	2.09
30	303	3.30	8.4	1.0	8.4	2.13
25	298	3.36	8.7	1.0	8.7	2.16

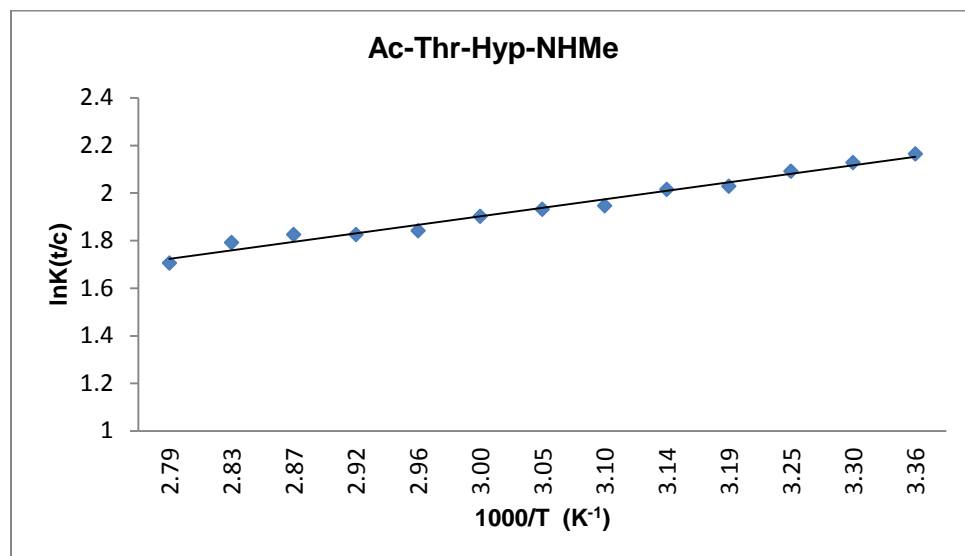


Figure 3.21: Van't Hoff plot for the *cis*→*trans* isomerization of Thr-Pro amide bond of Ac-Thr-Hyp-NHMe (**62**) in D<sub>2</sub>O

Table 3.21: Thr-Pro amide isomer equilibrium constant  $K_{t/c}$  at various temperatures for Ac-Thr-[( $\alpha$ ,1-4)GlcNAc]Hyp-NHMe (**63**)

T (°C)	T (K)	1000/T	Integration of Thr-Hy		$K_{t/c}$	$\ln K_{t/c}$
			<i>trans</i>	<i>cis</i>		
85*	358	2.79	10.9	1.9	5.7	1.75
80	353	2.83	11.1	1.4	7.9	2.07
75	348	2.87	11.4	1.2	9.5	2.25
70	343	2.92	11.1	1.2	9.3	2.22
65	338	2.96	7.7	0.9	8.6	2.15
60	333	3.00	10.8	1.1	9.8	2.28
55	328	3.05	9.3	1	9.3	2.23
50	323	3.10	7.7	0.8	9.6	2.26
45	318	3.14	11.6	1.1	10.5	2.36
40	313	3.19	9.2	0.8	11.5	2.44
35	308	3.25	11.4	1	11.4	2.43
30	303	3.30	10.5	0.8	13.1	2.57
25	298	3.36	11.9	0.9	13.2	2.58

\*This data point was eliminated due to the poor resolution of the designated  $^1\text{H}$  NMR signal at 85 °C.

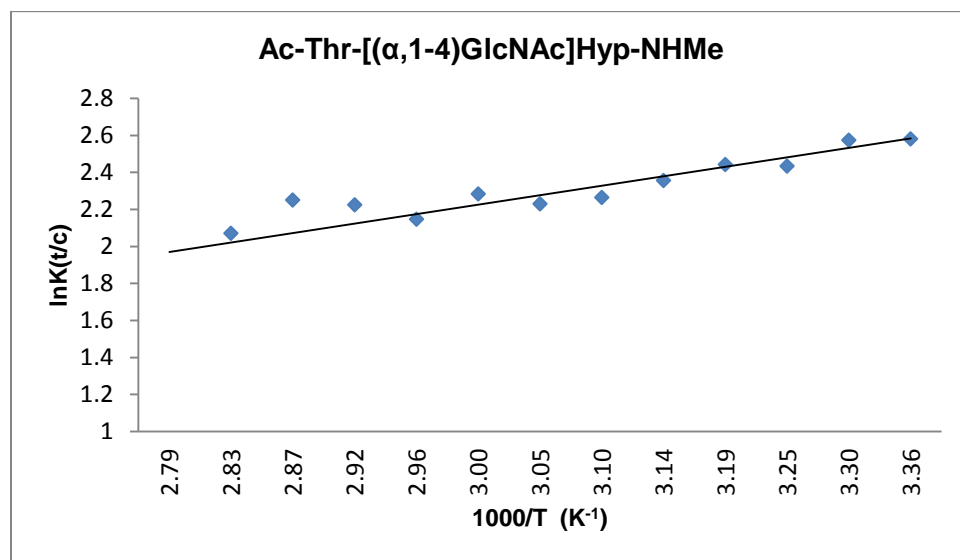


Figure 3.22: Van't Hoff plot for the *cis*→*trans* isomerization of Thr-amide bond of Ac-Thr-[( $\alpha$ ,1-4)GlcNAc]Hyp-NHMe (**63**) in  $\text{D}_2\text{O}$



Table 3.22: Thr-Pro amide isomer equilibrium constant  $K_{t/c}$  at various temperatures for Ac-[( $\alpha$ ,1-4)GlcNAc]-NHMe (**89**)

T (°C)	T (K)	1/T x 10 <sup>-3</sup>	Integration of methylamide CH <sub>3</sub>		$K_{t/c}$	$\ln K_{t/c}$
			<i>trans</i>	<i>cis</i>		
*85	358	2.79	1.9	0.6	3.2	1.14
80	353	2.83	2.0	0.8	2.5	0.97
75	348	2.87	2.1	0.8	2.6	0.96
70	343	2.92	2.1	0.8	2.6	0.94
65	338	2.96	2.1	0.7	3.0	1.03
60	333	3.00	2.1	0.7	3.0	1.04
55	328	3.05	2.1	0.7	3.0	1.10
50	323	3.10	2.1	0.8	2.6	1.02
45	318	3.14	2.2	0.8	2.8	1.09
40	313	3.19	2.1	0.7	3.0	1.05
35	308	3.25	2.1	0.6	3.5	1.21
30	303	3.30	2.0	0.6	3.3	1.19
25	298	3.36	2.0	0.6	3.3	1.18

\*This data point was eliminated due to the poor resolution of the designated <sup>1</sup>H NMR signal at 85 °C.

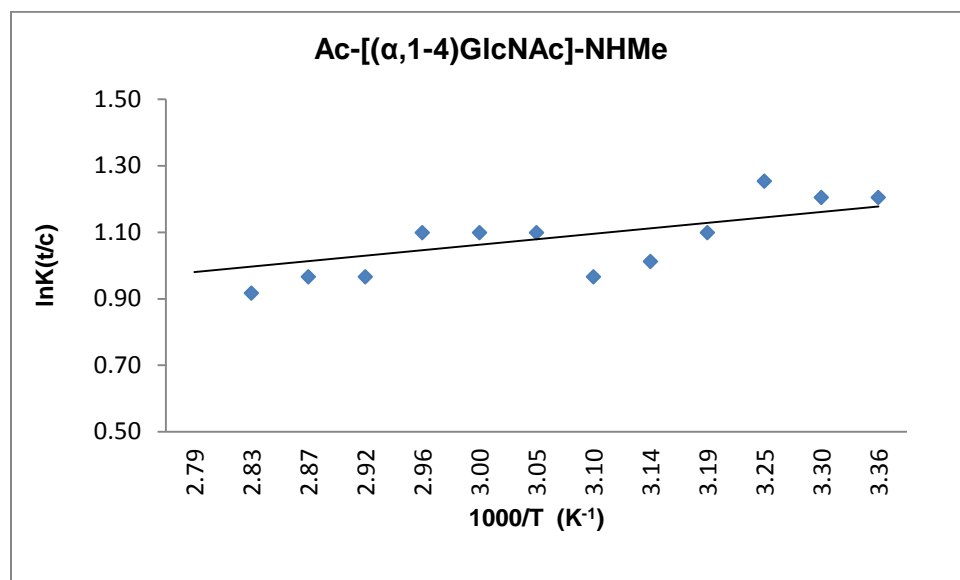


Figure 3.23: Van't Hoff plot for the *cis*→*trans* isomerization of proline amide bond of Ac-Hyp(GlcNAc)-NHMe (**89**) in D<sub>2</sub>O

### 3.8.3 Magnetization Transfer NMR Experiments

Samples of **61**, **62**, **63**, and **89** were prepared in D<sub>2</sub>O at concentrations between 0.02 M and 0.03 M. Experiments were performed over several temperatures (60-75 °C) on a Varian 700 MHz NMR spectrometer and the temperature was calibrated using an ethylene glycol standard.

Depending on the resolution of <sup>1</sup>H NMR signals, the threonine H<sub>γ</sub> doublet or the *N*-methylamide of the *trans* rotamer doublet was selectively inverted using a 58 ms pulse. Relaxation delay (d<sub>1</sub>) of 20 s, acquisition time of 2.12 s, inversion pulse power (satpwr) of -13, detection pulse power (tpwr) of 59 and detection pulse width (pw) of 8.9 μs were used. In each experiment inversion transfer spectra were measured at 23-28 d<sub>2</sub> values from 0-20 s and the number of points 32K and number of scans 128.

The data from the inversion transfer experiments were fitted using the CIFIT program.<sup>76</sup> The initial estimates of rate, T<sub>1</sub>, M<sub>0</sub> and M<sub>α</sub> were fed to the CIFIT mechanism file. The CIFIT program then conducts a least-squares minimization on the difference between the integration versus time curves in the data file and the curves predicted by the McConnell-Bloch equations given the initial guesses in the mechanism file.

T<sub>1</sub> = Spin lattice relaxation time

M<sub>0</sub> = Initial Magnetization

M<sub>α</sub> = Equilibrium Magnetization

Tables 3.23-3.41 show the integration vs. d<sub>2</sub> obtained from magnetization inversion transfer data and figures 3.24-3.42 display the inversion recovery of inverted *trans* and non inverted *cis* proton signals.

Table 3.23: Integration vs.  $d_2$  Ac-Thr-Hyp-NHMe (**62**) at 60 °C

$d_2$ (s)	Integration		$d_2$ (s)	Integration	
	<i>trans</i>	<i>cis</i>		<i>trans</i>	<i>cis</i>
0.1403	-0.43	0.31	2.1781	1.67	0.34
0.1977	-0.28	0.29	2.5853	1.78	0.35
0.2346	-0.19	0.29	3.0687	1.86	0.36
0.2785	-0.09	0.28	3.6424	1.92	0.37
0.3924	0.14	0.28	4.3234	1.95	0.37
0.4657	0.27	0.27	5.1318	1.97	0.38
0.5528	0.42	0.27	7.2301	1.97	0.37
0.7788	0.72	0.27	8.5819	1.96	0.37
0.9245	0.91	0.28	10.180	1.95	0.37
1.0993	1.08	0.29	12.091	1.94	0.37
1.5460	1.40	0.31	14.352	1.93	0.37
1.8350	1.55	0.33			

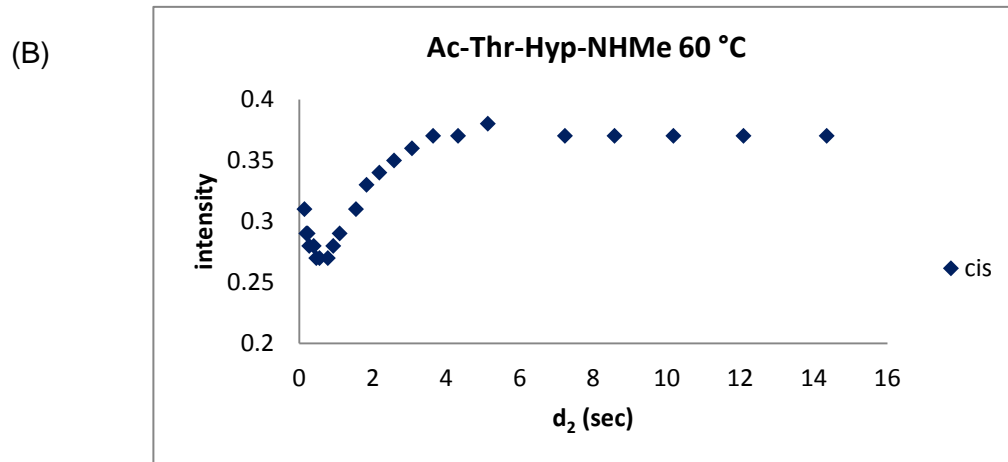
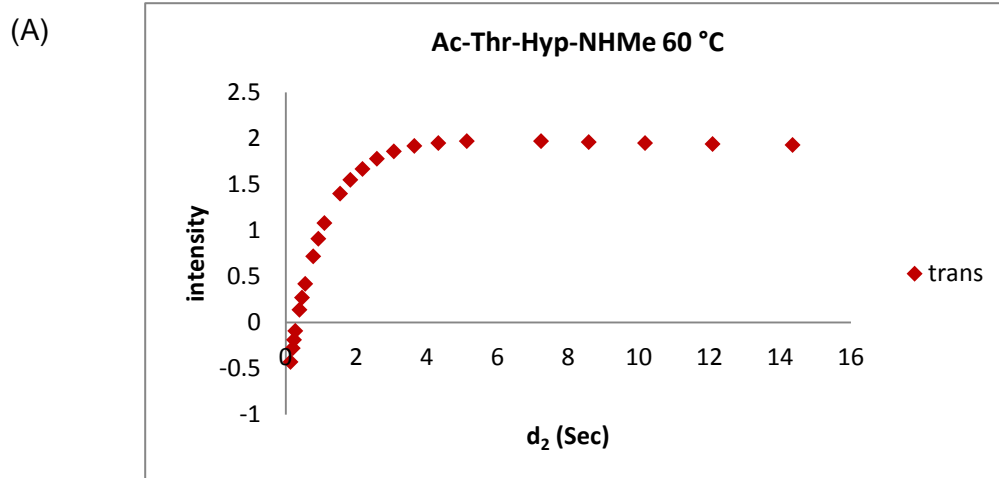


Figure 3.24: Inversion recovery of (A) inverted *trans* Thr-Hy doublet and (B) non-inverted *cis* Thr-Hy doublet of compound **62** at 60 °C

Table 3.24: Integration vs.  $d_2$  Ac-Thr-Hyp-NHMe (**62**) at 65 °C

$d_2$ (s)	Integration		$d_2$ (s)	Integration	
	<i>trans</i>	<i>cis</i>		<i>trans</i>	<i>cis</i>
0.1403	-0.23	0.26	2.1781	1.62	0.35
0.1977	-0.02	0.26	2.5853	1.71	0.37
0.2346	0.09	0.26	3.0687	1.78	0.38
0.2785	0.17	0.25	3.6424	1.83	0.38
0.3924	0.36	0.25	4.3234	1.86	0.39
0.4657	0.47	0.25	5.1318	1.88	0.39
0.5528	0.59	0.25	7.2301	1.87	0.39
0.7788	0.84	0.26	8.5819	1.85	0.39
0.9245	0.98	0.27	10.180	1.85	0.39
1.0993	1.12	0.28	12.091	1.85	0.39
1.5460	1.39	0.31	14.352	1.84	0.39
1.8350	1.51	0.33			

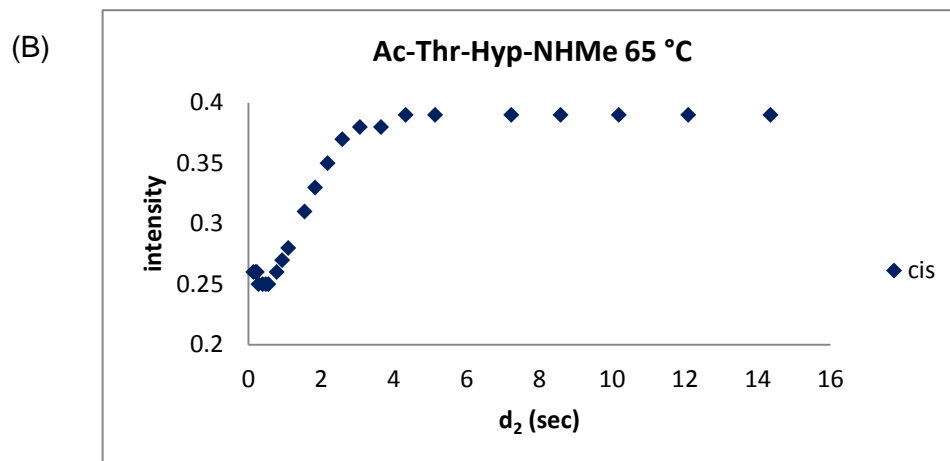
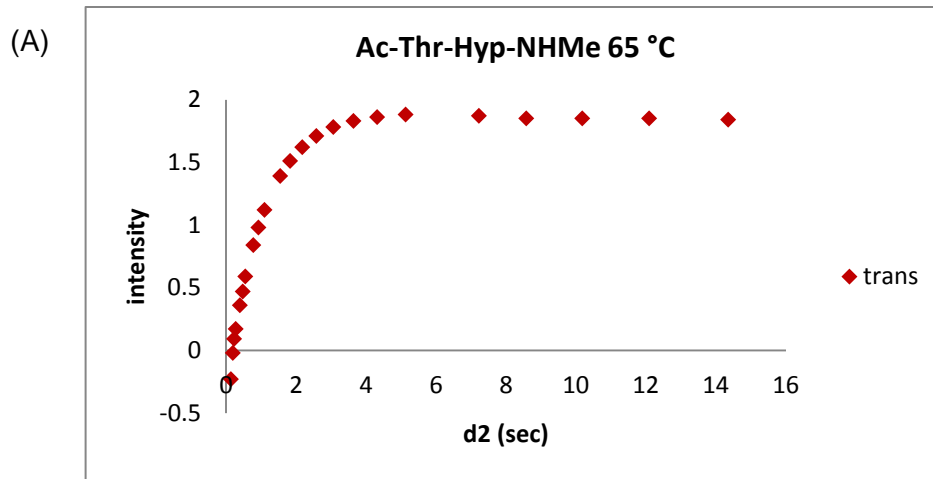
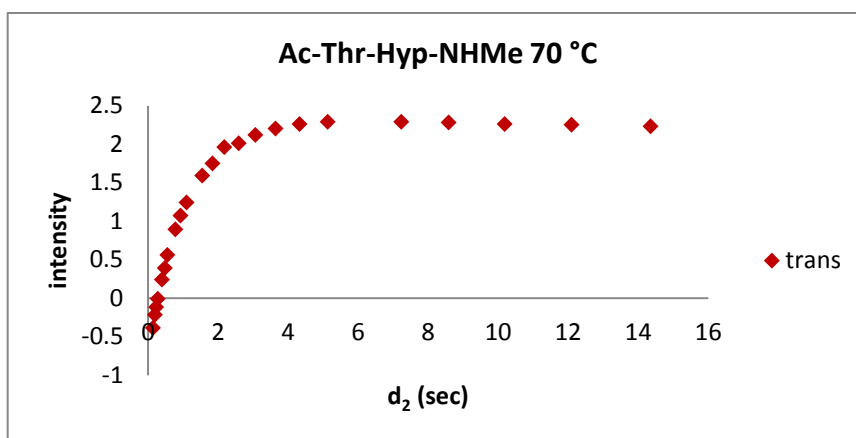


Figure 3.25: Inversion recovery of (A) inverted *trans* Thr-Hyp doublet and (B) non-inverted *cis* Thr-Hyp doublet of compound **62** at 65 °C

Table 3.25: Integration vs.  $d_2$  Ac-Thr-Hyp-NHMe (**62**) at 70 °C

Integration			Integration		
$d_2$ (s)	<i>trans</i>	<i>cis</i>	$d_2$ (s)	<i>trans</i>	<i>cis</i>
0.1403	-0.39	0.28	2.1781	1.96	0.39
0.1977	-0.22	0.25	2.5853	2.01	0.4
0.2346	-0.12	0.24	3.0687	2.12	0.42
0.2785	-0.01	0.23	3.6424	2.2	0.43
0.3924	0.24	0.22	4.3234	2.26	0.43
0.4657	0.39	0.22	5.1318	2.29	0.44
0.5528	0.56	0.22	7.2301	2.29	0.44
0.7788	0.89	0.24	8.5819	2.28	0.43
0.9245	1.07	0.26	10.180	2.26	0.43
1.0993	1.24	0.28	12.091	2.25	0.42
1.5460	1.59	0.32	14.352	1.96	0.39
1.8350	1.75	0.35			

(A)



(B)

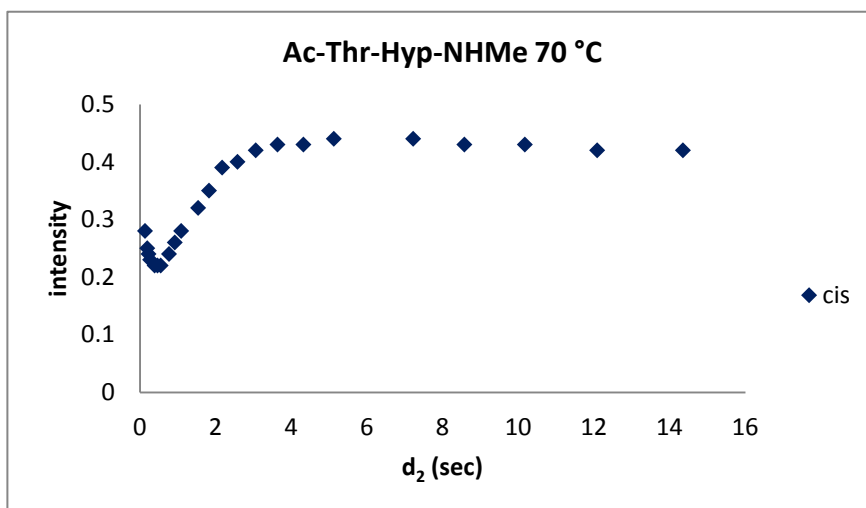


Figure 3.26: Inversion recovery of (A) inverted *trans* Thr-Hy doublet and (B) non-inverted *cis* Thr-Hy doublet of compound **62** at 70 °C

Table 3.26: Integration vs.  $d_2$  Ac-Thr-Hyp-NHMe (**62**) at 75 °C

Integration			Integration		
$d_2$ (s)	<i>trans</i>	<i>cis</i>	$d_2$ (s)	<i>trans</i>	<i>cis</i>
0.1403	-0.39	0.17	2.1781	1.79	0.26
0.1977	-0.22	0.14	2.5853	1.92	0.28
0.2346	-0.12	0.13	3.0687	2.03	0.29
0.2785	-0.01	0.13	3.6424	2.11	0.3
0.3924	0.22	0.12	4.3234	2.16	0.31
0.4657	0.36	0.12	5.1318	2.19	0.31
0.5528	0.51	0.12	7.2301	2.2	0.31
0.7788	0.81	0.15	8.5819	2.19	0.31
0.9245	0.98	0.17	10.180	2.18	0.32
1.0993	1.15	0.18	12.091	2.17	0.34
1.5460	1.49	0.23	14.352	2.17	0.33
1.8350	1.65	0.25			

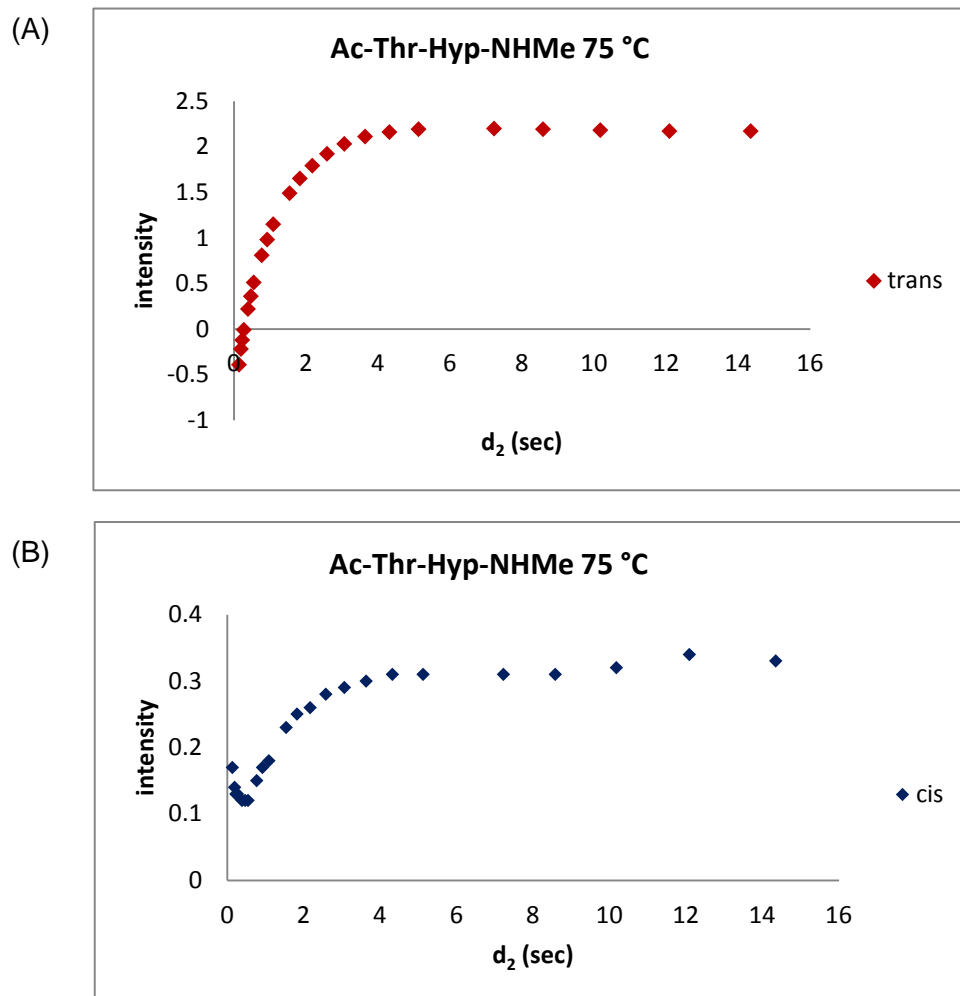


Figure 3.27: Inversion recovery of (A) inverted *trans* Thr-Hy doublet and (B) non-inverted *cis* Thr-Hy doublet of compound **62** at 75 °C

Table 3.27: Data for Eyring Analysis for rotation about the Ac-Hyp amide bond of Ac-Hyp-NHMe (62)

T (°C)	T (K)	1000/T (K <sup>-1</sup> )	k (s <sup>-1</sup> )	k/T	lnk/T	Rln(k/T)	Rln(k/T) - Rln(kB/h)
60	333.16	3.0016	0.1416	0.0004	-7.7634	-15.449	-62.629
65	338.16	2.9572	0.2050	0.0006	-7.4083	-14.742	-61.922
70	343.16	2.9141	0.3000	0.0008	-7.0422	-14.014	-61.194
75	348.16	2.8722	0.4861	0.0013	-6.5740	-13.0823	-60.262

$R$  = gas constant (8.314 J K<sup>-1</sup>mol<sup>-1</sup>)  
 $k_B$  = Boltzmann constant (1.381x10<sup>-23</sup> J K<sup>-1</sup>)  
 $h$  = Planck's constant (6.626x10<sup>-34</sup> J s)  
 $k$  = reaction rate (reported in the CIFIT output files)

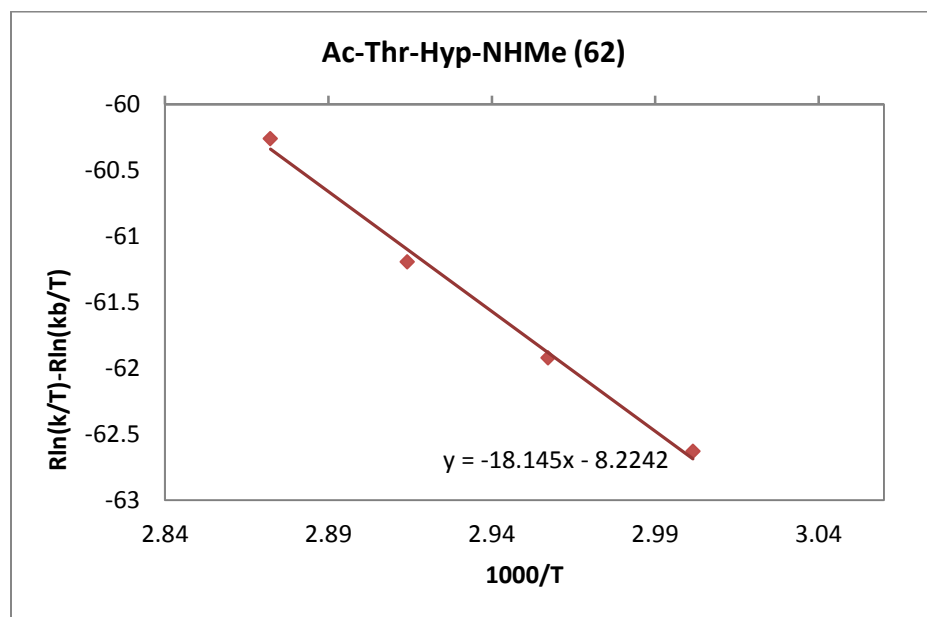


Figure 3.28: Eyring plot for rotation about the Thr-Hyp amide bond of Ac-Thr-Hyp-NHMe (62)

$\Delta H^\ddagger$  and  $\Delta S^\ddagger$  were calculated by fitting the data of the Eyring plots to the following equation;

$$R\ln(k/T) - R\ln(kB/h) = (-\Delta H^\ddagger/R)(1/T) + \Delta S^\ddagger/R$$

$\Delta G^\ddagger$  was calculated from  $\Delta G^\ddagger = -\Delta H^\ddagger - T\Delta S^\ddagger$

$\Delta H^\ddagger = 18.1$  kcal/mol,  $\Delta S^\ddagger = -8.2$  cal/mol.K,  $\Delta G^\ddagger$  (300 K) = 20.7 kcal/mol

Table 3.28: Integration vs.  $d_2$  Ac-Hyp[( $\alpha$ ,1-4)GlcNAc]-NHMe (**89**) at 60 °C

$d_2$ (s)	Integration			Integration		
	<i>trans</i>	<i>cis</i>		$d_2$ (s)	<i>trans</i>	<i>cis</i>
0.000	-10.00	7.652		0.800	1.150	5.49
0.005	-10.27	6.994		1.000	3.220	5.40
0.010	-10.96	6.401		1.500	7.100	5.42
0.050	-9.617	6.863		2.000	10.25	5.66
0.100	-8.740	6.570		4.000	16.42	6.72
0.150	-7.710	6.370		6.000	18.51	7.36
0.200	-6.740	6.450		8.000	19.37	7.59
0.250	-5.870	6.210		12.00	19.72	7.50
0.400	-3.750	5.870		16.00	19.45	7.37
0.600	-1.210	5.660				

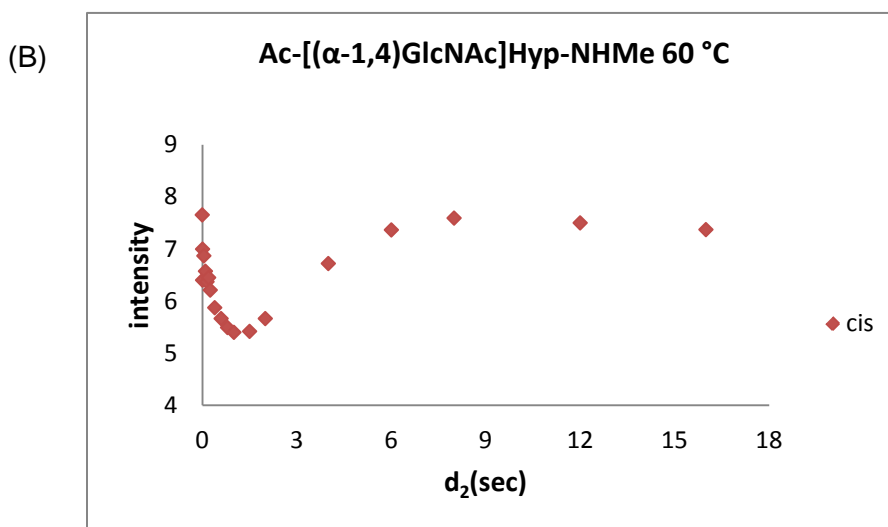
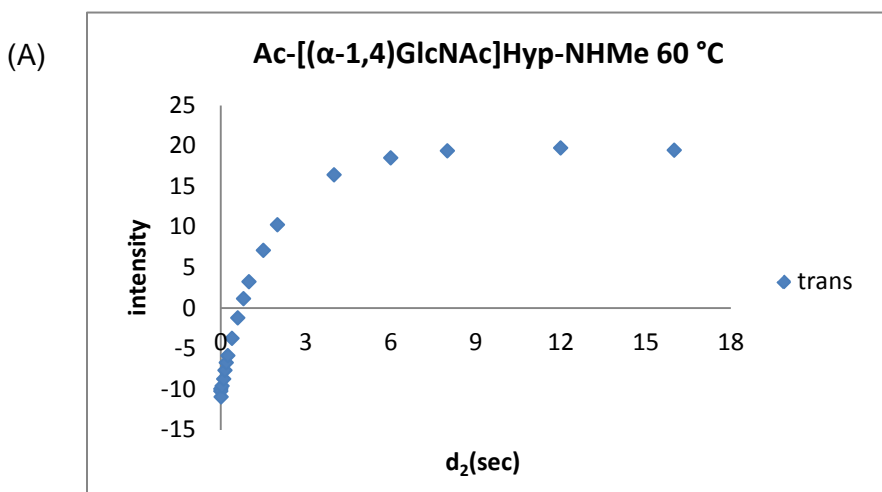


Figure 3.29: Inversion recovery of (A) inverted *trans* GlcNAc-H1 doublet and (B) non-inverted *cis* Thr-Hy doublet of compound **89** at 60 °C



Table 3.29: Integration vs.  $d_2$  Ac-Hyp[( $\alpha$ ,1-4)GlcNAc]-NHMe (**89**) at 65 °C

$d_2$ (s)	Integration		$d_2$ (s)	Integration	
	<i>trans</i>	<i>cis</i>		<i>trans</i>	<i>cis</i>
0.000	-10.00	8.466	0.800	3.760	7.227
0.005	-9.121	9.170	1.000	5.810	7.157
0.010	-8.870	9.174	1.500	9.851	7.258
0.050	-8.016	9.017	2.000	12.69	7.304
0.100	-6.963	8.682	4.000	18.82	8.768
0.150	-5.895	8.321	6.000	21.02	9.434
0.200	-5.092	8.107	8.000	21.98	9.665
0.250	-4.056	7.863	12.00	22.40	9.887
0.400	-1.560	7.451	16.00	22.40	9.676
0.600	1.140	7.310			

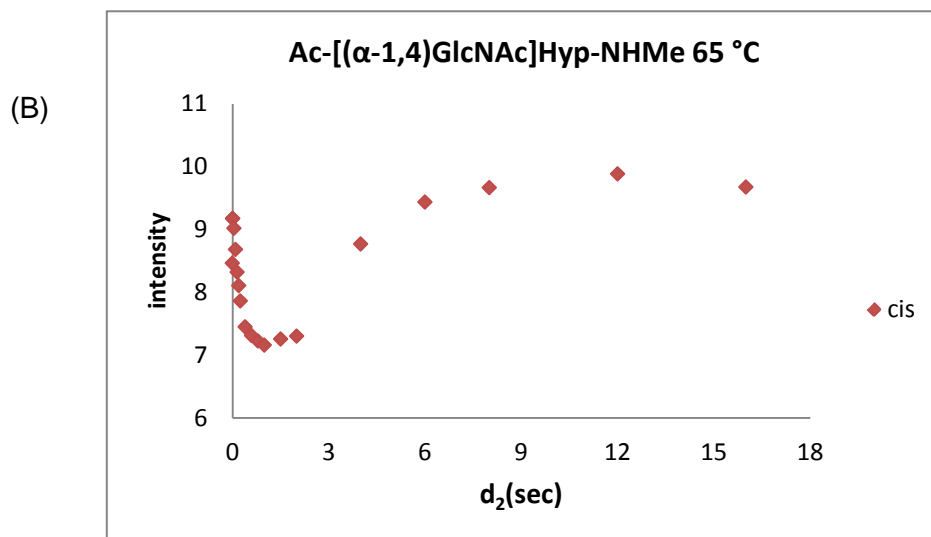
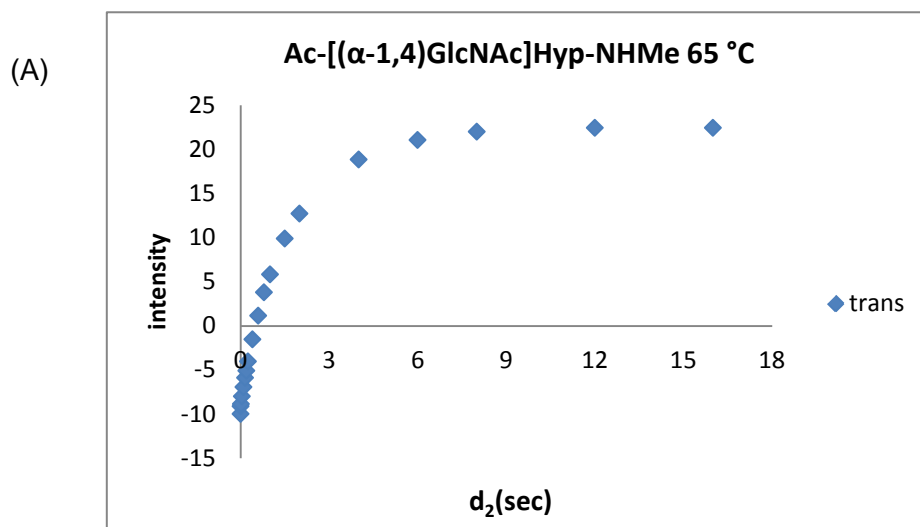


Figure 3.30: Inversion recovery of (A) inverted *trans* GlcNAc-H1 doublet and (B) non-inverted *cis* Thr-Hy doublet of compound **89** at 65 °C

Table 3.30: Integration vs.  $d_2$  Ac-Hyp[( $\alpha$ ,1-4)GlcNAc]-NHMe (**89**) at 70 °C

Integration			Integration		
$d_2$ (s)	<i>trans</i>	<i>cis</i>	$d_2$ (s)	<i>trans</i>	<i>cis</i>
0.00	-10.00	8.466	1.50	6.871	3.430
0.10	-10.84	6.727	2.00	9.410	3.850
0.20	-8.729	5.691	3.00	13.19	4.952
0.25	-6.025	4.374	4.00	15.59	5.865
0.40	-3.754	3.845	5.00	17.19	6.564
0.60	-1.045	3.439	6.00	18.04	6.788
0.80	1.246	3.293	7.00	18.34	6.767
1.00	3.332	3.248	8.00	18.85	6.892

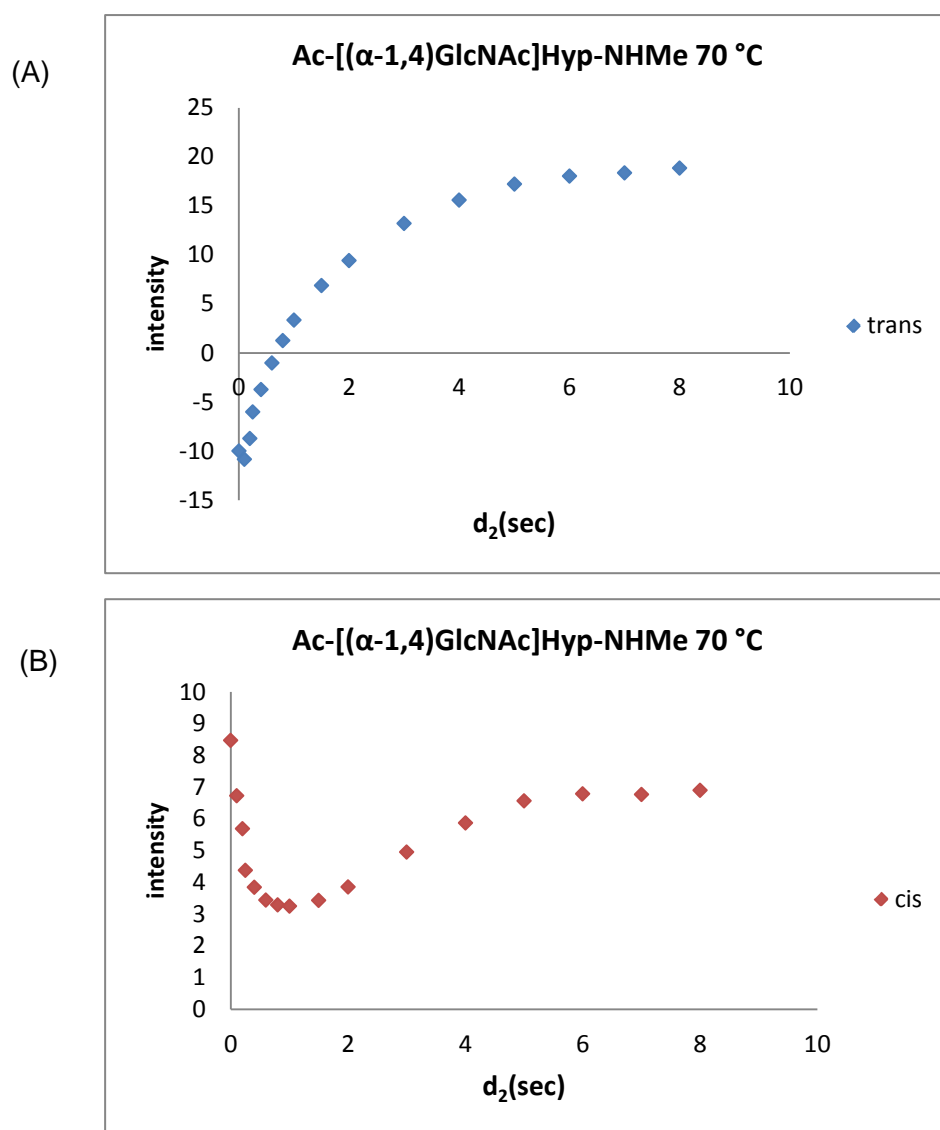


Figure 3.31: Inversion recovery of (A) inverted *trans* GlcNAc-H1 doublet and (B) non-inverted *cis* Thr-Hy doublet of compound **89** at 70 °C

Table 3.31: Integration vs.  $d_2$  Ac-Hyp[( $\alpha$ ,1-4)GlcNAc]-NHMe (**89**) at 75 °C

Integration			Integration		
$d_2$ (s)	<i>trans</i>	<i>cis</i>	$d_2$ (s)	<i>trans</i>	<i>cis</i>
0.00	-10.00	8.466	1.50	9.874	5.351
0.10	-9.832	9.005	2.00	12.44	5.836
0.20	-7.207	7.645	3.00	16.09	7.136
0.25	-3.828	6.106	4.00	18.71	7.826
0.40	-1.024	5.323	5.00	21.43	9.512
0.60	2.032	4.724	6.00	22.70	9.945
0.80	4.374	4.631	7.00	22.35	9.236
1.00	6.455	4.811	8.00	22.96	9.458

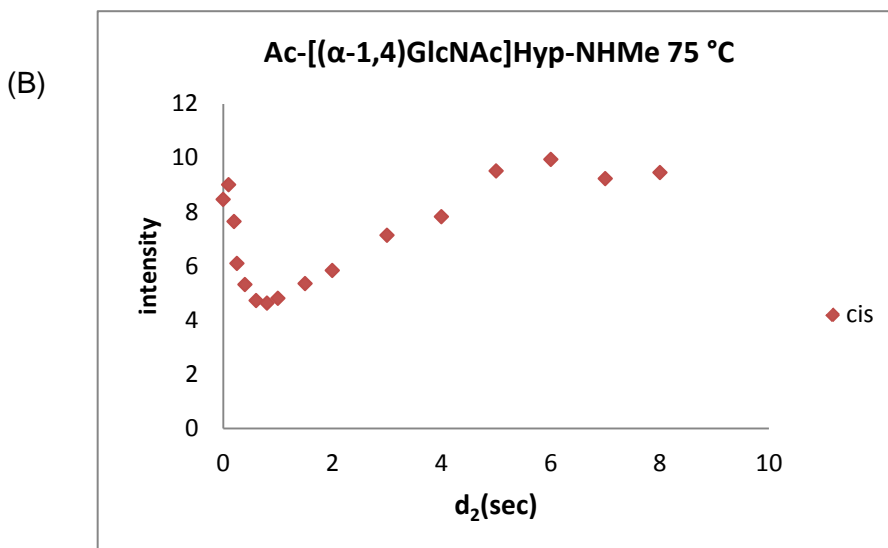
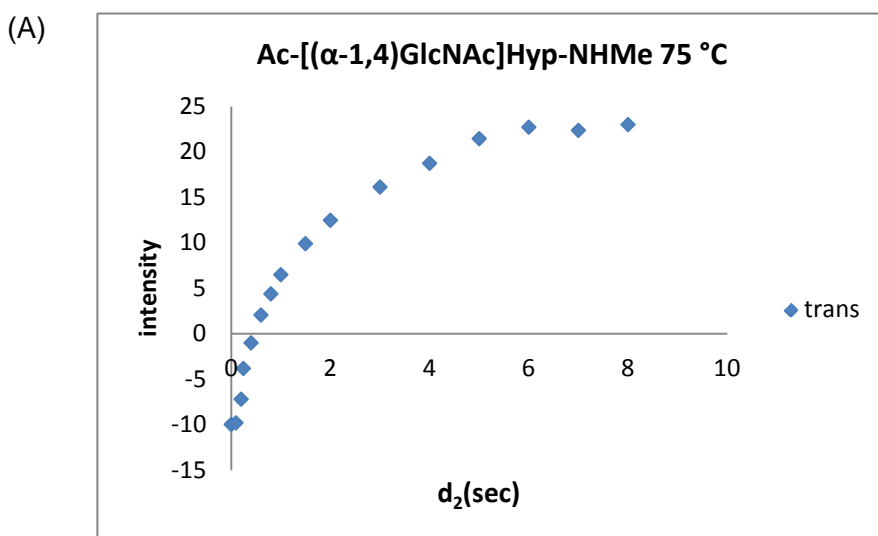


Figure 3.32: Inversion recovery of (A) inverted *trans* GlcNAc-H1 doublet and (B) non-inverted *cis* Thr-Hy doublet of compound **89** at 75 °C

Table 3.32: Integration vs.  $d_2$  Ac-Hyp[( $\alpha$ ,1-4)GlcNAc]-NHMe (**89**) at 80 °C

Integration			Integration		
$d_2$ (s)	<i>trans</i>	<i>cis</i>	$d_2$ (s)	<i>trans</i>	<i>cis</i>
0.00	-10.00	9.763	1.50	12.53	4.736
0.10	-10.73	8.945	2.00	15.67	5.806
0.20	-9.641	9.797	3.00	23.41	8.699
0.25	-7.608	8.662	4.00	27.14	10.02
0.40	-5.986	7.213	5.00	28.48	10.35
0.60	-4.161	6.616	6.00	30.03	11.04
0.80	-2.305	6.181	7.00	30.74	11.60
1.00	-0.869	5.674	8.00	12.53	4.736

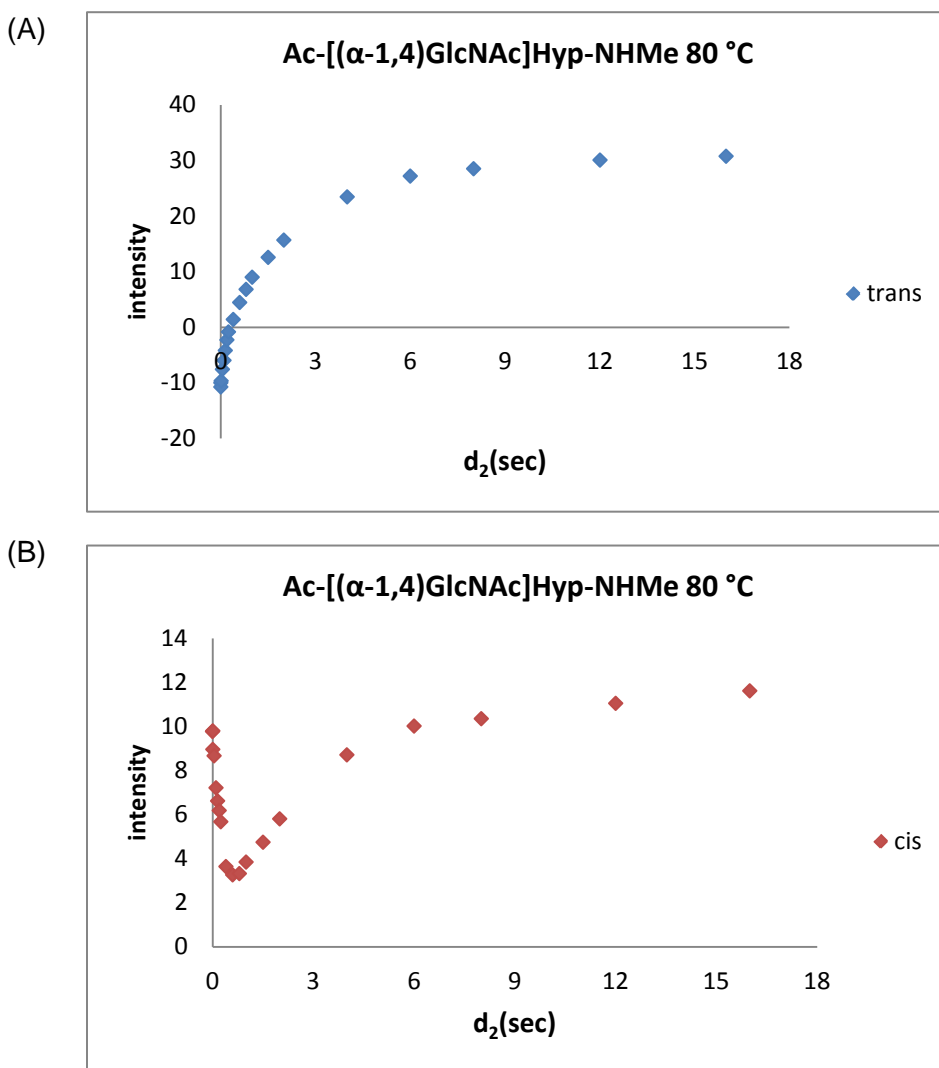


Figure 3.33: Inversion recovery of (A) inverted *trans* GlcNAc-H1 doublet and (B) non-inverted *cis* Thr-Hy doublet of compound **89** at 80 °C

Table 3.33: Data for Eyring analysis for rotation about the Ac-Hyp amide bond of Ac-Hyp[( $\alpha$ ,1-4)GlcNAc]-NHMe (**89**)

T (°C)	T (K)	1000/T (K <sup>-1</sup> )	k (s <sup>-1</sup> )	k/T	lnk/T	Rln(k/T)	Rln(k/T) – Rln(kB/h)
60	333.16	3.0016	0.1513	0.0004	-7.6971	-15.317	-62.497
65	338.16	2.9572	0.1768	0.0005	-7.5563	-15.037	-62.217
70	343.16	2.9141	0.4622	0.0013	-6.6100	-13.154	-60.334
75	348.16	2.8722	0.5054	0.0015	-6.5351	-13.005	-60.185
80	353.16	2.8316	0.7258	0.0021	-6.1874	-12.313	-59.493

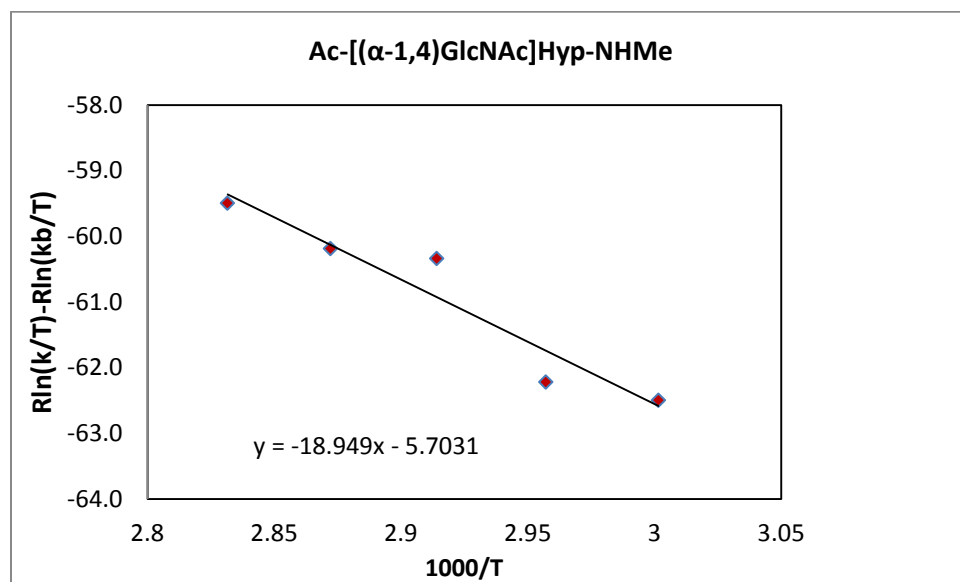


Figure 3.34: Eyring plot for the rotation of Ac-Hyp amide bond of Ac-Hyp[( $\alpha$ ,1-4)GlcNAc]-NHMe (**89**)

$\Delta H^\ddagger$  and  $\Delta S^\ddagger$  were calculated by fitting the data of the Eyring plots to the following equation;

$$R\ln(k/T) - R\ln(kB/h) = (-\Delta H^\ddagger/R)(1/T) + \Delta S^\ddagger/R$$

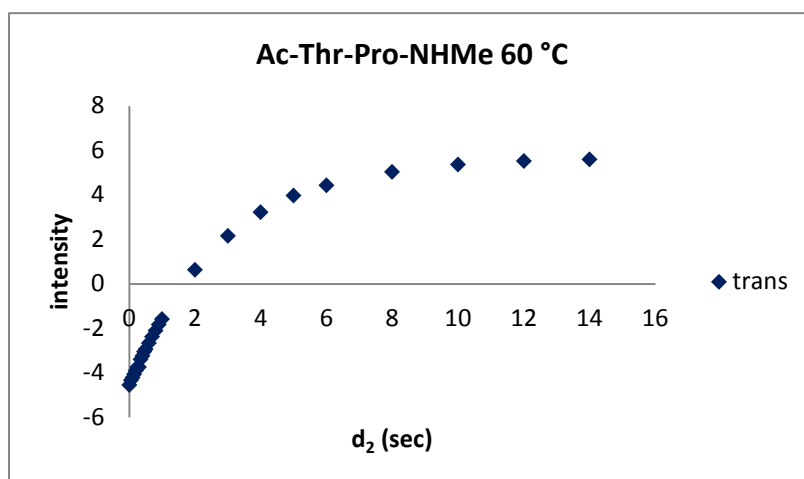
$\Delta G^\ddagger$  was calculated from  $\Delta G^\ddagger = -\Delta H^\ddagger - T\Delta S^\ddagger$

$\Delta H^\ddagger = 18.9$  kcal/mol,  $\Delta S^\ddagger = -5.7$  cal/mol.K,  $\Delta G^\ddagger$  (300 K) = 20.6 kcal/mol

Table 3.34: Integration vs.  $d_2$  Ac-Thr-Pro-NHMe (**61**) at 60 °C

$d_2$ (s)	Integration		$d_2$ (s)	Integration	
	<i>trans</i>	<i>cis</i>		<i>trans</i>	<i>cis</i>
0.01	-4.55	2.82	0.8	-2.11	2.97
0.05	-4.34	2.82	0.9	-1.84	2.99
0.10	-4.22	2.86	1.0	-1.6	3.01
0.15	-4.06	2.87	2.0	0.62	3.03
0.20	-3.91	2.9	3.0	2.15	3.02
0.25	-3.75	2.91	4.0	3.21	3.00
0.30	-3.75	2.91	5.0	3.96	3.00
0.35	-3.41	2.92	6.0	4.42	2.94
0.40	-3.25	2.92	8.0	5.03	2.90
0.45	-3.06	2.9	10	5.36	2.87
0.50	-2.94	2.93	12	5.52	2.83
0.60	-2.67	2.95	14	5.58	2.79
0.70	-2.38	2.95			

(A)



(B)

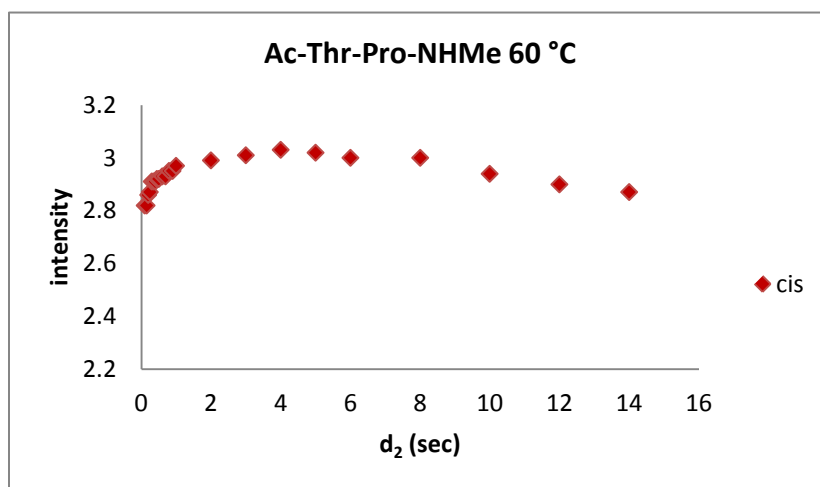


Figure 3.35: Inversion recovery of (A) inverted *trans* Ac-Thr singlet and (B) non-inverted *cis* Ac-Threonine singlet of compound **61** at 60 °C

Table 3.35: Integration vs.  $d_2$  Ac-Thr-Pro-NHMe (**61**) at 65 °C

Integration			Integration		
$d_2$ (s)	<i>trans</i>	<i>cis</i>	$d_2$ (s)	<i>trans</i>	<i>cis</i>
0.01	-3.07	2.55	0.8	5.67	2.40
0.05	-1.93	2.69	0.9	6.03	2.29
0.10	-0.39	2.75	1.0	6.13	2.29
0.15	1.52	2.75	2.0	6.23	2.36
0.20	2.61	2.71	3.0	6.34	2.36
0.25	4.01	2.63	4.0	6.64	2.31
0.30	4.91	2.49	5.0	6.82	2.20
0.35	5.01	2.43	6.0	6.88	2.09
0.40	5.12	2.44	8.0	6.90	2.02
0.45	5.22	2.46	10	5.72	2.37
0.50	5.41	2.39	12	5.67	2.40
0.60	5.61	2.35	14	6.74	2.02
0.70	5.72	2.37			

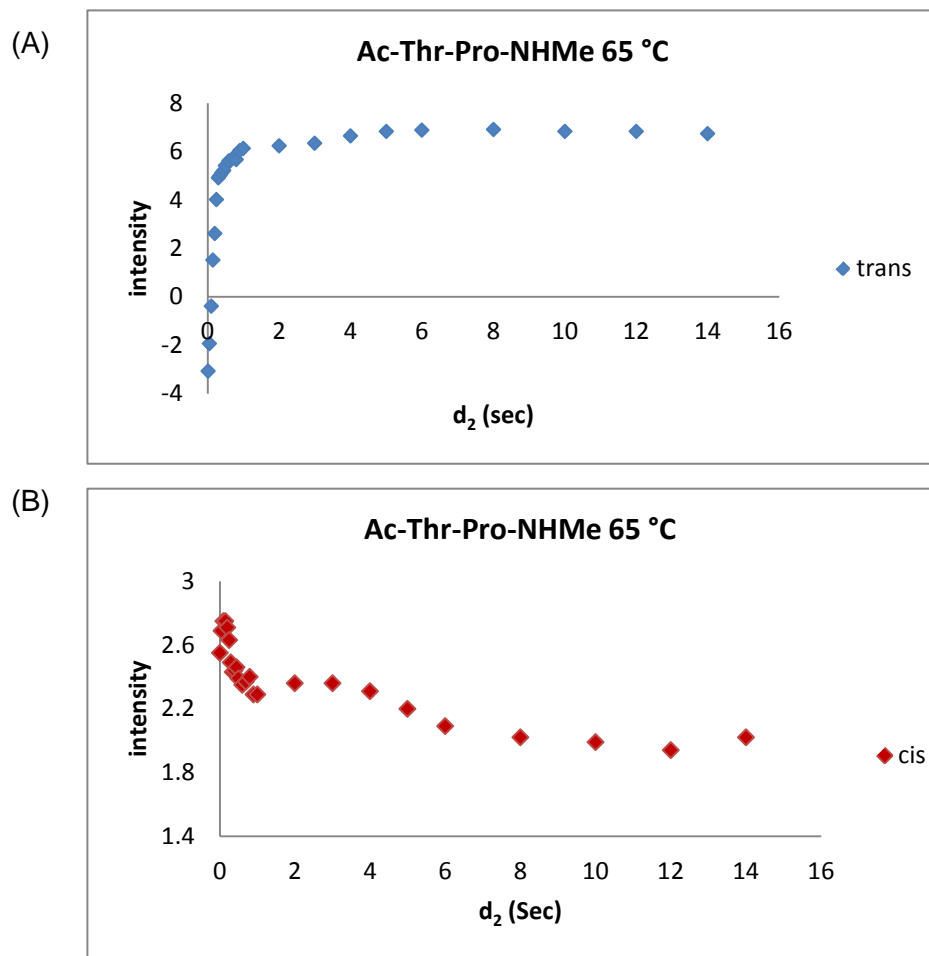


Figure 3.36: Inversion recovery of (A) inverted *trans* Ac-Thr singlet and (B) non-inverted *cis* Ac-Threonine singlet of compound **61** at 65 °C

Table 3.36: Integration vs.  $d_2$  Ac-Thr-Pro-NHMe (**61**) at 70 °C

Integration			Integration		
$d_2$ (s)	<i>trans</i>	<i>cis</i>	$d_2$ (s)	<i>trans</i>	<i>cis</i>
0.01	-4.40	2.69	0.8	-2.38	2.87
0.05	-4.32	2.74	0.9	-2.16	2.89
0.10	-4.22	2.79	1.0	-1.88	2.82
0.15	-4.01	2.76	2.0	0.06	2.88
0.20	-3.91	2.80	3.0	1.52	2.91
0.25	-3.78	2.83	4.0	2.62	2.94
0.30	-3.66	2.83	5.0	3.38	2.90
0.35	-3.52	2.83	6.0	3.95	2.91
0.40	-3.42	2.87	8.0	4.75	2.90
0.45	-3.26	2.84	10	5.06	2.84
0.50	-3.15	2.87	12	3.55	0.98
0.60	-2.82	2.8	14	3.53	0.94
0.70	-2.60	2.83			

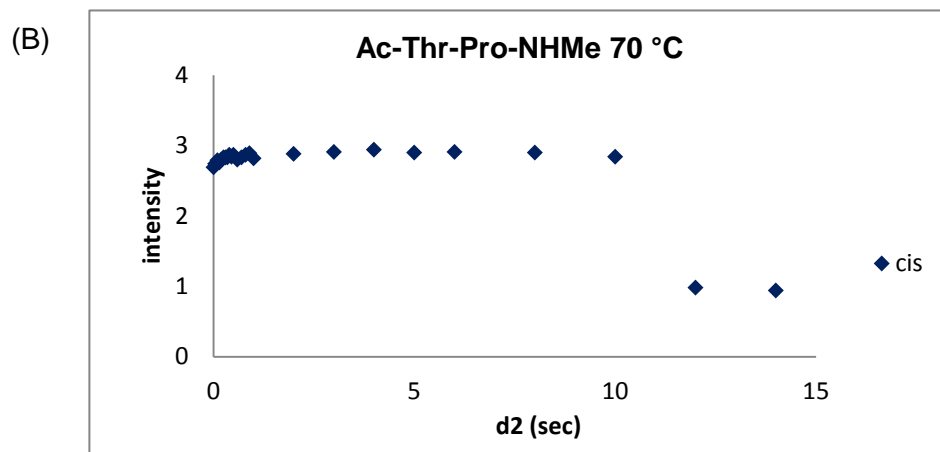
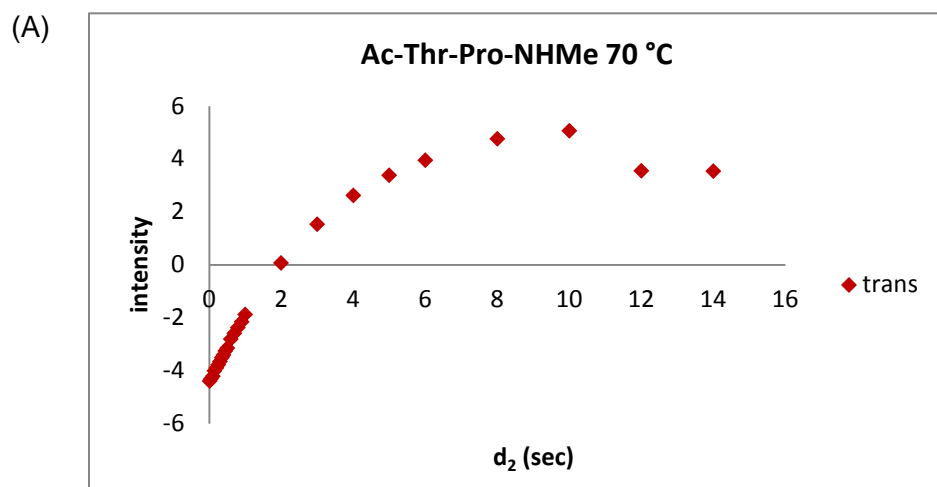


Figure 3.37: Inversion recovery of (A) inverted *trans* Ac-Thr singlet and (B) non-inverted *cis* Ac-Threonine singlet of compound **61** at 70 °C



Table 3.37: Integration vs.  $d_2$  Ac-Thr-Pro-NHMe (**61**) at 75 °C

$d_2$ (s)	Integration		$d_2$ (s)	Integration		
	<i>trans</i>	<i>cis</i>		<i>trans</i>	<i>cis</i>	
0.01	-4.65	2.98	0.8	-2.52	3.06	
0.05	-4.52	2.94	0.9	-2.24	3.09	
0.10	-4.26	2.87	1.0	-2.02	3.04	
0.15	-4.08	2.85	2.0	-0.02	3.07	
0.20	-4.01	2.91	3.0	1.50	3.11	
0.25	-3.89	2.92	4.0	2.63	3.12	
0.30	-3.73	2.93	5.0	3.42	3.13	
0.35	-3.63	2.95	6.0	4.11	3.14	
0.40	-3.48	2.95	8.0	4.82	3.07	
0.45	-3.36	2.98	10	5.37	3.09	
0.50	-3.22	2.98	12	5.67	3.12	
0.60	-2.97	2.99	14	5.62	2.99	
0.70	-2.74	3.02				

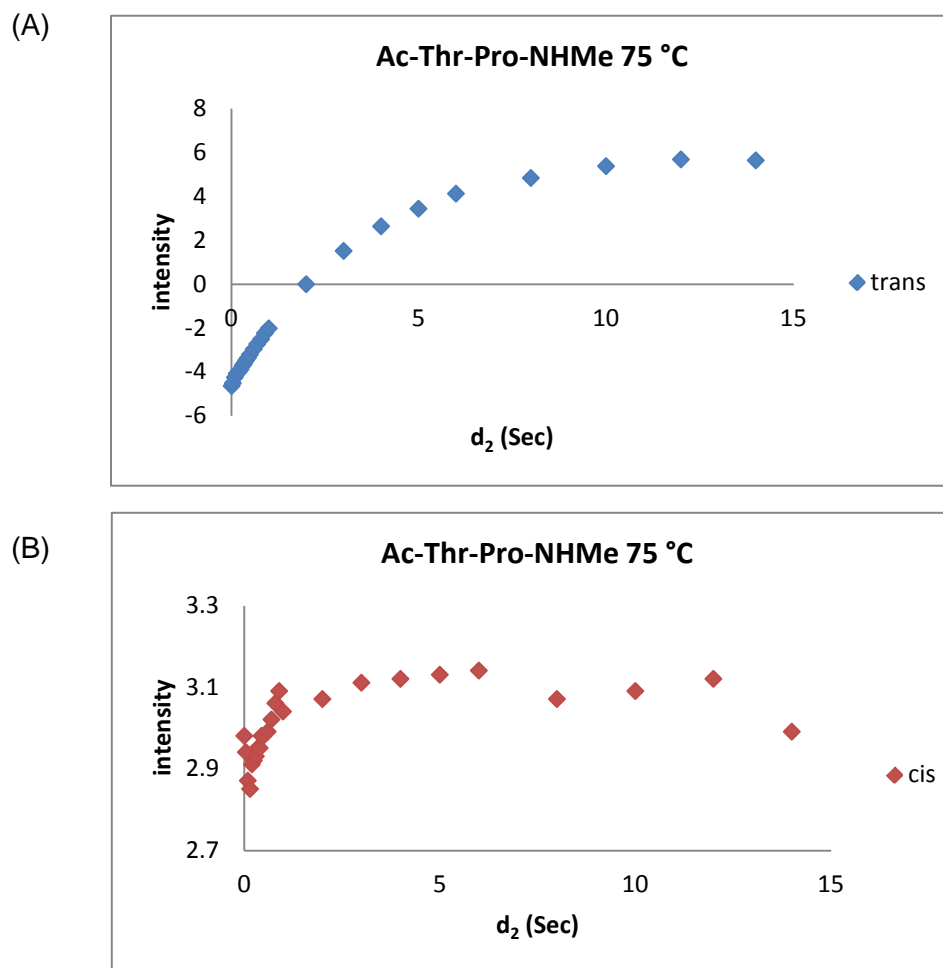
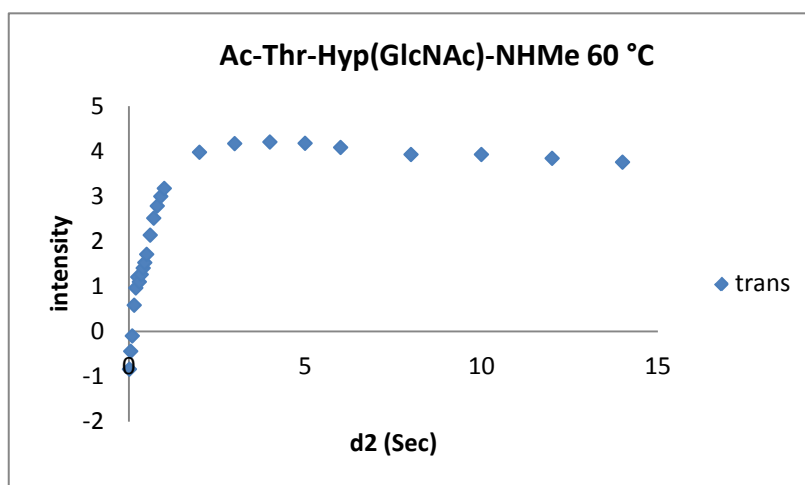


Figure 3.38: Inversion recovery of (A) inverted *trans* Ac-Thr singlet and (B) non-inverted *cis* Ac-Threonine singlet of compound **61** at 75 °C

Table 3.38: Integration vs.  $d_2$  Ac-Thr-Hyp(GlcNAc)-NHMe (**63**) at 60 °C

Integration			Integration		
$d_2$ (s)	<i>trans</i>	<i>cis</i>	$d_2$ (s)	<i>trans</i>	<i>cis</i>
0.01	-0.84	0.77	0.8	2.78	0.84
0.05	-0.44	0.77	0.9	2.99	0.86
0.10	-0.1	0.76	1.0	3.17	0.87
0.15	0.58	0.76	2.0	3.97	1.01
0.20	0.96	0.75	3.0	4.16	1.08
0.25	1.20	0.75	4.0	4.2	1.07
0.30	1.10	0.70	5.0	4.17	1.04
0.35	1.26	0.72	6.0	4.08	1.00
0.40	1.40	0.73	8.0	3.92	0.96
0.45	1.52	0.74	10	3.92	0.98
0.50	1.71	0.78	12	2.51	0.82
0.60	2.13	0.78	14	3.75	0.88
0.70	2.51	0.82			

(A)



(B)

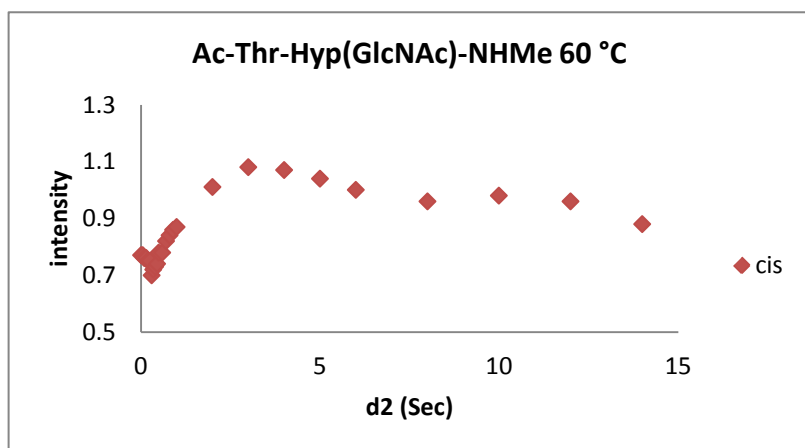


Figure 3.39: Inversion recovery of (A) inverted *trans* Thr-Hy doublet and (B) non-inverted *cis* Thr-Hy doublet of compound **63** at 60 °C

Table 3.39: Integration vs.  $d_2$  Ac-Thr-Hyp(GlcNAc)-NHMe (**63**) at 65 °C

Integration			Integration		
$d_2$	<i>trans</i>	<i>cis</i>	$d_2$	<i>trans</i>	<i>cis</i>
0.01	-0.46	1.04	0.8	2.34	0.91
0.05	-0.13	1.06	0.9	2.33	1.24
0.10	0.16	1.19	1.0	2.54	1.06
0.15	0.34	1.13	2.0	3.61	0.90
0.20	0.52	0.98	3.0	4.02	0.80
0.25	0.76	0.71	4.0	4.13	0.78
0.30	0.91	0.48	5.0	4.18	0.75
0.35	0.96	0.42	6.0	3.73	0.79
0.40	1.23	0.42	8.0	3.66	0.79
0.45	1.48	0.62	10	3.80	0.77
0.50	1.61	0.84	12	3.80	0.73
0.60	1.96	0.89	14	3.77	0.66
0.70	2.14	0.92			

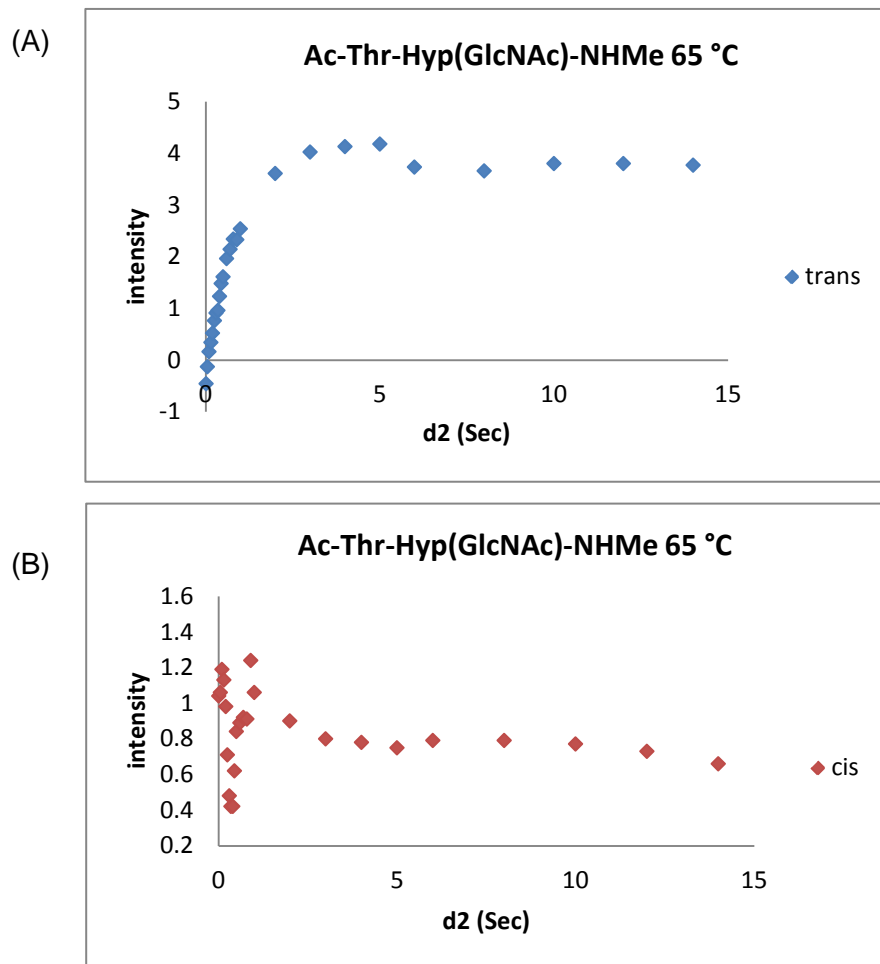


Figure 3.40: Inversion recovery of (A) inverted *trans* Thr-Hyp doublet and (B) non-inverted *cis* Thr-Hyp doublet of compound **63** at 65 °C

Table 3.40: Integration vs.  $d_2$  Ac-Thr-Hyp(GlcNAc)-NHMe (**63**) at 70 °C

$d_2$	Integration		$d_2$	Integration	
	<i>trans</i>	<i>cis</i>		<i>trans</i>	<i>cis</i>
0.01	-0.24	0.54	0.7	2.54	0.72
0.05	0.19	0.70	0.8	2.60	0.77
0.10	0.55	0.64	0.9	2.74	0.8
0.15	0.80	0.55	1.0	2.93	0.82
0.20	1.01	0.54	2.0	3.75	0.99
0.25	1.20	0.56	3.0	3.99	1.02
0.30	1.36	0.56	4.0	3.96	1.06
0.35	1.60	0.57	5.0	3.85	1.06
0.40	1.72	0.60	6.0	3.81	1.04
0.45	1.84	0.62	8.0	3.77	1.00
0.50	1.96	0.64	10	3.57	1.01
0.60	2.24	0.68			

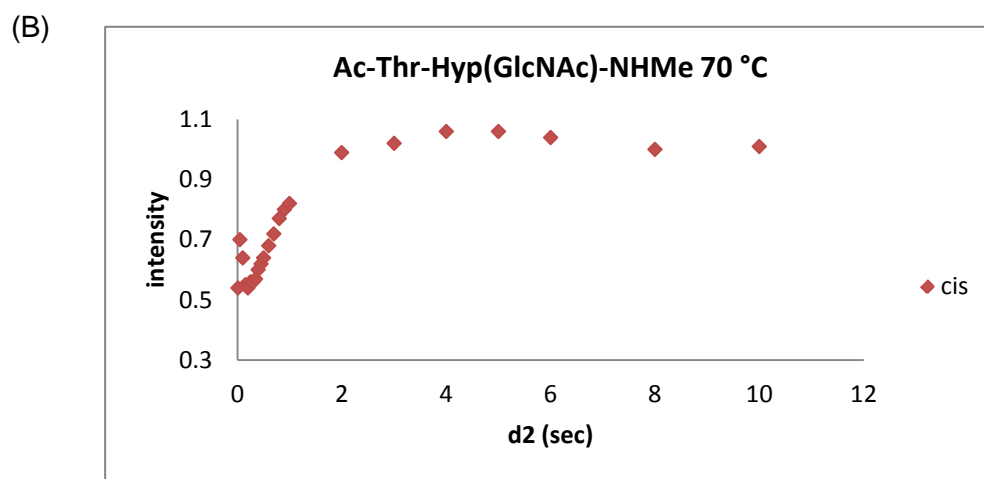
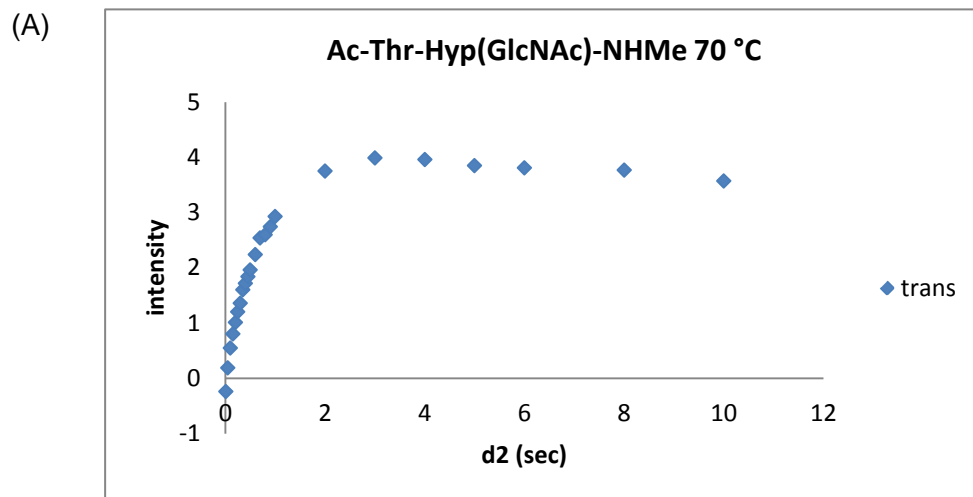


Figure 3.41: Inversion recovery of inverted *trans* Thr-Hy doublet (A) and non-inverted *cis* Thr-Hy doublet (B) at 70 °C

Table 3.41: Integration vs.  $d_2$  Ac-Thr-Hyp(GlcNAc)-NHMe (**63**) at 75 °C

Integration			Integration		
$d_2$	<i>trans</i>	<i>cis</i>	$d_2$	<i>trans</i>	<i>cis</i>
0.049	-2.70	2.94	0.06	-5.37	3.29
0.050	-3.22	3.14	0.061	-5.20	3.17
0.051	-3.76	3.33	0.062	-5.02	3.10
0.052	-4.23	3.43	0.063	-5.05	3.15
0.053	-4.47	3.43	0.064	-5.06	3.15
0.054	-4.81	3.45	0.065	-4.89	3.09
0.055	-4.98	3.45	0.066	-4.63	3.08
0.056	-5.16	3.45	0.067	-4.23	2.88
0.057	-5.26	3.40	0.068	-3.98	2.89
0.058	-5.33	3.37	0.069	-3.99	3.02
0.059	-5.36	3.28	0.070	-3.56	2.88

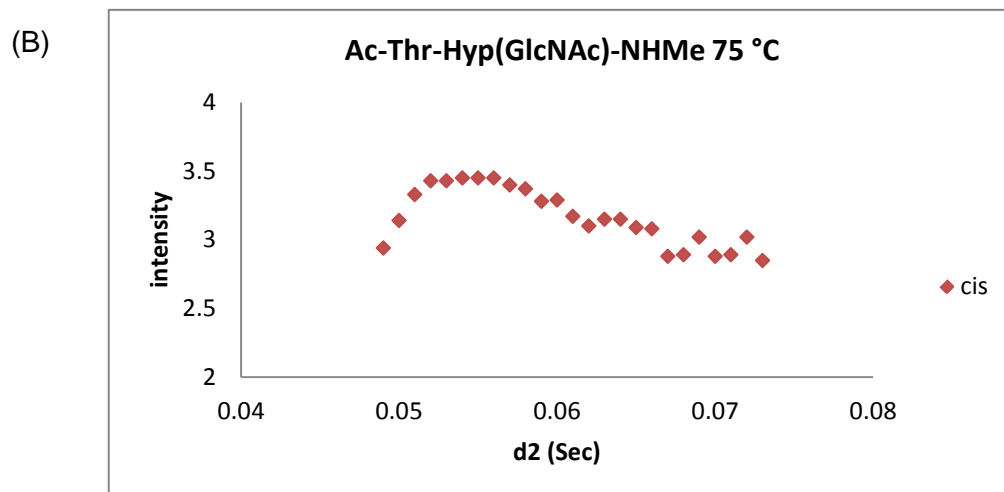
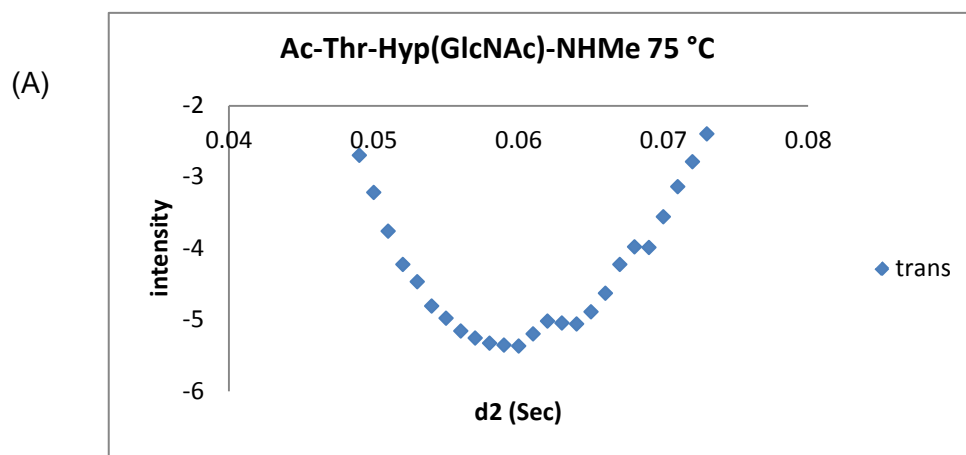
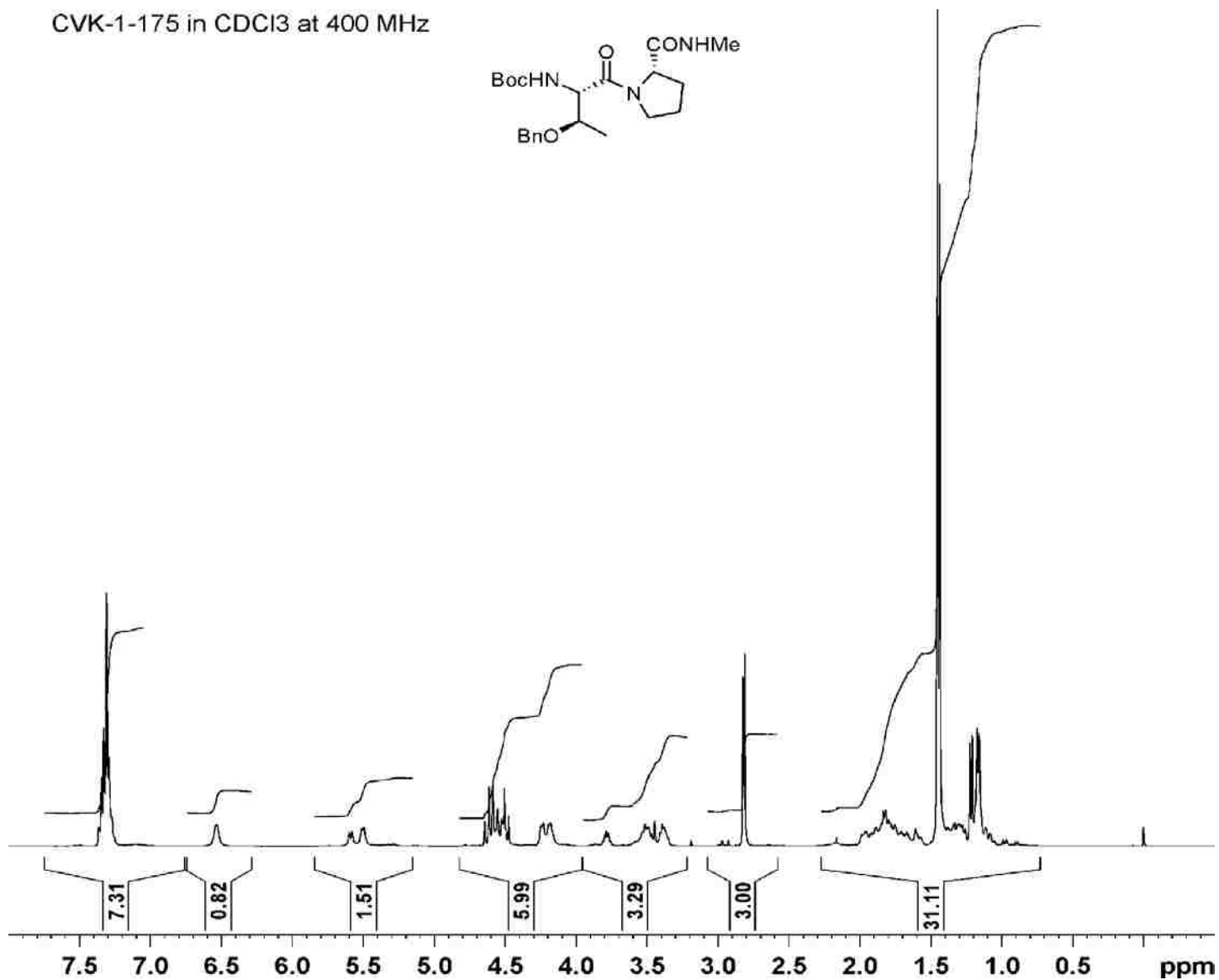
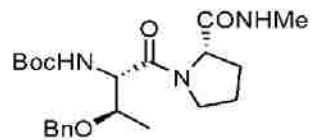


Figure 3.42: Inversion recovery of (A) inverted *trans* Thr-Hy doublet and (B) non-inverted *cis* Thr-Hy doublet of compound **63** at 75 °C

3.8.4  $^1\text{H}$  and  $^{13}\text{C}$  NMR Spectra

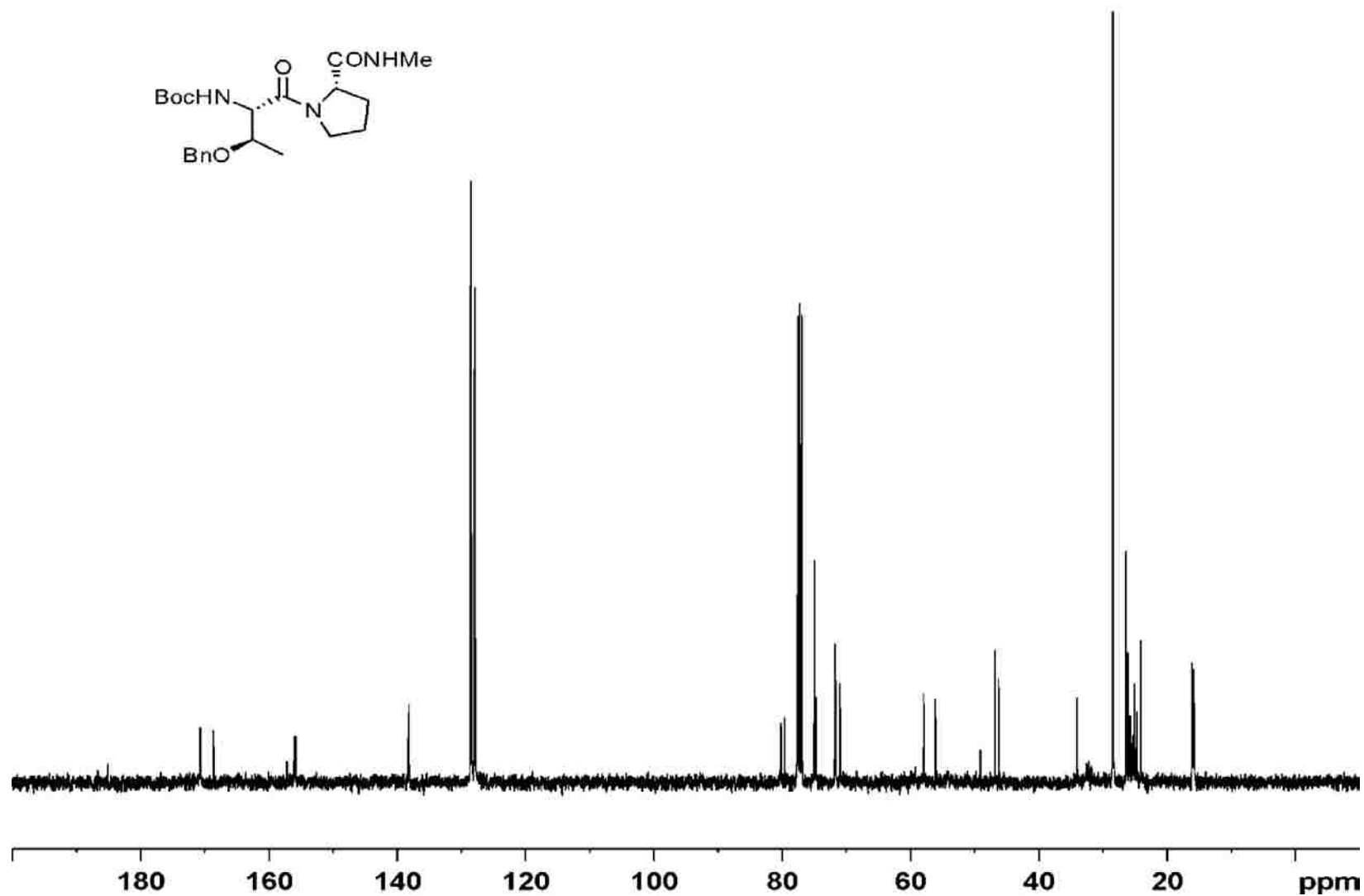
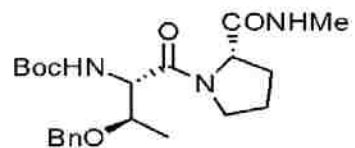
Boc-Thr(OBn)-Pro-NHMe (**67**)

CVK-1-175 in  $\text{CDCl}_3$  at 400 MHz



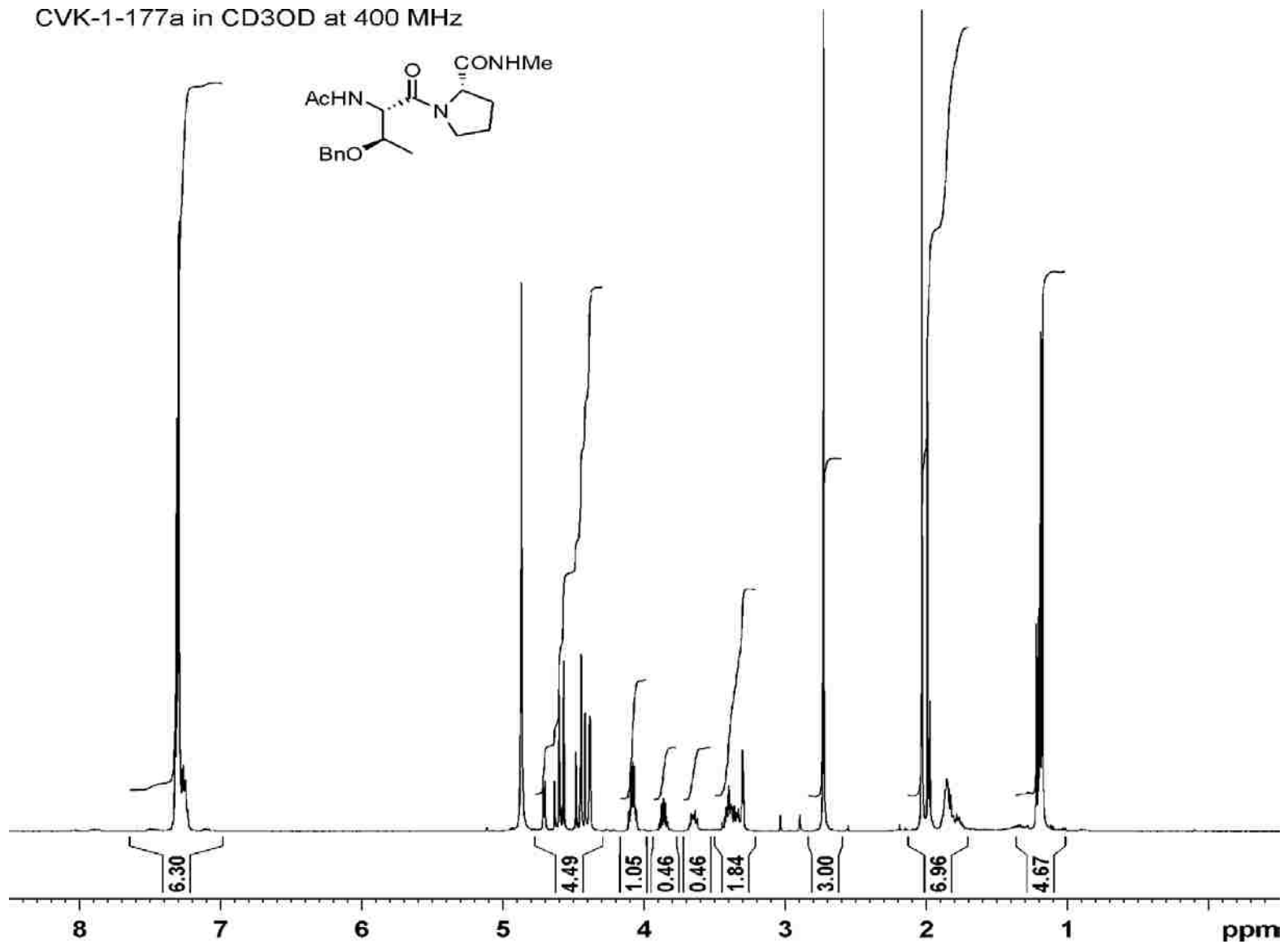
Boc-Thr(OBn)-Pro-NHMe (67)

CVK-1-175 in CDCl<sub>3</sub> at 100 MHz



Ac-Thr(OBn)-Pro-NHMe (68)

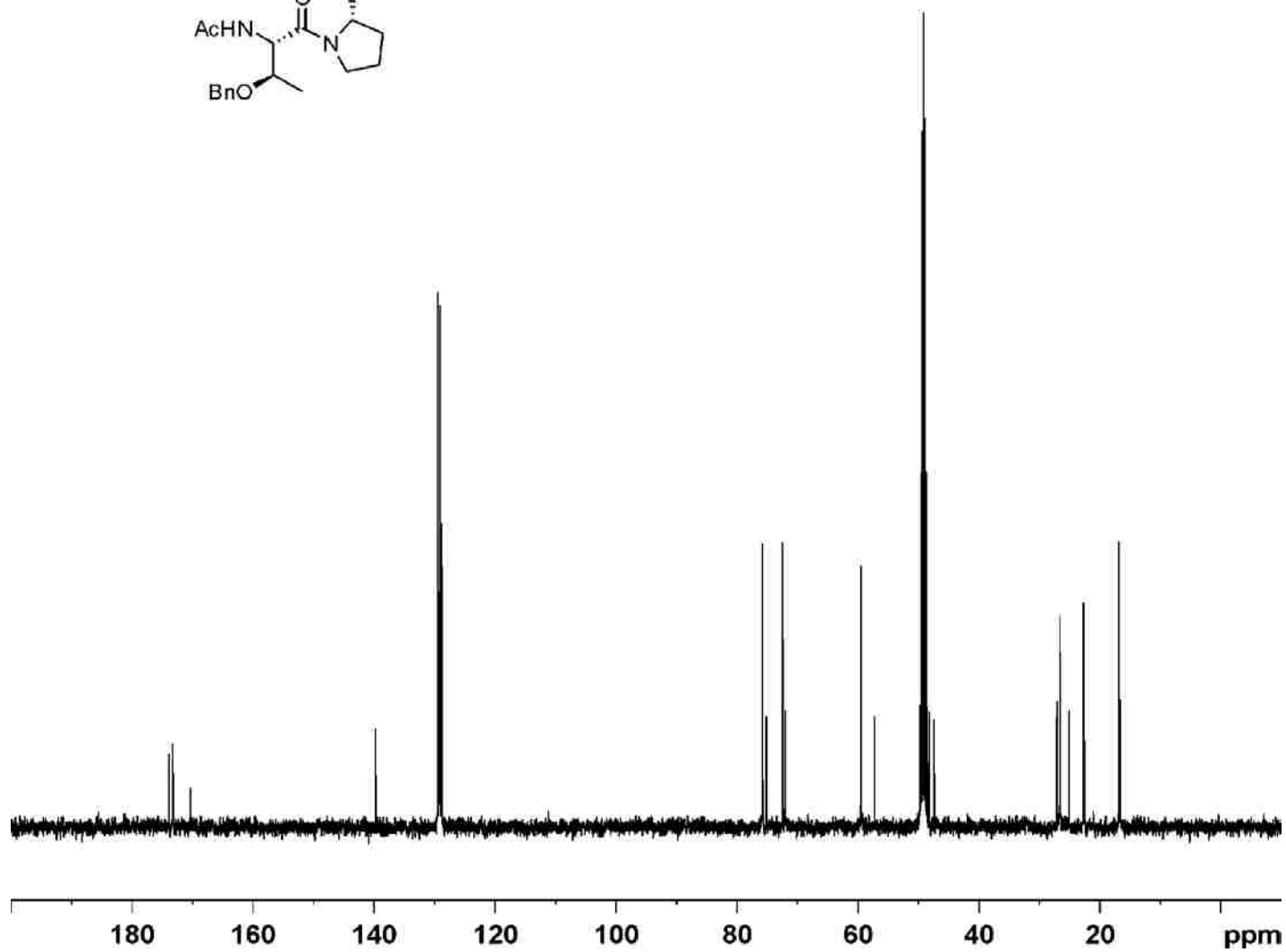
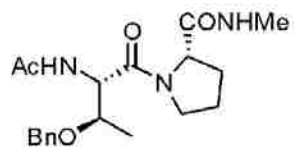
CVK-1-177a in CD3OD at 400 MHz





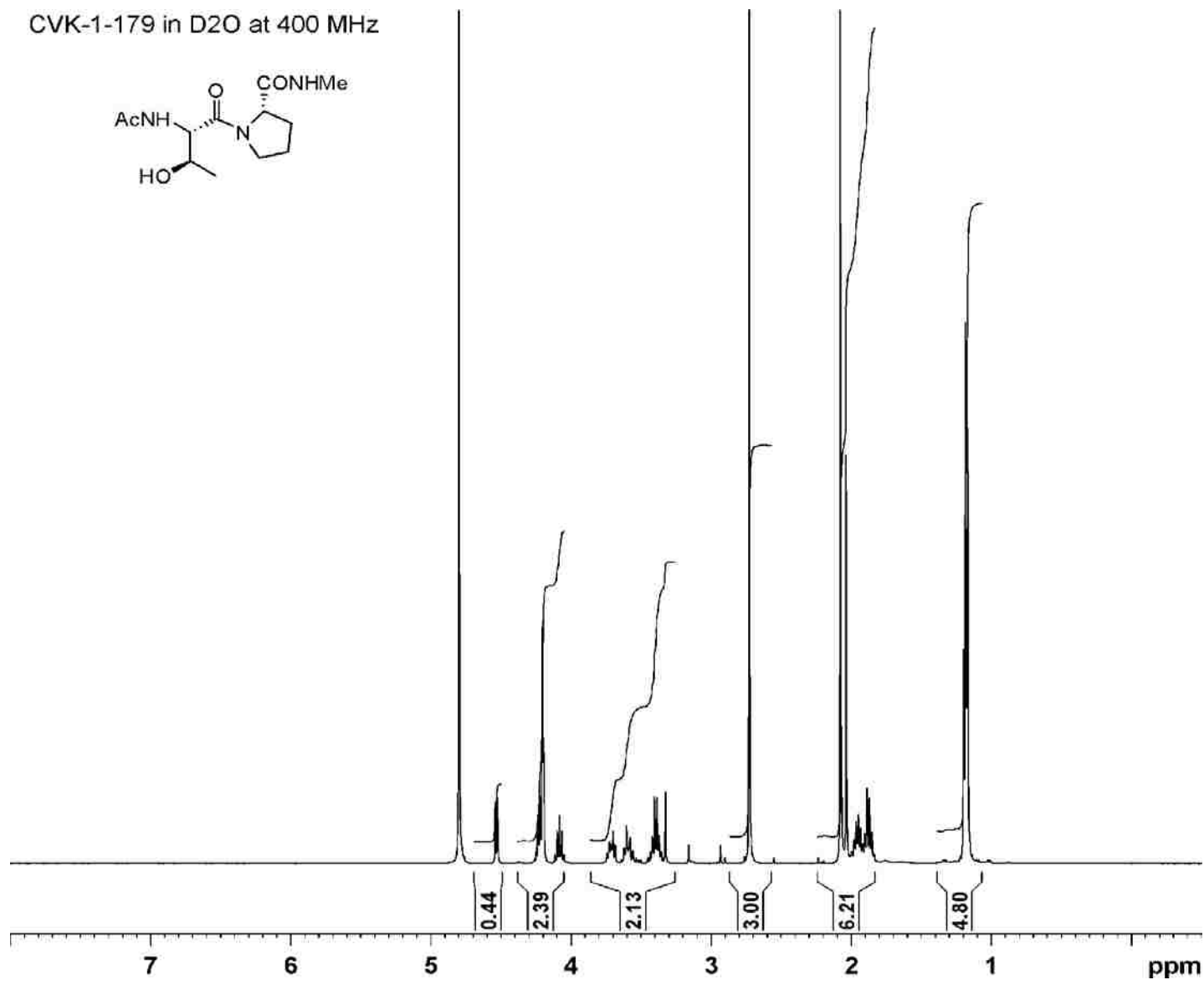
Ac-Thr(OBn)-Pro-NHMe (68)

CVK-1-177a in CD3OD at 100 MHz

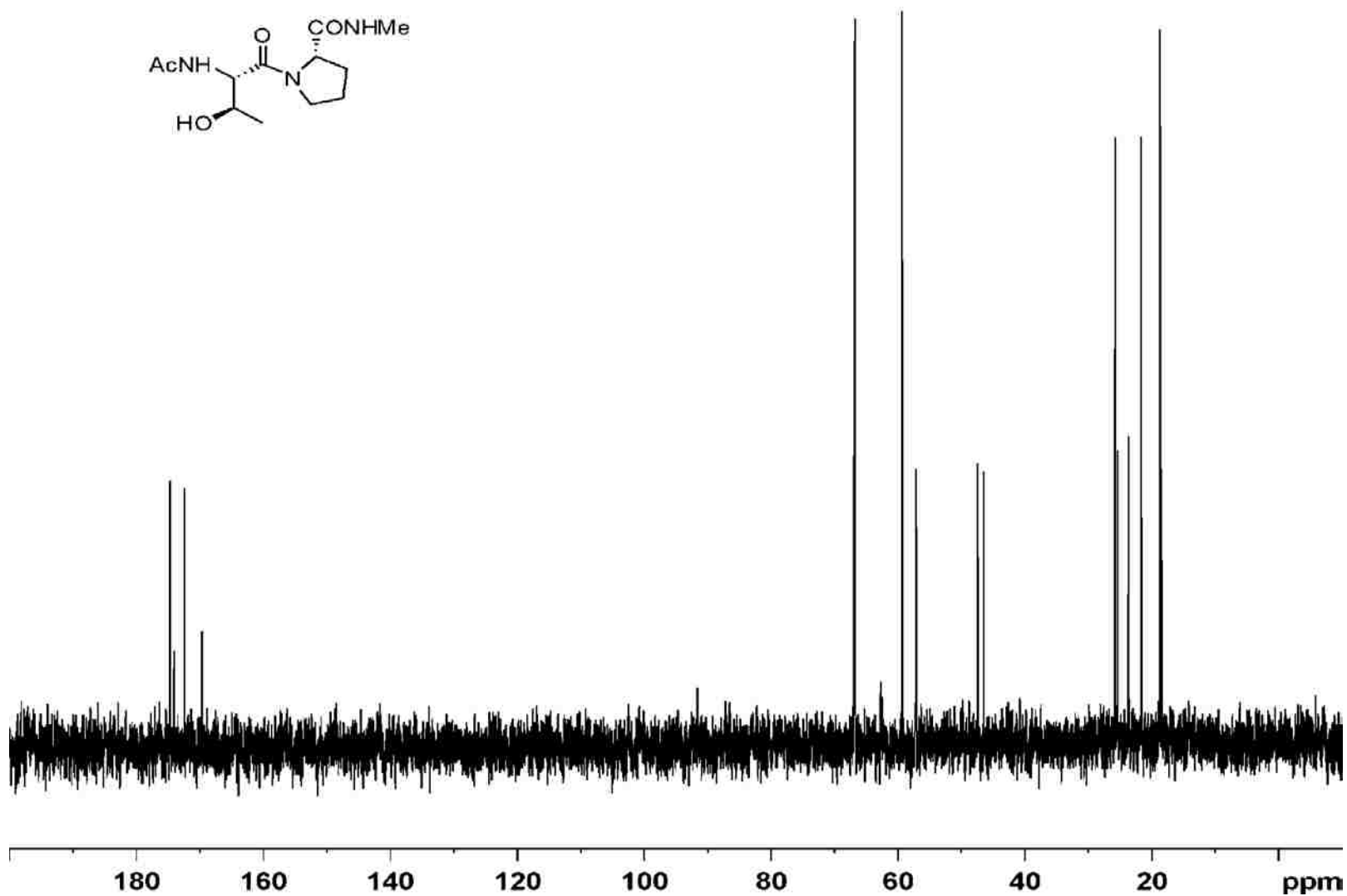
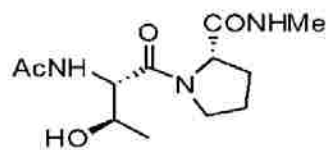


Ac-Thr-Pro-NHMe (61) – unreferenced

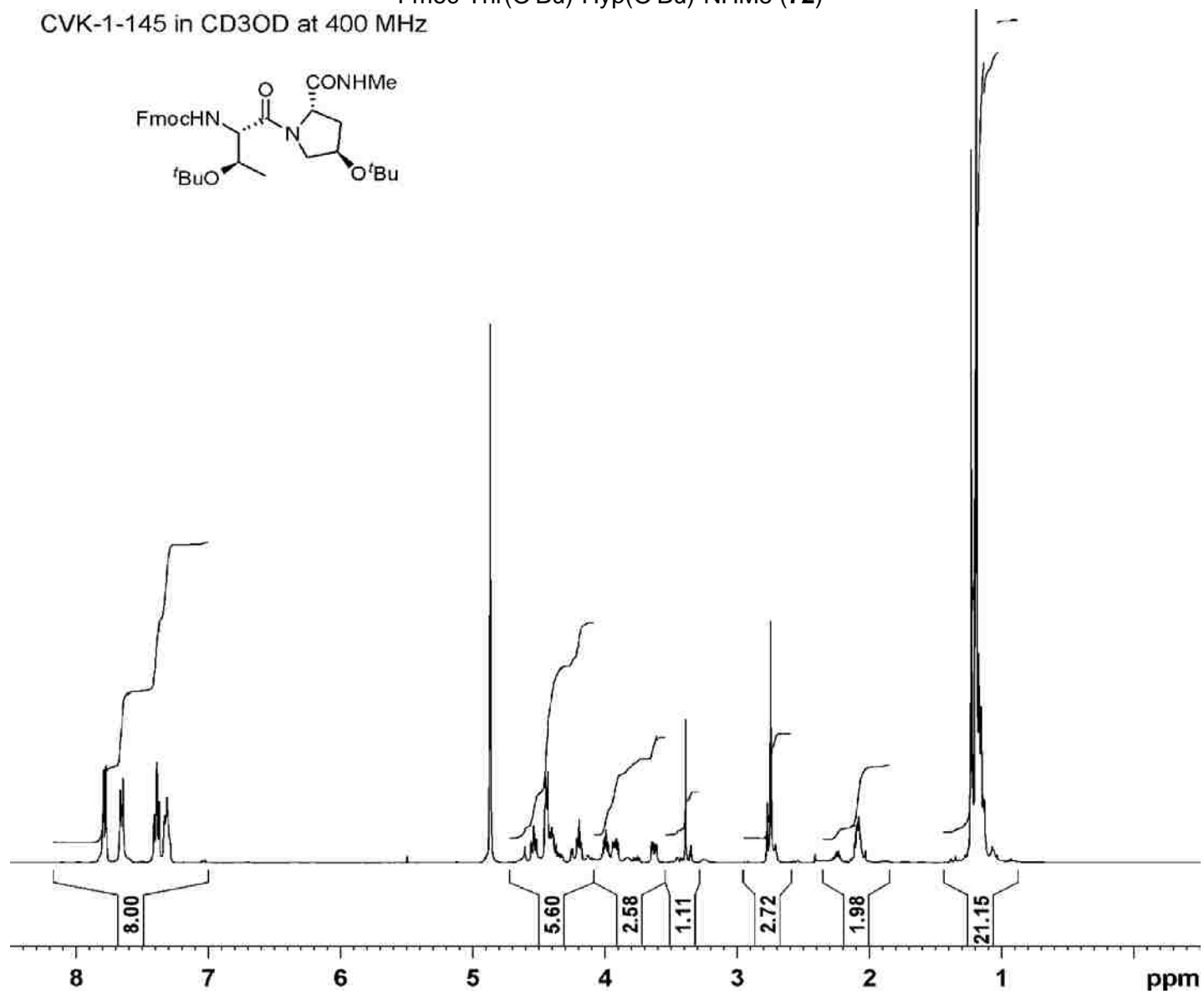
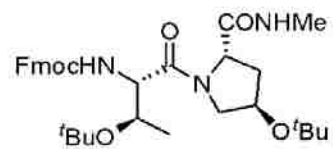
CVK-1-179 in D2O at 400 MHz



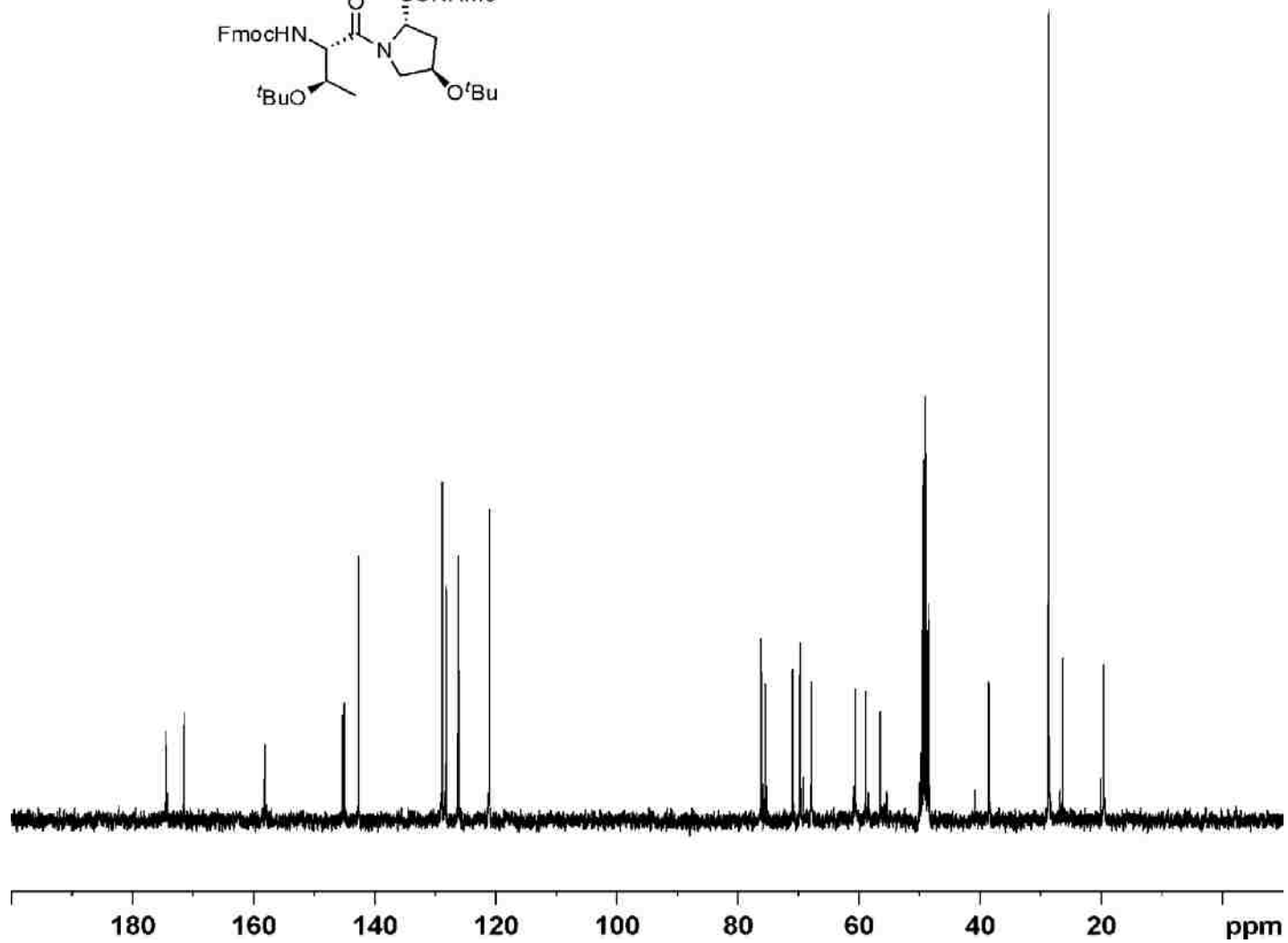
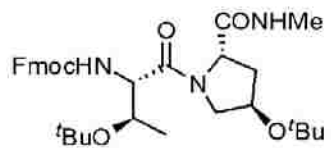
CVK-1-179 in D<sub>2</sub>O at 100 MHz Ac-Thr-Pro-NHMe (61) – unreferenced



Fmoc-Thr(O<sup>t</sup>Bu)-Hyp(O<sup>t</sup>Bu)-NHMe (72)  
CVK-1-145 in CD<sub>3</sub>OD at 400 MHz

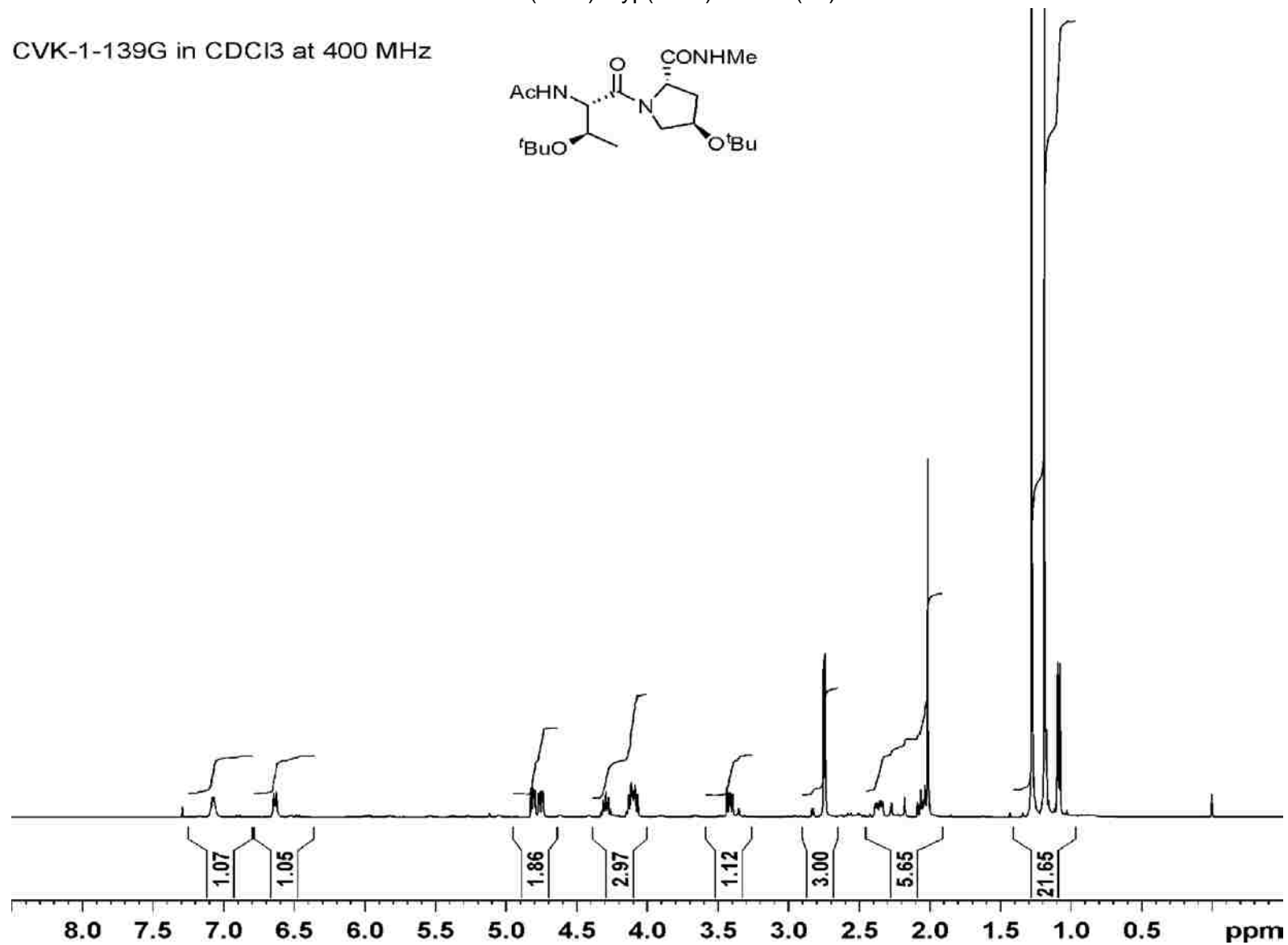
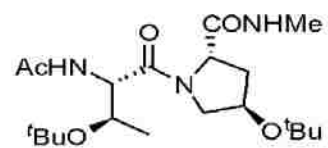


Fmoc-Thr(O<sup>t</sup>Bu)-Hyp(O<sup>t</sup>Bu)-NHMe (72)  
CVK-1-145 in CD3OD at 100 MHz



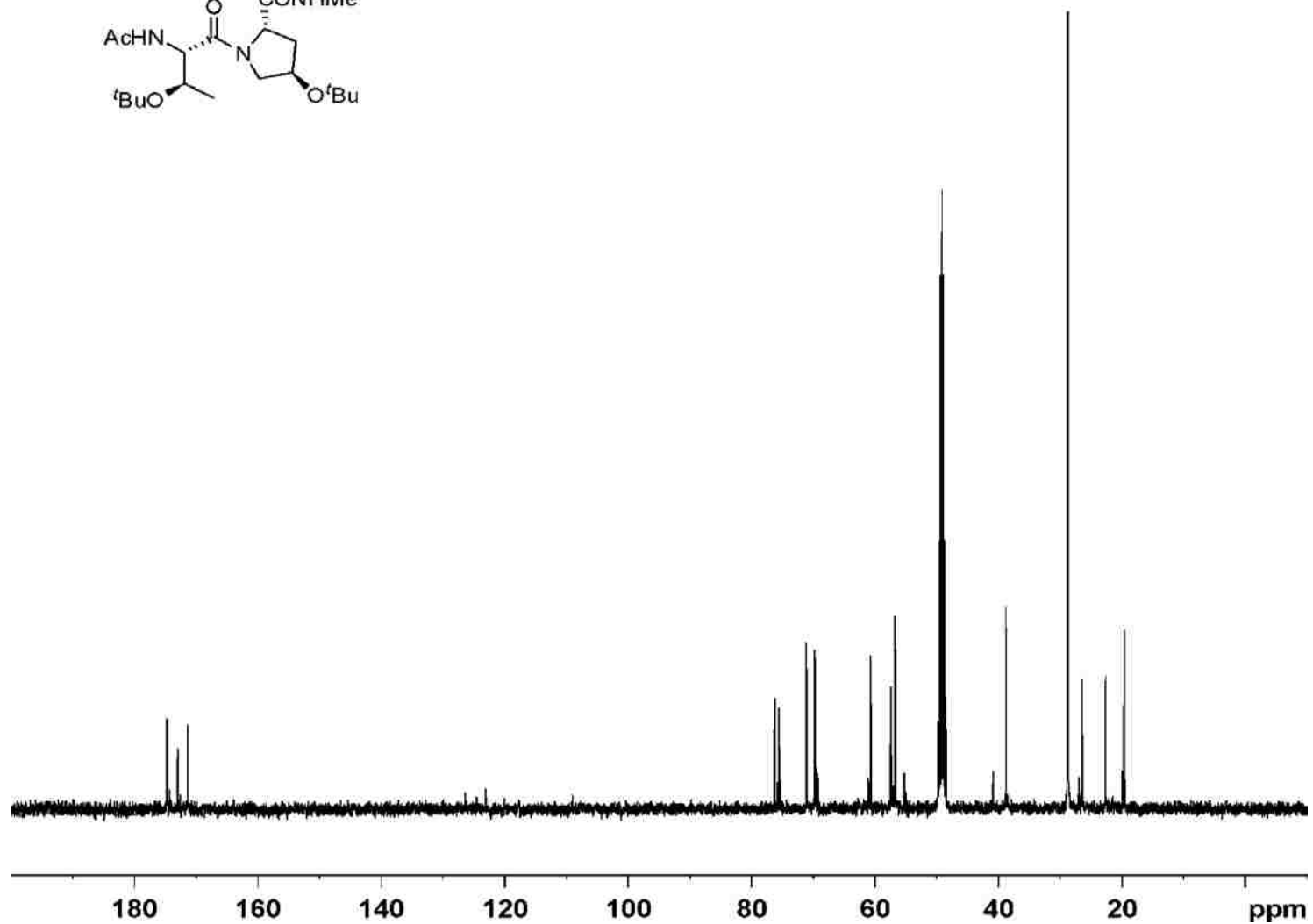
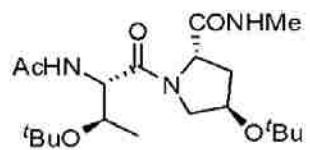
Ac-Thr(O<sup>t</sup>Bu)-Hyp(O<sup>t</sup>Bu)-NHMe (73)

CVK-1-139G in CDCl<sub>3</sub> at 400 MHz



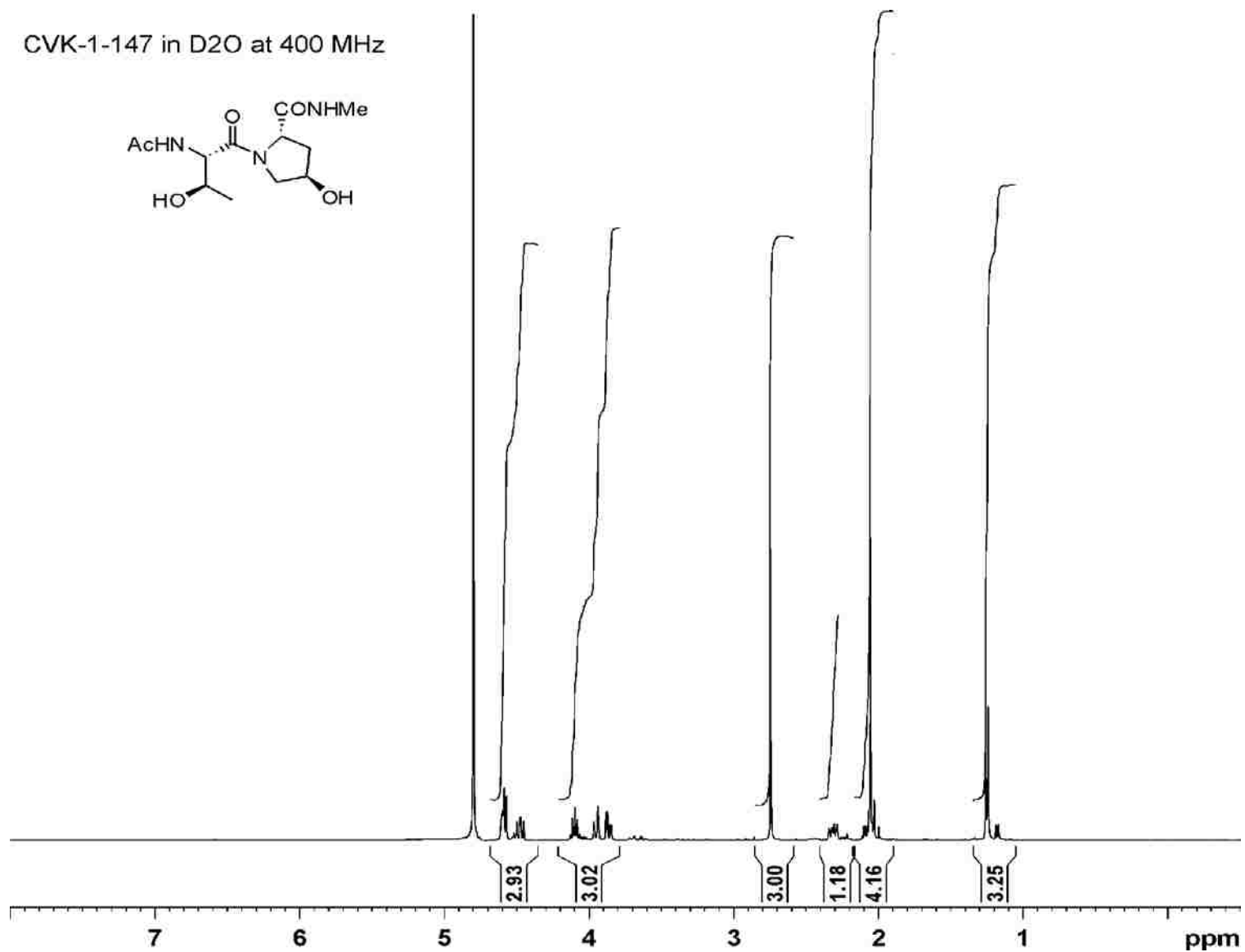
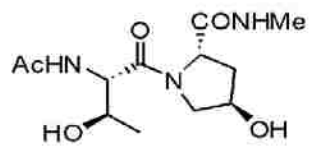
Ac-Thr(O<sup>t</sup>Bu)-Hyp(O<sup>t</sup>Bu)-NHMe (73)

CVK-1-139G in CDCl<sub>3</sub> at 100 MHz



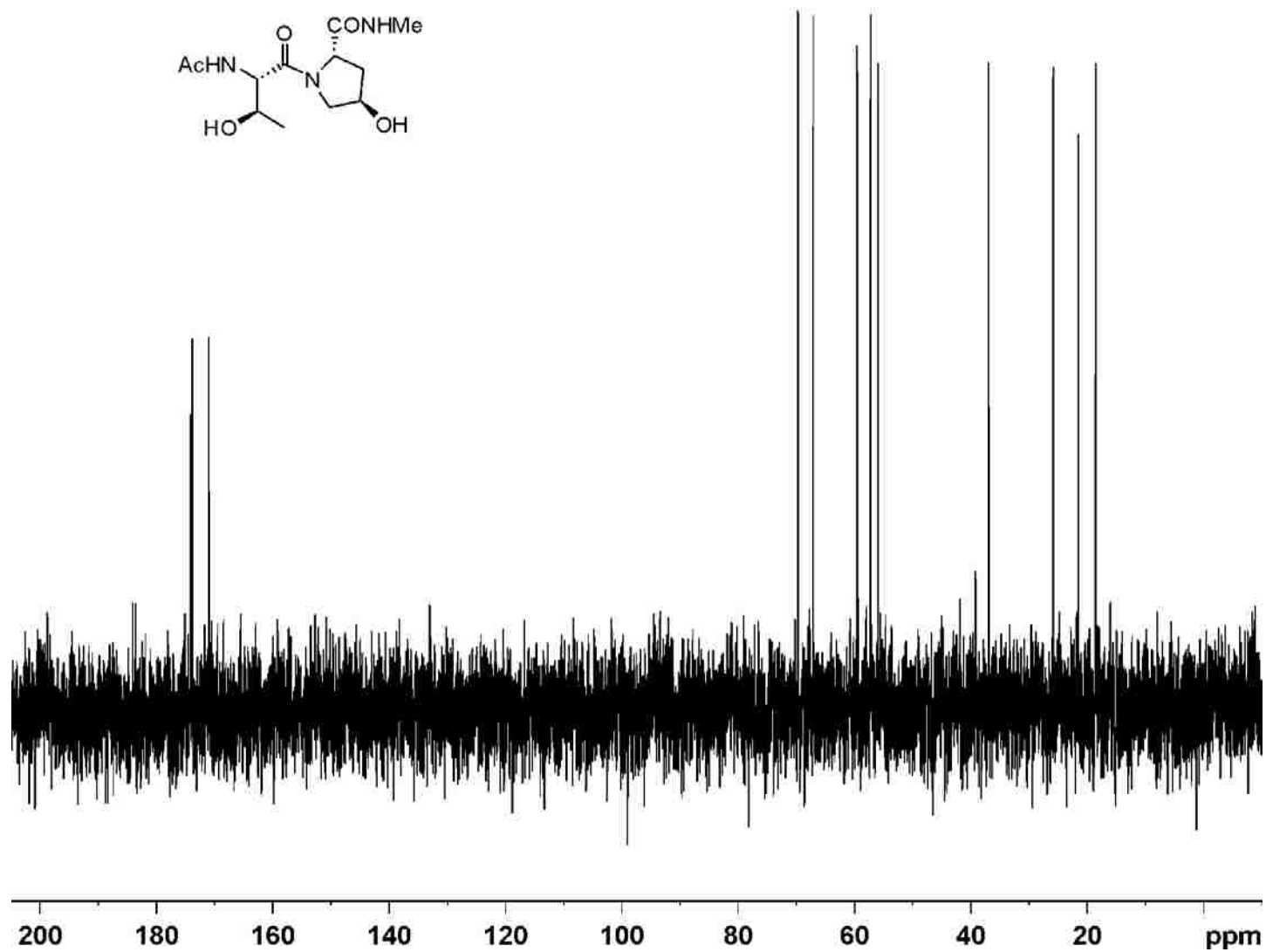
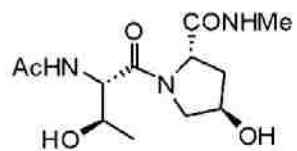
Ac-Thr-Hyp-NHMe (62)- unreferenced

CVK-1-147 in D2O at 400 MHz



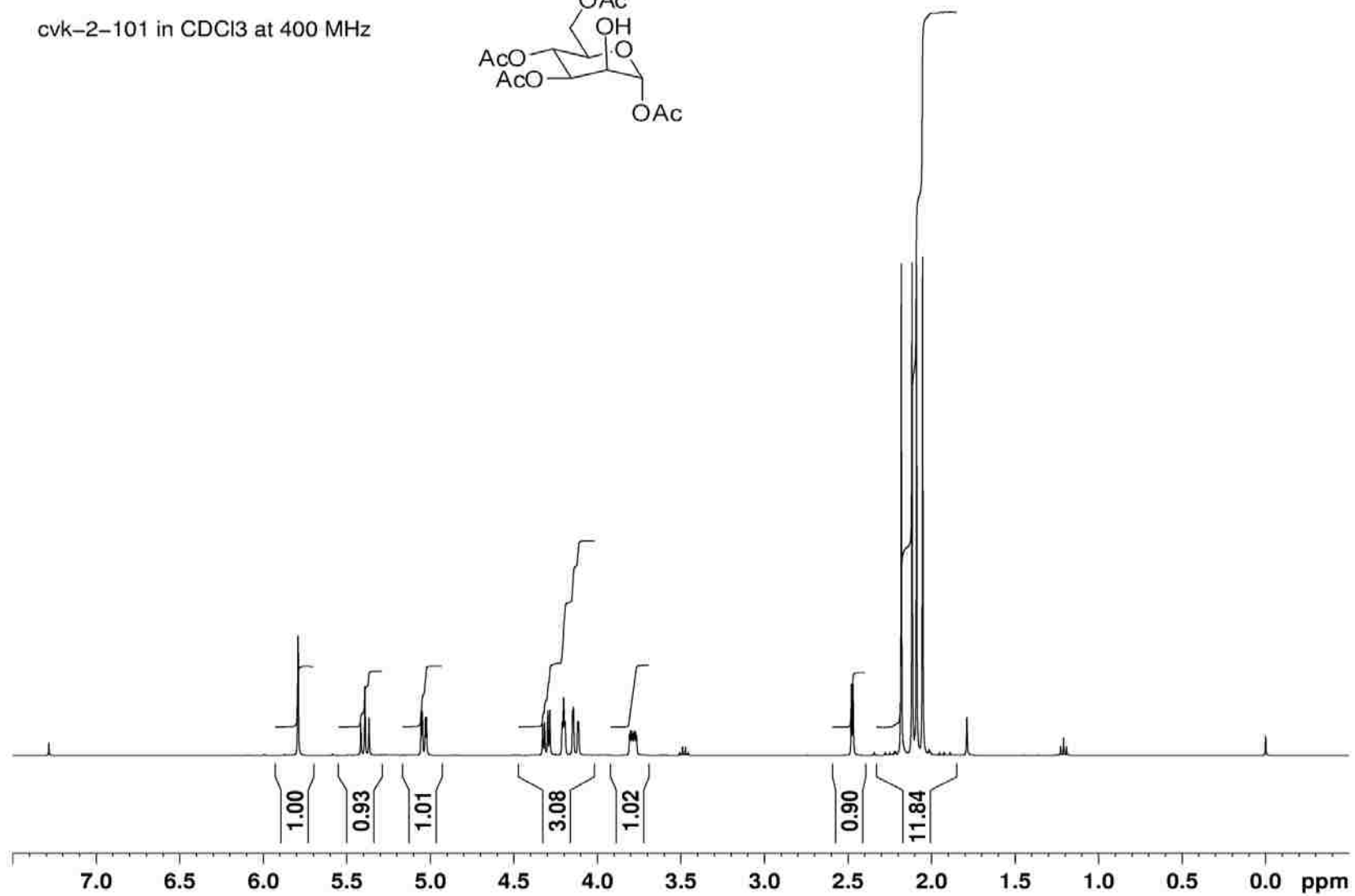
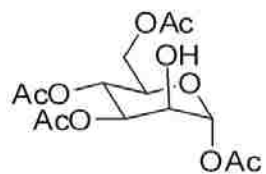


Ac-Thr-Hyp-NHMe (62)- unreferenced  
CVK-1-147 in D2O at 100 MHz



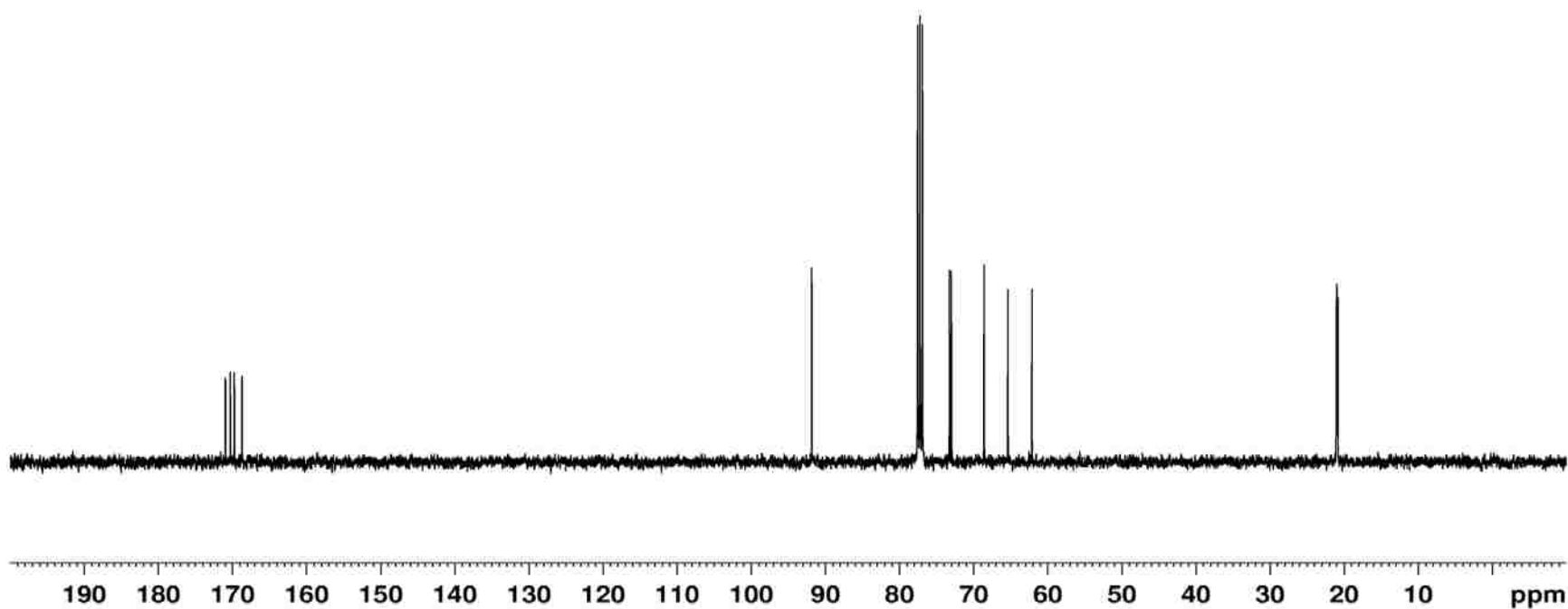
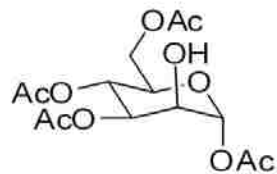
1,3,4,6-Tetra-O-acetylmannose (**75**)

cvk-2-101 in CDCl<sub>3</sub> at 400 MHz



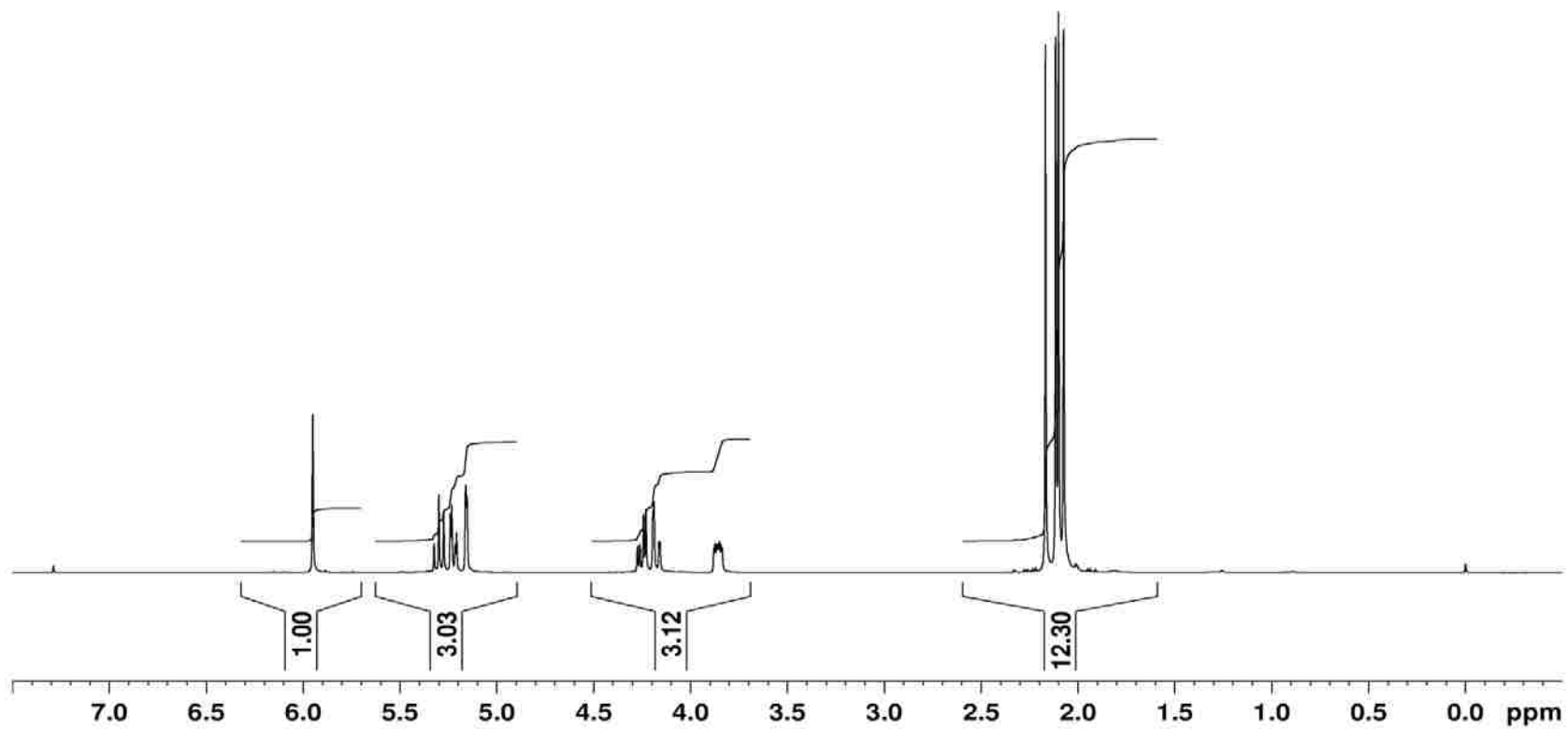
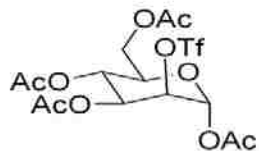
1,3,4,6-Tetra-O-acetylmannose (**75**)

cvk-2-101 in CDCl<sub>3</sub> at 100 MHz



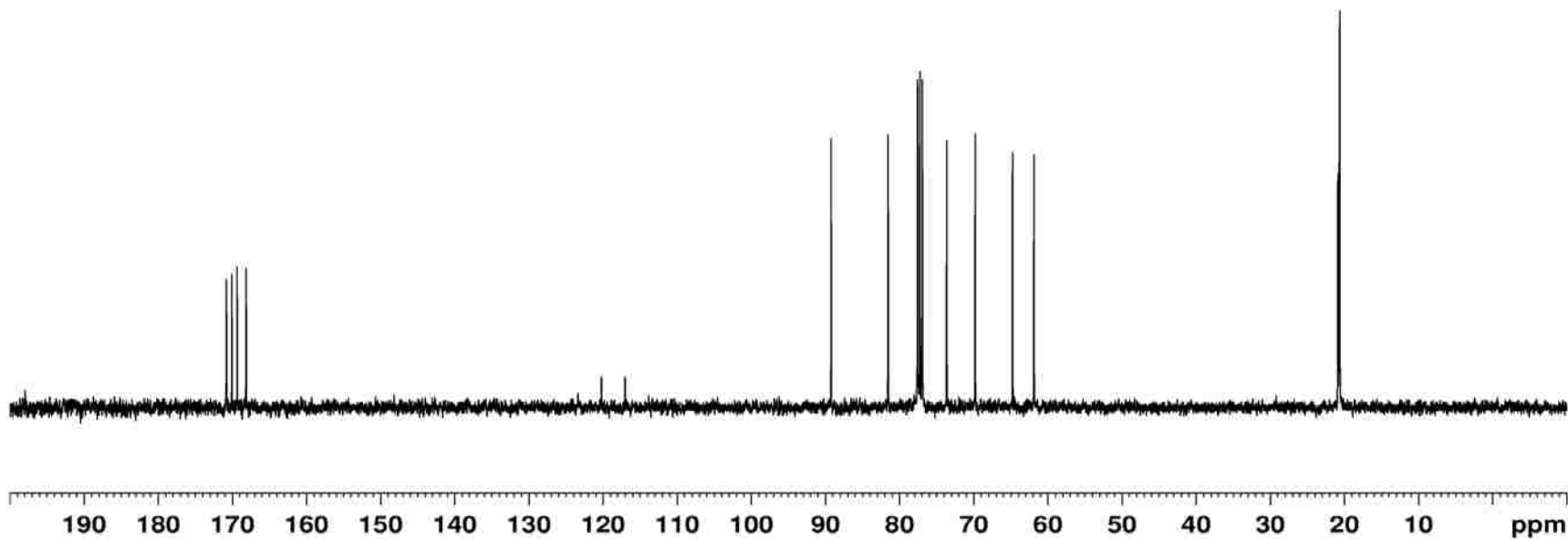
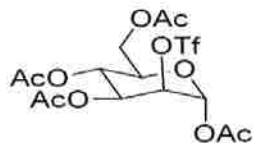
1,3,4,6-tetra-O-acetyl-trifluorosulfonyl- $\beta$ -D-glucopyranose (**76**)

cvk-2-106 in CDCl<sub>3</sub> at 100 MHz



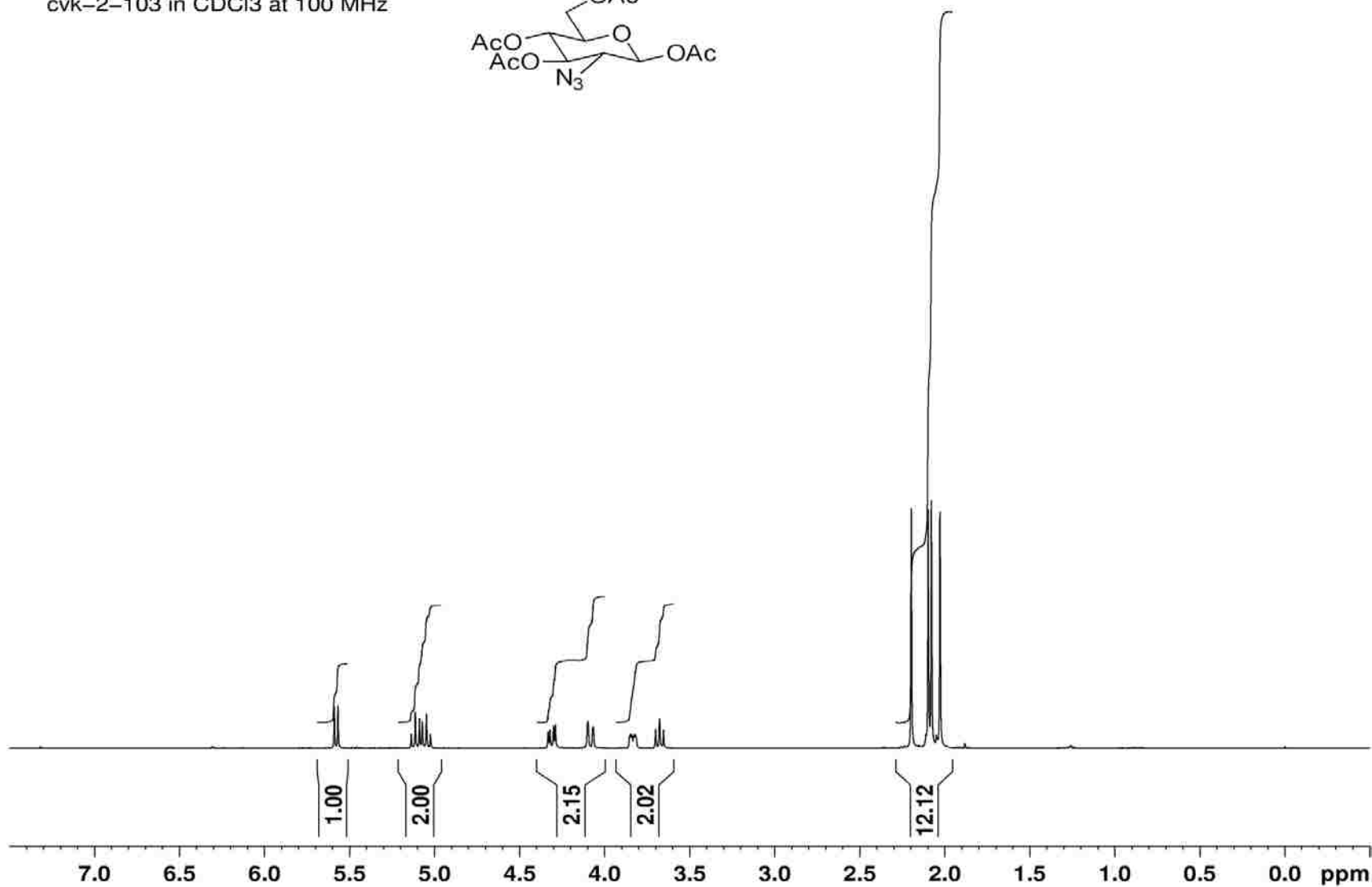
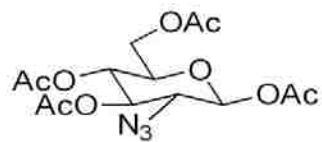
1,3,4,6-tetra-*O*-acetyl-trifluorosulfonyl- $\beta$ -*D*-glucopyranose (**76**)

cvk-2-106 in CDCl<sub>3</sub> at 100 MHz



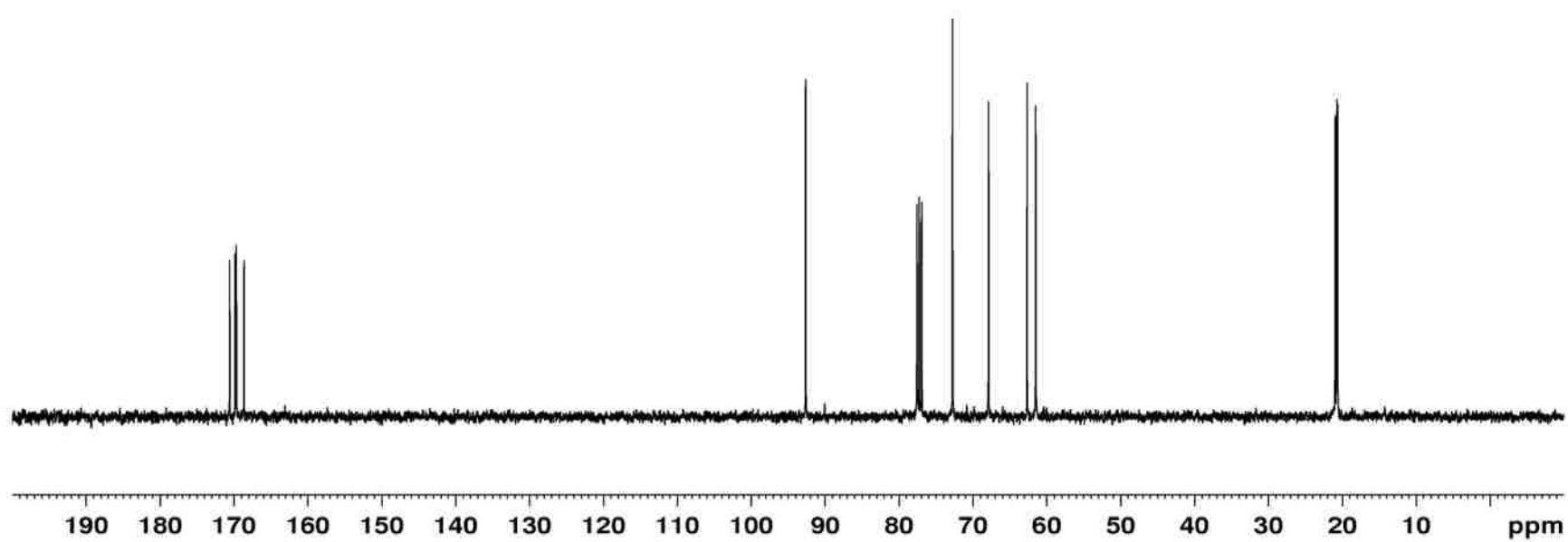
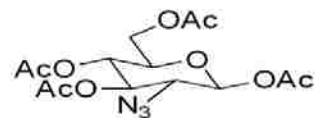
2-Azido-1,3,4,6-tetra-*O*-acetyl- $\beta$ -*D*-glucopyranose (**77**)

cvk-2-103 in CDCl<sub>3</sub> at 100 MHz

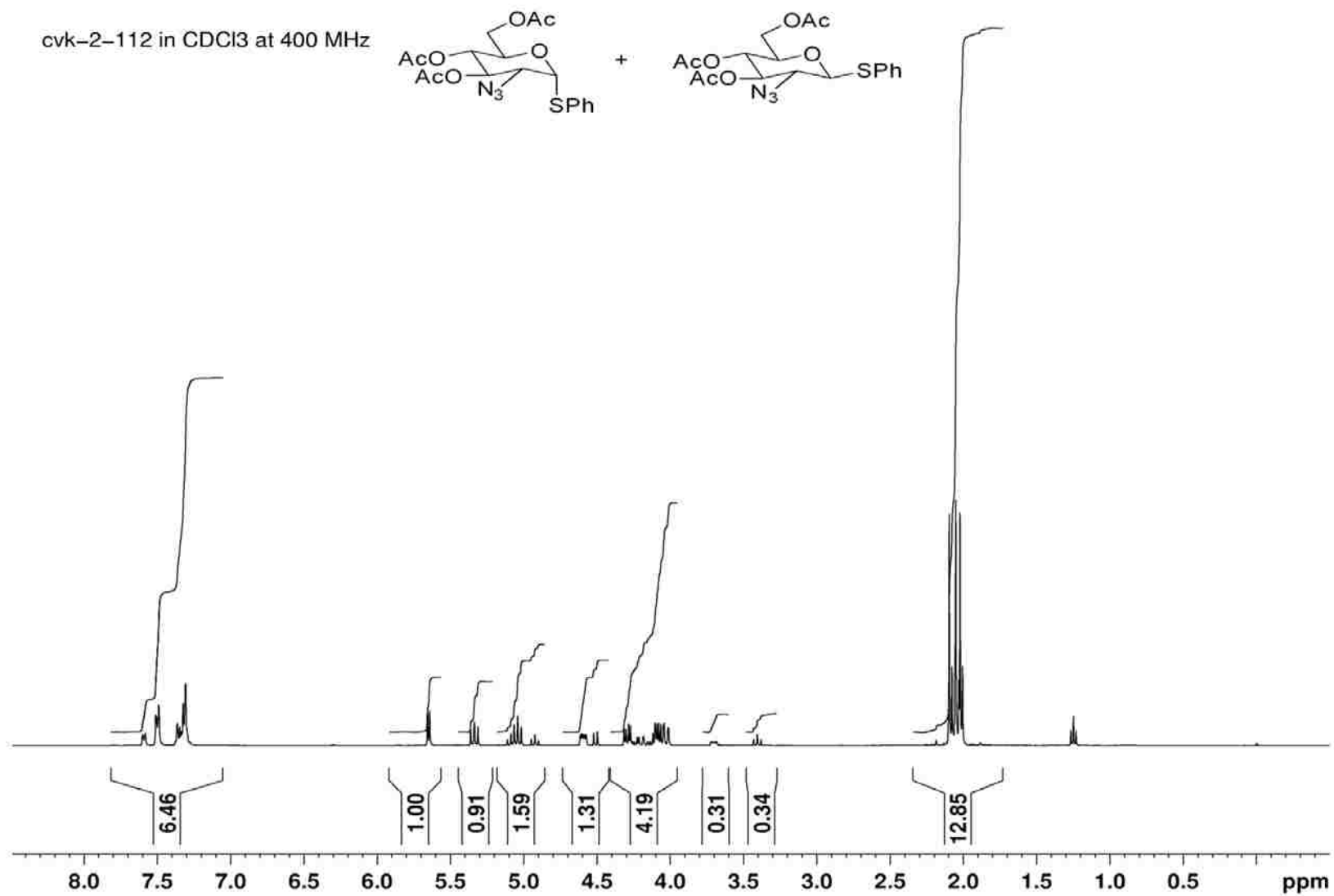


2-Azido-1,3,4,6-tetra-*O*-acetyl- $\beta$ -*D*-glucopyranose (**77**)

cvk-2-103 in CDCl<sub>3</sub> at 100 MHz



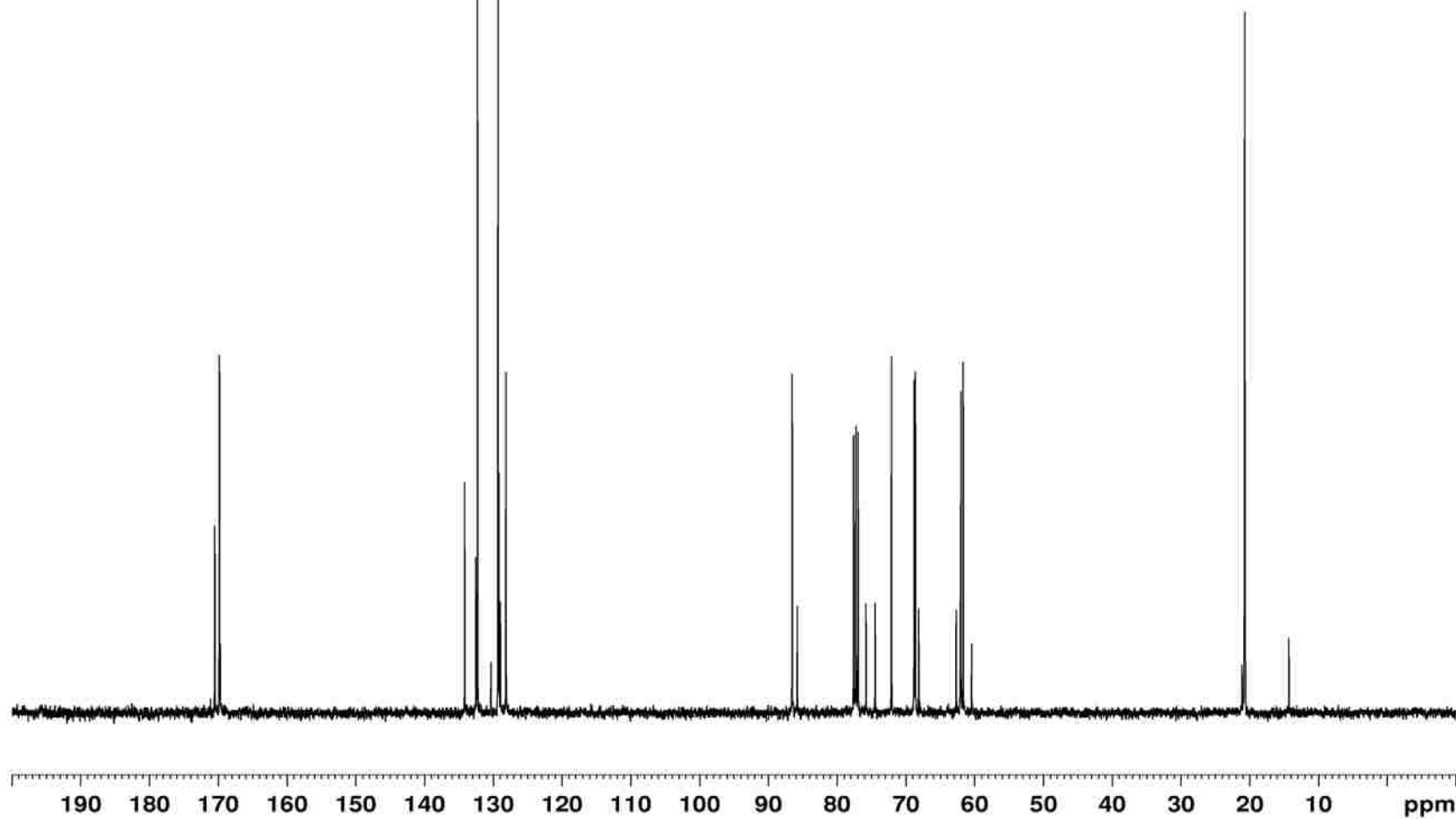
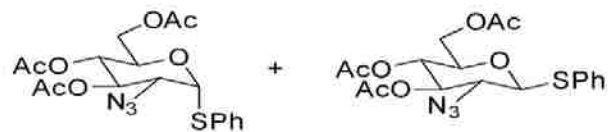
Thiobenzyl [2-azido-tri-O-acetyl-gluco]pyranose (**78**)





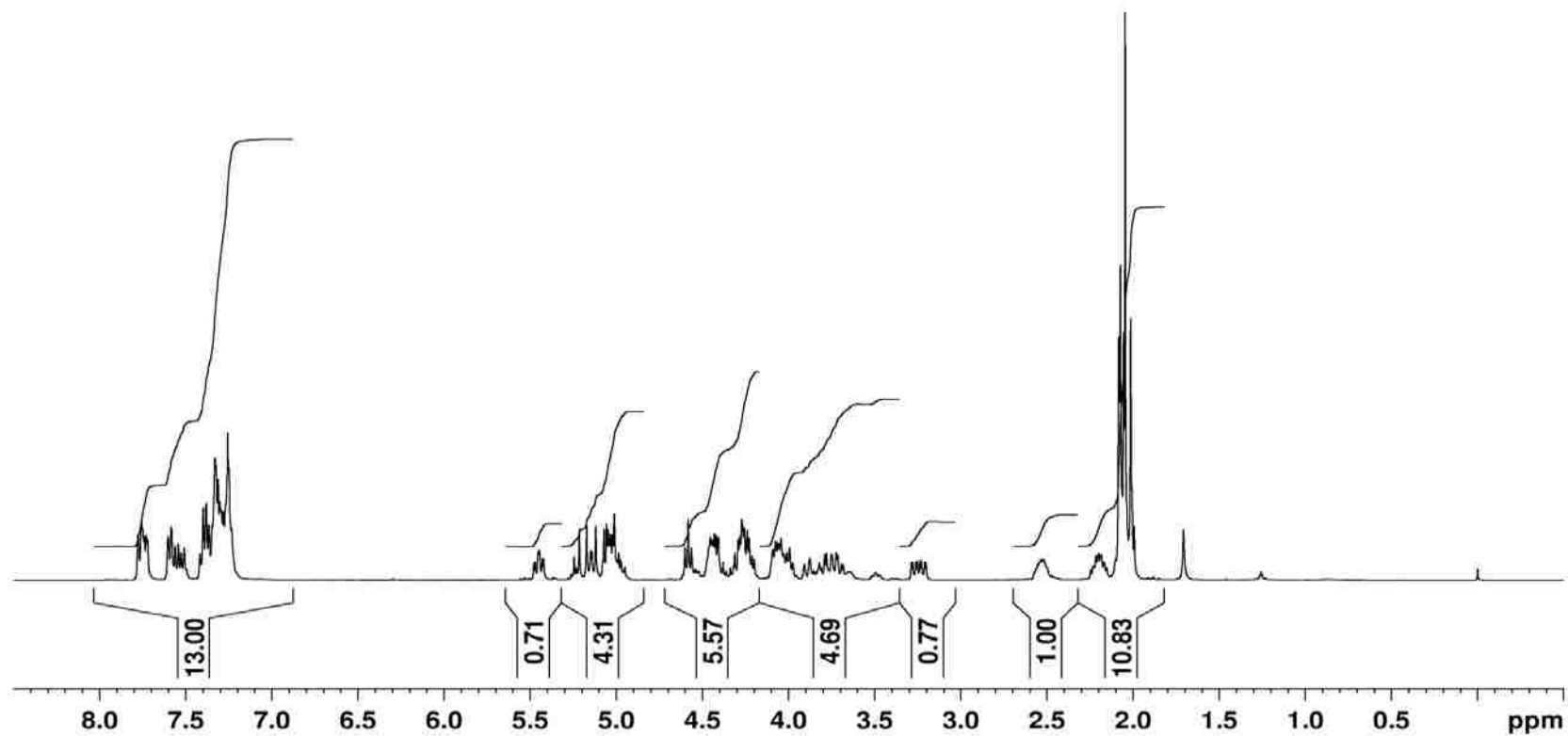
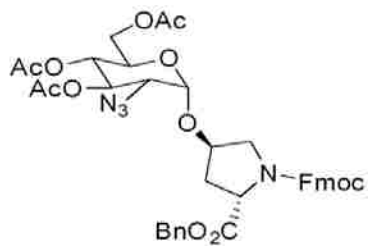
Thiobenzyl [2-azido-tri-O-acetyl-gluco]pyranose (**78**)

cvk-2-112 in CDCl<sub>3</sub> at 100 MHz



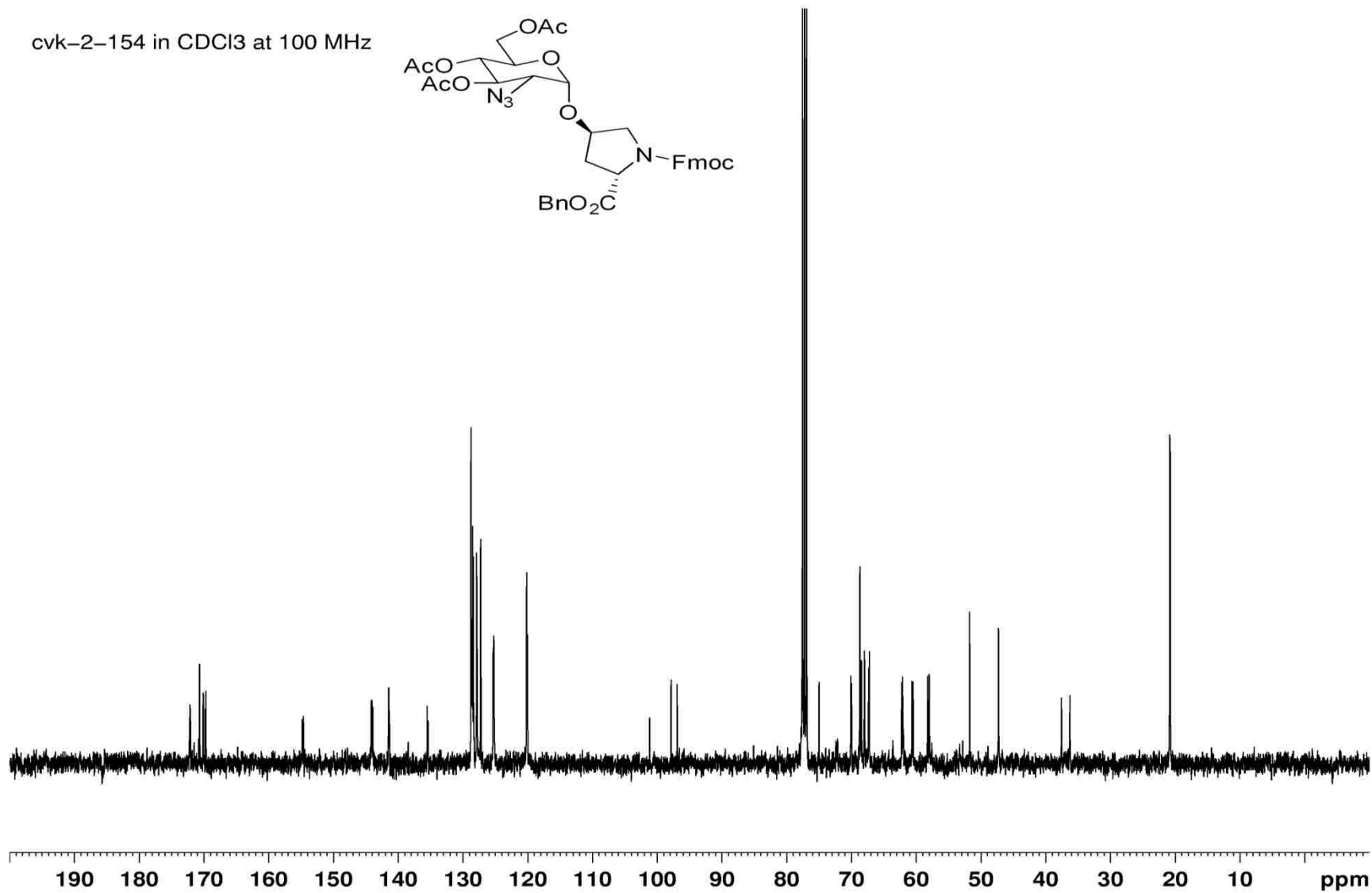
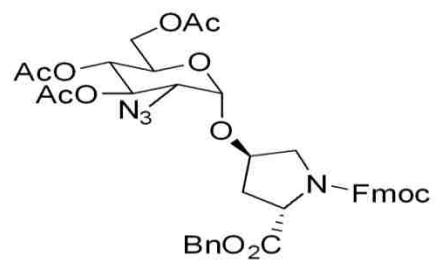
Fmoc-Hyp-4-O-(2-azido-3,4,6-tetra-O-acetyl- $\alpha$ -D-glucopyranosyl)-OBn (**80**)

cvk-2-154 in CDCl<sub>3</sub> at 400 MHz



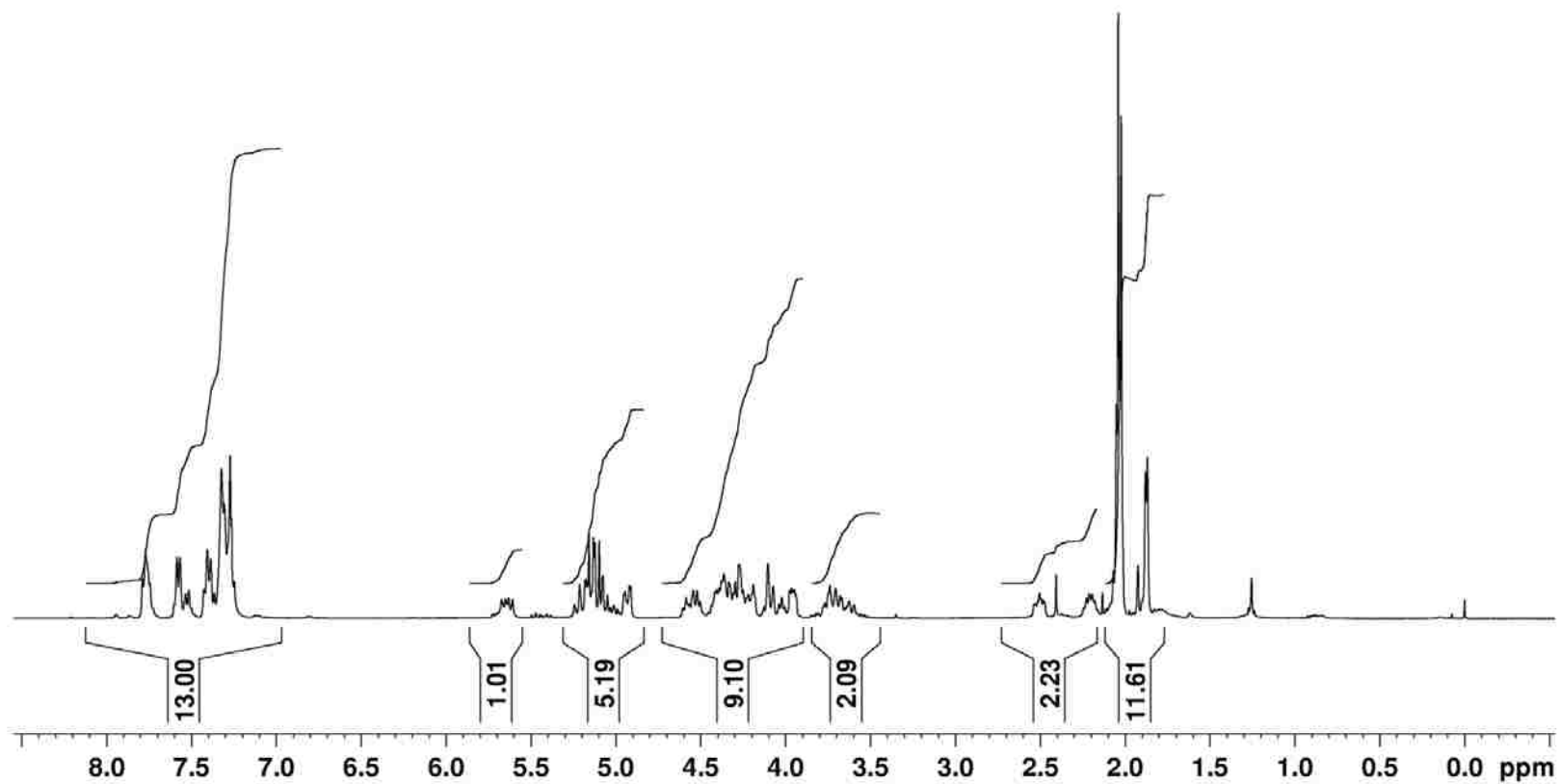
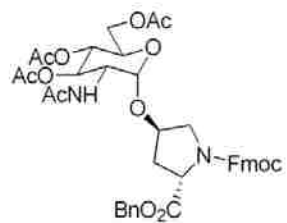
Fmoc-Hyp-4-O-(2-azido-3,4,6-tetra-O-acetyl- $\alpha$ -D-glucopyranosyl)-OBn (**80**)

cvk-2-154 in CDCl<sub>3</sub> at 100 MHz



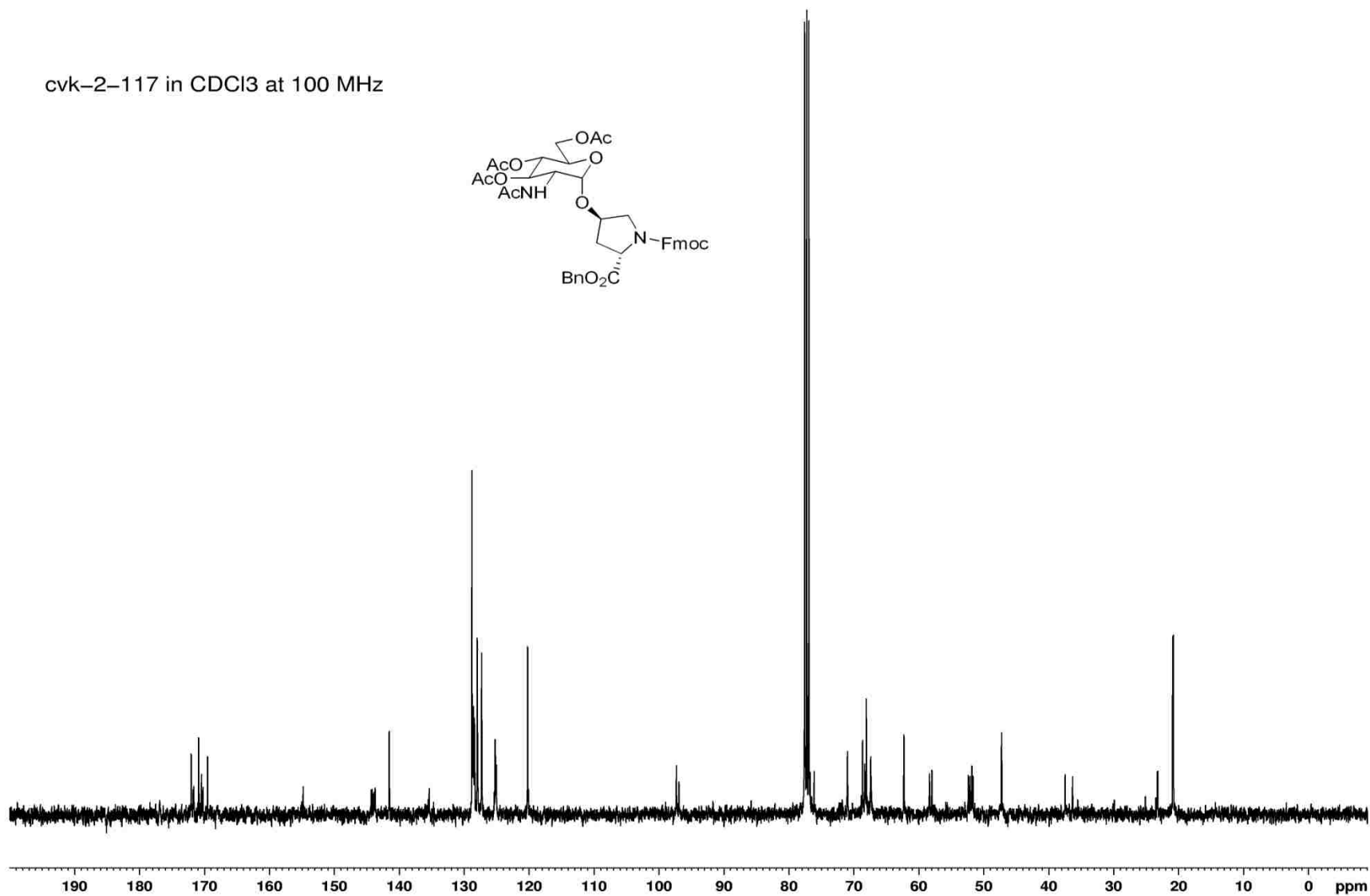
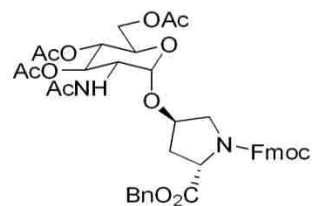
Fmoc-Hyp-[( $\alpha$ ,1-4)GlcNAc(OAc)<sub>4</sub>]-OBn (**81**)

cvk-2-117 in CDCl<sub>3</sub> at 400 MHz



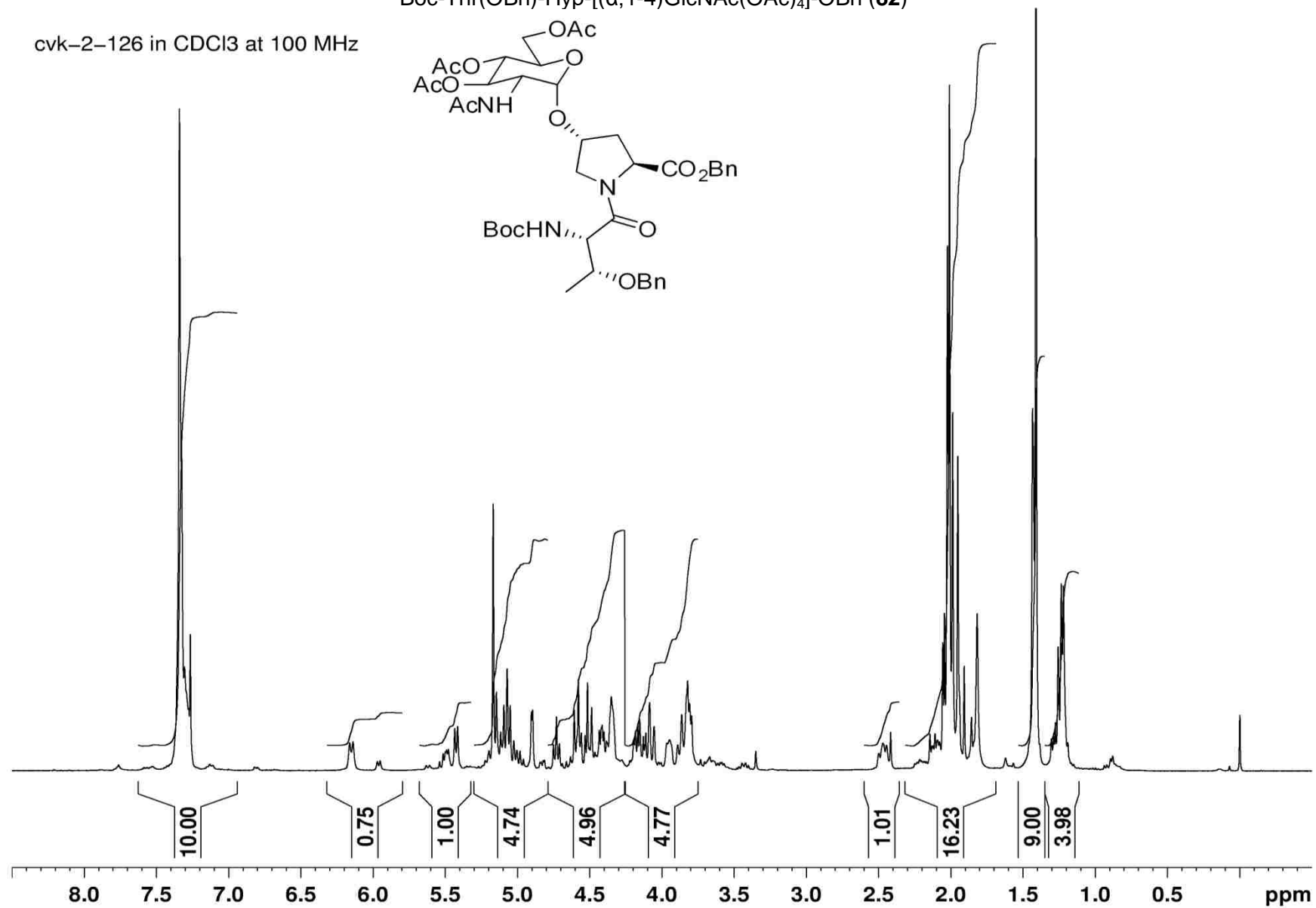
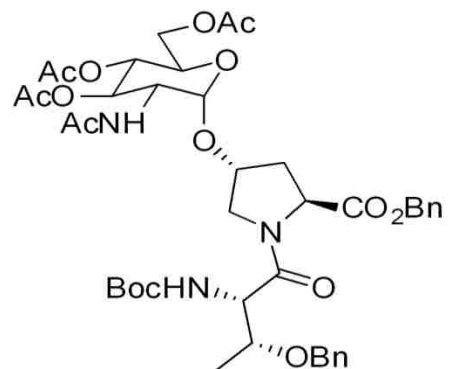
Fmoc-Hyp-[( $\alpha$ ,1-4)GlcNAc(OAc)<sub>4</sub>]-OBn (**81**)

cvk-2-117 in CDCl<sub>3</sub> at 100 MHz



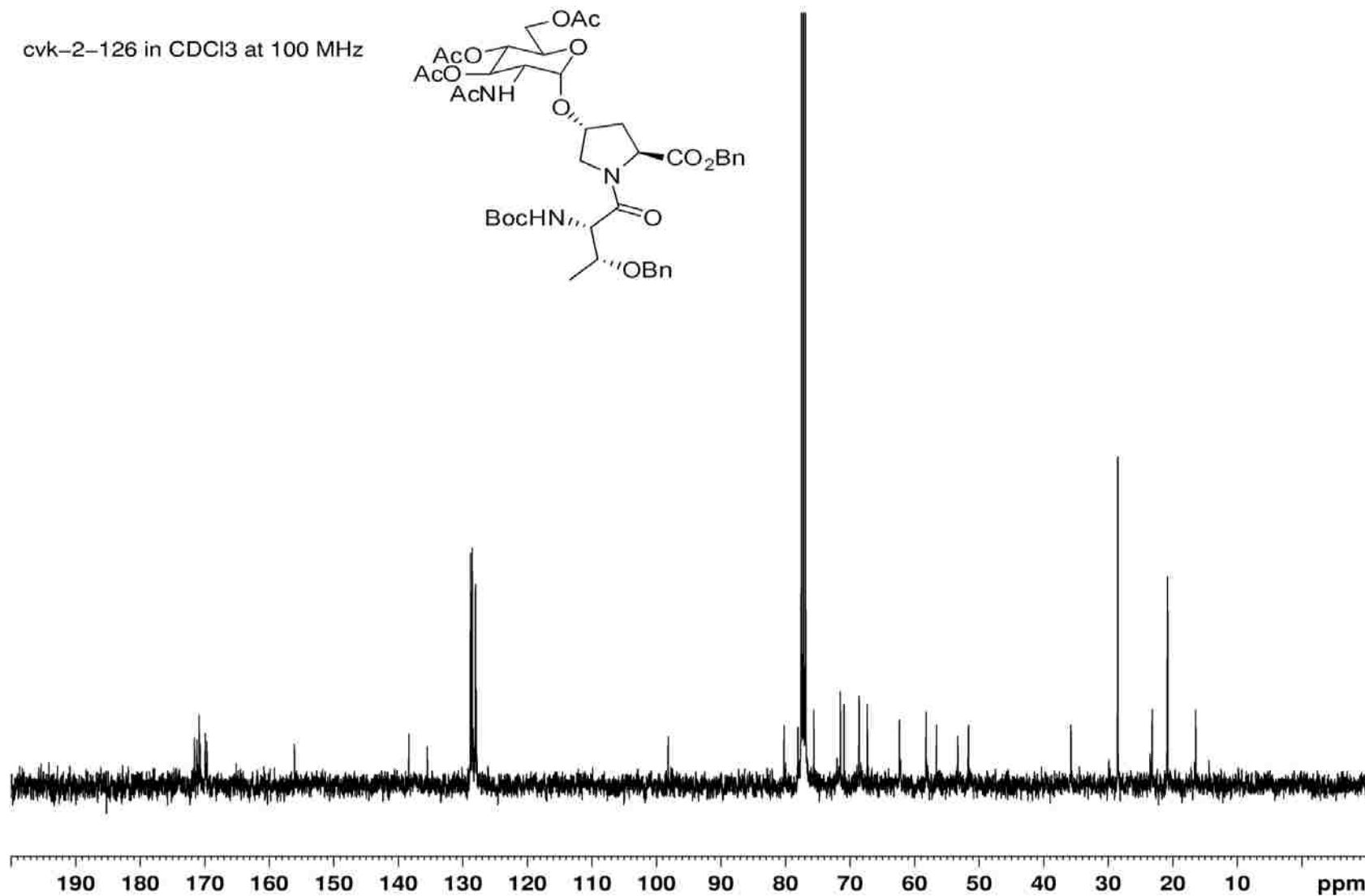
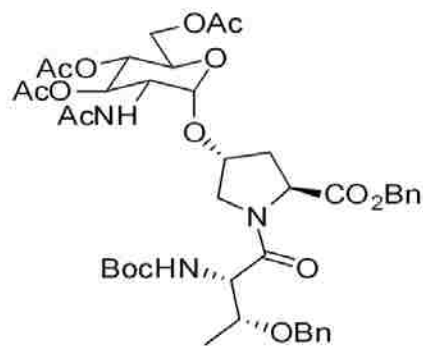
Boc-Thr(OBn)-Hyp-[( $\alpha$ ,1-4)GlcNAc(OAc)<sub>4</sub>]-OBn (**82**)

cvk-2-126 in CDCl<sub>3</sub> at 100 MHz



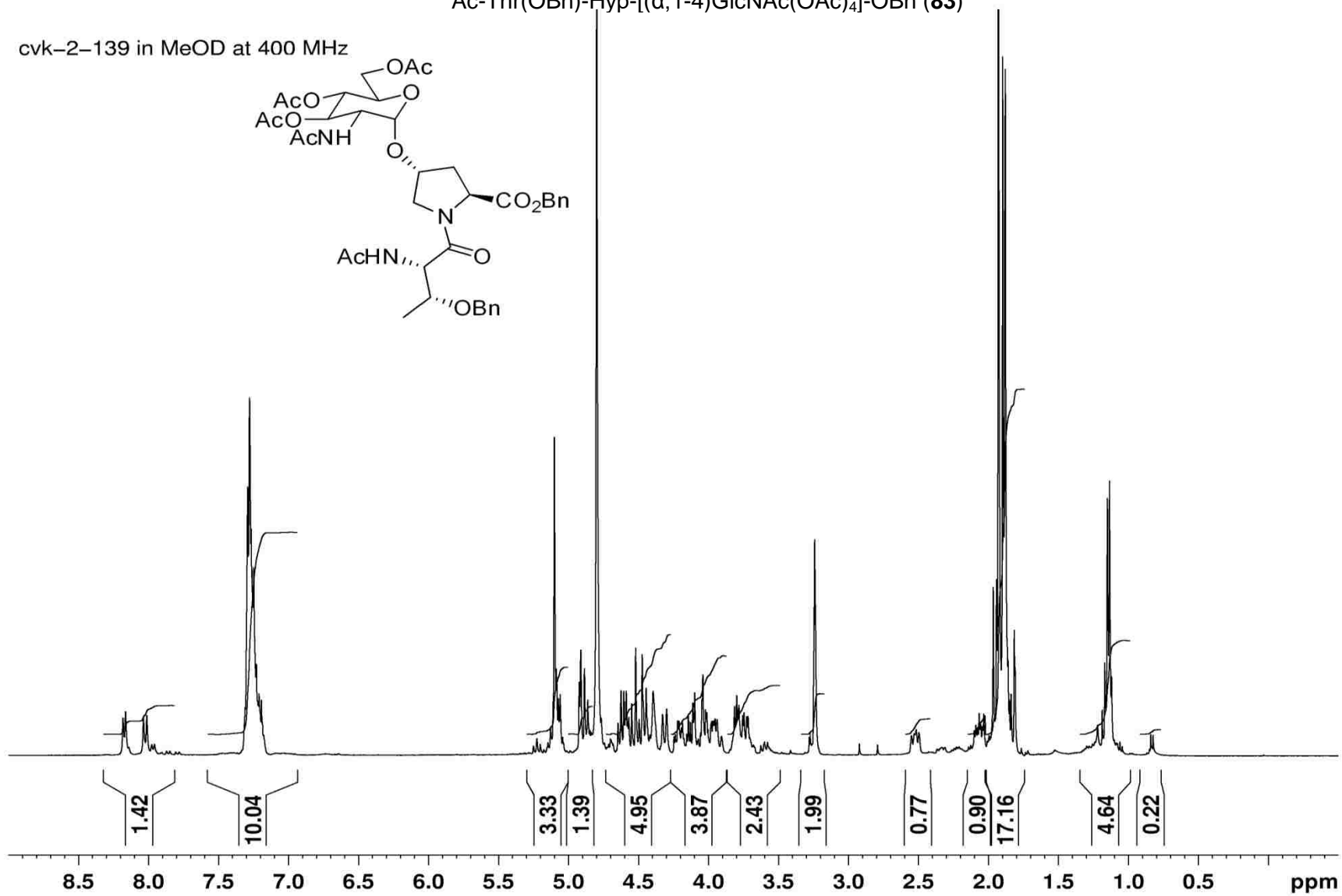
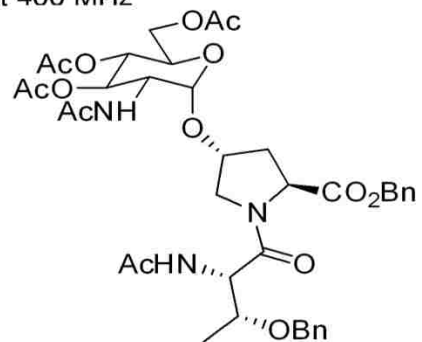
Boc-Thr(OBn)-Hyp-[( $\alpha$ ,1-4)GlcNAc(OAc)<sub>4</sub>]-OBn (**82**)

cvk-2-126 in CDCl<sub>3</sub> at 100 MHz



Ac-Thr(OBn)-Hyp-[( $\alpha$ ,1-4)GlcNAc(OAc)<sub>4</sub>]-OBn (**83**)

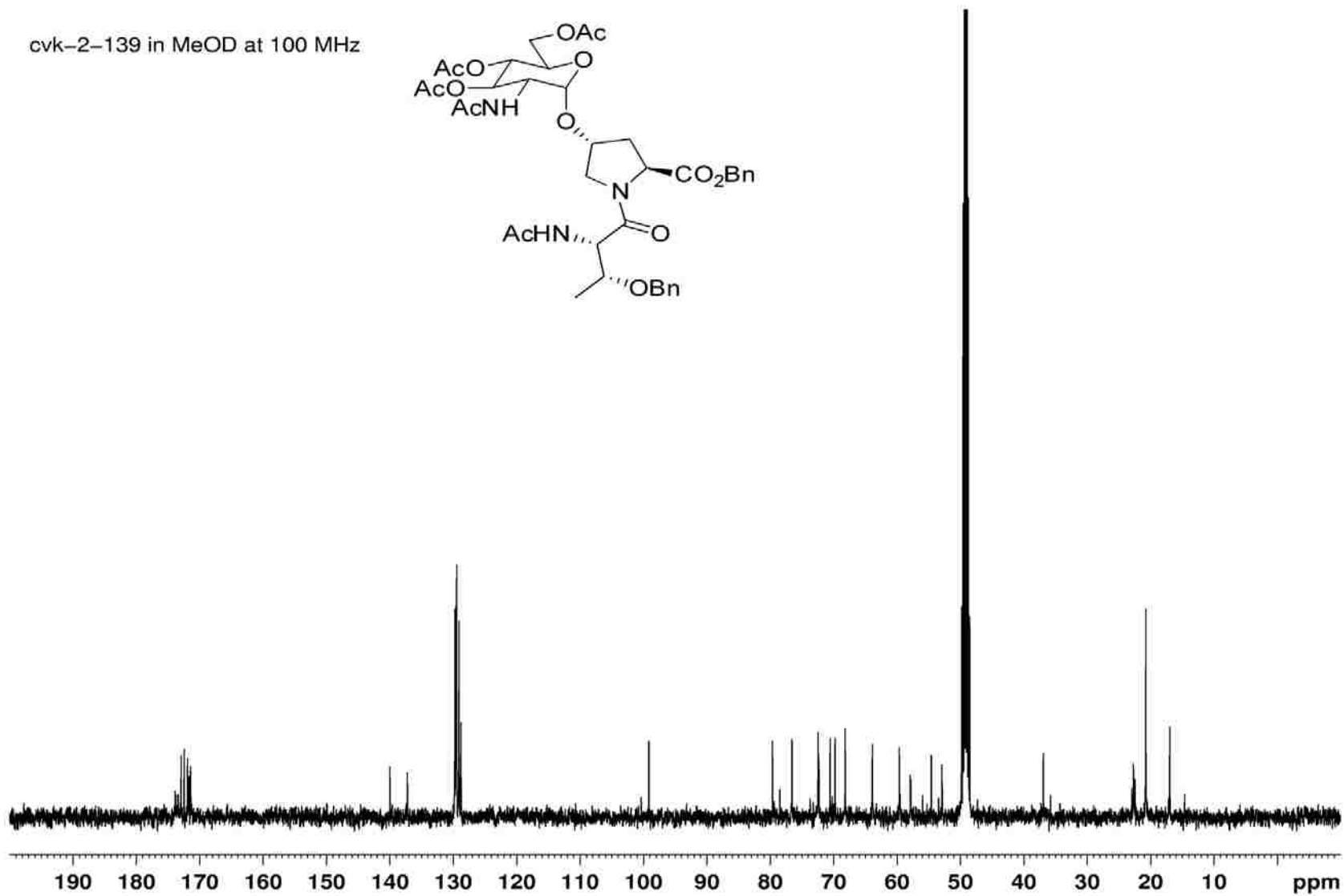
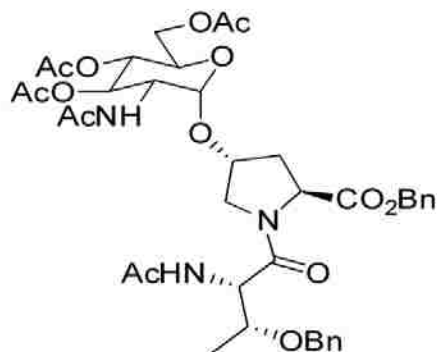
cvk-2-139 in MeOD at 400 MHz





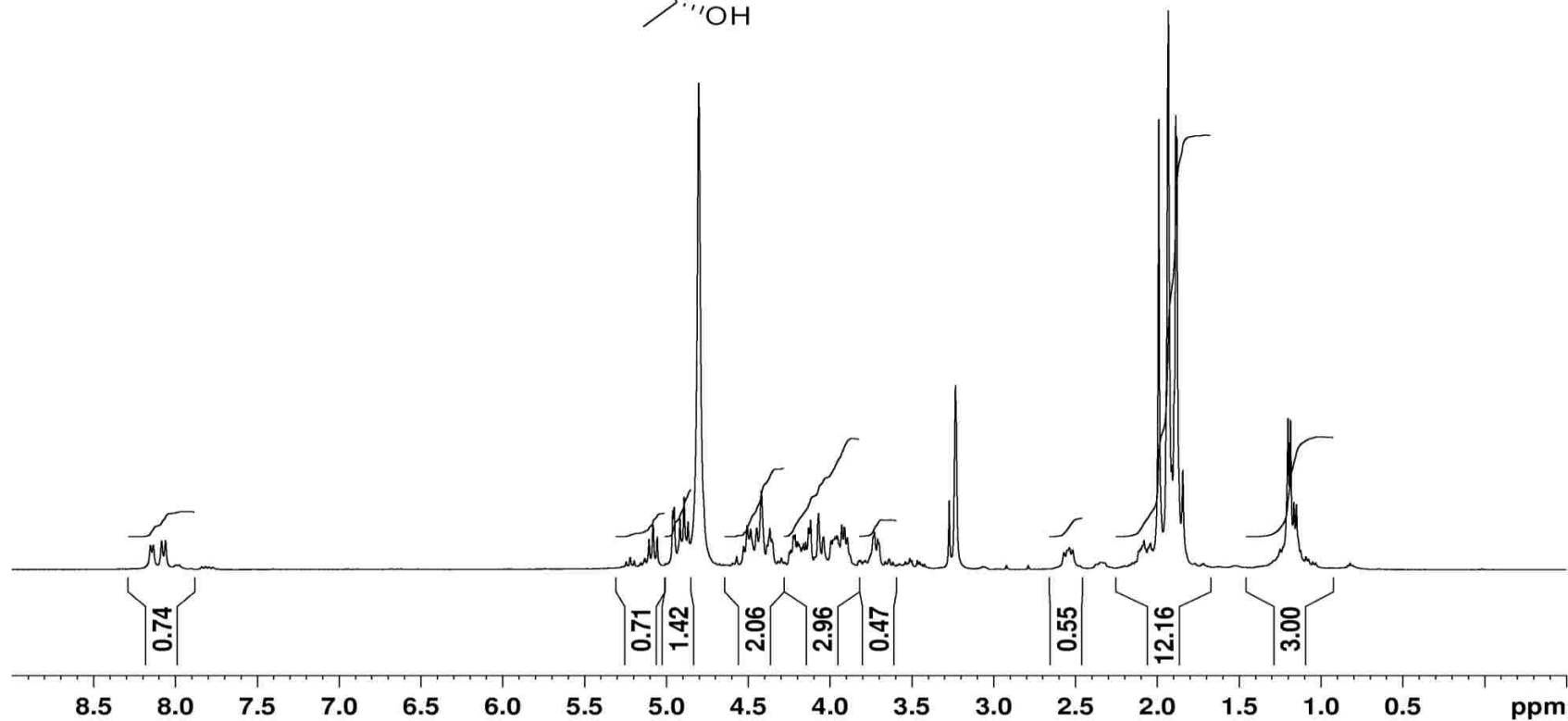
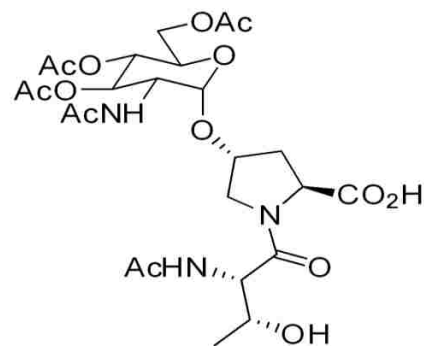
Ac-Thr(OBn)-Hyp-[( $\alpha$ ,1-4)GlcNAc(OAc)<sub>4</sub>]-OBn (**83**)

cvk-2-139 in MeOD at 100 MHz



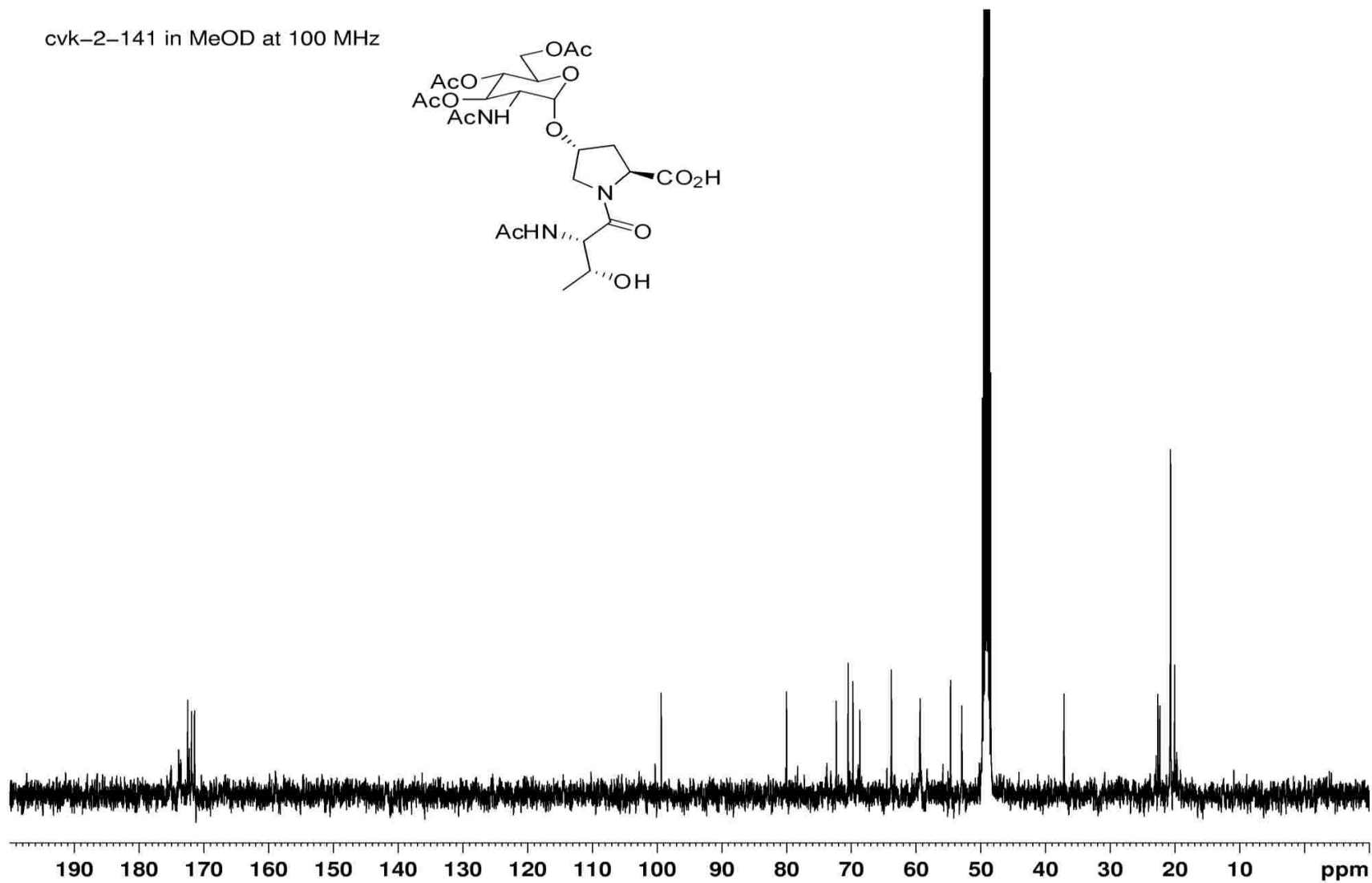
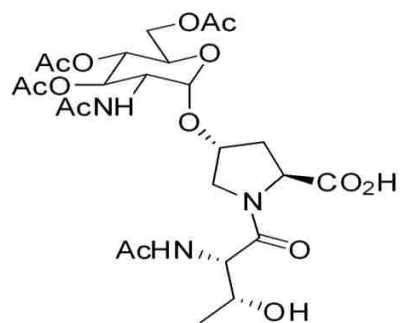
Ac-Thr-Hyp-[( $\alpha$ ,1-4)GlcNAc(OAc)<sub>4</sub>]-OH (**84**)

cvk-2-141 in MeOD at 400 MHz



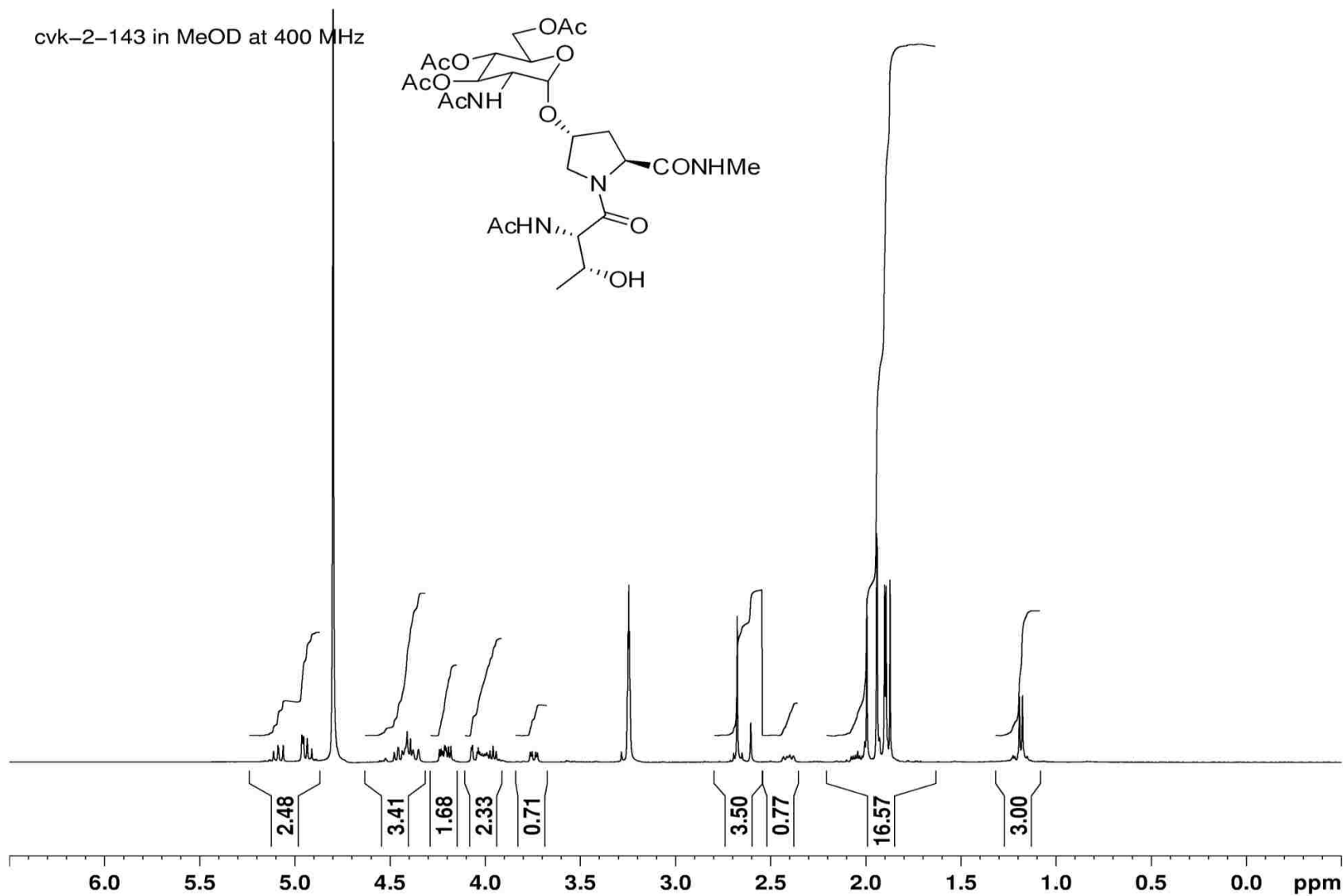
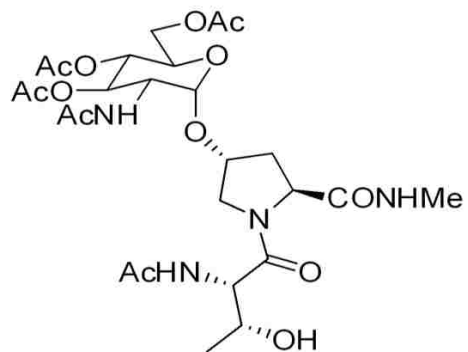
Ac-Thr-Hyp-[( $\alpha$ ,1-4)GlcNAc(OAc)<sub>4</sub>]-OH (**84**)

cvk-2-141 in MeOD at 100 MHz



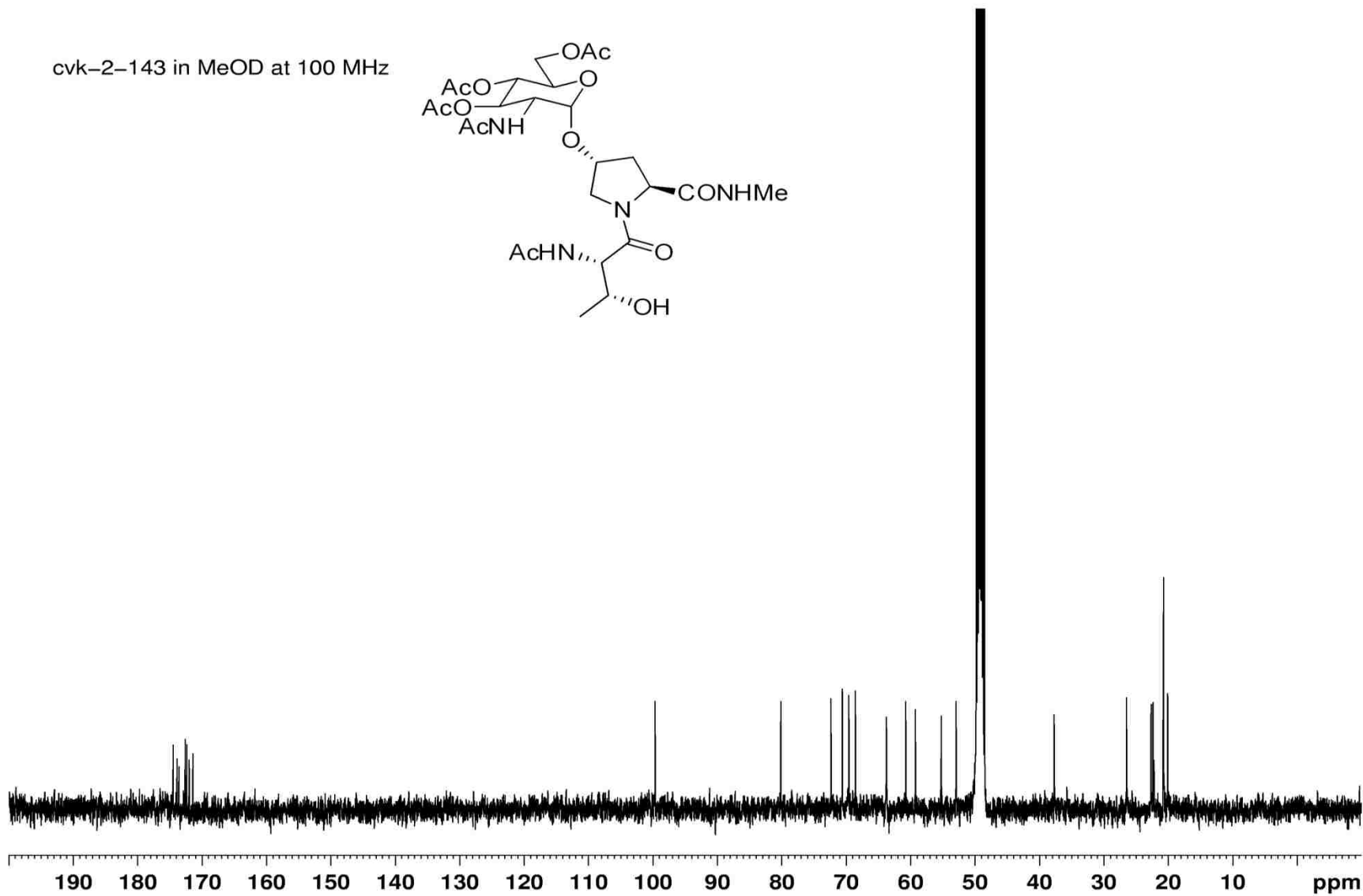
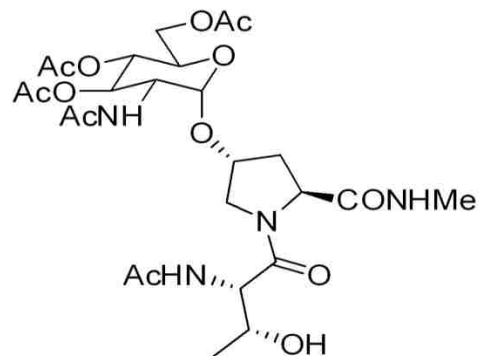
Ac-Thr-Hyp-[( $\alpha$ ,1-4)GlcNAc(OAc)<sub>4</sub>]-NHMe (**85**)

cvk-2-143 in MeOD at 400 MHz



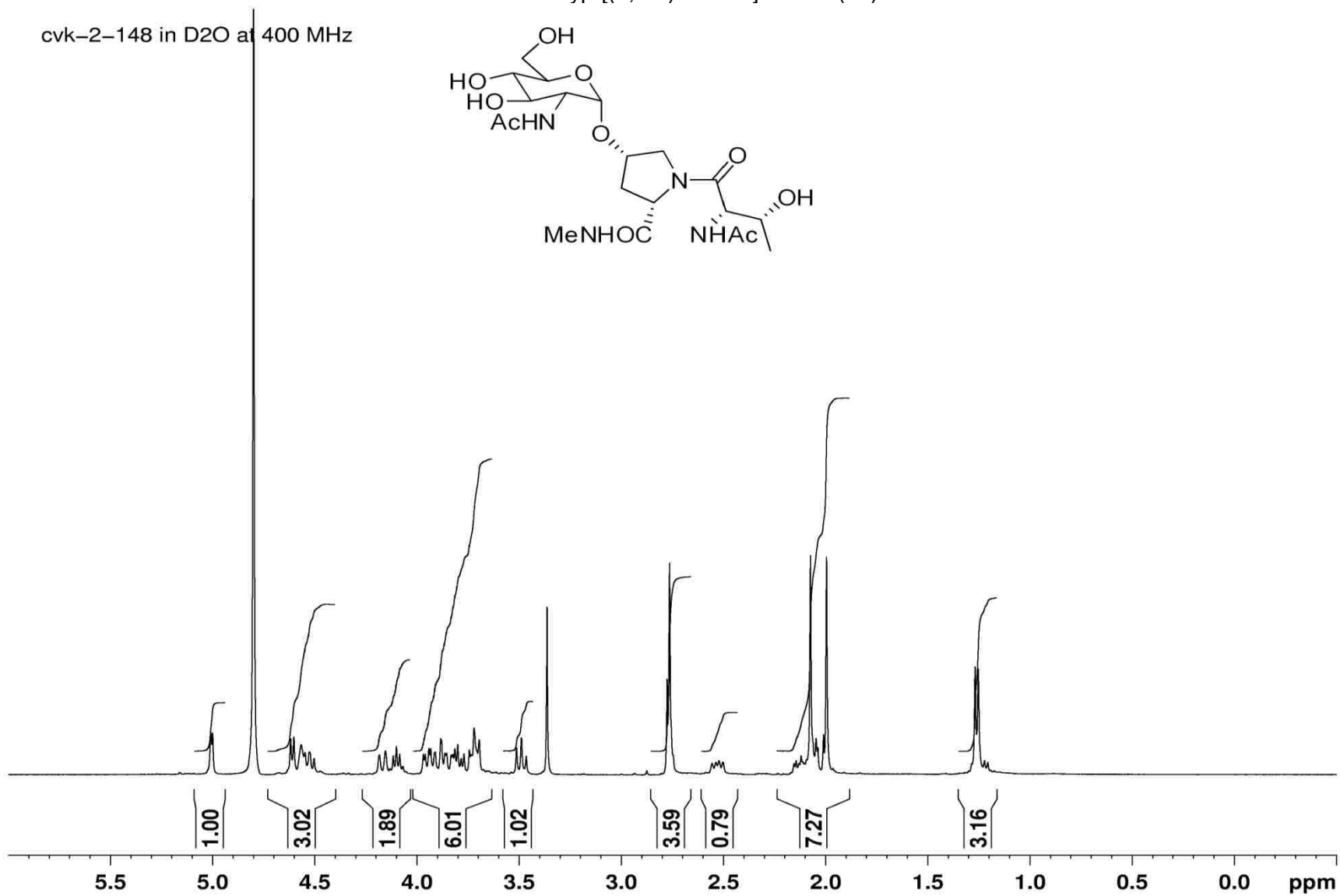
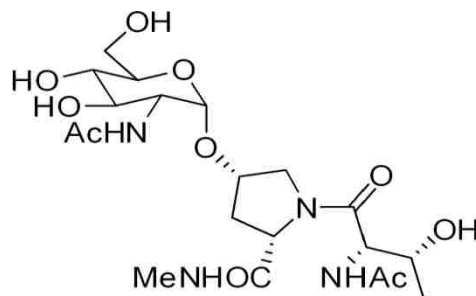
Ac-Thr-Hyp-[( $\alpha$ ,1-4)GlcNAc(OAc)<sub>4</sub>]-NHMe (85)

cvk-2-143 in MeOD at 100 MHz



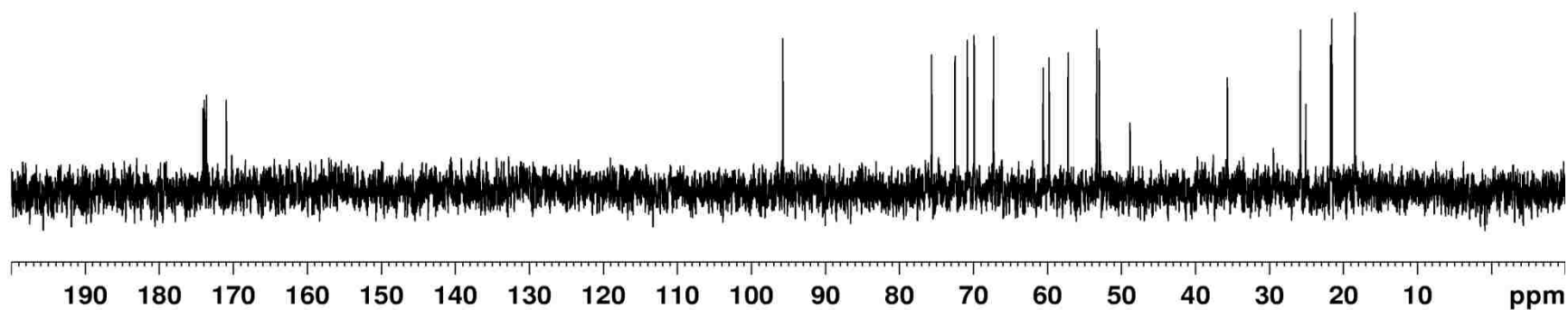
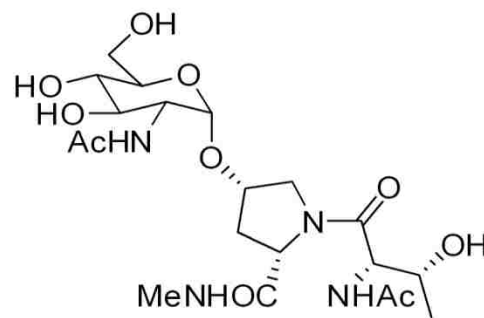
Ac-Thr-Hyp-[( $\alpha$ ,1-4)GlcNAc]-NHMe (**63**)

cvk-2-148 in D<sub>2</sub>O at 400 MHz



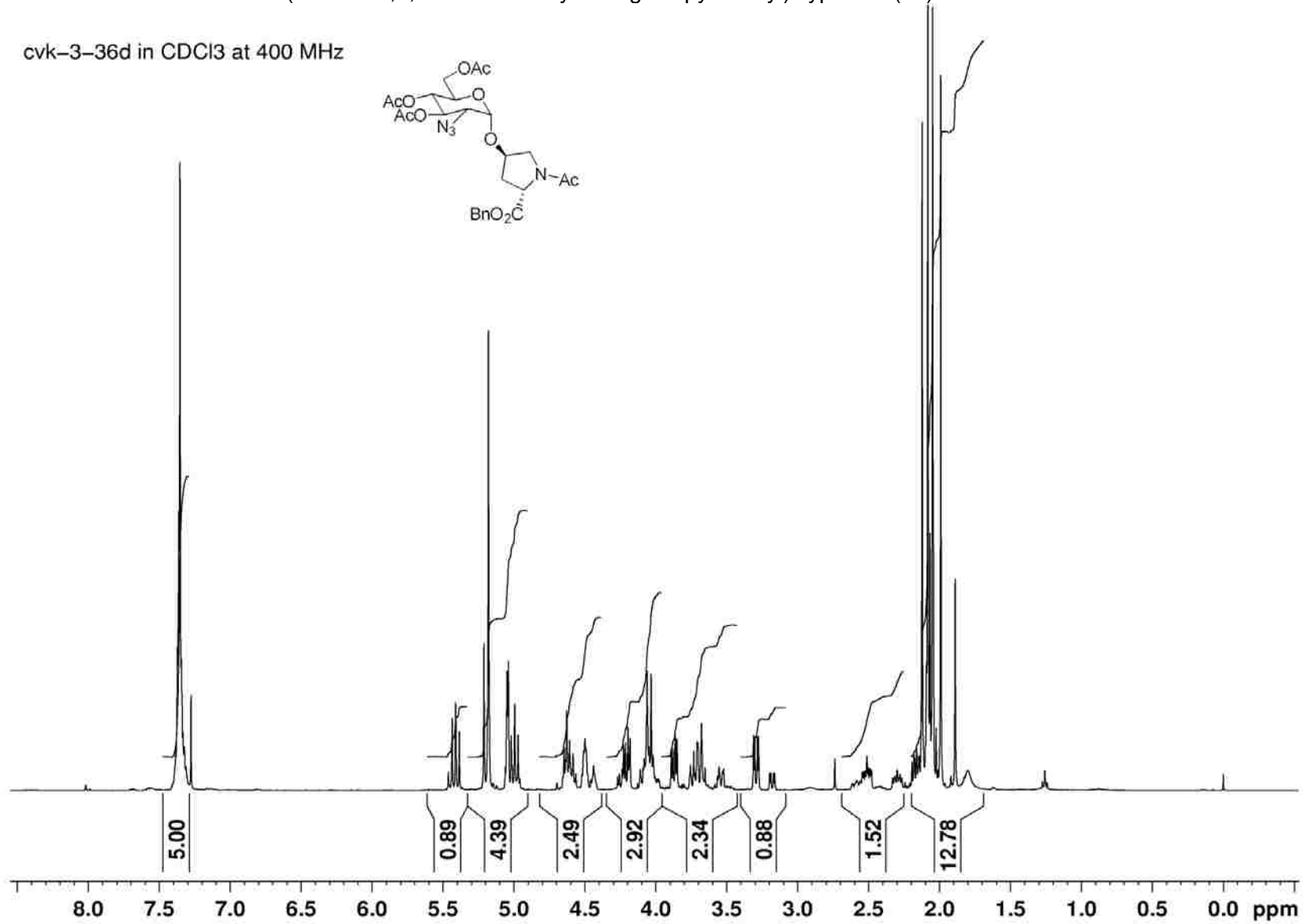
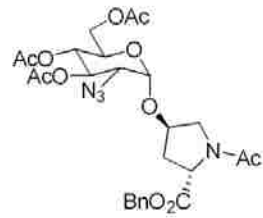
Ac-Thr-Hyp-[( $\alpha$ ,1-4)GlcNAc]-NHMe (**63**)

cvk-2-148 in D<sub>2</sub>O at 100 MHz



Ac-4-O-(2-azido-3,4,6-tetra-O-acetyl- $\alpha$ -D-glucopyranosyl)Hyp-OBn (**95**)

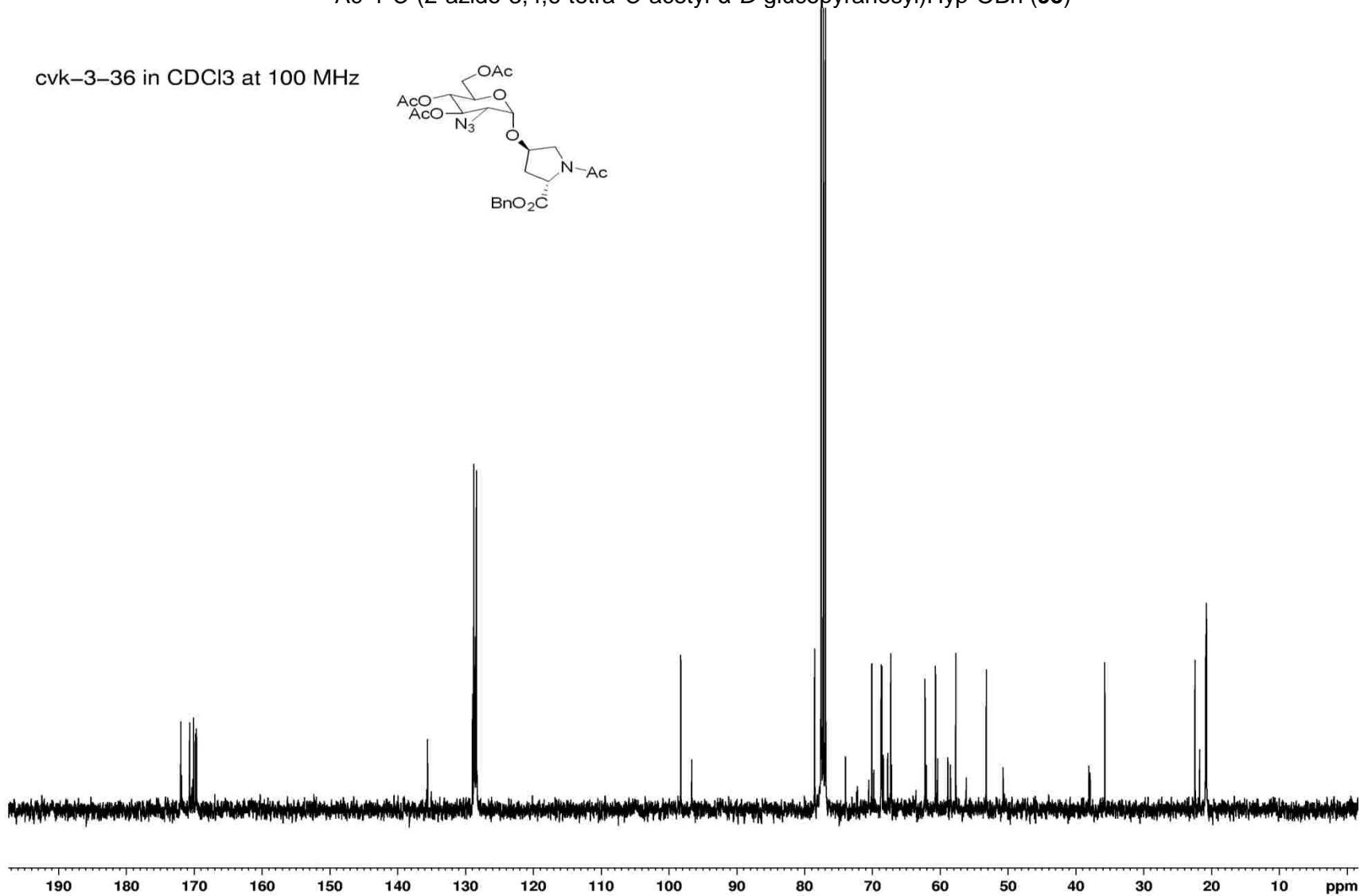
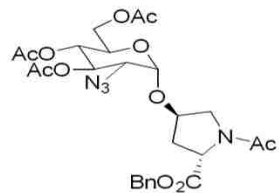
cvk-3-36d in CDCl<sub>3</sub> at 400 MHz



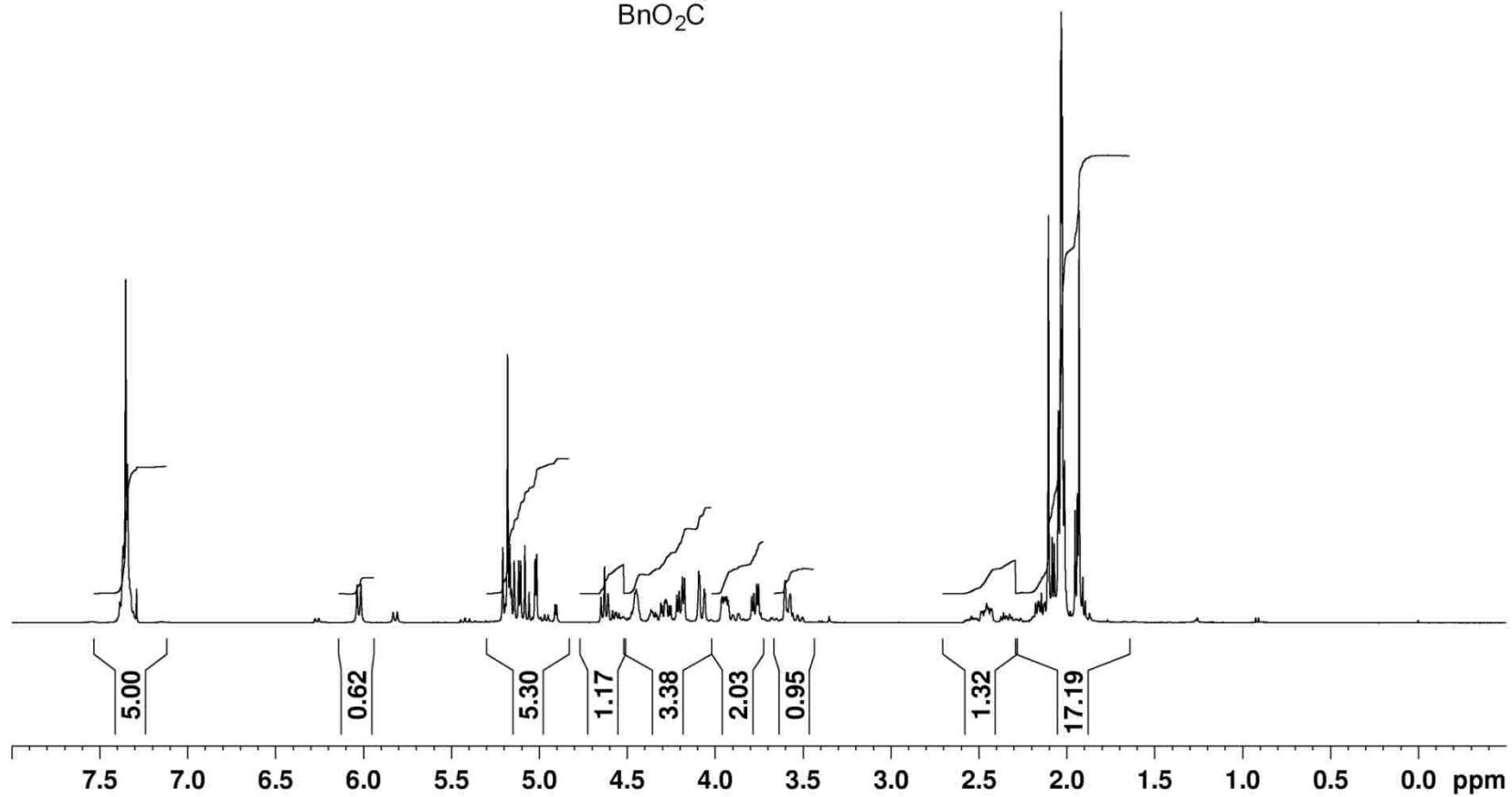
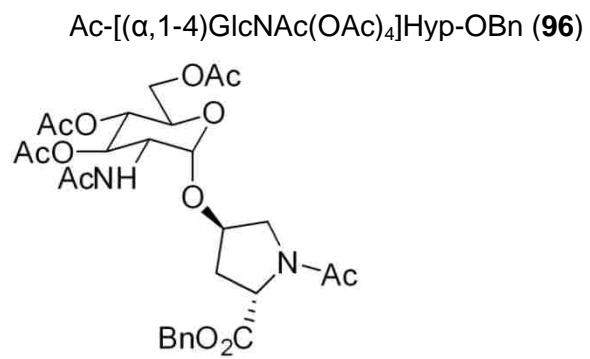


Ac-4-O-(2-azido-3,4,6-tetra-O-acetyl- $\alpha$ -D-glucopyranosyl)Hyp-OBn (**95**)

cvk-3-36 in CDCl<sub>3</sub> at 100 MHz

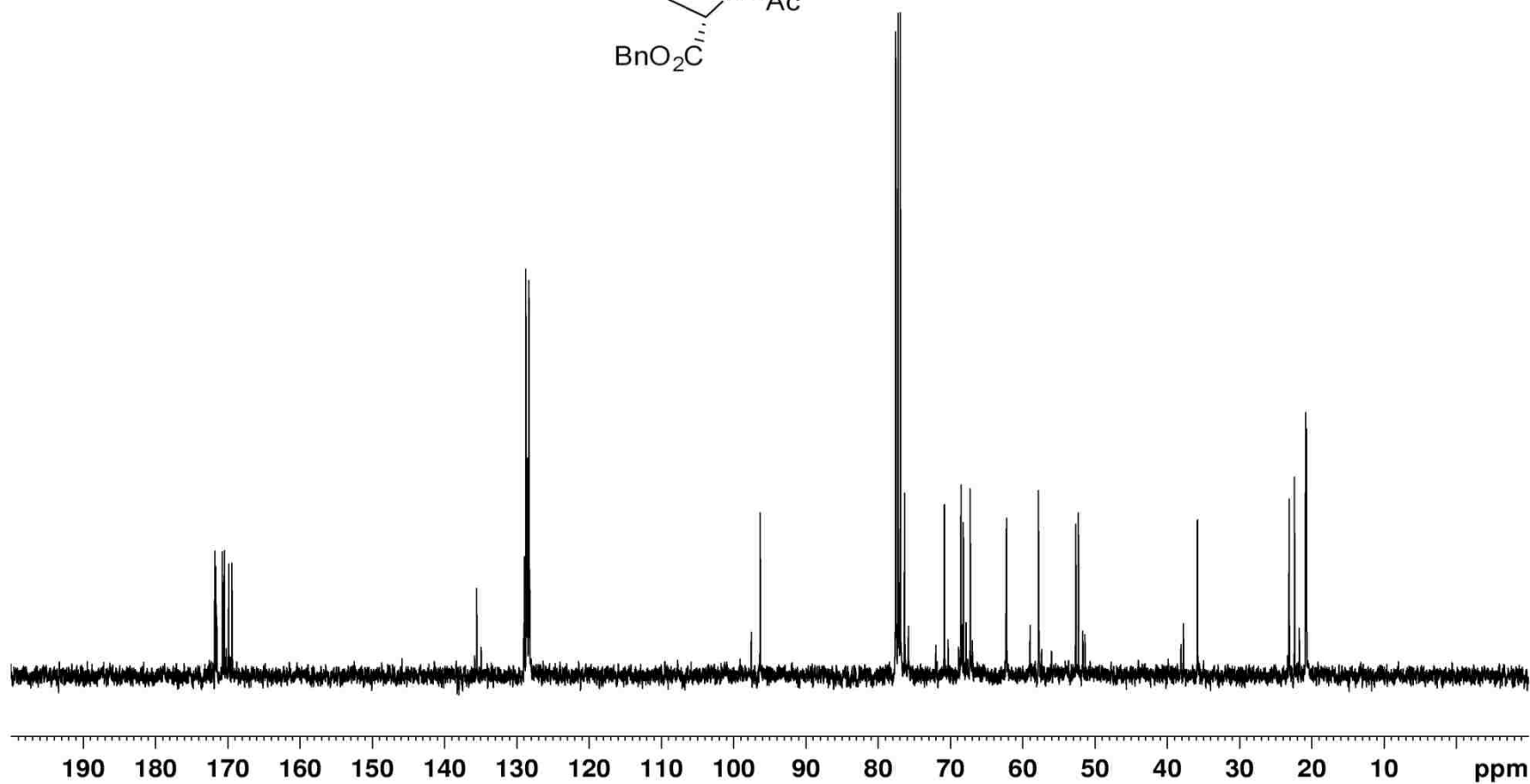
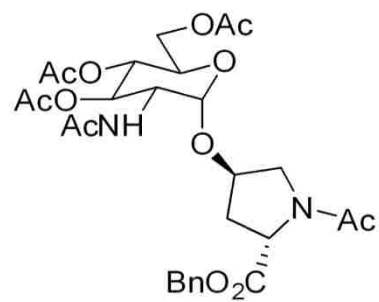


cvk-3-51 in CDCl<sub>3</sub> at 400 MHz



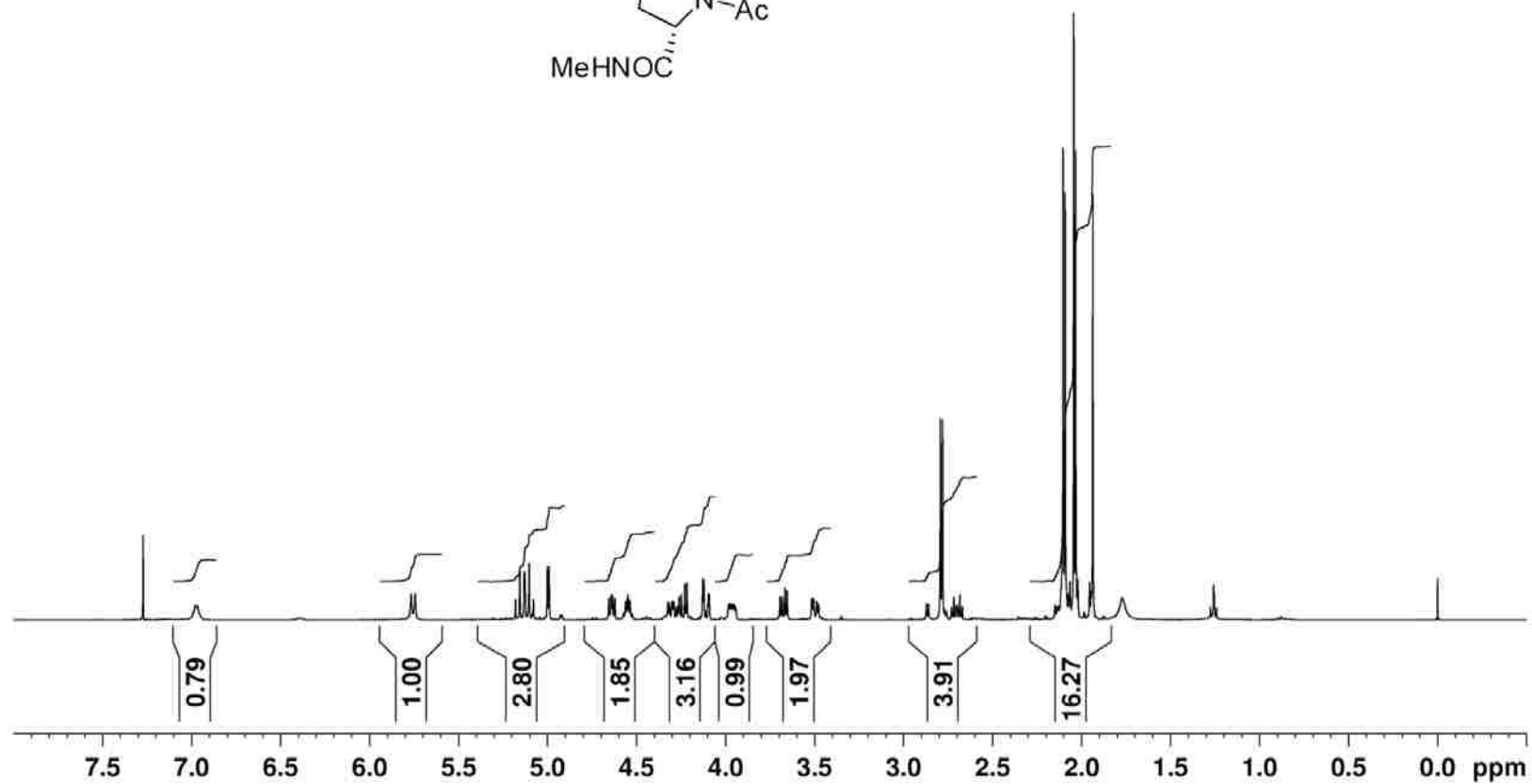
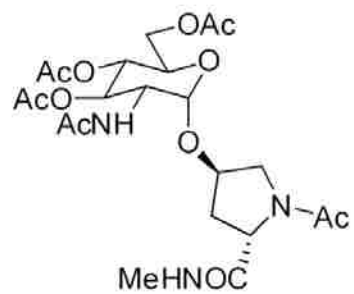
Ac-[( $\alpha$ ,1-4)GlcNAc(OAc)<sub>4</sub>]Hyp-On (**96**)

cvk-3-51 in CDCl<sub>3</sub> at 100 MHz



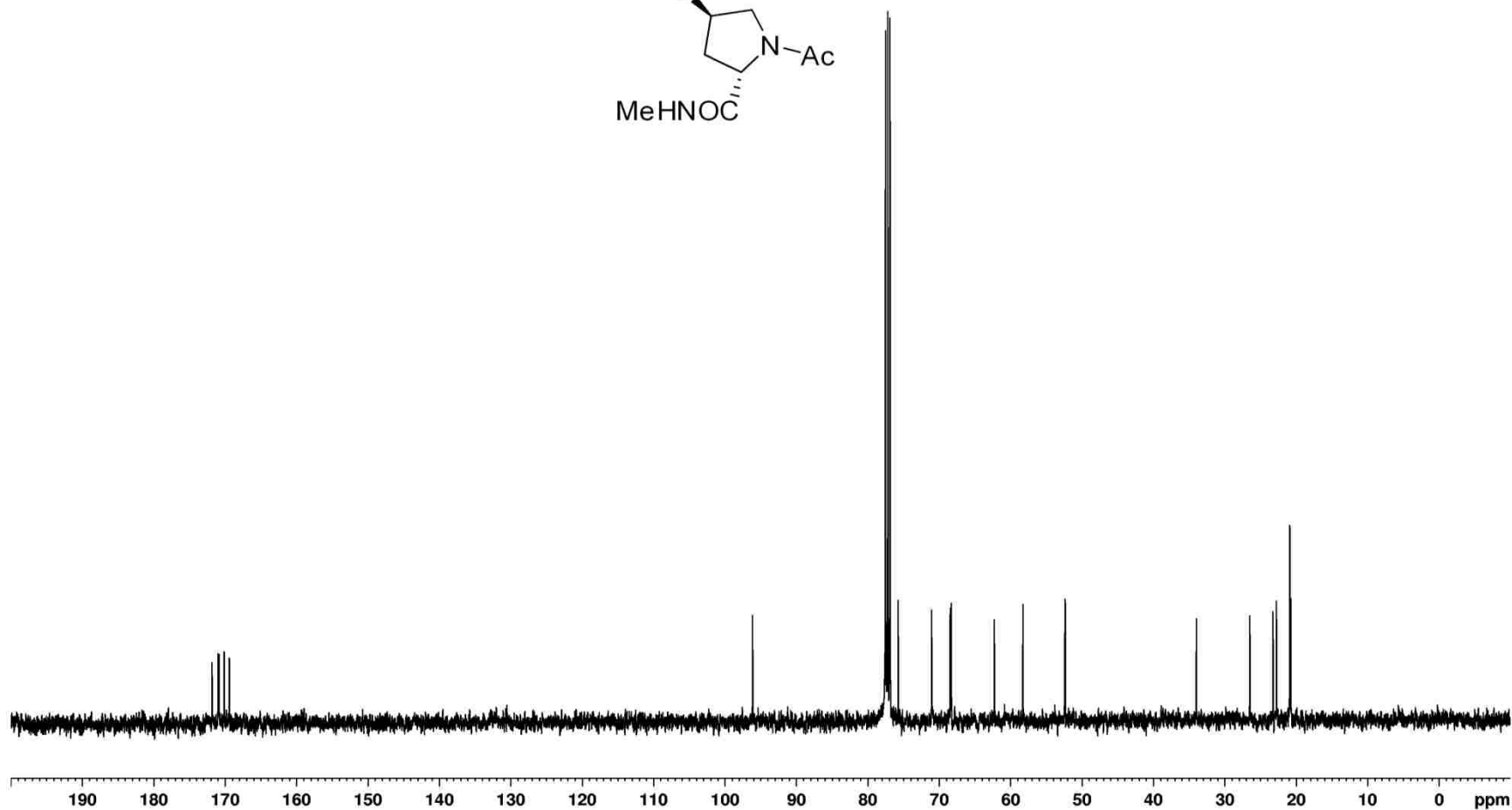
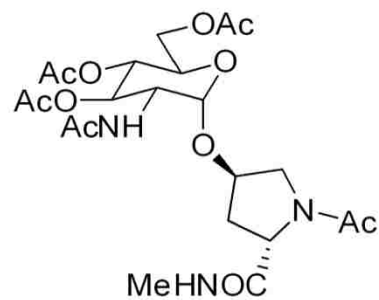
Ac-[( $\alpha$ ,1-4)GlcNAc(OAc)<sub>4</sub>]Hyp-NHMe (**98**)

cvk-3-68 in CDCl<sub>3</sub> at 400 MHz

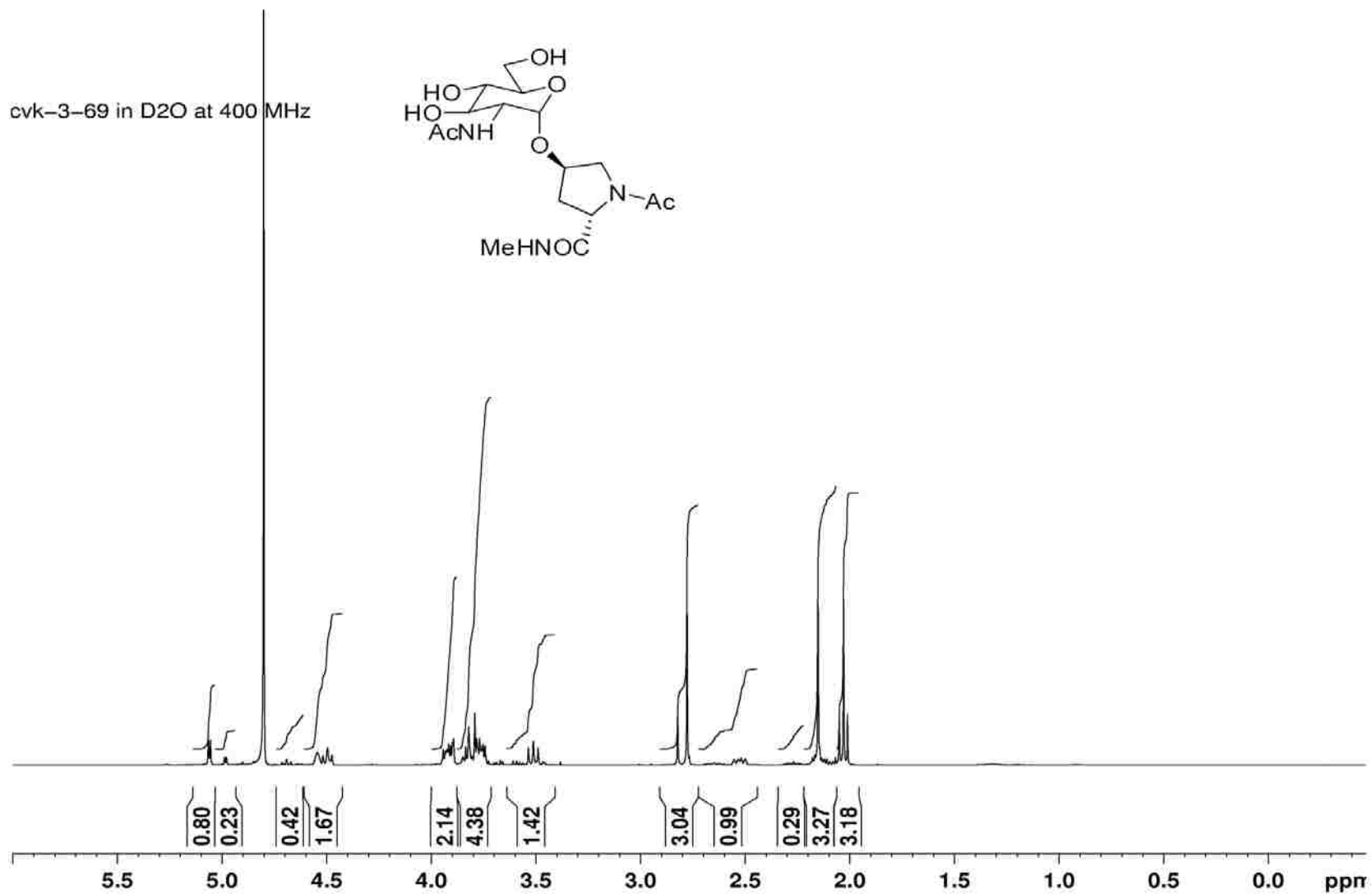


Ac-[( $\alpha$ ,1-4)GlcNAc(OAc)<sub>4</sub>]Hyp-NHMe (**98**)

cvk-3-68 in CDCl<sub>3</sub> at 100 MHz

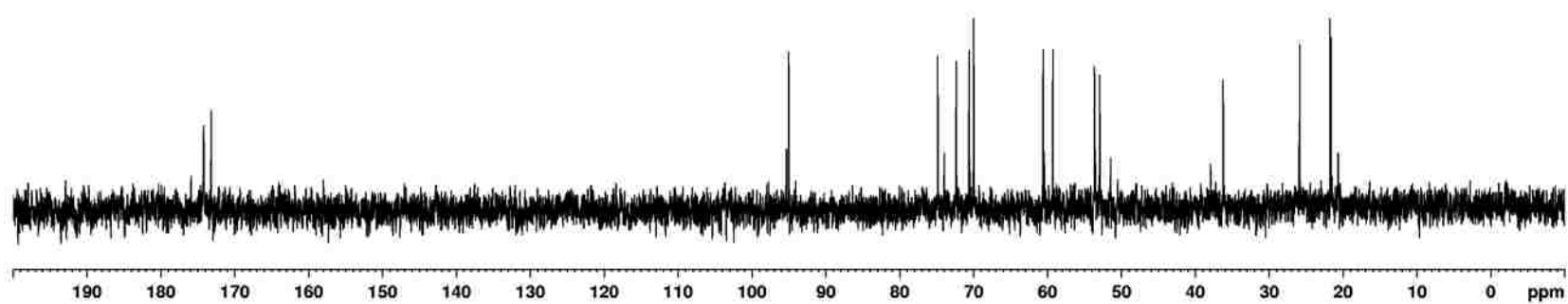
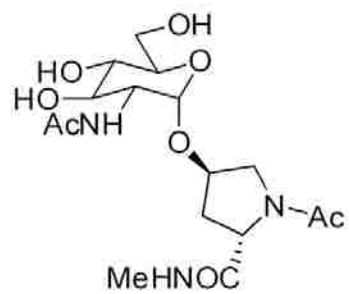


Ac-[( $\alpha$ ,1-4)-GlcNAc]-Hyp-NHMe (**89**)



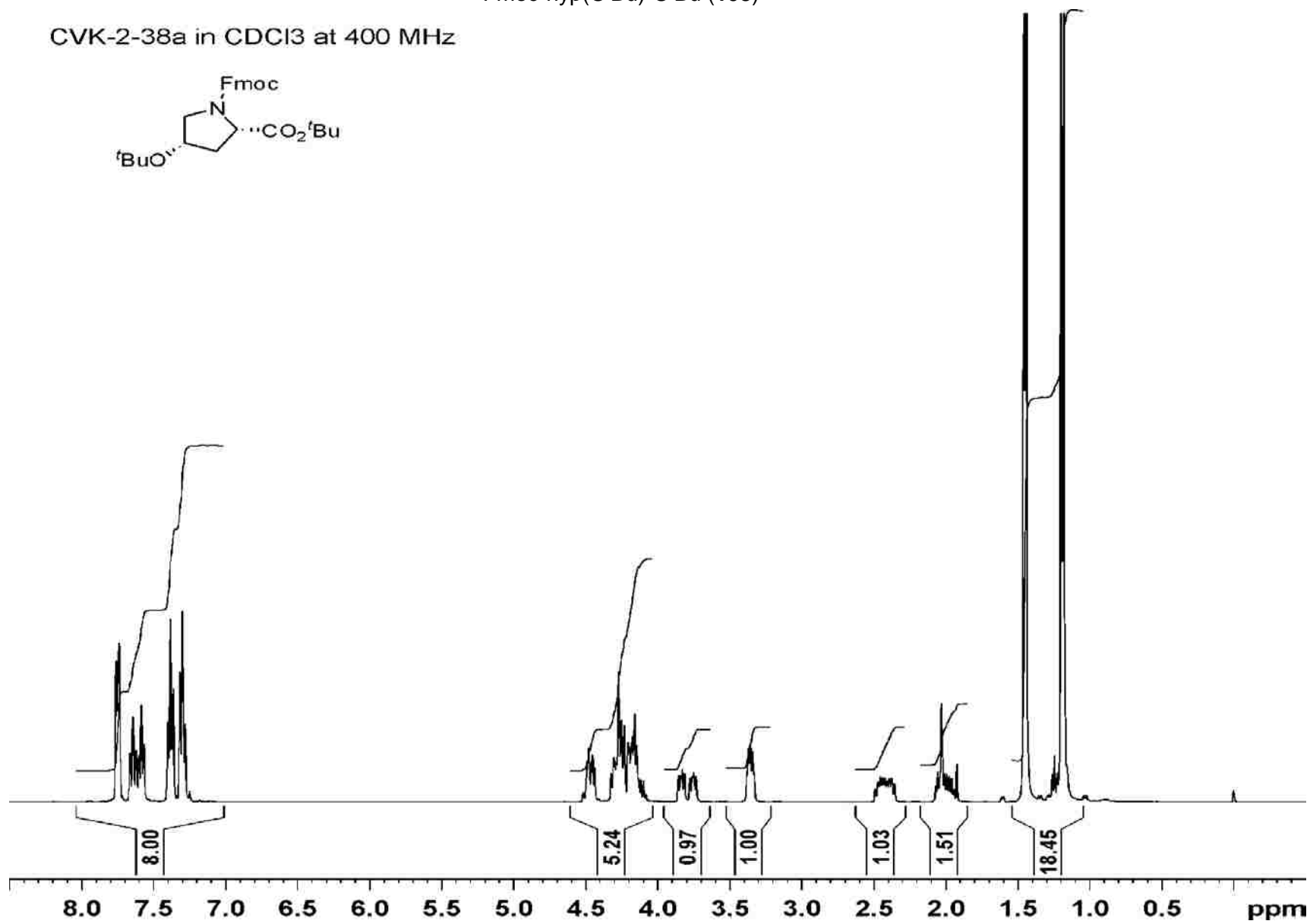
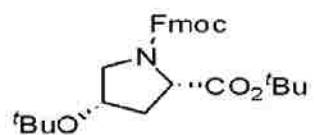
Ac-[( $\alpha$ ,1-4)-GlcNAc]-Hyp-NHMe (**89**)

cvk-3-69 in D<sub>2</sub>O at 100 MHz



Fmoc-hyp(O<sup>t</sup>Bu)-O<sup>t</sup>Bu (108)

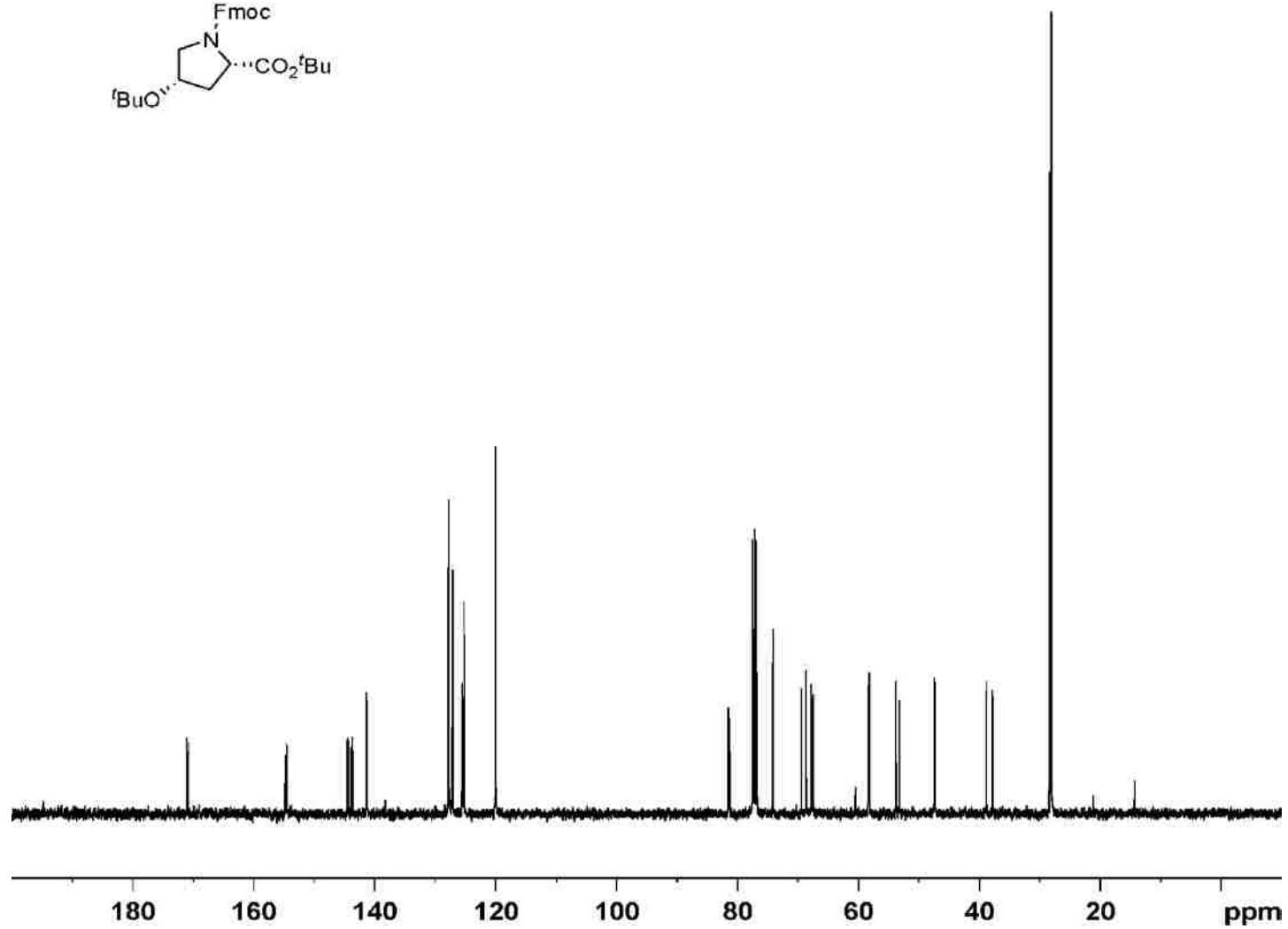
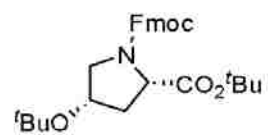
CVK-2-38a in CDCl<sub>3</sub> at 400 MHz





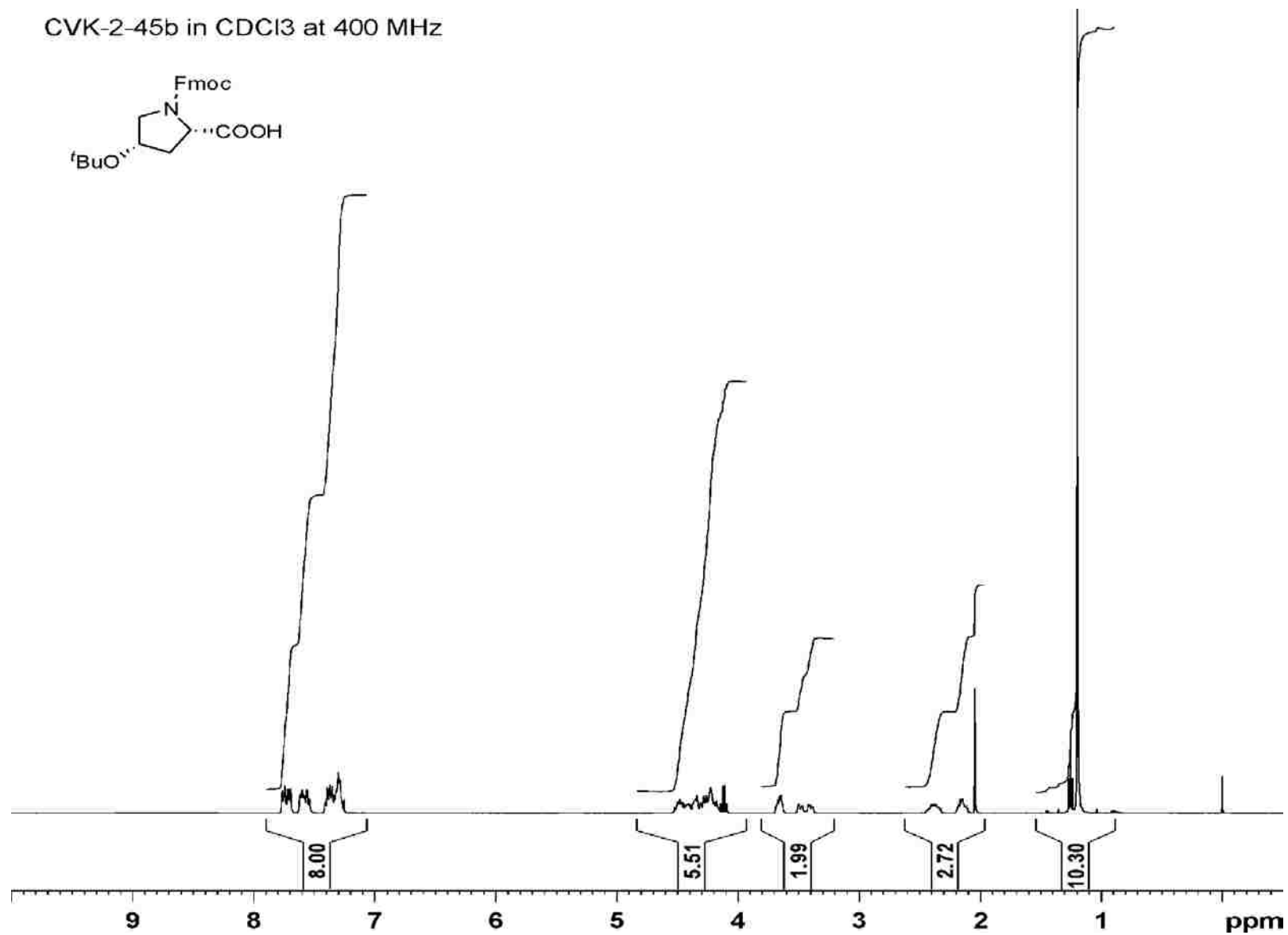
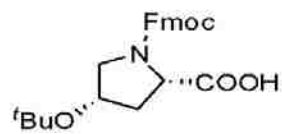
Fmoc-hyp(O<sup>t</sup>Bu)-O<sup>t</sup>Bu (108)

CVK-2-38a in CDCl<sub>3</sub> at 100MHz



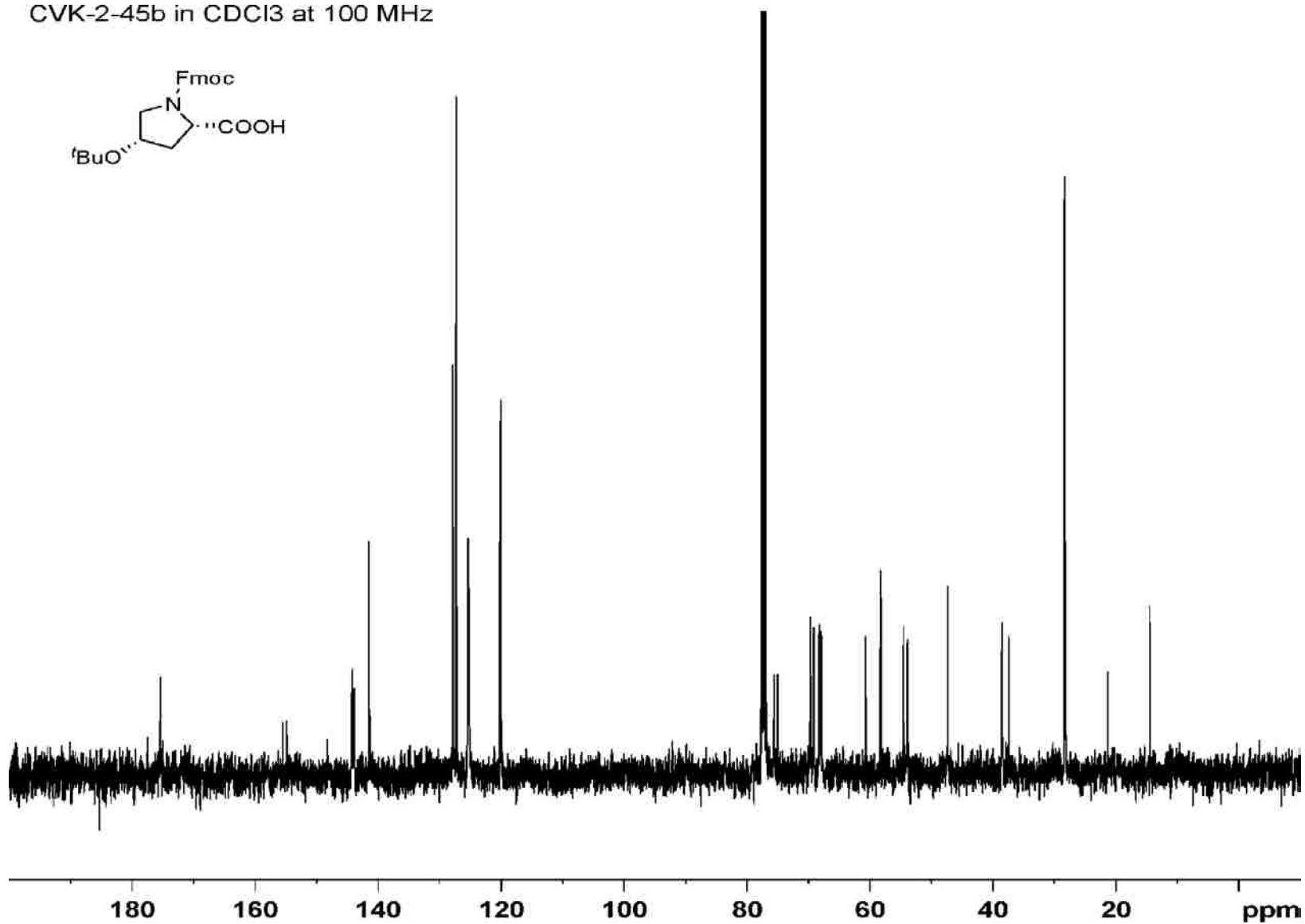
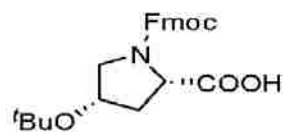
Fmoc-hyp(O<sup>t</sup>Bu)-OH (109)

CVK-2-45b in CDCl<sub>3</sub> at 400 MHz



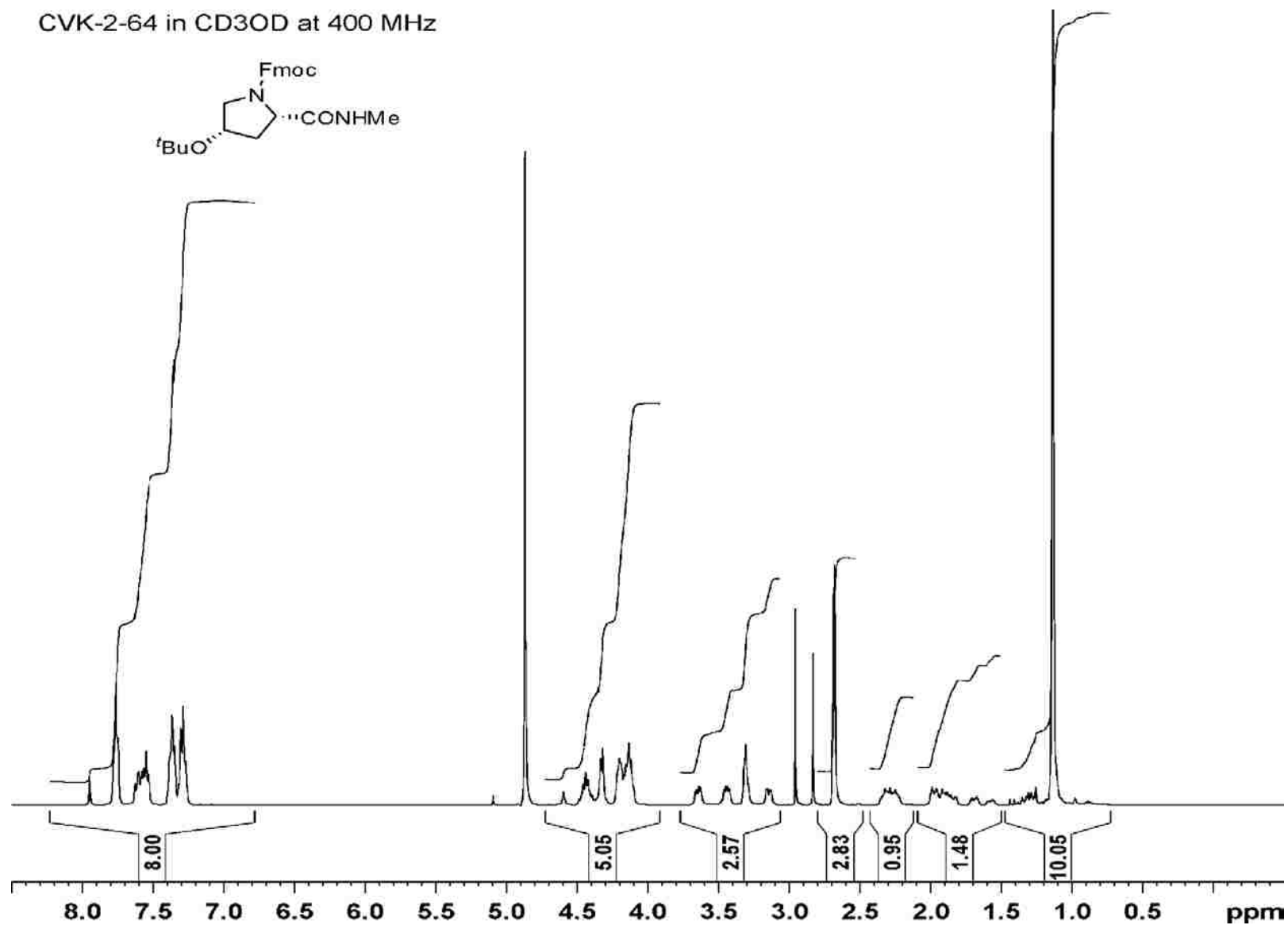
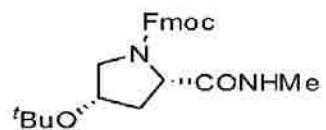
Fmoc-hyp(O<sup>t</sup>Bu)-OH (109)

CVK-2-45b in CDCl<sub>3</sub> at 100 MHz



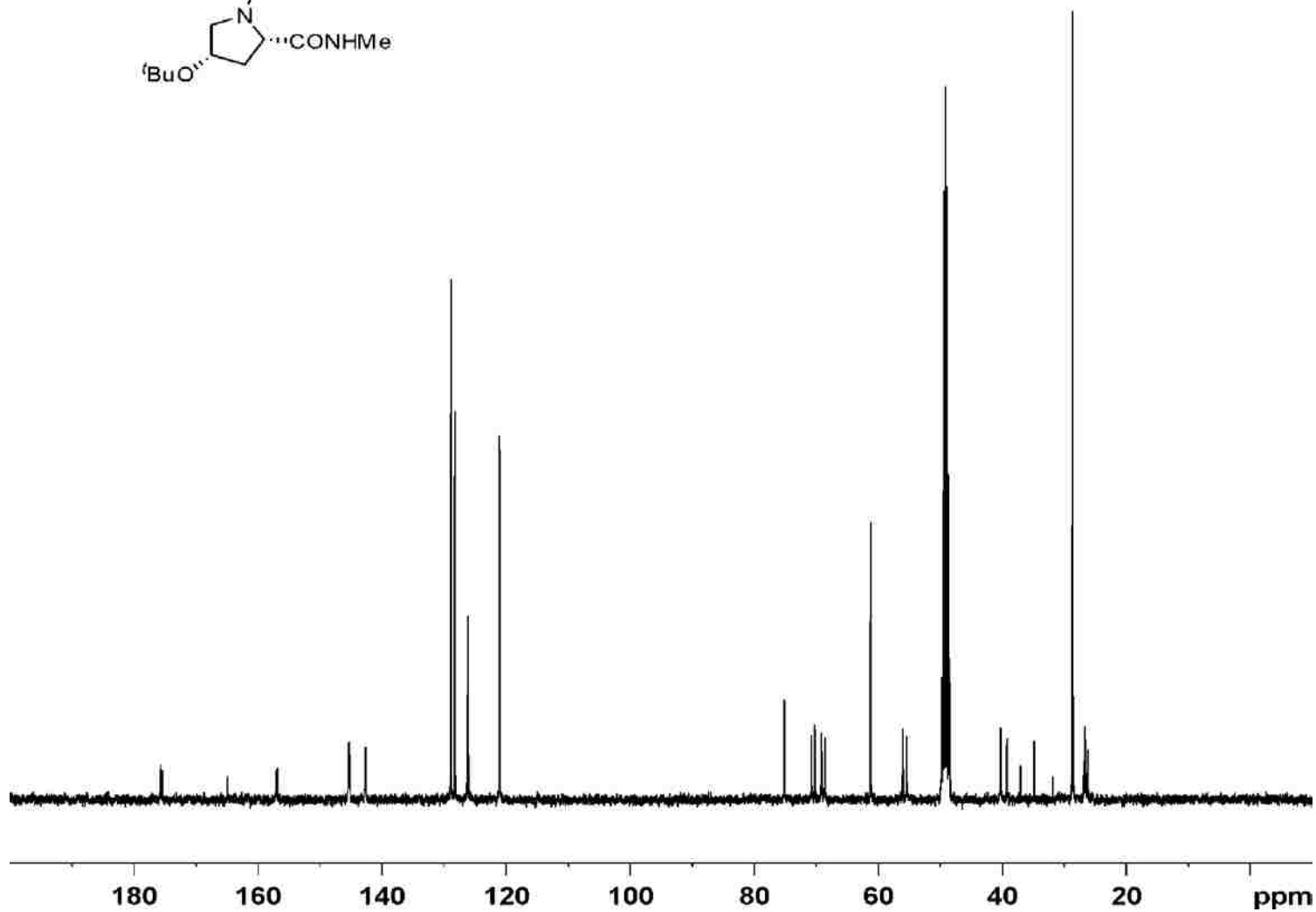
Fmoc-hyp(O<sup>t</sup>Bu)-NHMe (110)

CVK-2-64 in CD<sub>3</sub>OD at 400 MHz



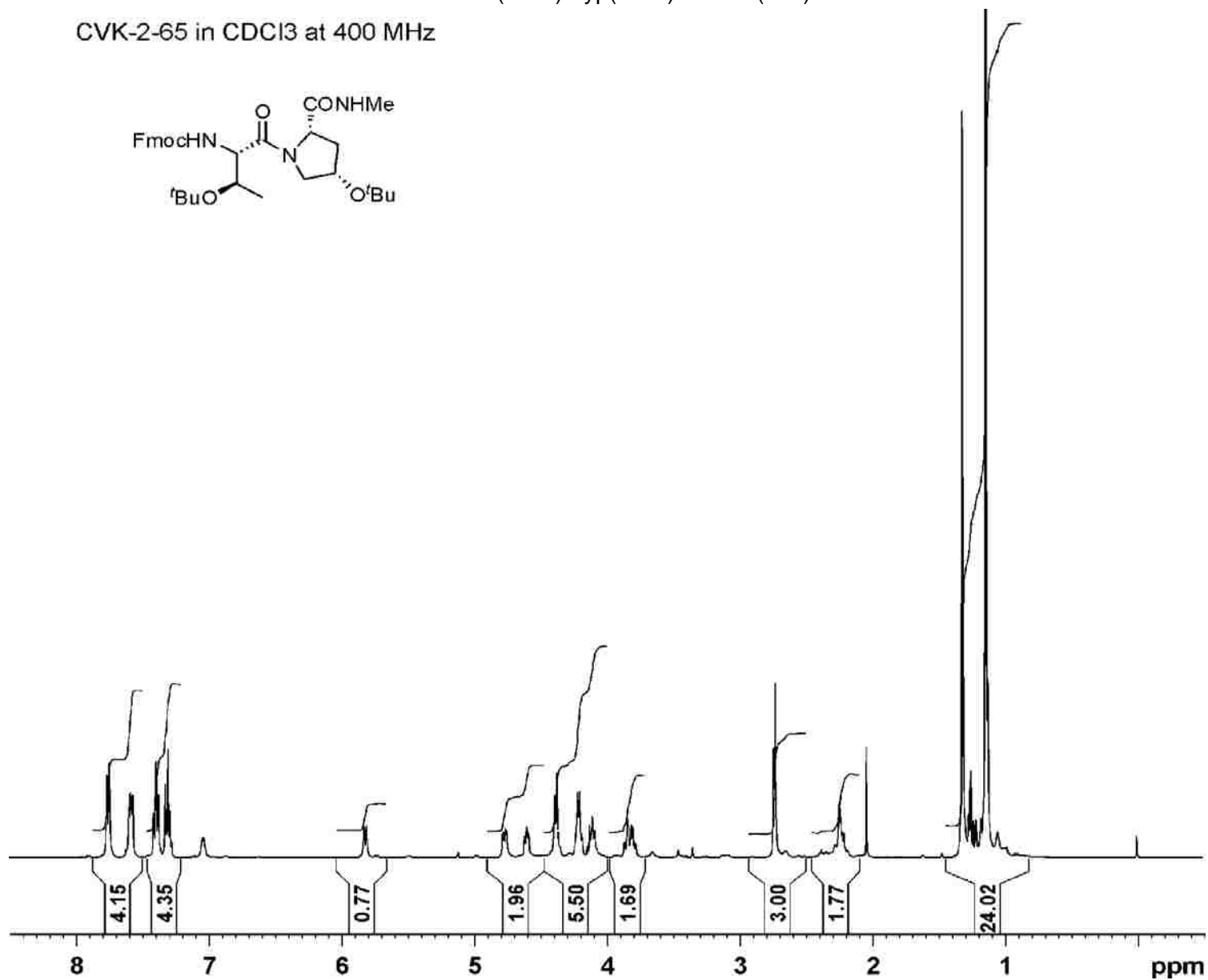
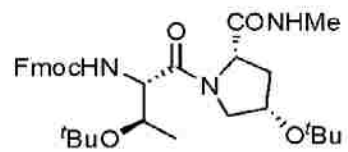
Fmoc-hyp(O<sup>t</sup>Bu)-NHMe (**110**)

CVK-2-64 in CD<sub>3</sub>OD at 100 MHz



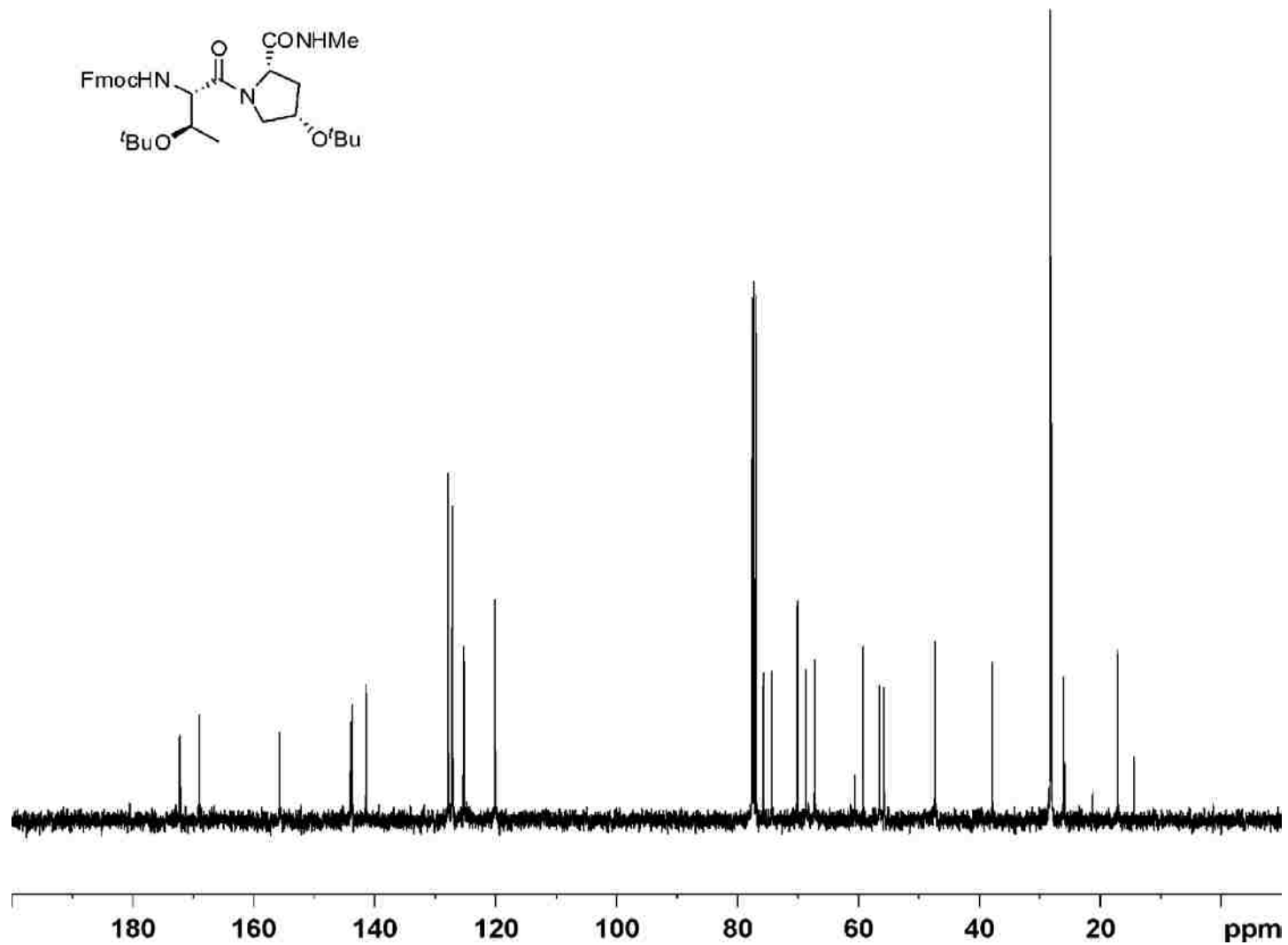
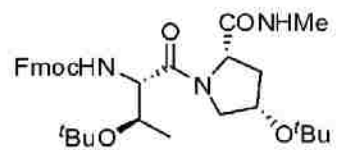
Fmoc-Thr(O<sup>t</sup>Bu)-hyp(O<sup>t</sup>Bu)-NHMe (111)

CVK-2-65 in CDCl<sub>3</sub> at 400 MHz



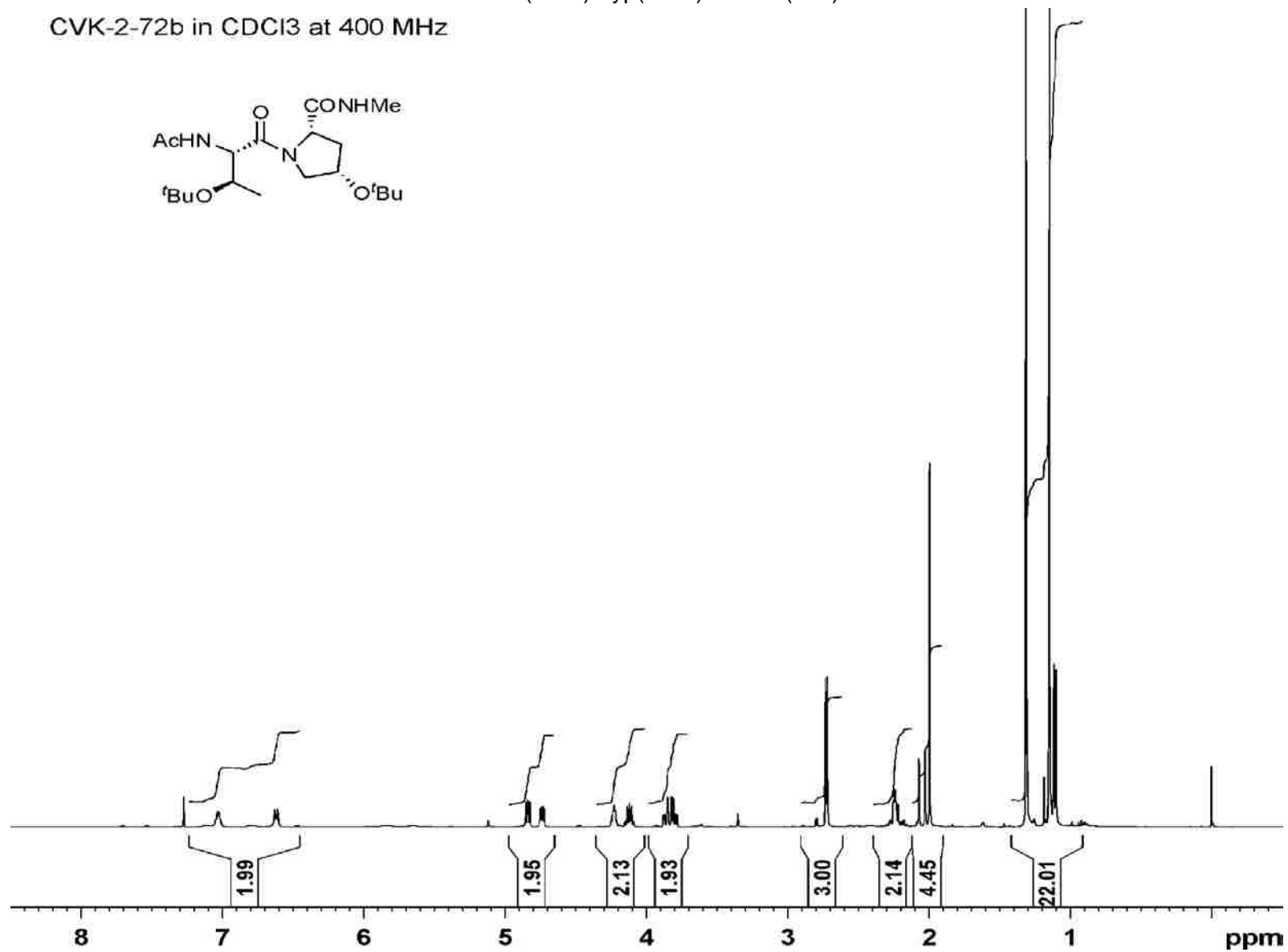
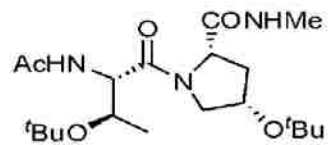
Fmoc-Thr(O<sup>t</sup>Bu)-hyp(O<sup>t</sup>Bu)-NHMe (111)

cvk-2-65 in CDCl<sub>3</sub> at 100 MHz



Ac-Thr(O<sup>t</sup>Bu)-hyp(O<sup>t</sup>Bu)-NHMe (112)

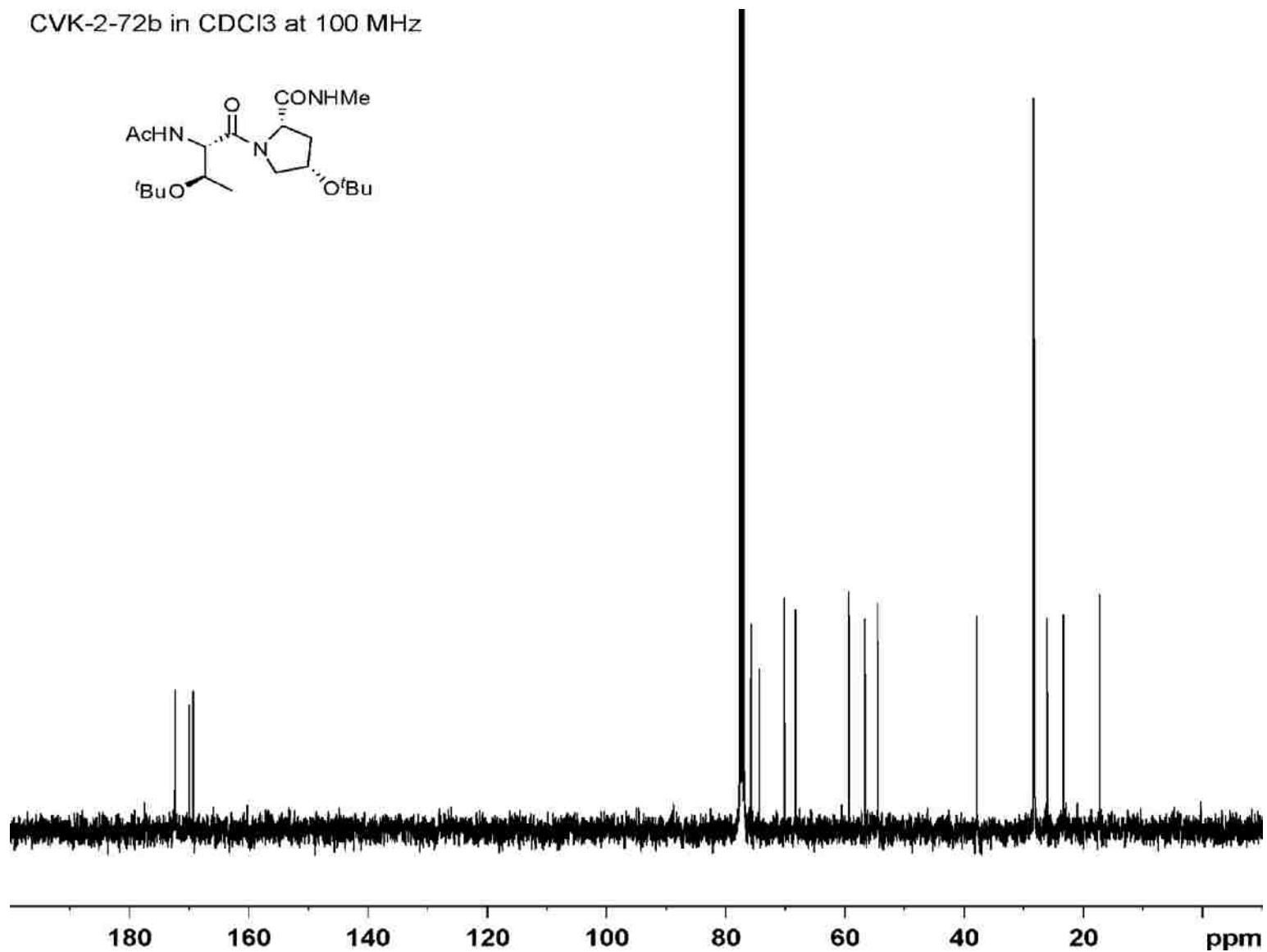
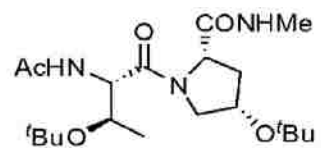
CVK-2-72b in CDCl<sub>3</sub> at 400 MHz





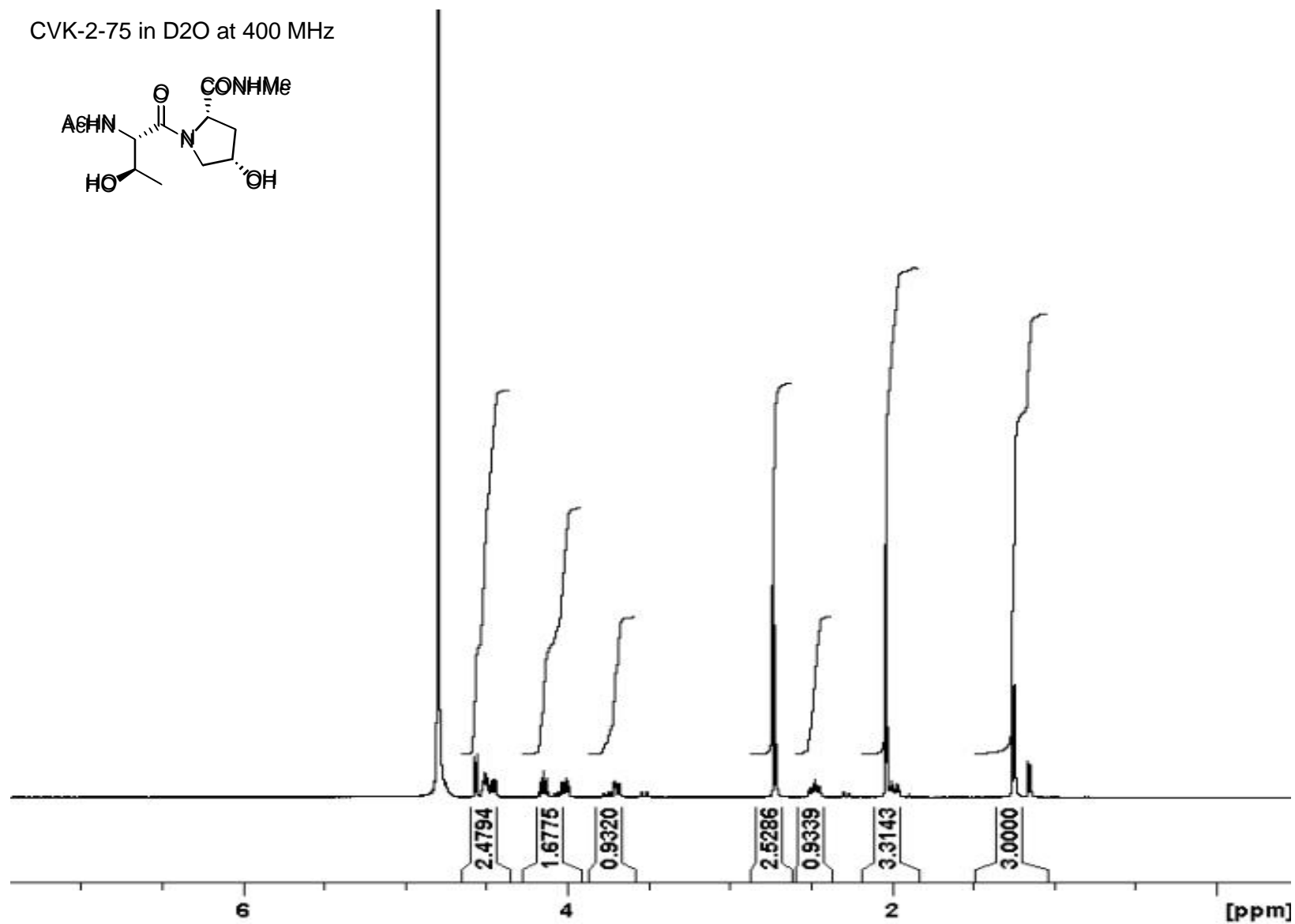
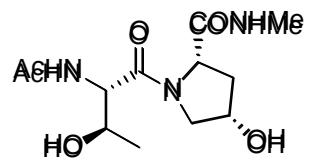
Ac-Thr(O<sup>t</sup>Bu)-hyp(O<sup>t</sup>Bu)-NHMe (112)

CVK-2-72b in CDCl<sub>3</sub> at 100 MHz



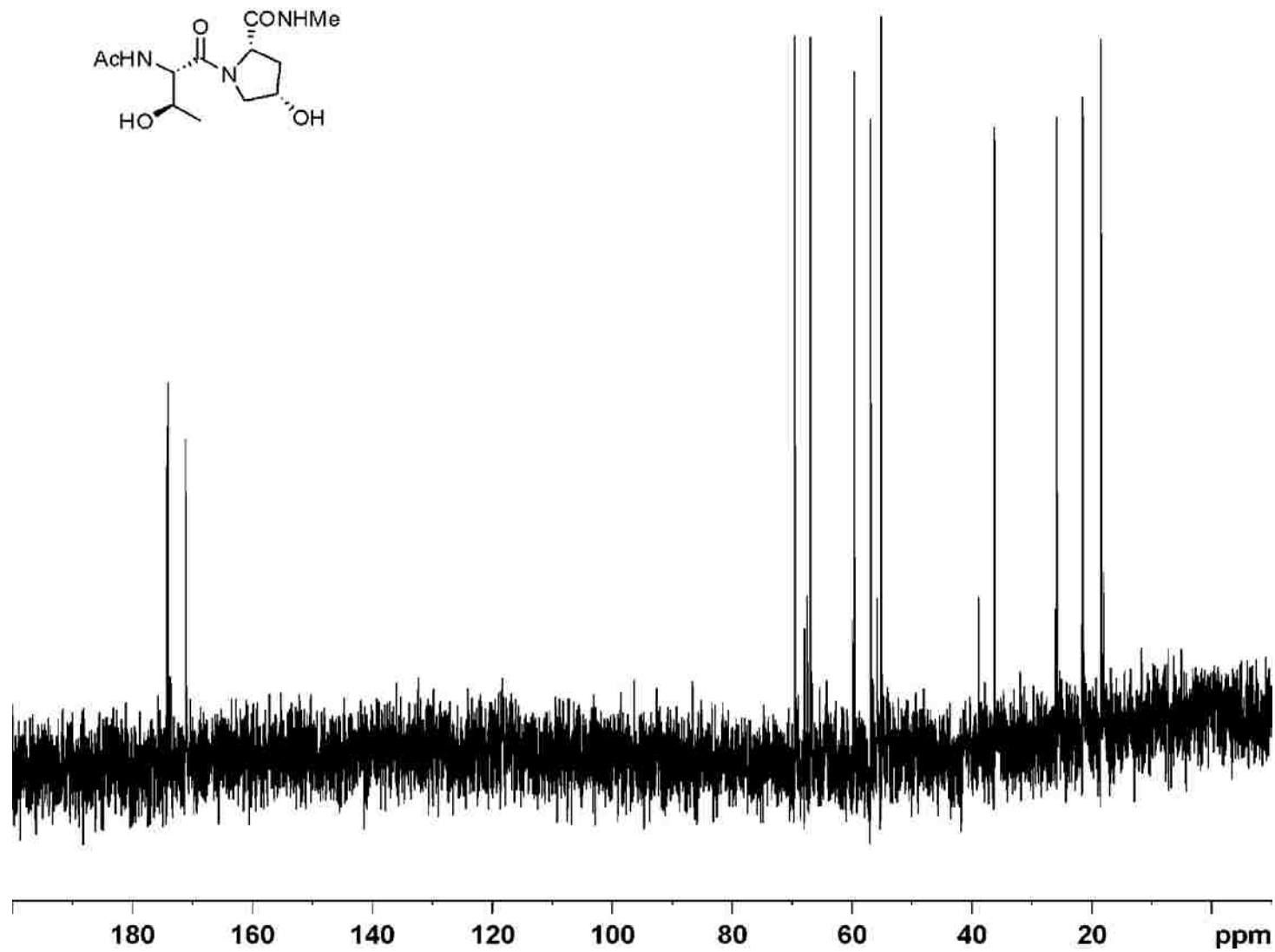
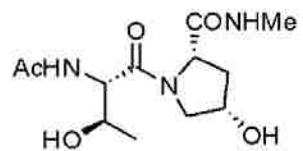
Ac-Thr-hyp-NHMe (106) - unreferenced

CVK-2-75 in D2O at 400 MHz



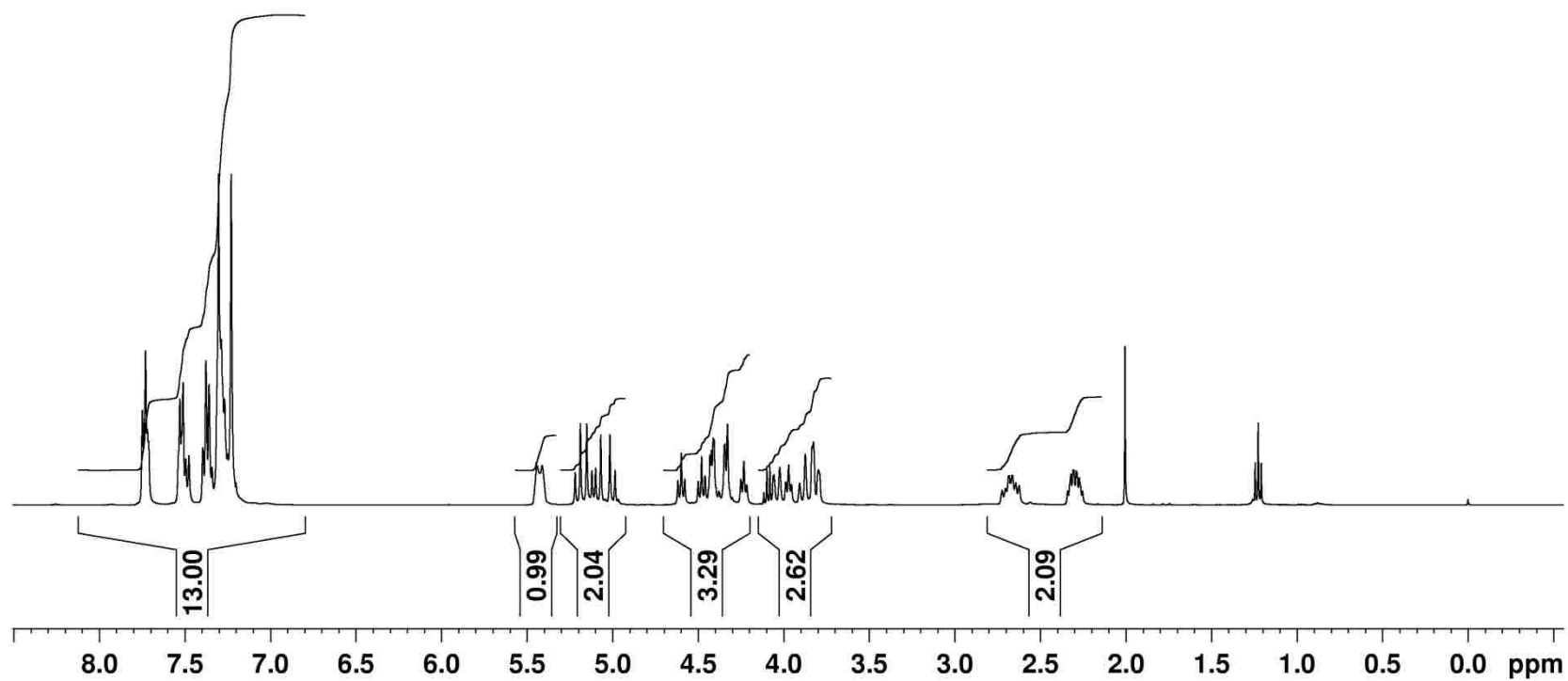
Ac-Thr-hyp-NHMe (**106**) - unreferenced

CVK-2-75 in D2O at 100 MHz



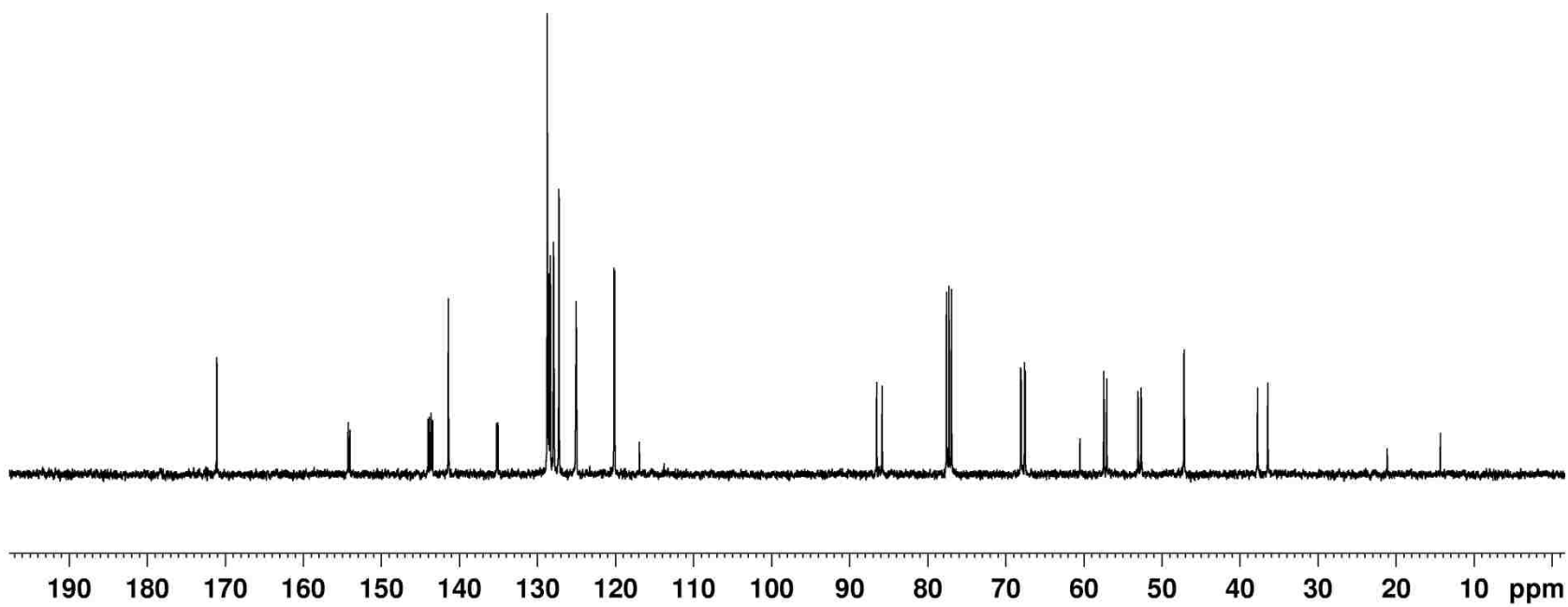
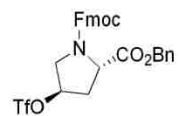
Fmoc-Hyp(OTf)-OBn (119)

cvk-2-121 in CDCl<sub>3</sub> at 400 MHz



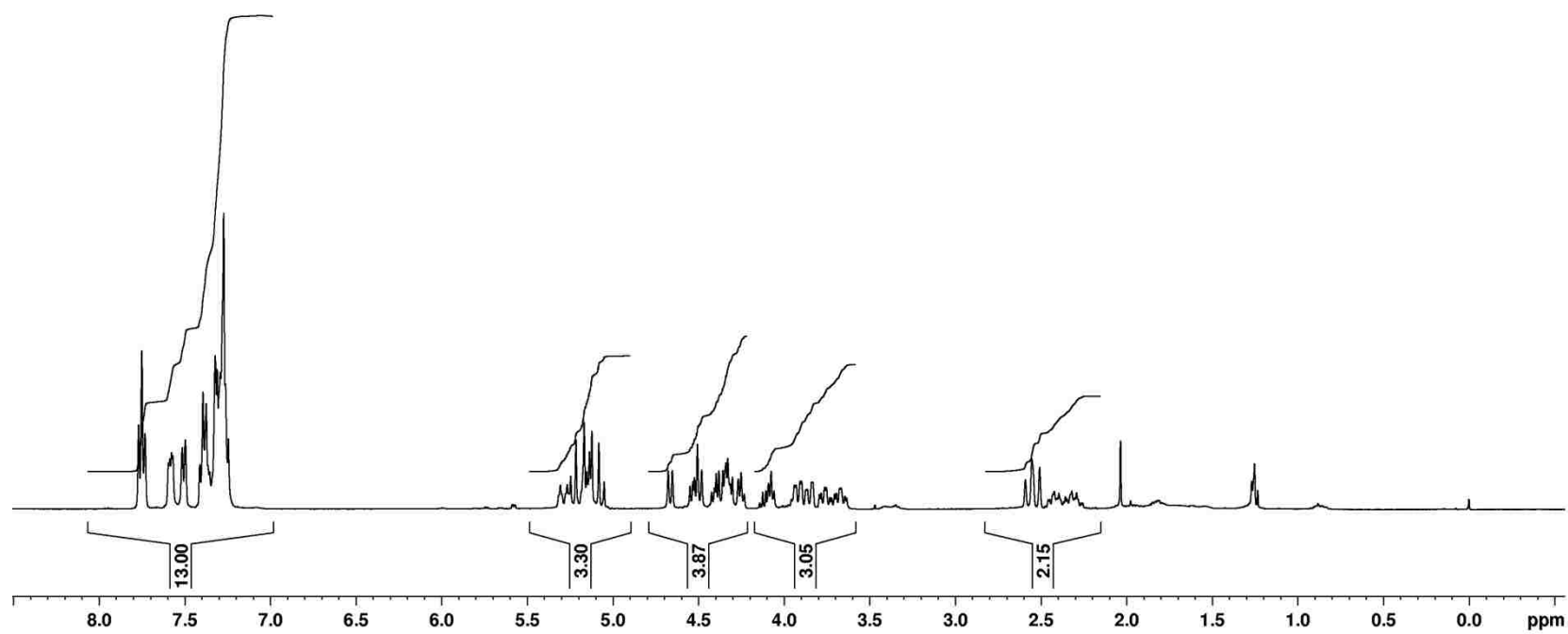
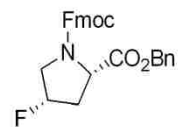
Fmoc-Hyp(OTf)-OBn (119)

cvk-2-122 in CDCl<sub>3</sub> at 100 MHz



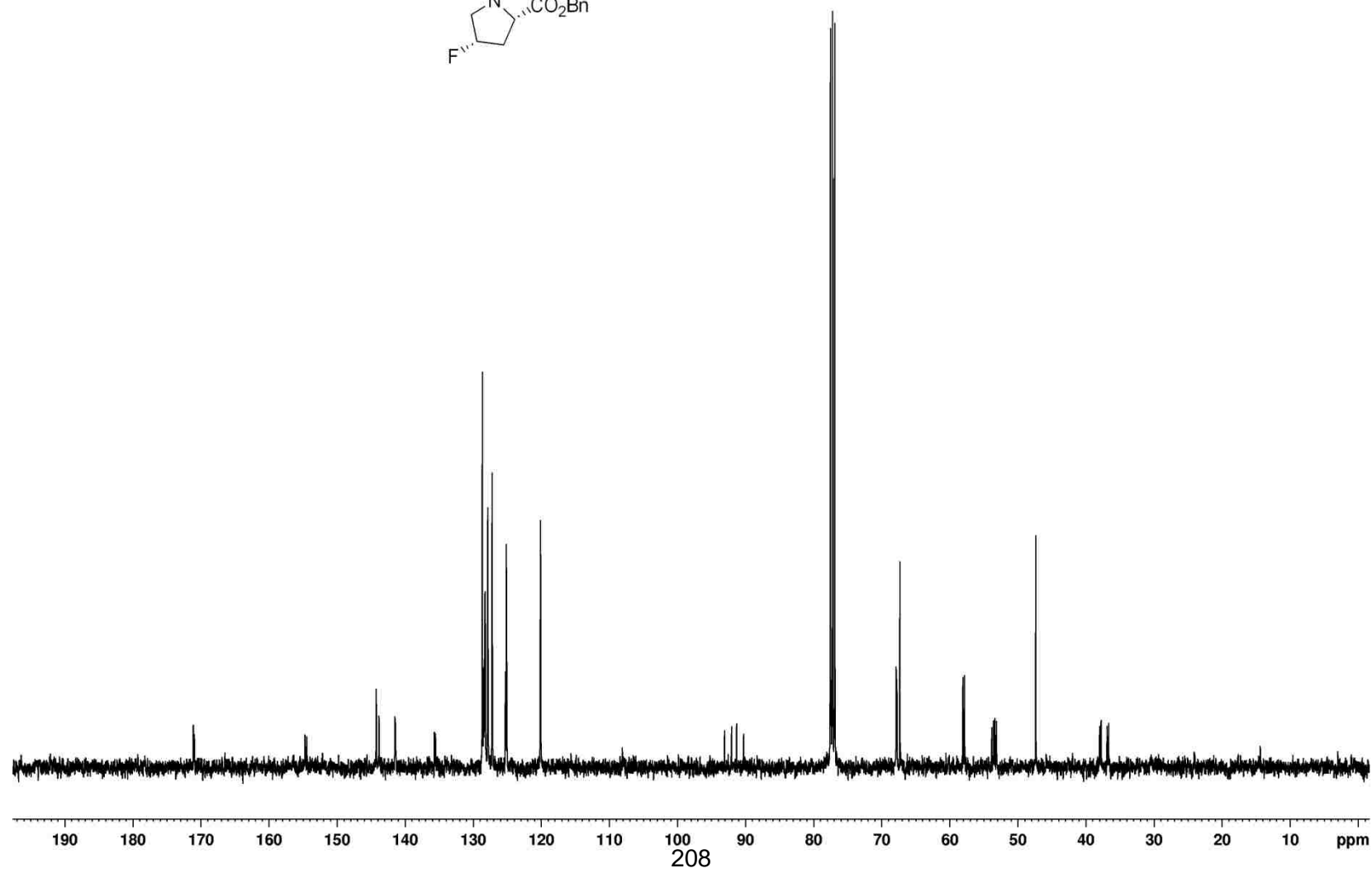
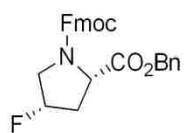
Fmoc-flp-OBn (118)

cvk-1-157 in CDCl<sub>3</sub> at 400 MHz



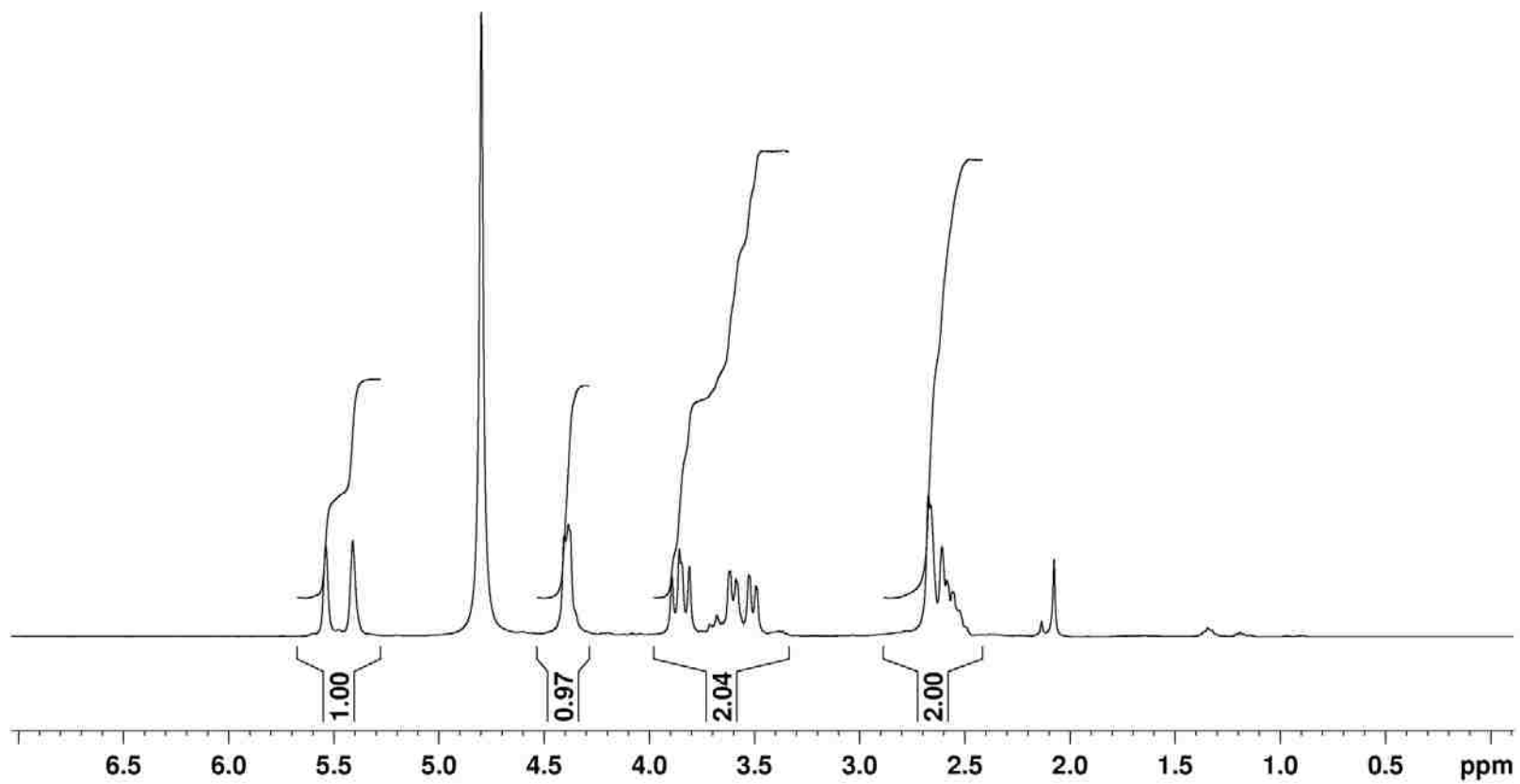
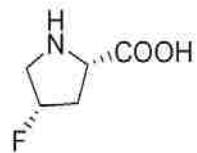
Fmoc-flp-OBn (118)

cvk-1-157 in CDCl<sub>3</sub> at 100 MHz



2S,4S-fluoroproline (121)

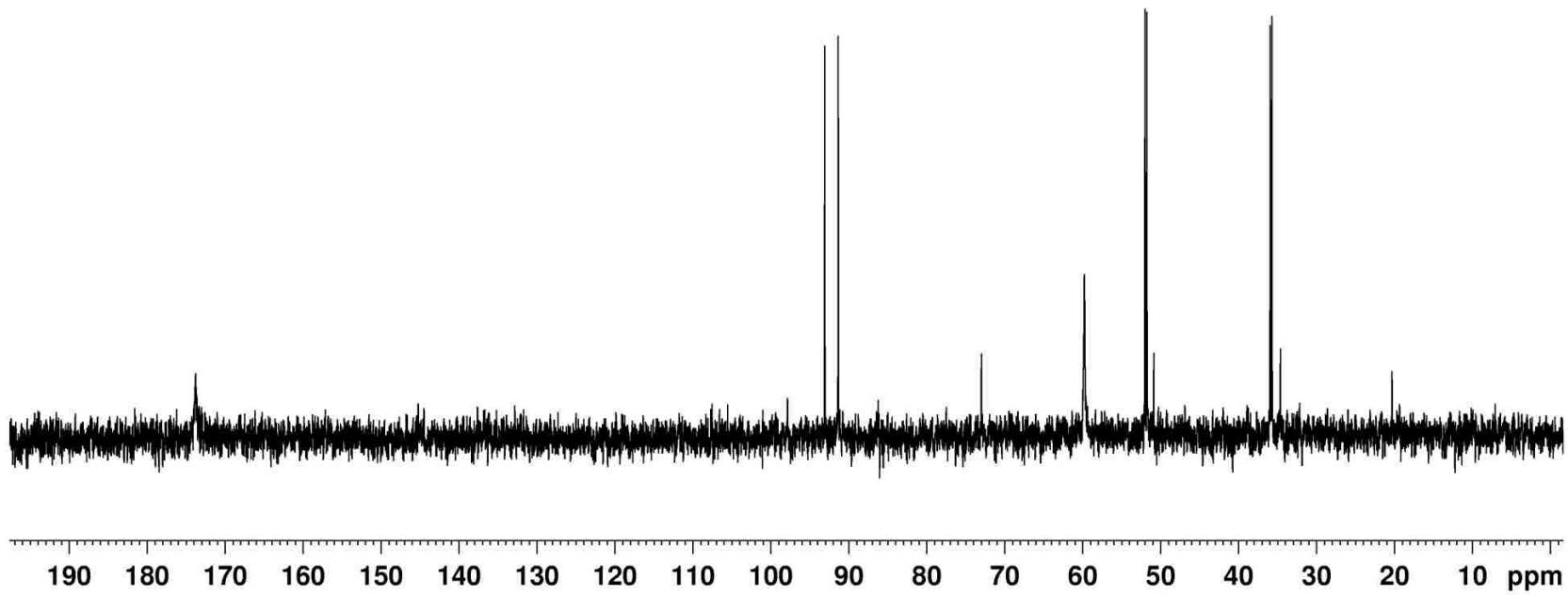
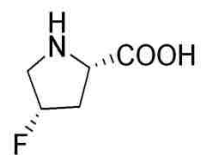
cvk-3-32 in H2O at 400 MHz





2S,4S-fluoroproline (121)

cvk-3-32 in H<sub>2</sub>O at 100 MHz



## CHAPTER 4 – SYNTHESIS OF AN $\alpha$ -HELICAL MIMETIC FOR THE 143-151 FRAGMENT OF SKP1

### 4.1 The $\alpha$ -Helix in Peptides and Proteins

Proteins organize at different levels, referred to as primary, secondary, tertiary and quaternary structure. The most common secondary structural element of proteins is the  $\alpha$ -helix, which constitutes more than 40% of the polypeptide structure in proteins.<sup>82</sup> The motif tends to be at least ten amino acid residues long (three turns).<sup>83</sup>  $\alpha$ -Helices play an important role in mediating protein-protein interactions in protein tertiary structure. Research has shown that helix geometry is determined by the primary amino acid sequence.<sup>84</sup> The helix is often associated with blocks of non-polar residues including Ala, Leu, Val, and Ile preferably at the  $i$ ,  $i+1$ ,  $i+4$ ,  $i+5$  positions with various other amino acids at other positions and Pro often at the  $N$ -terminus. These hydrophobic segments are typically less than 16 amino acids long.

According to the helix-coil transition theory,<sup>85</sup>  $\alpha$ -helices with short peptide chains (composed of less than ten amino acids) are unstable due to low nucleation probability. Stabilization of short peptides in an  $\alpha$ -helical conformation is challenging. Preorganization of amino acid residues in an  $\alpha$ -turn is expected to improve nucleation properties and initiate helix formation.<sup>86</sup>

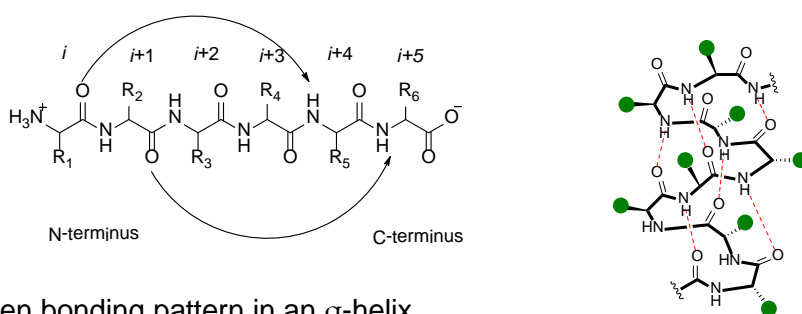


Figure 4.1: Hydrogen bonding pattern in an  $\alpha$ -helix

### 4.2 $\alpha$ -Helical Mimetics

Molecules that mimic the structure of  $\alpha$ -helices can be used for the inhibition of protein-protein interactions. In the design of mimetics, several features of the  $\alpha$ -helix are important

factors for consideration and incorporation.<sup>87</sup> In an  $\alpha$ -helix, a hydrogen bond between the C=O of the  $i$ th amino acid residue and the NH of the  $i+4$ th amino acid residue stabilizes the helical structure (Figure 4.1).<sup>88</sup> These hydrogen bonds are almost parallel to the axis of the  $\alpha$ -helix. The projecting side chains in the  $i$ ,  $i+4$ ,  $i+7/i+8$ , and  $i+11$  positions appear on the same side of the  $\alpha$ -helix and create an interface for intermolecular interactions with other proteins.<sup>89</sup>

The last decade has seen significant progress in the design and synthesis of peptidyl and nonpeptidyl helix mimetics. Different approaches have been investigated to stabilize short peptides in  $\alpha$ -helical conformations to enhance conformational rigidity, proteolytic stability, ability to penetrate the cell membrane and protein-like functionality in the resulting helical oligopeptide. These approaches can be divided into three categories: (1) helical surface mimetics, (2) helical foldamers and (3) stabilization of the native helix.<sup>86,90</sup> Some of these mimetics have been shown to bind their target protein with high affinity.<sup>91</sup>

#### 4.2.1 Helical Surface Mimetics

Helical surface mimetics are conformationally restricted molecules that present functional groups in a manner that topologically resembles the  $i$ ,  $i+4$ ,  $i+7$  pattern of side chain positioning along the face of an  $\alpha$ -helix.<sup>86</sup>

A report by Hamilton and coworkers in 2001 described the synthesis of the first entirely non-peptidyl  $\alpha$ -helix mimetic using a terphenyl scaffold (Figure 4.2) that can mimic the structural and recognition binding features of an  $\alpha$ -helix.<sup>92</sup> Their initial terphenyl scaffold has a *tris-ortho*-substituted terphenylene wherein the *o*-substituents mimic the side chains of  $i$ ,  $i + 4$ , and  $i + 7$  positions of an  $\alpha$ -helix.<sup>92</sup> To improve synthetic accessibility, solubility and flexibility, the initial design was extended to closely related structures including terpyridine, oligoamide, and terephthalamide derivatives.

Appropriately embellished scaffolds have been shown to effectively inhibit protein-protein interactions in pathways associated with human diseases. These protein-protein interactions can thus be important therapeutic targets.<sup>83</sup>

The B-cell lymphoma-2 (Bcl-2) family of proteins regulates apoptosis, which involves pro-survival and pro-death proteins. The BH3 domain of Bak is essential for the function of all pro-death proteins.<sup>93</sup> Hamilton and coworkers' terphenyl scaffold **123** (Figure 4.2) displayed good *in vitro* affinity with a  $K_i$  value of 0.114  $\mu\text{M}$  and derivatives of this scaffold have been shown to disrupt the binding of Bcl-xL to Bak in intact cells in human embryonic kidney 293 (HEK293) cells.<sup>94</sup>

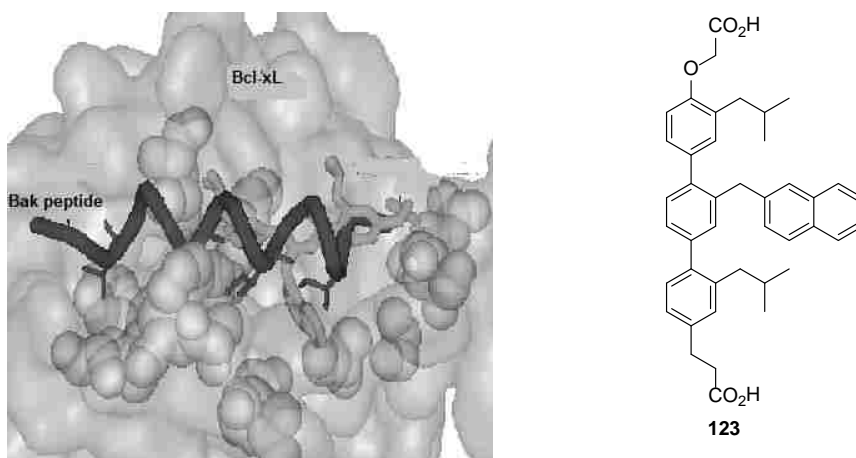


Figure 4.2 : X-ray crystal structure of the helical Bak BH3 domain of Bcl-xL protein.<sup>95</sup> Copyright 2006, John Wiley and Sons, reprinted with permission. Hamilton's  $\alpha$ -helix mimetic, terphenyl scaffold **123**

The crystal structure of calmodulin (CaM) (Figure 4.3) shows it bound to the smooth muscle myosin light chain kinase (smMLCK)  $\alpha$ -helical peptide through *i*, *i*+4, and *i*+7 residues of the helix. Hamilton and coworkers' terphenyl scaffold **124** (Figure 4.3) was shown to inhibit the CaM-smMLCK interaction with an  $\text{IC}_{50}$  of 800 nM.<sup>92</sup>

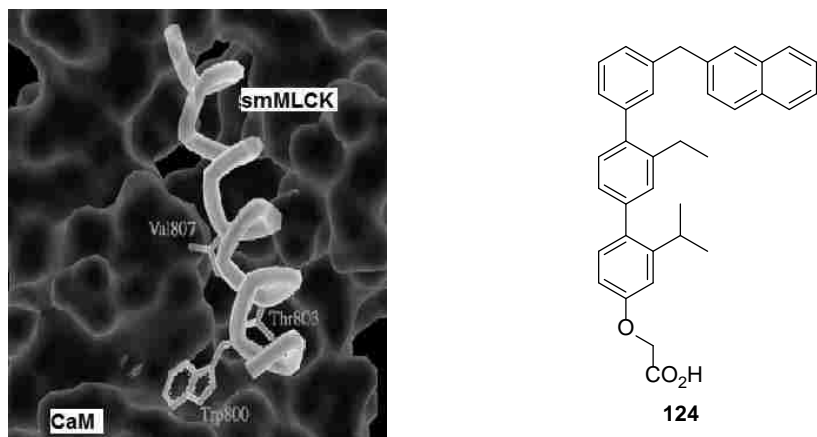


Figure 4.3: X-ray crystal structure of smMLCK binding region of the CaM. Copyright 2006, John Wiley and Sons, reprinted with permission and the  $\alpha$ -helical mimetic **124**

Deregulation of tachykinin receptors (TR) leads to epilepsy, Alzheimers disease and schizophrenia. The pioneering work of Horwell *et al.* used a 1,1,6-trisubstituted indane template (Figure 4.4) to mimic the  $i, i+1$  arrangement of an  $\alpha$ -helix of the mammalian tachykinin receptor. Their  $\alpha$ -helical mimetic, with undisclosed structure, had micromolar affinity for the tachykinin target and its neuroreceptor NK<sub>2</sub>.<sup>96</sup>

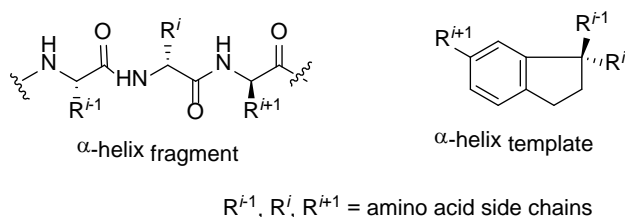


Figure 4.4: The indane template mimicking an  $\alpha$ -helix

#### 4.2.2 Helical Foldamers

$\beta$ -Peptide helices and peptoids come under the classification of helical foldamers which are capable of adopting conformations similar to natural proteins (Figure 4.5).

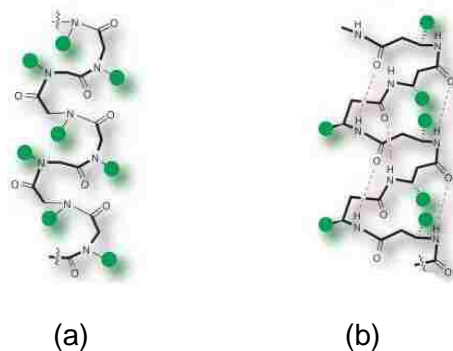


Figure 4.5:  $\alpha$ -Helices derived from foldamers:(a) peptoids,(b)  $\beta$ -peptides.<sup>88d</sup> Copyright 2008, ACS Publications, reprinted with permission

#### 4.2.3 Helix Stabilization Methods - Hydrogen Bond Surrogates

Stabilization of the native helix is based on pre-organizing amino acid residues to initiate helix formation by the introduction of side chain crosslinks and hydrogen bond surrogates (HBS) (Figure 4.6).

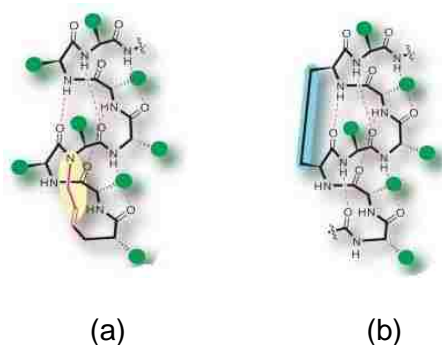


Figure 4.6:  $\alpha$ -Helices derived from helix stabilization: (a) HBS  $\alpha$ -helices, (b) Side chain crosslinked  $\alpha$ -helices.<sup>97</sup> Copyright 2008, ACS Publications, reprinted with permission

In 1999 Cabezas and Satterwait proposed stabilization of an  $\alpha$ -helix by replacing the weak  $i \rightarrow i+4$  hydrogen bond with a covalent linkage. They synthesized hydrazone-linked peptides by replacing a hydrogen bond with a N=C double bond (blue, Figure 4.7), and the C-N atoms of the backbone with the CH<sub>2</sub>-CH<sub>2</sub> group (red, Figure 4.7). Although this yielded a 13-membered ring, covalently bonded helical turn of the  $\alpha$ -helix neither hydrogen bond length nor angles are precisely mimicked by the double bond.<sup>98</sup> An attractive feature of this strategy is that

the cross-link made by the covalent linkage is inside the helix, thus not blocking the molecular recognition sites on the surface of the molecule.

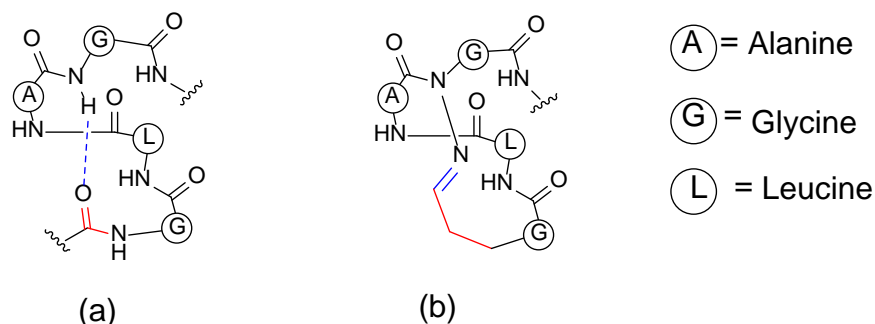
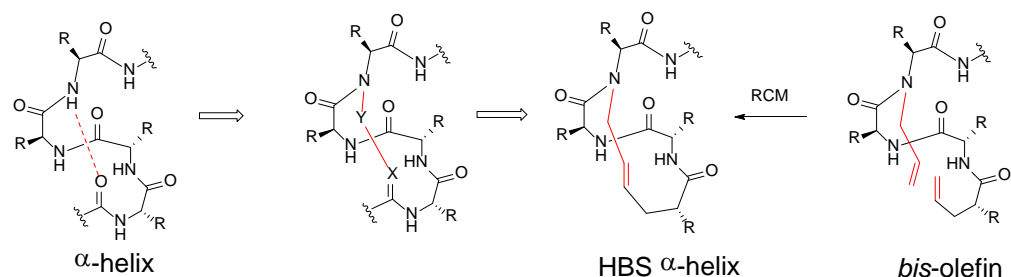


Figure 4.7: Hydrogen bond mimetics: (a) Native peptide highlighting the ( $i$ ,  $i+4$ ) H-bond (b) *N*-terminal hydrazone mimetic

In 2005, Arora and coworkers used the same general concept to lock short peptides in  $\alpha$ -helical conformations by invoking a different hydrogen bond surrogate (HBS). Their strategy involved replacement of the first hydrogen bond between amino acid residues  $i$  and  $i+4$  of an  $\alpha$ -helix with a covalent carbon-carbon bond, introduced during a ring-closing metathesis reaction (Scheme 4.1).<sup>88d</sup> They investigated the helicity of the constrained and control peptides by circular dichroism (CD) spectroscopy (Figure 4.8). The CD spectra of the HBS  $\alpha$ -helical mimetic displays double minima which is characteristic of  $\alpha$ -helices. The HBS  $\alpha$ -helical mimetic has been shown to bind with the Bak BH3 domain of Bcl-xL with high affinity. Synthesis of HBS systems by the groups of Cabezas and Arora have been limited to short peptides that terminate with the end of the  $\alpha$ -helix. Compared to Cabezas' hydrazone strategy, the Arora method affords a more stable bond that cannot be cleaved hydrolytically.<sup>88d</sup>



Scheme 4.1: HBS Strategy<sup>99</sup>

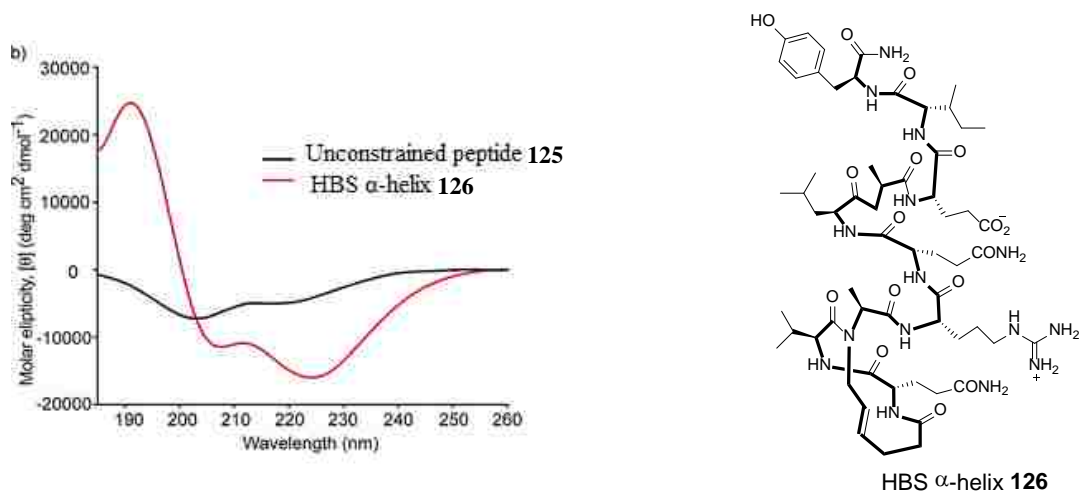


Figure 4.8: CD spectra of unconstrained peptide, Ac-QVARQLAEIY-NH<sub>2</sub> (**125**), and HBS  $\alpha$ -helix mimetic **126** used to demonstrate proof of principle for the hydrogen bond surrogate strategy by Arora.<sup>99</sup> Copyright 2008, ACS Publications, reprinted with permission.

In 2009 Vernall *et al.* introduced the first hydrogen bond replacement at an internal helical turn, where an ethylene linkage substitutes for an internal ( $i \rightarrow i+4$ ) hydrogen bond (Figure 4.9).<sup>100</sup> This ethylene bridge resulted a distance of 3.8 Å between the backbone C( $i$ ) and N( $i+4$ ) atoms, which is slightly less than the corresponding H-bond length (4.0 Å). The resulting modified peptide demonstrated increased helicity and thermal and proteolytic stability, but a decrease in biological activity, compared to the unmodified Galanin(1-16) peptide.<sup>100</sup> Galanin is an endocrine neuropeptide consisting of 29 amino acids in most mammals, but in humans there is an extra serine residue at the C-terminus (**127**). Galanin was selected for study because it plays roles in cancer, obesity, arthritis and diabetes<sup>101</sup> and the synthesis of a galanin mimetic via a side chain lactam approach had already been reported in literature.<sup>102</sup> Furthermore, the



galanin 1-16 *N*-terminal oligopeptide (Figure 4.9) has demonstrated partial helical structure responsible for its biological activity.<sup>103</sup>

(a) H-GWTLNSAGYLLGPHAVGNHRSFSDKNGLT(S)-OH (127)

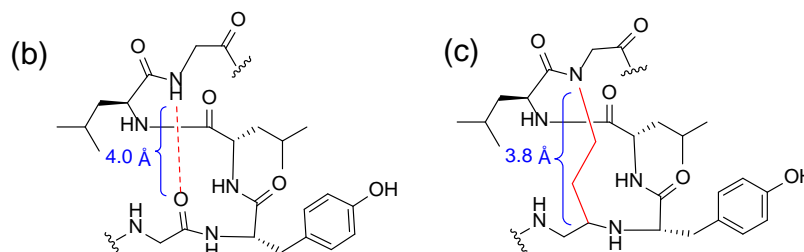


Figure 4.9: (a) Galanin sequence in humans; (b) Peptide partial sequence GYLLG showing *i*→*i*+4 H-bond; (c) H-bond mimetic with an internal ethylene bridge

### 4.3 The $\alpha$ -Helix of Skp1

Enzyme kinetics parameters for the glycosyltransferase Gnt1, determined by West and coworkers are shown in Table 4.1.<sup>18</sup> This study was performed to gain insight into the mechanism of the reaction catalyzed by Gnt1. Peptide substrates investigated were Skp1A-Myc, the full length protein from strain HW120 that is hydroxylated, but not glycosylated at Pro<sup>143</sup>, and the synthetic 23-mer peptide which has the sequence corresponding to residues 135-155 of Skp1 with 4-Hyp at the center of the peptide.

The  $K_m$  of an enzyme substrate indicates the affinity of the enzyme for that substrate. Gnt1 exhibits unusually low  $K_m$  values, in the submicromolar range, for both its natural donor (UDP-GlcNAc) and acceptor (Skp1A-Myc) substrates, a reflection of its location in the cytoplasm. The studies showed that the  $K_m$  value for the 23-mer was four orders of magnitude higher compared to that of Skp1A-Myc. While a low  $V_{max}$  value was observed for the 23-mer, the value was within an order of magnitude relative to the full length protein.<sup>18</sup>

Table 4.1: Enzyme kinetics parameters for the glycosyltransferase Gnt1

Substrate	$K_m$ ( $\mu\text{M}$ )	$V_{max}$ (nmol/h/mg)
UDP-GlcNAc	0.16	8.0
Skp1A-Myc	0.56	12.6
23-mer Peptide	1600	4.2

The relatively high  $K_m$  value for the synthetic 23-mer peptide (Table 4.1) indicates a poor binding affinity for the Gnt1 enzyme. Nevertheless, a reasonable  $V_{max}$  value indicates that the oligopeptide has the necessary features to be processed as a substrate.<sup>18, 104</sup> Our hypothesis was that the low binding affinity is due to a lack of secondary structure in the 23-mer. The lack of Gnt1 inhibition by bisubstrate analog **17** (Chapter 2) was another sign that we needed to improve recognition. Affinity for the various enzymes in the Skp1 hydroxylation/glycosylation pathway might be improved for small peptide substrates and inhibitors by constraining residues 143-151 in a helical arrangement, as occurs in the full length protein.

#### 4.4 A HBS $\alpha$ -Helical Mimetic for the 143-151 Peptide of Skp1

In Skp1, Pro<sup>143</sup> is located at the *N*-terminus of the  $\alpha$ -helix with four consecutive Glu residues immediately following Pro (Figure 4.10a). Preceding Pro<sup>143</sup> is a segment of random coil. We believe that this Glu-rich helix is likely to be important for binding to the Gnt1 enzyme active site. Additionally, we wanted to include four amino acids in the *C*-terminal direction and six amino acids in the *N*-terminal direction since it is also likely that conformation of the prolyl peptide bond is important for recognition. The amino acid sequence that we attempt to mimic in the  $\alpha$ -helix is IKNDFTPEEEEQIRK (Figure 4.10b). We initially followed the HBS concept advanced by Arora to emulate the Glu-rich  $\alpha$ -helix designed in peptide **129**.

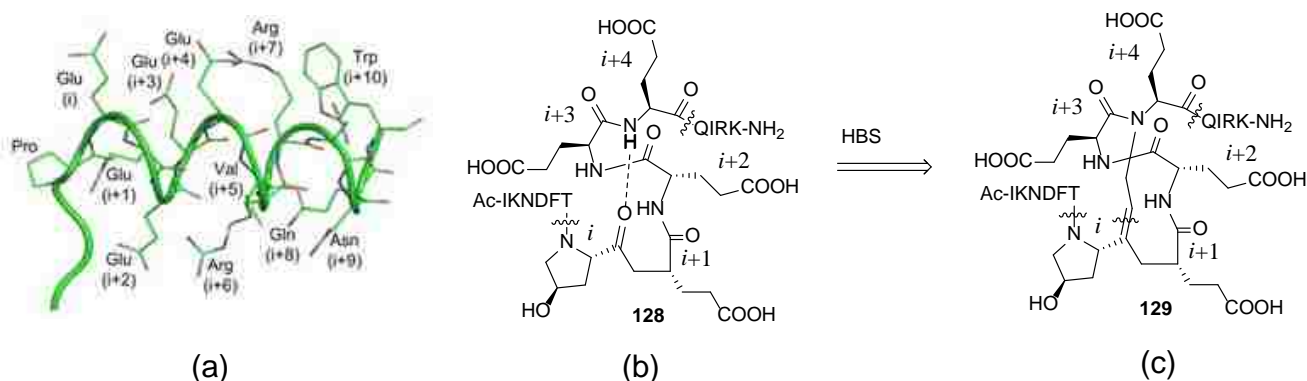
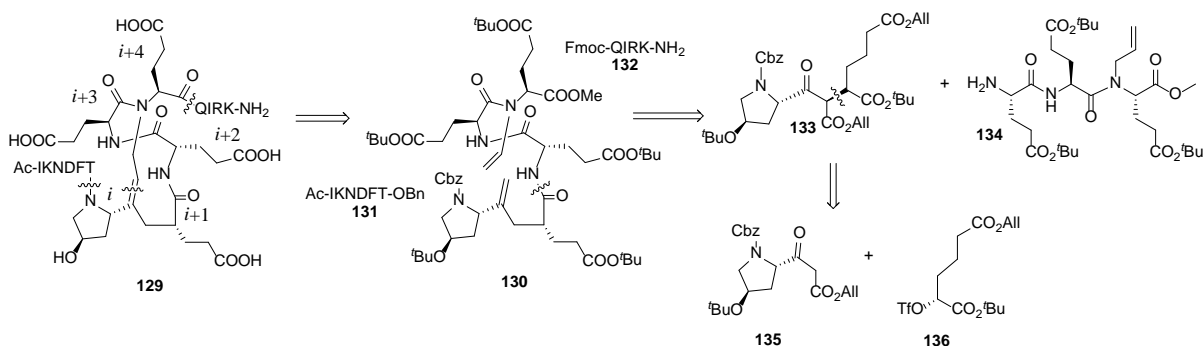


Figure 4.10: (a) Crystal structure of the Skp1 alpha helix of *Arabidopsis thaliana*, (b) Glu-rich  $\alpha$ -helix stabilized by hydrogen bonds (**128**); (c)  $\alpha$ -helical mimetic with covalent bonds (**129**)

#### 4.5 Retrosynthetic Analysis of an Arora-Type $\alpha$ -Helical Mimetic for Skp1

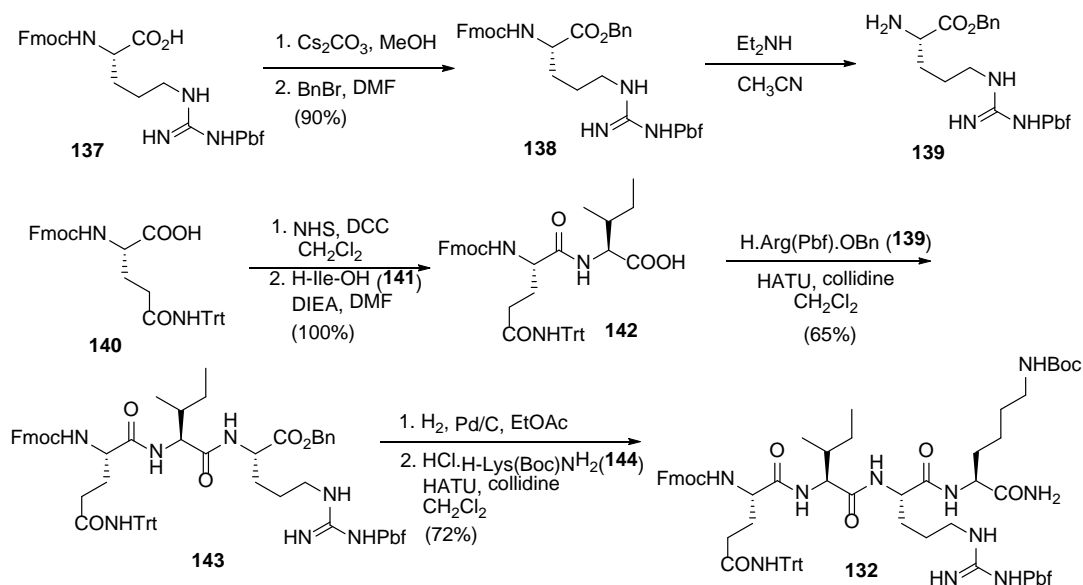
Our retrosynthetic analysis for the  $\alpha$ -helix mimetic **129** is depicted in Scheme 4.2. As illustrated, a disconnection has to be made to afford the diene **130**, a precursor to ring closing metathesis (RCM) and the oligopeptide fragments **131** and **132**. Compound **130** is a linear pseudo-pentapeptide that can be modified to make the initial turn of the helix by applying the HBS approach and invoking the RCM reaction. Fragment **130** can be further disconnected to yield a Pro-Glu dipeptide isostere **133** and a Glu-Glu-Glu tripeptide **134**. The *N*-terminal dipeptide isostere **133** can be further disconnected to reveal the  $\beta$ -ketoester **135** and the triflate ester **136**.



Scheme 4.2: Retrosynthetic analysis of HBS system

#### 4.6 Synthesis of the C-Terminal Fmoc-QIRK-NH<sub>2</sub> Tetrapeptide 132

The arginine building block **139** was synthesized by protecting the C-terminus of a commercially available arginine building block **137** as the benzyl ester **138**, followed by removal of the Fmoc protecting group (Scheme 4.3). Starting with commercially available Fmoc-Asn(Trt)OH (**140**) we prepared the dipeptide acid **142** using the NHS/DCC coupling method. Dipeptide acid **142** and amine **139** were coupled to generate tripeptide **143**. The QIR tripeptide **143** was subjected to hydrogenolysis and the free acid was then coupled with lysine building block **144** to give the QIRK oligopeptide **132** in 72% yield (Scheme 4.3). Both [2+1] and [3+1] peptide couplings to produce QIR and QIRK respectively were achieved utilizing HATU and 2,4,6-collidine. We chose HATU, because it is a highly effective peptide coupling reagent which, used in combination with 2,4,6-collidine, minimizes the potential racemization at C $\alpha$  of the C-terminal residue in each carboxyl component.<sup>105</sup> After reversed phase HPLC purification the identity of Fmoc-QIRK-NH<sub>2</sub> (**132**) was confirmed by mass spectrometry. Further characterization of the tetrapeptide **132** was performed using <sup>1</sup>H NMR, <sup>13</sup>C NMR and 2D-NMR spectroscopic data.



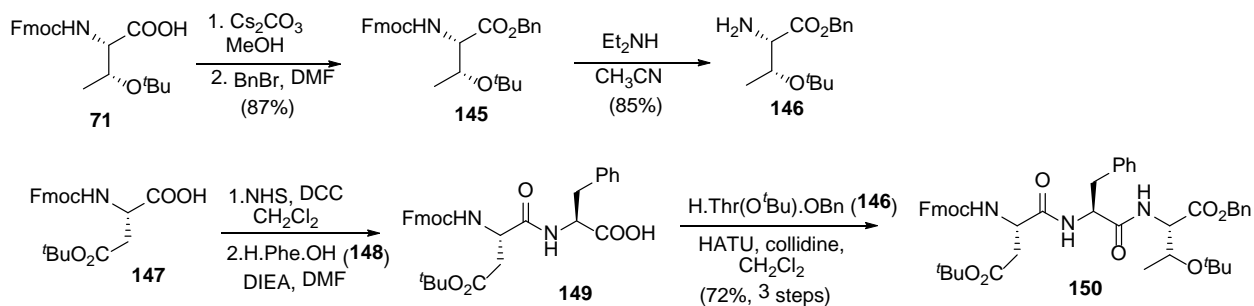
Scheme 4.3: Synthesis of QIRK peptide **132**

## 4.7 Synthesis of Fmoc-IKNDFT-OBn hexapeptide 171

For the synthesis of the Fmoc-Ile-Lys(Boc)-Asn(Trt)-Asp(O<sup>t</sup>Bu)-Phe-Thr(<sup>t</sup>Bu)-OBn oligopeptide our plan was to perform a [3+3] fragment coupling. The synthesis of the two tripeptide fragments will be discussed first.

### 4.7.1 Synthesis of Fmoc-Asp(O<sup>t</sup>Bu)-Phe-Thr(<sup>t</sup>Bu)-OBn (150)

We prepared H-Thr(<sup>t</sup>Bu)-OBn (**146**) by protecting the C-terminus of commercially available Fmoc-Thr(<sup>t</sup>Bu)-OH **71** as the benzyl ester **145**, followed by removal of the Fmoc protecting group (Scheme 4.4). For the synthesis of tripeptide **150** we coupled the commercially available aspartic acid **147** with phenylalanine **148** using an NHS/DCC coupling. The dipeptide acid **149** was then coupled to threonine **146** to give tripeptide **150** in good yield.

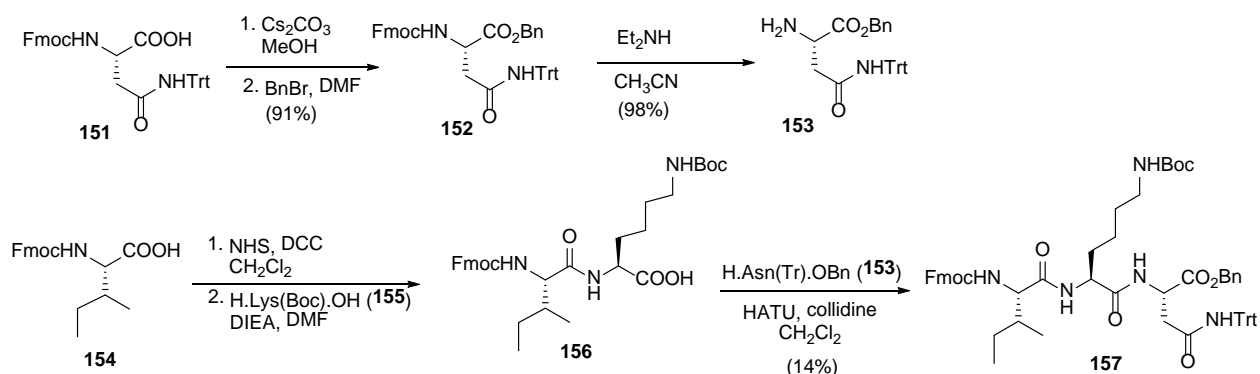


Scheme 4.4: Synthesis of peptide **150**

### 4.7.2 Synthesis of Fmoc-Ile-Lys(Boc)-Asn(Trt)-OBn (157)

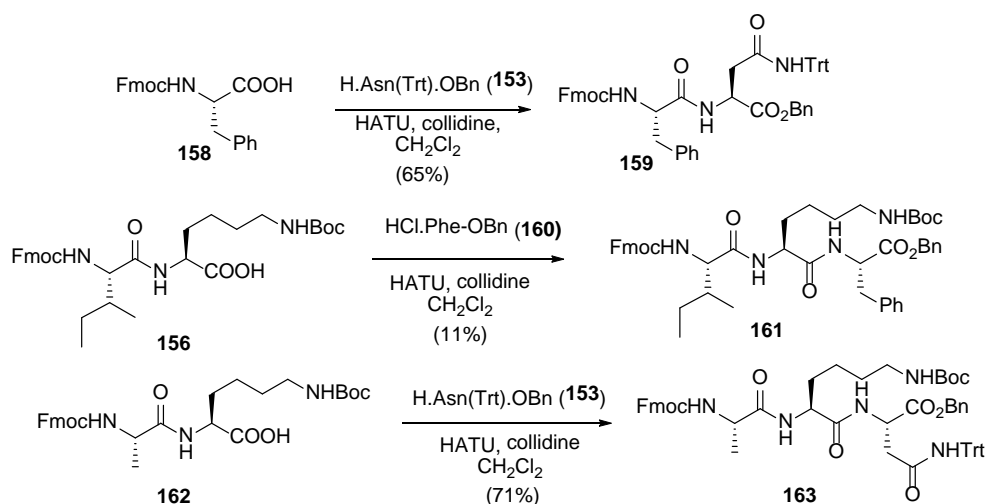
The H-Asn(Trt)-OBn (**153**) was synthesized by protecting the C-terminus of a commercially available arginine building block **151** as the benzyl ester **152**, followed by removal of the Fmoc protecting group (Scheme 4.5). To prepare the tripeptide **157**, we made the dipeptide acid **156** using NHS/DCC coupling of the commercially available Fmoc-Ile-OH (**154**) with H-Lys(Boc)-OH (**155**). The IK dipeptide acid **156** was then coupled to the asparagine

building block **153** as described above for the assembly of other tripeptides to afford tripeptide **157**, in only 14% yield.



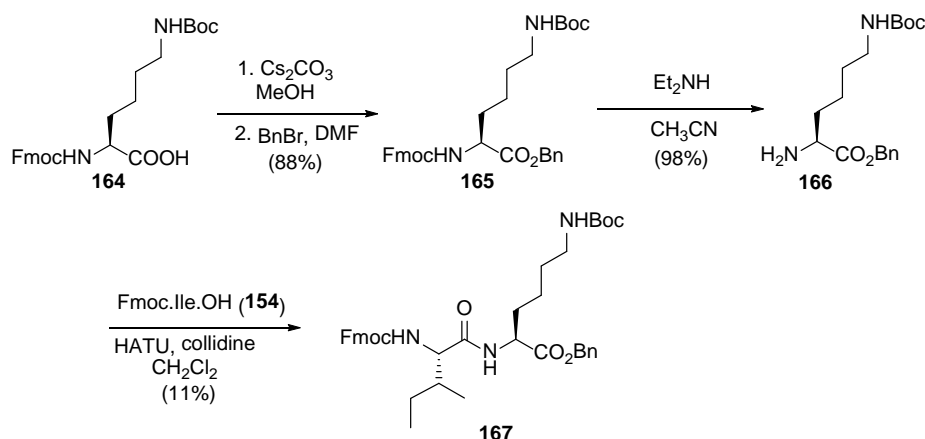
Scheme 4.5: Synthesis of peptide **157**

The poor yield could be due to steric hindrance provided by the trityl protecting group of the asparagine side chain. To probe this we tried to couple each “half of the problem” with phenylalanine residues. Specifically, Fmoc-Phe-OH (**158**) was coupled with H-Asn(Trt)-OBn (**153**) in reasonable yield. Dipeptide acid **156** was coupled with **153** in low yield (Scheme 4.6). We also coupled the asparagine amine **153** with Fmoc-Ala-Lys(Boc)-OH (**162**) that was available in our lab from the Mefp1 project,<sup>106</sup> with the Asn amine **153** to give **163** in 71% yield.



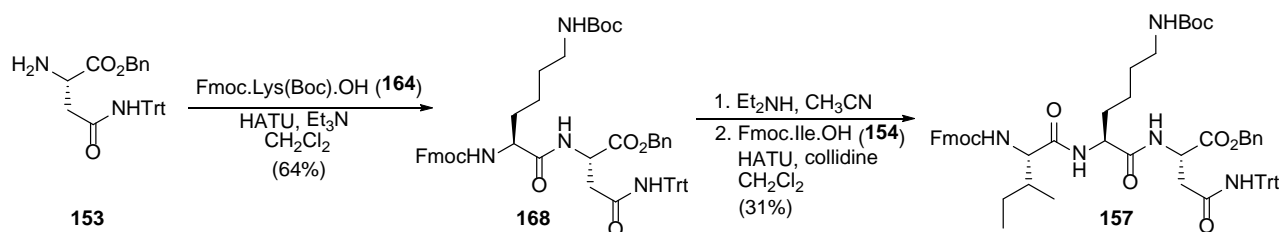
Scheme 4.6: Model studies

These combined results suggested to us that the isoleucine residue is the culprit in terms of steric hindrance, not the asparagine trityl group. Therefore we prepared the dipeptide **167** (Scheme 4.7) which could be purified by flash chromatography. Even with the amine **166**, coupling with isoleucine **154** gave only 11% of the IK dipeptide **167**. We also tried the same coupling reaction using PyBroP as the coupling reagent and DIEA as the base, which gave us a 20% yield of dipeptide **167**.



Scheme 4.7: Synthesis of dipeptide **167**

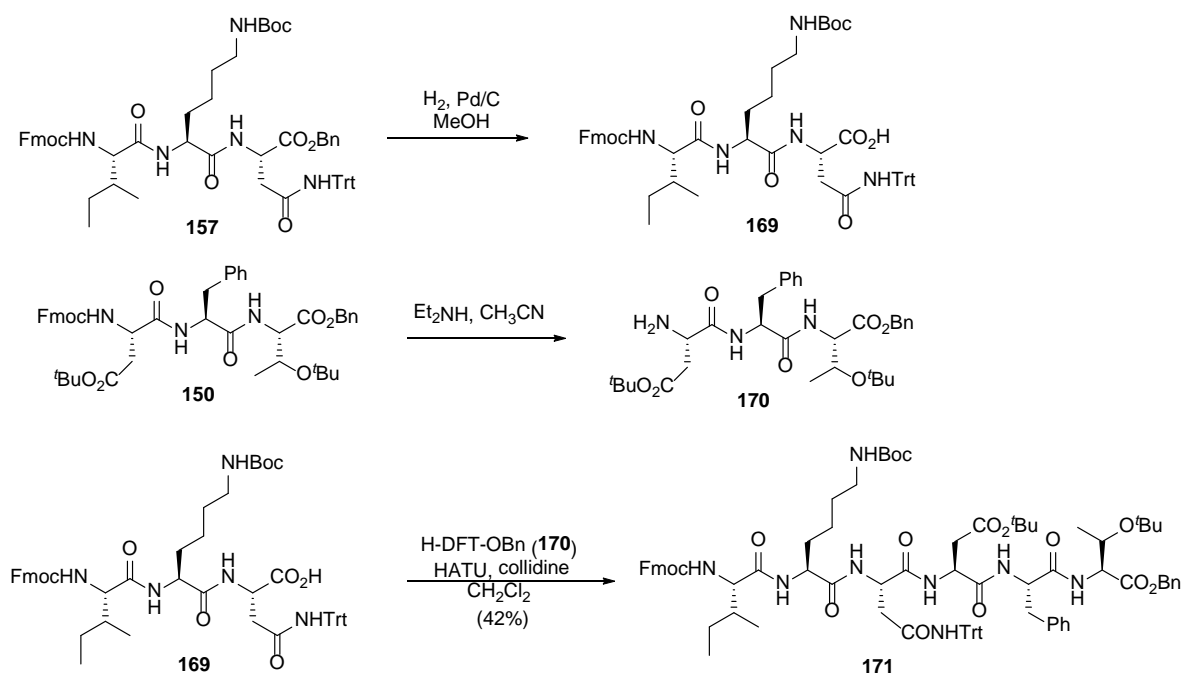
As we were unable to achieve a decent yield for the dipeptide **167**, our next strategy was to couple Fmoc-Lys(Boc)-OH (**164**) and H-Asn(Tr)-OBn (**153**) first (Scheme 4.8). This reaction gave 64% of the Fmoc-KN-OBn dipeptide **168** which was then coupled with Fmoc-Ile-OH (**154**) to give tripeptide **157** in 31% yield. This stepwise approach was the most effective way to prepare the tripeptide, although the overall yield still leaves a lot to be desired.



Scheme 4.8: Synthesis of the tripeptide **157**

### 4.7.3 [3+3] Fragment coupling

Having synthesized the two tripeptide fragments we next cleaved the benzyl ester of the Fmoc-IKN-OBn tripeptide (**157**) using standard catalytic hydrogenolysis to get the free acid **169**. The removal of the Fmoc protecting group of tripeptide **150** was performed using diethylamine. The synthesis of the Fmoc-IKNDFT-OBn hexapeptide **171** was achieved coupling the free amine **170** with the free acid **169** utilizing HATU as the coupling reagent with collidine as the base (Scheme 4.9).

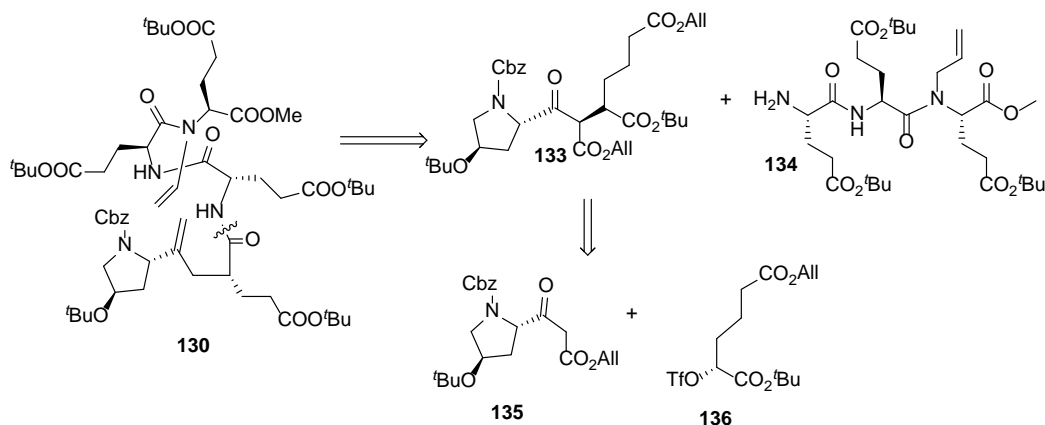


Scheme 4.9: Synthesis of Fmoc-Ile-Lys(Boc)-Asn(Trt)-Asp(O<sup>t</sup>Bu)-Phe-Thr(<sup>t</sup>Bu)-OBn (**171**)

## 4.8 The Central Peptidomimetic Fragment: Previous Alkylation of Related $\beta$ -Ketoesters

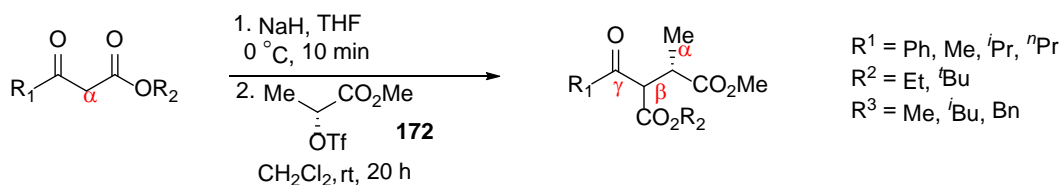
According to our retrosynthetic analysis in Scheme 4.10, our approach to the  $\alpha$ -helical mimetic **130** involves the coupling of Pro-Glu dipeptide isostere **133** with the Glu-Glu-Glu tripeptide **134**. The Pro-Glu dipeptide isostere **133** can be synthesized via alkylation of  $\beta$ -keto ester **135** with the electrophile **136**.





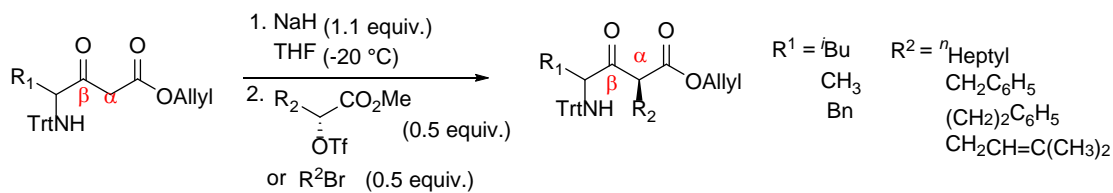
Scheme 4.10: Retrosynthetic analysis of the diene precursor **130**

A 1995 report by Hoffman and Kim described a general protocol for the stereoselective synthesis of  $\gamma$ -keto acids which have an alkyl group at C $\alpha$ .<sup>48</sup> They introduced the alkyl group by stereospecific alkylation using a triflate ester (Scheme 4.11). They reported that optically pure 2-triflate esters are good alkylating agents for  $\beta$ -keto ester enolates and the product  $\alpha$ -alkyl- $\gamma$ -keto esters are generally produced in good yields and high ee's with inversion of configuration. In this report they used both ethyl and *tert*-butyl  $\beta$ -keto esters.<sup>48</sup>



Scheme 4.11: Synthesis of  $\alpha$ -alkyl- $\gamma$ -keto esters

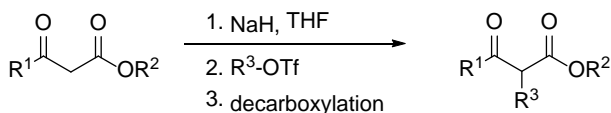
Later reports (1998 and 2002) by Hoffman and coworkers used allyl  $\beta$ -keto esters in preference to *tert*-butyl  $\beta$ -keto esters, because allyl  $\beta$ -keto esters can be cleaved and decarboxylated simultaneously using Pd(0).<sup>49, 107</sup> With the  $\beta$ -keto allyl esters they generated the anion at -20 °C, and performed the alkylation using both triflate and bromide electrophiles to get the alkylated product in 65-78% yields with triflate esters and 71-76% yields with bromides (Scheme 4.12).<sup>107-108</sup> Reaction with bromide electrophiles required a higher temperature and longer reaction time.



Scheme 4.12: Synthesis of  $\alpha$ -alkyl- $\gamma$ -keto esters

Since this pioneering work by Hoffman a number of examples of this reaction have been reported (Table 4.2). All four groups reported a similar approach for the alkylation of the  $\beta$ -keto ester, viz. the S<sub>N</sub>2 nucleophilic substitution of the triflate by the sodium carbanion.

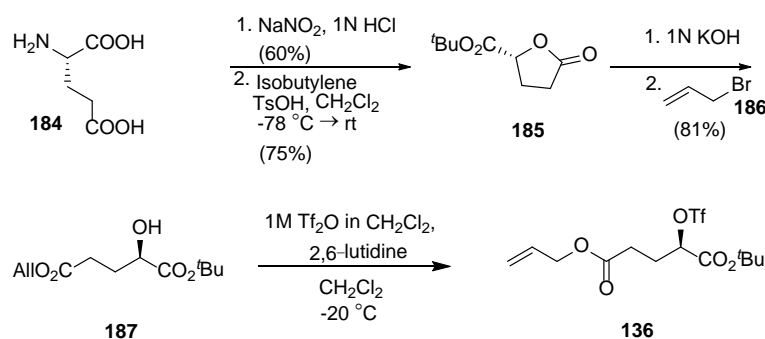
Table 4.2: Alkylation of  $\beta$ -keto esters



	$\beta$ -Keto Ester	Triflate	Product	Yield %
Worland and coworkers <sup>109</sup>	 <b>173</b>	 <b>174</b>	 <b>175</b>	54
Wong and coworkers <sup>110</sup>	 <b>176</b>	 <b>177</b>	 <b>178</b>	71
Kobayashi and coworkers <sup>111</sup>	 <b>179</b>	 <b>180</b>	 <b>181</b>	71
Laronze and coworkers <sup>112</sup>	 <b>182</b>	 <b>180</b>	 <b>183</b>	65

## 4.9 Synthesis of Triflate 136

*L*-Glutamic acid (**184**) was converted to the lactone **185** by deamination of glutamic acid, via the diazonium salt. The free side chain acid was subsequently protected as a *tert*-butyl ester.<sup>113</sup> Hydrolysis of lactone **185** with potassium hydroxide gave the potassium carboxylate salt that was reacted with allyl bromide to give **187** (Scheme 4.13).



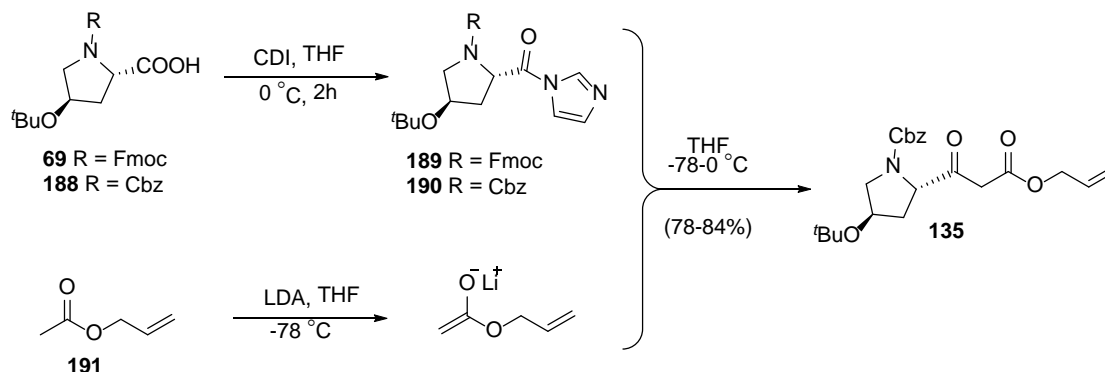
Scheme 4.13: Synthesis of triflate ester **136**

To convert the alcohol **187** into the corresponding triflate **136** we initially treated **187** with neat triflic anhydride in pyridine as solvent. The *tert*-butyl ester was cleaved under these conditions. We subsequently used a solution of triflic anhydride in dichloromethane and 2,6-lutidine as the base (Scheme 4.13).<sup>109-110</sup> Formation of **136** under these conditions was confirmed by TLC, but compound **136** was not stable to prolonged exposure to silica gel during column chromatography.

## 4.10 Synthesis of the $\beta$ -Ketoester Dipeptide Isostere

Synthesis of  $\beta$ -keto-ester **135** was initially investigated by combining imidazolide **189** with the lithium enolate of allyl acetate **191**. We observed Fmoc cleavage under these conditions, perhaps due to free diisopropylamine. We changed the proline *N* $\alpha$  protecting group to carbobenzyloxy (Cbz) and successfully transformed commercially available **188** into  $\beta$ -keto-ester **135** by converting **188** to the corresponding acylimidazolide. Subsequent displacement

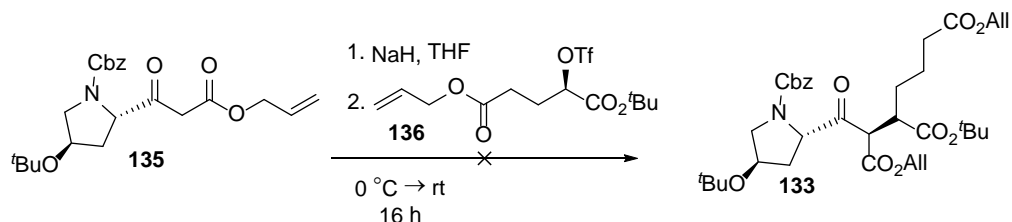
with the lithium enolate of allyl acetate afforded  $\beta$ -keto ester **135** (Scheme 4.14). This acylation can be conducted on 600 mg scale.



Scheme 4.14: Synthesis of  $\beta$ -keto-ester **135**

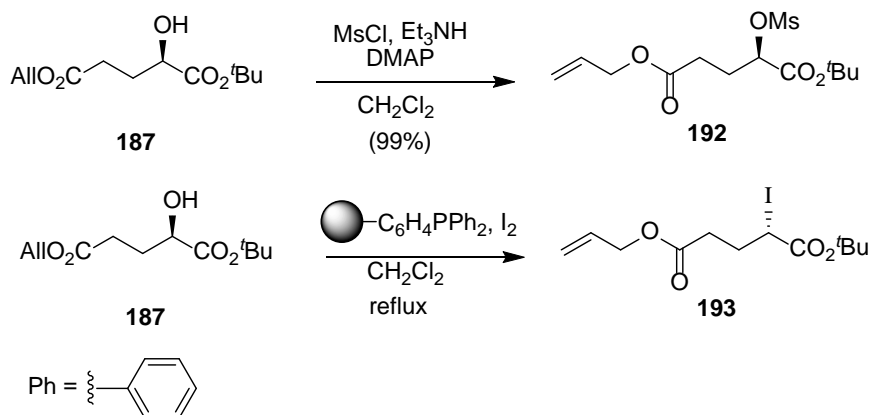
To introduce the alkyl group at C $\alpha$  of the  $\beta$ -keto ester **135** our initial effort was directed towards the generation of the carbanion of **135** and S<sub>N</sub>2 reaction with triflate **136**. Triflate **136** should react stereospecifically with the nucleophilic anion generated from **135** to give the inverted configuration.

Since we were unable to perform chromatographic purification of triflate ester **136** the product was subjected directly to condensation with the sodium anion of **135** (Scheme 4.15). We did not observe the formation of **133**, but after flash chromatography we were able to recover alcohol **187** and **135**. If the solution of **136** was acidic, that could lead to the quenching of the anion derived from **135**. We also tried the condensation of **136** with the lithium enolate of **135** derived by treatment with LDA, but again we recovered **187** and **135**.



Scheme 4.15: Attempted Synthesis of **133**

We also synthesized the mesylate **192** and iodide **193** (Scheme 4.16) as these are stable to silica and could be purified. The alkylation utilizing these two electrophiles was also unsuccessful.



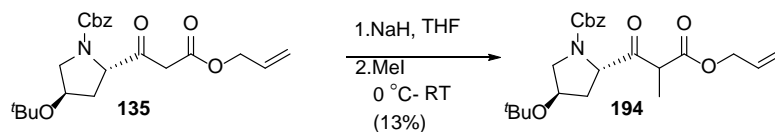
Scheme 4.16: Synthesis of electrophiles **192** and **193**

We tried different reaction conditions and different electrophiles for the alkylation of **135**, as summarized in Table 4.3.

Table 4.3: Conditions used for the alkylation of **135**

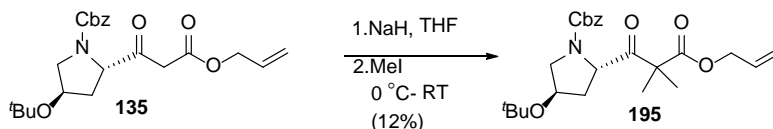
Electrophile / Number of equivalents	Base / Number of equivalents	Temperature (°C)	Comments
Triflate <b>136</b> / 1.2 Triflate <b>136</b> / 1.2 Triflate <b>136</b> / 1.2	NaH / 1.2 NaH / 2.2 LDA / 5	0-RT -20 -20	Recovered <b>187</b> and <b>135</b> after flash chromatography
Mesylate <b>192</b> / 1.2 Mesylate <b>192</b> / 1.2	LDA / 3 LDA / 5	-78 -78-RT	
Iodide <b>193</b> / 1.5 Iodide <b>193</b> / 1.5 Iodide <b>193</b> / 1.5	NaH / 1.2 LDA / 5 LiHMDS / 2.2	0-RT -78 -78	Recovered <b>187</b> and <b>135</b> after flash chromatography

Since we were unable to achieve this alkylation we were in doubt about the formation of the anion from **135**. To check the formation of the anion we attempted methylation of the sodium anion of **135** and isolated the methylated **194** in 13% yield (Scheme 4.17).



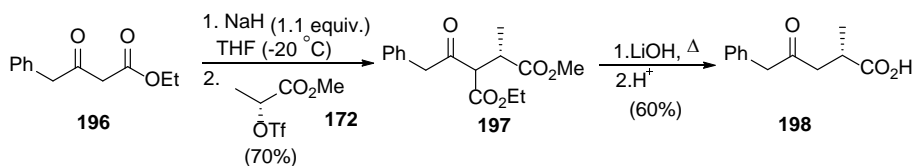
Scheme 4.17: Synthesis of **194**

In all our attempts we added sodium hydride to a solution of compound **135** in THF. As we got a very low yield for the methylation we next tried adding a solution of **135** to a suspension of sodium hydride in THF followed by the addition of methyl iodide. We observed mostly the dimethylated product **195** (12%) (Scheme 4.18) and very little of the monomethylated product. Lowering the reaction temperature to -20 °C did not help.



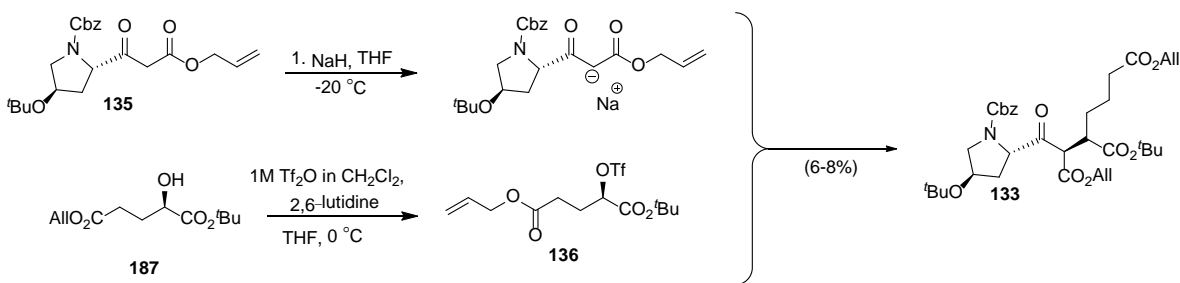
Scheme 4.18: Methylation of **135**

We reproduced a literature example of the Hoffman alkylation (Scheme 4.19) using commercially available reagents using the same reaction conditions and exact same scale (1.45 mmol) as they reported and we were able to get **198** in 42% yield over two steps, which is close to their reported yield (44%).



Scheme 4.19: Alkylation of **196**

Since we were able to successfully execute these protocols on a 1.45 mmol scale we tried the alkylation of our actual substrate (Scheme 4.20) utilizing the same reaction conditions with 250 mg scale. We were able to get the desired product **133** in 6-8% yield. Earlier we had been conducting this alkylation in 0.1 mmol scale and this was apparently too small to be effective.



Scheme 4.20: Alkylation of **135**

We decided to abandon the synthesis of the  $\alpha$ -helical mimetic using the Arora Group's approach because we couldn't improve the yield of the alkylation reaction (Scheme 4.20) to make **133** in reasonable quantities for elaboration to the HBS mimetic

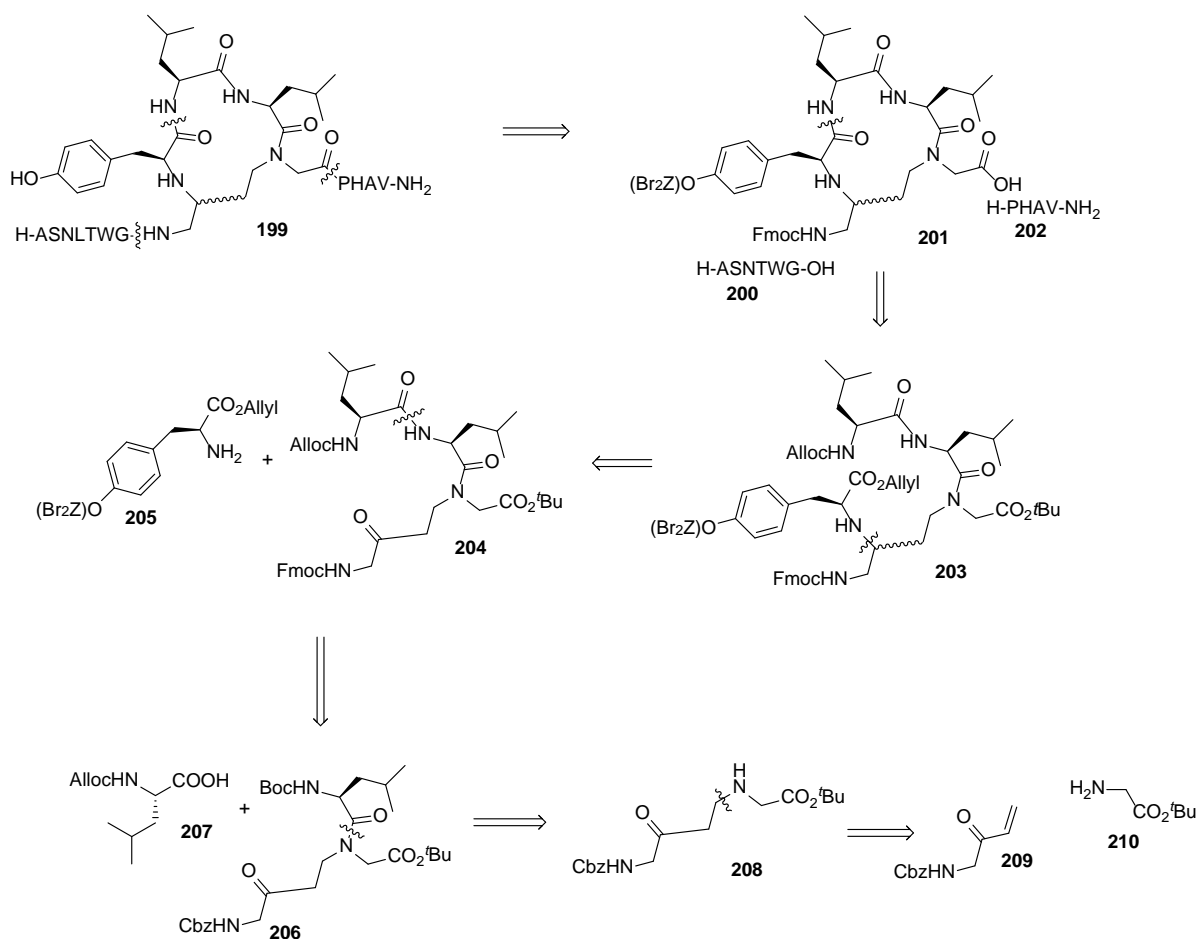
#### 4.11 Ethylene Isostere Approach of Vernall *et al.* for an $\alpha$ -Helical Mimetic for the 143-151 Peptide of Skp1

Our second approach to an  $\alpha$ -helical mimetic for the 143-151 peptide featured the strategy of Vernall *et al.* (Scheme 4.21).<sup>100</sup> As described in §4.2.3, they replaced the internal hydrogen bond with a covalent ethylene bridge in the  $\alpha$ -helical mimetic.

##### 4.11.1 Synthesis of an $\alpha$ -Helical Mimetic by Vernall *et al.*

The strategy of Vernall *et al.* was to preorganize the helical turn by synthesizing a cyclic pentapeptide mimetic. They incorporated a hexapeptide **200** (H-ASNLTWG-OH) at the *N*-terminus and a tetrapeptide **202** (H-PHAV-NH<sub>2</sub>) at the *C*-terminus of the cyclic pentapeptide

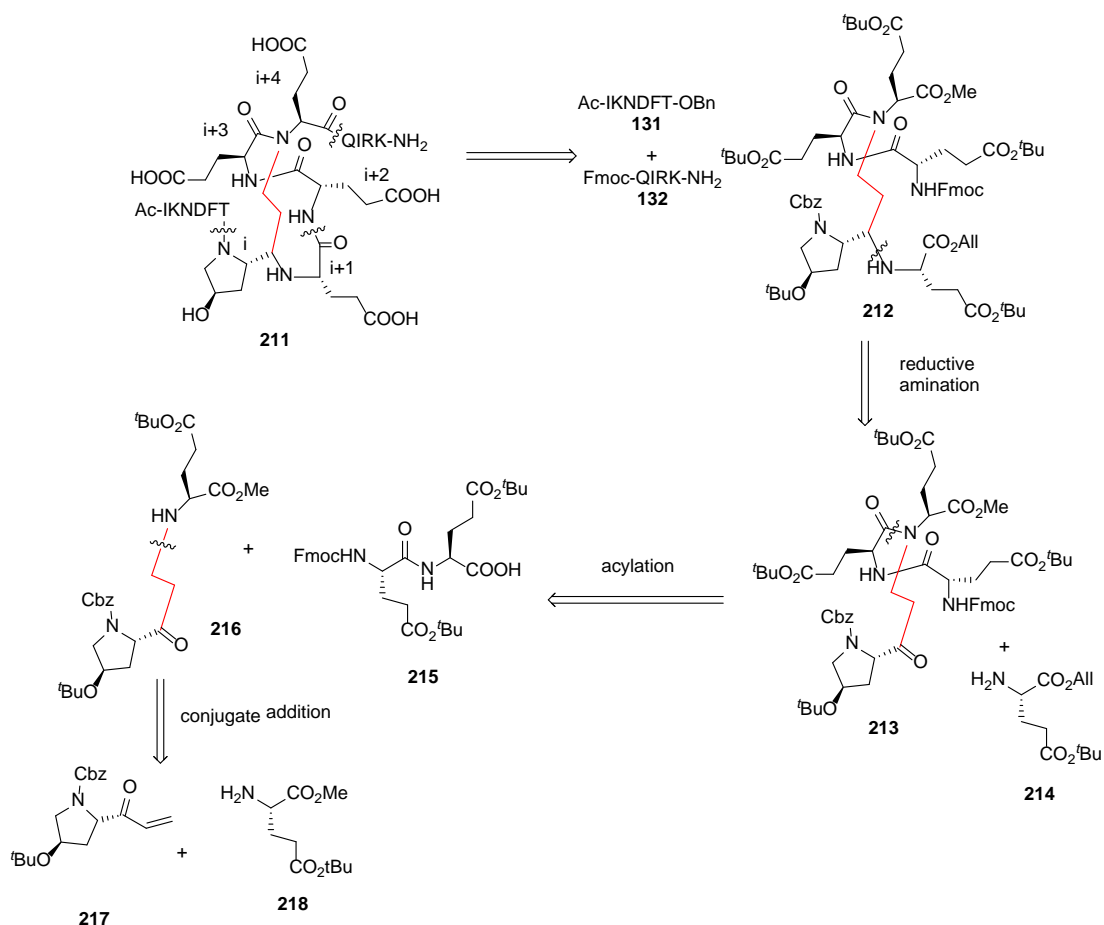
mimetic **201** (Scheme 4.21). According to their retrosynthetic analysis the first two disconnections are these amide bonds. The following disconnection of the pentapeptide mimetic **201** was the amide bond between tyrosine and leucine to reveal protected linear pseudo pentapeptide **203**. The second disconnection led to reductive amination precursors **204** and **205**. Tripeptide **204** was accessible via acylation of an amine derived from **206**, followed by a swap of Cbz group for Fmoc. Compound **206** was further disconnected to reveal ketone **208** that would arise from conjugated addition of amine **210** to  $\alpha,\beta$ -unsaturated ketone **209** (Scheme 4.21).



Scheme 4.21: Retrosynthetic analysis  $\alpha$ -helical mimetic for Galanin 1-16



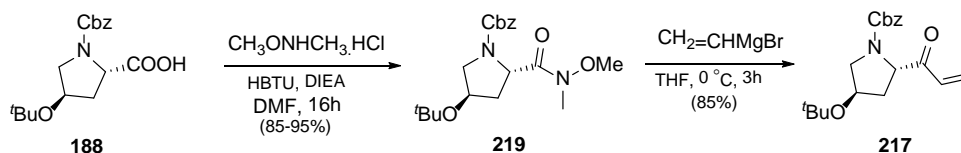
Our new retrosynthetic analysis (Scheme 4.22) was based on the strategy detailed by Vernall *et al.* (Scheme 4.21). Disconnection of the *N*- and *C*-terminal peptide fragments give the same *N*-terminal hexapeptide **131** and the *C*-terminal tetrapeptide **132** fragments that we had already prepared in our efforts toward the Arora-type HBS. Our next disconnection was the amide bond between the *i*+1 and *i*+2 residues to give the pseudo pentapeptide **212**. Disconnection of the C-N bond in **212** will give the linear Pro-Glu-Glu-Glu tetrapeptide isostere **213** which can be further simplified to reveal Pro-Glu dipeptide isostere **216** and Glu-Glu dipeptide **215**. The dipeptide isostere can be simplified to afford conjugate addition precursors **217** and **218**.



Scheme 4.22: Retrosynthetic analysis of second generation  $\alpha$ -helical mimetic with a saturated ethylene bridge

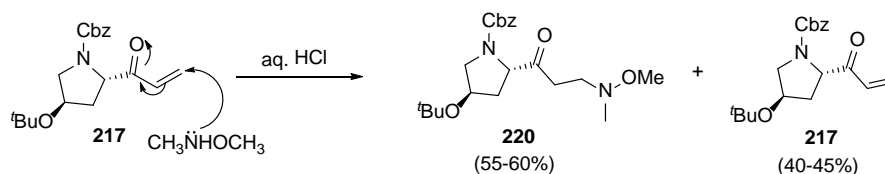
#### 4.11.2 Synthesis of the Dipeptide Isostere 216

The synthesis of the dipeptide isostere **216** began with the commercially available Cbz-Hyp(O<sup>t</sup>Bu)-OH (**188**). This was converted to Weinreb amide **219** which was then treated with vinylmagnesium bromide to give  $\alpha,\beta$ -unsaturated ketone **217** (Scheme 4.23).



Scheme 4.23: Synthesis of **217**

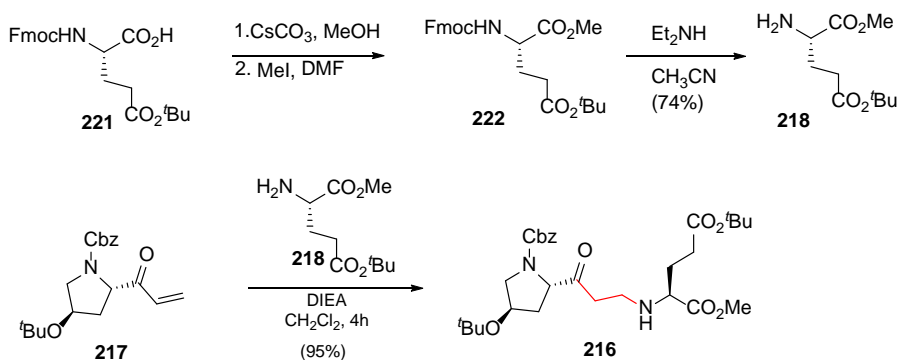
Initially, Grignard addition of vinyl magnesium bromide to Weinreb amide **219** gave us vinyl ketone **217** in low yield (40-45%). The experimental procedure for the analogous transformation in the work of Vernall *et al.* called for the quenching of the reaction with 1M HCl solution. In our case the major product isolated from this mixture was compound **220**, arising from conjugate addition of liberated *N,O*-dimethyl hydroxylamine to the desired product,  $\alpha,\beta$ -unsaturated ketone **217** (Scheme 4.24).



Scheme 4.24: Conjugate addition to **217**

To minimize the formation of compound **220** we quenched the reaction mixture with acetic anhydride, which trapped the released *N,O*-dimethyl hydroxylamine. For large scale reactions it was hard to get rid of excess acetic anhydride in the workup. We tried several different workup conditions to optimize this reaction. The best we could achieve is 85% by dropwise addition of the reaction mixture to an equal volume of an ice cold mixture of 1M HCl and acetic anhydride.

We prepared H-Glu(O<sup>t</sup>Bu)-OMe (**218**) by protecting the C-terminus of commercially available Fmoc-Glu(O<sup>t</sup>Bu)-OH (**221**) as the methyl ester **222**, followed by removal of the Fmoc protecting group. The  $\alpha,\beta$ -unsaturated ketone **217** was subjected to the conjugate addition with amine **218** to give **216** in 95% yield (Scheme 4.25).



Scheme 4.25: Synthesis of **216**

The <sup>1</sup>H NMR of compound **216** shows that the molecule exists as a 3:2 mixture of rotamers. Without an amide bond C-terminal to the “proline” of compound **216**, there is a much weaker backbone stereoelectronic effect that arises due to the  $n \rightarrow \pi^*$  interaction of the between the oxygen lone pair of the *N*-terminal amide C=O ( $n$ , nonbonding) and the antibonding orbital ( $\pi^*$ ) of the following *C*-terminal C=O (Figure 4.9). This  $n \rightarrow \pi^*$  interaction is weaker for a *C*-terminal amide than an ester<sup>65</sup> since the carbonyl carbon is less electrophilic. In compound **216** bearing a keto this  $n \rightarrow \pi^*$  interaction is weaker still.

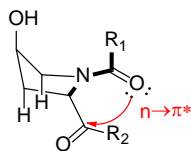
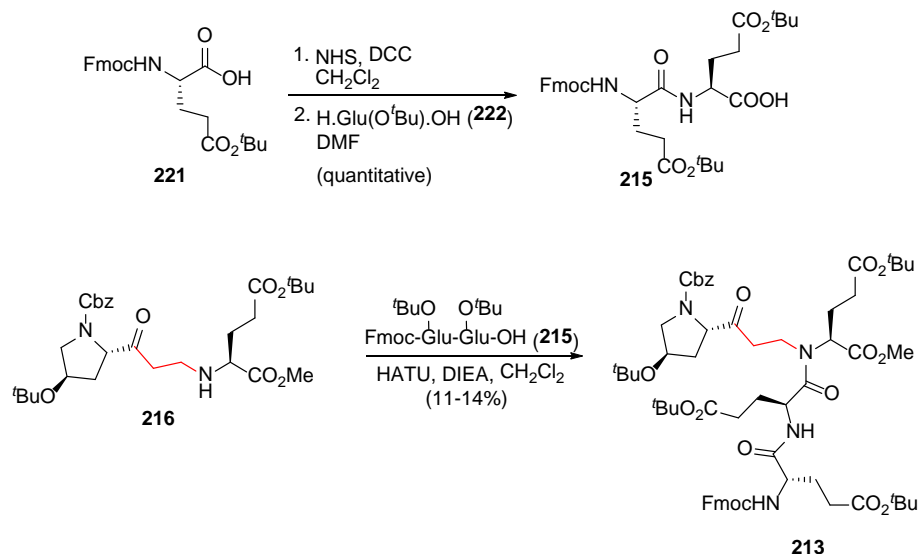


Figure 4.11: The  $n \rightarrow \pi^*$  interaction

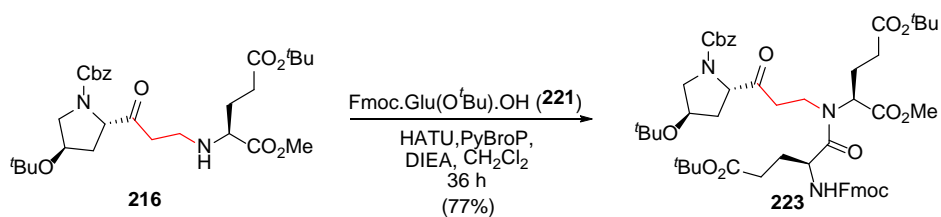
### 4.11.3 Synthesis of the Tetrapeptide Isostere 213

For elaboration to the tetrapeptide isostere **213** our initial plan was to couple the secondary amine **216** with Fmoc-Glu(<sup>t</sup>Bu)-Glu(<sup>t</sup>Bu)-OH (**215**). We prepared the dipeptide **215** using a standard NHS, DCC coupling (Scheme 4.26). Initially we tried the dipeptide segment coupling using HATU and collidine, conditions that should minimize the potential racemization.<sup>105</sup> Under these conditions we didn't observe the formation of **213**. When we used DIEA as the base in the coupling reaction the tetrapeptide mimetic **213** was obtained in very low yield (11-14%). We also tried PyBroP as the coupling reagent with DIEA, which also gave **223** in 14% yield.



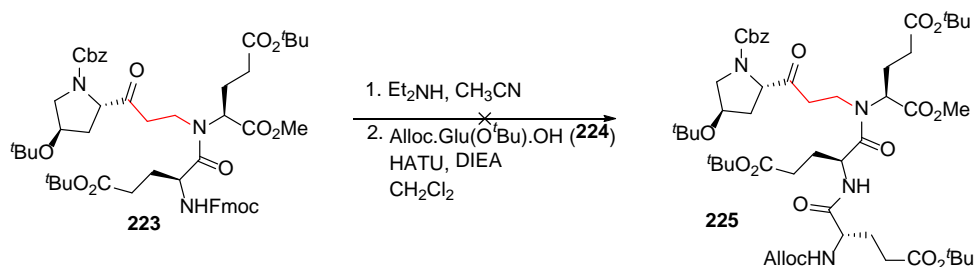
Scheme 4.26: Synthesis of **213**

As we worked to improve the coupling of dipeptide acid **215** with the secondary amine **216** we simultaneously investigated coupling one Glu residue at a time (Scheme 4.27) by analogy to Vernall *et al.* First, we tried HATU as the coupling reagent but that only give us 20% of the tripeptide mimetic **223**. We also tried PyBroP coupling reagent and that gave us **223** in 60% yield. When we used a mixture of HATU and PyBroP we were able to get **223** in 77% yield. Bizarrely, neither reagent alone gave such good results.



Scheme 4.27: Synthesis of **224**

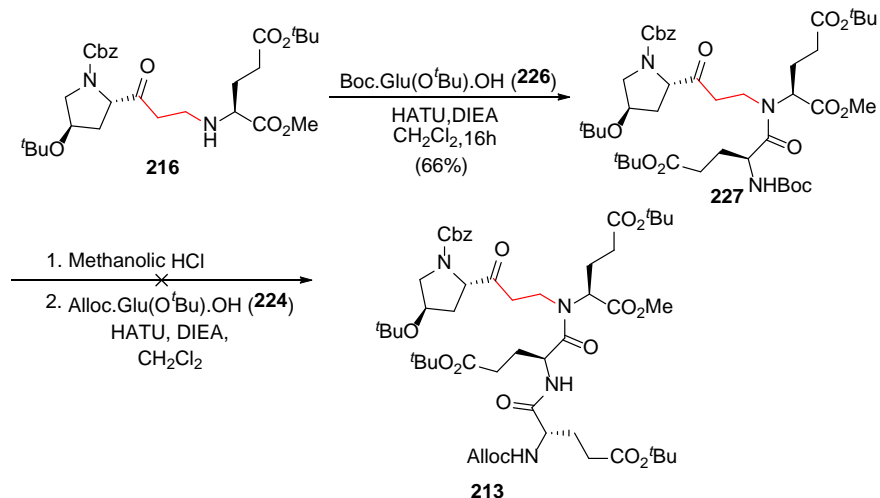
Next we removed the Fmoc protecting group from **223** and attempted the coupling of the resulting free amine with Alloc-Glu(O<sup>t</sup>Bu)-OH (**224**) (Scheme 4.28). This reaction didn't give us the desired **225** and we observed fragmentation of tripeptide mimetic **225**; the exact nature of the fragment products were not established.



Scheme 4.28: Attempted synthesis of tetrapeptide mimetic

We thought this might be due to nucleophilic attack of the free amine derived from **223** at the ketone carbonyl. Therefore, after Fmoc deprotection of **223** and chromatography, we acidified relevant fractions to generate a hydrochloride salt. This did not give any improvement.

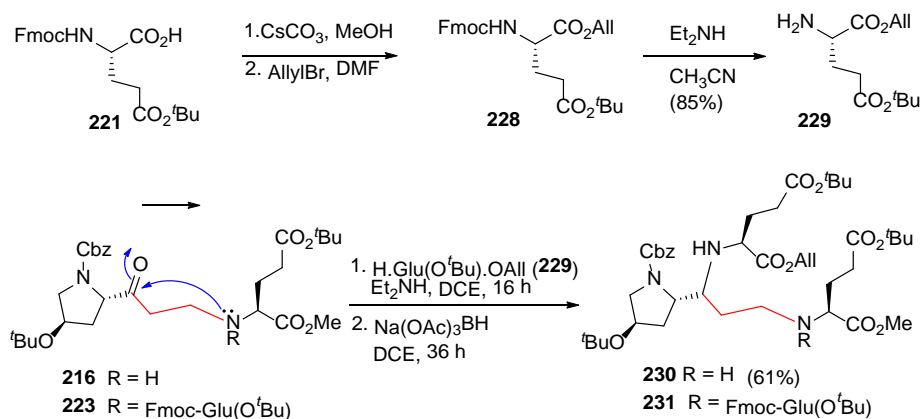
We also prepared the Boc-protected tripeptide isostere **227** (Scheme 4.29). The Boc deprotection was attempted using methanolic hydrogenchloride and the free amine was then treated with Alloc-Glu(O<sup>t</sup>Bu)-OH (**224**) for the coupling (Scheme 4.29). This gave us a gluey mixture of products which could not be purified using chromatography.



Scheme 4.29: Attempted synthesis of tetrapeptide mimetic **213**

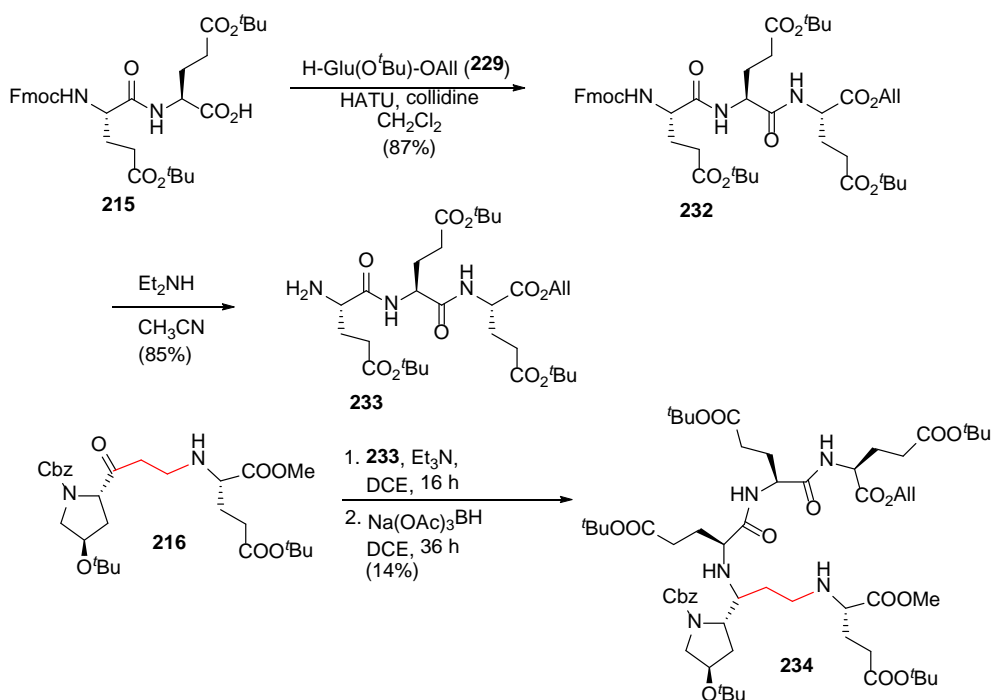
As we struggled with attachment of the Glu-Glu dipeptide **215** to isostere **216** we began to simultaneously explore the reductive amination of the ketone **216** with amine **239** using sodiumtriacetoxymethylborohydride in the presence of triethylamine as the base (Scheme 4.30). We prepared H-Glu(O<sup>t</sup>Bu)-OAll (**229**) by protecting the C-terminus of **221** as the allyl ester (**228**), followed by removal of the Fmoc protecting group. Reductive amination of **216** with **229** gave us product **230** in reasonable yield. With this promising result we next tried the reductive amination of tripeptide isostere **223** (Scheme 4.30). Even after five days after the addition of sodiumtriacetoxymethylborohydride we did not observe the formation of **231**, but recovered the starting materials **223** and **229**.

According to these results, the reductive amination is working in the presence of a secondary amine (**216** → **230**, Scheme 4.30). Intramolecular condensation (Scheme 4.30, blue arrows) is apparently not a concern since it would lead to four membered ring. Moreover, this probably reflects the hindered/non-nucleophilic nature of the secondary amine.



Scheme 4.30: Reductive amination

Next we tried the reductive amination of **216** with tripeptide amine H-Glu(O<sup>t</sup>Bu)-Glu(O<sup>t</sup>Bu)-Glu(O<sup>t</sup>Bu)-OAll (**233**). We prepared tripeptide **233** by coupling amine **229** to dipeptide **215** followed by Fmoc deprotection. We were able to get the desired product **234** for the reductive amination in 14% yield (Scheme 4.31).

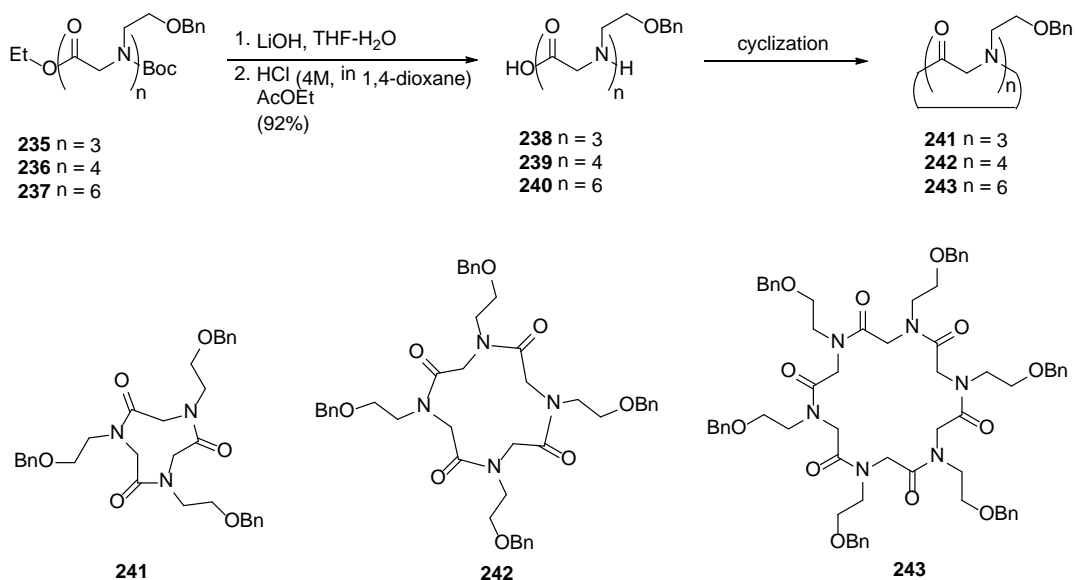


Scheme 4.31: Reductive amination of **216**

#### 4.11.4 Peptide cyclization

Success of cyclization reactions is based on the choice of the coupling reagents and the solvent. Most commonly used coupling reagents are HATU, Benzotriazol-1-yloxy)tris(dimethylamino)phosphonium hexafluorophosphate (BOP), benzotriazol-1-yloxytripyrrolidinophosphonium hexafluorophosphate (PyBOP), pentafluorophenyl diphenylphosphinate (FDPP) and EDC. The most commonly used solvents for peptide cyclizations are dimethylformamide and dichloromethane. To minimize epimerization at C $\alpha$  of the C-terminal residue and cyclodimer formation, cyclization is typically carried out under highly dilute conditions.<sup>114</sup>

In 2008 Maulucci *et al.* reported the synthesis of nine (**241**), twelve (**242**) and eighteen (**243**) membered cyclic  $\alpha$ -peptoids by cyclization of secondary amines **238-240** (Scheme 4.32).<sup>115</sup>

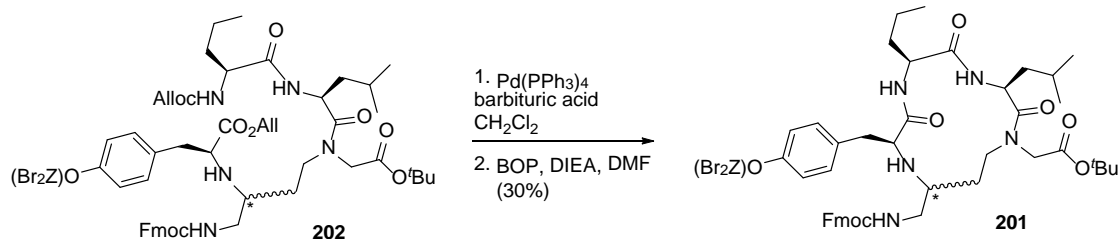


Scheme 4.32: Cyclization of  $\alpha$ -Peptoids

They treated the linear peptoids **235-237** with lithium hydroxide to deprotect the acid and hydrogenchloride to remove the Boc group. They utilized dimethylformamide as the solvent in







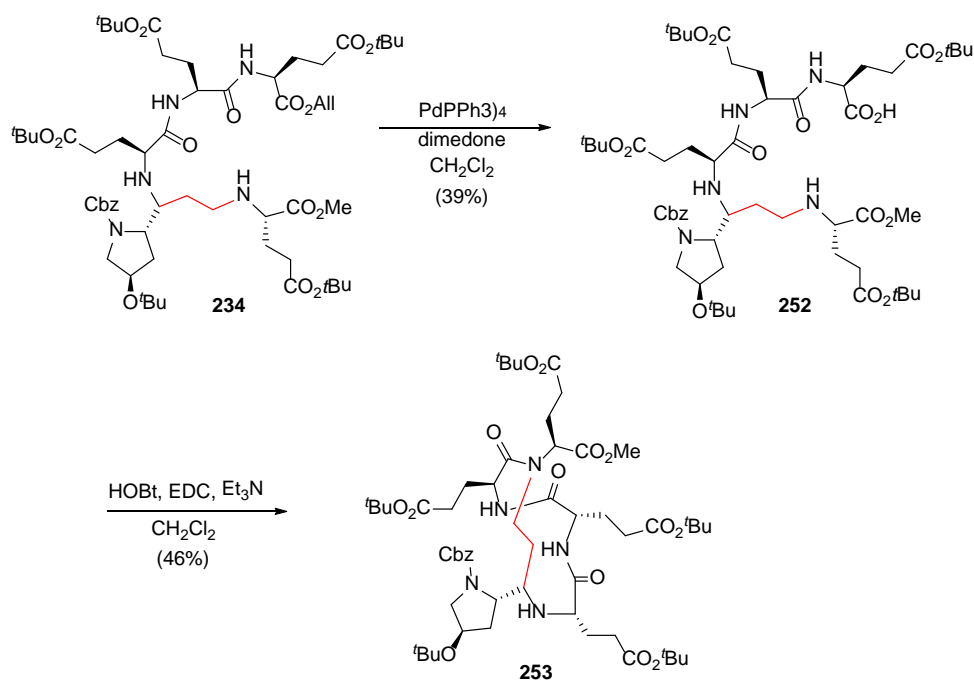
Scheme 4.34: Cyclization of **202**

#### 4.11.5 Cyclization of the tetrapeptide mimetic **234**

Cyclization of the linear tetrapeptide mimetic **234** can be achieved by removing the allyl ester protecting group utilizing Pd(0) and coupling of the resulting free acid with the secondary amine next to the ethylene bridge. This cyclization step will be another challenging step in the synthesis as the targeted amine is a hindered secondary amine. The cyclization of the **234** will result in a 13 membered ring.

With limited quantities of compound **234** in hand next we removed the allyl ester protecting group using tetrakis(triphenylphosphine)palladium(0) and dimedone. This reaction was performed on 3-5 mg scale. Initially, the resulting free acid **252** was directly taken to carry out the cyclization reaction. First we tried the cyclization under very dilute conditions, using HATU and collidine with dichloromethane as the solvent (Scheme 4.35). We ran the reaction for 2-3 days and checked the formation of **253** by ESI-MS. The molecular ion peak of **253** was not discernable in the mass spectrum but the molecular ion peak corresponding to the free acid **252** was present. We tried to purify the reaction mixture using reversed phase HPLC. The purification was difficult due to the byproducts including triphenylphosphine traces. Nothing isolated from this protocol showed much promise in terms of compound **253** according to <sup>1</sup>H NMR analysis.

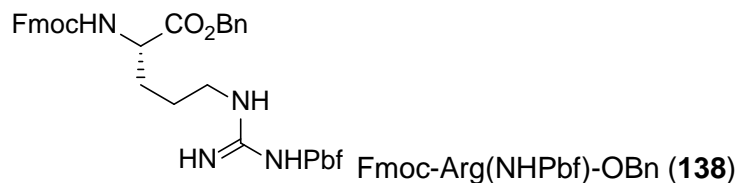
In subsequent reactions we took the time to purify acid **252** by flash chromatography prior to cyclization. We utilized dichloromethane and dimethylformamide solvent mixture and HOBt with EDC coupling reagent and diisopropylethylamine as the base. After four days we recovered starting material **252** but not the desired product **253**. We next tried the cyclization of **252** using dimethylformamide as the sole solvent and EDC as the coupling reagent in the presence of HOBt and triethylamine. We carried out the reaction on same scale under moderately dilute conditions. After 2 days we were able to isolate a new compound that is less polar than the starting acid **252** that appears to be the desired compound **253** by  $^1\text{H}$  NMR.



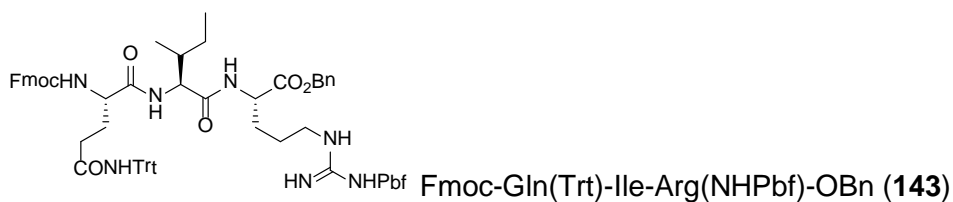
Scheme 4.35: Cyclization to produce **253**

## 4.12 Experimental Section

### 4.12.1 Synthetic Procedures



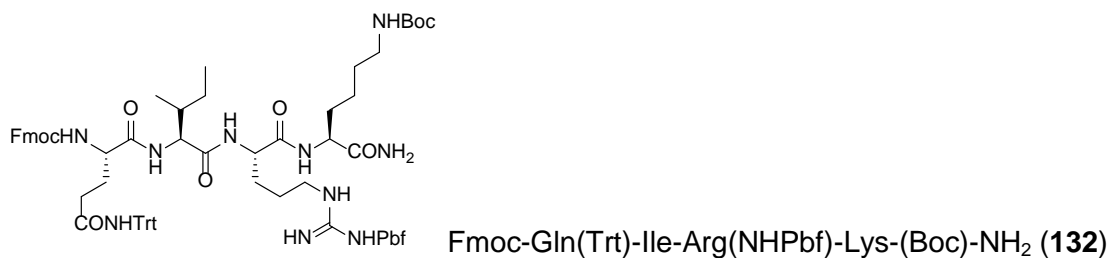
Cesium carbonate (76 mg, 0.23 mmol, 0.5 equiv.) was added to a solution of Fmoc-Arg(NHPbf)-OH (**137**) (300 mg, 0.46, 1.0 equiv.) in dry MeOH (3 mL) at 0 °C. The reaction mixture was stirred 20 min at 0 °C then 2 h at RT. The solvent was removed and the residue dissolved in DMF (3 mL). Benzyl bromide (56  $\mu$ L, 79 mg, 0.46 mmol, 1.0 equiv.) was added to the mixture and stirring continued overnight. The mixture was diluted with EtOAc (30 mL) and washed with water (30 mL) and brine (30 mL) and dried over MgSO<sub>4</sub>. The filtrate was concentrated and purified using a flash column eluting with 2:1 EtOAc:Hexanes to yield Fmoc-Arg(NHPbf)-OBn (**138**) as a colorless foam (170 mg, 90%). *R<sub>f</sub>* 0.43 (2:1 EtOAc:hexanes). <sup>1</sup>H NMR (CDCl<sub>3</sub>, 400 MHz)  $\delta$  1.41 (s, 6H), 1.52-1.57 (m, 1H), 1.63-1.72 (m, 2H), 1.80-1.89 (m, 1H), 2.05 (s, 3H), 2.49 (s, 3H), 2.55 (s, 3H), 2.89 (s, 2H), 3.08-3.15 (m, 1H), 3.16-3.22 (m, 1H), 4.15 (t, *J* = 6.7 Hz, 1H), 4.35 (d, *J* = 6.8 Hz, 2H), 5.12 (s, 2H), 5.64 (d, *J* = 7.9 Hz, 1H), 5.96-6.03 (br m, 2H), 7.24-7.31 (m, 7H), 7.37 (t, *J* = 7.4 Hz, 2H), 7.54 (d, *J* = 7.4 Hz, 2H), 7.73 (d, *J* = 7.5 Hz, 2H); <sup>13</sup>C NMR (CDCl<sub>3</sub>, 100 MHz)  $\delta$  12.7, 18.2, 19.5, 25.2, 28.8, 30.5, 40.9, 43.4, 47.3, 67.4, 67.7, 86.6, 117.7, 120.2, 124.9, 125.3, 127.3, 128.0, 128.6, 128.8, 128.9, 132.5, 133.1, 135.1, 138.6, 141.5, 156.2, 158.9, 172.5. HRMS (+ESI) calcd for C<sub>41</sub>H<sub>47</sub>N<sub>4</sub>O<sub>7</sub>S (M+H)<sup>+</sup> : 739.3160; obsd: 739.3174.



*N*-Hydroxysuccinimide (75.4 mg, 0.65 mmol, 1.00 equiv.) was added to a solution of Fmoc-Gln(Trt)-OH (**140**) (400 mg, 0.65 mmol, 1.00 equiv.) in dry CH<sub>2</sub>Cl<sub>2</sub> (4 mL). The mixture was stirred for 10 mins, then DCC (134 mg, 0.65 mmol, 1.00 equiv.) was added and stirring continued for 4 h under N<sub>2</sub>. The mixture was filtered and the filtrate was concentrated to approximately 1 mL and placed in the freezer for 2 h. The mixture was refiltered, concentrated and dried. The residue was dissolved in DMF (5 mL), H-Ile-OH (86 mg, 0.65 mmol, 1.00 equiv.) was added followed by the addition of DIEA (114 μL, 84 mg, 0.65 mmol, 1.00 equiv.). The mixture was stirred overnight under N<sub>2</sub>. The reaction mixture was diluted with ethyl acetate (25 mL), washed with 1M HCl. The aqueous layer was back-extracted with ethyl acetate (20 mL). The organic layers were combined, washed with brine (40 mL), dried over MgSO<sub>4</sub>, filtered and concentrated to give Fmoc-Gln(Tr)-Ile-OH (**142**) (470 mg, 100%) that was used directly in the next step, without purification. *R<sub>f</sub>* 0.38 (9:1 CH<sub>2</sub>Cl<sub>2</sub>:MeOH)

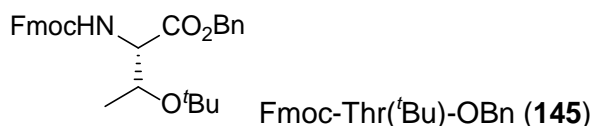
Diethylamine (1 mL) was added to a solution of Fmoc-Arg(NHPbf)-OBn (**138**) (120 mg, 0.16 mmol, 1 equiv.) in dry acetonitrile (1 mL). The reaction mixture was stirred for 2 h, concentrated and applied to a flash column eluting with 2:1 EtOAc to remove the Fmoc-biproductions and 9:1 CH<sub>2</sub>Cl<sub>2</sub>:MeOH to give H-Arg(NHPbf)-OBn (**139**) (83 mg). A solution of H-Arg(NHPbf)-OBn (**139**) (83 mg, 0.16 mmol, 1.00 equiv.) in dry CH<sub>2</sub>Cl<sub>2</sub> (2 mL) was added to a solution of Fmoc-Gln(Trt)-Ile-OH (**142**) (117 mg, 0.17 mmol, 1.05 equiv.) in dry CH<sub>2</sub>Cl<sub>2</sub> (3 mL). Collidine (43 μL, 39 mg, 0.32 mmol, 2.00 equiv.) and HATU (68 mg, 0.18 mmol, 1.05 equiv.) were added sequentially. The reaction mixture was stirred overnight under N<sub>2</sub>, concentrated and applied to a flash column eluting with 3:1 EtOAc:Hexanes to give **143** (128 mg, 65%, over 2

steps). The purity of the tripeptide was further conformed by HPLC (Econosil C-18 column, 4.6 mm diameter, 250 mm long) using flow rate of 1 mL min<sup>-1</sup>. The isocratic method was used (60% H<sub>2</sub>O, 40% acetonitrile). The tetrapeptide **143** was detected by UV absorption at 218 and 254 nm (*R<sub>T</sub>* = 11 min) *R<sub>f</sub>* 0.42 (3:1 EtOAc:hexanes). [ $\alpha$ ]<sub>D</sub><sup>25</sup> -0.097 (*c* 1.3, MeOH). <sup>1</sup>H NMR (CDCl<sub>3</sub>, 400 MHz)  $\delta$  0.76 (t, *J* = 7.0 Hz, 3H), 0.81 (d, *J* = 6.3, 3H), 0.94-1.12 (m, 2H), 1.23-1.32 (m, 3H), 1.42 (s, 6H), 1.55-1.68 (m, 1H), 1.69-1.80 (m, 1H), 1.88 (apt. d, *J* = 9.1 Hz, 2H), 2.05 (s, 3H), 2.37-2.43 (m, 2H), 2.46 (s, 3H), 2.53 (s, 3H), 2.85-3.06 (m, 2H), 2.89 (s, 2H), 4.10-4.14 (m, 2H), 4.27 (s, 2H), 4.36 (d, *J* = 8.0 Hz, 1H), 4.50-4.58 (br. s, 1H), 5.06 (2xd, *J* = 12.1 Hz, 2H), 5.76 (br. s, 1H), 5.95 (br. s, 1H), 6.18 (br. s, 1H), 7.15-7.35 (m, 24H), 7.53 (d, *J* = 7.1 Hz, 2H), 7.72 (d, *J* = 7.4 Hz, 2H); <sup>13</sup>C NMR (CDCl<sub>3</sub>, 100 MHz)  $\delta$  11.2, 12.7, 15.5, 18.2, 19.5, 25.05, 25.14, 25.8, 28.8, 29.6, 33.6, 34.0, 36.7, 40.4, 43.4, 47.2, 51.6, 54.3, 58.3, 67.2, 67.4, 70.8, 86.4, 117.5, 120.1, 124.6, 125.3, 127.2, 127.3, 127.9, 128.2, 128.5, 128.6, 128.8, 132.3, 133.5, 135.3, 138.4, 141.4, 143.8, 144.0, 144.4, 144.5, 156.3, 156.6, 158.7, 171.5, 171.9, 172.7. HRMS (+ESI) calcd for C<sub>71</sub>H<sub>80</sub>N<sub>7</sub>O<sub>10</sub>S (M+H)<sup>+</sup>: 1222.5682; obsd: 1222.5688.

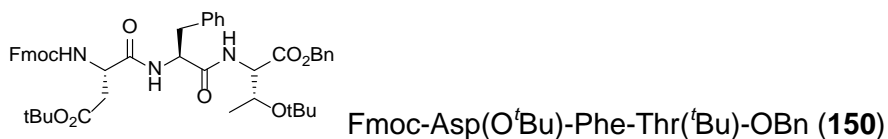


Palladium on carbon (10%, 20 mg) was added in one portion to a solution of Fmoc-Gln(Trt)-Ile-Arg(NHPbf)-OBn (**143**) (200 mg, 0.16 mmol, 1.00 equiv.) in MeOH (3 mL) and. The reaction flask was evacuated, then opened to an atmosphere of H<sub>2</sub> and stirred overnight. The catalyst was removed by filtering through a plug of Celite<sup>®</sup> in a Pasteur pipet. The filtrate was concentrated to give Fmoc-Gln(Trt)-Ile-Arg(NHPbf)-OH (154 mg, 83%). This was used to directly in the next reaction.

Fmoc-Gln(Trt)-Ile-Arg(NHPbf)-OH (154 mg, 0.136 mmol, 1.05 equiv.) was dissolved in dry CH<sub>2</sub>Cl<sub>2</sub> (4 mL), HCl salt of H-Lys(Boc)-NH<sub>2</sub> (**144**) (37 mg, 0.13 mmol, 1.00 equiv.) was added followed by the addition of HATU (55 mg, 0.14 mmol, 1.1 equiv.) and collidine (35 μL, 32 mg, 0.26 mmol, 2.00 equiv.) the reaction mixture stirred overnight under N<sub>2</sub>. The mixture was concentrated and the tetrapeptide isolated using flash column chromatography, eluting with 9:1 CH<sub>2</sub>Cl<sub>2</sub>:MeOH to give **132** as a colorless foam of (178 mg, 78%). For the purpose of characterization Fmoc-QIRK-NH<sub>2</sub> was further purified by injecting 5 mg of sample on RP-HPLC (Econosil C-18 column, 10 mm diameter, 250 mm long) using flow rate of 3 mL min<sup>-1</sup>. The gradient method used was as follows (% acetonitrile in H<sub>2</sub>O): 40-95% over 20 min; 95-40% over 5 min; 40% for 5 min. The tetrapeptide was detected by UV absorption at 218 and 254 nm (*R*<sub>T</sub> = 24 min). The relevant fractions were combined and freeze-dried to give trace amounts of **132** as a white solid. *R*<sub>f</sub> 0.58 (9:1 CH<sub>2</sub>Cl<sub>2</sub>: MeOH). [α]<sub>D</sub><sup>25</sup> -0.025 (c 0.35, MeOH). <sup>1</sup>H NMR (CDCl<sub>3</sub>, 400 MHz) δ 0.81 (apt. d, *J* = 4.6 Hz, 3H), 0.86 (apt. d, *J* = 6.6 Hz, 3H), 0.93-0.97 (br. m, 3H), 1.07-1.17 (br. m, 2H), 1.30 (apt. s, 2H), 1.40 (s, 3H), 1.44 (s, 3H), 1.48 (s, 9H), 1.69-1.75 (br. s, 8H), 1.77-1.88 (br. s, 2H), 1.90-1.98 (br. m, 2H), 2.11(s, 3H), 2.49 (s, 3H), 2.51 (apt. s, 1H), 2.56 (s, 3H), 3.03 (s, 2H), 3.11-3.19 (br. m, 2H), 4.08 (app. d, *J* = 2.5 Hz, 1H), 4.12 (br. s, 1H), 4.20-4.49 (br. m, 4H), 4.75 (br. s, 4.75), 5.56 (app. d, *J* = 4.2 Hz, 1H), 5.92 (br.s, 1H), 6.38 (1H), 7.19-7.61 (m, 26 H), 7.78 (d, *J* = 7.5 Hz, 2H); <sup>13</sup>C NMR (CDCl<sub>3</sub>, 100 MHz) δ 11.3, 12.7, 15.7, 18.2, 19.6, 23.8, 25.5, 28.7, 28.8, 31.6, 33.9, 36.3, 40.8, 43.5, 47.3, 53.3, 54.2, 54.9, 55.1, 67.4, 70.9, 79.7, 86.6, 117.7, 120.2, 124.8, 125.3, 125.4, 127.3, 128.0, 128.2, 128.8, 132.4, 138.4, 141.5, 143.9, 144.0, 144.3, 144.4, 144.5, 156.9, 157.5, 158.9, 172.0, 172.1, 172.9, 173.4, 175.2. HRMS (+ESI) calcd for C<sub>75</sub>H<sub>95</sub>N<sub>10</sub>O<sub>12</sub>S (M+H)<sup>+</sup>: 1359.6846; obsd: 1359.6863.



Cesium carbonate (123 mg, 0.4 mmol, 0.5 equiv.) was added to a solution of Fmoc-Thr(<sup>t</sup>Bu)-OH (**71**) (300 mg, 0.75, 1.0 equiv.) in dry MeOH (3 mL) at 0 °C. Reaction mixture stirred 20 min at 0 °C then 1 h at RT. The solvent was removed and the residue dissolved in DMF (3 mL). Benzyl bromide (90  $\mu$ L, 128 mg, 0.75 mmol, 1.0 equiv.) was added to the mixture and stirred overnight. The mixture was then diluted with EtOAc (30 mL) and washed with water (30 mL) and brine (30 mL) and dried over MgSO<sub>4</sub>. The filtrate was concentrated and purified using a flash column eluting with 3:1 Hexanes:EtOAc to yield Fmoc-Thr-OBn (**145**) as a colorless oil (87%). *R*<sub>f</sub> 0.47 (3:1 Hexanes:EtOAc). <sup>1</sup>H NMR (CDCl<sub>3</sub>, 400 MHz)  $\delta$  1.08 (s, 8.1 H) [1.02 (s, 0.9 H)], 1.21 (d, *J* = 6.2 Hz, 2.7 H) [1.14 (d, *J* = 6.2 Hz, 0.3H)], 4.22-4.23 (m, 2H), 4.31 (apt. d, *J* = 1.76 Hz, 1H), 4.34 (dd, *J* = 10.5, 7.7 Hz, 1H), 4.40 (d, *J* = 7.2 Hz, 1H), 4.43 (d, *J* = 7.2 Hz, 1H), 5.05 (d, *J* = 12.2 Hz, 1H), 5.20 (d, *J* = 12.2 Hz, 1H), 5.66 (d, *J* = 9.6 Hz, 0.9H) [5.40 (d, *J* = 9.4 Hz, 0.1 H)], 7.27-7.39 (m, 9H), 7.60-7.63 (m, 2H), 7.72 (d, *J* = 7.52 Hz, 2H); <sup>13</sup>C NMR (CDCl<sub>3</sub>, 100 MHz)  $\delta$  21.0, 28.4, 28.5, 47.3, 60.1, 67.4, 67.5, 74.2, 120.1, 125.2, 125.3, 127.2, 127.8, 128.5, 128.6, 128.7, 135.2, 141.4, 143.9, 144.2, 156.9, 171.1.

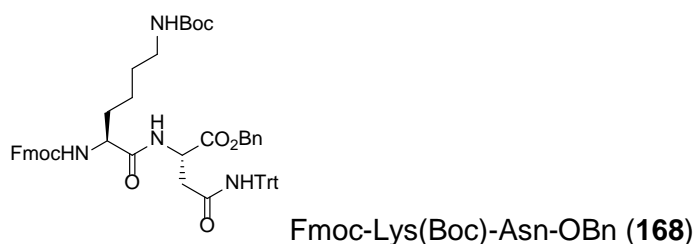


*N*-Hydroxysuccinimide (84 mg, 0.73 mmol, 1.0 equiv.) was added to a solution of Fmoc-Asp(O<sup>t</sup>Bu)-OH (**147**) (300 mg, 0.73 mmol, 1.0 equiv.) in dry CH<sub>2</sub>Cl<sub>2</sub> (4 mL). The mixture was stirred for 10 mins, then DCC (151 mg, 0.73 mmol, 1.0 equiv.) was added and stirring continued for 4 h under N<sub>2</sub>. The mixture was filtered and the filtrate was concentrated to approximately 1 mL and placed in the freezer for 2 h. The mixture was refiltered, concentrated and dried. The residue was dissolved in DMF (5 mL). Phenylalanine (121 mg, 0.73 mmol, 1.0 equiv.) was added followed by the addition of DIEA (128  $\mu$ L, 94 mg, 0.73 mmol, 1.0 equiv.). The reaction was stirred overnight under N<sub>2</sub>. The reaction mixture was diluted with ethyl acetate (25 mL) and



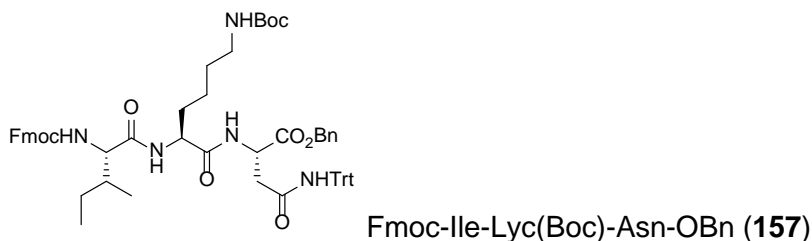
washed with 1M HCl. The aqueous layer was back-extracted with ethyl acetate (20 mL). The organic layers were combined, washed with brine (40 mL), dried over MgSO<sub>4</sub>, filtered and concentrated to give Fmoc-Asp(O<sup>t</sup>Bu)-Phe-OH (**149**) 411 mg that was used in subsequent reactions, without purification. *R<sub>f</sub>* 0.30 (9:1 CH<sub>2</sub>Cl<sub>2</sub>:MeOH).

H-Thr(<sup>t</sup>Bu)OBn (**146**) (153 mg, 0.58 mmol, 1.0 equiv.) in DMF (2 mL) was added to a solution of Fmoc-Asp(O<sup>t</sup>Bu)-Phe-OH (355 mg, 0.63 mmol, 1.1 equiv.) in DMF (2 mL). Collidine (167 μL, 153 mg, 0.126 mmol, 2.0 equiv.) and HATU (240 mg, 0.63 mmol, 1.1 equiv.) were added sequentially. The reaction mixture was stirred overnight under N<sub>2</sub>, concentrated and applied to a flash column eluting with 1:1 EtOAc:hexanes to give **150** (365 mg, 72%, over 2 steps). *R<sub>f</sub>* 0.65 (1:1 EtOAc:hexanes). [α]<sub>D</sub><sup>25</sup> -0.006 (c 0.70, MeOH). <sup>1</sup>H NMR (CDCl<sub>3</sub>, 400 MHz) δ 1.06 (s, 9H), 1.10 (d, *J* = 5.8 Hz, 3H), 1.46 (s, 9H), 2.61 (dd, *J* = 16.8, 6.1 Hz, 1H), 2.85 (dd, *J* = 16.8, 4.3 Hz, 1H), 3.04 (dd, *J* = 13.9, 6.6 Hz, 1H), 3.11 (dd, *J* = 13.9, 6.6 Hz, 1H), 4.15-4.23 (m, 2H), 4.32-4.44 (m, 2H), 4.48- 4.55 (m, 2H), 4.72 (dd, *J* = 13.9, 6.7 Hz, 1H), 5.03 (d, *J* = 12.2 Hz, 1H), 5.18 (d, *J* = 12.2 Hz, 1H), 5.97 (d, *J* = 8.3 Hz, 1H), 6.54 (d, *J* = 8.7 Hz, 1H), 7.19 - 7.44 (m, 14H), 7.60 (app. d, *J* = 4.9 Hz, 2H), 7.78 (d, *J* = 7.5 Hz, 2H); <sup>13</sup>C NMR (CDCl<sub>3</sub>, 100 MHz) δ 20.9, 28.1, 28.4, 37.6, 38.4, 47.2, 51.2, 54.7, 58.1, 60.5, 67.4, 74.2, 81.9, 120.1, 125.2, 127.0, 127.2, 127.9, 128.7, 129.6, 135.2, 136.5, 141.4, 143.8, 143.9, 156.1, 170.3, 170.3, 170.9, 171.0. HRMS (+ESI) calcd for C<sub>47</sub>H<sub>56</sub>N<sub>3</sub>O<sub>9</sub> (M+H)<sup>+</sup>: 806.4011; obsd: 806.4020.



H-Asn(Trt)-OBn (**153**) (207 mg, 0.45 mmol, 1.00 equiv.) in dry CH<sub>2</sub>Cl<sub>2</sub> (1 mL) was added to a solution of Fmoc-Lys(Boc)-OH (**164**) (230 mg, 0.49 mmol, 1.10 equiv.) in dry CH<sub>2</sub>Cl<sub>2</sub> (2 mL).

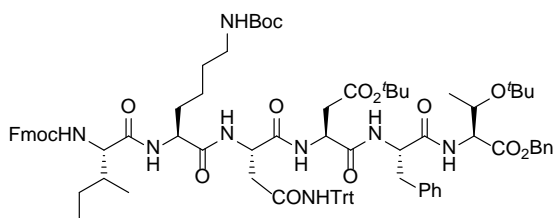
Triethylamine (126  $\mu$ L, 92 mg, 0.90 mmol, 2.00 equiv.) and HATU (187 mg, 0.49 mmol, 1.10 equiv.) were added sequentially. The reaction mixture was stirred overnight under nitrogen, concentrated and applied to a flash column eluting with 1:1 Hexanes:EtOAc to give Fmoc-Lys(Boc)-Asn(Trt)-OBn (**168**) (196 mg, 64%).  $R_f$  0.51 (1:1 Hexanes:EtOAc).  $^1\text{H}$  NMR ( $\text{CDCl}_3$ , 400 MHz)  $\delta$  1.23-1.36 (m, 4H), 1.42 (s, 9H), 1.49-1.76 (m, 2H), 2.79 (br. s, 1H), 2.99 (br. s, 1H), 3.08-3.14 (m, 2H), 4.07-4.10 (m, 1H), 4.18 (t,  $J = 6.9$  Hz, 1H), 4.32 (d,  $J = 7.3$  Hz, 2H), 4.63 (br. s, 1H), 4.87-4.89 (m, 1H), 5.03 (d,  $J = 12.3$  Hz, 1H), 5.08 (d,  $J = 12.3$  Hz, 1H), 5.52 (d,  $J = 7.0$  Hz, 1H), 6.82 (s, 1H), 7.12-7.40 (m, 22 H), 7.38 (t,  $J = 7.3$  Hz, 2H), 7.57 (t,  $J = 7.4$  Hz, 2H), 7.74 (d,  $J = 7.4$  Hz, 2H);  $^{13}\text{C}$  NMR ( $\text{CDCl}_3$ , 100 MHz)  $\delta$  22.4, 28.6, 29.6, 32.8, 38.2, 40.1, 47.3, 49.2, 54.8, 67.2, 67.8, 71.2, 79.2, 120.1, 125.4, 127.3, 127.4, 127.9, 128.2, 128.5, 128.6, 128.8, 128.8, 135.3, 141.5, 144.0, 144.1, 144.4, 156.2.



Diethylamine (2 mL) was added to a solution of Fmoc-Lys(Boc)-Asn-OBn (**168**) (196 mg, 0.21 mmol) in dry acetonitrile (2 mL). The reaction mixture was stirred under nitrogen for 2 h. The reaction mixture was concentrated and concentrated again four times with acetonitrile to give H-Lys(Boc)-Asn-OBn (148 mg). This was used in the next step without further purification.

Fmoc-Ile-OH (**154**) (82 mg, 0.23 mmol, 1.1 equiv.) was added to a solution of H-Lys(Boc)-Asn-OBn (148 mg, 0.21 mmol, 1.0 equiv.) in dry  $\text{CH}_2\text{Cl}_2$  (3 mL) followed by the addition of 2,4,6-collidine (40  $\mu$ L, 55 mg, 0.42 mmol, 2.0 equiv.) and HATU (88 mg, 0.23 mmol, 1.1 equiv.). The reaction mixture was stirred overnight under nitrogen. The reaction mixture was concentrated and applied to a flash column eluting with 1:1 Hexanes:EtOAc to yield Fmoc-Ile-

Lys(Boc)-Asn-OBn (**157**) (31%).  $R_f$  0.30 (1:1 Hexanes:EtOAc).  $^1\text{H}$  NMR ( $\text{CDCl}_3$ , 400 MHz)  $\delta$  0.87 (s, 3H), 0.89 (s, 3H), 1.02-1.11 (m, 1H), 1.16-1.34 (m, 4H), 1.39 (s, 9H), 1.45-1.50 (m, 2H), 1.56-1.66 (m, 1H), 1.77-1.89 (m, 1H), 2.72 (d,  $J = 15.5$  Hz, 1H), 2.81-3.00 (m, 2H), 3.05 (d,  $J = 15.5$  Hz, 1H), 4.07 (t,  $J = 7.6$  Hz, 1H), 4.17 (t,  $J = 6.8$  Hz, 1H), 4.25-4.40 (m, 3H), 4.70 (br. s, 1H), 4.85-4.91 (m, 1H), 5.01 (d,  $J = 12.3$  Hz, 1H), 5.06 (d,  $J = 12.3$  Hz, 1H), 5.58 (d,  $J = 8.5$  Hz, 1H), 6.83 (s, 1H), 6.86 (apt. d,  $J = 7.4$  Hz, 1H), 7.11-7.27 (m, 22H), 7.37 (t,  $J = 7.6$  Hz, 4H) 7.73 (d,  $J = 7.11$ , 2H);  $^{13}\text{C}$  NMR ( $\text{CDCl}_3$ , 100 MHz)  $\delta$  11.5, 15.7, 22.3, 25.0, 28.6, 29.4, 32.8, 37.6, 38.1, 40.1, 47.3, 49.1, 52.9, 59.9, 67.2, 67.7, 71.1, 79.1, 119.9, 120.1, 121.2, 125.4, 127.3, 127.4, 127.9, 128.1, 128.2, 128.4, 128.6, 128.7, 128.8, 135.3, 141.4, 143.9, 144.2, 144.4, 144.5, 156.2, 156.5, 169.8, 170.7, 171.4. HRMS (+ESI) calcd for  $\text{C}_{62}\text{H}_{70}\text{N}_5\text{O}_9$  ( $\text{M}+\text{H}$ ) $^+$ : 1028.5168; obsd: 1028.5162.



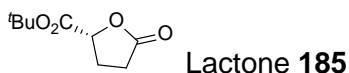
Fmoc-Ile-Lyc(Boc)-Asn-Asp(O<sup>t</sup>Bu)-Ph-Thr-OBn  
(**171**)

*Fmoc-Ile-Lys(Boc)-Asn(Trt)-OH* (**169**): Palladium on carbon (10%, 20 mg) was added in one portion to a solution of *Fmoc-Ile-Lys(Boc)-Asn(Trt)-OBn* (**157**) (32 mg, 0.03 mmol, 1.00 equiv.) in MeOH (2 mL) and. The reaction flask was evacuated, then opened to an atmosphere of  $\text{H}_2$  and stirred overnight. The catalyst was removed by filtering through a plug of Celite<sup>®</sup> in a Pasteur pipet, washing well with MeOH. The filtrate was concentrated to give *Fmoc-Ile-Lys(Boc)-Asn-OH*. This was used directly in the coupling reaction.

*H-Asp(O<sup>t</sup>Bu)-Phe-Thr(O<sup>t</sup>Bu)-OBn* (**170**): Diethylamine (2 mL) was added to a solution of *Fmoc-Asp(O<sup>t</sup>Bu)-Ph-Thr(O<sup>t</sup>Bu)-OBn* (**150**) (24 mg, 0.03 mmol) in dry acetonitrile (2 mL). The reaction mixture was stirred under nitrogen for 2 h. The reaction mixture was concentrated and again

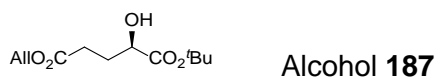
concentrated four times with acetonitrile to give H-Asp(O<sup>t</sup>Bu)-Ph-Thr-OBn (**170**). This was used in the coupling reaction without further purification.  $R_f$  0.59 (9:1 CH<sub>2</sub>Cl<sub>2</sub>:MeOH)

*Coupling reaction:* Collidine (8  $\mu$ L, 7 mg, 0.05 mmol, 2 equiv.) and HATU (11 mg, 0.03 mmol, 1.1 equiv.) were added to a solution of Fmoc-Ile-Lys(Boc)-Asn-OH (**169**) (21 mg, 0.03 mmol, 1 equiv.) in DMF (1 mL). A solution of H-Asp(O<sup>t</sup>Bu)-Ph-Thr-OBn (**170**) (18 mg, 0.03 mmol, 1.1 equiv.) in dry CH<sub>2</sub>Cl<sub>2</sub> (1 mL) was added to the DMF mixture. The reaction mixture was stirred overnight under nitrogen, concentrated and diluted with EtOAc (5 mL). The organic layer washed with brine (3 x 10 mL), dried over MgSO<sub>4</sub>, filtered, and concentrated. The residue was applied to a flash column eluting with 1:1 EtOAc:Hexanes then with 9:1 CH<sub>2</sub>Cl<sub>2</sub>:MeOH to give hexapeptide **171** (45mg, 42%).  $R_f$  0.45 (9:1 CH<sub>2</sub>Cl<sub>2</sub>:MeOH). <sup>1</sup>H NMR (CDCl<sub>3</sub>, 400 MHz)  $\delta$  0.80-0.92 (m, 9H), 1.04 (s, 9H), 1.05-1.10 (m, 4H), 1.35-1.59 (m, 1H), 1.42 (s, 18 H), 1.74-1.87 (m, 1H), 1.99-2.16 (m, 1H), 2.16-2.34 (m, 4H), 2.52-2.72 (m, 2H), 2.90-3.15 (m, 3H), 3.58-3.69 (m, 1H), 4.06-4.24 (m, 2H), 4.38-4.51 (m, 1H), 4.64-4.76 (m, 3H), 5.04 (d,  $J$  = 12.1 Hz, 1H), 5.12-5.21 (m, 1H), 6.56-6.60 (m, 1H), 7.17-7.44 (m, 33H).

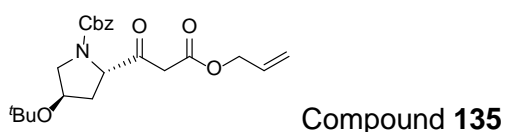


A solution of sodium nitrite (1.41, 20.4 mmol, 1.5 equiv.) in water (7 mL) was added over 15 min to a stirred mixture of D-Glutamic acid (2.0 g, 13.6 mmol, 1 equiv.) in dioxane:1M HCl (5 mL:16 mL) maintaining the internal temperature at 0-5 °C. Upon completion of addition the ice bath was removed, the mixture was warmed to RT and stirred overnight. The mixture was concentrated, the residue was dissolved in EtOAc (10 mL) and filtered to remove the white solid. The filtrate was dried over MgSO<sub>4</sub>, filtered and concentrated. The residue was dissolved in CH<sub>2</sub>Cl<sub>2</sub> (20 mL), and *p*-toluenesulfonic acid (5.3 g, 27.4 mmol, 2.1) was added.

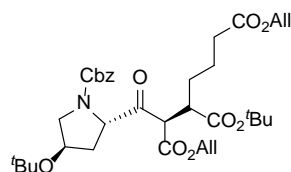
In a separate two-neck flask isobutylene (40 mL) was condensed at -78 °C. The main reaction contents were then transferred over to the two-neck flask over 15 min and stirred 4 d. the reaction mixture was concentrated diluted with CH<sub>2</sub>Cl<sub>2</sub> (30 mL) and washed with sat' aq. NaHCO<sub>3</sub> (2 x 40 mL). The organic layer was dried over MgSO<sub>4</sub>, filtered and concentrated. The residue was applied to a flash column eluting with 2:1 Hexanes:EtOAc to give **185** (1.1 g, 43% over 2 steps). *R<sub>f</sub>* 0.50 (1:1 EtOAc: Hexane). <sup>1</sup>H NMR (CDCl<sub>3</sub>, 400 MHz) δ 1.50 (s, 9H), 2.24-2.30 (m, 1H), 2.48-2.64 (m, 3H), 4.79-4.83 (m, 1H); <sup>13</sup>C NMR (CDCl<sub>3</sub>, 100 MHz) δ 26.1, 27.0, 28.2, 83.4, 169.2, 176.4.



Aqueous potassium hydroxide (1N, 1 mL) was added to a solution of **185** (160 mg, 0.86 mmol, 1 equiv.) in 1,4-dioxane (1 mL) at 0 °C. The reaction mixture was stirred for 5 h at rt and freeze-dried. The residue was dissolved in anhydrous DMF (2 mL) and cooled to 0 °C. Allyl bromide (90 μL, 125 mg, 1.03 mmol, 1.2 equiv.) was added and the mixture stirred overnight at rt under N<sub>2</sub>. The reaction mixture was diluted with EtOAc (30 mL) and washed with water (40 mL). The organic layer was dried over MgSO<sub>4</sub>, filtered and concentrated. The residue was applied to a flash column eluting with 1:1 hexanes:EtOAc to give **187** (210 mg, 81%). *R<sub>f</sub>* 0.66 (1:1 hexanes:EtOAc). <sup>1</sup>H NMR (CDCl<sub>3</sub>, 400 MHz) δ 1.49 (s, 9H), 1.85-1.95 (m, 1H), 2.10-2.18 (m, 1H), 2.41-2.57 (m, 2H), 3.20 (d, *J* = 5.4 Hz, 1H), 4.09 (td, *J* = 8.0, 4.5 Hz, 1H), 4.59 (dt, *J* = 5.7, 1.3 Hz, 2H), 5.22 (dd, *J* = 10.5, 1.3 Hz, 1H), 5.34 (ddd, *J* = 17.2, 3.0, 1.5 Hz, 1H), 5.87-5.97 (m, 1H); <sup>13</sup>C NMR (CDCl<sub>3</sub>, 100 MHz) δ 28.0, 29.5, 29.7, 65.1, 69.6, 82.5, 118.1, 132.2, 172.8, 173.9. HRMS (+ESI) calcd for C<sub>12</sub>H<sub>20</sub>NaO<sub>5</sub> (M+Na)<sup>+</sup>: 267.1208; obsd: 267.1247.



Carbonyldiimidazole (111 mg, 0.68, 1.1 equiv.) was added to a solution of proline **188** (200 mg, 0.62 mmol, 1.0 equiv.) in anhydrous THF (2 mL). The reaction mixture was stirred for 2 h. In a separate flask allyl acetate (335  $\mu$ L, 310 mg, 3.1 mmol, 5.0 equiv.) was added to a freshly prepared LDA (1.25 mL, 3.2 mmol, 5.0 equiv.) in THF (1 mL) at -78 °C and stirred for 5 min. The activated acid mixture was added dropwise to the allyl acetate, LDA mixture over 10 min. The reaction mixture was stirred overnight under nitrogen and quenched with 0.5 M HCl (3 drops from pipette). The reaction mixture was concentrated, diluted with CH<sub>2</sub>Cl<sub>2</sub> (30 mL), washed with 1 M HCl (30 mL), and brine (30 mL) and dried over MgSO<sub>4</sub>, concentrated. The residue was applied to a flash column eluting with 3:1 Hexanes:EtOAc to give  $\beta$ -keto-ester **135** (217 mg, 84%). *R<sub>f</sub>* 0.26(1:3 EtOAc: Hexane). <sup>1</sup>H NMR (CDCl<sub>3</sub>, 400 MHz)  $\delta$  1.16 [1.17] (s, 9H), 2.04-2.19 (m, 2H), 3.32 [3.55] (dd, *J* = 10.8, 4.8 Hz, 1H), 3.38 (d, *J* = 2.1 Hz, 1H), 3.6-3.7 (m, 2H), 4.25 (p, *J* = 5.1 Hz, 1H), 4.52-4.63 (m, 1H), 5.09 (dd, *J* = 17.4, 7.4 Hz, 2H), 5.23-5.35 (m, 2H), 5.84-5.95 (m, 1H), 7.29-7.31 (m, 5H); <sup>13</sup>C NMR (CDCl<sub>3</sub>, 100 MHz)  $\delta$  28.4, 36.7 [37.8], 47.1 [46.1], 3.9 [54.7], 64.1, 66.1, 67.3 [67.5], 69.5 [68.6], 74.5 [74.4], 119.0 [119.1], 128.0, 128.3, 128.4, 128.7, 128.8, 131.7, 131.8, 136.6, 155.6 [154.4], 167.0 [166.6], 202.7 [202.4].

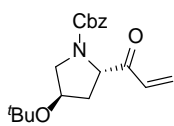


Dipeptide isostere **133**

To a stirred suspension in of NaH (25 mg, 1.04 mmol, 1.5 equiv.) in dry THF (1 mL) at -20 °C,  $\beta$ -keto ester **135** (280 mg, 0.69 mmol, 1.1 equiv.) in dry THF (1 mL) was added and the reaction mixture was stirred for 10 min under nitrogen maintaining the temperature at -20 °C.

In a separate flask triflate **136** was prepared by adding 2,6-lutidine (80  $\mu$ L, 74 mg, 0.69 mmol, 1.1 equiv.) to a solution of alcohol **187** (185mg, 0.63 mmol, 1 equiv.) in dry THF (1 mL) at 0 °C and the reaction mixture was stirred for 10 min under nitrogen. The mixture was added

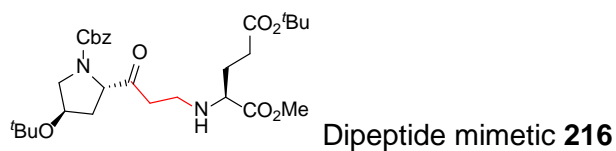
dropwise to the NaH and  $\beta$ -keto ester mixture. The reaction mixture gradually warmed to RT and stirred for 3.5 h under nitrogen. The reaction was quenched by adding 0.5M HCl (3 drops from pipette), concentrated and diluted with EtOAc (15 mL). The organic layer washed with 1M HCl (15 mL), and brine (15 mL), dried over MgSO<sub>4</sub> and concentrated. The residue was applied to a flash column with 3:1 Hexanes:EtOAc to give **133** (49 mg, 11%). *R<sub>f</sub>* 0.69 (2:1 Hexanes:EtOAc). <sup>1</sup>H NMR (CDCl<sub>3</sub>, 400 MHz)  $\delta$  1.18 [1.19] (s, 9H), 1.51 (s, 9H), 1.67-1.70 (m, 2H), 1.86-2.23 (m, 2h), 2.39-2.43 (m, 2H), 2.64-2.62 (m, 2H), 2.94 (s, 1H), 3.33 [3.42] (dd, *J* = 10.7, 4.9 Hz, 1H), 3.75-3.80 (m, 1H), 4.11-4.13 (m, 1H), 4.23 [4.27] (t, *J* = 5.5 Hz, 1H), 4.52-4.70 (m, 3H), 4.84 [4.77] (dd, *J* = 8.6, 4.9 Hz, 1H), 5.07-5.18 (m, 4H), 5.25-5.30 (m, 2H), 5.37 (d, *J* = 17.1 Hz, 1H), 5.83-5.99 (m, 1H), 7.32-7.39 (m, 10H); <sup>1</sup>H NMR (CDCl<sub>3</sub>, 400 MHz)  $\delta$  25.1, 25.4, 25.7, 28.5, 33.4, 33.7, 33.8, 33.8, 38.3 [38.9], 54.0 [54.5], 56.0, 60.9, 61.0 [61.1], 66.3, 66.9, 67.2, 67.6, 68.6, 69.5, 74.3, 119.1 [119.2], 127.9, 128.2, 128.3, 128.4, 128.5, 128.7, 128.8, 128.9, 129.0, 130.3, 131.6, 131.9, 132.7, 136.1 [136.9], 153.7, 155.0, 172.7. HRMS (+ESI) calcd for C<sub>35</sub>H<sub>49</sub>NO<sub>10</sub> (M+H)<sup>+</sup>: 644.3356; obsd: 644.3395.



Cbz-Hyp(<sup>t</sup>Bu)- $\alpha$ -enylcarbamate **217**

*N,O*-Dimethylhydroxylamine hydrochloride (138 mg, 1.41 mmol, 1.5 equiv.) was added to a solution of Cbz-Hyp(O<sup>t</sup>Bu)-OH (**188**) (300 mg, 0.94 mmol, 1.0 equiv.) in DMF (3 mL) followed by the addition of HBTU (425 mg, 1.12 mmol, 1.2 equiv.) and DIEA (328  $\mu$ L, 243 mg, 1.88 mmol, 2.0 equiv.). The reaction mixture was stirred overnight under nitrogen. The solvent was removed and the residue dissolved in EtOAc (20 mL), washed with 1M HCl (2 x 20 mL), sat'd aq. NaHCO<sub>3</sub> (20 mL) and brine (20 mL). The organic layer was dried over MgSO<sub>4</sub>, filtered and concentrated to give Weinreb amide (**219**) (322 mg) that was used directly in the next step, without purification. *R<sub>f</sub>* 0.33 (1:1 EtOAc:Hexanes).

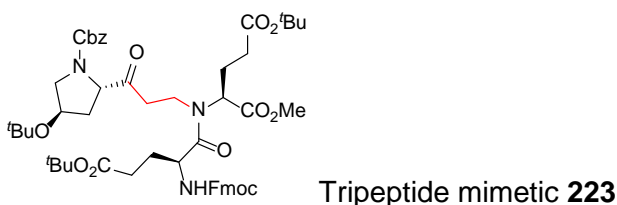
Vinyl magnesium bromide (1.7 mL, 1.67 mmol, 2.0 equiv.) was added in two portions over 1 h to a solution of Weinreb amide **219** (322 mg, 0.88 mmol, 1.0 equiv.) in anhydrous THF (10 mL) at -10 °C. The reaction mixture warmed to 0 °C and stirred for 3 h under nitrogen maintaining the temperature at 0 °C. The reaction was quenched by adding the reaction mixture dropwise to a solution of acetic anhydride (5 mL) and acetic acid (5 mL) at 0 °C. The combined solution was washed with water (30 mL) and the organic layer separated and washed with 1M HCl (2x30 mL) and brine (30 mL). The organic layer was dried over MgSO<sub>4</sub>, filtered and concentrated. The residue was applied to a flash column eluting with 1:1 Hexanes:EtOAc to give **217** (248 mg, 85%). *R<sub>f</sub>* 0.56 (1:1 Hexanes:EtOAc). <sup>1</sup>H NMR (CDCl<sub>3</sub>, 400 MHz) δ 1.16 (s, 9H), 1.94-2.04 (m, 1H), 2.08-2.20 (m, 1H), 3.32 (dd, *J* = 10.7, 5.2 Hz, 0.5H) [3.44 (dd, *J* = 11.04, 4.1 Hz, 0.5H)], 3.74-3.79 (m, 1H), 4.20-4.26 (m, 1H), 4.68-4.74 (m, 0.5H) [4.83 (dd, *J* = 8.9, 4.6 Hz, 0.5H)], 5.05 (s, 1H), 5.13 (d, *J* = 12.5 Hz, 1H), 5.16 (d, *J* = 12.5 Hz, 1H) 5.81 (2d, *J* = 9.82 Hz, 1H), 6.25-6.53 (m, 2H), 7.22-7.36 (m, 5H); <sup>13</sup>C NMR (CDCl<sub>3</sub>, 100 MHz) δ 28.5, 37.1 [38.2], 53.7 [54.6], 62.0 [62.2], 67.3, 68.7 [69.5], 74.3, 74.4 128.0, 128.1, 128.2, 128.5, 128.7, 130.1, 130.2, 132.5, 133.4, 136.9 [136.5], 155.2 [154.5], 198.7 [198.6]. HRMS (+ESI) calcd for C<sub>16</sub>H<sub>27</sub>NaO<sub>7</sub> (M+Na)<sup>+</sup>: 354.1649; obsd: 354.1667.



A solution mixture of H-Glu(O<sup>t</sup>Bu)-OMe (**218**) (130 mg, 0.6 mmol, 1.4 equiv.) and DIEA (166 μL, 123 mg, 0.95 mmol, 2.2 equiv.) in dry CH<sub>2</sub>Cl<sub>2</sub> (2 mL) was added dropwise to a solution of **217** in dry CH<sub>2</sub>Cl<sub>2</sub> (2 mL). The reaction mixture was stirred for 3.5 h at RT under nitrogen, concentrated and the residue applied to a flash column eluting with 1:2 EtOAc:Hexanes and then with 1:1 EtOAc:Hexanes to give the dipeptide mimetic **216** (236 mg, 95%). *R<sub>f</sub>* 0.36 (1:1 Hexanes:EtOAc). <sup>1</sup>H NMR (CDCl<sub>3</sub>, 400 MHz) δ 1.16 (s, 9H), 1.44 (s, 9H), 1.72-2.14 (m, 4H),

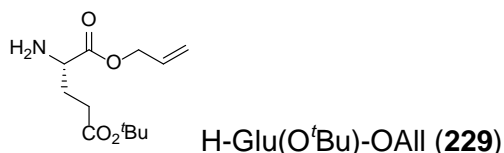


2.29 (apt. p,  $J = 7.7$  Hz, 2H), 2.43-2.52 (m, 1H), 2.62-2.71 (m, 2H), 2.73-2.79 [2.90-2.96] (m, 1H), 3.14 [3.23] (dd,  $J = 7.9, 5.7$  Hz, 1H), 3.31 (dd,  $J = 10.8, 5.0$  Hz, 0.5H) [3.43 (dd,  $J = 10.8, 3.9$  Hz, 0.5H)], 3.68-3.72 (m, 1H), 3.71 (s, 3H), 4.20-4.25 (m, 1H), 4.46 (app.dd,  $J = 8.4, 6.1$  Hz, 0.5 H) [4.53 (dd,  $J = 8.4, 5.5$  Hz, 0.5H)], 5.01-5.16 (m, 2H), 7.23-7.36 (m, 5H);  $^{13}\text{C}$  NMR ( $\text{CDCl}_3$ , 100 MHz)  $\delta$  28.3, 28.5, 28.6, 32.1 [32.0], 36.7 [37.7], 40.9 [40.1], 42.7 [42.5], 52.1, 53.9 [54.7], 61.1, 63.8, 67.4 [67.5], 69.5 [68.7], 74.3 [74.4], 80.5, 80.6, 128.1, 128.4, 128.7, 136.8, 155.3, 155.4, 172.6, 175.4. HRMS (+ESI) calcd for  $\text{C}_{29}\text{H}_{45}\text{N}_2\text{O}_8$  ( $\text{M}+\text{H}$ ) $^+$  : 549.3170; obscd: 549.3185.



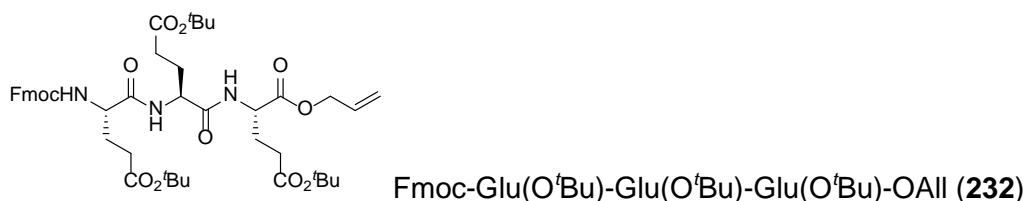
A solution of Fmoc-Glu-OH (**221**) (80 mg, 0.18 mmol, 1.5 equiv.) in dry  $\text{CH}_2\text{Cl}_2$  (2 mL) was added to a solution of **216** (67 mg, 0.12 mmol, 1 equiv.) in dry  $\text{CH}_2\text{Cl}_2$  (2 mL), followed by the addition of DIEA (54  $\mu\text{L}$ , 40 mg, 0.31 mmol, 2.5 equiv.) and HATU (56 mg, 0.15 mmol, 1.2 equiv.). The reaction mixture was stirred for 2 days under  $\text{N}_2$ , concentrated and applied to a flash column eluting with 1:1 EtOAc:Hexanes to give **223** (90 mg, 77%).  $R_f$  0.28 (1:1 Hexanes:EtOAc).  $^1\text{H}$  NMR ( $\text{CDCl}_3$ , 400 MHz)  $\delta$  1.16 [1.17] (s, 9H), 1.44 [1.45] (s, 18H), 1.71-1.90 (m, 4H), 1.93-2.13 (m, 4H), 2.25-2.45 (m, 2H), 2.43-2.53 (m, 2H), 2.63-2.79 [2.91-2.97] (m, 2H), 3.24 [3.15] (app.dd,  $J = 6.2, 7.4$  Hz, 1H), 3.39-3.42 (m, 0.9H) [3.31 (dd,  $J = 10.8, 4.9$  Hz, 0.1 H)], 3.49-3.65 (m, 1.8 H) [3.44 (app. t,  $J = 6.1$  Hz, 0.2 H)], 3.69-3.73 (m, 1H), 3.72 (s, 3H), 4.20-4.25 (m, 2H), 4.35 (d,  $J = 7.2$  Hz, 2H), 4.44-4.57 (m, 1H), 5.00-5.16 (m, 2H), 5.80 (d,  $J = 8.4$  Hz, 1H), 7.25-7.41 (m, 9H), 7.60 (t,  $J = 6.2$  Hz, 2H), 7.75 (d,  $J = 7.5$  Hz, 2H);  $^{13}\text{C}$  NMR ( $\text{CDCl}_3$ , 100 MHz)  $\delta$  24.2, 26.1, 27.9, 28.2, 28.3, 28.4, 30.9, 31.9 [31.8], 36.5 [37.7], 40.7 [39.9], 42.5 [42.3], 46.1 [46.5], 47.3, 51.9 [51.8], 53.7 [54.5], 60.9, 63.6, 67.1, 67.2 [67.4], 69.3 [68.6], 74.2 [74.3], 80.7, 120.0, 125.3, 127.2, 127.8, 127.9, 128.1, 128.2, 128.6, 136.7 [136.3], 141.4,

144.1, 143.9, 155.2 [154.3], 156.2, 170.0, 172.3 [172.4], 175.3 [175.2]. HRMS (+ESI) calcd for  $C_{53}H_{69}N_3NaO_{13}$  (M+H)<sup>+</sup> : 979.4762; obsd: 979.4860.



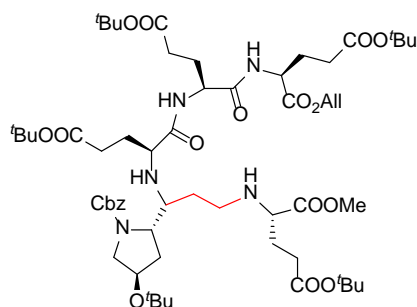
Cesium carbonate (192 mg, 0.58 mmol, 0.50 equiv.) was added to a solution of Fmoc-Glu-OH (**221**) (500 mg, 1.14 mmol, 1.00 equiv.) in dry MeOH (4 mL) at 0 °C. The reaction mixture was stirred for 20 min at 0 °C then 2 h at RT. The solvent was removed and the residue dissolved in DMF (4 mL). Allyl bromide (100  $\mu$ L, 138 mg, 1.14 mmol, 1.0 equiv.) was added to the mixture which was stirred overnight. The mixture was diluted with EtOAc (30 mL) and washed with water (30 mL) and brine (30 mL) and dried over MgSO<sub>4</sub>. The filtrate was concentrated to yield Fmoc-Glu-OAll (**228**) as a colorless solid. (420 mg, 80%). This was used directly in the next step, without purification.  $R_f$  0.73 (1:1 EtOAc:hexanes).

Diethylamine (2 mL) was added to a solution of **228** (420 mg, 1.14 mmol) in dry acetonitrile (2 mL). The reaction mixture was stirred for 6 h under nitrogen, concentrated and applied to a flash column eluting with 2:1 EtOAc:Hexanes to elute the Fmoc-protected products and then with 9:1 CH<sub>2</sub>Cl<sub>2</sub>:MeOH to give H-Glu-OAll (**229**) (283 mg, 85% over 2 steps).  $R_f$  0.69 (9:1 CH<sub>2</sub>Cl<sub>2</sub>:MeOH). <sup>1</sup>H NMR (CDCl<sub>3</sub>, 400 MHz)  $\delta$  1.24 (s, 9H), 1.54-1.65 (m, 1H), 1.81-1.87 (m, 1H), 2.17 (app. t,  $J$  = 7.5 Hz, 2H), 3.26-3.32 (m, 1H), 4.38-4.43 (m, 2H), 5.05 (dd,  $J$  = 10.4, 1.2 Hz, 1H), 5.13 (dd,  $J$  = 17.2, 1.4 Hz, 1H), 5.67-5.78 (m, 1H); <sup>13</sup>C NMR (CDCl<sub>3</sub>, 100 MHz)  $\delta$  28.1, 29.9, 31.7, 53.8, 65.5, 80.3, 118.6, 131.9, 172.3, 175.4.



*N*-Hydroxysuccinimide (109 mg, 0.94 mmol, 1.0 equiv.) was added to a solution of Fmoc-Glu(O<sup>t</sup>Bu)-OH (**221**) (400 mg, 0.94 mmol, 1.0 equiv.) in dry CH<sub>2</sub>Cl<sub>2</sub> (4 mL). The mixture was stirred for 10 min, then DCC (194 mg, 0.94 mmol, 1.0 equiv.) was added and stirring continued for 4 h under N<sub>2</sub>. The mixture was filtered and the filtrate was concentrated to approximately 1 mL and placed in the freezer for 2 h. The mixture was refiltered, concentrated and dried. The residue was dissolved in DMF (5 mL). H-Glu(O<sup>t</sup>Bu)-OH (191 mg, 0.94 mmol, 1.0 equiv.) was added followed by the addition of DIEA (180 μL, 133 mg, 1.03 mmol, 1.1 equiv.). The reaction was stirred overnight under N<sub>2</sub>. The reaction mixture was diluted with ethyl acetate (25 mL) and washed with 1M HCl. The aqueous layer was back-extracted with ethyl acetate (20 mL). The organic layers were combined, washed with brine (40 mL), dried over MgSO<sub>4</sub>, filtered and concentrated to give Fmoc-Glu(O<sup>t</sup>Bu)-Glu(O<sup>t</sup>Bu)-OH (**215**) 480 mg that was used in subsequent reactions, without purification. *R*<sub>f</sub> 0.32 (9:1 CH<sub>2</sub>Cl<sub>2</sub>:MeOH).

A solution of H-Glu(O<sup>t</sup>Bu)-OAll (**229**) (50 mg, 0.36 mmol, 1.1 equiv.) in CH<sub>2</sub>Cl<sub>2</sub> (1 mL) was added to a solution of **215** (169 mg, 0.27 mmol, 1.0 equiv.) in CH<sub>2</sub>Cl<sub>2</sub> (2 mL), followed by the addition of DIEA (112 μL, 83 mg, 0.64 mmol, 2.0 equiv.) and HATU (159 mg, 0.42 mmol, 1.3 equiv.). The reaction mixture was stirred overnight under N<sub>2</sub>, concentrated and applied to a flash column eluting with 2:1 Hexanes:EtOAc to give **232** (226 mg, 87%) (*R*<sub>f</sub> 0.32 (9:1 CH<sub>2</sub>Cl<sub>2</sub>:MeOH). <sup>1</sup>H NMR (CDCl<sub>3</sub>, 400 MHz) δ 1.42 (s, 9H), 1.44 (s, 9H), 1.46 (s, 9H), 1.89-2.02 (m, 3H), 2.05-2.21 (m, 3H), 2.24-2.47 (m, 6H), 4.21 (t, *J* = 6.9 Hz, 1H), 4.33-4.43 (m, 1H), 4.47 (dd, *J* = 13.0, 7.1 Hz, 1H), 4.56 (dd, *J* = 13.0, 7.7 Hz, 1H), 4.62 (d, *J* = 5.8 Hz, 2H), 5.24 (dd, *J* = 10.4, 1.0 Hz, 1H), 5.32 (dd, *J* = 17.2, 1.3 Hz, 1H), 5.83-5.93 (m, 2H), 7.26-7.33 (m, 3H), 7.40 (t, *J* = 7.4 Hz, 2H), 7.60 (d, *J* = 7.2 Hz, 2H), 7.76 (d, *J* = 7.5 Hz, 2H); <sup>13</sup>C NMR (CDCl<sub>3</sub>, 400 MHz) δ 27.2, 28.0, 28.3, 28.4, 31.7, 31.9, 32.0, 47.4, 52.2, 52.3, 54.9, 66.3, 67.4, 81.1, 81.4, 119.2, 120.2, 125.4, 127.3, 128.0, 131.8, 141.5, 144.0, 144.1, 156.5, 171.1, 171.4, 171.5, 172.3, 173.2, 173.4. HRMS (+ESI) calcd for C<sub>45</sub>H<sub>6</sub>N<sub>3</sub>NaO<sub>12</sub> (M+Na)<sup>+</sup>: 858.4184; obsd: same.

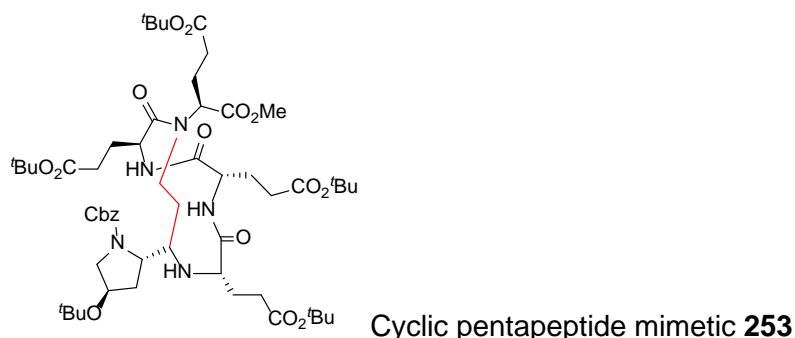


Pseudo pentapeptide mimetic **234**

*H*-Glu(O<sup>t</sup>Bu)-Glu(O<sup>t</sup>Bu)-(O<sup>t</sup>Bu)-OAll (**233**): Diethylamine (1.5 mL) was added to a solution of **232** (144 mg, 0.18 mmol) in dry acetonitrile (1.5 mL). The reaction mixture was stirred for 4 h under nitrogen, concentrated and applied to a flash column eluting with 2:1 EtOAc:Hexanes to elute the Fmoc-related products and then with 9:1 CH<sub>2</sub>Cl<sub>2</sub>:MeOH to give **233** (96 mg). *R<sub>f</sub>* 0.64 (9:1 CH<sub>2</sub>Cl<sub>2</sub>:MeOH).

A solution of *H*-Glu(O<sup>t</sup>Bu)-Glu(O<sup>t</sup>Bu)-(O<sup>t</sup>Bu)-OAll (**233**) (96 mg, 0.17 mmol, 1.30 equiv.) in dichloroethane (1 mL) was added to a solution of dipeptide mimetic **216** (71 mg, 0.13 mmol, 1.00 equiv.) in dichloroethane (1 mL), followed by the addition of Et<sub>3</sub>N (54 μL, 41 mg, 0.4 mmol, 3.00 equiv.). The reaction mixture was stirred overnight under nitrogen. The solvent was removed and the residue was dissolved in dichloroethane (3 mL). Sodiumtriacetoxymethylborohydride (72 mg, 0.33 mmol, 2.60 equiv.) was added to the reaction mixture and stirring continued for 2 d under nitrogen. The reaction mixture was concentrated, diluted with EtOAc (10 mL) and washed with sat'd aq. NaHCO<sub>3</sub> (10 mL). The organic layer was dried over MgSO<sub>4</sub>, filtered, concentrated and applied to a flash column eluting with 1:1 EtOAc:Hexanes to give **234** (16 mg, 11%). *R<sub>f</sub>* 0.63 (3:1 EtOAc:Hexanes). <sup>1</sup>H NMR (CDCl<sub>3</sub>, 400 MHz) δ 1.18 (s, 9H), 1.46 (s, 36H), 1.81 (dd, *J* = 14.0, 7.1 Hz, 1H), 1.89-2.04 (m, 4H), 2.06-2.20 (m, 3H), 2.28-2.42 (m, 9H), 2.50-2.69 (m, 2H), 2.78-2.89 (m, 2H), 3.10[2.99] (t, *J* = 6.4 Hz, 1H), 3.33-3.37 (m, 1H), 3.50 (dd, *J* = 8.2, 5.3 Hz, 2H), 3.77 (s, 3H), 4.25 (app.t, *J* = 5.5 Hz, 1H), 4.41-4.50 (m, 2H), 4.58-4.64 (m, 5H), 5.03-5.18 (m, 3H), 5.26 (dd, *J* = 10.4, 1.1 Hz, 1H), 5.34 (d, *J* = 17.2 Hz, 1H), 5.86-5.94 (m, 1H), 7.10-7.38

(m, 7H), 7.91 [7.82] (d, J = 8.2 Hz, 1H). HRMS (ESI+) calcd for C<sub>59</sub>H<sub>95</sub>N<sub>5</sub>NaO<sub>17</sub> (M+Na)<sup>+</sup> : 1169.6654; obsd: 1069.5869.

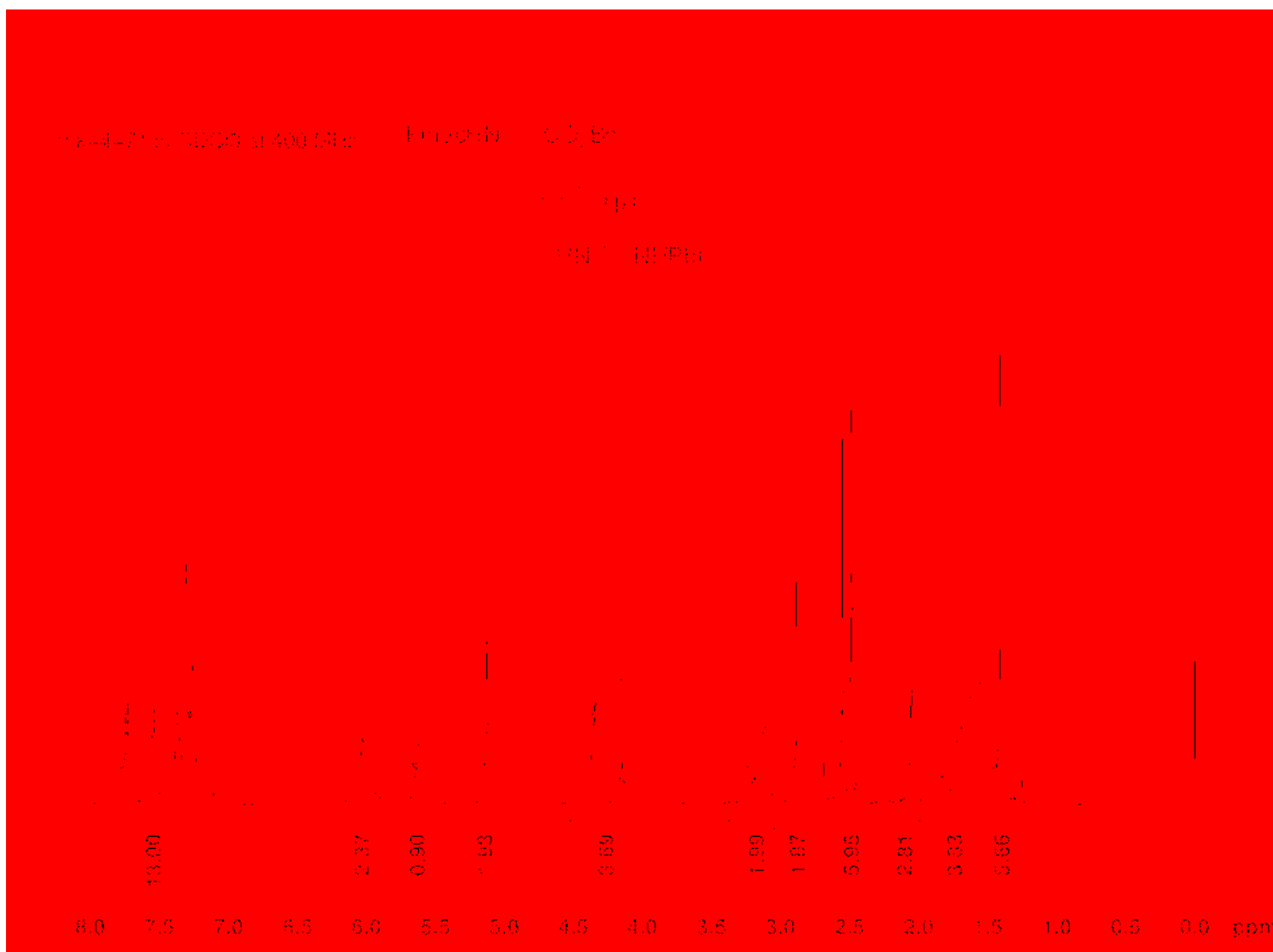


*Tetrakis*(triphenylphosphine)palladium(0) (0.8 mg, 0.0007 mmol, 0.10 equiv.) and dimedone (2 mg, 0.014 mmol, 2.00 equiv.) were added to a solution of **234** (8 mg, 0.007 mmol, 1.00 equiv.) in CH<sub>2</sub>Cl<sub>2</sub> (2 mL). The reaction mixture was stirred 16 h under N<sub>2</sub>, concentrated and applied to a flash column eluting with 9:1 CH<sub>2</sub>Cl<sub>2</sub>:MeOH to remove the triphenylphosphine-related biproducts and then flushed with 4:1 CH<sub>2</sub>Cl<sub>2</sub>:MeOH to get the free acid **253** (3 mg, 39%).

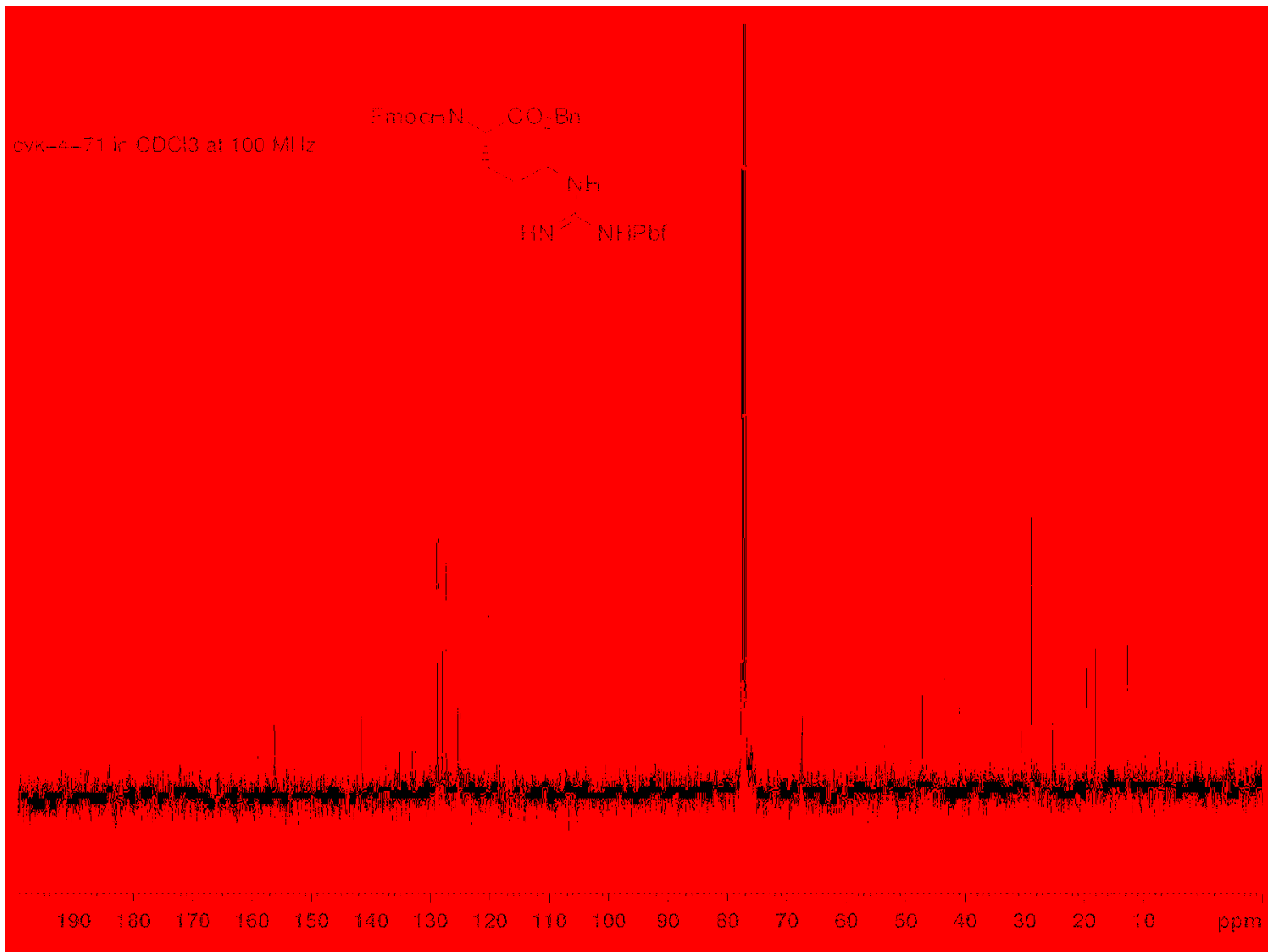
1-Ethyl-3-(3-dimethylaminopropyl)carbodiimide hydrochloride (3 mg, 0.012 mmol, 4.00 equiv.) and Et<sub>3</sub>N (1.5 μL, 1 mg, 0.009 mmol, 3.00 equiv.) were added to a solution of free acid **252** (3 mg, 0.003 mmol, 1.00 equiv.) in DMF (1.5 mL), followed by HOBt (2 mg, 0.012 mmol, 4.00 equiv.). The reaction mixture was stirred under nitrogen for 2 d, concentrated and applied to a flash column eluting with 2:1 EtOAc:Hexanes and then 9:1 CH<sub>2</sub>Cl<sub>2</sub>:MeOH to give **253** (1.5 mg, 46%). *R<sub>f</sub>* 0.47 (9:1 CH<sub>2</sub>Cl<sub>2</sub>:MeOH).

## 4.12.2 $^1\text{H}$ and $^{13}\text{C}$ NMR Spectra

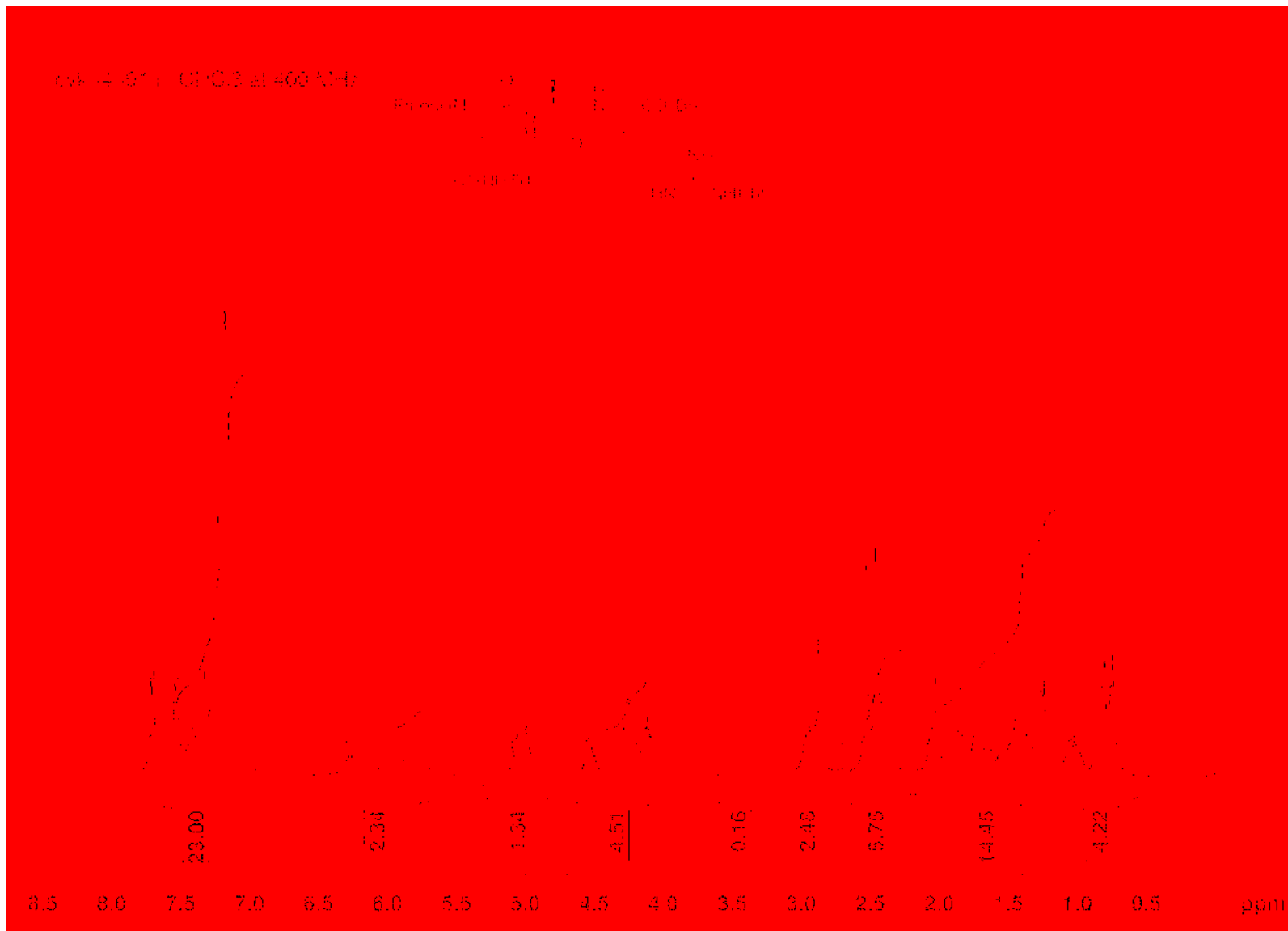
### Fmoc-Arg(NHPbf)-OBn (**138**)



Fmoc-Arg(NHPbf)-OBn (138)



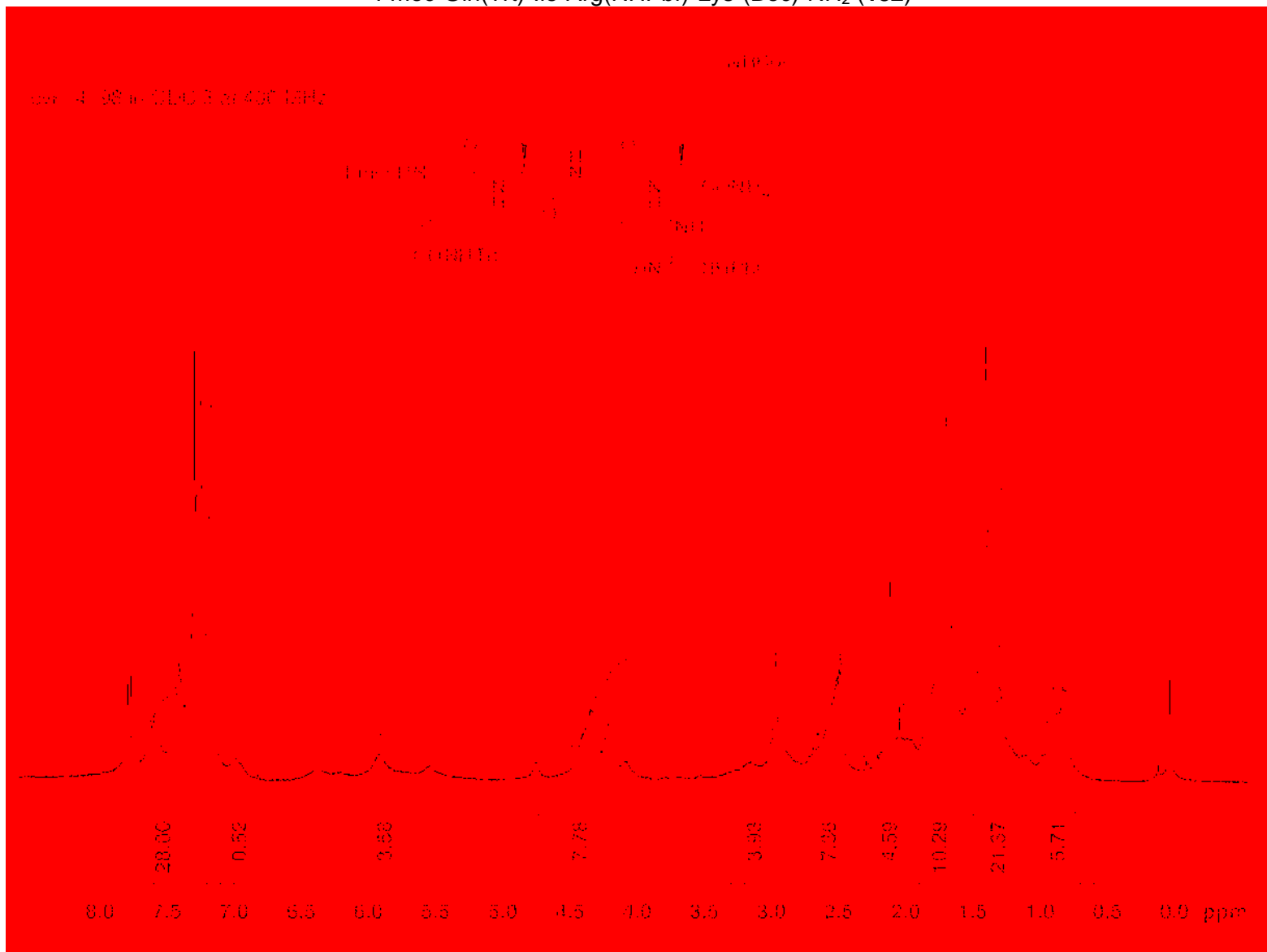
Fmoc-Gln(Trt)-Ile-Arg(NHPbf)-OBn (143)







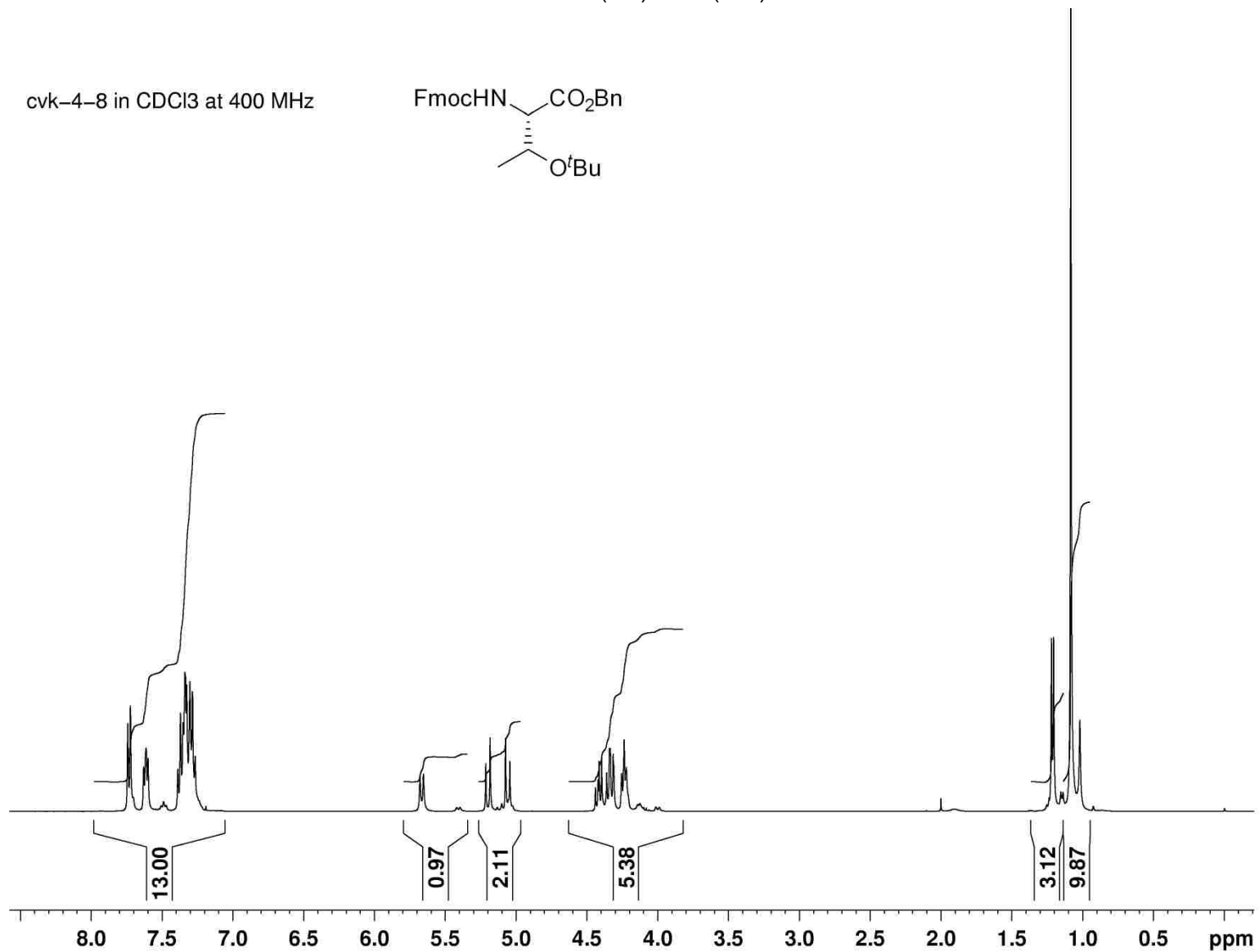
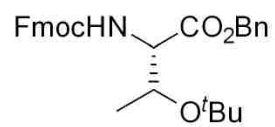
Fmoc-Gln(Trt)-Ile-Arg(NHPbf)-Lys-(Boc)-NH<sub>2</sub> (132)



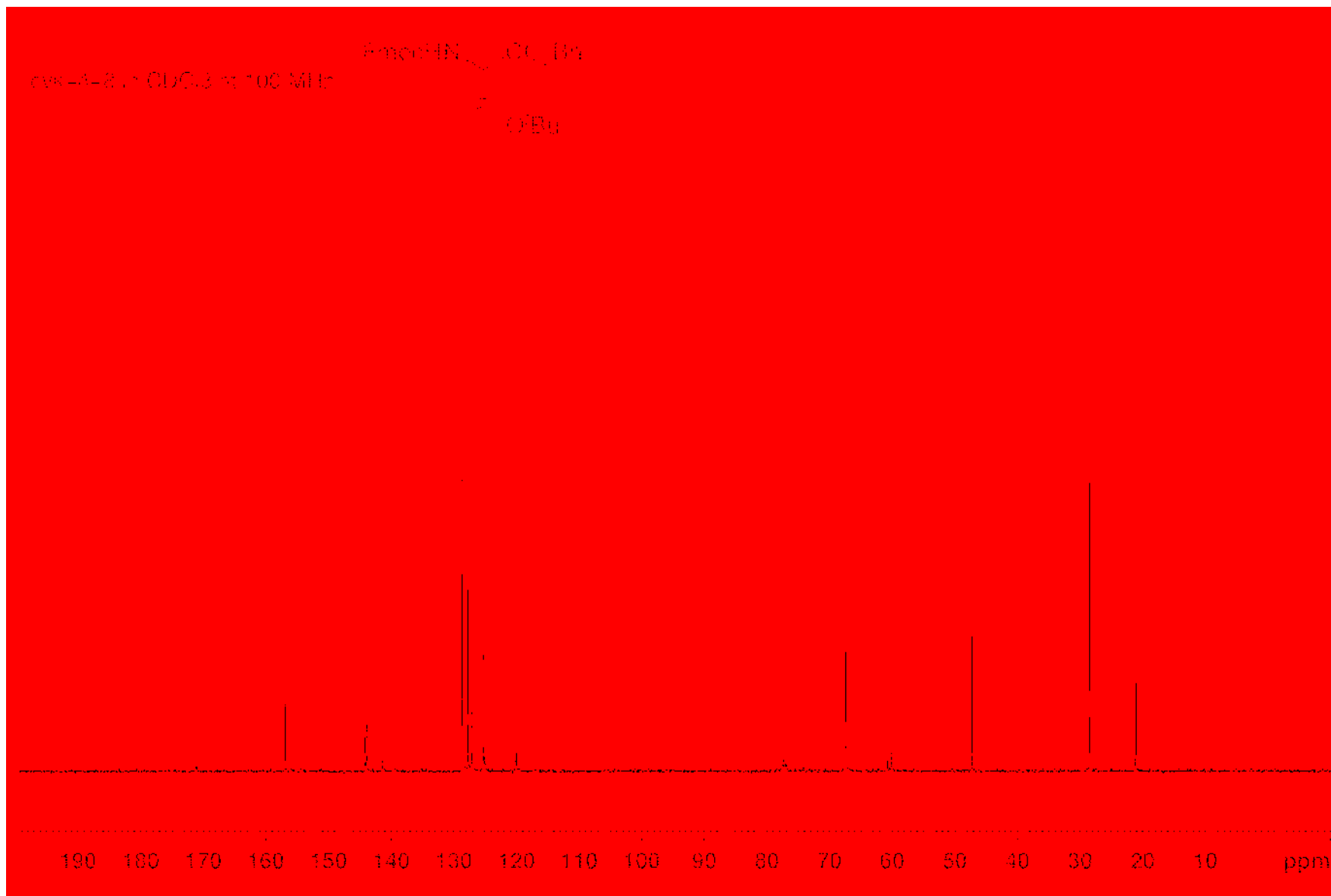


Fmoc-Thr(<sup>t</sup>Bu)-OBn (145)

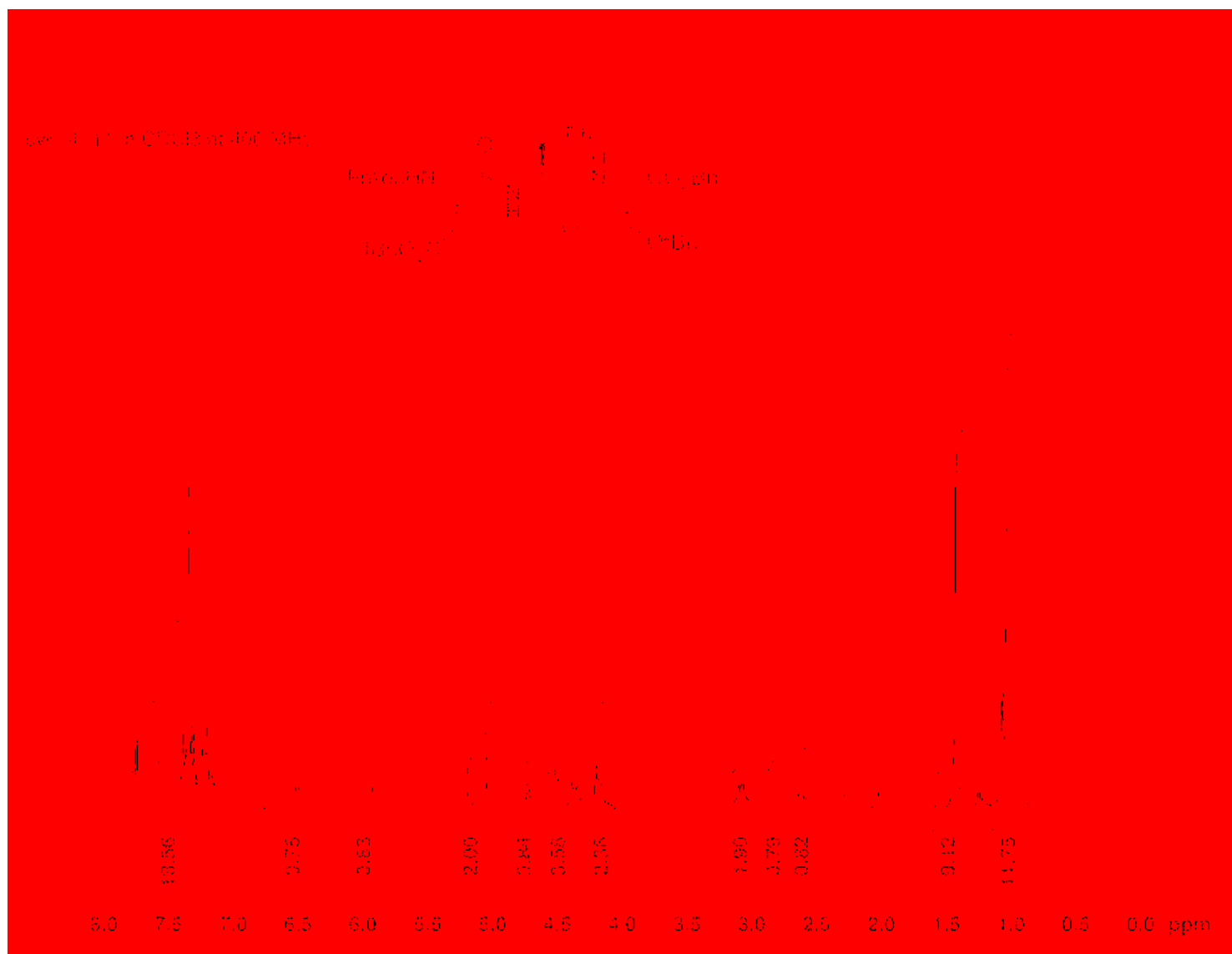
cvk-4-8 in CDCl<sub>3</sub> at 400 MHz



Fmoc-Thr(<sup>t</sup>Bu)-OBn (145)



Fmoc-Asp(O<sup>t</sup>Bu)-Phe-Thr(<sup>t</sup>Bu)-OBn (**150**)



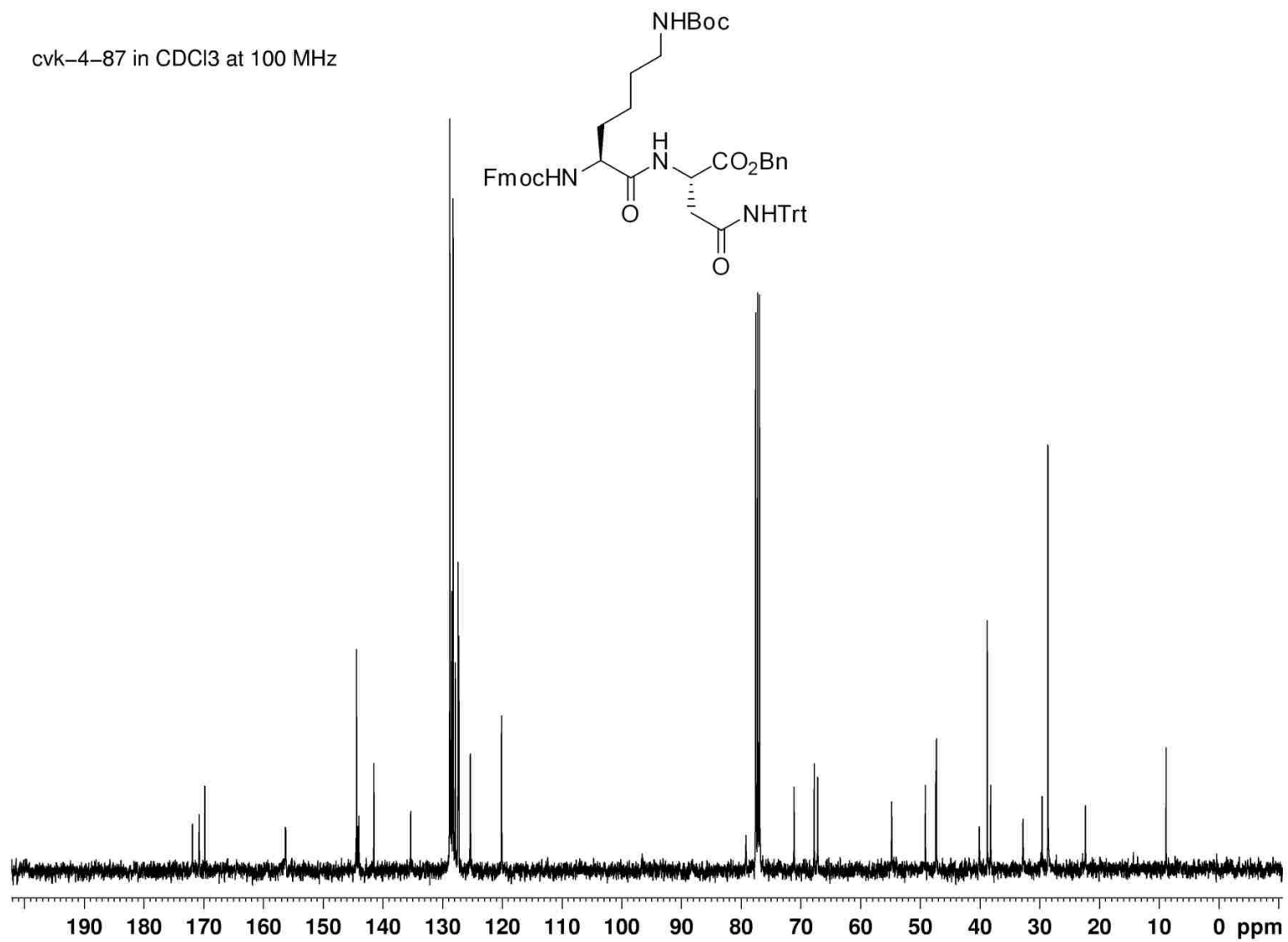




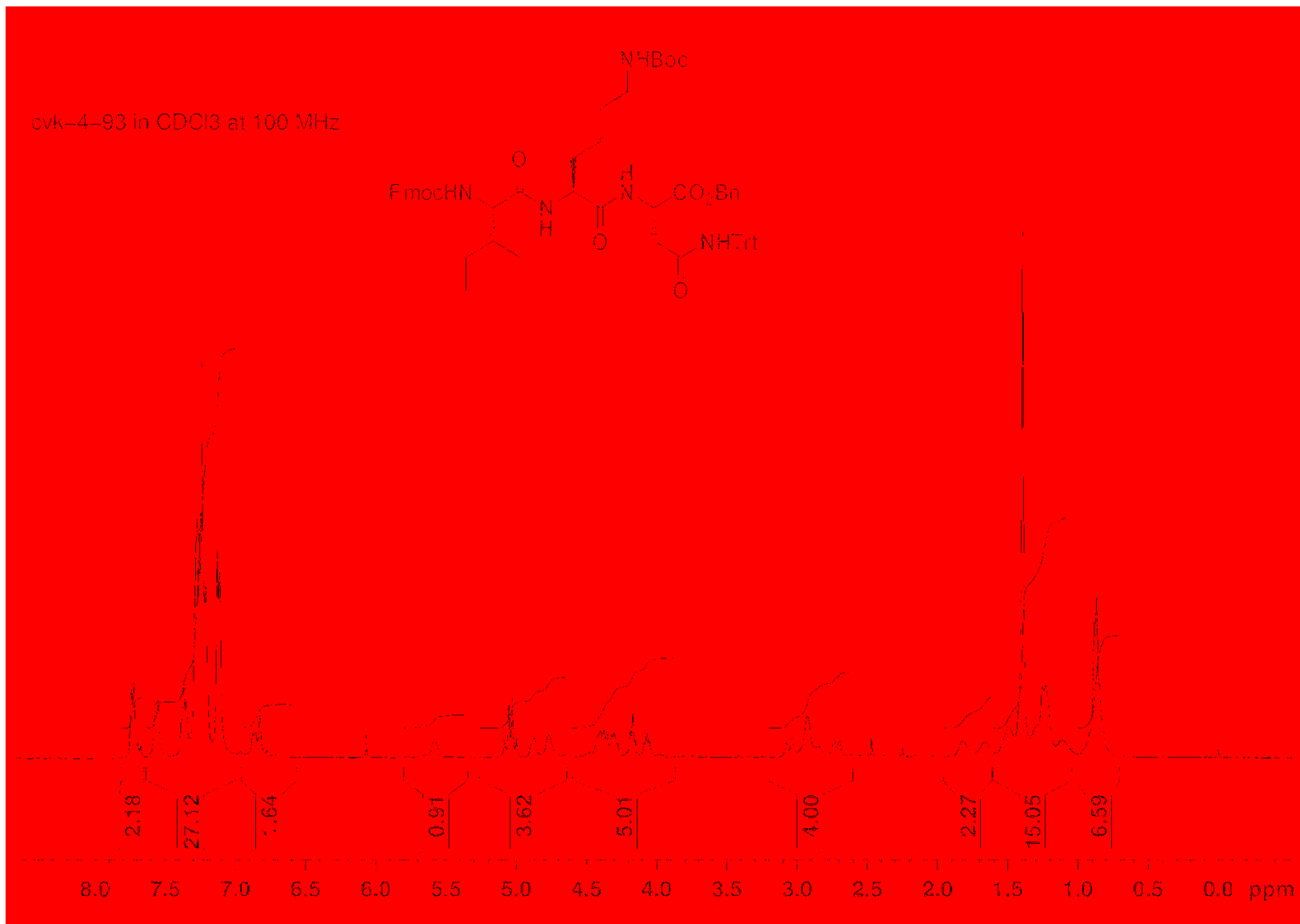


Fmoc-Lys(Boc)-Asn-OBn (**168**)

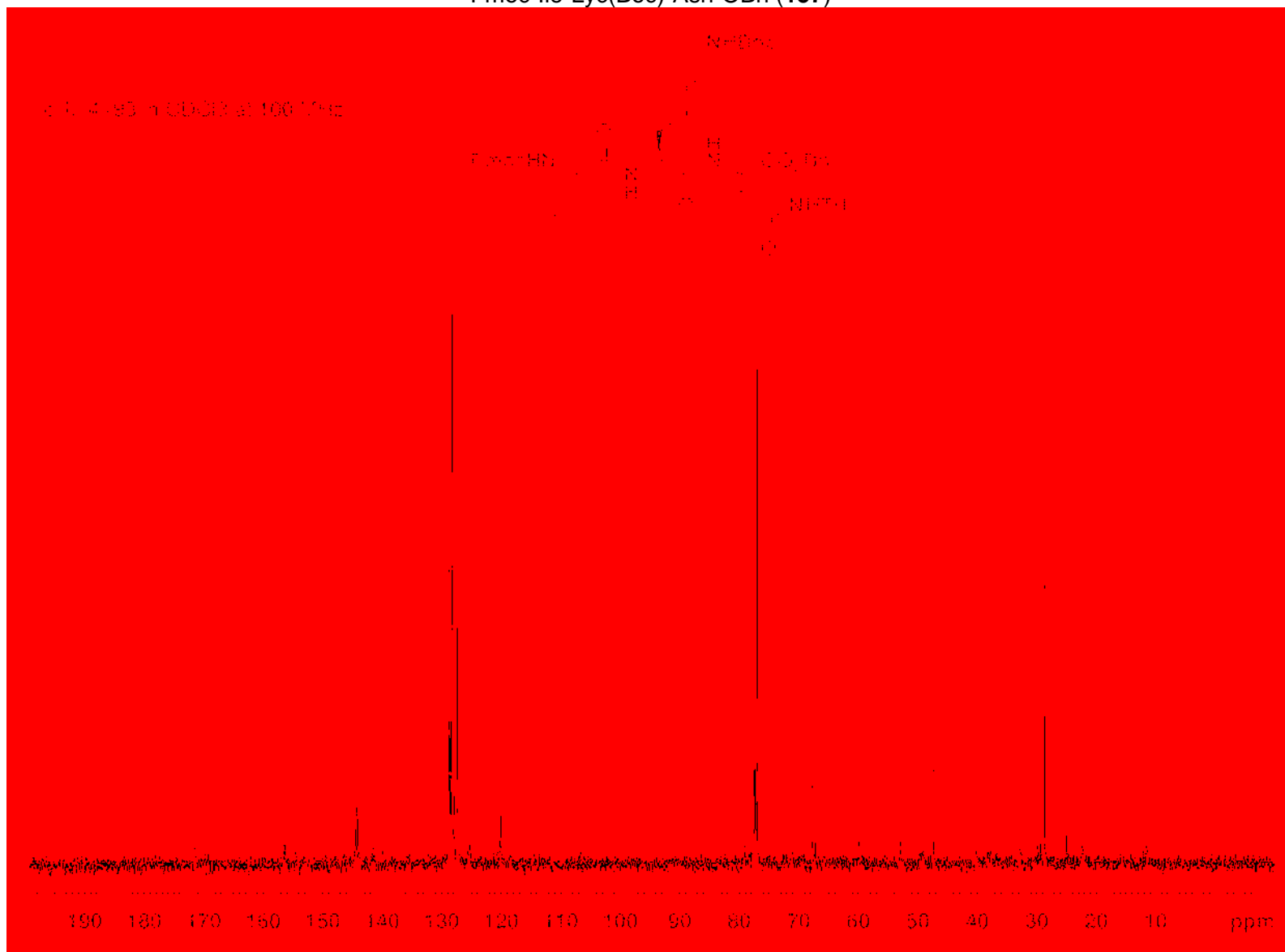
cvk-4-87 in CDCl<sub>3</sub> at 100 MHz



Fmoc-Ile-Lyc(Boc)-Asn-OBn (157)



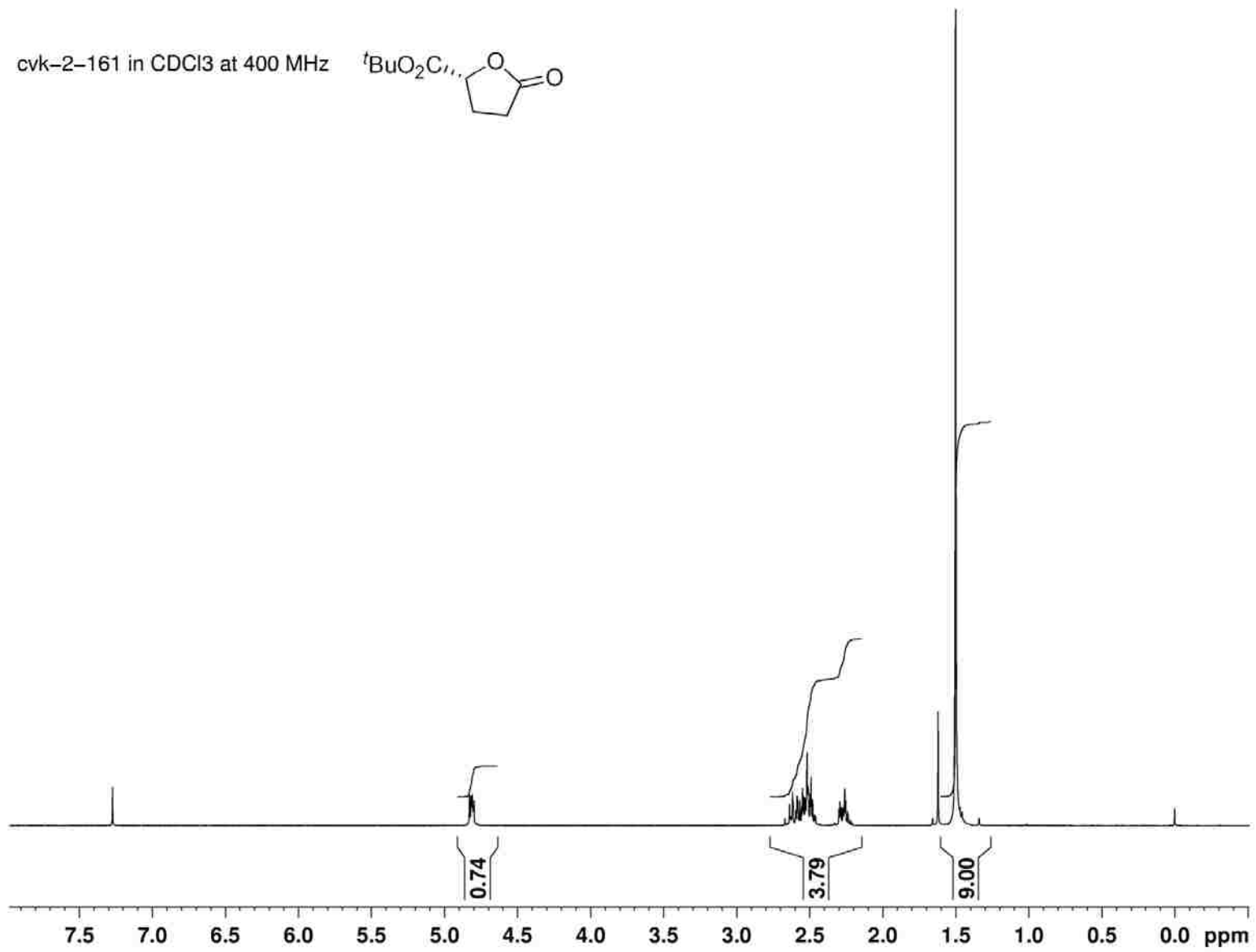
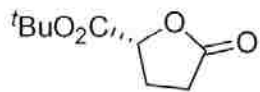
Fmoc-Ile-Lyc(Boc)-Asn-OBn (157)





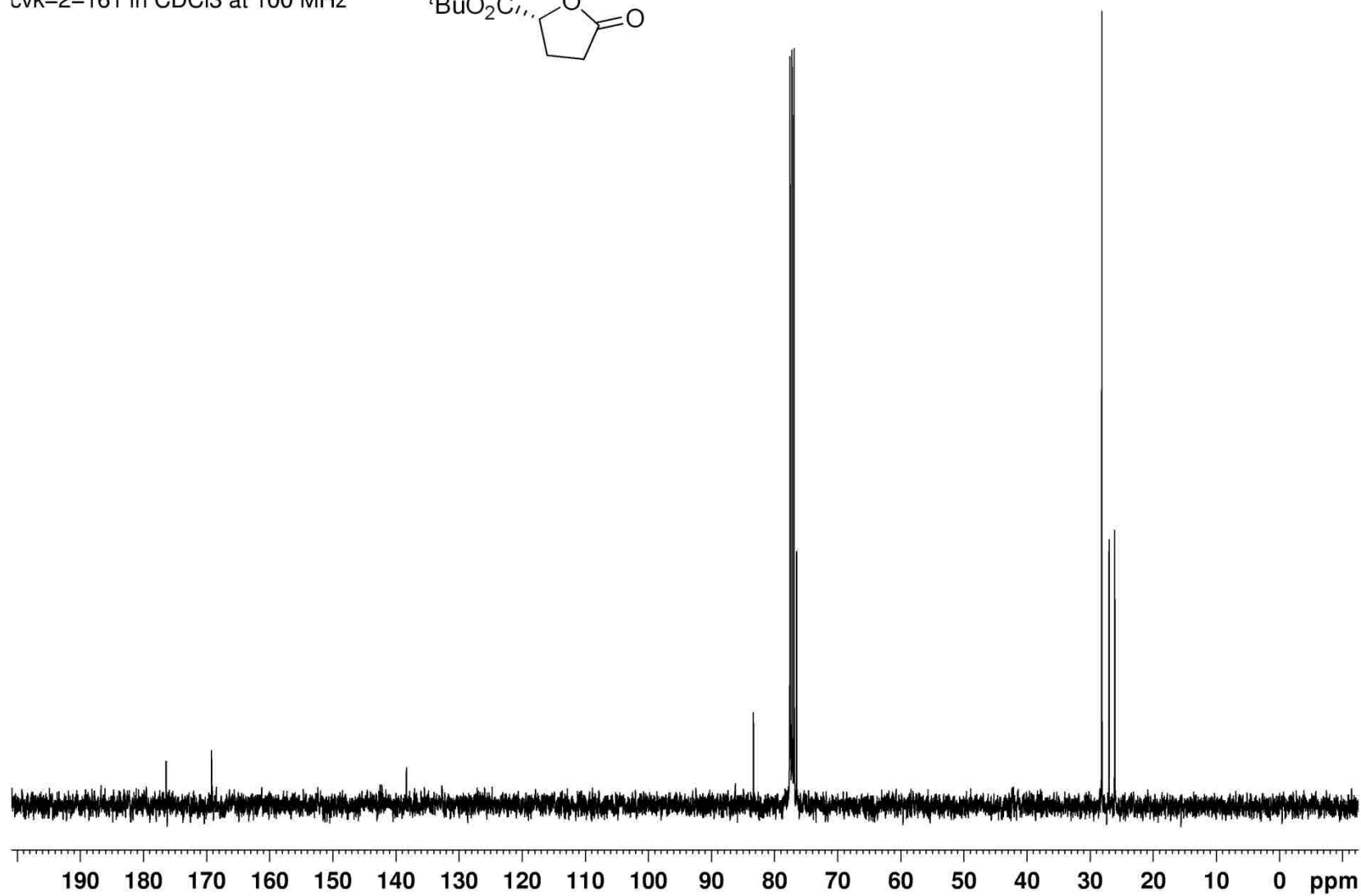
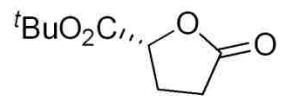
Lactone 185

cvk-2-161 in CDCl<sub>3</sub> at 400 MHz



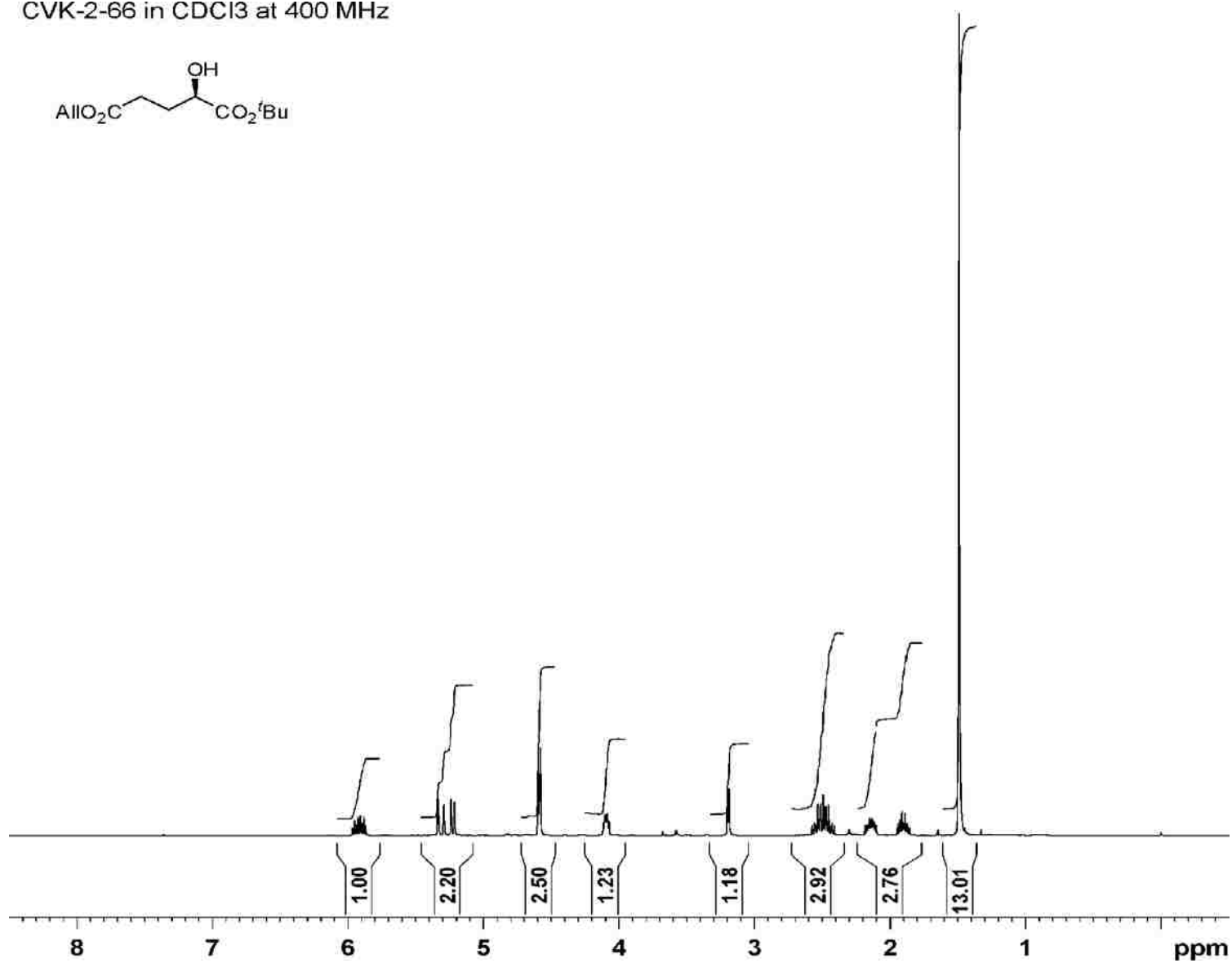
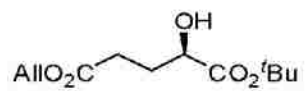
Lactone 185

cvk-2-161 in CDCl<sub>3</sub> at 100 MHz



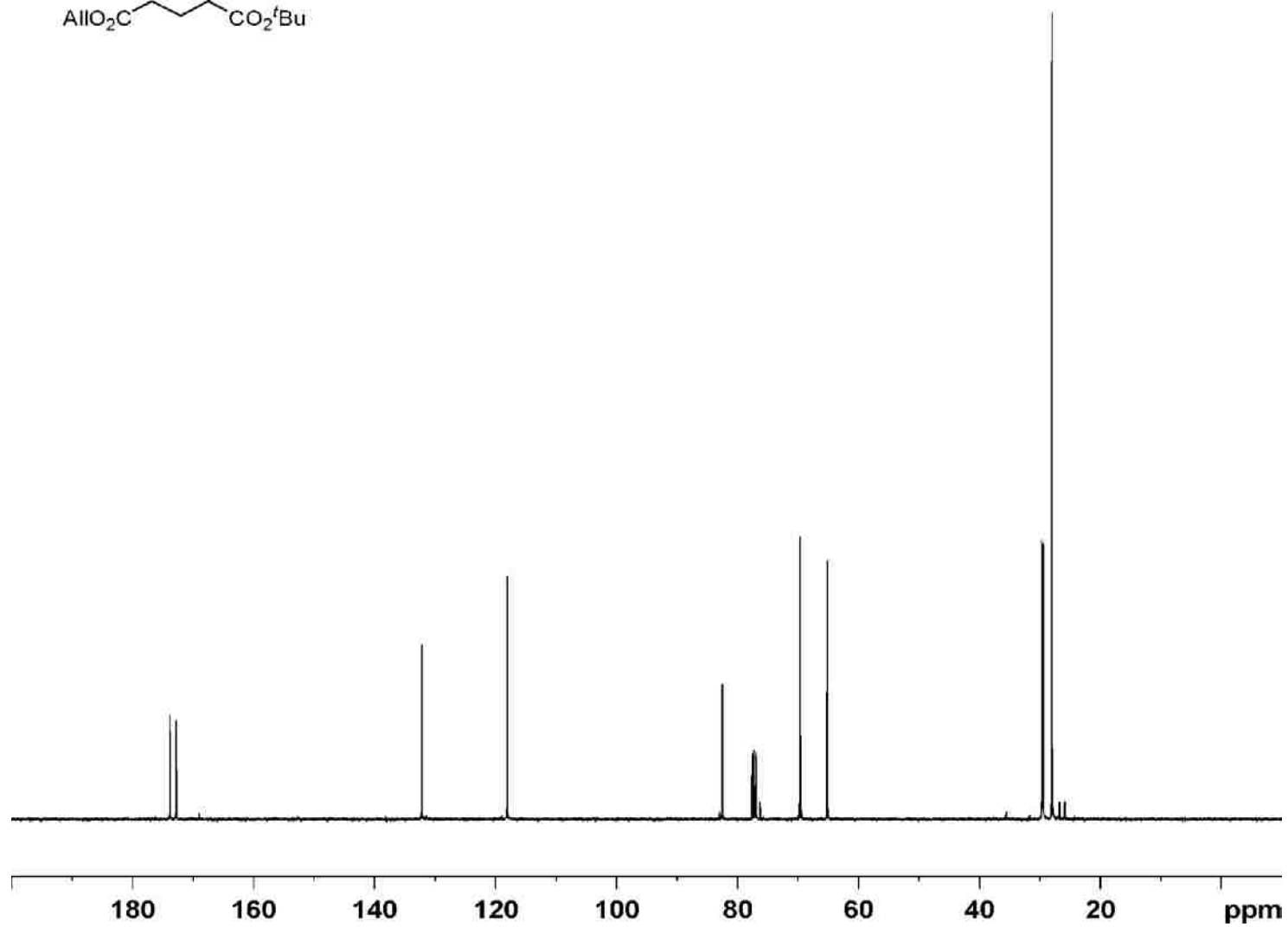
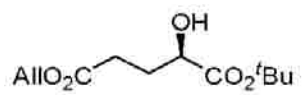
Alcohol 187

CVK-2-66 in CDCl<sub>3</sub> at 400 MHz



Alcohol 187

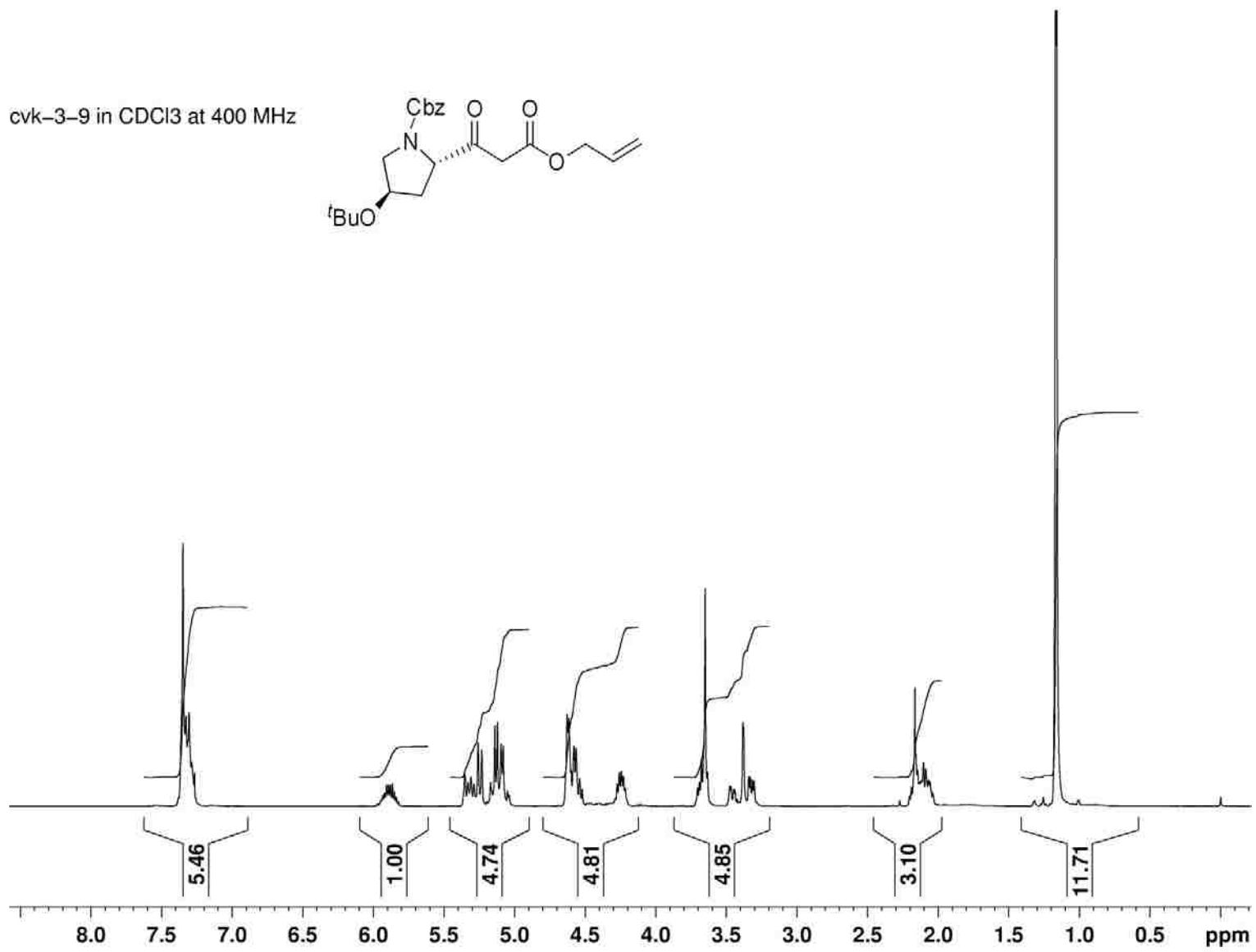
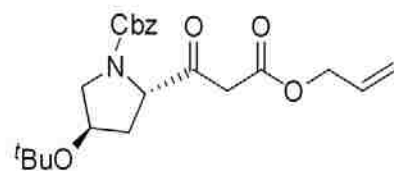
CVK-2-66 in CDCl<sub>3</sub> at 100 MHz





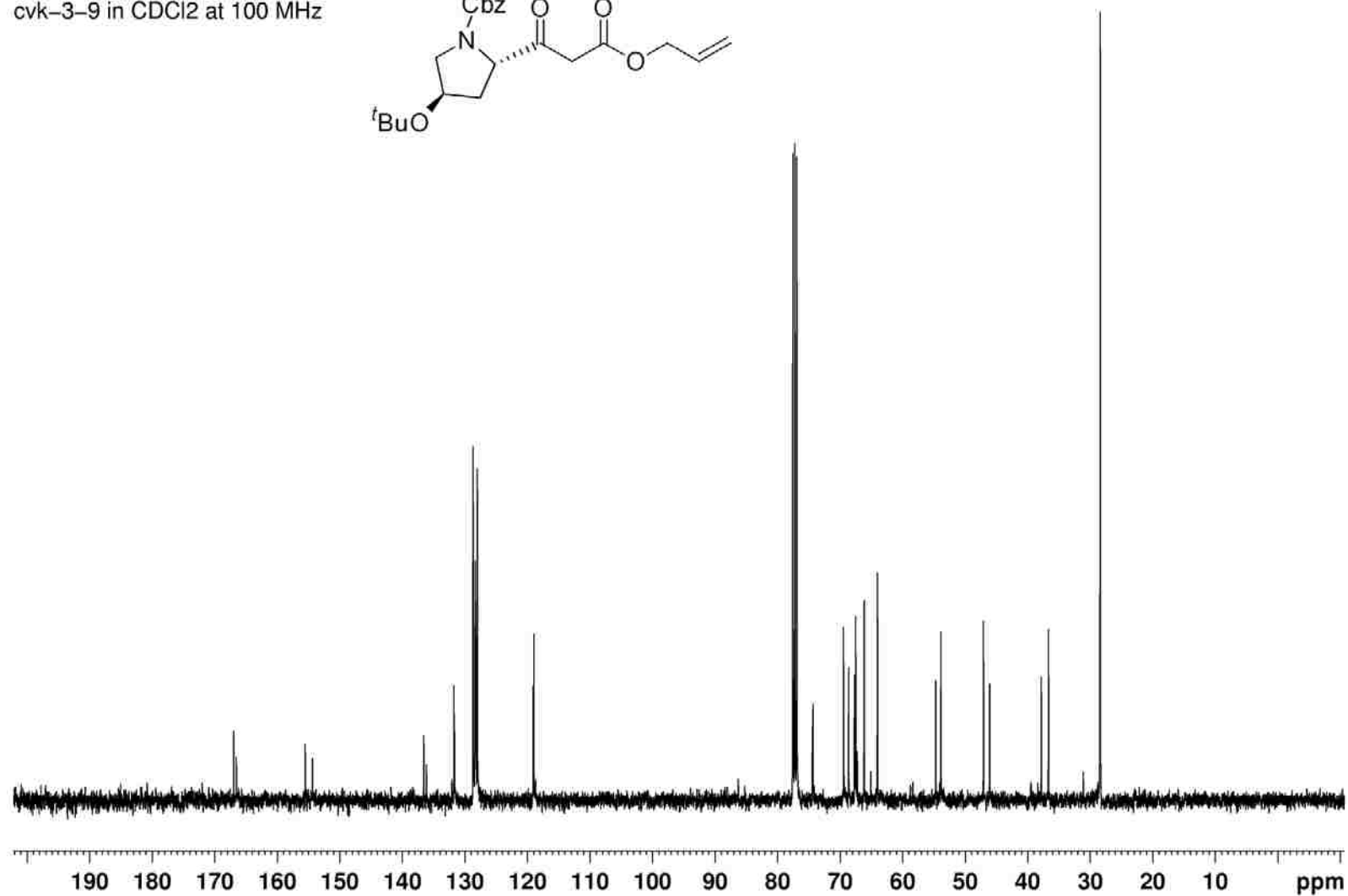
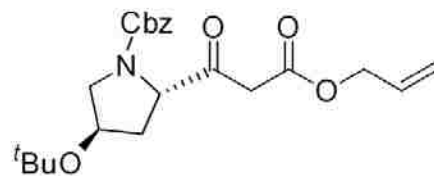
Compound 135

cvk-3-9 in CDCl<sub>3</sub> at 400 MHz



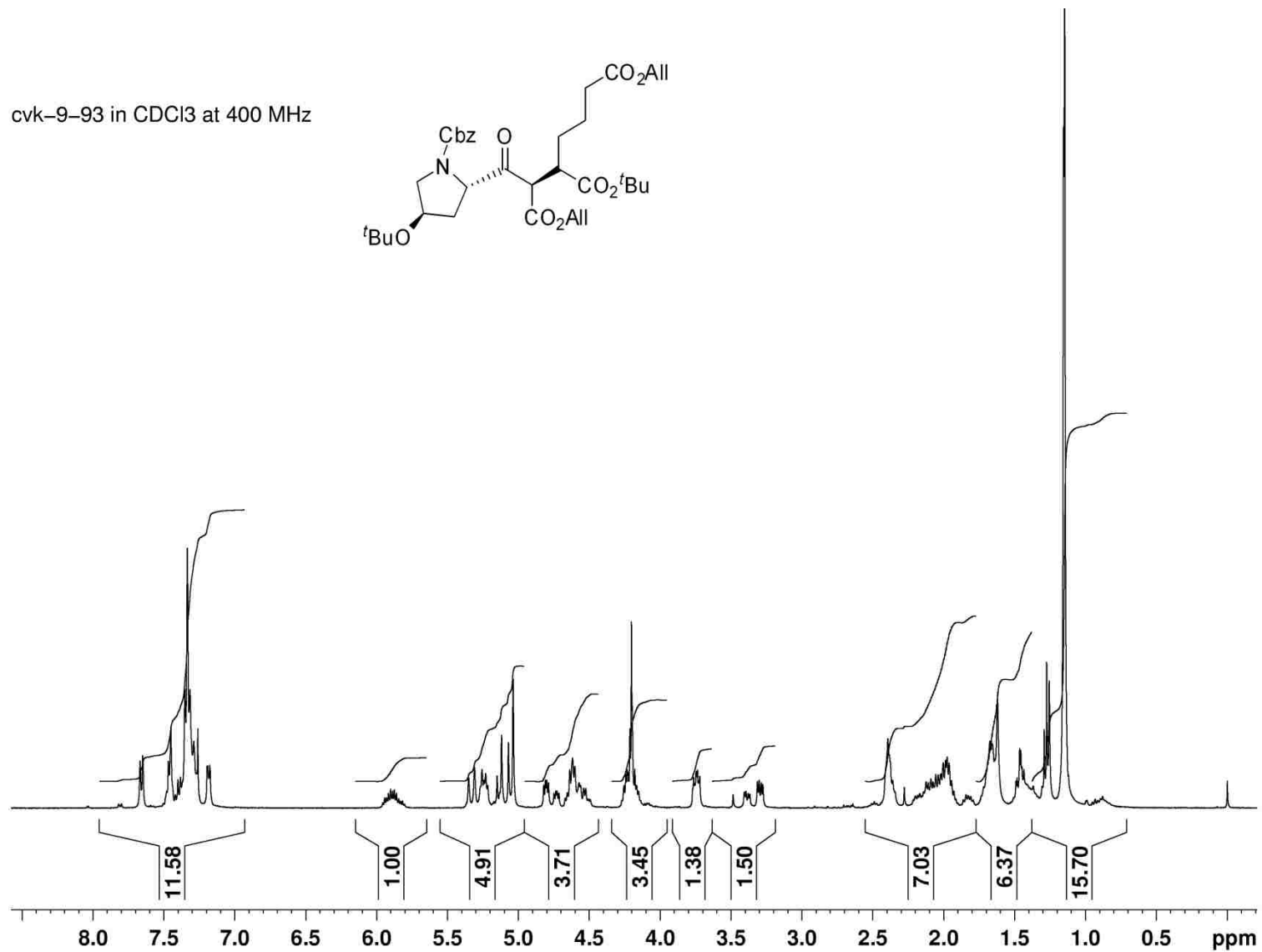
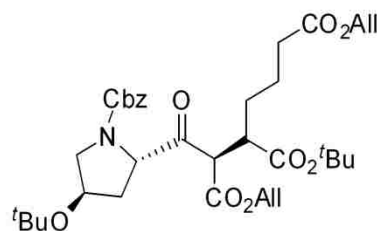
Compound 135

cvk-3-9 in CDCl<sub>2</sub> at 100 MHz



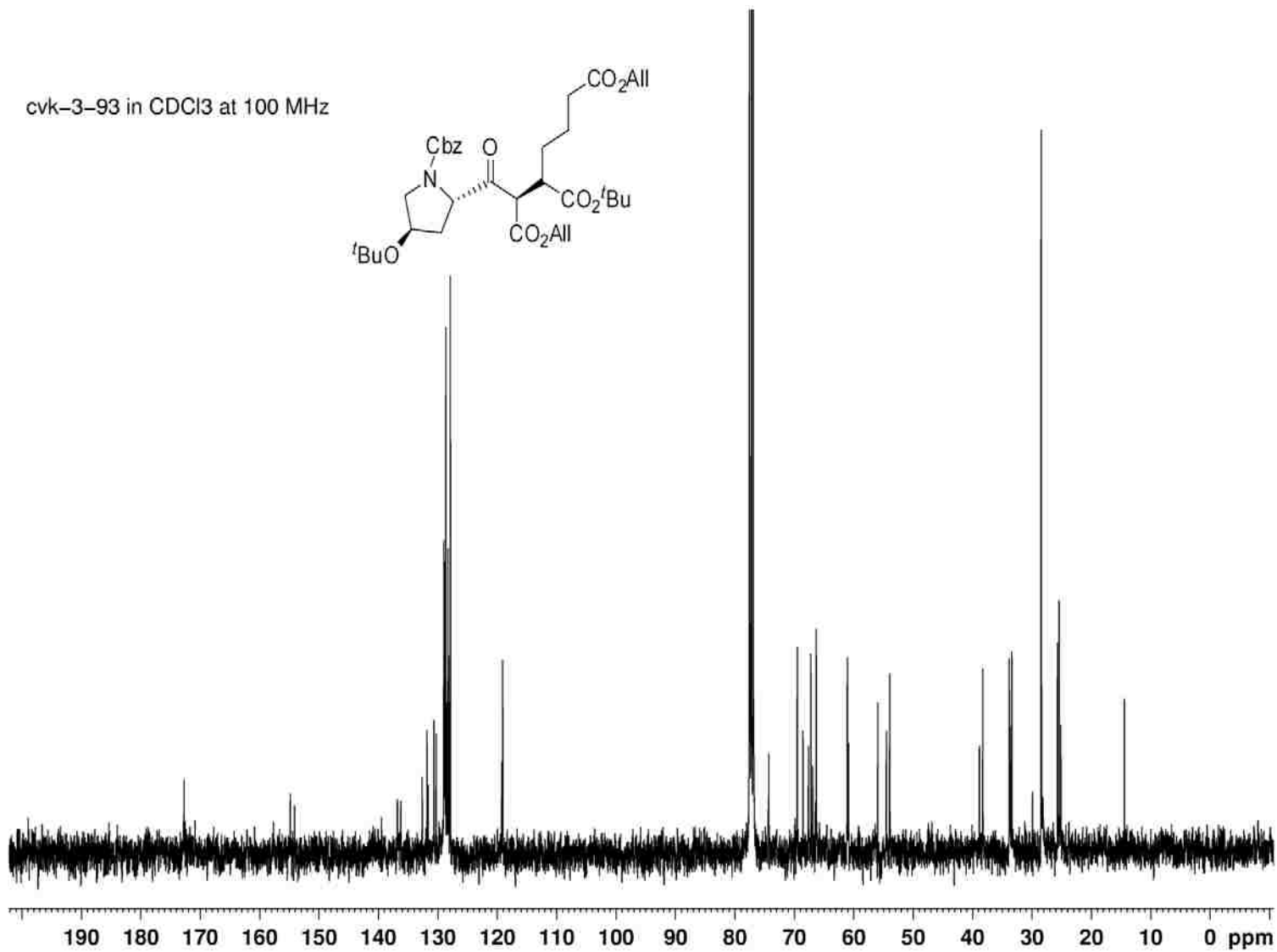
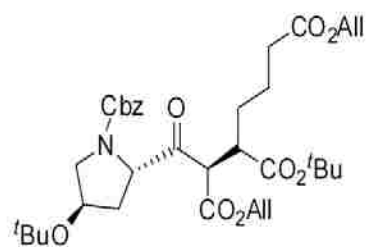
Dipeptide isostere 133

cvk-9-93 in CDCl<sub>3</sub> at 400 MHz

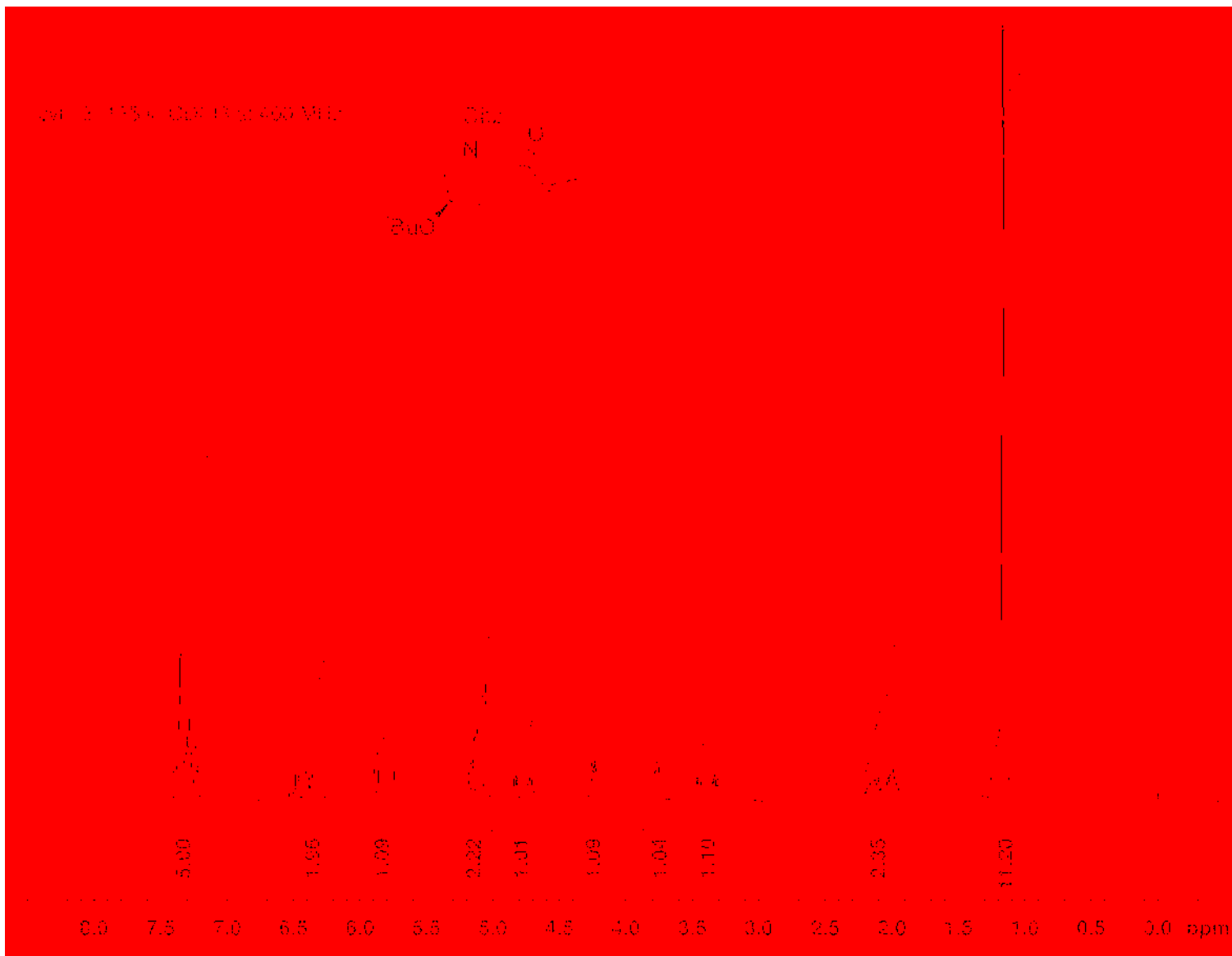


Dipeptide isostere 133

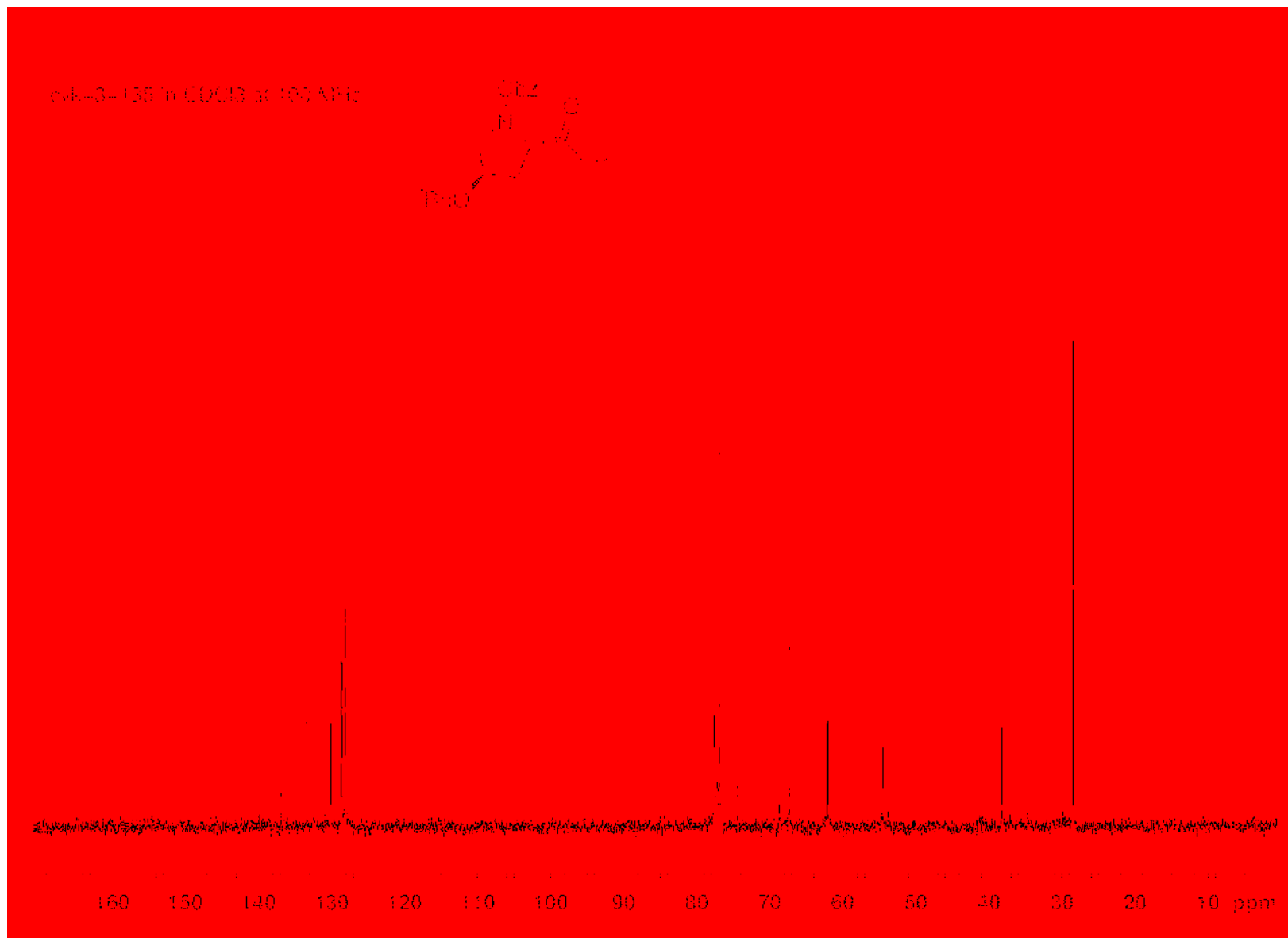
cvk-3-93 in CDCl<sub>3</sub> at 100 MHz



Cbz-Hyp(<sup>t</sup>Bu)- $\alpha$ -enylcarbamate **217**

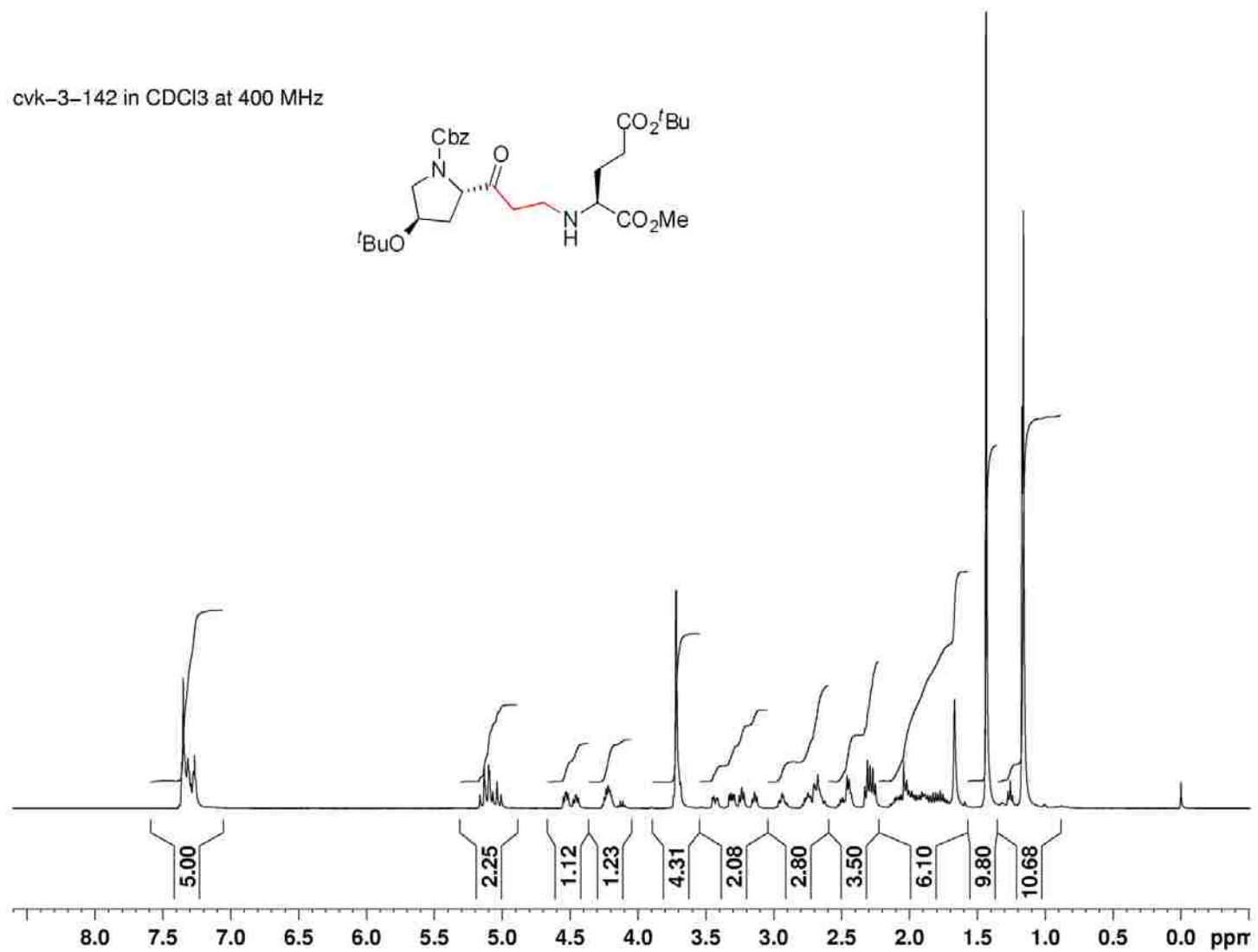
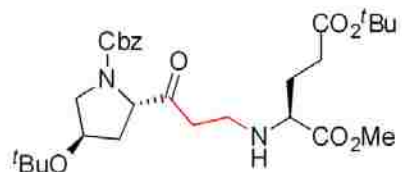


Cbz-Hyp(<sup>t</sup>Bu)- $\alpha$ -enylcarbamate **217**



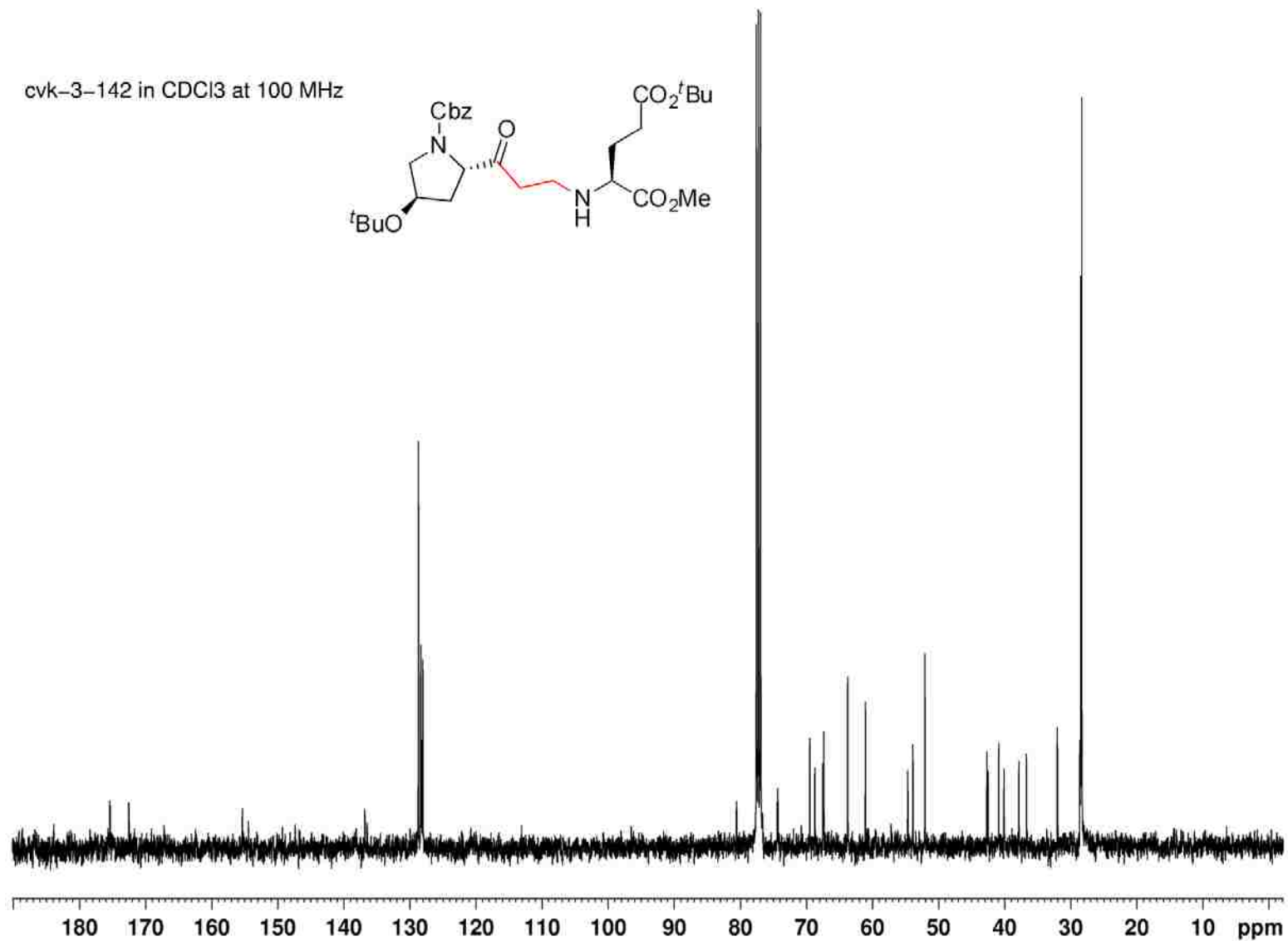
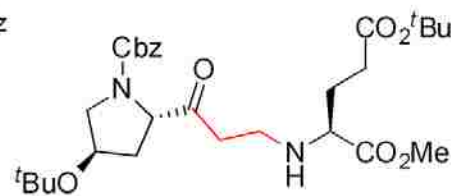
Dipeptide mimetic **216**

cvk-3-142 in CDCl<sub>3</sub> at 400 MHz



Dipeptide mimetic **216**

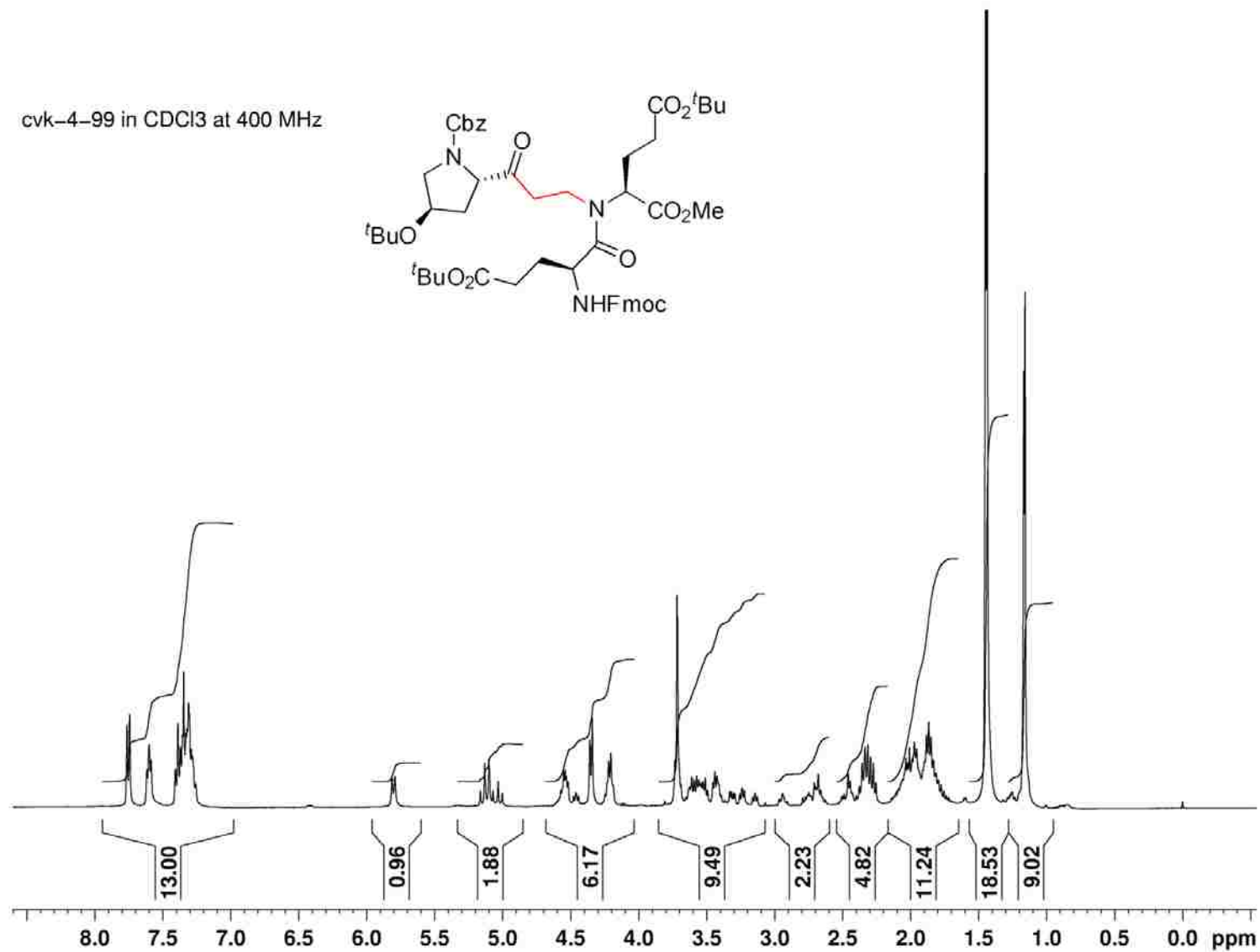
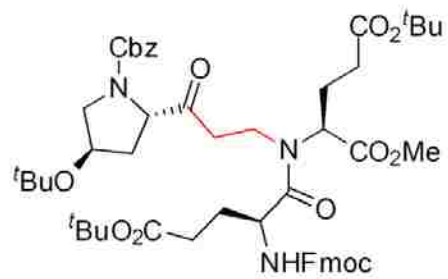
cvk-3-142 in CDCl<sub>3</sub> at 100 MHz





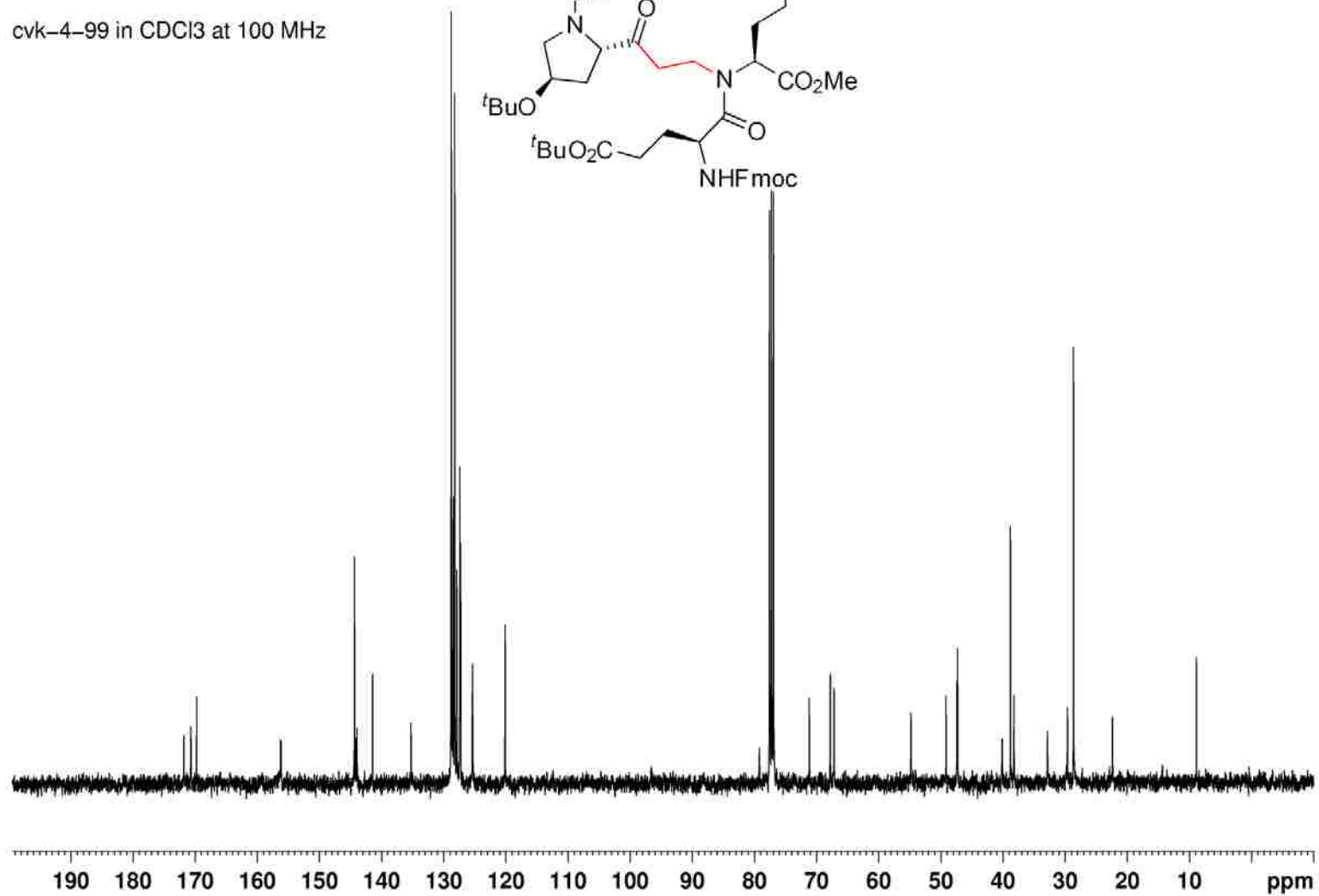
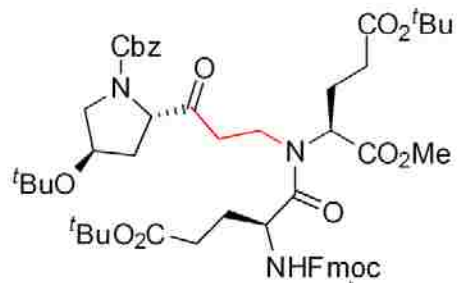
Tripeptide mimetic **223**

cvk-4-99 in CDCl<sub>3</sub> at 400 MHz

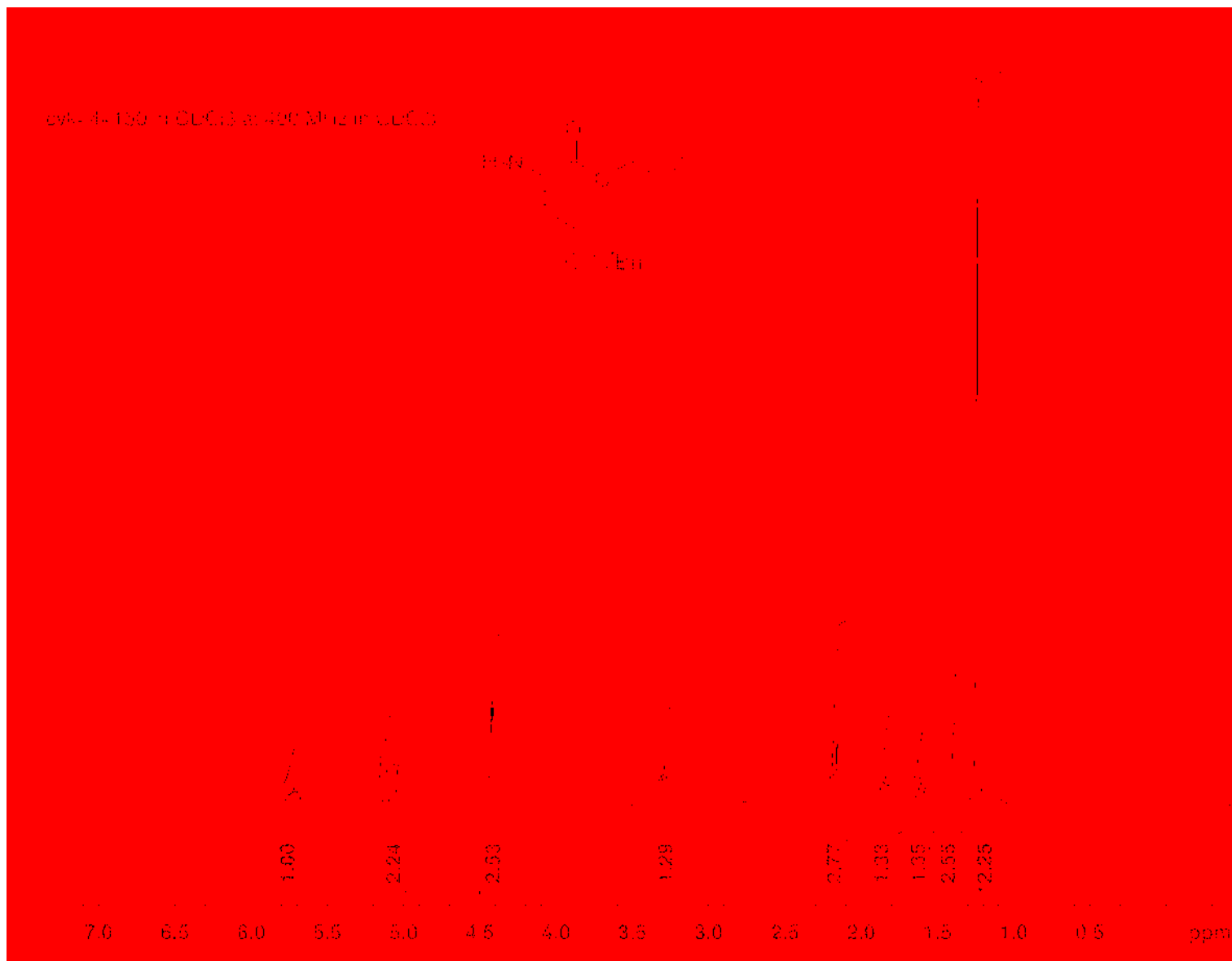


Tripeptide mimetic **223**

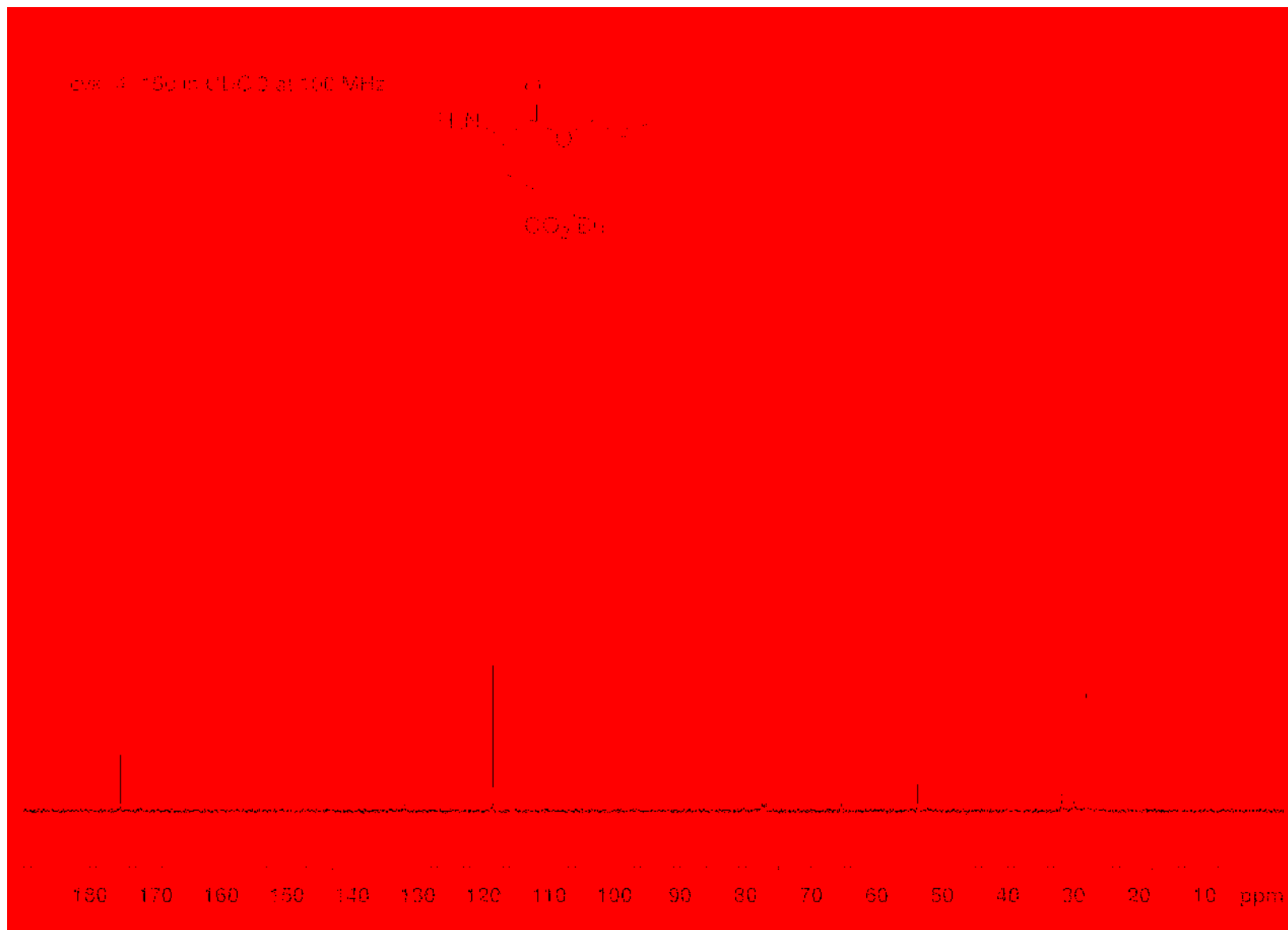
cvk-4-99 in CDCl<sub>3</sub> at 100 MHz



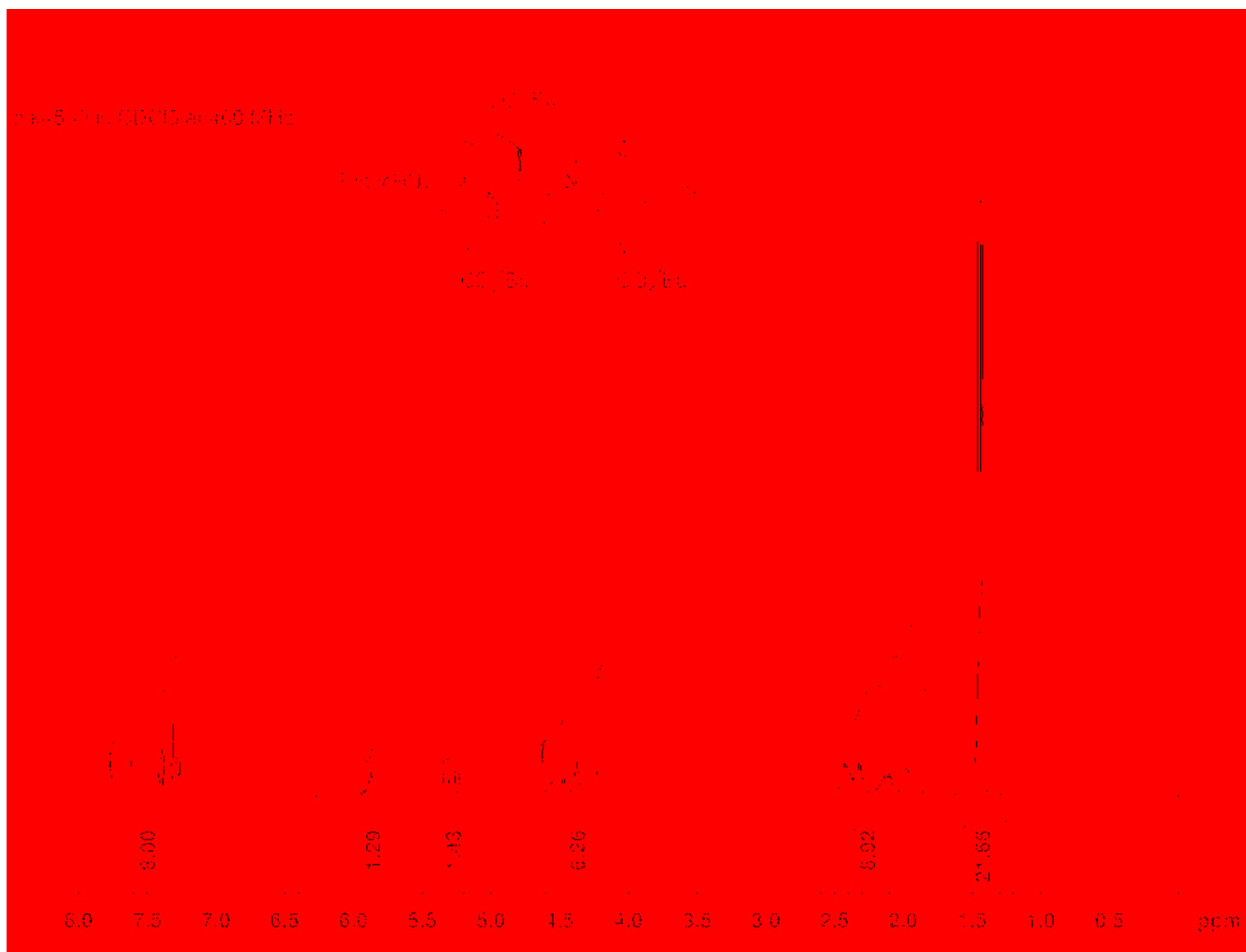
H-Glu-OAlI 229



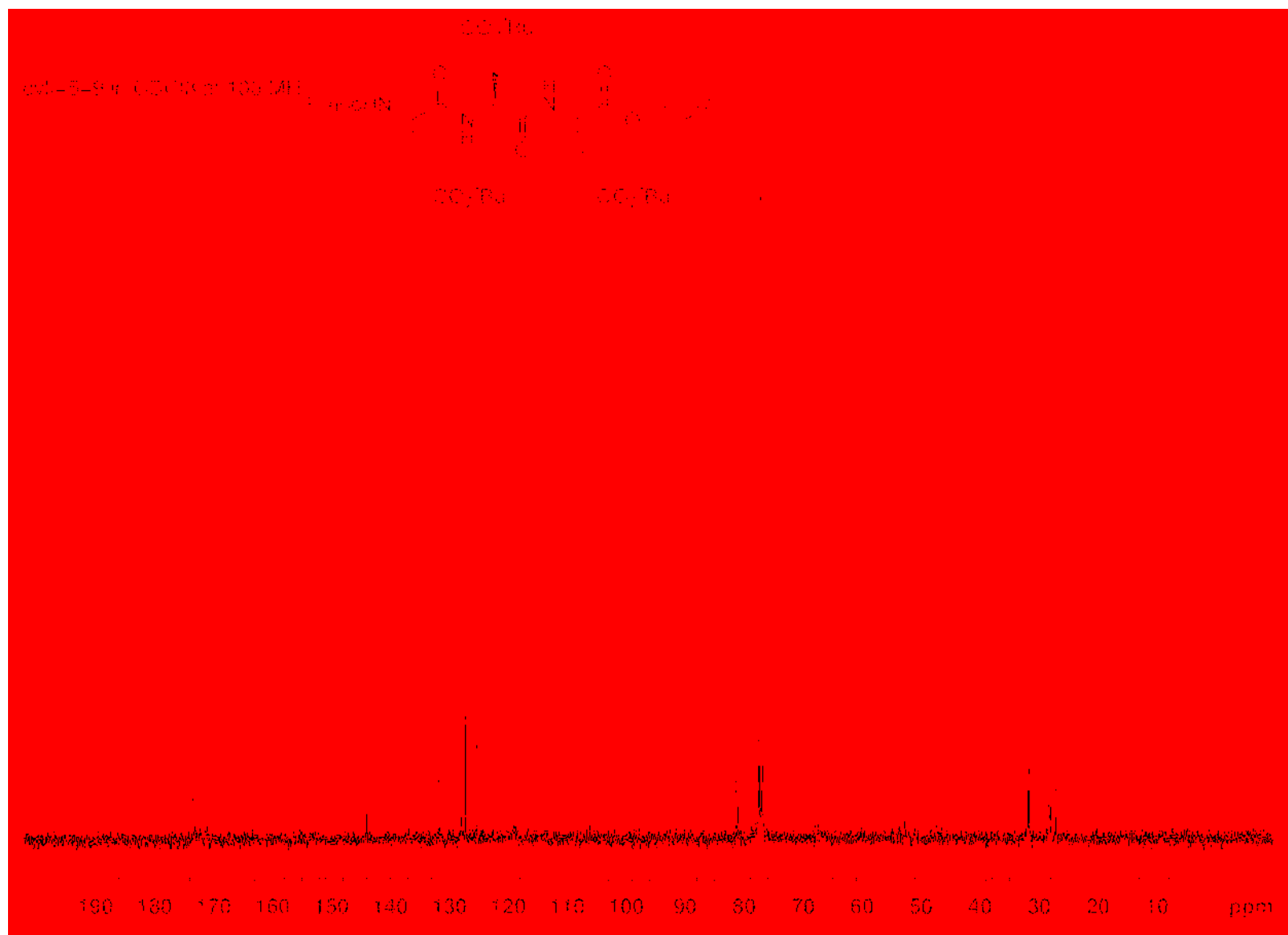
# H-Glu-OAlI 229



Fmoc-Glu(O<sup>t</sup>Bu)-Glu(O<sup>t</sup>Bu)-Glu(O<sup>t</sup>Bu)-OAll (232)

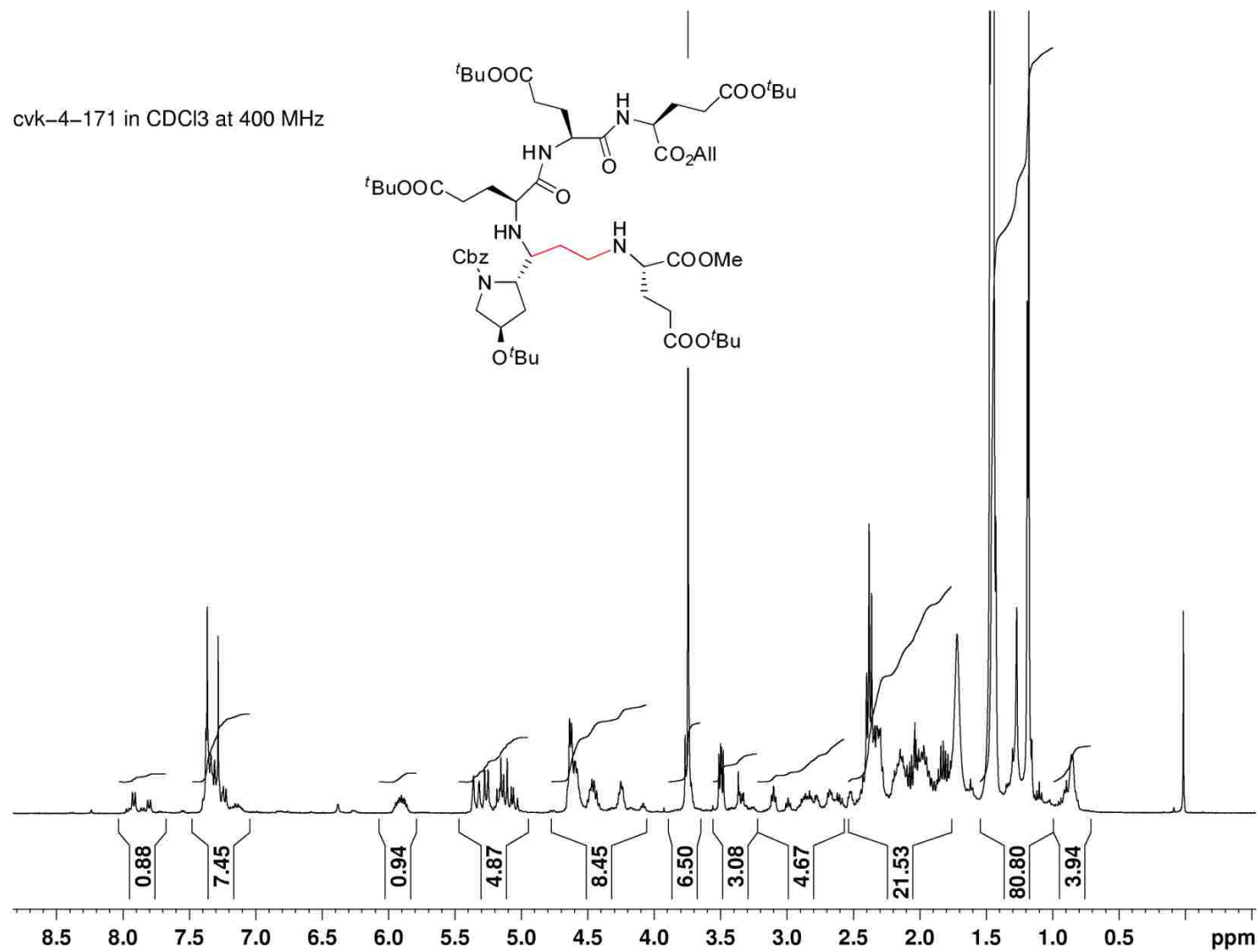


Fmoc-Glu(O<sup>t</sup>Bu)-Glu(O<sup>t</sup>Bu)-Glu(O<sup>t</sup>Bu)-OAll (232)



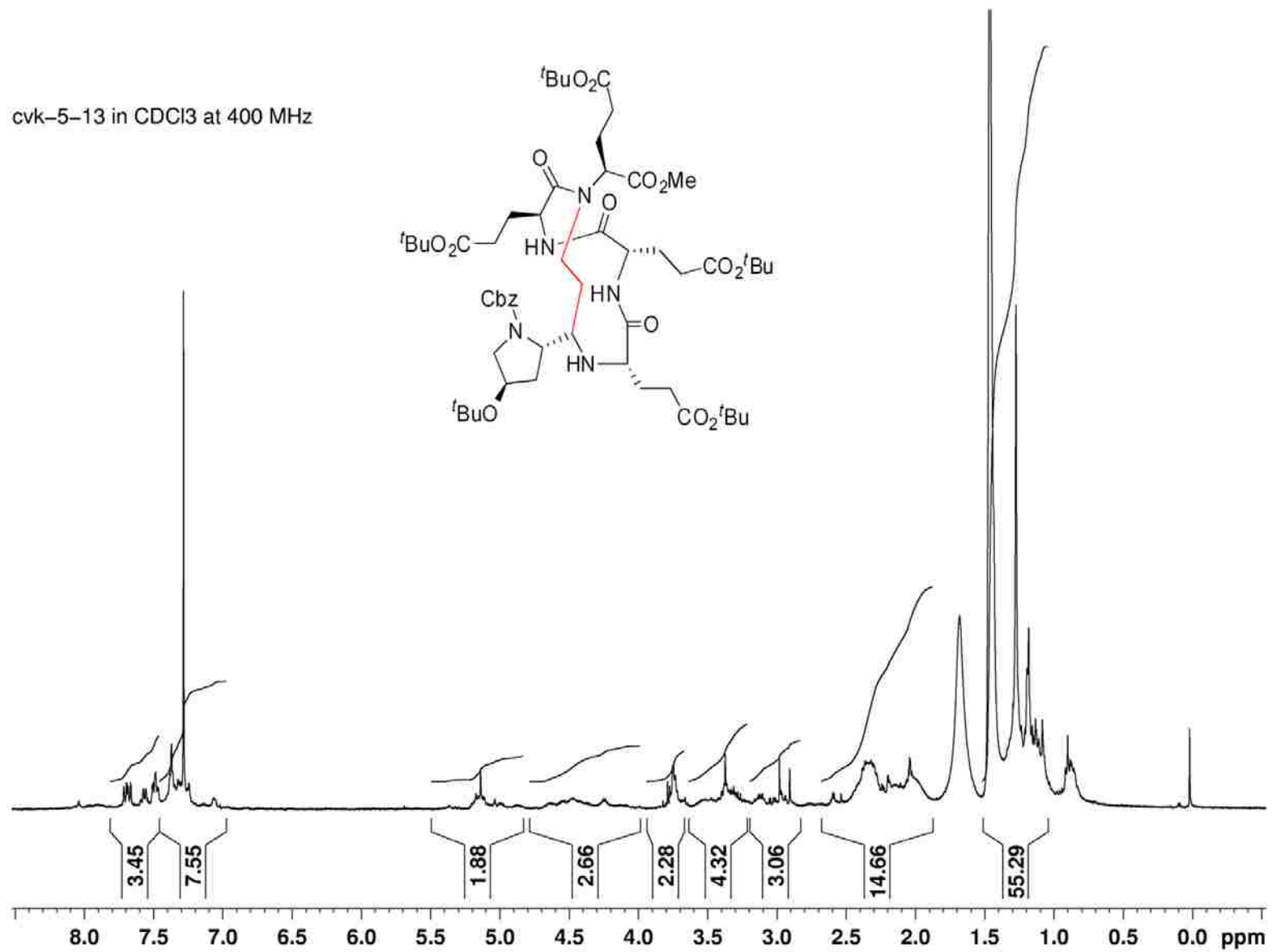
Pseudo pentapeptide mimetic **234**

cvk-4-171 in CDCl<sub>3</sub> at 400 MHz



Cyclic pentapeptide mimetic **253**

cvk-5-13 in CDCl<sub>3</sub> at 400 MHz

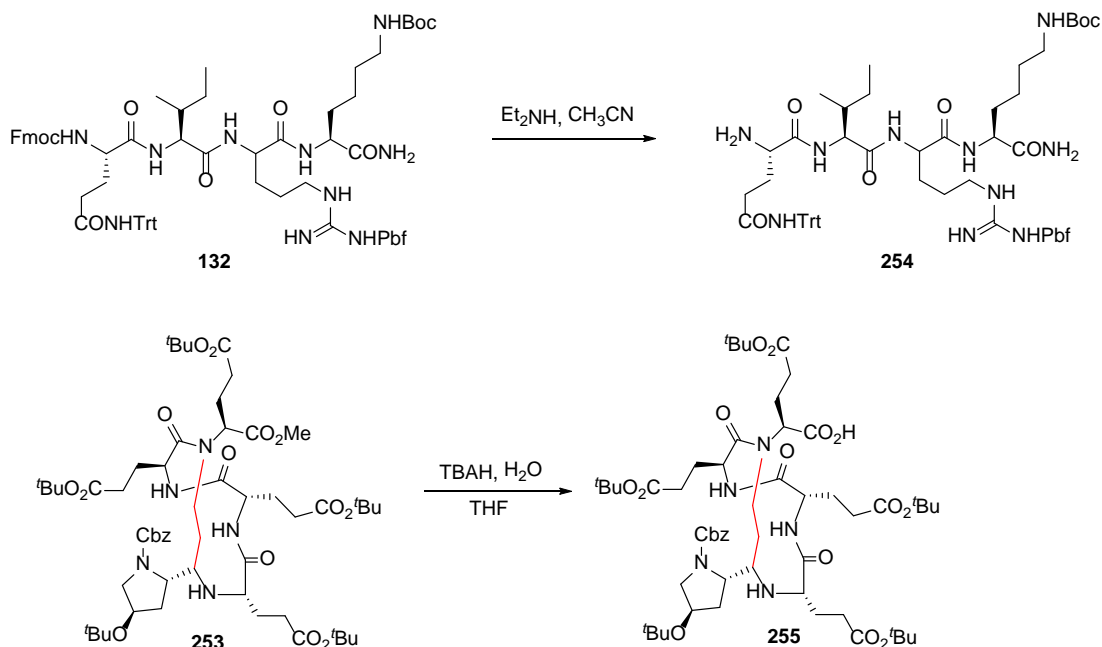




## CHAPTER 5: FUTURE WORK

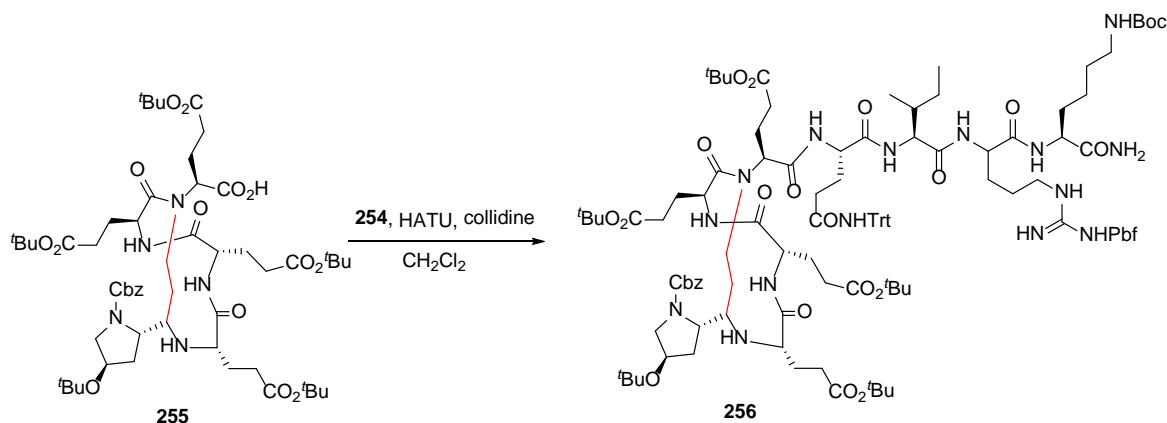
### 5.1 Coupling of *N*-terminal and *C*-terminal Oligopeptides to the Cyclic Pentapeptide Mimetic

With the cyclic pentapeptide mimetic **253** in hand, what remains to be done is coupling of the oligopeptides either side of this fragment to afford the 15-mer containing the mimetic motif. Our preparation of these oligopeptides is depicted in Scheme 5.1. The Fmoc protecting group of the QIRK tetrapeptide **132** will be removed using diethylamine to give the free amine **254**. The methyl ester of cyclic pentapeptide mimetic **253** will be hydrolyzed utilizing tetrabutylammonium hydroxide (TBAH) to give the free acid **255**.



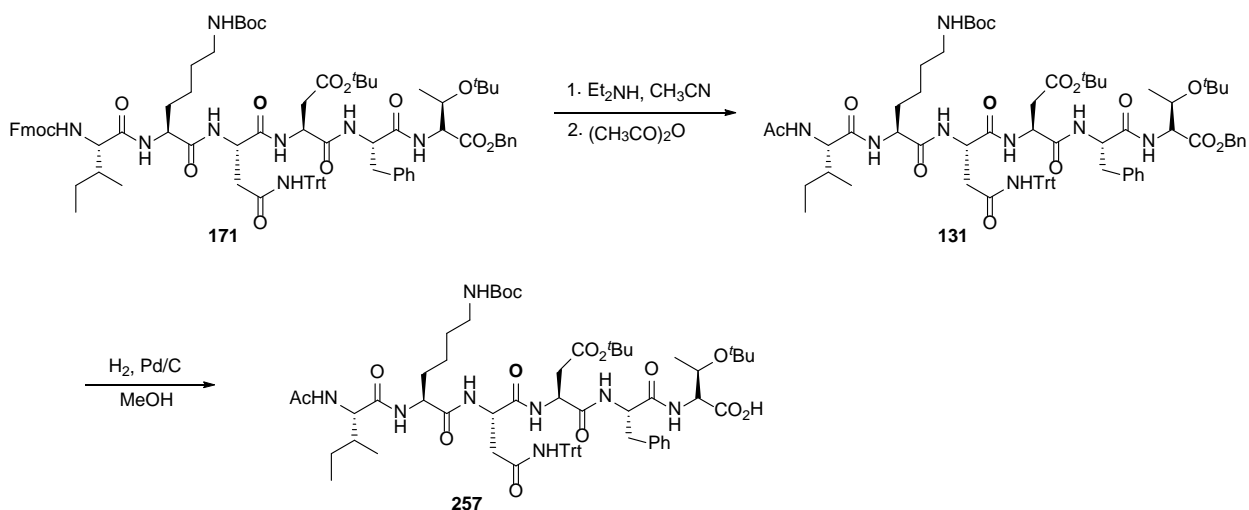
Scheme 5.1: Preparation of fragments **254** and **255**. Ethylene bridge is highlighted in red

The free acid **255** will then be coupled with the amine **254** to afford Cbz-[HypE]\*EEEQIRK-NH<sub>2</sub> ([HypE]\* denotes the isosteric replacement for the amide).



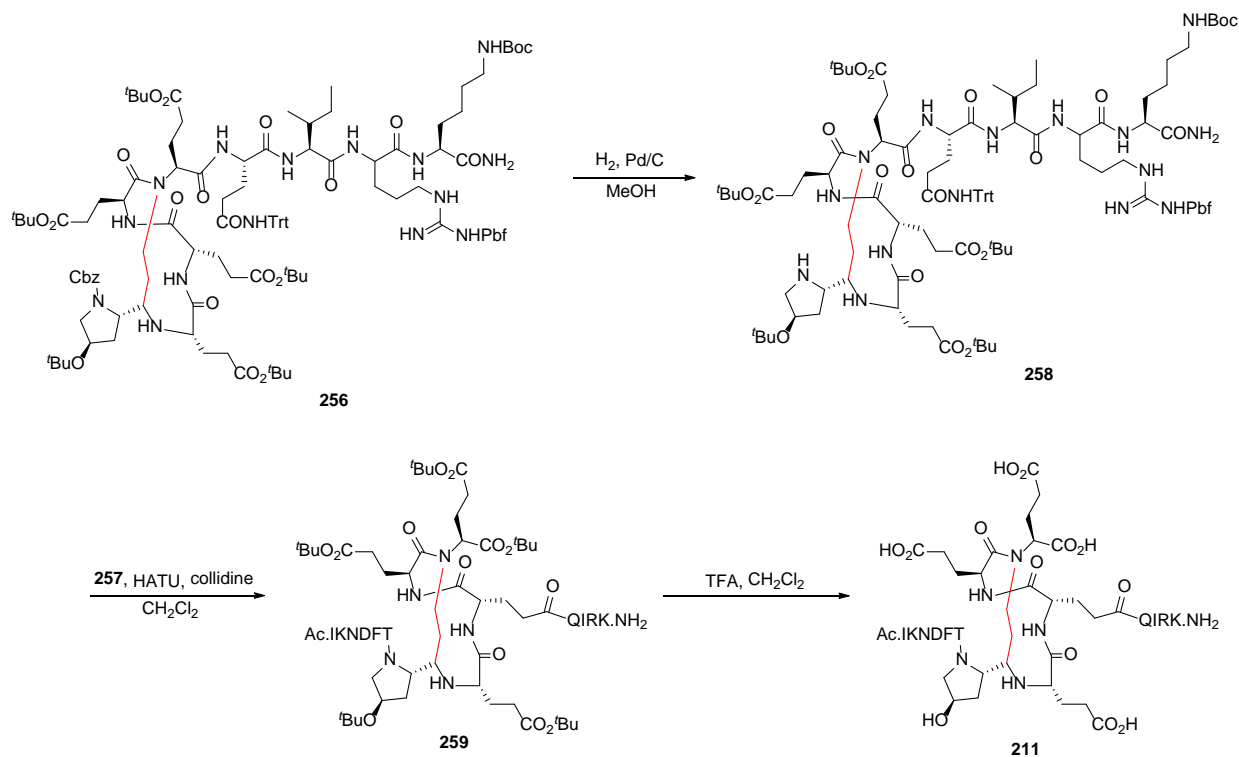
Scheme 5.2: Coupling of **254** and **255**

The Fmoc protecting group of the hexapeptide **171** will be removed and the free amine will be acetylated to give **131**. Hydrogenolysis will be used to remove the benzyl ester of hexapeptide **131** afford free acid **257**.



Scheme 5.3: Preparation of fragment **257**

The Cbz group of mimetic **256** will be removed by hydrogenolysis. The amine **258** will then be coupled to acid **257** using HATU as coupling reagent and collidine as base to give Ac-IKNDFT[HypE]\*EEEQIRK-NH<sub>2</sub> (**259**). The global deprotection of **259** will be carried out using TFA in dichloromethane to give  $\alpha$ -helical mimetic **211** (Scheme 5.4).



Scheme 5.4: Plan to complete the synthesis of **211**

## 5.2 Circular Dichroism

Circular Dichroism (CD) is used to investigate the secondary structure of peptides and proteins. In proteins there are two characteristic electronic transitions:  $n \rightarrow \pi^*$  (an electronically forbidden but magnetically permitted transition) and  $\pi \rightarrow \pi^*$  of the amide chromophore. These transitions show circular dichroism maxima at 215-230 nm and minima at 185-200 nm respectively.<sup>117</sup> The CD spectra of  $\alpha$ -helices shows one characteristic positive band ( $\sim 190$  nm, due to  $\pi \rightarrow \pi^*$ ) and two negative bands (at 208 nm and 222 nm due to the  $\pi \rightarrow \pi^*$  and  $n \rightarrow \pi^*$  transition respectively)<sup>118</sup> (Figure 5.1).

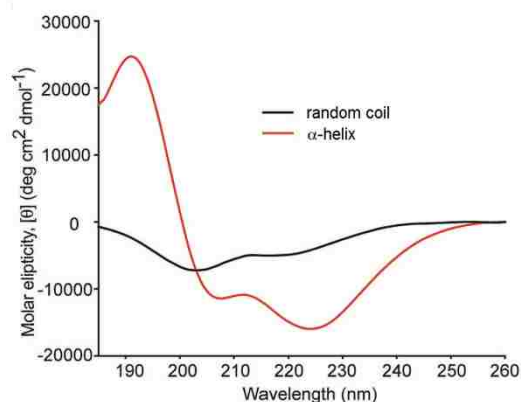
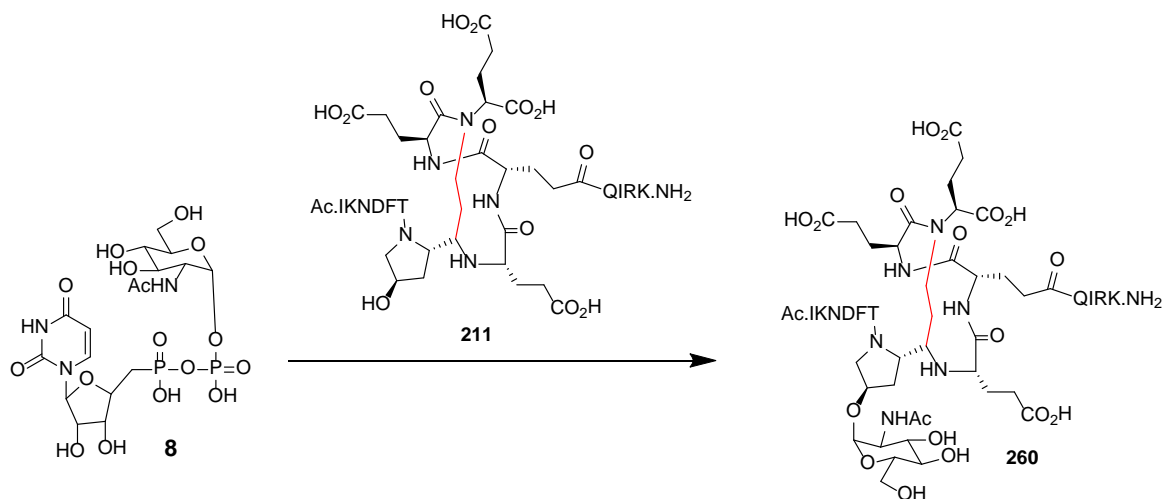


Figure 5.1: CD spectra of an  $\alpha$ -helix and a random coil

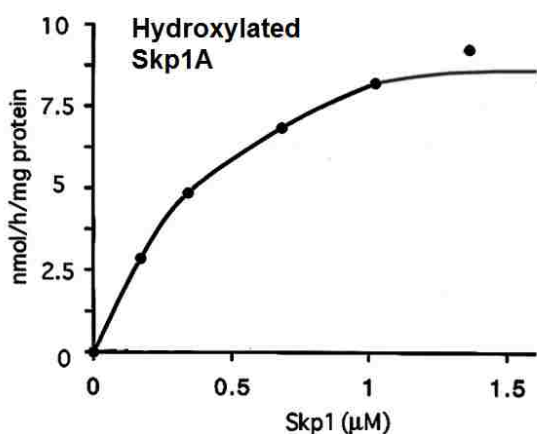
Both the Arora<sup>88d</sup> and Alewood<sup>100</sup> Groups performed CD spectroscopy to study the secondary structure of their  $\alpha$ -helical mimetics. Both groups reported that their  $\alpha$ -helical mimetics showed the desired secondary structural characteristics (§ 4.2.3). We will also perform CD spectroscopy studies for the  $\alpha$ -helical mimetic H-IKNDFT[HypE]\*EEEQIRK-NH<sub>2</sub> (**211**) to verify secondary structure consistent with an  $\alpha$ -helix.

### 5.3 Enzyme Assays

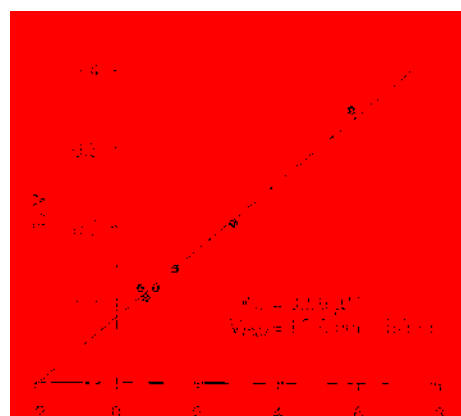
The future direction of this project depends on the activity of the  $\alpha$ -helical mimetic **211**. The  $\alpha$ -helical mimetic will be evaluated as a substrate for Gnt1 in the West Laboratory using *in vitro* reactions. Enzyme assays will be utilized to measure the affinity of the  $\alpha$ -helical mimetic for Gnt1. The rate of the reaction (Scheme 5.5) will be measured with increasing substrate concentration. These data will then be fitted to the Michaelis-Menten equation and  $V_{\max}$  and  $K_m$  values will be determined as illustrated for the full length protein in Figure 5.2. If the  $\alpha$ -helical mimetic shows an increase in affinity (lower  $K_m$ ) for the Gnt1 enzyme relative to the untemplated peptide, this will validate our hypothesis that the  $\alpha$ -helix is an important feature of the region of Skp1 substrates that bind to the active site of Gnt1.



Scheme 5.5: GlcNAc-Hyp linkage with the  $\alpha$ -helical mimetic **211**



(a)



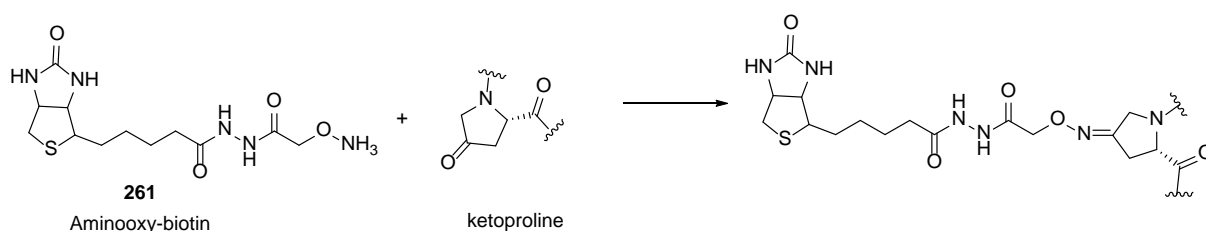
(b)

Figure 5.2: Kinetic analysis of the Skp1-HypPro GlcNAc transferase with respect to Skp1 adapted from Teng-umnuay *et al.*<sup>18</sup> (a) Plot for the Michaelis-Menten Kinetics, (b) Lineweaver-Burke analysis

#### 5.4 P4H1 Substrates

As described in §3.7 studies by both the Raines<sup>79</sup> and Schofield<sup>12b</sup> Groups have shown that 2S,4S-fluoroproline (flp) is a substrate for P4H1. In collaboration with West, we want to explore other potential pathways of P4H1 in *Dictyostelium discoideum* as occur in human PHDs including HIF $\alpha$ . This will be investigated using flp (**121**). 2S,4S-Fluoroproline (**121**) might be incorporated into a short peptide sequence and used to study its processing by the P4H1 of

*Dictyostelium discoideum*. If this affords the 4-oxo-prolyl product (Ketoproline, Scheme 5.3) we could trap it with **261**, an aminoxy derivative of biotin. Since ketones are rare in proteins, **261** will react selectively to form an oxime (Scheme 5.6), as reported by Ramakrishnan *et al.* for coupling with a keto-glycan.<sup>119</sup> To detect the aminoxy biotin conjugated ketoproline we can use the same method that Ramakrishnan *et al.* used to detect the aminoxy biotin conjugated glycoprotein. This will involve experiments with a probe containing streptavidin conjugated to horseradish peroxidase (HRP) and measurement of the presence of biotin indirectly via production of a chemiluminescent species by HRP.<sup>119</sup>



Scheme 5.6: Trapping of ketoproline with aminoxy-biotin **261**

We might also feed flp to *Dictyostelium discoideum* and look for its incorporation into Skp1. The incorporation might affect the activity of the non-glycosylated Skp1. In 2008, Budisa and coworkers replaced the ten Pro residues in *Enhanced Green Fluorescent Protein (EGFP)* with flp. The mutant protein was shown to fold faster than the wild type protein.<sup>120</sup> In 2011, a report by Rubini *et al.* demonstrated the incorporation of Flp into human ubiquitin using an auxotrophic *E. coli* strain JM83 that is deficient in proline biosynthesis. They substituted all three Pro residues (Pro<sup>19</sup>, Pro<sup>37</sup>, Pro<sup>38</sup>) in the ubiquitin sequence. Their results showed that the fluorinated protein undergoes polyubiquitination and its biological activity is fully retained.<sup>121</sup> In 2004 Contecello and coworkers demonstrated the efficient incorporation of flp in to *E. coli* cells.<sup>122</sup> We will focus the search using *Dictyostelium discoideum* strains in which P4H1 is exclusively induced in prestalk and prespore cells.<sup>10</sup> Our plan is to follow the same approach as Contecello and coworkers which is semi-auxotrophic for Pro when grown in a



Following this example we could incorporate a nucleotide recognition element, UDP-GlcNAc, to the  $\alpha$ -helical mimetic to improve inhibitor binding affinity. Moreover it is important to consider the ability of these compounds to traverse the cell membrane. Most substrate analogs that inhibit glycosyltransferases *in vitro* fail in cellular systems. This is due to the polyhydroxylated nature of carbohydrates which prevents their uptake across the cell membrane. Esko and coworkers demonstrated that “pro-drugs” in the form of peracetylated carbohydrates are a useful strategy. In the same manner that acetylsalicylic acid serves as a precursor to salicylic acid, inside the cell the acetate esters can be hydrolyzed by esterases to release the polyhydroxylated drug.<sup>125125</sup> Another factor we have to consider is the bioavailability of **213**. Peptidyl drugs usually doesn't have good bioavailability. If the Glu-rich  $\alpha$ -helix proved to be important for effective binding, then we might need to replace the oligopeptide with a peptidomimetic such as oligopyridine or oligopyridylamide as described by Hamilton and coworkers (§4.2.1). Considering these three factors we might envision inhibitor **264** (Figure 5.5).

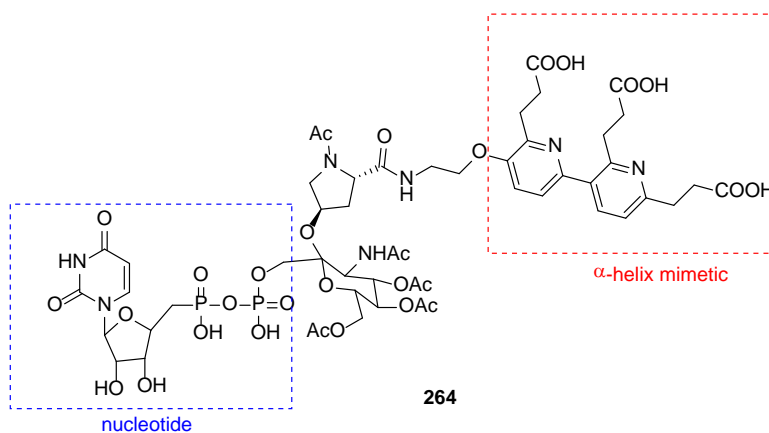


Figure 5.5: Futuristic target



## REFERENCES

1. Ramage, R.; Green, J.; Muir, T. W.; Ogunjobi, O. M.; Love, S.; Shaw, K., "Synthetic, structural and biological studies of the ubiquitin system: the total chemical synthesis of ubiquitin," *Biochem. J* **1994**, *299*, 151-158.
2. van der Wel, H.; Ercan, E.; West, C. M., "The Skp1 prolyl hydroxylase from *Dictyostelium* is related to the hypoxia-inducible factor- $\alpha$  class of animal prolyl 4-hydroxylases," *J. Biol. Chem.* **2005**, *280*, 14645-14655.
3. Rieser, E.; Cordier, S. M.; Walczak, H., "Linear ubiquitination: a newly discovered regulator of cell signaling," *Trends in Biochemical Sciences* **2013**, *38*, 94-102.
4. (a) Zheng, N.; Schulman, B. A.; Song, L.; Miller, J. J.; Jeffrey, P. D.; Wang, P.; Chu, C.; Koepf, D. M.; Elledge, S. J.; Paganok, M.; Conaway, R. C.; Conaway, J. W.; Harper, J. W.; Pavletich, N. P., "Structure of the Cul1-Rbx1-Skp1-F-boxSkp2 SCF ubiquitin ligase complex," *Nature* **2002**, *416*, 703-709; (b) Hershko, A.; Ciechanover, A., "The ubiquitin system," *Annu. Rev. Biochem.* **1998**, *67*, 425-479; (c) Sadowski, M.; Sarcevic, B., "Mechanisms of mono- and poly-ubiquitination: Ubiquitination specificity depends on compatibility between the E2 catalytic core and amino acid residues proximal to the lysine," *Cell Div.* **2010**, *5*, 1-19.
5. West, C. M., "Evolutionary and functional implications of the complex glycosylation of Skp1, a cytoplasmic/nuclear glycoprotein associated with polyubiquitination," *Cell. Mol. Life. Sci.* **2003**, *60*, 229-240.
6. West, C. M.; van der Wel, H.; Gaucher, E. A., "Complex glycosylation of Skp1 in *Dictyostelium*: implications for the modification of other eukaryotic cytoplasmic and nuclear proteins," *Glycobiology* **2002**, *12*, 17R-27R.
7. Zhang, D.; van der Wel, H.; Johnson, J. M.; West, C. M., "Skp1 prolyl 4-hydroxylase of *Dictyostelium* mediates glycosylation-independent and -dependent responses to O<sub>2</sub> without affecting Skp1 stability," *J. Biol. Chem.* **2012**, *287*, 2006-2016.
8. (a) Wang, Z. A.; van der Wel, H.; Vohra, Y.; Buskas, T.; Boons, G.-J.; West, C. M., "Role of a cytoplasmic dual-function glycosyltransferase in O<sub>2</sub> regulation of development in *Dictyostelium*," *J. Biol. Chem.* **2009**, *284*, 28896-28904; (b) West, C. M.; Wang, Z. A.; van der Wel, H., "A cytoplasmic prolyl hydroxylation and glycosylation pathway modifies Skp1 and regulates O<sub>2</sub>-dependent development in *Dictyostelium*," *Biochim. Biophys. Acta.* **2010**, *1800*, 160-171.
9. Wang, Z. A.; Singh, D.; van der Wel, H.; West, C. M., "Prolyl hydroxylation- and glycosylation-dependent functions of Skp1 in O<sub>2</sub>-regulated development of *Dictyostelium*," *Dev. Biol.* **2011**, *349*, 283-295.
10. West, C. M.; van der Wel, H.; Wang, Z. A., "Prolyl 4-hydroxylase-1 mediates O<sub>2</sub> signaling during development of *Dictyostelium*," *Development* **2007**, *134*, 3349-3358.
11. Gorres, K. L.; Raines, R. T., "Prolyl 4-hydroxylase," *Crit. Rev. Biochem. Mol. Biol.* **2010**, *45*, 106-124.

12. (a) Loenarz, C.; Mecinovic, J.; Chowdhury, R.; McNeill, L. A.; Flashman, E.; Schofield, C. J., "Evidence for a stereoelectronic effect in human oxygen sensing," *Angew. Chem. Int. Ed.* **2009**, *48*, 1784-1787; (b) Chowdhury, R.; McDonough, M. A.; Mecinovic, J.; Loenarz, C.; Flashman, E.; Hewitson, K. S.; Domene, C.; Schofield, C. J., "Structural basis for binding of hypoxia-inducible factor to the oxygen-sensing prolyl hydroxylases," *Structure* **2009**, *17*, 981-989.
13. Gonzalez-Yanes, B.; Cicero, J. M.; Brown, R. D. J.; West, C. M., "Characterization of a cytosolic fucosylation pathway in *Dictyostelium*," *J. Biol. Chem* **1992**, *267*, 9595-9605.
14. Teng-umnuay, P.; Morris, H. R.; Dell, A.; Panico, M.; Paxton, T.; West, C. M., "The cytoplasmic F-box binding protein Skp1 contains a novel pentasaccharide linked to hydroxyproline in *Dictyostelium*," *J. Biol. Chem.* **1998**, *273*, 18242-18249.
15. Sassi, S.; Sweetinburgh, M.; Erogul, J.; Zhang, P.; Teng-Umnuay, P.; West, C. M., "Analysis of Skp1 glycosylation and nuclear enrichment in *Dictyostelium*," *Glycobiology* **2001**, *11*, 283-295.
16. Mauger, A. B., "Naturally occurring proline analogues," *J. Nat. Prod.* **1996**, *59*, 1205-1211.
17. van der Wel, H.; Johnson, J. M.; Xu, Y.; Karunaratne, C. V.; Wilson, K. D.; Vohra, Y.; Boons, G.-J.; Taylor, C. M.; Bendiak, B. K.; West, C. M., "Requirements for Skp1 processing by cytosolic prolyl 4(trans)-hydroxylase and  $\alpha$ -N-acetylglucosaminyltransferase enzymes involved in O<sub>2</sub>-signaling in *Dictyostelium*," *Biochemistry* **2011**, *50*, 1700-1713.
18. Teng-umnuay, P.; van der Wel, H.; West, C. M., "Identification of a UDP-GlcNAc: Skp1-hydroxyproline GlcNAc-transferase in the cytoplasm of *Dictyostelium*," *J. Biol. Chem* **1999**, *274*, 36392-36402.
19. van der Wel, H.; Morris, H. R.; Panico, M.; Paxton, T.; Dell, A.; Kaplan, L.; West, C. M., "Molecular cloning and expression of a UDP-N-acetylglucosamine(GlcNAc):hydroxyproline polypeptide GlcNAc-transferase that modifies Skp1 in the cytoplasm of *Dictyostelium*," *J. Biol. Chem.* **2002**, *277*, 46328-46337.
20. West, C. M.; van Der Wel, H.; Sassi, S.; Gaucher, E. A., "Cytoplasmic glycosylation of protein-hydroxyproline and its relationship to other glycosylation pathways," *Biochim. Biophys. Acta.* **2004**, *1673*, 29-44.
21. West, C. M.; van der Wel, H.; Blader, I. J., "Detection of cytoplasmic glycosylation associated with hydroxyproline," *Methods Enzymol.* **2006**, *417*, 389-404.
22. Koshland, D. E., "Stereochemistry and the mechanism of enzymatic reactions," *Biol. Rev. Camb. Phil. Soc.* **1953**, *28*, 416-436.
23. Lairson, L. L.; Henrissat, B.; Davies, G. J.; Withers, S. G., "Glycosyltransferases: structures, functions, and mechanisms," *Annu. Rev. Biochem.* **2008**, *77*, 521-555.
24. (a) Taylor, C. M.; Karunaratne, C. V.; Xie, N., "Glycosides of hydroxyproline: Some recent, unusual discoveries," *Glycobiology* **2012**, *22*, 757-767; (b) Ketcham, C.; Wang, F.; Fisher, S. Z.; Ercan, A.; van der Wel, H.; Locke, R. D.; Sirajud-Douhah, K.; Matta, K. L.; West, C. M., "Specificity of a soluble UDP-galactose:Fucoside  $\alpha$ 1,3-galactosyltransferase that modifies the cytoplasmic glycoprotein Skp1 in *Dictyostelium*," *J. Biol. Chem.* **2004**, *279*, 29050-29059.

25. (a) Izumi, M.; Yuasa, H.; Hashimoto, H., "Bisubstrate analogues as glycosyltransferase inhibitors," *Current Topics in Medicinal Chemistry* **2009**, *9*, 87-105; (b) Compain, P.; Martin, O. R., "Carbohydrate mimetics-based glycosyltransferase inhibitors," *Bioorg. Med. Chem.* **2001**, *9*, 3077-3092.
26. Pesnot, T.; Jørgensen, R.; Palcic, M. M.; Wagner, G. K., "Structural and mechanistic basis for a new mode of glycosyltransferase inhibition," *Nature Chem. Bio.* **2010**, *6*, 321-323.
27. Gross, B. J.; Kraybill, B. C.; Walker, S., "Discovery of O-GlcNAc transferase inhibitors," *J. Am. Chem. Soc.* **2005**, *127*, 14588-14589.
28. Palcic, M. M.; Heerzel, L. D.; Srivastava, O. P.; Hindsgaul, O., "A bisubstrate analog inhibitor for  $\alpha(1-2)$ -fucosyltransferase," *J. Biol. Chem.* **1989**, *264*, 17174-17181.
29. Kamps, B. M.; Veenemana, G. H.; van der Marela, G. A.; van Boeckela, C. A. A.; van Boom, G. A., "Design and synthesis of a trisubstrate analogue for  $\alpha(1\rightarrow3)$ fucosyltransferase: A potential inhibitor," *Tetrahedron* **1995**, *51*, 8397-8406.
30. Jung, K.-H.; Schmidt, R. R., Glycosyltransferase Inhibitors, in Carbohydrate-Based Drug Discovery C.-H. Wong, Ed., **2005**, Wiley-VCH Verlag GmbH & Co. KGaA, Weinheim, FRG.
31. West, C. M., unpublished results.
32. Whitworth, G. E.; Macauley, M. S.; Stubbs, K. A.; Dennis, R. J.; Taylor, E. J.; Davies, G. J.; Greig, I. R.; Vocadlo, D. J., "Analysis of PUGNAc and NAG-thiazoline as transition state analogues for human O-GlcNAcase: Mechanistic and structural insights into inhibitor selectivity and transition state poise," *J. Am. Chem. Soc.* **2007**, *129*, 635-644.
33. Knapp, S.; Vocadlo, D.; Gao, Z.; Kirk, B.; Lou, J.; Withers, S. G., "NAG-thiazoline, an N-Acetyl-b-hexosaminidase inhibitor that implicates acetamido participation," *J. Am. Chem. Soc.* **1996**, *118*, 6804-6805.
34. Knapp, S.; Myers, D. S., " $\alpha$ -GlcNAc thioconjugates," *J. Org. Chem.* **2001**, *66*, 3636-3638.
35. (a) Swamy, K. C. K.; Kumar, N. N. B.; Balaraman, E.; Kumar, K. V. P. P., "Mitsunobu and related reactions: Advances and applications," *Chem. Rev.* **2009**, *109*, 2551-2651; (b) Schips, C.; Ziegler, T., "A practical one pot synthesis of new S-glycosyl amino acid building blocks for combinatorial neoglycopeptide synthesis," *J. Carbohydr. Chem.* **2005**, *24*, 773-778.
36. (a) Thayer, D. A.; Yu, H. N.; Galan, M. C.; Wong, C.-H., "A general strategy toward S-linked glycopeptides," *Angew. Chem. Int. Ed.* **2005**, *44*, 4596-4599; (b) Rye, C. S.; Withers, S. G., "The synthesis of a novel thio-linked disaccharide of chondroitin as a potential inhibitor of polysaccharide lyases," *Carbohydr. Res.* **2004**, 699-703; (c) Scheffler, G.; Behrendt, M. E.; Schmidt, R. R., "Investigation on leaving group based intra-versus intermolecular glycoside bond formation," *Eur. J. Org. Chem.* **2000**, 3527-3539; (d) Johnston, B. D.; Pinto, B. M., "Synthesis of thio-linked disaccharides by 1 $\rightarrow$ 2 intramolecular thioglycosyl migration: Oxacarbenium versus episulfonium ion intermediates," *J. Org. Chem.* **2000**, *65*, 4607-4617; (e) Knapp, S.; Myers, D. S., "Synthesis of  $\alpha$ -GalNAc thioconjugates from an  $\alpha$ -GalNAc Mercaptan," *J. Org. Chem.* **2002**, *67*, 2995-2999; (f) Zhu, X.; Schmidt, R. R., "Efficient synthesis of S-linked glycopeptides in aqueous solution by a convergent strategy," *Chem. Eur. J.* **2004**, *10*, 875-887;

(g) Turnbull, W. B.; Field, R. A., "Thio-oligosaccharides of sialic acid-synthesis of an a(2-3) sialyl galactoside via a gulofuranose/galactopyranose approach," *J. Chem. Soc. Perkin Trans. 1*, **2000**, 1859-1866.

37. Dembinski, R., "Recent advances in the Mitsunobu reaction: Modified reagents and the quest for chromatography-free separation," *Eur. J. Org. Chem.* **2004**, 2763-2772.

38. Ohnishi, Y.; Ichikawa, M.; Ichikawa, Y., "Facile synthesis of *N*-Fmoc-serine-*S*-GlcNAc: A potential molecular probe for the functional study of *O*-GlcNAc," *Bioorg. Med. Chem. Lett.* **2000**, *10*, 1289-1291.

39. Falconer, R. A.; Jablonkai, I.; Toth, I., "Efficient synthesis of thioglycosides via a Mitsunobu condensation," *Tetrahedron Lett.* **1999**, *40*, 8663-8666.

40. Shi, Y. J.; Hughes, D. L.; McNamara, J. M., "Stereospecific synthesis of chiral tertiary alkyl-aryl ethers via Mitsunobu reaction with complete inversion of configuration," *Tetrahedron Lett.* **2003**, *44*, 3609-3611.

41. Schumacher, K. K.; Jiang, J.; Joullie, M. M., "Synthetic studies toward astins A, B and C. Efficient syntheses of *cis*-3,4-dihydroxyprolines and (-)-(3*S*,4*R*)-dichloroproline esters," *Tetrahedron Asym.* **1998**, *9*, 47-53.

42. Webb, T. R.; Eigenbrot, C., "Conformationally restricted arginine analogues," *J. Org. Chem.* **1991**, *56*, 3009-3016.

43. Berger, Y.; Dehmlow, H.; Blum-Kaelin, D.; Kitas, E. A.; Löffler, B.-M.; Aebi, J. D.; Juillerat-Jeanneret, L., "Endothelin-Converting Enzyme-1 Inhibition and Growth of Human Glioblastoma Cells," *J. Med. Chem.* **2005**, *48*, 483-498.

44. Lange, U. E. W.; Baucke, D.; Hornberger, W.; Mack, H.; Seitz, W.; Hoffken, H. W., "Orally active thrombin inhibitors. Part 2: Optimization of the P2-moiety," *Bioorg. Med. Chem. Lett.* **2006**, *16*, 2648-2653.

45. Qiu, X. L.; Qing, F. L., "Synthesis of 3'-deoxy-3'-difluoromethyl azanucleosides from *trans*-4-hydroxy-L-proline," *J. Org. Chem.* **2005**, *70*, 3826-3837.

46. Oh, C.-H.; Cho, J.-H., "Synthesis and biological evaluation of 1 $\beta$ -methylcarbapenems having guanidino moieties," *Eur. J. Med. Chem.* **2006**, *41*, 50-55.

47. Cadamuro, S. A.; Reichold, R.; Kusebauch, U.; Musiol, H.-J.; Renner, C.; Tavan, P.; Moroder, L., "Conformational properties of 4-mercaptoproline and related derivatives," *Angew. Chem. Int. Ed.* **2008**, *47*, 2143-2146.

48. Hoffman, R. V.; Kim, H.-O., "The stereoselective synthesis of 2-alkyl  $\alpha$ -keto acid and heterocyclic ketomethylene peptide isostere core units using chiral alkylation by 2-triflyloxy esters," *J. Org. Chem.* **1995**, *60*, 5107-5113.

49. Hoffman, R. V.; Tao, J., "A stereocontrolled synthesis of monofluoro ketomethylene dipeptide isosteres," *Tetrahedron Lett.* **1998**, *39*, 4195-4198.

50. (a) Jenkins, C. L.; Raines, R. T., "Insights on the conformational stability of collagen," *Nat. Prod. Rep.* **2002**, *19*, 49-59; (b) Wolfe, S., "Gauche effect. Stereochemical consequences of adjacent electron pairs and polar bonds," *Acc. Chem. Res.* **1972**, *5*, 102-111.
51. Wolfe, S., "Gauche effect. Stereochemical consequences of adjacent electron pairs and polar bonds," *Acc. Chem. Res.* **1972**, *5*, 102-111.
52. Hur, S.; Bruice, T. C., "The mechanism of *cis-trans* isomerization of prolyl peptides by cyclophilin," *J. Am. Chem. Soc.* **2002**, *124*, 7303-7313.
53. Song, J.; Burrage, K.; Yuan, Z.; Huber, T., "Prediction of *cis/trans* isomerization in proteins using PSI-BLAST profiles and secondary structure information," *BMC Bioinformatics* **2006**, *7*, 124-137.
54. Bretscher, L. E.; Jenkins, C. L.; Taylor, K. M.; DeRider, M. L.; Raines, R. T., "Conformational stability of collagen relies on a stereoelectronic effect," *J. Am. Chem. Soc.* **2001**, *123*, 777-778.
55. Berg, R. A.; Prockop, D. J., "The thermal transition of a non-hydroxylated form of collagen. Evidence for a role for hydroxyproline in stabilizing the triple-helix of collagen" *Biochem. Biophys. Res. Comm.* **1973**, *52*, 115-120.
56. Ramachandran, G. N.; Bansala, M.; Bhatnagar, R. S., "A hypothesis on the role of hydroxyproline in stabilizing collagen structure". *Biochem. Biophys. Acta-Protein Structure* **1973**, *322*, 166-171.
57. Bella, J.; Eaton, M.; Brodsky, B.; Berman, H. M., "Crystal and molecular structure of a collagen-like peptide at 1.9 Å resolution," *Science* **1994**, *266*, 75-81.
58. Brinckmann, J.; Notbohm, H.; Müller, P. K., "*Collagen: Primer in structure, processing, and assembly*," **2005**, Springer Berlin Heidelberg.
59. Beausoleil, E.; Lubell, W. D., "Steric effects on the amide isomer equilibrium of prolyl peptides. Synthesis and conformational analysis of *N*-acetyl-5-*tert*-butylproline *N*-methylamides," *J. Am. Chem. Soc.* **1999**, *118*, 12902-12908.
60. Eberhardt, E. S.; Panasik, J. N.; Raines, R. T., "Inductive effects on the energetics of prolyl peptide bond isomerization: Implications for collagen folding and stability," *J. Am. Chem. Soc.* **1996**, *118*, 12261-12266.
61. Holmgren, S. K.; Bretscher, L. E.; Taylor, K. M.; Raines, R. T., "A hyperstable collagen mimic," *Chem. Biol.* **1999**, *6*, 63-70.
62. Andreotti, A. H.; Kahne, D., "The effects of glycosylation on peptide backbone conformation," *J. Am. Chem. Soc.* **1993**, *115*, 3352-3353.
63. Liang, R.; Andreotti, A. H.; Kahne, D., "Sensitivity of glycopeptide conformation to carbohydrate chain length," *J. Am. Chem. Soc.* **1995**, *117*, 10395-10396.
64. Renner, C.; Alefelder, S.; Bae, J. H.; Budisa, N.; Huber, R.; Moroder, L., "Fluoroprolines as tools for protein design and engineering," *Angew. Chem. Int. Ed.* **2001**, *40*, 923-925.

65. Taylor, C. M.; Hardré, R.; Edwards, P. J. B.; Park, J. H., "Factors affecting conformation in proline-containing peptides," *Org. Lett.* **2003**, *5*, 4413-4416.
66. Taylor, C. M.; Hardré, R.; Edwards, P. J. B., "The impact of pyrrolidine hydroxylation on the conformation of proline-containing peptides," *J. Org. Chem.* **2005**, *70*, 1306-1315.
67. Jr. Panasik, N.; Eberhardt, E. S.; Edison, A. S.; Powell, D. R.; Raines, R. T., "Inductive effects on the structure of proline residues," *Int. J. Pep. Prot. Res.* **1994**, *44*, 262-269.
68. (a) Lamport, D. T. A., "Hydroxyproline-O-glycosidic linkage of the plant cell wall glycoprotein extensin," *Nature* **1967**, *216*, 1322-1324; (b) Lamport, D. T. A., "Structure, biosynthesis and significance of cell wall glycoproteins," *Recent Adv. Phytochem.* **1977**, *11*, 79-115.
69. Owens, N. W.; Braun, C.; O'Neil, J. D.; Marat, K.; Schweizer, F., "Effects of glycosylation of (2S,4R)-4-hydroxyproline on the conformation, kinetics, and thermodynamics of prolyl amide isomerization," *J. Am. Chem. Soc.* **2007**, *129*, 11670-11671.
70. Koehn, F. E.; Longley, R. E.; Reed, J. K., "Microcolins A and B, new immunosuppressive peptide from the blue-green alga *Lyngbya majuscula*," *J. Nat. Prod.* **1992**, *55*, 613-619.
71. Owens, N. W.; Lee, A.; Marat, K.; Schweizer, F., "The implications of (2S,4S)-hydroxyproline 4-O-glycosylation for prolyl amide isomerization," *Chem. Eur. J.* **2009**, *15*, 10649-10657.
72. Deferrari, J. O.; Gros, E. G.; Mastronardi, I. O., "Methylation of carbohydrates bearing base-labile substituents, with diazomethane-boron trifluoride etherate : II. A new synthesis of 2-O-methyl-D-mannose," *Carbohydr. Res.* **1967**, *4*, 432-434.
73. (a) Gerig, J. T.; McLeod, R. S., "Conformations of *cis*- and *trans*-4-fluoro-Yl-proline in aqueous solution," *J. Am. Chem. Soc.* **1973**, *95*, 5725-5729; (b) Cai, M.; Huang, Y.; Liu, J.; Krishnamoorthi, R., "Solution conformations of proline rings in proteins studied by NMR spectroscopy," *J. Biom. NMR* **1995**, *6*, 123-128.
74. Jenkins, C. L.; McCloskey, A. I.; Guzei, I. A.; Eberhardt, E. S.; Raines, R. T., "O-Acylation of hydroxyproline residues: Effect on peptide bond isomerization and collagen stability," *Biopolymers* **2005**, *80*, 1-8.
75. Morris, M. B.; Ralston, J. G. B.; Biden, T. J.; Browne, C. L.; King, G. F.; Iismaa, T. P., "Structural and biochemical studies of human galanin: NMR evidence for nascent helical structures in aqueous solution," *Biochemistry* **1995**, *34*, 4538-4545.
76. Williams, T. J.; Kershaw, A. D.; Li, V.; Wu, X., "An inversion recovery NMR kinetics experiment," *J. Chem. Educ.* **2011**, *88*, 665-669.
77. Beausoleil, E.; Sharma, R.; Michnick, S. W.; Lubell, W. D., "Alkyl 3-position substituents retard the isomerization of prolyl and hydroxyprolyl amides in water," *J. Org. Chem.* **1998**, *63*, 6572-6578.

78. Jenkins, C. L.; Bretscher, L. E.; Guzei, I. A.; Raines, R. T., "Effect of 3-hydroxyproline residues on collagen stability," *J. Am. Chem. Soc.* **2003**, *125*, 6422-6427.
79. Chorghade, M. S.; Mohapatra, D. K.; Sahoo, G.; Gurjar, M. K.; Mandlecha, M. V.; Bhoite, N.; Moghe, S.; Raines, R. T., "Practical syntheses of 4-fluoroprolines," *J. Fluor. Chem.* **2008**, *129*, 781-784.
80. Hodges, J. A.; Raines, R. T., "Stereo-electronic effects on collagen stability: The dichotomy of 4-fluoroproline diastereomers," *J. Am. Chem. Soc.* **2003**, *125*, 9262-9263.
81. (a) Demange, L.; Ménez, A.; Dugave, C., "Practical synthesis of Boc and Fmoc protected 4-fluoro and 4-difluoroprolines from *trans*-4-hydroxyproline," *Tetrahedron Lett.* **1998**, *39*, 1169-1172; (b) Demange, L.; Cluzeau, J.; Ménez, A.; Dugave, C., "Synthesis of optically pure *N*-Boc-protected (2*R*,3*R*)- and (2*R*,3*S*)-3-fluoroprolines," *Tetrahedron Lett.* **2001**, *42*, 651-653; (c) Tran, T. T.; Patino, N.; Condom, R.; Frogier, T.; Guedj, R., "Fluorinated peptides incorporating a 4-fluoroproline residue as potential inhibitors of HIV protease," *J. Fluor. Chem.* **1997**, *82*, 125-130.
82. Shaginian, A.; Whitby, L. R.; Hong, S.; Hwang, I.; Farooqi, B.; Searcey, M.; Chen, J.; Vogt, P. K.; Boger, D. L., "Design, synthesis, and evaluation of an  $\alpha$ -helix mimetic library targeting protein-protein interactions," *J. Am. Chem. Soc.* **2009**, *131*, 5564-5572.
83. Davis, J. M.; Tsou, L. K.; Hamilton, A. D., "Synthetic non-peptide mimetics of  $\alpha$ -helices," *Chem. Soc. Rev.* **2007**, *36*, 326-334.
84. Barlow, D. J.; Thornton, M., "Helix geometry in proteins," *J. Mol. Biol.* **1988**, *201*, 601-619.
85. Zimm, B. H.; Bragg, J. K., "Theory of the phase transition between helix and random coil in polypeptide chains," *J. Chem. Phys.* **1959**, *31*, 526-535.
86. Henchey, L. K.; Jochim, A. L.; Arora, P. S., "Contemporary strategies for the stabilization of peptides in the  $\alpha$ -helical conformation," *Curr. Opin. Chem. Biol.* **2008**, *12*, 692-697.
87. Davis, J. M.; Tsou, L. K.; Hamilton, A. D., "Synthetic non-peptide mimetics of  $\alpha$ -helices," *Chem. Soc. Rev.* **2007**, *36*, 326-334.
88. (a) Dimartino, G.; Wang, D.; Chapman, R. N.; Arora, P. S., "Solid-phase synthesis of hydrogen-bond surrogate-derived  $\alpha$ -helices," *Org. Lett.* **2005**, *7*, 2389-2392; (b) Wang, D.; Chen, K.; Kulp III, J., L.; Arora, P. S., "Evaluation of biologically relevant short  $\alpha$ -helices stabilized by a main-chain hydrogen-bond surrogate," *J. Am. Chem. Soc.* **2006**, *128*, 9248-9256; (c) Wang, D.; Chen, K.; Dimartino, G.; Arora, P. S., "Nucleation and stability of hydrogen-bond surrogate-based  $\alpha$ -helices," *Org. Biomol. Chem.* **2006**, *21*, 4074-4081; (d) Patgiri, A.; Andrea, L. J.; Arora, P. S., "A hydrogen bond surrogate approach for stabilization of short peptide sequences in  $\alpha$ -helical conformation," *Acc. Chem. Res.* **2008**, *41*, 1289-1300.
89. Restorp, P.; Jr. Rebek, J., "Synthesis of  $\alpha$ -helix mimetics with four side-chains," *Bioorg. Med. Chem. Lett.* **2008**, *18*, 5909-5911.
90. Garner, J.; Harding, M. M., "Design and synthesis of  $\alpha$ -helical peptides and mimetics," *Org. Biomol. Chem.* **2007**, *5*, 3577-3585.

91. Henchey, L. K.; Porter, J. R.; Ghosh, I.; Arora, P. S., "High specificity in protein recognition by hydrogen-bond-surrogate  $\alpha$ -helices: selective inhibition of the p53/MDM2 complex," *Chem. Bio. Chem* **2010**, *11*, 2104-2107.
92. Orner, B. P.; Ernst, J. T.; Hamilton, A. D., "Toward proteomimetics: Terphenyl derivatives as structural and functional mimics of extended regions of an  $\alpha$ -helix," *J. Am. Chem. Soc.* **2001**, *123*, 5382-5383.
93. Reed, J. C., "Double identity for proteins of the Bcl-2 family," *Nature* **1997**, *387*, 773-776.
94. Yin, H.; Lee, G.-i.; Sedey, K. A.; Kutzki, O.; Park, H. S.; Orner, B. P.; Ernst, J. T.; Wang, H.-G.; Sebt, S. M.; Hamilton, A. D., "Terphenyl-based bak BH3  $\alpha$ -helical proteomimetics as low-molecular-weight antagonists of Bcl-xL," *J. Am. Chem. Soc.* **2005**, *127*, 10191-10196.
95. Yin, H.; Lee, G.-I.; Hamilton, A. D., "Alpha-helix mimetics in drug discovery,". In *Drug Discovery Research: New Frontiers in the Post-Genomic Era*, Huang, Z., Ed. **2007**, 280-298, John Wiley & Sons, Inc.
96. Horwell, D. C.; Howson, W.; Ratcliffe, G. S.; Willems, H. M. G., "The design of dipeptide helical mimetics: The synthesis, tachykinin receptor affinity and conformational analysis of 1,1,6-trisubstituted indanes," *Bioorg. & Med. Chem.* **1996**, *33*, 33-42.
97. Jochim, A. L.; Arora, P. S., "Assessment of helical interfaces in protein-protein interactions," *Mol. BioSyst.* **2009**, *5*, 924-926.
98. Cabezas, E.; Satterthwait, A. C., "The hydrogen bond mimic approach: Solid-phase synthesis of a peptide stabilized as an  $\alpha$ -helix with a hydrazone link," *J. Am. Chem. Soc.* **1999**, *121*, 3862-3875.
99. Patgiri, A.; Jochim, A. L.; Arora, P. S., "A hydrogen bond surrogate approach for stabilization of short peptide sequences in alpha-helical conformation," *Acc. Chem. Res.* **2008**, *41*, 1289-1300.
100. Vernall, A. J.; Cassidy, P.; Alewood, P. F., "A single  $\alpha$ -helical turn stabilized by replacement of an internal hydrogen bond with a covalent ethylene bridge," *Angew. Chem. Int. Ed.* **2009**, *48*, 5675-5678.
101. Mitsukawa, K.; Lu, X.; Bartfai, T., "Galanin, galanin receptors and drug targets," *Cell. Mol. Life Sci.* **2008**, *65*, 1796-1805.
102. Carpenter, K. A.; Schmidt, R.; Yu, S. Y.; Hodzic, L.; Pou, C.; Payza, K.; Godbout, C.; Brown, W.; Roberts, E., "The glycine1 residue in cyclic lactam analogues of galanin(1-16)-NH<sub>2</sub> is important for stabilizing an N-terminal helix," *Biochem.* **1999**, *38*, 15295-15304.
103. Morris, M. B.; Ralston, J. G. B.; Biden, T. J.; Browne, C. L.; King, G. F.; Iismaa, T. P., "Structural and biochemical studies of human galanin: NMR evidence for nascent helical structures in aqueous solution," *Biochem.* **1995**, *34*, 4538-4545.



104. Teng-umnuay, P.; Morris, H. R.; Dell, A.; Panico, M.; Paxton, T.; West, C. M., "The cytoplasmic F-box binding protein Skp1 contains a novel pentasaccharide linked to hydroxyproline in *Dictyostelium*," *J. Biol. Chem.* **1998**, *273*, 18242-18249.
105. Carpino, L. A., "1-Hydroxy-7-azabenzotriazole. An efficient peptide coupling additive," *J. Am. Chem. Soc.* **1993**, *115*, 4397-4398.
106. Taylor, C. M.; Weir, C. A., "Synthesis of the repeating decapeptide unit of Mefp1 in orthogonally protected form," *J. Org. Chem.* **2000**, *65*, 1414-1425.
107. Hoffman, R. V.; Maslouh, N.; Lee, F. C., "Highly stereoselective syntheses of syn- and anti-1,2-amino alcohols," *J. Org. Chem.* **2002**, *67*, 1045-1056.
108. Hoffman, R. V.; Tao, J., "A stereocontrolled synthesis of monofluoro ketomethylene sipeptide isosteres," *Tetrahedron Lett.* **1998**, *39*, 4195-4198.
109. Dragovich, P. S.; Prins, T. J.; Zhou, R.; Fuhrman, S. A.; Patick, A. K.; Matthews, D. A.; Ford, C. E.; Meador III, J. W.; Ferre, R. A.; Worland, S. T., "Structure-based design, synthesis, and biological evaluation of irreversible human rhinovirus 3C protease inhibitors. 3. structure-activity studies of ketomethylene-containing peptidomimetics," *J. Med. Chem.* **1999**, *42*, 1203-1212.
110. Shie, J.-J.; Fang, J.-M.; Kuo, T.-H.; Kuo, C.-J.; Liang, P.-H.; Huang, H.-J.; Wu, Y.-T.; Jan, J.-T.; Cheng, Y.-S. E.; Wong, C.-H., "Inhibition of the severe acute respiratory syndrome 3CL protease by peptidomimetic alpha,beta-unsaturated esters," *Bioorganic & Medicinal Chemistry* **2005**, *13*, 5240-5252.
111. Murakami, N.; Wang, W.; Tamura, S.; Kobayashi, M., "Synthesis and biological property of carba and 20-Deoxo analogues of arenastatin A," *Biorg. Med. Chem. Lett.* **2000**, *10*, 1823-1826.
112. Auge, F.; Hornebeck, W.; Decarme, M.; Laronze, J.-Y., "Improved gelatinase a selectivity by novel zinc binding groups containing galardin derivatives," *Biorg. Med. Chem. Lett.* **2003**, *13*, 1783-1786.
113. (a) Markgraf, J. H.; Davis, H. A., "Steric course of lactonization in the deamination of glutamic acid: An organic mechanism experiment," *J. Chem. Educ.* **1990**, *67*, 173-174; (b) Zhang, D.-W.; Luo, Z.; Liu, G.-J.; Weng, L.-H., " $\alpha$  N-O turn induced by fluorinated  $\alpha$ -aminoxy diamide: synthesis and conformational studies," *Tetrahedron* **2009**, *65*, 9997-10001; (c) Levy, S. G.; Jacques, V.; Zhou, K. L.; Kalogeropoulos, S.; Schumacher, K.; Amedio, J. C.; Scherer, J. E.; Witowski, S. R.; Lombardy, R.; Koppetsch, K., "Development of a multigram asymmetric synthesis of 2-(*R*)-2-(4,7,10-*tris tert*-Butylcarboxymethyl-1,4,7,10-*tetraazacyclododec-1-yl*)-pentanedioic acid, 1-*tert*-Butyl Ester, (*R*)-*tert*-Bu<sub>4</sub>-DOTAGA," *Org. Process Res. Dev.* **2009**, *13*, 535-542; (d) Cai, X.; Chorghade, M. S.; Fura, A.; Grewal, G. S.; Jauregui, K. A.; Lounsbury, H. A.; Scannell, R. T.; Yeh, C. G.; Young, M. A.; Yu, S., "Synthesis of CMI-977, a potent 5-lipoxygenase inhibitor," *Org. Proc. Res. Dev.* **1999**, *3*, 73-76.
114. Ehrlich, A.; Heyne, H. U.; Winter, R.; Beyermann, M.; Haber, H.; Carpino, L. A.; Bienert, M., "Cyclization of all-L-pentapeptides by means of 1-hydroxy-7-azabenzotriazole-derived uronium and phosphonium reagents," *J. Org. Chem.* **1996**, *61*, 8831-8838.

115. Maulucci, N.; Izzo, I.; Bifulco, G.; Aliberti, A.; De Cola, C.; Comegna, D.; Gaeta, C.; Napolitano, A.; Pizza, C.; Tedesco, C.; Flot, D.; De Riccardis, F., "Synthesis, structures, and properties of nine-, twelve-, and eighteen-membered *N*-benzyloxyethyl cyclic  $\alpha$ -peptoids," *Chem. Commun.* **2008**, 3927-3929.
116. Shin, S. B. Y.; Yoo, B.; Todaro, L. J.; Kirshenbaum, K., "Cyclic Peptoids," *J. Am. Chem. Soc.* **2007**, *129*, 3218-3225.
117. (a) Woody, R. W., "Circular dichroism," *Method. Enzymol.* **1995**, *246*, 34-71; (b) Woody, R. W.; Koslowski, A., "Recent developments in the electronic spectroscopy of amides and  $\alpha$ -helical polypeptides," *Biophys. Chem.* **2002**, *101*, 535-551.
118. (a) Corrêa, D. H. A.; Ramos, C. H. I., "The use of circular dichroism spectroscopy to study protein folding, form and function," *Afr. J. Biochem. Res.* **2009**, *3*, 164-173; (b) Bulheller, B. M.; Rodgerb, A.; Hirst, J. D., "Circular and linear dichroism of proteins," *Phys. Chem. Chem. Phys.* **2007**, *9*, 2020-2035.
119. Qasba, P. K.; Boeggeman, E.; Ramakrishnan, B., "Site-specific linking of biomolecules via glycan residues using glycosyltransferases," *Biotechnol Prog.* **2008**, *24*, 520-526.
120. Steiner, T.; Hess, P.; Bae, J. H.; Wiltschi, B.; Moroder, L.; Budisa, N., "Synthetic biology of proteins: tuning GFPs folding and stability with fluoroproline," *PLoS One* **2008**, *27*, 1680-1695.
121. Crespo, M. D.; Rubini, M., "Rational design of protein stability: Effect of (2*S*,4*R*)-4-fluoroproline on the stability and folding pathway of ubiquitin," *PLoS One* **2011**, *6*, 19425-19433.
122. Kim, W.; George, A.; Evans, M.; Conticello, V. P., "Cotranslational incorporation of a structurally diverse series of proline analogues in an *Escherichia coli* expression system," *Chem. biochem.* **2004**, *5*, 928-936.
123. Franke, J.; Kessin, R., "A defined minimal medium for axenic strains of *Dictyostelium discoideum*," *Proc. Natl. Acad. Sci. USA* **1977**, *74*, 2157-2161.
124. Waldscheck, B.; Streiff, M.; Notz, W.; Kinzy, W.; Schmidt, R. R., " $\alpha$ (1-3)-Galactosyltransferase inhibition based on a new type of disubstrate analogue," *Angew. Chem. Int. Ed.* **2001**, *40*, 4007-4011.
125. (a) Sarkar, A. K.; Fritz, T. A.; Taylor, W. H.; Esko, J. D., "Disaccharide uptake and priming in animal cells: inhibition of sialyl Lewis X by acetylated Gal  $\beta$  1- $\rightarrow$ 4GlcNAc  $\beta$ -*O*-naphthalenemethanol," *Proc. Natl. Acad. Sci. USA.* **1995**, *92*, 3323-3327; (b) Sarkar, A. K.; Rostand, K. S.; Jain, R. K.; Matta, K. L.; Esko, J. D., "Fucosylation of disaccharide precursors of sialyl LewisX inhibit selectin-mediated cell adhesion," *J. Biol. Chem.* **1997**, *272*, 25608-25616; (c) Sarkar, A. K.; Brown, J. R.; Esko, J. D., "Synthesis and glycan priming activity of acetylated disaccharide," *Carbohydr. Res.* **2000**, *329*, 287-300.

## APPENDIX: LETTERS OF PERMISSION



**Book:** Drug Discovery Research: New Frontiers in the Post-Genomic Era  
**Chapter:** Computer-Aided Drug Design  
**Author:** Grace Shiahuy Chen, Ji-Wang Chern  
**Publisher:** John Wiley and Sons  
**Date:** Nov 2, 2006  
Copyright © 2007 John Wiley & Sons, Inc.

Logged in as:  
Chamini Karunaratne



### Order Completed

Thank you very much for your order.

This is a License Agreement between Chamini V Karunaratne ("You") and John Wiley and Sons ("John Wiley and Sons"). The license consists of your order details, the terms and conditions provided by John Wiley and Sons, and the [payment terms and conditions](#).

[Get the printable license.](#)

License Number	3243810773704
License date	Oct 07, 2013
Licensed content publisher	John Wiley and Sons
Licensed content publication	Wiley eBooks
Licensed content title	Computer-Aided Drug Design
Book title	Drug Discovery Research: New Frontiers in the Post-Genomic Era
Licensed copyright line	Copyright © 2007 John Wiley & Sons, Inc.
Licensed content author	Grace Shiahuy Chen, Ji-Wang Chern
Licensed content date	Nov 2, 2006
Start page	89
End page	107
Type of use	Dissertation/Thesis
Requestor type	University/Academic
Format	Print and electronic
Portion	Figure/table
Number of figures/tables	2
Original Wiley figure/table number(s)	x-ray crystal structure
Will you be translating?	No
Total	0.00 USD



**Title:** A Hydrogen Bond Surrogate Approach for Stabilization of Short Peptide Sequences in  $\alpha$ -Helical Conformation

**Author:** Anupam Patgiri, Andrea L. Jochim, and Paramjit S. Arora

**Publication:** Accounts of Chemical Research

**Publisher:** American Chemical Society

**Date:** Oct 1, 2008

Copyright © 2008, American Chemical Society

Logged in as:  
Chamini Karunaratne



### PERMISSION/LICENSE IS GRANTED FOR YOUR ORDER AT NO CHARGE


This type of permission/license, instead of the standard Terms & Conditions, is sent to you because no fee is being charged for your order. Please note the following:

- Permission is granted for your request in both print and electronic formats, and translations.
- If figures and/or tables were requested, they may be adapted or used in part.
- Please print this page for your records and send a copy of it to your publisher/graduate school.
- Appropriate credit for the requested material should be given as follows: "Reprinted (adapted) with permission from (COMPLETE REFERENCE CITATION). Copyright (YEAR) American Chemical Society." Insert appropriate information in place of the capitalized words.
- One-time permission is granted only for the use specified in your request. No additional uses are granted (such as derivative works or other editions). For any other uses, please submit a new request.

If credit is given to another source for the material you requested, permission must be obtained from that source.



**Chapter:** Detection of Cytoplasmic Glycosylation Associated with Hydroxyproline  
**Book:** Methods in Enzymology, Volume 417  
**Author:** Christopher M. West, Hanke van der Wel, Ira J. Blader  
**Publisher:** Elsevier  
**Date:** 2006  
 Copyright © 2006, Elsevier

Logged in as:  
 Chamini Karunaratne  


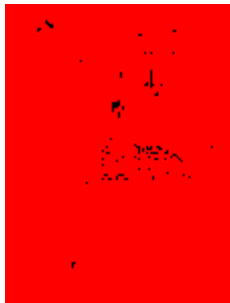
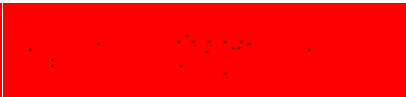
## Order Completed

Thank you very much for your order.

This is a License Agreement between Chamini V Karunaratne ("You") and Elsevier ("Elsevier"). The license consists of your order details, the terms and conditions provided by Elsevier, and the [payment terms and conditions](#).

[Get the printable license](#).

License Number	3243820347506
License date	Oct 07, 2013
Licensed content publisher	Elsevier
Licensed content publication	Elsevier Books
Licensed content title	Methods in Enzymology, Volume 417
Licensed content author	Christopher M. West, Hanke van der Wel, Ira J. Blader
Licensed content date	2006
Number of pages	16
Type of Use	reuse in a thesis/dissertation
Portion	figures/tables/illustrations
Number of figures/tables/illustrations	1
Format	both print and electronic
Are you the author of this Elsevier chapter?	No
Will you be translating?	No
Order reference number	
Title of your thesis/dissertation	Structural and synthesis studies of the Pro143 region of Skp1 in Dictyostelium discoideum
Expected completion date	Dec 2013
Estimated size (number of pages)	300
Elsevier VAT number	GB 494 6272 12
Permissions price	0.00 USD
VAT/Local Sales Tax	0.00 USD / 0.00 GBP
Total	0.00 USD



**Title:** A cytoplasmic prolyl hydroxylation and glycosylation pathway modifies Skp1 and regulates O2-dependent development in *Dictyostelium*

**Author:** Christopher M. West, Zhuo A. Wang, Hanke van der Wel

**Publication:** Biochimica et Biophysica Acta (BBA) - General Subjects

**Publisher:** Elsevier

**Date:** February 2010

Copyright © 2010, Elsevier

Logged in as:  
Chamini Karunaratne



### Order Completed

Thank you very much for your order.

This is a License Agreement between Chamini V Karunaratne ("You") and Elsevier ("Elsevier"). The license consists of your order details, the terms and conditions provided by Elsevier, and the [payment terms and conditions](#).

[Get the printable license.](#)

License Number	3243820530164
License date	Oct 07, 2013
Licensed content publisher	Elsevier
Licensed content publication	Biochimica et Biophysica Acta (BBA) - General Subjects
Licensed content title	A cytoplasmic prolyl hydroxylation and glycosylation pathway modifies Skp1 and regulates O2-dependent development in <i>Dictyostelium</i>
Licensed content author	Christopher M. West, Zhuo A. Wang, Hanke van der Wel
Licensed content date	February 2010
Licensed content volume number	1800
Licensed content issue number	2
Number of pages	12
Type of Use	reuse in a thesis/dissertation
Portion	figures/tables/illustrations
Number of figures/tables/illustrations	1
Format	both print and electronic
Are you the author of this Elsevier article?	No
Will you be translating?	No
Order reference number	
Title of your thesis/dissertation	Structural and synthesis studies of the Pro143 region of Skp1 in <i>Dictyostelium discoideum</i>
Expected completion date	Dec 2013
Estimated size (number of pages)	300
Elsevier VAT number	GB 494 6272 12

Permissions price	0.00 USD
VAT/Local Sales Tax	0.00 USD / 0.00 GBP
Total	0.00 USD



**Title:** Requirements for Skp1 Processing by Cytosolic Prolyl 4(trans)-Hydroxylase and  $\alpha$ -N-Acetylglucosaminyltransferase Enzymes Involved in O2 Signaling in Dictyostelium

**Author:** Hanke van der Wel, Jennifer M. Johnson, Yuechi Xu, Chamini V. Karunaratne, Kyle D. Wilson, Yusuf Vohra, Geert-Jan Boons, Carol M. Taylor, Brad Bendiak, and Christopher M. West

**Publication:** Biochemistry

**Publisher:** American Chemical Society

**Date:** Mar 1, 2011

Logged in as:  
Chamini Karunaratne



Copyright © 2011, American Chemical Society

#### PERMISSION/LICENSE IS GRANTED FOR YOUR ORDER AT NO CHARGE

This type of permission/license, instead of the standard Terms & Conditions, is sent to you because no fee is being charged for your order. Please note the following:

- Permission is granted for your request in both print and electronic formats, and translations.
- If figures and/or tables were requested, they may be adapted or used in part.
- Please print this page for your records and send a copy of it to your publisher/graduate school.
- Appropriate credit for the requested material should be given as follows: "Reprinted (adapted) with permission from (COMPLETE REFERENCE CITATION). Copyright (YEAR) American Chemical Society." Insert appropriate information in place of the capitalized words.
- One-time permission is granted only for the use specified in your request. No additional uses are granted (such as derivative works or other editions). For any other uses, please submit a new request.



If credit is given to another source for the material you requested, permission must be obtained from that source.



**Title:** A hyperstable collagen mimic  
**Author:** Steven K Holmgren, Lynn E Bretscher, Kimberly M Taylor, Ronald T Raines  
**Publication:** Chemistry & Biology  
**Publisher:** Elsevier  
**Date:** February 1999  
Copyright © 1999, Elsevier

Logged in as:  
Chamini Karunaratne  
Account #:  
3000704758

### Order Completed

Thank you very much for your order.

This is a License Agreement between Chamini V Karunaratne ("You") and Elsevier ("Elsevier"). The license consists of your order details, the terms and conditions provided by Elsevier, and the [payment terms and conditions](#).

[Get the printable license.](#)

License Number	3250571498364
License date	Oct 16, 2013
Licensed content publisher	Elsevier
Licensed content publication	Chemistry & Biology
Licensed content title	A hyperstable collagen mimic
Licensed content author	Steven K Holmgren, Lynn E Bretscher, Kimberly M Taylor, Ronald T Raines
Licensed content date	February 1999
Licensed content volume number	6
Licensed content issue number	2
Number of pages	8
Type of Use	reuse in a thesis/dissertation
Portion	figures/tables/illustrations
Number of figures/tables/illustrations	1
Format	both print and electronic

Are you the author of this Elsevier article?	No
Will you be translating?	No
Order reference number	
Title of your thesis/dissertation	Structural and synthesis studies of the Pro143 region of Skp1 in Dictyostelium discoideum
Expected completion date	Dec 2013
Estimated size (number of pages)	300
Elsevier VAT number	GB 494 6272 12
Permissions price	0.00 USD
VAT/Local Sales Tax	0.00 USD / 0.00 GBP
Total	0.00 USD

# Copyright Permission Policy

These guidelines apply to the reuse of articles, figures, charts and photos in the *Journal of Biological Chemistry*, *Molecular & Cellular Proteomics* and the *Journal of Lipid Research*.

## For authors reusing their own material:

Authors need **NOT** contact the journal to obtain rights to reuse their own material. They are automatically granted permission to do the following:

- Reuse the article in print collections of their own writing.
- Present a work orally in its entirety.
- Use an article in a thesis and/or dissertation.
- Reproduce an article for use in the author's courses. (If the author is employed by an academic institution, that institution also may reproduce the article for teaching purposes.)
- Reuse a figure, photo and/or table in future commercial and noncommercial works.
- Post a copy of the paper in PDF that you submitted via BenchPress.
- Link to the journal site containing the final edited PDFs created by the publisher.

EXCEPTION: If authors select the Author's Choice publishing option:

- The final version of the manuscript will be covered under the Creative Commons Attribution license (CC BY), the most accommodating of licenses offered. [Click here for details.](#)
- The final version of the manuscript will be released immediately on the publisher's website and PubMed Central.

Please note that authors must include the following citation when using material that appeared in an ASBMB journal:

"This research was originally published in Journal Name. Author(s). Title. *Journal Name*. Year; Vol:pp–pp. © the American Society for Biochemistry and Molecular Biology."

## For other parties using material for noncommercial use:

Other parties are welcome to copy, distribute, transmit and adapt the work — at no cost and without permission — for noncommercial use as long as they attribute the work to the original source using the citation above.

Examples of noncommercial use include:

- Reproducing a figure for educational purposes, such as schoolwork or lecture presentations, with attribution.
- Appending a reprinted article to a Ph.D. dissertation, with attribution.

## **For other parties using material for commercial use:**

Navigate to the article of interest and click the "Request Permissions" button on the middle navigation bar. (See diagram at right.) It will walk you through the steps for obtaining permission for reuse.

Examples of commercial use by parties other than authors include:

- Reproducing a figure in a book published by a commercial publisher.
- Reproducing a figure in a journal article published by a commercial publisher.

Updated March 20, 2013

## THE VITA

Chamini Vichithra Karunaratne was born in Colombo, Sri Lanka, to Upali Karunaratne and Irine Karunaratne. She received her Bachelor of Science in Chemistry from the University of Colombo in August 2006. She later worked as an Assistant Lecturer at the University of Colombo and as a Teaching Assistant at Open University, Sri Lanka. In Fall 2008, she was accepted to Graduate School Doctoral Program at Louisiana State University in the Department of Chemistry where she is currently a doctoral candidate in organic chemistry working under the direction of Dr. Carol M. Taylor. Her graduate dissertation work involved the synthesis of an  $\alpha$ -helical mimetic for Skp1 and structural studies of Pro<sup>143</sup> region of Skp1 protein. Chamini is a member of the American Chemical Society.